Theoretical Condensed Matter Physics
Principal Investigators' Meeting
August 14–16, 2018
Gaithersburg, Maryland

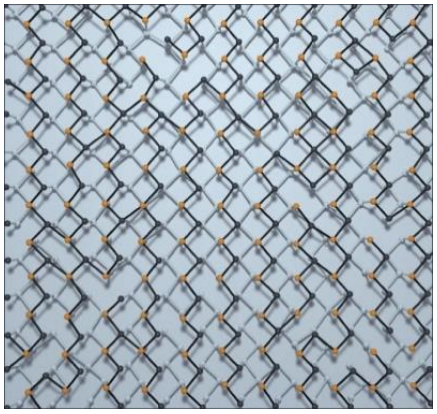

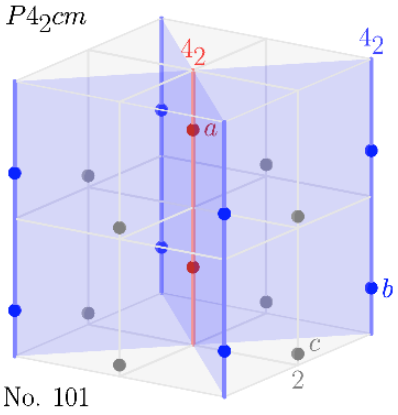

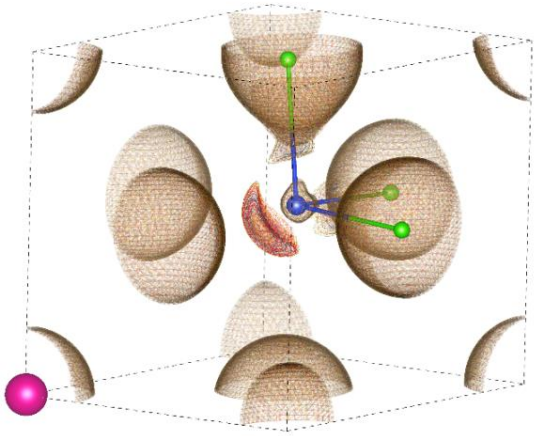

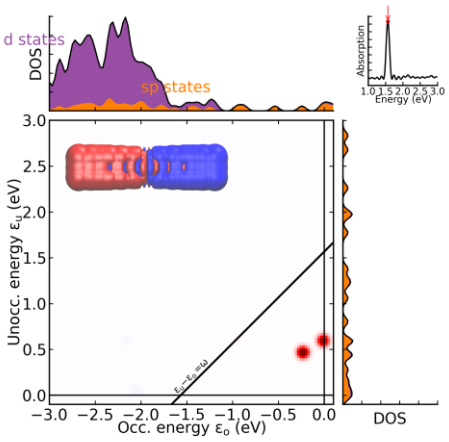

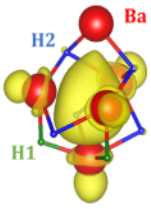

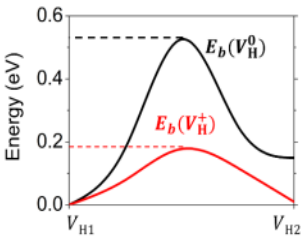

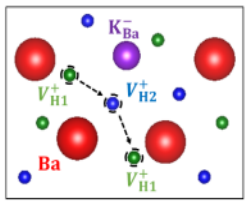

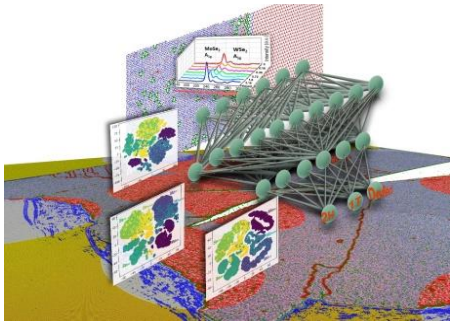

Office of Basic Energy Sciences
Division of Materials Sciences and Engineering

U.S. DEPARTMENT OF ENERGY | Office of Science

On the Cover

Top left: Salvador Barraza-Lopez, Univ. of Arkansas: Snapshot of a 12x12 SnSe monolayer at room temperature. M. Mehboudi, A.M. Dorio, W. Zhu, A. van der Zande, H.O.H. Churchill, A.A. Pacheco-Sanjuan, E.O. Harriss, P. Kumar, and S. Barraza-Lopez, Nano Lett. 16, 1704 (2016).

Top right: Michael Hermele, Univ. of Colorado: Topological phases protected by the geometrical symmetries of crystal lattices can be built from simpler lower-dimensional states, arranged in a crystalline pattern. S.-J. Huang, H. Song, Y.-P. Huang, and M. Hermele, Phys. Rev. B 96, 205106 (2017), Editor's Suggestion.

Middle left: Walter Lambrecht, Case Western Reserve Univ.: Total valence charge density for the relaxed distorted halide perovskite $RbGeCl_3$. Lone-pair s-electron makes this material a ferro-electric semiconductor. S. K. Radha, C. Bahandari, and W. R. L. Lambrecht, Phys. Rev. Materials 2, 063605 (2018).

Middle right: Rahman Talat, Univ. of Central Florida: Transition Contribution Maps for the plasmonic peak at 1.57 eV arising from an array of three Au chains each consisting of 14 atoms (unpublished).

Bottom left: Chris Van de Walle, UC Santa Barbara: The high hydride ionic conductivity in BaH_2 is explained by diffusion through a vacancy mechanism, and can be enhanced by doping with alkali metals such as K. A. J. E. Rowberg, L. Weston, and C. G. Van de Walle, Chemistry of Materials 30, 5878 (2018).

Bottom right: Priya Vashishta, Univ. Southern California: Materials Genome Innovation for Computational Software (MAGICS). Machine learning analysis using three layer feed-forward neural network (FNN) during fracture-induced 2H to 1T structural phase transformation in $MoSe_2$ monolayer. Deeper hidden layers of FNN network show successful refinement of classification of Mo and Se atoms belonging to 2H, 1T and defect structures. The FNN model is able to detect each phase with 97% accuracy (unpublished).

This document was produced under contract number DE-SC0014664 between the U.S. Department of Energy and Oak Ridge Associated Universities.

The research grants and contracts described in this document are supported by the U.S. DOE Office of Science, Office of Basic Energy Sciences, Materials Sciences and Engineering Division.

Foreword

This volume is a collection of 4-page research summaries of research projects currently supported by the Theoretical Condensed Matter Physics (TCMP) Program, Materials Sciences and Engineering (MSE) Division in the Office of Basic Energy Sciences (BES) of the U.S. Department of Energy (DOE). It is the program summary prepared for the fourth biennial TCMP Principal Investigators' meeting, held August 14–16, 2018, at the Marriott Washingtonian Center in Gaithersburg, Maryland.

The purpose of the Principal Investigators' (PI) meeting is to bring together researchers supported by the BES TCMP program in order to foster an awareness of the research of others in the program, facilitate the exchange of new results and research highlights, promote new ideas and collaborations among participants and BES scientific user facilities, and identify and pursue new scientific opportunities and new frontiers. The meeting also provides an opportunity for the program managers and MSE/BES management to get a comprehensive overview of the program, which provides opportunities to identify program needs and potential new research directions.

BES supports fundamental research to understand, predict, and ultimately control matter and energy at the electronic, atomic, and molecular levels and fundamental research that provides the foundations for new energy technologies relevant to DOE's missions in energy, environment and national security. Condensed matter theory plays a key role in both the discovery of new organizing principles and the clarification of the origin of newly discovered phenomena.

The TCMP program supports theoretical research efforts in the areas of quantum materials, materials discovery, non-equilibrium transport and ultrafast response, and fundamental research in materials related to energy technologies. Ongoing efforts include research to advance our understanding of strongly correlated electron systems, quantum phase transitions, topological states, computational and data driven materials design, magnetism, superconductivity, wide-bandgap semiconductors, thermoelectric materials, optical response, and neutron and photon scattering. Support for the development of new field theoretical approaches and computational methods includes research in the areas of quantum Monte Carlo techniques, beyond standard density functional theory implementations, dynamical mean field theory, self-consistent GW methods, and density matrix renormalization group theory.

The research supported by the TCMP program expanded recently to include research relevant to the Materials Genome Initiative and now includes support for large projects in computational materials sciences. These projects are developing experimentally validated, robust, open-source software for materials discovery and new ways to make the data available to the materials community. An emphasis of the software development research is to generate community codes that can transition to exascale computers. Additionally, high-performance computing science projects are being supported in partnership with the Office of Advanced Scientific Computing in the Office of Science at DOE. In FY-18, the TCMP program expanded its research support in the area of quantum information science to include research focused on the discovery of new quantum systems and the development of quantum computing capabilities relevant to BES.

We thank all the meeting participants for their active contributions in sharing their ideas and

research accomplishments. We wish to thank Teresa Crockett in MSE and Linda Severs at the Oak Ridge Institute for Science and Education (ORISE) for their excellent work providing all the logistical support for the meeting.

Dr. James W. Davenport & Dr. Matthias J. Graf
Program Managers, Theoretical Condensed Matter Physics
Materials Sciences and Engineering Division, Office of Basic Energy Sciences
Office of Science, U.S. Department of Energy

Table of Contents

AGENDA

2018 Theoretical Condensed Matter Physics
Principal Investigators' Meeting
Materials Sciences and Engineering Division, Office of Basic Energy Sciences
U. S. Department of Energy
Marriott Washingtonian Center, Gaithersburg MD

MONDAY, AUGUST 13, 2018

*****Arrival, Dinner on Your Own*****

TUESDAY, AUGUST 14, 2018

7:00 – 8:30 am	*****Breakfast*****
8:30 – 8:40 am	Matthias Graf, Program Manager, Theoretical Condensed Matter Physics Introduction
Session I	**Title: Topology and Quantum Hall** Chair: Liang Fu, Massachusetts Institute of Technology
8:40 – 9:10 am	Michael Hermele, University of Colorado *Classifications and Constructions of Crystalline Topological Phases*
9:10 – 9:40 am	Arun Bansil, Northeastern University *Toward a First-Principles Description of Stronger Correlations: Stripe and Magnetic Phases in Cuprates to Topological Materials*
9:40 – 10:10 am	Ravindra Bhatt, Princeton University *Engineering Fermi Surfaces of Composite Fermions*
10:10 – 10:30 am	*****Break*****
10:30 – 11:00 am	Jainendra Jain, Pennsylvania State University *Progress towards Quantitative Understanding of the Fractional Quantum Hall Effect*
11:00 – 11:30 am	Rebecca Flint, Iowa State University *Heavy Fermion Physics in Non-Kramers Doublet Materials*
11:30 – 12:00 pm	Linda Horton, Director, Materials Sciences and Engineering Division *BES Program Updates*
12:00 – 1:00 pm	*****Working Lunch***** Jim Davenport, *Ask the Program Manager: Questions, Comments and Thoughts on the Program followed by Poster Session Preview*

Session II	**Title: Computational Materials Physics** Chair: Talat Rahman, University of Central Florida
1:00 – 1:30 pm	Paul Kent, Oak Ridge National Laboratory *Towards Predictive Calculations of Functional Materials*
1:30 – 2:00 pm	Steven Louie, Lawrence Berkeley National Laboratory & University of California Berkeley *Ab Initio Theory and Computation of Excited-State Phenomena at C2SEPEM: Trions, Biexcitons, and Shifted Currents*
2:00 – 2:30 pm	Samuel Trickey, University of Florida *Free Energy Density Functional Theory for Matter under Extreme Conditions*
2:30 – 3:00 pm	Cai-Zhuang Wang, Ames Laboratory *First-Principles Calculation of Correlated Electron Systems based on Gutzwiller Many-Body Wavefunctions*
3:00 – 3:30 pm	***Break***
Session III	**Title: 2D/Nanoscale Materials Physics** Chair: Salvador Barraza-Lopez, University of Arkansas
3:30 – 4:00 pm	Hai-Ping Cheng, University of Florida *First-Principles Studies of Spin-Dependent Charge Transport in Gated 2D Systems*
4:00 – 4:30 pm	Chris Marianetti, Columbia University *Computing Phonons and Their Interactions from First Principles*
4:30 – 5:00 pm	Eugene Mishchenko, University of Utah *Many-Body Depolarization Effect in Metallic Nanotubes*
5:00 – 5:30 pm	Chris Van de Walle, University of California Santa Barbara *Physics and Applications of Hydrogen Interactions with Materials*
5:30 – 6:00 pm	Alex Zunger, University of Colorado *Symmetry Unconstrained Density Functional as a Route for Predicting Magnetism, Gaping, Structural Distortions and Doping in Binary and Ternary 3d Oxides*
6:15 – 7:30 pm	***Working Dinner*** *Scientific Highlights of the Day: Discussion and Input from Attendees*
7:30 – 9:30 pm	***Poster Session I***

WEDNESDAY, AUGUST 15, 2018

7:00 – 8:00 am	***Breakfast***
Session IV	**Title: Superconductivity & Complex Order** Chair: Nandini Trivedi, Ohio State University
8:00 – 8:30 am	Piers Coleman, Rutgers University *Interactions Meet Topology: The Challenge of Topological Kondo Materials*
8:30 – 9:00 am	Rafael Fernandes, University of Minnesota *Quantum Monte Carlo Simulations of Competing Orders Near an Antiferromagnetic Quantum Critical Point*
9:00 – 9:30 am	Adriana Moreo, Oak Ridge National Laboratory & University of Tennessee *New Directions in the Study of Iron Superconductors*
9:30 – 10:00 am	Ziqiang Wang, Boston College *Quantum Anomalous Vortex and Majorana Zero Mode in Fe(Te,Se) Superconductors*
10:00 – 10:30 am	Eun-Ah Kim, Cornell University *Machine Learning Quantum Emergence*
10:30 – 10:45 am	***Break***
Session V	**Title: Transport & Non-Equilibrium** Chair: Aditi Mitra, New York University
10:45 – 11:15 am	Anton Andreev, University of Washington Seattle *Longitudinal Negative Magnetoresistance in Conventional and Topological Conductors*
11:15 – 11:45 am	Andrew Jordan, University of Rochester *Mesoscopic Thermoelectrics and Quantum Measurement Engines*
11:45 – 12:15 pm	Dimitri Kharzeev, Brookhaven National Laboratory & Stony Brook University *Chiral Materials: Anomaly-Induced Transport and Optical Response*
12:15 – 12:45 pm	Yaroslav Tserkovnyak, UCLA *Hydrodynamics of Topological Fields in Insulators*
12:45 – 1:30 pm	***Working Lunch*** Matthias Graf, *TCMP Program Update followed by Poster Session Preview*

Session VI	**Title: Quantum Information Science** Chair: Garnet Chan, California Institute of Technology
1:30 – 2:00 pm	James Freericks, Georgetown University *A Primer on Quantum Computing for the Condensed Matter Theorist*
2:00 – 2:30 pm	Harold Baranger, Duke University *Waveguide QED: Photon Correlations, Capture, and Production*
2:30 – 3:00 pm	Claudio Chamon, Boston University *Controlling Topological Zero Modes for Photons and Majoranas*
3:00 – 3:30 pm	Leonid Glazman, Yale University *Two-Terminal Conductance via Majorana Fermions*
3:30 – 4:00 pm	Valerii Vinokour, Argonne National Laboratory *Fundamental Thermodynamic Frontiers of Quantum Information*
4:00 – 4:30 pm	***Break***
Session VII	**Title: Time Dependence** Chair: Emanuel Gull, University of Michigan
4:30 – 5:00 pm	Thomas Devereaux, SLAC National Accelerator Laboratory & Stanford University *Theoretical Understanding of Photon Spectroscopies in Correlated Materials In and Out of Equilibrium*
5:00 – 5:30 pm	Sahar Sharifzadeh, Boston University *Investigating Excited-States Near Defects with Many-Body Perturbation Theory*
5:30 – 6:00 pm	Michel Van Veenendaal, Northern Illinois University *X-ray Spectroscopy on Excited and Decaying Systems*
6:15 – 7:30 pm	***Working Dinner*** *Scientific Highlights of the Day: Discussion and Input from Attendees*
7:30 – 9:30 pm	***Poster Session II***

THURSDAY, AUGUST 16, 2018

7:00 – 8:00 am	***Breakfast***
Session VIII	**Title: Frustration & Disorder** Chair: Sidney Nagel, University of Chicago
8:00 – 8:30 am	Leon Balents, University of California Santa Barbara *Observing a Quantized Thermal Hall Effect in a Chiral Spin Liquid*
8:30 – 9:00 am	Natalia Perkins, University of Minnesota *Quantum Spin Liquid in the Semiclassical Regime*
9:00 – 9:30 am	Patrick Lee, Massachusetts Institute of Technology *1T-TaS_2 as a 45-Year-Old Quantum Spin Liquid and a Potential Unconventional Superconductor*
9:30 – 10:00 am	Inna Ponomareva, University of South Florida *Uncovering Peculiar Features of Phase Transitions from Advanced Simulations*
10:00 – 10:15 am	*** **Break***
Session IX	**Title: Strongly Correlated Electrons & Magnetic Systems** Chair: Victor Galitski, University of Maryland
10:15 – 10:45 am	Thomas Maier, Oak Ridge National Laboratory & University of Tennessee *Emergent Behavior in Correlated Quantum Matter: Numerical Studies of Single- and Multi-orbital Hubbard Models*
10:45 – 11:15 am	Carsten Ullrich, University of Missouri *Spin Waves in Chiral Two-Dimensional Electron Systems: Larmor's Theorem Revisited*
11:15 – 11:45 am	Eugene Chudnovsky, City University of New York *Skyrmion Glass in Disordered 2D Systems and Quantum Tunneling of Skyrmions*
11:45 – 12:15 pm	Michel Pleimling, Virginia Tech *Relaxation Processes in Systems of Interacting Skyrmions*
12:15 – 12:30 pm	**Wrap-up, debriefing, evaluation** *Meeting feedback, suggestions for future meetings*

Poster Session I

Tuesday, August 14

7:30 – 9:30 PM

1. **Philip B. Allen**, Stony Brook University
   Static and Dynamic Thermal Effects in Solids

2. **Salvador Barraza-Lopez**, University of Arkansas
   Quantum Phenomena in Few-Layer Group-IV Monochalcogenides: Interplay among Structural, Thermal, Optical, Spin, and Valley Properties in 2D

3. **Igor Bondarev**, North Carolina Central University
   Plasmon-Mediated Photophysics of Complex Hybrid Nanostructures

4. **James Chelikowsky**, University of Texas
   Computational Theory Applied to Nanostructures: Superconducting and Ferromagnetic Amorphous Carbon

5. **Valentino Cooper**, Oak Ridge National Laboratory
   Materials Theory

6. **Alexander Finkel'stein**, Texas A&M University
   Flexural Phonons in Supported Graphene: From Pinning to Localization (Electron Cooling at Low Temperatures)

7. **Liang Fu**, Massachusetts Institute of Technology
   Superconductivity and Density Wave in Twisted Bilayer Graphene

8. **Victor Galitski**, University of Maryland
   Cavity Superconductor-Polaritons

9. **Giulia Galli** (presenter **Marco Govoni**), University of Chicago/Argonne National Laboratory
   The Midwest Integrated Center for Computational Materials (MICCoM)

10. **Stephan Haas**, University of Southern California
    Topological Protection of Coherence in a Dissipative Environment

11. **Olle Heinonen**, Argonne National Laboratory
    Condensed Matter Theory: Skyrmions, Topological Hall Effect, and Spin-Flip Scattering

12. **Rajiv Kalia**, University of Southern California
    Self-Healing Ceramics and Mechanical Metamaterials

13. **Gabriel Kotliar**, Brookhaven National Laboratory / Rutgers University
Correlation Effects and Magnetism in Actinides: Elements and Compounds

14. **Yuli Lyanda-Geller**, Purdue University
The Hunt for Non-Abelian Statistics

15. **Allan MacDonald** (presenter **Qian Niu**), University of Texas
Spin-Orbit Torque as a Faraday Gauge Feld on the Bloch Sphere

16. **Eugene Mele**, University of Pennsylvania
Structure and Electronic Properties of Dirac Materials

17. **Kristin Persson** (presenter **Shyam Dwaraknath**), Lawrence Berkeley National Laboratory
The Materials Project

18. **Nandini Trivedi**, The Ohio State University
Novel Phases and Dynamics of Multi-orbital Mott Insulators

19. **Dong-ning Sheng**, California State University, Northridge
Novel Fractional Quantum Hall Effect and New Topological Phase in Interacting Systems

20. **Christian Van de Walle**, University of California, Santa Barbara
Computational Studies of Hydrogen Interactions with Materials

21. **Priya Vashishta**, University of Southern California
Computational Synthesis of Materials Software Project – MAGICS

22. **Michael Widom**, Carnegie University
Thermodynamic Stability of Solid Solutions and High Entropy Alloys: The BCC to HCP Transition is Driven by a Jahn-Teller-Peierls Instability

23. **Lilia Woods**, University of South Florida
Fluctuation Induced Interactions in Novel Materials

24. **Ruqian Wu**, University of California, Irvine
First Principle Investigations for Magnetic Properties of Innovative Materials

25. **Guoping Zhang**, Indiana State University
All-Optical Spin Switching, Ultrafast Demagnetization and High-Harmonic Generations in Magnetic Materials

26. **Igor Zutic**, University at Buffalo
Proximitized Materials

27. **Thomas Maier**, Oak Ridge National Laboratory
Computational Framework for Unbiased Studies of Correlated Electron Systems

28. **Anubhav Jain**, Lawrence Berkeley National Laboratory
High-Throughput and Data-Driven Materials Discovery Tools with Application to Thermoelectric Materials Design

29. **Senthil Todadri**, Massachusetts Institute of Technology
Correlated Electronic States in Twisted Bilayer Graphene

Poster Session II

Wednesday, August 15

7:30 – 9:30 PM

1. **Alexander Balatsky**, Los Alamos National Laboratory
   Integrated Modeling of Novel Materials

2. **Laurent Bellaiche** (presenter **Bin Xu**), University of Arkansas
   Atomistic Theories and Simulations of Multiferroics

3. **Garnet Chan**, California Institute of Technology
   Condensed Phase Quantum Embedding and Quantum Many-Body Methods

4. **Alexander Chernyshev**, University of California, Irvine
   Broad Magnons in α-$RuCl_3$

5. **Adrian Feiguin**, Northeastern University
   Excitonic Density Waves, Bi-excitons and Orbital Selective Superconductivity in Correlated Two-Orbital Models

6. **Emanuel Gull**, University of Michigan, Ann Arbor
   Simulation of Correlated Lattice and Impurity Systems Out of Equilibrium

7. **Alexey Kovalev**, University of Nebraska, Lincoln
   Boundary Twists, Instabilities, and (Anti)Skyrmion Creation

8. **Aditi Mitra**, New York University
   Nonequilibrium Phenomena in Topological Insulators: Central Charge of Periodically Driven Critical Kitaev Chains

9. **Sidney Nagel**, University of Chicago
   Design of Functional Materials Based on New Principles of Disorder

10. **Michael Norman** (presenter **Konstantin Matveev**), Argonne National Laboratory
    Condensed Matter Theory: Viscosity of One-Dimensional Quantum Liquids

11. **Michael Norman** (presenter **Hyowon Park**), Argonne National Laboratory
    Condensed Matter Theory: Dynamical Mean Field Theory Study of Emergent Phase Diagrams in Transition Metal Oxides

12. **Warren Pickett**, University of California, Davis
    Symmetry Effects on the Interplay between Strong Correlation and Spin-Orbit Coupling

13. **Srinivas Raghu**, SLAC National Accelerator Laboratory
Atomic Engineering Oxide Heterostructures: Materials by Design

14. **Andrew Rappe**, University of Pennsylvania
Physical Analysis of the Bulk Photovoltaic Effect for Solar Harvesting Materials

15. **Fernando Reboredo**, Oak Ridge National Laboratory
Extending the Reach of Computational-Theoretical Methods to Materials at the Energy Frontier

16. **John Rehr**, University of Washington
New Dimension in the Theory of Excited States and X-ray Spectra

17. **Sashi Satpathy** (presenter **Sayantika Bhowal**), University of Missouri
Emerging Phenomena in the Strong Spin-Orbit Coupled Systems: Electric Field Tuning of the Anomalous Hall Effect at the Oxide Interfaces

18. **Richard Scalettar**, University of California, Davis
Phonon Dispersion and the Competition between Pairing and Charge Order

19. **Sahar Sharifzadeh**, Boston University
Electronic and Optical Properties of Borophene, a Two-Dimensional Transparent Metal

20. **Qimiao Si**, Rice University
Orbital-Selective Electron Correlations and Unconventional Superconductivity

21. **Charles Stafford**, University of Arizona
Many-Body Theory of Energy Transport and Conversion at the Nanoscale

22. **Talat Rahman**, University of Central Florida
Theoretical and Computational Studies of Functional Nanomaterials

23. **Alexei Tsvelik**, Brookhaven National Laboratory
Condensed Matter Theory

24. **Giovanni Vignale** (presenter **Mohammad Zarenia**), University of Missouri
Time-Dependent Density Functional Theory and Quantum Continuum Mechanics

25. **Ziqiang Wang**, Boston College
Disorder and Interaction in Correlated Electron Systems

26. **Jiadong Zang**, University of New Hampshire
Interfacial Magnetic Skyrmions and Proximity Effects

27. **Shengbai Zhang**, Rensselaer Polytechnic Institute
Fundamental Properties of Electronic Materials: From Novel 2D Materials to Band Alignment at Interfaces

28. **Eugene Chudnovsky**, The City University of New York
Skyrmion Glass in Disordered 2D Systems and Quantum Tunneling of Skyrmions

29. **Andreas Glatz**, Argonne National Laboratory
Quantum Mesoscopic Materials

30. **James Freericks**, Georgetown University
Theory for Pump/Probe Experiments in Quantum Materials

31. **Walter Lambrecht**, Case Western Reserve University
Lattice Dynamics and Phase Stability in Halide Perovskites

32. **Murray Daw**, Clemson University
First Principles Calculation of Vibrational Mode Lifetimes in Complex Materials

Transport and Optical Properties of Chiral Quantum Materials

Principal Investigator: Alexandre Abanov
Department of Physics and Astronomy and Simons Center for Geometry and Physics, Stony Brook University

Co-PI: Dmitri Kharzeev
Department of Physics and Astronomy, Stony Brook University
and
Department of Physics and RIKEN-BNL Research Center,
Brookhaven National Laboratory

Keywords: magneto-transport in Dirac and Weyl semimetals, topology and hydrodynamics, modeling QCD effects in condensed matter systems

Project Scope: To study condensed matter systems using approaches universally known in condensed-matter and nuclear physics combining them with more recent topological methods. In this project the focus is on a particular subset of new materials known as chiral materials. The three directions of research are: D1: Magnetotransport in Dirac/Weyl semimetals; D2: Topology and hydrodynamics of strongly interacting condensed matter systems; D3: Modeling QCD effects in condensed matter physics.

The proposed research explores broad interdisciplinary connections between condensed matter physics and nuclear/particle physics. The hydrodynamics and topology might hold the key to understanding many universal dynamical properties of systems at vastly different scales, from femto-meter (quarks and gluons of Quantum Chromo-Dynamics), to nanometer (e.g., cold atoms, quantum hall effect, topological insulators and graphene), to parsec (e.g., magnetic helicity and polarization of cosmic microwave background in cosmology). The projects outlined in this proposal will lead to more systematic understanding of quantum anomaly related phenomena and can result in important new effects and practical applications in condensed matter physics and beyond.

Recent progress

Quantum oscillations in chiral magnetic conductivity In strong magnetic field the longitudinal magnetoconductivity in 3D chiral materials has been shown by Kharzeev and his student S.Kaushik to exhibit a new type of quantum oscillations arising from the chiral magnetic effect (CME) [1]. They have demonstrated that the non-linear relation between the density of chiral charge and the chiral chemical potential induces a new type of quantum oscillations in longitudinal magnetoconductivity of Dirac and Weyl (semi)metals. In strong magnetic fields and in materials that approximately preserve chirality (when the chirality flipping time is much longer than the scattering time), these new quantum oscillations dominate over the SdH ones. The phase of these quantum CME oscillations differs from the SdH oscillations by $\pi/2$ which makes it possible to isolate them in experiment.

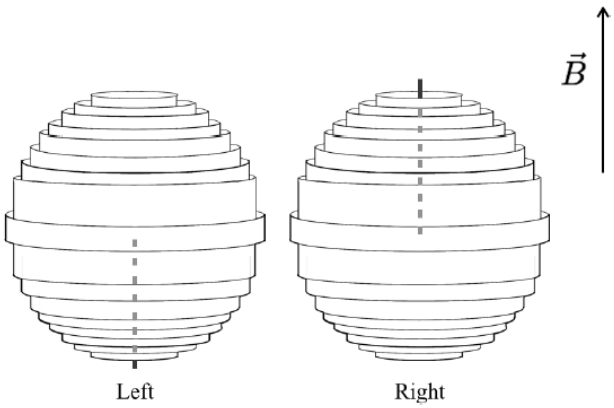

Fig.1 Fermi surface of a Dirac metal in an external magnetic field; from G.Monteiro, A.Abanov, D.Kharzeev, Phys. Rev. B92, 165109 (2015).

Helical magnetic effect and photocurrent in Weyl semimetals The helical magnetic effect is proposed to exist in Weyl semimetals by Kharzeev in collaboration with his Stony Brook student Y.Kikuchi, R.Meyer and RIKEN-BNL postdoc Y.Tanizaki [2]. Namely, the helicity imbalance in asymmetric Weyl semimetals in a magnetic field results in generation of photocurrent. It is found that due to the large density of states in a magnetic field, the helical magnetic effect might induce a remarkably large photocurrent for the incident THz frequency light. In usual symmetric Weyl semimetals in a magnetic field, the particles and holes produced by an incident light in different Weyl cones have opposite helicities and hence move in opposite directions, canceling each others's contributions to the photocurrent. However this cancelation does not occur if the Weyl semimetal possesses both a broken particle-hole symmetry and a broken spatial inversion symmetry.

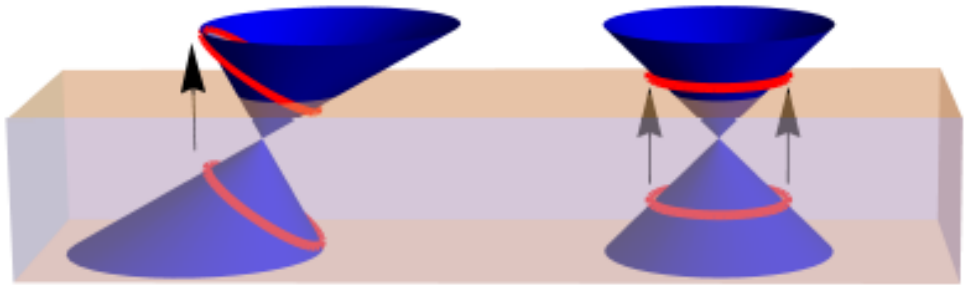

Fig.2 Non-zero photocurrent in asymmetric Weyl semimetal (left) and zero photocurrent in a symmetric Weyl semimetal (right) [2].

The resulting generation of photocurrent has been called in [2] the helical magnetic effect because it is induced by the helicity imbalance in a magnetic field. Due to the large density of states in a magnetic field, the helical magnetic effect induces a remarkably large photocurrent for incident THz frequency light. The computation has been performed by using the Chiral Kinetic Theory that

incorporates the effect of chiral anomaly through the non-trivial Berry curvature originating from the Weyl points. The large magnitude of the proposed photocurrent in the THz frequency range suggests a potential application of asymmetric Weyl semimetals for creating THz photosensors.

Weakly nonlinear dispersive surface waves for incompressible fluids with odd viscosity The theory of weakly nonlinear dispersive surface waves for incompressible fluids with odd viscosity is constructed by Abanov with collaborators T. Can and S. Ganeshan [3]. These surface waves have a chiral nature and have common features with edge states of quantum Hall fluids. After modifying this theory to be applicable to quantum Hall, one can use it to identify Hall viscosity effects on edge dynamics of quantum Hall droplets.

It was found [4] that the presence of odd viscosity creates a singular vortical boundary layer at the free surface of the fluid. This layer modifies the pressure at the surface of the fluid. The latter modification results in chiral surface waves propagating in one direction only. The direction of the propagation depends on the sign of odd viscosity. The dispersion of surface waves is quadratic and is given by $\Omega = -2\nu_o k^2$. In [3] we also studied the nonlinear theory of such surface waves. In weakly nonlinear limit we derived the equations governing surface wave dynamics. The system of equations turned out to be Hamiltonian, energy conserving system. Moreover, in an additional, so-called small angle approximation, the system of equations is simplified and reduces to a single equation which is proposed to be named chiral Burgers equation. This is a new equation related to known complex Burgers equation but having additional analyticity requirements. The chiral Burgers equation possesses very peculiar multi-pole solutions and can be used to study the formation of surface singularities of the nonlinear boundary dynamics. These results are published in SciPost Physics journal.

Chiral magnetic effect without chirality source in asymmetric Weyl semimetals The chiral magnetic effect in “conventional” chiral materials (symmetric Dirac and Weyl semimetals) in addition to the background magnetic field requires a chirality imbalance between the Fermi energies of the left- and right-handed fermions. However as shown recently by Kharzeev with his Stony Brook student Y. Kikuchi and R. Meyer, asymmetric Weyl semimetals offer a new possibility to induce the chiral magnetic effect that does not require a chirality source [4]. The reason is that an out-of-equilibrium state of an asymmetric Weyl semimetal driven by an AC electric field develops the chirality asymmetry due to the different densities of states in the left- and right-handed Weyl cones.

Dynamics of vortices in chiral fluids: the chiral propulsion effect The dynamics of vortex filaments in chiral fluids has been investigated by Kharzeev with collaborators Y. Hirono and A. Sadofyev [5]. They have found that in the fluids with a non-zero magnetic helicity the chiral Hasimoto solitions on the vortices get propelled along the vortex in the direction determined by their chirality (“the chiral propulsion effect”). The dynamics of the soliton propagation has been found to be integrable, and described by Hirota-type equation.

Future plans

Optical properties of Weyl semimetals in external electric and magnetic fields Chiral quasiparticles in three-dimensional chiral materials strongly couple to circularly polarized light, that opens possibilities for a number of novel phenomena. Kharzeev, with his students S. Kaushik and E. Philip, will study the rotation of polarization of light going through the Weyl semimetal that is placed in external electric and magnetic fields. If the scalar product of electric and magnetic fields is non-zero, this external field configuration induces a chirality imbalance, that leads to a number of interesting phenomena including the Faraday and Kerr effects.

The effect of parity odd viscosity on hydrodynamic surface waves in two-dimensional incompressible fluids The Quantum Hall Effects (both integer and fractional) are the most striking experimental discoveries in the condensed matter physics in the last 50 years. Recently it was recognized (so far only theoretically) that in addition to the Hall conductivity the other quantity dubbed the Hall viscosity is also expressible in units related to Planck's constant. The Hall viscosity is the non-dissipative part of a viscous stress tensor in 2D systems. Both the Hall conductivity and the Hall viscosity are not the properties unique to quantum physics. These responses are known to be present in classical fluids if the parity symmetry is violated. A particular field of relevance of Hall viscosity to classical fluids is the rapidly growing field of chiral active fluids - fluids with an external source of angular momentum. In classical domain the Hall viscosity is often referred to as odd viscosity. In incompressible fluids the odd viscosity is hard to observe as in the bulk of the fluid it just redefines the pressure of the fluid by adding to it the vorticity dependent part. However, even in incompressible fluid odd viscosity manifests itself on free surfaces. The PI, together with Stony Brook students, will investigate the effect of parity odd viscosity on hydrodynamic surface waves in two-dimensional incompressible fluids.

Chiral magnetic wave propagation in asymmetric Weyl semimetals The chiral magnetic wave is a collective gapless excitation emerging in chiral materials that results from the chiral anomaly. Previously Kharzeev and H.-U.Yee proposed its existence and studied its properties in symmetric Weyl semimetals and non-Abelian plasmas. Kharzeev with student S. Kaushik plan to investigate the chiral magnetic wave in asymmetric Weyl semimetals, where it can exhibit novel properties, including anisotropic velocity. They will work out numerical predictions for the forthcoming experimental studies of chiral magnetic wave in symmetric and asymmetric Weyl semimetals.

References

[1] Sahal Kaushik and Dmitri E. Kharzeev,
Quantum Oscillations in the Chiral Magnetic Conductivity, Phys. Rev. B 95, 235136 (2017)

[2] Dmitri E. Kharzeev, Yuta Kikuchi, Reńe Meyer, and Yuya Tanizaki,
Giant photocurrent in asymmetric Weyl semimetals from the helical magnetic effect, Phys. Rev. B 98, 014305 (2018)

[3] Alexander G. Abanov, Tankut Can, Sriram Ganeshan,
Odd surface waves in two-dimensional incompressible fluids, SciPost Physics 5 (1) 010 (2018)

[4] Dmitri E. Kharzeev, Yuta Kikuchi, and Reńe Meyer, *Chiral magnetic effect without chirality source in asymmetric Weyl semimetals,* European Journal of Physics B91 (5), 83 (2018)

[5] Yuji Hirono, Dmitri E. Kharzeev, and Andrey V. Sadofyev, *Dynamics of vortices in chiral media: the chiral propulsion effect*, Phys. Rev. Lett, in press

Static and Dynamic Thermal Effects in Solids

Philip B. Allen, Stony Brook University

Keywords: Thermal Conductivity, Thermal Shifts, Polaron, Pyroelectric

Project Scope

There are two main projects under current investigation. 1. Nonlocal effects in lattice thermal conductivity are particularly interesting because phonon mean free paths are very diverse and some phonons travel long distances before scattering. 2. Spectral functions for electrons (for example, lineshapes measured in photoemission) are altered in various ways by electron-phonon interactions.

Recent Progress

1. Molecular dynamics simulations enable computation of local temperature versus position when heat is added in spatially varying fashion. The figure shows a nice example[1]. If transport obeyed the local Fourier law $j = -\kappa\nabla T$, then T(x) would vary linearly between insertion and removal. The curvature indicates nonlocal conduction $j(x) = -\mp\int dx'\kappa(x,x')\nabla T(x')$. I have used Boltzmann transport theory to formulate a proper nonlocal theory. This enables nonlocal conductivity to be extracted from such simulations.

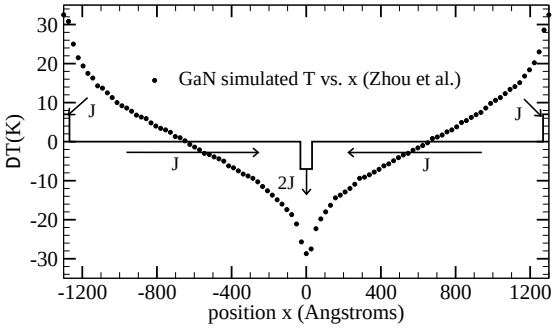

Temperature shift versus position when heat is added in periodically spaced slabs of width 70Å at x=1300+2600nÅ. Equal heat is removed periodically at x=2600nÅ. From X. W. Zhou *et al*.[1]

One of the issues in such theories is the question of whether (or how) temperature can be defined. Perebeinos and I have recently examined this carefully[2]. The local energy is well defined, and determined by the local distribution function $N_Q(x,t)$ by $U(x,t) = \Sigma_Q \omega_Q N_Q$. Then temperature in Boltzmann theory is defined by $U(x,t) = \Sigma_Q \omega_Q n_Q(T(x,t))$ **(A)**, where n_Q is the Bose-Einstein distribution. However, if the full Boltzmann equation is approximated by the relaxation time approximation (RTA) for scattering, then an alternative definition of temperature is possible, namely $(dU/dt)_{scatt} = 0 \rightarrow \Sigma_Q \omega_Q n_Q(T(x,t))/\tau_Q$ **(B)**, where τ_Q is the relaxation time. This is automatically true in the full theory because each collision conserves energy. In RTA applied to nonlocal situations, conditions **A** and **B** cannot both be satisfied. Either **A** or **B** can be used to define temperature. We compare results from these two separate choices. For thermal conductivity, the results are fairly similar. We find that version **B** is somewhat preferable. We also find singularity issues when trying to extract local results from the nonlocal theory, and are still working to fully understand the problems.

2. Electron spectral functions as seen in x-ray photoemission have been examined for many years. In addition to the "quasiparticle peaks" showing holes left in the occupied levels (*e.g.* valence states), there can be additional structure, for example, a series of plasmon satellites which appear at the quasiparticle energy of the photohole, plus multiples of the plasmon energy. A conventional many-body Green's function theory ("GW" being the logical choice) gives a spectral function $A(k,\omega)=(-1/\pi)$ x Im $G(k,\omega)$ which is surprisingly bad. It gives only a single plasmon satellite, and not at the correct energy. Langreth[2] was able to show that omitted higher-order graphs are summed exactly by a cumulant (exponential) re-summation of the low-order graphs, provided that the quasiparticle band is dispersionless (*e.g.*, a core hole). Others[3] have found since that the cumulant procedure works surprisingly well for valence states and seems to correct the errors of the GW procedure.

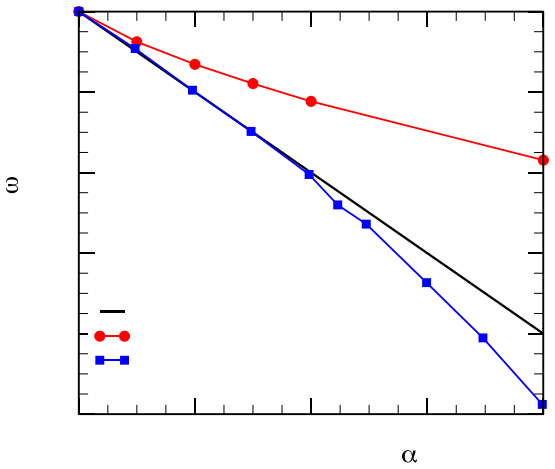

Quasiparticle energy of the Fröhlich polaron, as a function of the Fröhlich coupling constant: Monte Carlo results[5] (blue squares), cumulant results (black line), and the badly misplaced Dyson-Migdal version (red circles). From ref. 5.

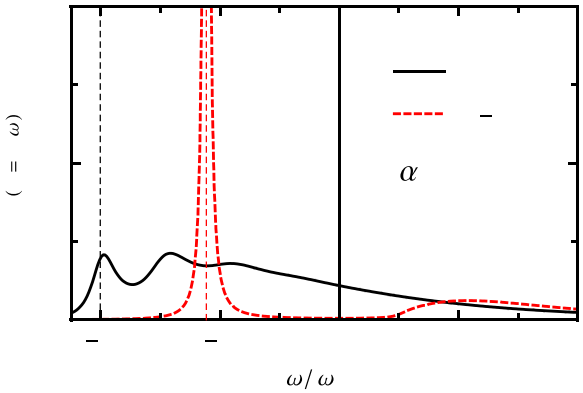

Fröhlich Hamiltonian spectral function using the cumulant (in black) and the Dyson-Migdal approach (dashed, in red) for $\alpha = 4.01$ (typical of the conduction-band minimum of LiF). The cumulant curve shows three well-resolved peaks. The one at $-4\omega_{LO}$ is the quasiparticle peak (agreeing with Monte Carlo and Rayleigh-Schrödinger theory); the other two are part of a chain of LO phonon satellites. The Dyson-Migdal version puts the quasiparticle peak close to $-2\omega_{LO}$, and misplaces the satellite badly. From ref. 5.

Recent progress in photoemission has enabled structure on millivolt scales to be resolved. In polar semiconductors, the singular Fröhlich coupling of electrons to small Q LO phonons has been resolved as satellites to the quasiparticle peaks of the doped electrons or holes. Surprisingly, the standard (Migdal-type) Green's function procedure again fails badly, both by having only one LO phonon satellite at a misplaced energy, and also by misplacing the quasiparticle peak. With European collaborators, my student Nery and I[4] have studied this in detail, and find much improved agreement with Monte Carlo calculations[5] and with experiment, by using the cumulant method. There is no known method of deriving this approximation or proving its reliability, so I regard it as a useful *ad hoc* device that is justified by agreement with experiment or more accurate theories such as quantum Monte Carlo. I think DFT should also be described this way.

Future Plans

It is a little worrisome to disclose the most interesting future plans here. One reason is that I try to find simple ideas that are not yet in the literature. There is always a worry of being scooped, usually by distant scientists with no way of knowing they were competing with me. However, even perfectly honest known competitors have ideas that arose somewhere but the origin has been forgotten. I know that people have put ideas in my head that I later misremember as being my own. Future plans are in my renewal proposal; I am willing to discuss them privately. I am willing to risk one simple idea here, because I think I will be able to finish it rapidly enough. This is to use cumulants to look at the spectral function of phonons. Apparently there has not yet been any exploration of how a cumulant approach will alter the spectral function of bosonic excitations. Anharmonicity causes $A(k,\omega)$ for phonons to deviate from simple Lorentzian form. Neutron scattering resolution has improved sufficiently that now phonon line shapes can sometimes be trusted to contain information separable from noise and from the quasiparticle peak. I think no one knows how good the standard anharmonic perturbation theory is for such line shapes, and whether a cumulant resummation will alter the answer significantly, or whether this alteration will be an improvement. All these questions can now be addressed by theory, and possibly I will have preliminary results to present at the August meeting.

References

1. X. W. Zhou, S. Aubry, R. E. Jones, A. Greenstein, and P. K. Schelling, Towards more accurate molecular dynamics calculation of thermal conductivity: Case study of GaN bulk crystals, Phys. Rev. B **79**, 115201 (2009).

2. D. C. Langreth, Singularities in the x-ray spectra of metals, Phys. Rev. B **1**, 471 (1970).

3. F. Aryasetiawan, L. Hedin, and K. Karlsson, Multiple Plasmon Satellites in Na and Al Spectral Functions from Ab Initio Cumulant Expansion, Phys. Rev. Lett. **77**, 2268 (1996).

4. Jean Paul Nery, Philip B. Allen, Gabriel Antonius, Lucia Reining, Anna Miglio, and Xavier Gonze, "Quasiparticles and phonon satellites in spectral functions of semiconductors and insulators: Cumulants applied to full first principles theory and Fröhlich polaron", Phys. Rev. B **97**, 115145:1-19 (2018).

5. A. S. Mishchenko, N. V. Prokof'ev, A. Sakamoto, and B. V. Svistunov, Diagrammatic quantum Monte Carlo study of the Fröhlich polaron, Phys. Rev. B **62**, 6317 (2000).

Publications (August 2016 – July 2018)

1. P. B. Allen and V. Perebeinos, "Temperature in a Peierls-Boltzmann Treatment of Nonlocal Phonon Heat Transport", submitted. (arXiv:1803.10757).

2. Philip B. Allen, "Analysis of nonlocal phonon thermal conductivity simulations showing the ballistic to diffusive crossover", Phys. Rev. B **97**, 134307 (2018).

3. Jean Paul Nery, Philip B. Allen, Gabriel Antonius, Lucia Reining, Anna Miglio, and Xavier Gonze, "Quasiparticles and phonon satellites in spectral functions of semiconductors and insulators: Cumulants applied to full first principles theory and Fröhlich polaron", Phys. Rev. B **97**, 115145:1-19 (2018).

4. Philip B. Allen and Warren E. Pickett, "Accidental degeneracy in k-space, geometrical phase, and the perturbation of π by spin-orbit interactions", Physica C: Superconductivity and its Applications, 549, 102-106 (2018).

5. Betul Pamuk, Philip B. Allen, and M.-V. Fernandez-Serra, "Insights into the Structure of Liquid Water from Nuclear Quantum Effects on Density and Compressibility of Ice Polymorphs", J. Phys. Chem. B **122**, 5694-5706 (2018).

6. Dong-Bo Zhang, Philip B. Allen, Tao Sun, and Renata M. Wentzcovitch, "Thermal conductivity from phonon quasiparticles with subminimal mean free path in the $MgSiO_3$ perovskite", Phys. Rev. B **96**, 100302(R):1-5 (2017).

7. Philip B. Allen and Jean Paul Nery, "Low-temperature semiconductor band-gap thermal shifts: T^4 shifts from ordinary acoustic and T^2 from piezoacoustic coupling," Phys. Rev. B **95**, 035211:1-9 (2017).

8. Jean Paul Nery and Philip B. Allen, "Influence of Fröhlich polaron coupling on renormalized electron bands in polar semiconductors. Results for zincblende GaN," Phys. Rev. B **94**, 115135:1-8 (2016).

9. Jian Liu, Maria V. Fernández-Serra, and Philip B. Allen, "Special Quasi-ordered Structures: role of short-range order in the semiconductor alloy $(GaN)_{1-x}(ZnO)_x$," Phys. Rev. B **93**, 054207:1-8 (2016).

10. Jian Liu, Maria V. Fernández-Serra, and Philip B. Allen, "First-principles study of pyroelectricity in GaN and ZnO," Phys. Rev. B 93, 081205(R):1-6, (2016). Erratum, 2018.

Electron transport in topologically nontrivial conductors and nanosystems

PI: Anton Andreev, University of Washington, Seattle, WA

Keywords: Electron transport, magnetoresistnce, chiral anomaly, hydrodynamic effects

Project Scope

The project aims to develop theory of electron transport and photogalvanic phenomena in Weyl and Dirac semimetals, two-dimensional transition metal dichalcogenides, and nanoelectronic devices based on them. Another goal of the proposed work is to investigate manifestations of momentum conserving electron-electron scattering in transport properties of nanoelectronic devices in which the electron liquid lacks Galilean invariance, and to develop a hydrodynamic theory of charge and energy transport in these systems. The proposed work is organized along the following directions.

Electronic properties of Weyl semimetals and nanodevices based on them. In many of the recently discovered Weyl semimetals the electron-electron interaction constant is small. At the same time the characteristic values of the electron Fermi momenta and the distance between the Weyl nodes in momentum space are much smaller than the Brillouin zone size. In this situation only the coupling of electrons to the low wavelength phonons needs to be considered. This enables construction of a detailed theory of electron and phonon transport, which will be developed as part of the proposed work. Such a theory would be very useful in interpreting the rapidly growing body of experimental data on Weyl and Dirac semimetals, in which many aspects of electron transport are still not understood.

Hydrodynamic charge and energy transport in conductors lacking Galilean invariance. In recent experiments on boron nitride encapsulated graphene and metal-based nanodevices evidence for hydrodynamic flow has been reported. In these systems the electron liquid lacks Galilean invariance. The PI is developing a hydrodynamic theory of charge and energy transport in conductors in which the electron liquid lacks Galilean invariance.

Photogalvanic phenomena in nanodevices based on transition metal dichalcogenides. The PI would like to develop a theory of photogalvanic phenomena in two-dimensional transition metal dichalcogenides focusing on the edge phenomena and the regime of sub-band gap photoexcitation resonant with the trion absorption line.

Recent Progress

Klein tunneling and magnetoresistance of p-n junctions in Weyl semimetals [with Songci Li and Boris Spivak]. We studied the zero temperature conductance and magnetoconductance of ballistic p-n junctions in Weyl semimetals. Electron transport is mediated by Klein tunneling between n- and p- regions. The chiral anomaly that is realized in Weyl semimetals plays a crucial role in the magnetoconductance of the junction. With the exception of field orientations where the angle between B and the junction plane is small, magnetoconductance is positive and linear in B at both weak and strong magnetic fields. In contrast, magnetoconductance in conventional p-n junctions is always negative. This work has been published as a Rapid Communication in Physical Review B, Phys. Rev. B 94, 081408 (2016).

Viscous magnetoresistance of correlated electron liquids [with Alex Levchenko and Hong-Yi Xie]. We developed a theory of magnetoresistance of two-dimensional electron systems in a smooth disorder potential in the hydrodynamic regime. Our theory applies to two-dimensional semiconductor structures with strongly correlated carriers when the mean free path due to electron-electron collisions is sufficiently short. The dominant contribution to magnetoresistance arises from the modification of the flow pattern by the Lorentz force, rather than the magnetic field dependence of the kinetic coefficients of the electron liquid. The resulting magnetoresistance is positive and quadratic at weak fields. Although the resistivity is governed by both viscosity and thermal conductivity of the electron fluid, the magnetoresistance is controlled by the viscosity only. This enables extraction of viscosity of the electron liquid from magnetotransport measurements. This work has been published as Rapid Communication in Physial Review B, and selected as Editor's Suggestion. Phys. Rev. B 95, 121301 (2017).

Anomalous Hall Effect in type-I Weyl metals [with Jacob Steiner and Dima Pesin]. We studied the ac anomalous Hall conductivity $\sigma_{xy}(\omega)$ of a Weyl semimetal with broken time-reversal symmetry. Even in the absence of free carriers these materials exhibit a "universal" anomalous Hall response determined solely by the locations of the Weyl nodes. We showed that the free carriers, which are generically present in an undoped Weyl semimetal, give an additional contribution to the ac Hall conductivity. We elucidated the physical mechanism of the effect and developed a microscopic theory of the free carrier contribution to $\sigma_{xy}(\omega)$. The latter can be expressed in terms of a small number of parameters (the electron velocity matrix, the Fermi energy , and the tilt of the Weyl cone). The resulting $\sigma_{xy}(\omega)$ has resonant features at frequencies commensurate by the chemical potential of the carriers, which may be used to separate the free carrier response from the filled-band response using, for example, the Kerr effect measurements. This may serve as diagnostic tool to characterize the doping of individual valleys. This work was published in Phys. Rev. Lett. **119**, 036601

(2017).

Longitudinal negative magnetoresistance and magneto-transport phenomena in conventional and topological conductors [with Boris Spivak], Recently a large negative longitudinal (parallel to the magnetic field) magnetoresistance was observed in Weyl and Dirac semimetals. It is believed to be related to the chiral anomaly, associated with the topologically-protected gapless electron band structure in these materials. We showed that in a certain range of parameters negative longitudinal magnetoresistance can also exist in conventional centrosymmetric and time-reversal invariant conductors, lacking the topological protection of the gapless electron spectrum and the chiral anomaly. We also discussed the magnetic field enhancement of the longitudinal components of the thermal conductivity and thermoelectric tensors. This work was published in Phys. Rev. Lett. **120**, 026601 (2018).

Two-fluid hydrodynamics and sound modes in one-dimensional quantum liquids [with K. A. Matveev]. Many properties of one-dimensional quantum liquids may be understood within the Luttinger liquid framework. In this description the elementary excitations are bosons, which correspond to quanta of density and spin waves in the liquid. At finite temperature the collisions between these elementary excitations result in relaxation of the gas of excitations to local thermal equilibrium. Since the collisions between the excitations conserve their energy and momentum, the equilibrium state of the gas is characterized by the temperature T and the hydrodynamic velocity of the gas of excitations u_{ex}. At much longer time scales, corresponding the backscattering relaxation time τ, u_{ex} becomes equal to the velocity of the liquid as a whole, u. However, at shorter time scales the two velocities need not be equal, and the motion of the liquid is described by a two fluid hydrodynamics similar to the one developed for superfluid helium. Using the two fluid hydrodynamics we showed that at in a broad frequency range one-dimensional quantum liquids support two sound modes. In liquids consisting of spin-1/2 fermions these modes are first and second sound that correspond to respectively, density and temperature waves. In liquids consisting of spinless or spin-polarized particles the two sound modes are hybrids of the first and second sound modes and involve oscillations of both density and temperature. This results in a striking prediction: An initial local density disturbance will split into four pulses, that will propagate at two different speeds in opposite directions. The results of this work were published in two recent papers: Phys. Rev. Lett. **119**, 266801 (2017), and Phys. Rev. Lett. **121**, 026803 (2018). An article on the second work was recently featured in phys.org: https://phys.org/news/2018-07-unusual-quantum-liquids.html

Future Plans

I will work on the theory of magnetoresistance in the hydrodynamic regime in materials lacking Galilean invariance. I am also developing a theory of electrical *ac*-conducticity in superconductors due to inelastic electron scattering. Together with Konstantin Matveev I will study attenuation of the sound modes in quantum one-dimensional liquids.

Publications (August 2016 – July 2018)

1) Songci Li, A. V. Andreev, and B. Z. Spivak, *Klein tunneling and magnetoresistance of p-n junctions in Weyl semimetals*, Phys. Rev. B 94, 081408(R) (2016).

2) Alex Levchenko, Hong-Yi Xie, A. V. Andreev, *Viscous magnetoresistance of correlated electron liquids*, Phys. Rev. B 95, 121301(R) (2017). Selected as Editor's Suggestion.

3) J. F. Steiner, A. V. Andreev, and D. A. Pesin, *Anomalous Hall Efect in type-I Weyl metals,* Phys. Rev. Lett. 119, 036601 (2017).

4) K. A. Matveev, and A. V. Andreev, *Second sound in one dimensional electron liquids*, Phys. Rev. Lett. 119, 266801 (2017).

5) A. V. Andreev, and B. Z. Spivak, *Longitudinal negative magnetoresistance and magneto-transport phenomena in conventional and topological conductors*, Phys. Rev. Lett. **120**, 026601 (2018).

6) K. A. Matveev, and A. V. Andreev, *Hybrid sound modes in one-dimensional quantum liquids*, Phys. Rev. Lett., **121,** 026803 (2018). [An article on this work was featured in featured in phys.org: https://phys.org/news/2018-07-unusual-quantum-liquids.html]

Integrated Modeling of Novel Materials

PI A. Balatsky, Co-PI J. X. Zhu (Los Alamos)

Keywords: Dirac Materials, dynamics phase transition, critical point, multiferroics, interface, superconductivity, topological states

Project Scope

Complex electronic materials show strong electronic correlations and strong electronic coupling to lattice and spin multiple degrees of freedom. Our focus is to understand competing interactions in order to control material properties, predict novel states, and investigate the temporal response in Dirac Materials (DM). Dirac Materials include graphene, unconventional superconductors, and topological systems. We envisage that a command of competing interactions will allow us to make universal response predictions of DM to external fields and chemical dopants. Our understanding of external fields will allow us to probe the time response in pumped and driven DM. Material systems with competing interactions at interfaces will also fall into our focus. Interfaces provide a versatile platform to search for novel states resulting from competing couplings. Towards this end, we envisage using a theoretical understanding developed in this work to predict new functionalities in low dimensional materials.

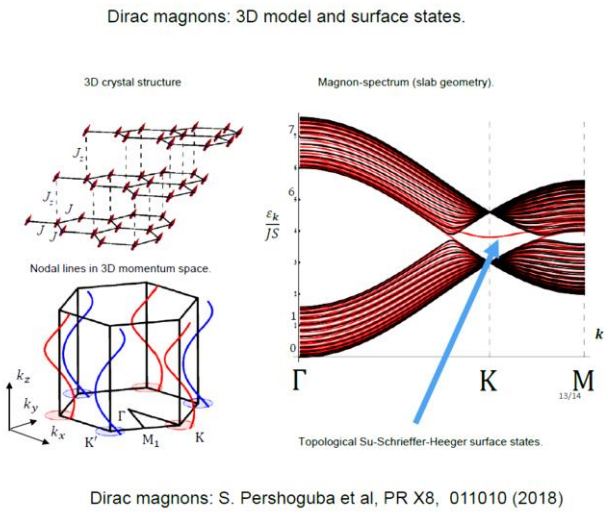

Fig.1
(a) The 3D lattice structure of CrBr3. The honeycomb layers are composed of Cr atoms and are stacked in ABC order. (b) The band structure: Dirac nodal lines wind around the corners of the Brillouin zone. (c) Magnon energy spectrum for a 25-layer slab of a three-dimensional material. Results for open vs closed boundary conditions are shown with red and black lines.

Recent Progress

1. Topologically protected dynamical quantum phase transitions

Topological phases of insulators and nodal Dirac and Weyl materials and their classification is an inherently time-independent notion as its analysis is rooted in static wavefunctions. Its implication in non-equilibrium quantum dynamics is therefore non-trivial and still a largely uncharted area of research. In this work, we marry these two fields each under intensive current interest, and show that static topological information, encoded in an initial wavefunction and a time-independent driving Hamiltonian, has a profound implication in the ensuing quench dynamics. In particular, it

fully determines if the dynamics can host robust dynamical quantum phase transitions, which are recurrent singularities in Loschmidt echos, the time domain analogue of equilibrium phase transitions. The fundamental mathematical reason can be traced back to the global nature of topological information --- in contrast with traditional order parameters which are encoded locally --- and we show that this global character enables the retrieval of topological information from *any* fraction of the full Hilbert space. [1,2]

2. Dynamic Multiferroicity of Ferroelectric Quantum Critical Points

The connections and symmetries between electric and magnetic phenomena are well known in electromagnetism. In solid state systems, electric polarization resulting from a spatial modulation of atomic spins, via the Dzyaloshinskii-Moriya interaction, is well established. The reciprocal effect of magnetic moments induced by rotating electric dipoles - dynamical multiferroicity - was introduced recently (2017), with rotation dynamics driven by external fields.

We consider inherent rotations, such as might occur at low temperatures near a ferroelectric quantum critical point (FE QCP), characterised by the slowing of rotating electric dipoles, and find a divergence in the magnetic susceptibility at a finite distance from the FE QCP indicating the appearance of a region with magnetic signatures as a result of paraelectric fluctuations. This new `multiferroic paraeletric' phase is of fundamental interest due to its relation to the nature of the FE QCP. It also has important technological implications since it demonstrates the potential to control a FE QCP using magnetic rather than electric fields, opening exciting avenues for investigation and possible applications.[3]

3. Dirac Magnons

We addressed the questions of stability and interaction effects on Dirac nodes for the case of boson Dirac materials: excitations possessing helical Dirac-like dispersion, Fig.1. The discovery of the Dirac electron dispersion in graphene led to the question of the Dirac cone stability with respect to interactions. Coulomb interactions between electrons were shown to induce a logarithmic renormalization of the Dirac dispersion. We considered a specific case of ferromagnets consisting of van der Waals-bonded stacks of honeycomb layers, e.g., chromium trihalides CrX_3 (X=F, Cl, Br and I), that display two spin wave modes with energy dispersion similar to that for the electrons in graphene. At the single-particle level, these materials resemble their fermionic counterparts. To address the role of interacting Dirac magnons, we expand the theory of ferromagnets beyond the standard Dyson theory [F. J. Dyson, General Theory of Spin-Wave Interactions, Phys. Rev. **102**, 1217 (1956), F. J. Dyson, Thermodynamic Behavior of an Ideal Ferromagnet, Phys. Rev. **102**, 1230 (1956)] to the case of non-Bravais honeycomb layers. We found that magnon-magnon interactions lead to a significant momentum-dependent

renormalization of the bare band structure in addition to strongly momentum-dependent magnon lifetimes. We show that our theory qualitatively accounts for hitherto unexplained anomalies in nearly half-century-old magnetic neutron-scattering data for CrBr3 [W. B. Yelon and R. Silberglitt, Renormalization of Large-Wave-Vector Magnons in Ferromagnetic CrBr3 Studied by Inelastic Neutron Scattering: Spin-Wave Correlation Effects, Phys. Rev. B **4**, 2280 (1971), E. J. Samuelsen, *et al.*, Spin Waves in Ferromagnetic CrBr3 Studied by Inelastic Neutron Scattering, Phys. Rev. B **3**, 157 (1971)]. We also show that honeycomb ferromagnets display dispersive surface and edge states, unlike their electronic analogs.[4]

Future Plans

We plan to investigate

1. Competing interactions and dynamics of magnetism and strain of the bulk materials and interfaces.
2. Predict and investigate the properties of new organic Dirac materials.
3. The symmetry and topology of the odd frequency superconducting state (Berezinskii pairing) in multiband, driven and topological materials.
4. The dynamics of transient excitonic states, superluminescence and polariton effects in Dirac materials.

References

[1] Z. Huang and A. V. Balatsky, *Dynamical quantum phase transitions: Role of topological nodes* , Physical Review Letters **117**, 086802 (2016).

[2] Z. Huang, W. Zhu, D. P. Arovas, J.-X. Zhu, and A. V. Balatsky, *Invariance of Topological Indices Under Hilbert Space Truncation*, Physical Review Letters **120,** 016403 (2018).

[3] K. Dunnett, J.-X. Zhu, N. A. Spaldin, V. Juricic, and A. V. Balatsky, *Dynamic multiferroicity of a ferroelectric quantum critical point*, arXiv:1808.xxxxx.

[4] Sergey S. Pershoguba, Saikat Banerjee, J. C. Lashley, Jihwey Park, Hans Ågren, Gabriel Aeppli, and Alexander V. Balatsky, *Dirac Magnons in Honeycomb Ferromagnets*, Phys. Rev. **X 8**, 011010 (2018).

Publications (August 2016 – July 2018)

[1]. Z. Huang and A. V. Balatsky, *Dynamical quantum phase transitions: Role of topological nodes* , Physical Review Letters **117**, 086802 (2016).

[2] Gregory Houchins, Charles Crook, Jian-Xin Zhu, A. Balatsky et al., *Voltage-dependent spin flip in magnetically substituted graphene nanoribbons: Towards the realization of graphene-based spintronic devices*, Physical Review B 95, 155450 (2017)

[3]. Z. Huang, W. Zhu, D. P. Arovas, J.-X. Zhu, and A. V. Balatsky, *Invariance of Topological Indices Under Hilbert Space Truncation*, Physical Review Letters **120,** 016403 (2018).

[4]. T La Martina, JX Zhu, AV Balatsky, JT Haraldsen, *Dirac Nodes and Magnetic Order in M_2X_2 Transition-Metal Chalcogenides*, physica status solidi (RRL)–Rapid Research Letters, **1800**, 1800181 (2018).

[5]. C. B. Crook, G. Houchins, J-X. Zhu, A.V. Balatsky et al., *Spatial dependence of the super-exchange interactions for transition-metal trimers in graphene*, Journal of Applied Physics, **123**, 013903, (2018).

[6]. K. Dunnett, A. Narayan, N. A. Spaldin, and A. V. Balatsky, *Strain and ferroelectric soft-mode induced superconductivity in strontium titanate*, *Phys. Rev.* **B 97**, 144506 (2018).

[7]. Anna Pertsova and Alexander V. Balatsky, *Excitonic instability in optically pumped three-dimensional Dirac materials*, *Phys. Rev.* **B 97**, 075109 (2018).

[8] Sergey S. Pershoguba, Saikat Banerjee, J. C. Lashley, Jihwey Park, Hans Ågren, Gabriel Aeppli, and Alexander V. Balatsky, *Dirac Magnons in Honeycomb Ferromagnets*, Phys. Rev. **X 8**, 011010 (2018).

Theory of Fluctuating and Critical Quantum Matter

Leon Balents, University of California, Santa Barbara

Keywords: quantum criticality, frustration, strong correlations, spin liquid, mott transition

Project Scope

The proposal centers on the theory of phenomena in electronic materials involving strong quantum fluctuations, which arise due to frustration, exotic interactions, and strong correlations. The projects are divided roughly into two areas: phases of frustrated quantum magnets, and transport in correlated systems. All components are connected both to specific experiments and materials, and to general issues at the forefront of the theory of correlated quantum matter.

Recent Progress

Strongly correlated metals from SYK models:
Recent activity showed that the Sachdev-Ye-Kitaev (SYK) model[1], a very simple model of a quantum "cluster" with random all-to-all four-fermion interactions among N fermion modes, has remarkable properties. It shared features of black holes such as fast scrambling, and also describes a non-Fermi liquid state of a sort of "quantum dot". In our paper (pub.4), we show how to build a model of a strongly correlated metal using SYK models as the "atoms" of a lattice. This is a special sort of multi-orbital Hubbard model with interaction strength U in the SYK clusters and hopping strength t between them. We developed some new Keldysh formalism to fully attack the problem. We obtained a full solution including to electrical and thermal transport, and it is striking how many of the properties are similar to those of experimental correlated metals:

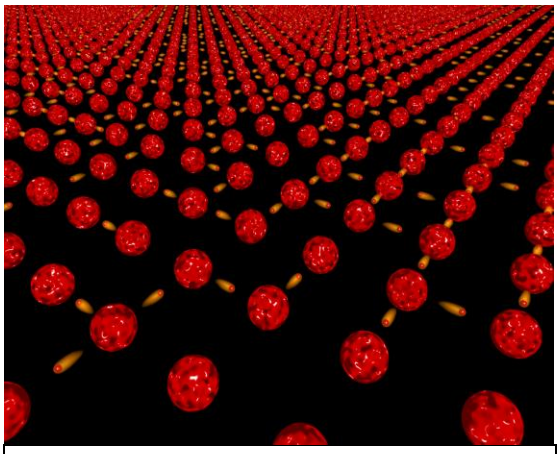

Artist's conception of the lattice of SYK "atoms" exchanging electrons.

- Small coherence scale $Ec = t^2/U$
- Large effective mass (Sommerfeld coefficient) $\gamma \sim m^*/m \sim U/t$
- Small quasiparticle weight $Z \sim t/U$
- T2 low-temperature resistivity with Kadowaki-Woods ratio A/γ^2 = constant
- linear in temperature resistivity at high temperature
- linear in temperature thermal "resistivity" T/κ at high temperature
- Fermi liquid Lorenz number $L = \kappa/(T\,\sigma) = \pi^2/3$ at low T
- non-Fermi liquid Lorenz number $L = \pi^2/8$ at high T

Our paper started a flurry of other works addressing correlated metals based on this approach.

Spin-orbit dimers and non-collinear phases in d^1 double perovskites: Our group a number of years earlier initiated the theoretical description of double perovskite materials with d^1 transition metal ions, formulating a model Hamiltonian and analyzing it within mean field theory. Recently we revisited (pub.3) the problem beyond mean field theory to address the observation[2] of gap formation in Ba_2YMoO_6. Using a variational approach and a complimentary analytical analysis, we obtained a remarkable non-magnetic disordered spin-orbit dimer phase, as well as possible non-collinear magnetic phases which may appear in the Ba_2BOsO_6 compounds with B=Na,Li.

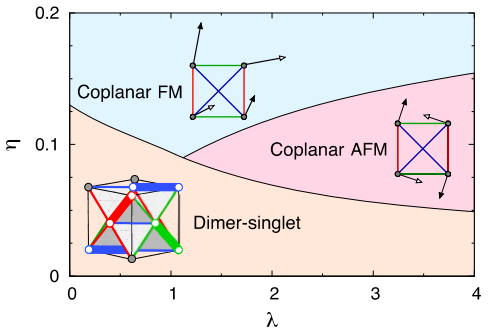

Phase diagram of our model of double perovskites.

Amplitude in the planar antiferromagnet $Na_{0.9}MnO_2$: We collaborated with Stephen Wilson's group at UCSB, who grew this S=2 antiferromagnetic chain material with weak easy axis anisotropy, and measured its excitations in neutron scattering (pub.6). In addition to the usual magnon modes, they observed a longitudinal excitation that is not predicted from spin wave theory. We showed that the semi-classical theory of a chain with weak Ising anisotropy has a magnon bound state and calculated its dispersion and weight, in agreement with experiment.

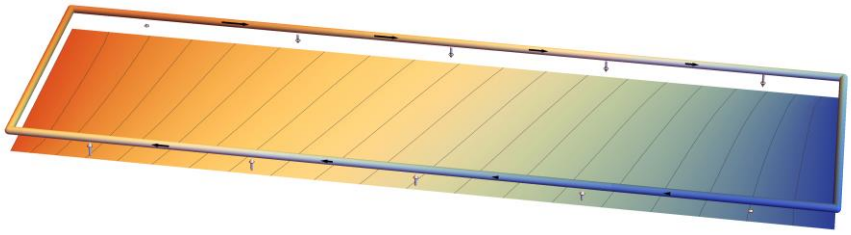

Thermal state of bulk (phonons) and edge (Majorana fermions) for a "Hall bar" model of $RuCl_3$. Heat flows both in the bulk and at the edge, and is exchanged between the two (vertical arrows). Lines in the Hall bar denote isotherms, and the color scale reflects temperature, as a net heat current is passed along the long direction of the bar.

Quantization of thermal Hall conductivity at small Hall angle: A recent experiment on $RuCl_3$, a 2d "Kitaev material", observed a remarkable quantized thermal Hall conductivity [3], which may be a smoking gun signature of a chiral Majorana fermions and a non-abelian topological phase. However, the observation was made under the unusual condition that the diagonal thermal conductivity is 1000 times larger than the Hall component, i.e. the Hall angle is order 10^{-3}. The standard theory, on which the prediction of the quantized thermal Hall effect is based, actually *fails* under these conditions. We developed a new theory (pub. 7) which shows that the effect can still occur but actually relies upon spin-phonon coupling: remarkably, thermalization between the Majorana fermions and phonons occurs which stabilizes the quantization, and renders it observable. Our calculations make many predictions for future experiments.

Future Plans

We will continue our investigations of promising frustrated magnetic systems, primarily in search of quantum spin liquids. For $RuCl_3$, we will study the role of disorder in the bulk, which affects the phonon heat transport, and show how it couples to the edge. We hope that this will explain the loss of quantization in lower thermal conductivity samples. We will also study the topological quantum phase transitions occurring on raising and lowering the magnetic field. What are the universality classes of these transitions, and how may they be revealed by ultra-low-energy probes such as magnetostriction, ultrasound attenuation, ac susceptibility, etc? Finally, the long term goal for this material is to understand how to directly reveal the non-abelian vortex excitations and Majorana fermions, by proposing new experiments that directly probe these particles. We have in mind engineering tunneling between Majorana edges, inducing local Ising anyons inside the bulk, and measuring the signatures of these using thermal transport and other probes.

We also are working on extending the theory of three dimensional spin liquids in for example pyrochlores to quantitative numerical calculations. To do so, we are developing the technology to carry out three dimensional variational Monte Carlo (VMC), one of the few techniques capable of studying reasonably large systems without a sign problem. This requires first analytical symmetry analysis to determine the projective symmetry group that controls the VMC wavefunctions. Then it must be incorporated into a VMC code – we have begun collaborating with the group of Federico Becca in Trieste to do so.

Finally, we will continue developing general methods to study dynamical quantities and conductivities in strongly correlated systems. This builds on our SYK work, as well as various approaches including numerical ones to study localized spin systems.

References

Put the list of references here using Times New Roman 10 pt. Please limit to no more than 5 papers. Provide full citation, including title and full author list.

[1] Sachdev, S. and Ye, J., *Gapless spin-fluid ground state in a random quantum Heisenberg magnet,* Physical review letters, ***70***, p.3339 (1993).

[2] De Vries, M.A., Mclaughlin, A.C. and Bos, J.W., *Valence bond glass on an fcc lattice in the double perovskite Ba_2YMoO_6*. Physical review letters, **104**, 177202 (2010).

[3] Y. Kasahara *et al, Majorana quantization and half-integer thermal quantum Hall effect in a Kitaev spin liquid,* Nature **559**, 227–231 (2018).

Publications (August 2016 – July 2018)

1. Röchner, Julia, Leon Balents, and Kai Phillip Schmidt. *Spin liquid and quantum phase transition without symmetry breaking in a frustrated three-dimensional Ising model*. Physical Review B **94**, 201111 (2016).
2. Li, Fei-Ye, Yao-Dong Li, Yong Baek Kim, Leon Balents, Yue Yu, and Gang Chen. *Weyl magnons in breathing pyrochlore antiferromagnets* Nature communications **7**, 12691 (2016).
3. Romhányi, Judit, Leon Balents, and George Jackeli. *Spin-Orbit Dimers and Noncollinear Phases in d 1 Cubic Double Perovskites*. Physical review letters **118**, 217202 (2017).
4. Song, Xue-Yang, Chao-Ming Jian, and Leon Balents. *Strongly correlated metal built from sachdev-ye-kitaev models*. Physical review letters **119**, 216601 (2017).
5. Parker, Edward, and Leon Balents. *Finite-temperature behavior of a classical spin-orbit-coupled model for $YbMgGaO_4$ with and without bond disorder*, Physical Review B **97**, 184413 (2018).
6. Dally, Rebecca L., Yang Zhao, Zhijun Xu, Robin Chisnell, M. B. Stone, Jeffrey W. Lynn, Leon Balents, and Stephen D. Wilson. *Amplitude mode in the planar triangular antiferromagnet $Na0.9MnO_2$*, Nature communications **9**, 2188 (2018).
7. Ye, Mengxing, Gábor B. Halász, Lucile Savary, and Leon Balents. *Quantization of the thermal Hall conductivity at small Hall angles*, arXiv:1805.10532 (2018).

Electronic Structure, Spectroscopy and Correlation Effects in Novel Materials

Principal Investigator: Arun Bansil; Co-PI: Robert S. Markiewicz
Physics Department, Northeastern University, Boston MA 02115
ar.bansil@northeastern.edu

Project Scope

This project concerns theoretical studies of electronic structure, spectroscopic response, and correlation effects in a wide variety of novel materials of current interest. Our overarching goal is to undertake realistic modeling of various highly resolved spectroscopies of materials for providing discriminating tests of competing theoretical scenarios, and as a rational basis for future experimentation. We emphasize that spectroscopies do not provide a direct map of electronic states, but act as a complex 'filter' or 'mapping' of the underlying spectrum. This link between electronic states and measured spectra—the 'matrix element effect'—is in general extremely complex, but a good understanding of this link is crucially important for fully exploiting various spectroscopies. Accordingly, we are working toward formulating and implementing increasingly sophisticated methodologies for making direct connection with angle-resolved photoemission (ARPES), resonant inelastic x-ray scattering (RIXS), scanning tunneling microscopy/spectroscopy (STM/STS), magnetic and non-magnetic Compton scattering, positron annihilation, neutron scattering and optical spectroscopies. Specific systems considered are topological insulators and other exotic topological phases of quantum matter, cuprates, pnictides, manganites, nano-particles, and 2D ultrathin films beyond graphene. Although the LDA provides an important baseline, 'beyond LDA' schemes are invoked for modeling the underlying electronic spectrum in correlated materials in order to incorporate the physics of superconducting orders, pseudogaps, impurities and nanoscale heterogeneities, and how matrix element effects can enhance/suppress related signatures in spectroscopies. The present project thus aims to help fill a critical gap in the available tools for understanding, analyzing and interpreting spectroscopies in wide use today, and to obtain through direct comparisons between theory and experiment new insights into electron correlation effects, Fermi surfaces, magnetism and related issues.

Recent Progress

First-principles Modeling of Cuprate High-Tc Superconductors

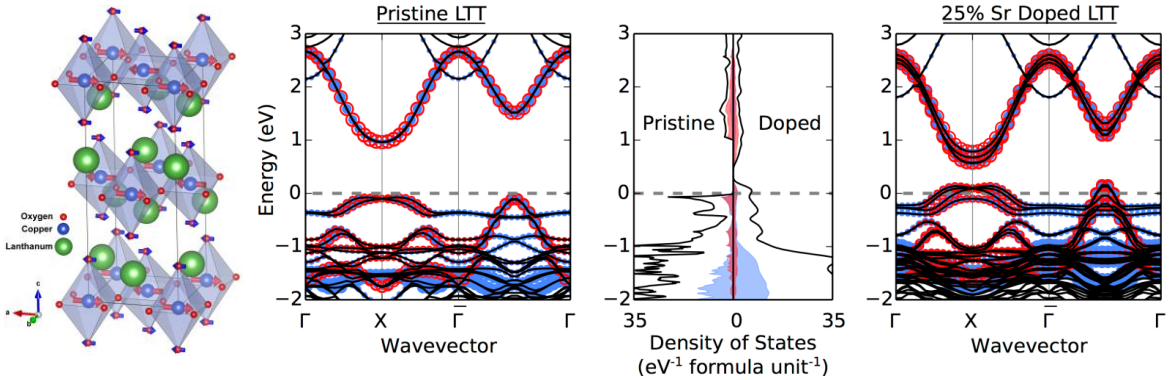

The figure above highlights the progress we have made in addressing the longstanding problem of obtaining a viable first-principles description of the electronic structures of cuprates. [1] We used the recently constructed strongly-constrained-and-appropriately-normed (SCAN) meta-GGA exchange-correlation functional to study the pristine (half-filled) La_2CuO_4 (LCO) and 25% Sr doped LCO as exemplar cuprates. For the first time, we reproduce correctly the insulating anti-ferromagnetic ground state of LCO and its transition to the metallic state with doping. No free parameters such as the Hubbard U are invoked. In LCO, we correctly capture the size of the optical band gap, value of the copper magnetic moment and its alignment in the cuprate plane, and the magnetic form factor in good accord with the corresponding experimental results. These results suggest that many of the so-called correlated materials, which have been believed traditionally to lie beyond the reach of the DFT framework, will likely be amenable to first-principles treatment.

Landscape of Competing Stripe and Magnetic Phases in Cuprates

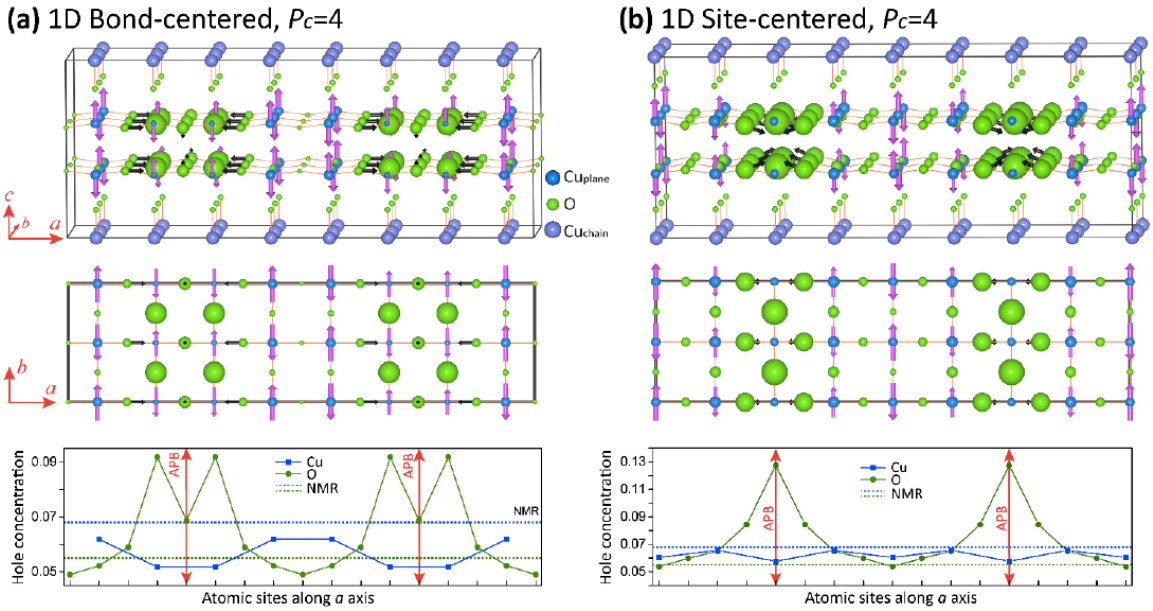

Encouraged by the preceding results on the La-cuprates, we have investigated on a first-principles basis the landscape of competing stripe and magnetic phases [2] in $YBa_2Cu_3O_6$ ($YBCO_6$) and $YBa_2Cu_3O_7$ ($YBCO_7$). Here, $YBCO_6$ is representative of pristine cuprates, while $YBCO_7$ lies around optimal doping deep in the superconducting dome in the pseudogap phase. Bond-centered as well as site-centered stripes of various charge and magnetic periodicities were considered. Here again no free parameters were used. The charge, spin and lattice degrees are treated on an equal footing, and all electrons are included in the computations. Notably, the existing literature on stripe phases is limited to the analysis of generic model Hamiltonians with a few orbitals, and neglects modifications of the electronic structure resulting from the couplings with the lattice, which our first-principles results show to be important in stabilizing various competing phases. 20 distinct, stable stripe phases are identified in $YBCO_7$ and 6 in $YBCO_6$. The ground state in $YBCO_6$ is reasonably well separated from the nearest stripe state by ~10 meV/planar-Cu. In sharp contrast, in $YBCO_7$, a large number of states are found to be nearly degenerate with the ground state. All stripe phases in $YBCO_7$ ($YBCO_6$) carry persistent Cu

moments of about 0.4 (0.5) μ_B/Cu. The strong spin-charge-lattice couplings indicated by our study suggest that phonons could play a substantial role in creating the superconducting glue in the cuprates.

Predicting Exotic Topological Phases of Quantum Matter

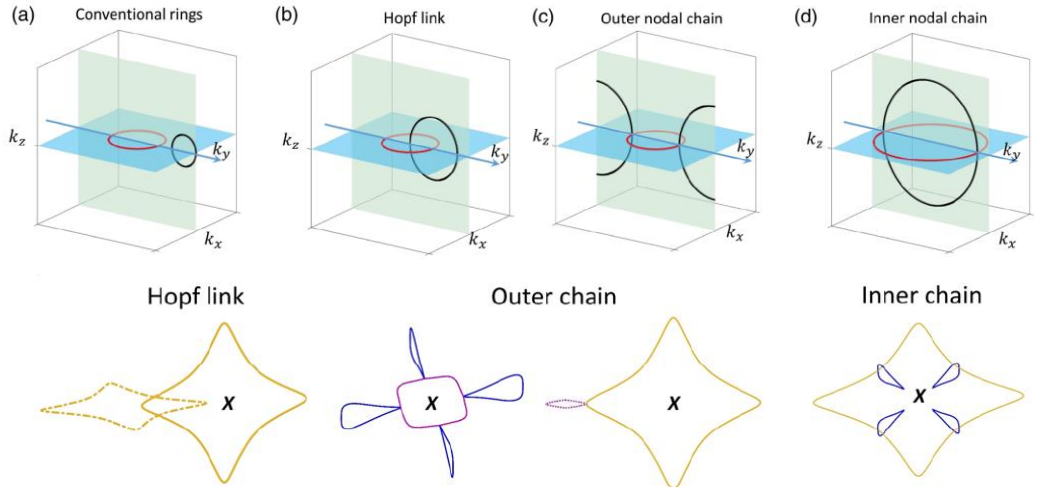

We have predicted a number of materials that can harbor exotic topological phases, including our successful realization of LaAlGe as a Type-II Weyl semimetal. [3-11] As an example, the figure above considers the case of Co_2MnGa, which we predict to harbor unusual linked line nodes. [4] Topological semimetals can be classified by the connectivity and dimensionality of the band crossings in momentum space. The band crossings of a Dirac or Weyl semimetal are 0D points, whereas the band crossings of a nodal-line semimetal are 1D closed loops. In Co_2MnGa, we find that the presence of perpendicular crystalline mirror planes can protect 3D band crossings characterized by nontrivial links such as a Hopf link or a coupled chain, giving rise to a variety of new types of topological semimetals. The top row in the figure shows schematics of various types of 3D links, while the bottom row gives the actual type of links predicted in Co_2MnGa.

A New Type of Rotationally Aligned Heterocrystal: Bi_2Se_3 on MoS_2

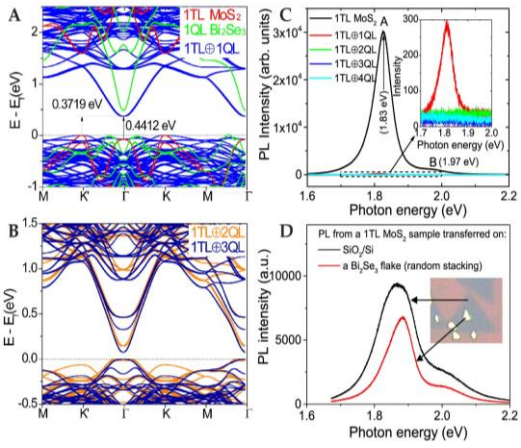

Vertical stacking of crystallographically commensurate materials is widely viewed as a promising approach for designing advanced functionalities using two-dimensional (2D) materials. We show that crystallographically dissimilar and incommensurate atomically-thin MoS_2 and Bi_2Se_3 layers can form rotationally-aligned stacks with long-range crystallographic order. [12] Our first-principles theoretical modeling predicts heterocrystal electronic band structures, which are quite distinct from those of the parent crystals (see panels A and B in the figure), characterized with an indirect band gap. Experiments reveal striking optical changes when Bi_2Se_3 is stacked layer-by-layer on monolayer MoS_2,

including 100% photoluminescence (PL) suppression (panel C), tunable transmittance-edge (1.1 eV→0.75 eV), suppressed Raman, and wide-band evolution of spectral transmittance. Disrupting the interface using a focused laser results in a spectacular reversal of PL (panel D), Raman, and transmittance, demonstrating for the first time that *in-situ* manipulation of interfaces can enable "reconfigurable" 2D materials. We also demonstrate sub-micrometer resolution, "laser-drawing" and "bit"-writing, and a novel laser-induced broadband light-emission in these heterocrystal sheets.

Finally, we note briefly a number of our further results as follows. (1) Bosonic entropy driven by a hidden van Hove singularity was shown to be the origin of pseudogap physics in cuprates [13]. (2) We demonstrated visualization of redox orbitals and their potentials in advanced lithium-ion battery materials using high-resolution X-ray Compton scattering [14]. (3) Through an analysis of scanning tunneling spectra from cubic perovskite oxide $SrVO_3$(001) thin films, we established a direct link between the observed atomic-scale interference patterns and the formation of a d_{xy}-derived surface state [15]. (4) We systematically explored topological properties of functionalized III-Bi honeycombs, and identified the presence of robust quantum anomalous Hall phases in TlBi films. [16]. (5) Longstanding questions concerning the nature of the positron state in CdSe quantum dots were resolved through a first-principles analysis of the positron annihilation spectra [17].

Planned activities

Highlights of ongoing/planned activities are as follows. (1) Along the lines of our studies of LSCO and YBCO cuprate superconductors described above, we are examining at the first-principles level the ground state electronic structures and the associated competing phases in wide classes of correlated materials such as the cuprates, Fe-based superconductors, nickelates and iridates. (2) Materials discovery effort toward predicting viable materials that can host Weyl, Dirac, Majorana and other more exotic fermions in a condensed matter setting, including strongly correlated systems. (3) Modeling and analysis of spin-textures of topological states in 2D and 3D topological materials and the associated ARPES and STS/STM spectra. (4) Thin-film materials beyond graphene, especially those with large spin-orbit coupling, their topological phases, and their quantum transport characteristics in the presence of external electric and magnetic fields. (5) Modeling and analysis of the doping and temperature dependencies of the electronic spectra of complex non-topological as well as topological materials using our comprehensive, beyond LDA intermediate coupling scheme and its multi-orbital extensions. (6) Modeling electronic structures of ordered and disordered phases of various Li-battery materials, and the associated inelastic x-ray scattering spectra to develop the potential of these techniques as unique, in situ/operando advanced characterization tools with the capability to probe closed electrochemical cells. (7) Modeling of K-, L- and M-edge RIXS spectra of cuprates and extensions of our methodology for treating dissipation effects and time-domain problems.

References

[1] J. W. Furness, Y. Zhang, C. Lane, I. G. Buda, B. Barbiellini, R. S. Markiewicz, A. Bansil, J. Sun: "An accurate first-principles treatment of doping-dependent electronic structure of high-temperature cuprate superconductors," Nature Communications Physics 1, 11 (2018).

[2] Y. Zhang, C. Lane, J. W. Furness, B. Barbiellini, R. S. Markiewicz, A. Bansil and J. Sun: "Landscape of competing stripe and magnetic phases in cuprates," Science (2018, submitted).

[3] S-Y. Xu, N. Alidoust, G. Chang, H. Lu, B. Singh, I. Belopolski, D. S. Sanchez, X. Zhang, G. Bian, H. Zheng, M-A. Husan, Y. Bian, S-M. Huang, C-H Hsu, T-R. Chang, H-T. Jeng, A. Bansil, T. Neupert, V. N. Strocov, H. Lin, S. Jia, M. Z. Hasan: "Discovery of Lorentz-violating type II Weyl fermions in LaAlGe," Science Advances 3, e1603266 (2017).

[4] G. Chang, Su-Y. Xu, X. Zhou, S-M. Huang, B. Singh, B. Wang, I. Belopolski, J. Yin, S. Zhang, A. Bansil, H. Lin, M. Z. Hasan; "Topological Hopf and chain link semimetal states and their application to Co_2MnGa." Physical Review Letters 119, 156401 (2017).

[5] G. Chang, S-Y. Xu, B. J. Wieder, D. S. Sanchez, S-M Huang, I Belopolski, T-R Chang, S. Zhang, A Bansil, H Lin, and M. Z. Hasan; "Unconventional Chiral Fermions and Large Topological Fermi Arcs in RhSi." Physical Review Letters 119, 206401 (2017).

[6] C-H Hsu, Y Fang, S Wu, Z-Q Huang, C P Crisostomo, Y-M Gu, Z-Z Zhu, H Lin, A Bansil, F-C Chuang, and L Huang; "Quantum anomalous Hall insulator phase in asymmetrically functionalized germanene," Physical Review B 96, 165426 (2017).

[7] S-M Huang, C-H Hsu, S-Y Xu, C-C Lee, S-Y Shiau, H Lin, and A Bansil: "Topological superconductor in quasi-one-dimensional $Tl_{2-x}Mo_6Se_6$," Physical Review B 97, 014510 (2018).

[8] G Chang, B Singh, S-Y Xu, G Bian, S-M Huang, C-H Hsu, I Belopolski, N Alidoust, D S Sanchez, H Zheng, H Lu, X Zhang, Y Bian, T-R Chang, H-T Jeng, A Bansil, H Hsu, S Jia, T Neupert, H Lin, and M Z Hasan: "Magnetic and noncentrosymmetric Weyl fermion semimetals in the RAlGe family of compounds (R=rare earth)," Physical Review B- Rapid Communication 97,041104 (2018).

[9] B Singh, X Zhou, H Lin and A Bansil: "Saddle-like topological surface states on the TT'X family of compounds (T, T' = Transition metal, X= Si, Ge)," Physical Review B 97, 075125 (2018).

[10] W C Yu, X Zhou, F-C Chuang, S A Yang, H Lin, A Bansil: "Nonsymmorphic cubic Dirac point and crossed nodal rings across ferroelectric phase transition in $LiOsO_3$," Phys. Rev. Materials-Rapid (2018).

[11] B Singh, G Chang, T-R Chang, S-M Huang, C Su, M-C Lin, H Lin, A Bansil: "Tunable double-Weyl Fermion semimetal state in the $SrSi_2$ materials class," Scientific Reports (2018).

[12] A Vargas, F Liu, C Lane, D Rubin, I Bilgin, Z Hennighausen, A Bansil, S Kar; "Tunable and laser-reconfigurable 2D heterocrystals obtained by epitaxial stacking of crystallographically incommensurate Bi_2Se_3 and MoS_2 atomic layers," Science Advances 3, e1601741 (2017).

[13] R. S. Markiewicz, I. G. Buda, P. Mistark, C. Lane and A. Bansil: "Entropic Origin of Pseudogap Physics and a Mott-Slater Transition in Cuprates," Scientific Reports 7, 44008 (2017).

[14] H Hafiz, K Suzuki, B Barbiellini, Y Orikasa, V Callewaert, S Kaprzyk, M Itou, K Yamamoto, R Yamada, Y Uchimoto, Y Sakurai, H Sakurai, A Bansil; "Visualizing redox orbitals and their potentials in advanced lithium-ion battery materials using high-resolution x-ray Compton scattering," Science Advances 3, e1700971(2017).

[15] Y Okada, S-Y Shiau, T-R Chang, G Chang, M Kobayashi, R Shimizu, H-T Jeng, S Shiraki, H Kumigashira, A Bansil, H Lin, and T Hitosugi; "Quasiparticle Interference on Cubic Perovskite Oxide Surfaces," Physical Review Letters 119, 086801 (2017).

[16] C P. Crisostomo, Z-Q Huang, C-H Hsu, F-C Chuang, H Lin, A Bansil: "Chemically-induced Large-Gap Quantum Anomalous Hall Insulator States in III-Bi Honeycombs," NPJ (Nature Partner Group) Computational Materials 3, 39 (2017).

[17] W Shi, V Callewaert, B Barbiellini, R Saniz, M Butterling, W Egger, M Dickmann, C Hugenschmidt, B Shakeri, R W Meulenberg, E Brück, B Partoens, A Bansil, and S W.H. Eijt: "Nature of the positron state in CdSe quantum dots," Physical Review Letters (2018).

Quantum Phases of Nanosystems: Non-Equilibrium Phenomena

Principal Investigator: Harold U. Baranger
Dept. of Physics, Duke University, Durham NC 27708-0305; baranger@phy.duke.edu

Keywords: quantum phases, nanoscale, nonequilibrium, quantum transport, phase transition

Project Scope

The focus of this project is *non-equilibrium* properties of *interacting quantum systems* realized in *nanoscale structures*. Nanoscale structures are ideal for studying non-equilibrium interacting systems because of the exquisite control over parameters that they provide, the natural interactions coming from electron confinement, and the ease in creating highly non-equilibrium conditions by applying a voltage bias. Indeed, in the last five years there has been an increasing number of experiments in engineered nanoscale systems that probe electron correlations. One long-term goal of this project is to understand non-equilibrium steady states near quantum critical points of quantum impurity models. Such models are paradigmatic many-body systems: they are tractable strongly interacting systems that still contain much of the interesting many-body physics and also apply to real materials. Several such models have been realized in experimental systems using quantum dots, normal and superconducting metallic grains, and quantum hall edge states. Beyond steady-state nonequilibrium phenomena, time-dependent effects have recently become accessible through microwave and optical techniques, opening a whole new range of nonequilibrium nanoscale problems. Finally, novel topological quantum states may be obtained by combining elements in different quantum phases, such as quantum hall (or spin hall) edges and superconductivity.

Recent Progress

Nonequilibrium I-V Curve at an Interacting Impurity Quantum Critical Point

Nonequilibrium properties of correlated quantum matter are being intensively investigated because of the rich interplay between the external drive and the many-body correlations. Of particular interest is the nonequilibrium behavior at a quantum critical point (QCP), where a system is delicately balanced between different ground states.

We have been studying a system that is fully accessible to both theory and experiment, and so provides an ideal setting for addressing steady-state nonequilibrium phenomena in correlated quantum matter. The system is a quantum dot coupled to resistive leads: a spinless resonant level interacting with an ohmic resistive environment (Fig. 1). A two-channel Kondo QCP occurs when the level is on resonance and symmetrically coupled to the leads. Although nonequilibrium effects at a QCP are typically out of reach, for this case we are able to overcome the theoretical and experimental challenges, providing [2,4] both an analytical calculation of the *I-V* curve at a QCP and experimental results to which the theory is compared. We believe these are the first experimental or theoretical results on *I-V* characteristics in the quantum critical region of a QCP [along path 1 in Fig. 1].

Using a bosonized representation, we first calculate the nonlinear *I-V* curve in the quantum critical region [2]. We show that it has a physically intuitive interpretation in terms of weak backscattering of non-interacting fermions coupled to a modified environment, thus arriving at the same *I-V* through dynamical Coulomb blockade theory. We then find the *I-V* curve using similar techniques for the cross-over from the QCP to the weakly coupling fixed point—path 2 in

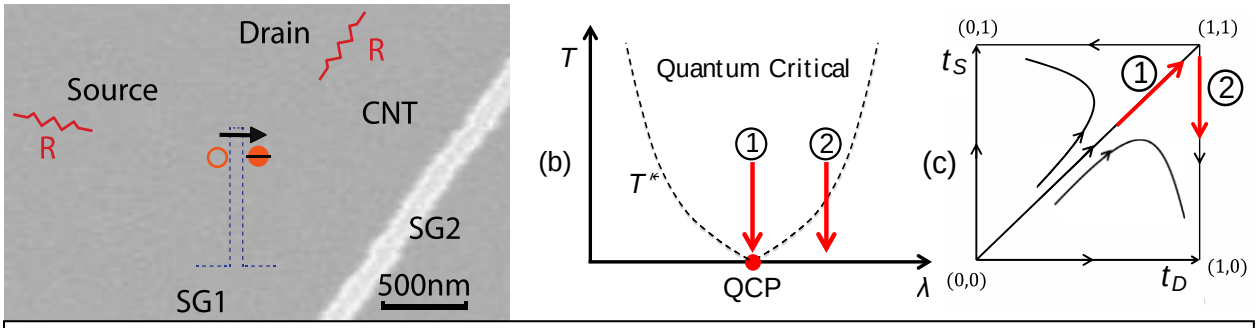

Fig. 1. (a) Schematic of the system overlaid on a SEM image of a sample measured. A quantum dot is formed in the carbon nanotube (CNT) segment between the source and drain leads. These resistive leads create a dissipative environment for electrons tunneling through the dot. The tunneling barriers can be tuned with the side gates SG1 and SG2. Applying a bias between the source and drain produces a nonequilibrium steady state.
(b) Diagram of the quantum critical region. When tuned to the QCP, the quantum critical region extends down to zero temperature (path 1), otherwise a crossover to one of the trivial ground states occurs (path 2).
(c) The RG flow of source and drain coupling (t_S, t_D) when the system is on resonance. For symmetric coupling, the flow is into the strong coupling fixed point (1,1) (path 1) corresponding to the QCP. A slight detuning leads to a crossover to a trivial fixed point (path 2).

Fig. 1 [4]. In both cases, the quantitative agreement between our theoretical and experimental results (Fig. 2), with no fitting parameter, is excellent.

Stabilization of a Majorana Zero Mode Through Quantum Frustration

Majorana zero modes (MZMs) are exotic self-conjugate edge excitations that are predicted to exist in non-trivial condensed matter structures. They have attracted wide interest because their non-Abelian statistics may be relevant for quantum computation. To observe MZMs, researchers have proposed several routes to effectively realize the celebrated toy model by Kitaev in which there is an MZM at each end of a one-dimensional wire. A requirement for interesting MZM phenomena is that the coupling between the two MZM be zero so that they are truly independent. As the wavefunctions in proposed systems may overlap too much, we consider ways in which an MZM can be stabilized.

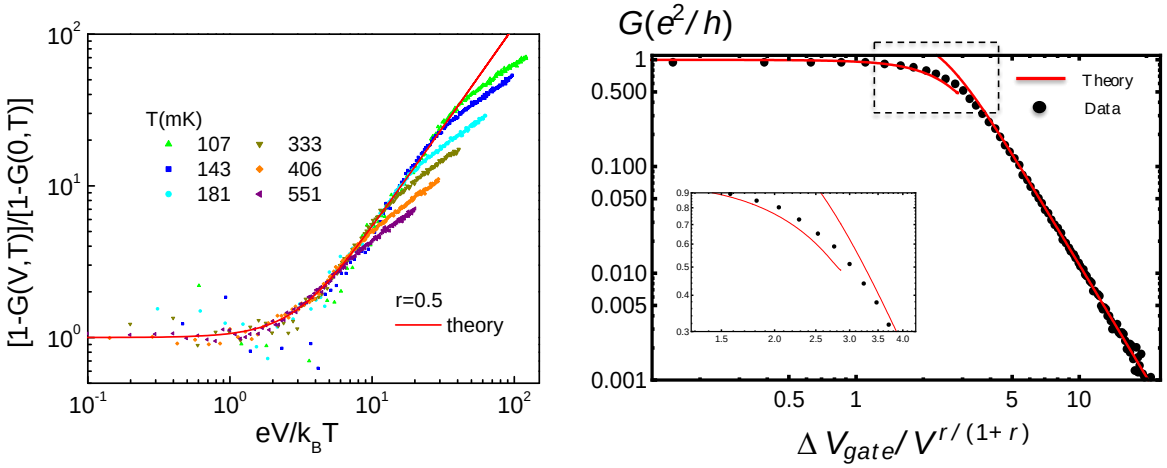

Fig. 2. (Left) Deviation from perfect conductance 1−G(V,T) for R/ R_Q =0.5. Here G(V,T) is the differential conductance G = (h/e^2)dI/dV. The symbols are the experimental results at the color-coded temperatures. The red line is the result of the full non-linear theory, in which there are no free parameters. Note the excellent agreement between the theory and data in both the crossover and power-law regimes.
(Right) Conductance in the non-equilibrium cross-over regime as a function of detuning of the resonant level. The theory in both the small and large detuned limits agrees very well with the data.

We show [5] that a MZM can be stabilized by hybridizing its partner with an effective two channel Kondo (2CK) state. Frustration inherent in the effective 2CK state leads to a decoupled Majorana degree of freedom which can naturally hybridize with one of a pair of MZM in a topological wire, thereby leaving an unpaired MZM at the other end of the wire.

Concretely, the system that we study (Fig. 3) consists of two (left and right) on-resonant quantum dots that couple to two interacting Majorana fermions on the same grounded topological superconducting wire. The right dot is connected to two dissipative leads with R = R_Q, thus creating an effective 2CK state with an isolated Majorana zero mode on the dot. We find that the conductance through the left dot is $e^2/2h$ independent of the coupling between the two MZM, thus showing that the left-hand MZM is stabilized in its non-trivial state.

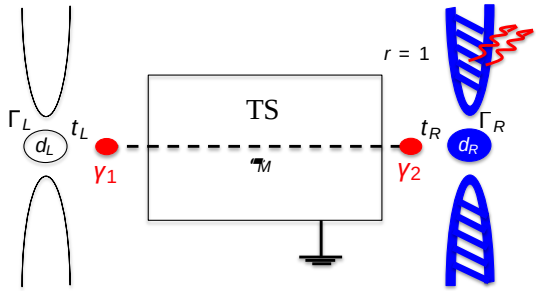

Fig. 3. Schematic of setup for stabilizing a MZM. A topological superconducting wire in its nontrivial state supports two MZM at its ends that may be hybridized. The unpaired Majorana associated with the 2CK state in the righthand dot pairs with one of the MZM, leaving the other one free. The conductance through the lefthand dot is one way to detect the unpaired, stabilized MZM.

Particle Production in the Non-Equilibrium Spin-Boson Model

One of the hallmarks of non-equilibrium phenomena in strongly interacting systems is the presence of a broad spectrum of excitations. Understanding the nonequilibrium state requires, then, characterizing this broad spectrum and how it is produced. As a canonical example which is experimentally accessible, we study the scattering of photons from a two-level emitter.

In a photonic system, for which the chemical potential is zero, the broad spectrum of excitations involves substantial particle production. Thus, as long as the coupling to the emitter is very strong, an injected few photon pulse generates many more (lower-energy) outgoing photons. The necessary experimental conditions for such a study have very recently been achieved for microwave photons coupled to superconducting qubits.

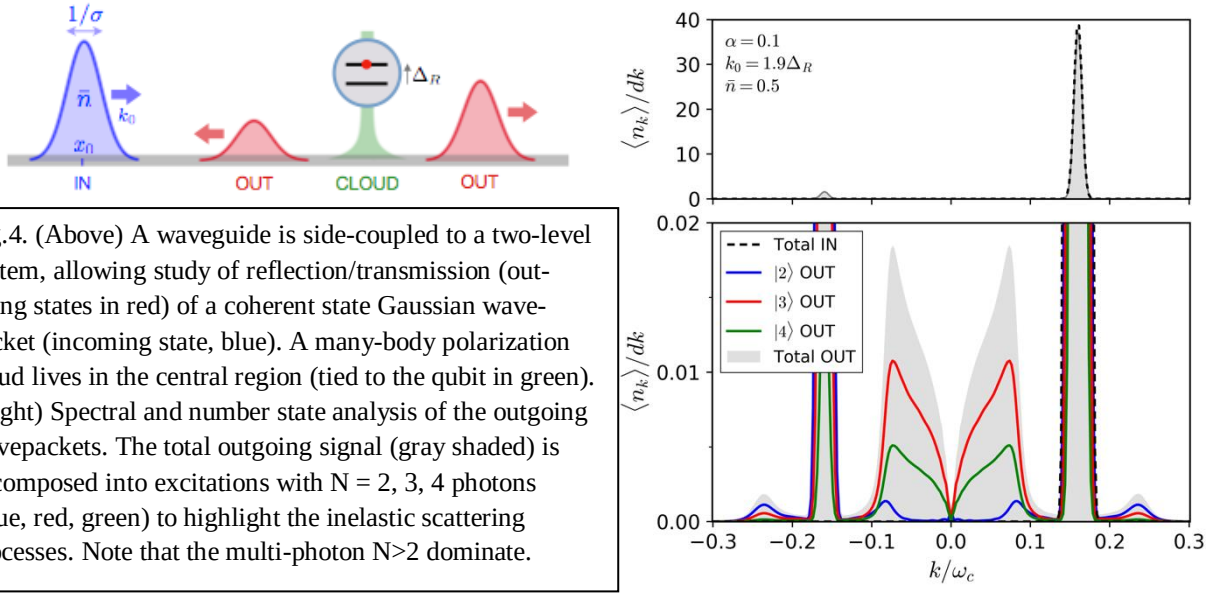

Fig.4. (Above) A waveguide is side-coupled to a two-level system, allowing study of reflection/transmission (outgoing states in red) of a coherent state Gaussian wavepacket (incoming state, blue). A many-body polarization cloud lives in the central region (tied to the qubit in green). (Right) Spectral and number state analysis of the outgoing wavepackets. The total outgoing signal (gray shaded) is decomposed into excitations with N = 2, 3, 4 photons (blue, red, green) to highlight the inelastic scattering processes. Note that the multi-photon N>2 dominate.

We have studied scattering of a photon pulse in the classic spin-boson problem in the ultra-strong coupling regime [3]. A numerically exact calculation is carried out using a novel and highly efficient time-dependent polaronic basis, which is then compared to results from using the rotating wave approximation standard in quantum optics in which there is no photon production. We find, indeed, that when the drive is off resonance, the leading contribution to the inelastic scattering comes from a process in which 3 outgoing photons are produced by a single incoming photon (see Fig. 4). As a result, for off-resonant inelastic phenomena, there is no regime of parameters in which the very commonly used rotating wave approximation is correct.

Future Plans

Nonequilibrium Effects at Quantum Critical Points

I am continuing to study nonequilibrium effects at QCP in nanosystems, now in more complex systems in which the physics is richer. First, we are investigating what happens when a spin degree of freedom is added to the quantum dot so that there is an interplay between the dissipative resonant level effects mentioned above and the Kondo effect. Second, there are very recent experimental realizations of the charge and spin multi-channel-Kondo QCP in nanostructures, and I plan to investigate non-equilibrium quantum transport in these. Both of these problems require a numerical approach, which with collaborators we are developing with time-dependent DMRG.

Quantum Hall and Superconductivity in Graphene

I plan to pursue a new way to produce interesting quantum states that can be probed with quantum transport in both equilibrium and highly non-equilibrium situations. The idea is to combine quantum Hall effect (QHE) edge states with superconductivity: because QHE occurs at low magnetic field in graphene (~1T), it can be combined with superconductors. Several experimental groups are actively pursuing this system; supercurrent, for instance, has recently been observed (e.g. group of G. Finkelstein, Duke).

This is an excellent system on which to build future studies of interesting quantum states and non-equilibrium effects. Because the 2DEG in graphene has structure—valley and sublattice degrees of freedom—the interaction with the superconductor has non-trivial effects. Non-equilibrium situations in which electrons are injected via the edge channels, as in the "electron quantum optics" experiments in regular 2DEG, would be particularly interesting. Finally, using fractional QHE edge states, novel quasi-particles, such as parafermions, may provide a useful low-energy description, and so could be probed out of equilibrium.

Publications (August 2016 – July 2018)

1. Gu Zhang, E. Novais, and H. U. Baranger, *Rescuing a Quantum Phase Transition with Quantum Noise*, Phys. Rev. Lett. **118**, 050402 (2017).
2. G. Zhang, C.-H. Chung, C. T. Ke, C.-Y. Lin, H. Mebrahtu, A. I. Smirnov, G. Finkelstein, and H. U. Baranger, *Universal Nonequilibrium I-V Curve at an Interacting Impurity Quantum Critical Point*, submitted, arXiv:1609.04765.
3. N. Gheeraert, X. H. H. Zhang, S. Bera, N. Roch, H. U. Baranger, and S. Florens, *Particle Production in Ultra-Strong Coupling Waveguide QED*, Phys. Rev. A in press, (2018).
4. Gu Zhang, E. Novais, and H. U. Baranger, *Non-Equilibrium Crossover near a Non-Fermi-Liquid Quantum Critical Point: Conductance of a Dissipative Quantum Dot*, in preparation (2018).
5. Gu Zhang and H. U. Baranger, *Stabilization of a Majorana Zero Mode through Quantum Frustration*, in preparation (2018).

Structural phase transitions and material properties of ferroic 2D materials

Salvador Barraza-Lopez, University of Arkansas, Fayetteville

Keywords: Ferroic behavior, two-dimensional materials, group-IV monochalcogenides

Project Scope: The goal is to study two-dimensional structural phase transitions in 2D materials that possess structural degeneracies, and the effects of these structural transitions on materials' properties. This work was spearheaded by the structural degeneracies in group-IV monochalcogenide monolayers discovered in my group (1) and experimentally verified already (2). Work on group-IV monochalcogenides is being done in collaboration with two experimental groups (Zhu, UIUC; and Parkin, MPI-Halle), and we are extending it onto other 2D materials. An important component of this work are of *ab-initio* molecular dynamics calculations using the NPT ensemble that help capture these transitions directly from first principles and without any bias in the model. A review article on this field appeared recently (3).

Recent Progress: We have moved from the determination of degeneracies (1), onto the demonstration of a ferro-to-paraelectric structural transition from *ab-initio*

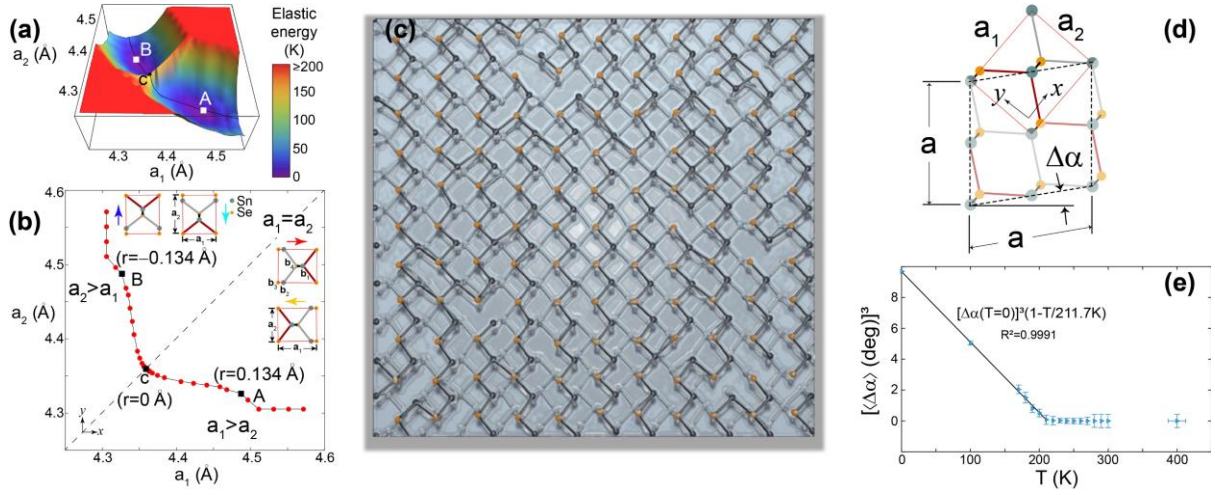

Figure 1. (a) Elastic energy landscape for a SnSe monolayer. Points A and B are degenerate. (b) Four degenerate ground states exist from the orientation of the electric dipole at the unit cell. (c) Still frame during the MD evolution. (d) Defining the rhombic angle Δα. (e) Thermal evolution of Δα.

molecular dynamics (4, 5). Figure 1 showcases our results, obtained on supercells containing 1024 atoms, on calculations that ran for 20,000 fs with a 1.5 fs resolution.

Defining the energy barrier *J* as the energy difference among points A and C in Fig. 1(a), the relation among *J* and the transition temperature *Tc* (in which the rhombic angle $\Delta\alpha$ defined in Fig. 1(d) becomes zero in Fig. 1(e)) is found as $Tc=1.4J$.

As part of the effort, we have contrasted the results we obtained with those from a published *ad-hoc* model, whose shortcomings are the use of only two out of the four degenerate ground states, and a "mean field disorder" term obtained on a single unit cell. Both assumptions over-constrain their Monte-Carlo model to yield $Tc=6J$, which is not supported from actual *ab-initio* MD, which not needing *ad-hoc* interactions sets the gold standard for the actual dynamics of these transitions. We showed that introduction of *ad-hoc* constraints raises *Tc* from its intrinsic value (5).

In another work, not related to the transition but still having to do with this material family, we demonstrated that the anisotropic mass of the valence band valley (Fig. 2(d) below) is responsible for anisotropic electric transport through hole-doped, bulk GeSe (6). This was a collaboration with Wenjuan Zhu' experimental team (Illinois).

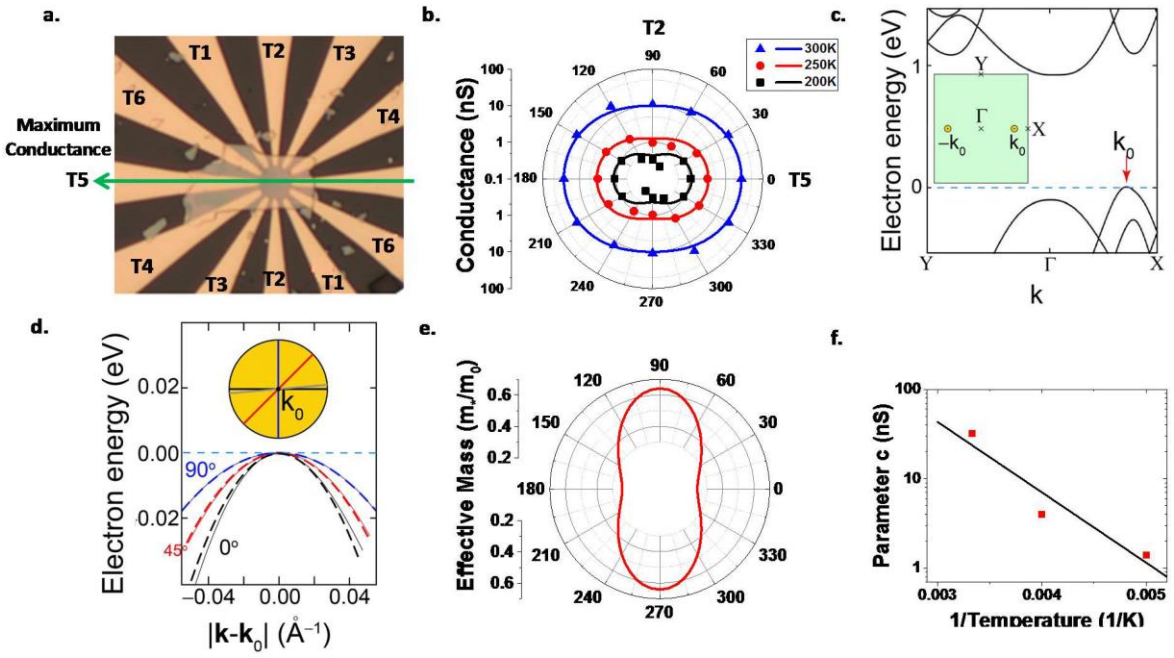

Figure 2. (a) Patterned leads onto a p-doped GeSe flake. (b) Anisotropic conductance; solid curves are a result from our model. (c) Valley responsible for transport. (d and e) Anisotropy of valley's effective mass m*. (f) Parameter to fit the conductance, from a mobility expression in terms of m*.

A characteristic of ferroic materials is to change their shape when the electronic density is altered, by illumination, because the change in electron density alters the intrinsic electric dipole and produces an anisotropic elastic response of the material

(Fig. 3), in an effect known as *photostriction*. Using constrained density functional theory, we depopulated a small charge density at the top of the valence band to populate the bottom of the conduction band, effectively simulating the excitation of carriers by illumination, and determined the structural changed that ensued as a result. We found that group-IV monochalcogenide monolayers SnS and SnSe sustain record amounts of anisotropic distortion upon illumination (7).

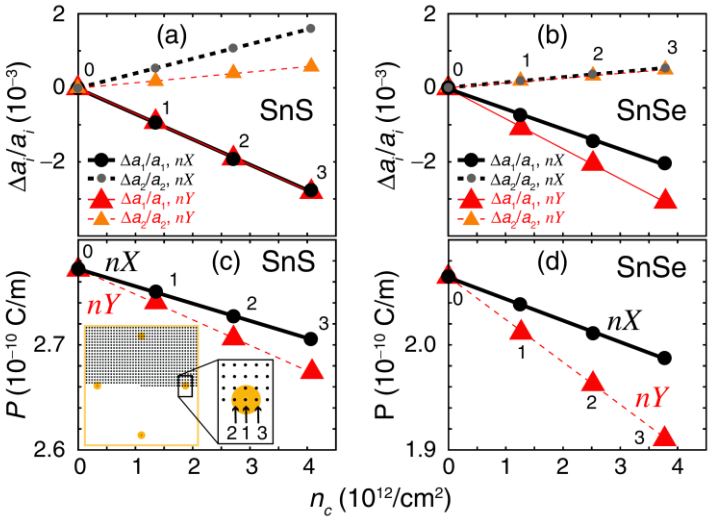

Figure 3. Changes of lattice parameters a_1 and a_2, and intrinsic polarization for SnS and SnSe upon excitation of carriers. The anisotropic change of lattice parameters observed is due to photostriction.

Review article: We wrote a review article solicited by Reports on Progress of Physics (8). Among other contents, we discussed the issue of structural degeneracies in two-dimensional materials.

Future Plans:

1. To make the in-house modifications we developed to perform NPT molecular dynamics broadly available.

2. Being isostructural and isoelectronic with phosphorene, the fact that no group has reported the creation of monolayers of group-IV monochalcogenides by mechanical exfoliation is mysterious. We are looking into how these materials degrade under ambient conditions. This will provide guidance onto potential new routes to creating these materials, which is imperative for this field to move forward with more vigor.

3. To expand the studies of structural transitions in 2D onto four additional material families; one work along this direction is under review already.

4. To continue to develop a collaboration effort with Dr. Kai Chang, the experimentalist behind the first demonstration of ferroic behavior in group-IV monochalcogenides, who is a scientist at Stuart Parkin's group at MPI-Halle.

References:

1. Mehboudi M, Dorio AM, Zhu W, van der Zande A, Churchill HOH, Pacheco-Sanjuan AA, Harriss EO, Kumar P, & Barraza-Lopez S (2016) Two-Dimensional Disorder in Black Phosphorus and Monochalcogenide Monolayers. Nano Letters 16(3):1704–1712.
2. Chang K, Liu J, Lin H, Wang N, Zhao K, Zhang A, Jin F, Zhong Y, Hu X, Duan W, Zhang Q, Fu L, Xue Q-K, Chen X, & Ji S-H (2016) Discovery of robust in-plane ferroelectricity in atomic-thick SnTe. Science 353(6296):274-278.
3. Cui C, Xue F, Hu W-J, & Li L-J (2018) Two-dimensional materials with piezoelectric and ferroelectric functionalities. npj 2D Materials and Applications 2(1):18.

Publications:

4. Mehboudi M, Fregoso BM, Yang Y, Zhu W, van der Zande A, Ferrer J, Bellaiche L, Kumar P, & Barraza-Lopez S (2016) Structural Phase Transition and Material Properties of Few-Layer Monochalcogenides. Physical Review Letters 117(24):246802.
5. Barraza-Lopez S, Kaloni TP, Poudel SP, & Kumar P (2018) Tuning the ferroelectric-to-paraelectric transition temperature and dipole orientation of group-IV monochalcogenide monolayers. Physical Review B 97(2):024110.
6. Yap WC, Yang Z, Mehboudi M, Yan J-A, Barraza-Lopez S, & Zhu W (2018) Layered material GeSe and vertical GeSe/MoS2 p-n heterojunctions. Nano Research 11(1):420-430.
7. Haleoot R, Paillard C, Kaloni TP, Mehboudi M, Xu B, Bellaiche L, & Barraza-Lopez S (2017) Photostrictive Two-Dimensional Materials in the Monochalcogenide Family. Physical Review Letters 118(22):227401.
8. Naumis GG, Barraza-Lopez S, Oliva-Leyva M, & Terrones H (2017) Electronic and optical properties of strained graphene and other strained 2D materials: a review. Reports on Progress in Physics 80(9):096501.

Atomistic Theories and Simulations of Multiferroics

Laurent Bellaiche, University of Arkansas

Keywords: Multiferroics and related systems; magnetism, electric field; energy storage

Project Scope

Multiferroics (MFE) form an important class of materials that possess coupled long-range-ordered electric and magnetic degrees of freedom. Such magneto-electric coupling is promising to design new devices taking advantage of the control of magnetic properties by the application of an electric field, or conversely, of the magnetic-field-induced change in electric properties.

The broad objective of this award revolves around three main issues, all involving multiferroics and related materials. First of all, we wish to understand (at a microscopic level) experimentally-found but poorly understood complex phenomena in MFEs. Secondly, we want to design novel multiferroics. Finally, we desire to explore the possibility of using multiferroics in new applications, by focusing on some of their properties that have been scarcely studied so far.

To achieve these objectives, several research projects on multiferroics and related compounds have been conducted or are being conducted, by continuing to develop and/or use different state-of-the-art first-principles-based schemes. Collaborations with internationally-recognized groups, having vital experimental programs on multiferroics, are also further strengthened, which allow us to ground our simulations and to fully, deeply understand the complex materials under investigation.

Recent Progress

I will focus here on a recent study that has attracted quite a lot of attention, but also indicate on page 4 of this abstract the other DOE-sponsored works that have been published since March 2017 alone. The study we focus here is ``Designing Lead-Free Antiferroelectrics for Energy Storage," Bin Xu, Jorge Iniguez and L. Bellaiche, Nature Communications 8, 15682 (2017).

We used our newly developed first-principles-based effective Hamiltonian method for $Bi_{1-x}R_xFeO_3$ (BRFO, R being a lanthanide, Nd in Ref. [1]) to study the energy storage properties of antiferroelectrics [1]. Antiferroelectrics are very promising for high-power energy storage, and we predicted that BRFO can potentially allow high energy densities (100–150 J cm^{-3}) and efficiencies (80–88%) for feasible electric fields upon experimental advances (2–3 MV cm^{-1}). Additionally, we derived a simple model to describe the energy density and efficiency of a general antiferroelectric material, providing a framework to assess the effect on the storage properties of variations in doping, electric field magnitude and direction, epitaxial strain, temperature, etc., which can facilitate future search of antiferroelectric materials for energy storage.

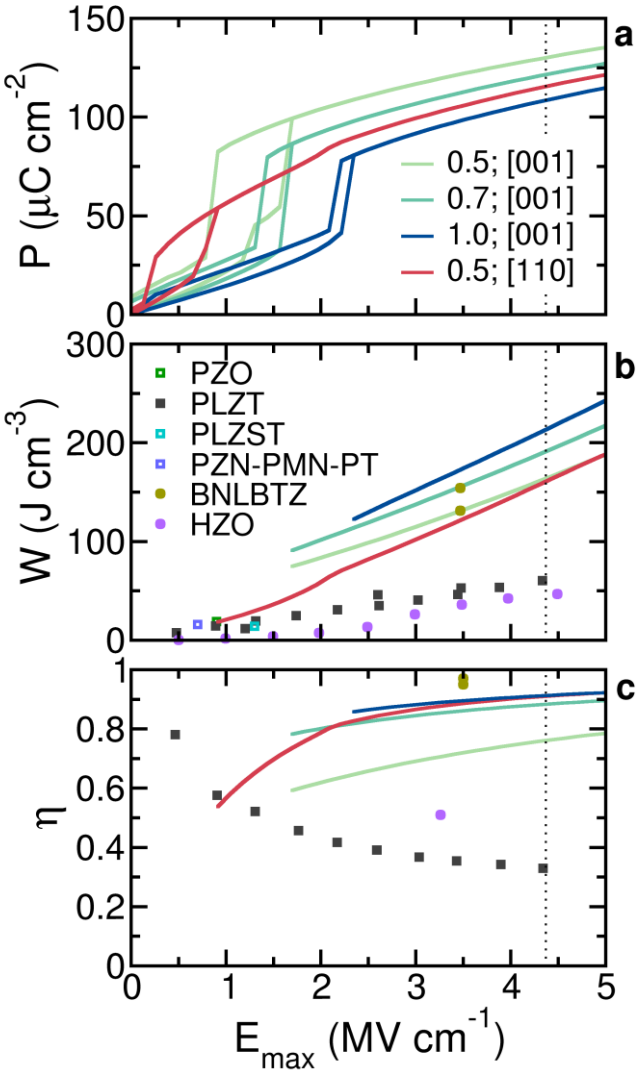

Figure captions: The computed energy storage performance of selected $Bi_{1-x}Nd_xFeO_3$ solid solutions. (a) The *P*–*E* hysteresis curves. (b) The energy density as a function of the magnitude of the maximum applied electric field, with the discrete symbols representing the best available experimental data from different types of materials, that is, lead-based ($PbZrO_3$, $(Pb,La)(Zr,Ti)O_3$, $(Pb,La)(Zr,Sn,Ti)O_3$ and $Pb(Zn_{1/3}Nb_{2/3})O_3$-$Pb(Mg_{1/3}Nb_{2/3})O_3$-$PbTiO_3$), and lead-free ($((Bi_{1/2}Na_{1/2})_{0.9118}La_{0.02}Ba_{0.0582}(Ti_{0.97}Zr_{0.03})O_3$ and $Hf_xZr_{1-x}O_2$) systems. (c) The efficiency as a function of the magnitude of the maximum applied electric field.

Future Plans

We will continue to investigate properties of mutiferroics and related systems. Examples of ongoing and future studies are as follows:

- Designing (via strain-engineering) new antiferroelectric systems with high energy storage density

- Designing new multiferroics and new type of ferroelectricity, via defect engineering.

- Investigating ultrafast switching of electrical polarization in multiferroics and related systems.

- Search for the so-called electromagnons in multiferroics.

- Discovery of multiferroic solid solutions that are ferroelectric and ferromagnetic.

- Joint theoretical and experimental collaboration on the effect of uniaxial stress on properties of multiferroic thin films.

- Investigation of the so-called polar metals under pressure and epitaxial strain, and in thin films' form.

- Understanding at a microscopic level of 2D ferroelectrics.

- Understanding at a microscopic level of 2D ferromagnets.

- Investigating magnetic properties of rare-earth iron garnets.

- Study of domains and domain walls in multiferroic thin films.

- Determining from first-principles the various magnetic interactions and their parameters allowing the existence of many different complex magnetic arrangements (different cycloids, antiferromagnetism with weak magnetization, etc..) in $BiFeO_3$–based systems.

References

1. ``Designing lead-free antiferroelectrics for energy storage," Bin Xu, Jorge Iniguez and L. Bellaiche, Nature Communications 8, 15682 (2017).

Publications quoting DOE support since March 2017

1. ``Novel Multiferroic Phases and Phenomena in Epitaxial (111) $BiFeO_3$ Films," Changsong Xu, Hongjun Xiang, and Laurent Bellaiche, Adv. Electron. Mater. 3, 1700332 (2017).
2. ``Rules and mechanisms governing octahedral tilts in perovskites under pressure," H. J. Xiang, Mael Guennou, Jorge Íñiguez, Jens Kreisel, and L. Bellaiche, Physical Review B 96, 054102 (2017).
3. ``Structural phases arising from reconstructive and isostructural transitions in high-melting-point oxides under hydrostatic pressure: A first-principles study,'' Hao Tian, Xiao-Yu Kuang, Ai-Jie Mao, Yurong Yang, Changsong Xu, S. Omid Sayedaghaee, and L. Bellaiche, Physical Review B, (Rapid Communications) 97, 020103(R) (2018).
4. ``Improper ferroelectricity at antiferromagnetic domain walls of perovskite oxides,'' Yali Yang, Hongjun Xiang, Hongjian Zhao, Alessandro Stroppa, Jincang Zhang, Shixun Cao, Jorge Íñiguez, L. Bellaiche, and Wei Ren, Physical Review B 96, 104431 (2017).
5. ``Toy model for uncommon spin–orbit-driven spin-torque terms," Charles Paillard, Raymond Walter, Surendra Singh, Brahim Dkhil and L Bellaiche, Journal of Physics: Condensed Matter 29, 254001 (2017).
6. `` Intrinsic polarization switching mechanisms in BiFeO3," Bin Xu, Vincent Garcia, Stephane Fusil, Manuel Bibes, and L. Bellaiche, Physical Review B 95, 104104 (2017).
7. ``Designing lead-free antiferroelectrics for energy storage," Bin Xu, Jorge Íñiguez and L. Bellaiche, Nature Communications 8, 15682 (2017).
8. ``Interface reconstruction with emerging charge ordering in hexagonal manganite," Shaobo Cheng, Changsong Xu, Shiqing Deng, Myung-Geun Han, Shanyong Bao, Jing Ma, Cewen Nan, Wenhui Duan, Laurent Bellaiche, Yimei Zhu and Jing Zhu, Science Advances 4, 4298 (2018).
9. ``Cooperative Couplings between Octahedral Rotations and Ferroelectricity in Perovskites and Related Materials," Teng Gu, Timothy Scarbrough, Yurong Yang, Jorge Iniguez, L. Bellaiche, and H. J. Xiang, Physical Review Letters 120, 197602 (2018).
10. ``Designing switchable near room-temperature multiferroics via the discovery of a novel magneto-electric coupling," J.S. Feng, Ke Xu, Laurent Bellaiche and H.J. Xiang, New Journal of Physics 20, 053025 (2018).
11. ``Understanding and revisiting the most complex perovskite system via atomistic simulations," Yali Yang, Bin Xu, Changsong Xu, Wei Ren and L. Bellaiche, Physical Review B 97, 174106 (2018).

Geometry, Disorder & Phase Transitions in Topological States of Matter

Principal Investigator: Dr. Ravindra Bhatt, Department of Electrical Engineering, Princeton University, Princeton, NJ 08544 (ravin@princeton.edu).

Co-Principal Investigators: Dr. F. Duncan M. Haldane, Department of Physics, Princeton University, Princeton, NJ 08544 (haldane@princeton.edu); Dr. Edward H. Rezayi, Department of Physics, California State University, Los Angeles, CA 90032 (erezayi@calstatela.edu); Dr. Kun Yang, Department of Physics and NHFML, Florida State University, Tallahassee, FL 32310 (kunyang@magnet.fsu.edu)

Keywords: Quantum Hall Effect, Composite Fermions, Phase Transitions, Quantum Entanglement, Disorder

Project Scope

Carried out in a synergistic manner, our project aims to provide a detailed understanding of topological phases and phase transitions in two-dimensional electron systems in the fractional quantum Hall (FQH) regime, as well as in related systems. This includes the quantum geometry characterizing the phases, effect of disorder (e.g. possibility of many-body localization), as well as response to strong external drives. We use a variety of numerical techniques in conjunction with fundamental theory to achieve our goals.

Research Accomplishments (7/16 – 6/18)

Research accomplishments are detailed in References [1-32]. A synopsis of the main accomplishments is given below.

(I) Fermi Surface Structure of Composite Fermions (CF)

A comprehensive numerical study of the composite Fermi liquid at $\nu = ½$ for a variety of zero-field band dispersions with and without rotational symmetry in the plane was carried out [9,13,17]. We used the Density Matrix Renormalization Group scheme on the infinite cylinder geometry (i-DMRG). We first studied [9] parabolic bands with mass anisotropy and Coulomb (1/r) interactions, and showed that the CF Fermi surface anisotropy (ratio of two principal Fermi momenta) is accurately given by the *square-root* of the anisotropy of the (non-interacting) zero-field Fermi surface, a *parameter-free result* confirmed by experiments on strained GaAs quantum wells [I. Jo *et al*., PRL **119**, 016402 (2017)]. The amount of anisotropy transfer from the zero-field dispersion to the CF Fermi surface depends on the form of electron-electron interaction, and agrees with analytical results for a model interaction from our previous grant period [K. Yang, PRB **88**, 241105 (2013)].

A second study [13] examined the limitations of manipulating quantum Hall phases using zero-field "band-structure engineering". In particular, we show that the Landau-levels formed of isotropic dispersions of any form have exactly the same eigenstates as for the canonical parabolic dispersion, and thus the composite fermion Fermi surface is *completely insensitive* to such distortions including Lifshitz transitions. We further show that multiple Fermi surfaces at zero-field could give rise to a single anisotropic composite Fermi surface at filling factor $\nu = ½$. Finally, we studied the effect of N-fold anisotropy of the zero-field dispersion on the composite fermion Fermi surface. It is found [17] that the anisotropy transferred to the composite Fermi surface decreases dramatically with N, so that the significant effect for the case of $N = 2$ (elliptical anisotropy), becomes very small (<1%) by $N = 6$. This is consistent with the result described above for rotationally isotropic deformations of parabolic bands, and can be

understood in part in terms of the generalized Haldane pseudopotential scheme for anisotropic systems [7]. More recently, the iDMRG scheme has been applied [31] to various gapped phases, and it is found that states within a given Jain sequence have similar responses to mass anisotropy, while those of different Jain sequences have different responses. This implies that members of a single Jain sequence are characterized by universal behavior.

(II) Lattice Formalism for Composite Fermi Liquid on a Torus

A new formulation of the Landau level problem in terms of a "lattice" of N_Φ^2 points (instead N_Φ Landau eigenfunctions) was used to develop a fast, lattice-based Monte Carlo method and evaluate properties of model wavefunctions [26]. Remarkably, it was found [23] that the Halperin-Lee-Read formulation of the $\nu = ½$ state [PRB **47,** 7312 (1993)] was almost particle-hole symmetric when implemented in the lowest Landau level formalism. Further, we identified [27] a many-body analog of the Berry phase associated with the adiabatic transport of a single quasiparticle around the Fermi surface, and found a topological "Z2" Berry phase factor of −1/+1 for odd/even winding numbers of the path around the Fermi surface, in accord with the Son's prediction [PRX **5,** 031027 (2015)]. We also identified a "Dirac cone"-like feature: the model state with a quasi-hole in an inversion-symmetric "Fermi sea" becomes less particle-hole-symmetric as the hole moves towards the interior, and becomes orthogonal to its particle-hole conjugate when the hole reaches the center. This provides the central point that defines the winding number of the adiabatic path of a CF quasihole. Two other related manuscripts have been written dealing with various aspects of Landau levels on a torus [30,32].

(III) Competing Phases and Phase Transitions in Clean QH Systems

A comprehensive numerical study was done [12] of the $\nu = 5/2$ state including Landau level mixing in an unbiased, self-consistent manner, and showed that the anti-Pfaffian is selected over its particle-hole conjugate, the Moore-Read Pfaffian state. This study demonstrated terms in the Hamiltonian missed by earlier studies and helped clear a long-standing debate.

An investigation [2] of the half-filled QH bilayer system with interlayer tunneling using the DMRG technique revealed a continuous transition from an Abelian (331) state to the non-Abelian Moore-Read state in the intermediate tunneling regime. This shows how to realize a non-Abelian state by coupling different degrees of freedom, as in QH bilayers.

Precise analogs of Landau levels occur in rotating cold atom systems, where in the limit of high rotations, particles are in lowest Landau levels. Two exact diagonalization studies were performed [10,23] to study phases and transitions occurring under different circumstances. In one [10], a single species of fermions at filling $\nu = 1$ interacting through a p-wave Feshbach resonance, are found to undergo a second order transition from $\nu = 1$ fermionic integer QH state to a $\nu = 1/4$ molecular bosonic FQH state for weak coupling. More interestingly, for strong coupling, an intermediate phase occurs, in which there is coherence between bosonic molecules and (unbound) fermion pairs. As a result, the system goes through two phase transitions, one second order and one first order. Subsequently, we studied [23] a system with two species of fermions with filling $\nu = 2$ interacting through an s-wave Feshbach resonance. By studying the nature of the gapless edge modes, a continuous transition from a $\nu = 2$ fermionic integer QH state of atoms to a $\nu = 1/2$ bosonic FQH state formed of diatomic molecules was found.

A variational Monte Carlo study of the Pomeranchuk instability towards nematic phases of electrons in higher Landau levels was carried out [28]. In agreement with experimental observations, an instability was found to occur at small layer widths for higher Landau levels $n = 1$ and 2, with greater instability for $n = 2$.

(IV) Quantum Entanglement, Disorder and Localization

A new technique was formulated to study the disorder-driven FQH to insulator transition, using entanglement entropy as a diagnostic [1,15]. This scheme offers significant speedup over previous methods using Chern numbers, as no averaging over boundary conditions is needed. Besides a more reliable determination of the transition point, the method allowed an estimation of critical exponents. The derivative of the entanglement entropy with respect to disorder appears to diverge at the transition in the thermodynamic limit, and a finite size scaling analysis provides an estimate of the correlation length critical exponent. The scheme was initially applied [1] to study the effect of uncorrelated disorder on the $\nu = 1/3$ FQH state with Haldane V_1 pseudopotential (pure Laughlin state). Subsequently, we studied [15] the experimentally more relevant Coulomb interaction and several fractions $\nu = 1/3, 1/5, 1/7, 2/5$, as well as the gapless $\nu = ½$ phase. Finite-size scaling works well for the gapped phases for the larger sizes studied, but the gapless $\nu = ½$ phase shows strong finite size effects, and poor scaling. Two separate projects [20,29] studied the issue of universality of the localization length exponent in plateau IQH transitions using two-dimensional methods.

We examined [4] the possibility of a many-body localization (MBL) transition in a disordered quantum Hall system projected to a single Landau level using exact diagonalization. The challenge here is that one needs the entire spectrum - not just ground and low lying states. The crossover to Poisson statistics for energy eigenvalues, characterizing the transition to an MBL phase, moves rapidly to higher disorder strengths as system size is increased, implying no transition in the thermodynamic limit. Besides informing other topological models, this has implications for the existence of mobility edges in many-body localized systems, a topic of considerable current interest. Several other projects on disordered systems and MBL in other models were carried out [3,5,11,22] to obtain a clearer understanding of disorder in topological models.

Future Plans

Numerical calculations are underway to test the predictions of the graviton mode for FQH states. We plan to extend our studies of competing FQH phases (e.g. the newly suggested PH Pfaffian in experiment) and transitions (e.g. towards nematic order) using the new Monte Carlo scheme as well as DMRG methods. We will perform studies of quantum Hall physics in fractions of a Landau level, including MBL in different Chern bands that result, and also study the effect of strong ac drives in the QH regime.

Publications (11/2016 – 6/2018; chronological)

1. *Quantum Entanglement as a diagnostic of phase transitions in disordered quantum Hall liquids,* Zhao Liu and R. N. Bhatt, Physical Review Letters **117**, 206801 (2016) – Editor's suggestion.

2. *Fractional quantum Hall bilayers at half filling: Tunneling-driven non-Abelian phase,* W. Zhu, Zhao Liu, F. D. M. Haldane and D. N. Sheng, Physical Review B **94**, 245147 (2016).

3. *Rare-region effects and dynamics near the many-body localization transition,* K. Agarwal, E. Altman, E. Demler, S. Gopalakrishnan, D. A. Huse and M. Knap, Annalen der Physik **529**, 1600326 (2017).

4. *Absence of many-body localization in a single Landau level,* Scott D. Geraedts and R. N. Bhatt, Physical Review B **95**, 054303 (2017).

5. *Emergent local integrals of motion without a complete set of eigenstates,* Scott D. Geraedts, R. N. Bhatt and Rahul Nandkishore, Physical Review B **95,** 064204 (2017).

6. *Fibonacci anyons and charge density order in 12/5 and 13/5 quantum Hall plateaus*, Roger S. K. Mong, Michael P. Zaletel, Frank Pollmann and Zlatko Papic, Physical Review B **95,** 115136 (2017).

7. *Generalized pseudopotentials for the anisotropic fractional quantum Hall effect,* Bo Yang, Z-Xiang Hu, Ching Hua Lee and Zlatko Papic, Physical Review Letters **118,** 146403 (2017).

8. *Quantum heat waves in a one-dimensional condensate,* K. Agarwal, E. G. Dalla Torre, J. Schmiedmayer and E. Demler, Physical Review B **95**, 195157 (2017).

9. *Numerical Study of anisotropy in a composite Fermi liquid,* Matteo Ippoliti, Scott D. Geraedts and R. N. Bhatt, Physical Review B **95**, 201104 (2017). – Rapid Communication.

10. *Topological quantum phase transition from a fermionic integer quantum Hall phase to a bosonic fractional quantum Hall phase through a p-wave Feshbach resonance,* Shiuan-Fan Liou, Zi-Xiang Hu and Kun Yang, Physical Review B **95,** 241106 (2017).

11. *Localization and transport in a strongly driven Anderson insulator,* Kartiek Agarwal, Sriram Ganeshan and R. N. Bhatt, Physical Review B **96,** 014201 (2017).

12. *Landau level mixing and the ground state of the v = 5/2 quantum Hall effect,* Edward H. Rezayi, Physical Review Letters **119,** 026801 (2017).

13. *Connection between Fermi contours of zero-field electrons and v = ½ composite fermions in two-dimensional systems,* Matteo Ippoliti, Scott D. Geraedts and R. N. Bhatt, Physical Review B **96,** 045145 (2017).

14. *Exotic non-Abelian topological defects in lattice fractional quantum Hall states,* Zhao Liu, Gunnar Moller and Emil J. Bergholtz, Physical Review Letters **119**, 106801 (2017).

15. *Evolution of quantum entanglement with disorder in fractional quantum Hall liquids,* Zhao Liu and R. N. Bhatt, Physical Review B **96,** 115111 (2017).

16. *Fermionic lattice realization of a bosonic integer quantum Hall state – trivial insulator transition and relation to the self-dual line in the easy plane NCCP1 model,* Scott Geraedts & O. I. Motrunich, Physical Review B **96**, 115137 (2017).

17. *Composite fermions in bands with n-fold rotational symmetry,* Matteo Ippoliti, Scott D. Geraedts and R. N. Bhatt, Physical Review B **96,** 115151 (2017).

18. *Investigating anisotropic quantum Hall states with bimetric geometry,* Andrey Gromov, Scott D. Geraedts and Barry Bradlyn, Physical Review Letters **119**, 146602 (2017).

19. *Heitler-London model for acceptor-acceptor interactions in doped semiconductors*, Adam C. Durst, Kyle C. Castoria and R. N. Bhatt, Physical Review B **96**, 155208 (2017).

20. *Integer quantum Hall transition in a fraction of a Landau level,* Matteo Ippoliti, Scott D. Geraedts and R. N. Bhatt, Physical Review B **97**, 014205 (2018).

21. *Disordered quantum spin chains with long-range antiferromagnetic interactions,* N. Moure, H-Y Lee, S. Haas, R. N. Bhatt and S. Kettemann, Physical Review B **97**, 014206 (2018).

22. *Effect of Hilbert space truncation on Anderson localization,* Akshay Krishna and R. N. Bhatt, Physical Review B **97,** 174205 (2018).

23. *Topological phase transition in a two-species fermion system: Effects of a rotating trap potential or a symmetric gauge field,* Shiuan-Fan Liou, Zi-Xiang Hu and Kun Yang, Physical Review B **97,** 245140 (2018).

24. *Fast preparation of critical ground states using superluminal fronts,* Kartiek Agarwal, R. N. Bhatt and S. L. Sondhi, Physical Review Letters **120,** 210604 (2018).

25. *Evidence for a topological "exciton Fermi sea" in bilayer graphene,* Michael P. Zaletel, Scott Geraedts, Zlatko Papic and Edward H. Rezayi, Physical review B **98,** 045113 (2018).

26. *Lattice Monte Carlo for quantum Hall states on a torus,* Jie Wang, Scott D. Geraedts, E. H. Rezayi and F. D. M. Haldane, arXiv1710.09729.

27. *Berry phase and model wavefunction in the half filled Landau level,* Scott D. Geraedts, Jie Wang, E. H. Rezayi and F. D. M. Haldane, arXiv1711.07864.

28. *Pomeranchuk instability of composite Fermi liquid,* Kyungmin Lee, Junping Shao, Eun-Ah Kim, F. D. M. Haldane and Edward H. Rezayi, arXiv:1802.08261

29. *Localization length exponent in two models of quantum Hall plateau transitions,* Qiong Zhu, Peng Wu, R. N. Bhatt and Xin Wan, arXiv:1804.00398.

30. *A modular-invariant modified Weierstrass sigma-function as a building block for lowest-Landau-level wavefunctions on a torus, F. D. M. Haldane, arXiv:1806.00876*

31. *Geometry of flux attachment in anisotropic fractional quantum Hall states,* Matteo Ippoliti, R. N. Bhatt and F. D. M. Haldane, arXiv:1806.03303.

32. The origin of holomorphic states in Landau levels from non-commutative geometry, and a new formula for their overlaps on a torus, F. D. M. Haldane, arXiv:1806.10106

Plasmon-Mediated Photophysics of Complex Hybrid Nanostructures

Principle investigator: Igor Bondarev, Professor, PhD, DSc (Habilitation)
Department of Math & Physics, North Carolina Central University, Durham, NC 27707
ibondarev@nccu.edu

Project Scope

This project focuses on the development of the rigorous theoretical description for collective electromagnetic phenomena and excited states in complex hybrid nanostructures of reduced dimensionality. Theory is being developed for the plasmon-mediated resonance photophysics phenomena in low-dimensional quantum materials such as quasi-2D heterostructures of metals and semiconductors, organic semiconductor crystalline films, and carbon nanotubes. Complex hybrid structures of reduced dimensionality are currently in the process of rapid experimental development. There is a strong need for theoretical support to unravel their functionalities. Fundamental understanding of the properties of the collective excitations and how individual constituents of complex systems communicate with one another in the near field, and how this reflects on the properties of the entire complex system, is a natural prerequisite for advances ranging from new technological applications to the development of new concepts for future generation nanomaterials engineering. The proposed program capitalizes on the new results and accomplishments from the preceding DOE funded effort on nanooptics and plasmonics with advanced carbon and organic semiconductor nanostructures of direct relevance to the national priority Materials Genome Initiative.

Recent Progress

Below are some highlights of the progress made in the past two years. A more comprehensive publication list is appended below the highlights.

Complexes of indirect excitons in quasi-2D van der Waals heterostructures – An analytical theory has been developed for the trion and biexciton states formed by indirect (dipolar) excitons in layered quasi-2D semiconductor heterostructures [Fig.1(a,b)]. The trion state under study is a charged three-particle Coulomb-bound electron-hole complex with two like-charge particles confined to one layer and the third unlike-charge particle confined to another layer. The charge-neutral biexciton state is a four-particle complex with an interesting charge separation feature where a pair of like charges is in one layer and another pair of like charges of an opposite sign is in another layer. The configuration space method developed earlier by the PI for quasi-1D excitonic systems [I.V.Bondarev, Mod. Phys. Lett. B 30, 1630006 (2016)] is now generalized to obtain the analytical expressions for the binding energies of these complexes as functions of the interlayer distance, the exciton reduced effective mass, and the effective dielectric constant of the system [Fig.1(c,d)]. The method captures the essential kinematics of the complex formation to reveal that the trion and biexciton binding energies, despite a rapid decrease with distance, can exceed 10 meV and a few tens of meV, respectively, for the interlayer distances ~3–5 Å typical of van der Waals heterostructures. The theory explains the experimental evidence reported lately for the two types of the trion states formed by direct and indirect excitons in bilayer systems (APS March Meeting 2018, Harvard group, unpublished). Biexcitons and trions formed by indirect excitons control the formation of strongly correlated (Wigner-like) electron-hole crystal structures. Significant binding energies predicted herewith suggest that this strongly correlated multiexciton phenomenon of Wigner crystallization can be realized in layered van der Waals heterostructures such as gapped double bilayer graphene and few-layer transition-metal dichalcogenide systems, to open up new avenues for nonlinear coherent optical control and spinoptronics applications with indirect excitons. Work done in collaboration with the Coulomb Lab at the University of Montpellier, FRANCE [Figure 1; I.V.Bondarev and M.R.Vladimirova, Physical Review B 97, 165419 (2018)]

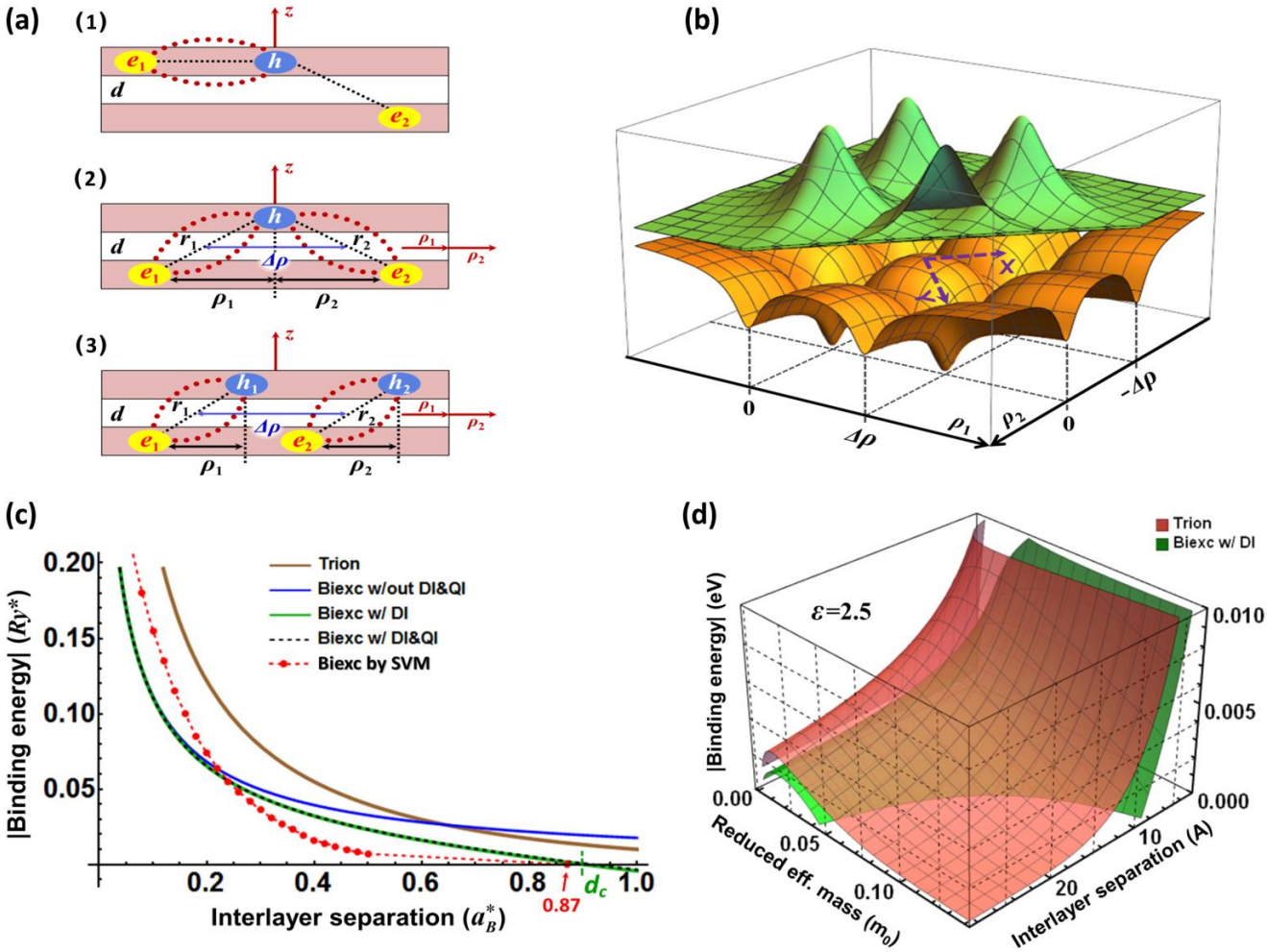

Fig. 1: **(a)** Sketches (1) and (2) show the difference between the trion formed by an electron and a *direct* exciton and that formed by an electron and an *indirect* exciton in a bilayer heterostructure with the interlayer distance *d*. Sketch (3) shows the biexciton complex of two *indirect* excitons. Exciton configurations (h-e_1) and (h-e_2) are inequivalent in (1) and are equivalent in (2) (and can be viewed as two indirect excitons sharing the same hole to form a negatively charged trion state), whereby the configuration space method can be used in case (2) to evaluate the ground-state binding energy of the corresponding trion complex. **(b)** Schematic of the tunnel exchange coupling for the two ground-state indirect excitons to form the trion (or biexciton) complex. The coupling occurs in the configuration space of the two independent in-plane relative e-h motion coordinates ρ_1 and ρ_2 of each of the excitons separated by the center-of-mass-to-center-of-mass distance $\Delta\rho$ [cf. Fig. 1 (a)]. The coupling is due to the tunneling of the system through potential barriers formed by the two single-exciton Coulomb interaction potentials (bottom) between the equivalent states represented by the isolated two-exciton wave functions shown on the top. **(c)** Binding energies (in atomic units) of the trion and biexciton complexes as functions of the interlayer distance. Biexciton binding energy is represented by the three different curves obtained analytically with no long-range interexciton interaction terms included, with only the dipolar interaction term included, and with both dipolar and quadrupolar interaction terms included, respectively. For comparison, also shown (red circles connected by dashes) is the biexciton binding energy obtained numerically with the stochastic variational method (SVM) by Meyertholen and Fogler [PRB78,235307]. **(d)** Binding energies of the trion and biexciton complexes as functions of the interlayer distance and the exciton reduced effective mass, obtained analytically in absolute units with ε = 2.5 (effective dielectric constant of the heterostructure).

I.V.Bondarev and M.R.Vladimirova, Phys. Rev. B 97, 165419 (2018)

Frenkel-CT exciton intermixing in crystalline organic semiconductor films – Motivated by the importance of the fundamental understanding of elementary excitations in crystalline organic thin films, the combined experimental and theoretical studies have been performed of the transient polarization dynamics for low-lying collective electron-hole states in α-copper phthalocyanine (CuPc). Phthalocyanines (Pc's) are organic materials with great potential both

for fundamental and for applied science. They are used in a variety of optoelectronics device applications such as low-cost organic photovoltaics, organic field-effect transistors, organic light-emitting diodes, and spinoptronic devices, to mention a few. Crystalline Metal-Pc thin film structures are typically composed of crystallites formed by the 1D periodic chains of planar molecules aligned in parallel face-to-face π-coupled stacks with the translation period much less than the shortest interstack distance. Each molecule features *two* Frenkel exciton states. The transient optical absorption is measured and the nonlinear optical response theory within the framework of the Frenkel-Charge-Transfer (Frenkel-CT) exciton intermixing model earlier developed by the PI and co-workers [I.V.Bondarev, et al., APL109,213302] is used to interpret the measurements. It is found that, initially excited in the molecular plane, the intramolecular Frenkel exciton polarization reorients with time to align along the molecular chain direction to form the Frenkel-CT coupled eigenstates of the 1D molecular crystal lattice. The process pinpoints the direction of the charge separation in crystalline CuPc. Such a charge separation mechanism is expected to occur in thin films made of the chains of face-to-face stacked organic molecules with negligible interactions between the chains. Being able to observe and monitor such processes is important for the physical understanding of the charge separation scenarios in organic thin film energy conversion devices and for the development of future organic optoelectronics applications in general. Work done in collaboration with the NC State University, USA [Figure 2; A.Popescu, R.A.Younts, B.Hoffman, T.McAfee, D.B.Dougherty, H.W.Ade, K.Gundogdu, and I.V.Bondarev, Nano Letters 17, 6056 (2017)]

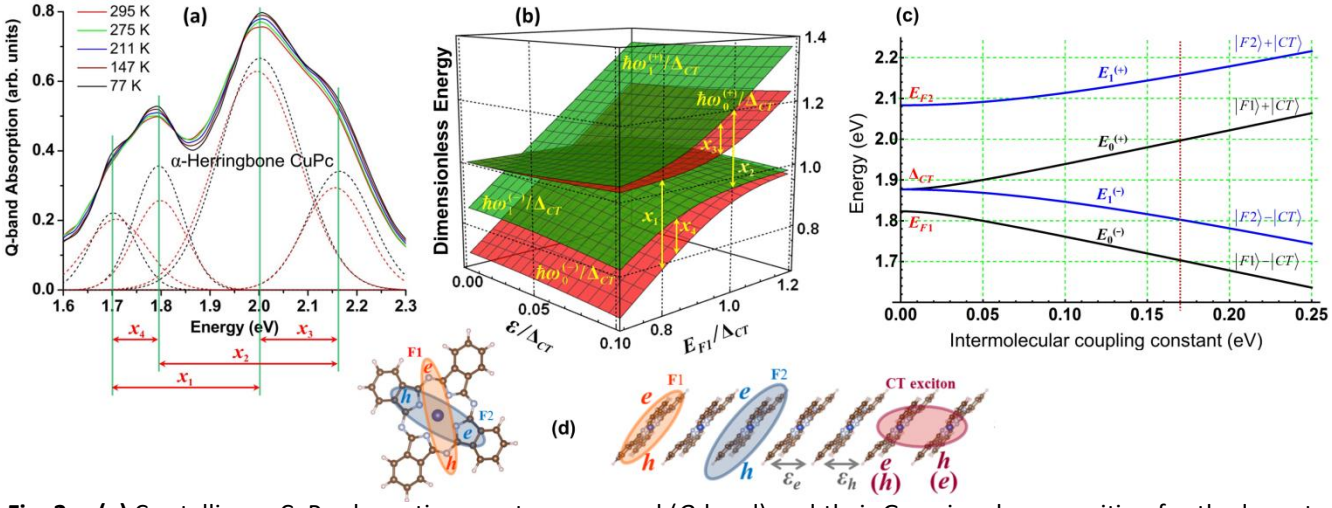

Fig. 2: **(a)** Crystalline α-CuPc absorption spectra measured (Q-band) and their Gaussian decomposition for the lowest (77 K, black dash) and highest (295 K, red dash) temperatures. **(b)** Dimensionless eigen energy level structure as given by the theory developed for the coupled Frenkel-CT exciton system [I.V.Bondarev, et al., APL109,213302]. In (a) and (b), $x_{1,2,3,4}$ are the same transition energies viewed from the absorption profile and from the theoretical eigen energy level structure of the Frenkel-CT coupled system, respectively. **(c)** Theoretical Frenkel-CT energy level splitting as a function of the intermolecular coupling constant. Vertical red dotted line shows the coupling constant obtained by comparing the theory with experiment. **(d)** Schematic of the single-molecule (F1,F2) and 1D-molecular-chain excitations studied.

A.Popescu, R.A. Younts, B.Hoffman, T.R.McAfee, D.Dougherty, H.W.Ade, K.Gundogdu, and I.V.Bondarev, Nano Lett. 17, 6056 (2017)

I.V.Bondarev, A.Popescu, R.A.Younts, B.Hoffman, T.R.McAfee, D.Dougherty, K.Gundogdu, and H.W.Ade, Appl. Phys. Lett. 109, 213302 (2016)

Exciton-plasmons in double wall carbon nanotubes – Exciton Bose-Einstein condensates (BECs), coherent many-particle states of excitons with zero translational momentum, have received considerable attention since their first theoretical prediction in the 1900's. This has been motivated by fundamental as well as practical interest. Fundamental interest comes from the aspiration to understand the physical nature of coherent collective electron-hole excitations in low-dimensional semiconductors. Practical interest is prompted by the need to develop sustainable and efficient coherent light emission sources using the photoluminescence of the

exciton Bose-Einstein condensates. We demonstrate theoretically the possibility for the exciton BEC effect in a double-walled semiconducting carbon nanotube (DWCN) system. Here the exciton condensation is enabled by the near-field coupling of the excitons residing on one tubule to the interband plasmon mode of a close excitation energy on the other coaxial tubule, to form the new type of hybridized bosonic type excitations — exciton-plasmons. The exciton-plasmon dispersion relation derived shows the intertube hybridization for the appropriately chosen DWCN combinations, with zero longitudinal momentum being the global energy minimum of the upper exciton-plasmon branch, to enable the exciton-plasmon BEC. This BEC effect will manifest itself as the highly coherent, narrow exciton emission resonance polarized along the DWCN symmetry axis (the largest polarizability direction of the system), which will be blue shifted from the exciton resonance energy by the Rabi splitting energy. The experimental observation of such a BEC effect will open up new avenues for the fundamental science and nanomaterials engineering applications with DWCNs. [I.V.Bondarev and A.Popescu, MRS Advances 2, 2401 (2017)]

Future Plans

Complexes of indirect excitons in quasi-2D van der Waals heterostructures – The main focus will be on the exciton Wigner crystallization theory development for layered quasi-2D semiconductor van der Waals heterostructures. Significant binding energies we predict for the trion complexes formed by indirect excitons are in excellent agreement with the experiments done at Harvard on planar semiconductor heterostructures obtained by stacking together two transition-metal dichalcogenide (TMD) monolayers with *h*-BN monolayers placed in-between to control the TMD interlayer distance (talk # E37.00013 presented at the APS March meeting in Los Angeles, CA on March 6, 2018). This suggests that the strongly correlated multiexciton phenomenon of the Wigner crystallization can be realized with the indirect excitons in layered van der Waals heterostructures such as gapped bilayer graphene and few-layer TMD systems. We will work to develop the conceptual understanding of how, under which conditions, such strongly correlated multiexciton Wigner structures can form and how stable they can possibly be. This is important for the development of nonlinear optics and spinoptronics applications with the new generation of advanced quantum materials of reduced dimensionality.

Publications

(2016-18)

I.V.Bondarev, H.Mousavi, and V.M.Shalaev, Optical response of finite-thickness ultrathin plasmonic films, MRS Communications 2018, *at press* (arXiv1806.00654, 2 Jun 2018)

I.V.Bondarev and M.R.Vladimirova, Complexes of dipolar excitons in layered quasi-two-dimensional nanostructures, Physical Review B **97**, 165419 (2018)

A.Popescu, R.A.Younts, B.Hoffman, T.R.McAfee, D.Dougherty, H.W.Ade, K.Gundogdu, and I.V.Bondarev, Monitoring charge separation processes in quasi-one-dimensional organic crystalline structures, Nano Letters **17**, 6056 (2017)

I.V.Bondarev and A.Popescu, Exciton Bose-Einstein condensation in double-walled carbon nanotubes, MRS Advances **2**, 2401 (2017)

I.V.Bondarev, A.Popescu, R.A.Younts, B.Hoffman, T.R.McAfee, D.Dougherty, K.Gundogdu, and H.W.Ade, Lowest energy Frenkel and charge transfer exciton intermixing in one-dimensional copper phthalocyanine molecular lattice, Applied Physics Letters **109**, 213302 (2016)

I.V.Bondarev, Configuration space method for calculating binding energies of exciton complexes in quasi-1D/2D semiconductors, Modern Physics Letters B **30**, 1630006 (2016)

M.F.Gelin and I.V.Bondarev, One-dimensional transport in hybrid metal-semiconductor nanotube systems, Physical Review B **93**, 115422 (2016)

Development of finite-temperature density functional theory

Principal Investigator: Professor Kieron Burke
Department of Chemistry and of Physics, University of California, Irvine, CA 92697
kieron@uci.edu

Keywords: Density functional theory, electronic structure, warm dense matter, exact conditions, excitations

Project Scope

Warm dense matter is a rapidly evolving field with applications in controlled fusion, planetary interiors, and other areas of high energy density physics. Over the past decade or so, molecular dynamics calculations driven by modern density functional theory have played a crucial role in bringing chemical realism to these applications, often (but not always) with excellent agreement with experiment.

Density functional theory (DFT) has become the most popular approach to electronic structure across disciplines, especially in material and chemical sciences. Last year, at least 30,000 papers used DFT to make useful predictions or give insight into an enormous diversity of scientific problems, ranging from battery development to solar cell efficiency and far beyond. The success of this field has been driven by usefully accurate approximations based on known exact conditions and careful testing and validation.

The aim of this project is to further develop both the formal and the practical tools of DFT to warm-dense matter conditions. This includes developing several new approaches for creating approximations, performing benchmark calculations to examine the importance of thermal corrections to ground-state approximations, and going beyond equilibrium conditions to understand the accuracy of present methods for extracting conductivities and other response properties.

Recent Progress

Understanding accuracy of the zero-temperature approximation:

At present, most WDM calculations use the zero-temperature approximation (ZTA), i.e., using a ground-state XC approximation in the finite-temperature KS equations, finding good to excellent agreement with experiment. We realized this is because ZTA is relatively accurate in both the low- and high-temperature limits, because at high temperatures, XC effects become relatively irrelevant. This feature is crucial, because the MKS orbitals, upon which calculations of conductivity sensitively depend, also become accurate in this limit. This feature is illustrated on a simple asymmetric Hubbard dimer, which can be solved exactly, and so is perfect for such illustrations.

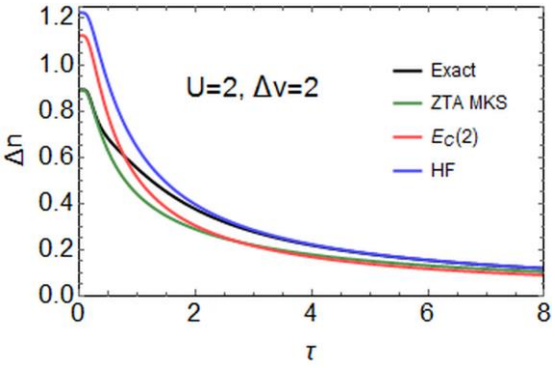

Difference in onsite densities as a function of temperature for an asymmetric Hubbard dimer with U = 2 and site-potential difference 2 (in units where the hopping parameter t = 1/2). The approximate calculations are all MKS-DFT equilibrium calculations where HF denotes Hartree-Fock, $E^{(2)}$ is a zero-temperature approximation (ZTA) including the high-density limit of correlation, and ZTA denotes using the exact ground-state XC.

Thermal stitching: Extending the reach of quantum fermion solvers:

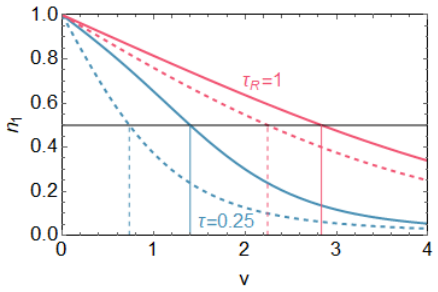

FIG. 1. n_1 vs. x at $\tau = 0.25$ (blue) and $\tau = 1$ (red). Solid lines are $U = 1$ and dashed are non-interacting, $U = 0$. The intersections with the horizontal line at $n_1 = 0.5$ give the v values that yield $n_1 = 0.5$ for the given temperature and interaction.

For quantum fermion problems, many accurate solvers are limited by the temperature regime in which they can be usefully applied. The Mermin theorem implies the uniqueness of an effective potential from which both the exact density and free energy at a target temperature can be found, via a calculation at a different, reference temperature. We derive exact expressions for both the potential and the free energy in such a calculation, and introduce three controllable approximations that reduce the cost of such calculations. We illustrate the effective potential and its free energy, and test the approximations, on the asymmetric two-site Hubbard model at finite temperature. The figure shows the exact thermal stitching potential, where a change in the potential in a hot calculation tricks the systems into producing the density at a cooler temperature [2].

Excitations from a new ensemble in DFT:

There are many known limitations to approximate TDDFT mathods (which was recently proven to apply to finite temperature DFT in the linear response regime), but TDDFT is a work-horse tool for WDM calculations, including both electrical and thermal conductivity and stopping power, for example. A particularly vexing case is that of double excitations, which are lost in the standard adiabatic approximations of TDDFT. In recent work [1], we developed a previously-unused ensemble method to directly correct KS transitions into the true excitations of a system. For single excitations, it is competive with standard TDDFT for accuracy, but it also produces double excitations. The cartoon shows the doubles for a Be atom. We followed this up with a thorough investigation using (what else) the Hubbard dimer[3].

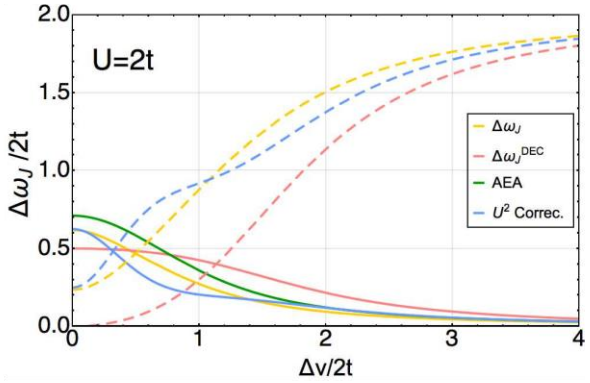

FIG. 2. Correction to the KS transitions of Fig. 1, both exact and various approximations, where solid lines are single excitations, dashed are double. The correction to the single turns off with increasing asymmetry, but not so the double excitation. The DEC/EEXX approximation correctly captures both effects. Also included is the leading correlation contribution, which further improves the results, when the system is weakly correlated.

Future Plans

The blue electron – We have found a very simple approach to calculate approximately (but rather accurately) the XC energy of a uniform gas via self-consistent calculations of an inhomogeneous gas, using the Ornstein-Zernicke trick from classical DFT (where it is an exact relation). This work is currently in progress.

Exploration of temperature scales – using the one-dimensional mimic of the three-dimensional world developed in collaboration with Steve White, we will illustrate the physical important temperature scales of MKS thermal DFT calculations, showing in particular that the ZTA becomes accurate at much lower temperature scales than those at which semiclassical treatments (Thomas-Fermi and beyond) apply.

Publications (all available at dft.uci.edu):

1. Direct extraction of excitation energies from ensemble density-functional theory Zeng-hui Yang, Aurora Pribram-Jones, Kieron Burke, Carsten A. Ullrich, Phys. Rev. Lett. **119**, 033003 (2017).
2. Thermal stitching: Extending the reach of quantum fermion solvers Justin C. Smith, Kieron Burke, Submitted arXiv:1801.01927 (2018).
3. Can ensemble density functional theory yield accurate double excitations? Francisca Sagredo, Kieron Burke, (Submitted, arXiv:1806.03392) (2018).

Controlling topological zero modes

Principal Investigator: Claudio Chamon
Department of Physics, Boston University
chamon@bu.edu

Project scope:

Quantum materials, those whose properties rely on intrinsically quantum mechanical effects such as interference or entanglement, hold the promise to serve as the building blocks for novel technologies for computing and energy applications. Topological materials, in particular, may provide ways to realize fault tolerant platforms for quantum computation and quantum information processing.

The goal of our research effort is to find a clean and direct demonstration of non-Abelian Berry phases from braiding topological zero modes. To this end, we study novel ways to control the position of topological zero modes that host excitations that accumulate non-Abelian Berry phases as they are exchanged or braided. The research effort includes the study of not only electronic systems, but also photonic systems, in which there is much control of the properties of specially-designed artificial structures. The expertise gained in these studies is currently being directed at systems whose zero modes host Majoranas, which can potentially serve as halfs of topological qubits.

Recent progress:

• *Non-Abelian braiding of light*

Many topological phenomena first proposed and observed in the context of electrons in solids have recently found counterparts in photonic and acoustic systems. In Publication #5 we presented non-Abelian Berry phases that can accumulate when coherent states of light are injected into "topological guided modes" in specially-fabricated photonic waveguide arrays. These modes are photonic analogues of topological zero modes in electronic systems. Light traveling inside spatially well-separated topological guided modes can be braided, leading to the accumulation of non-Abelian phases, which depend on the order that the guided beams are wound around each other. Notably, these effects survive the macroscopic photon occupation limit, and can be understood as wave phenomena and thus predicted directly from Maxwell's equations without resorting to quantization of light. We proposed an optical interference experiment to probe this non-Abelian braiding of light directly, and more recently we carried out detailed calculations in collaborations with Mik Rechtsman to design of a photonic crystal and interferometric scheme to be tested by his group at Penn State.

The zero modes we propose to realize are photonic analogues of Kekulé zero modes in graphene, which are bound to vortices in the complex order parameter $\Delta(r)$ describing a dimerization pattern in the hexagonal lattice (Fig. 1). The translation between electrons and photons is achieved by replacing the sites of the lattice with waveguides embedded in a bulk optical medium (e.g. fused silica), which are extended in the z direction and whose x-y positions mimic the 2D positions of the carbon atoms in the distorted graphene lattice. The wave equation for the paraxial propagation of light in such a waveguide array maps directly onto the time-dependent Schrödinger equation (SE), where the time coordinate t in the SE is replaced by the coordinate z along the direction of light propagation. This wave equation can be further mapped, using coupled mode theory, to a linear differential equation that is in one-to-one correspondence with the non-interacting tight-binding model of the electronic system. The waveguides themselves can therefore be thought of

as the world lines of the carbon atoms, with straight waveguides corresponding to a lattice that is static in time.

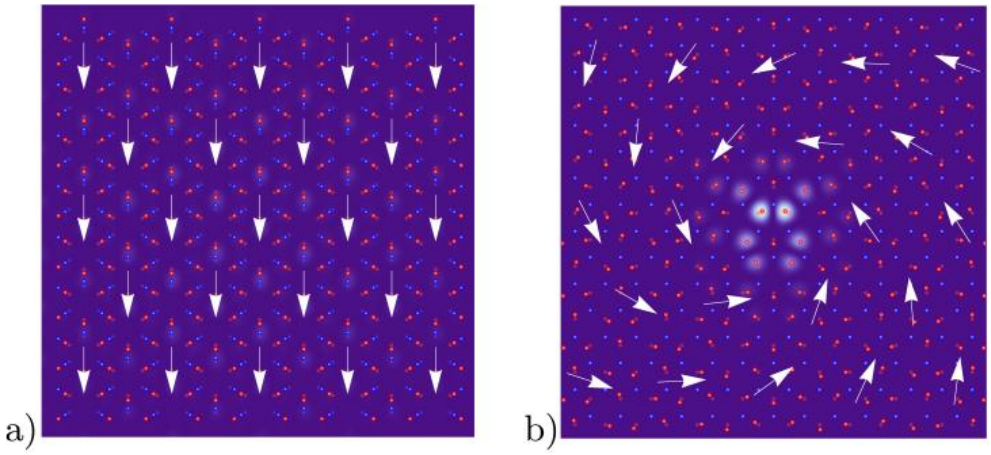

Figure 1: Topological guided modes in photonic crystals. Left: (a) Uniform Kekulé distortion in a hexagonal waveguide lattice at a slice of constant z. Sublattice A is colored red, while sublattice B is colored blue. The overlaid vector field represents the magnitude and direction of the order parameter $\Delta(r)$. The intensity pattern represents the amplitude of the electric field in each waveguide. (b) Waveguide lattice in the presence of a vortex in the Kekulé pattern, with an overlaid order-parameter vector field showing circulation around the vortex core. The background is an intensity plot of the localized zero-mode wavefunction.

The zero-mode solution is tightly localized near the core (size of order $1/\Delta$) of the vortex associated to a pattern of small displacements of the waveguides (see Fig. 1b). This means that light propagating in the zero mode travels as if confined to an "optical fiber" located at the vortex core, albeit with evanescent decay into neighboring waveguides in the same sublattice. However, the zero mode differs crucially from a mode in an optical fiber, both because it takes the distortion of an entire waveguide lattice to create, and because it depends on the topological nature of this distortion. These "topological guided modes" are responsible for the non-Abelian effects.

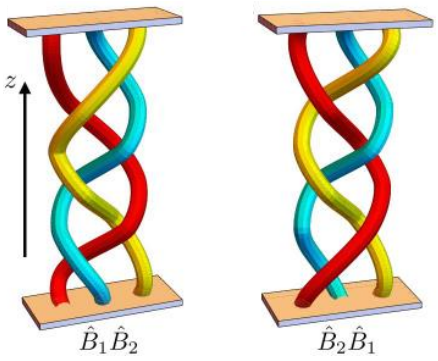

Figure 2: Depiction of the braids B_1B_2 and B_2B_1 used in the proposed experiment. The strands being braided represent the positions $R_i(z)$ of the three vortex cores, into which coherent light is injected. The order of the strands coincides on the input and output facets at the bottom and top, respectively.

Planned activities:

The planned effort for the future funding period will primarily concentrate on studying platforms that allow for moving Majorana zero modes, instead of photonic topological guided modes.

While the physical setting is quite different, the mathematical model is identical. In fact, the photonic systems inspire a simple way that allows one to move Majorana modes anywhere in two-dimensions, an ability that is lacking in present schemes.

We plan to study an architecture for building "logical" Majorana zero modes using "physical" Majorana zero modes at the Y-junctions of a hexagonal network of semiconducting quantum wires. These wires are deliberately chosen to be sufficiently short that the hybridization between the physical Majorana zero modes localized at their endpoints would give rise to hybridization (hopping). These hopping amplitudes can be controlled externally by, for instance, applied gate voltages. Selecting hopping amplitudes associated to a Kekulé vortex pattern should yield an emergent Majorana zero mode bound to the vortex core, whose position could be moved adiabatically by programming the values of the hopping amplitudes to change as functions of time. These Majorana zero modes are the "logical" Majorana zero modes emerging from an architecture that should enable braiding without ever selectively moving "physical" Majorana zero modes.

Carrying out the above studies in full detail constitute the initial part of the work plan.

Publications: DOE support, explicitly referred to as "DOE Grant DEFG02-06ER46316", is acknowledged in every publication listed below.

1. "Fractional (Chern and topological) insulators"
   T. Neupert, C. Chamon, T. Iadecola, L. H. Santos, and C. Mudry,
   Proceedings of the Nobel symposium on "New forms of matter: topological insulators and superconductors", Physica Scripta 2015, 014005 (2015)

2. "Two-component structure in the entanglement spectrum of highly excited states"
   Z.-C. Yang, C. Chamon, A. Hamma, and E. R. Mucciolo,
   Phys. Rev. Lett. 115, 267206 (2015)

3. "Non-Abelian topological spin liquids from arrays of quantum wires or spin chains"
   P.-H. Huang, J.-H. Chen, P. R. S. Gomes, T. Neupert, C. Chamon, and C. Mudry,
   Phys. Rev. B 93, 205123 (2016)

4. "Wire constructions of Abelian topological phases in three or more dimensions "
   T. Iadecola, T. Neupert, C. Chamon, and C. Mudry,
   Phys. Rev. B 93, 195136 (2016)

5. "Non-Abelian braiding of light "
   T. Iadecola, T. Schuster, and C. Chamon,
   Phys. Rev. Lett. 117, 073901 (2016)

6. "Dissipationless conduc- tance in a topological coaxial cable "
   T. Schuster, T. Iadecola, C. Chamon, R. Jackiw, and S.-Y. Pi,
   Phys. Rev. B 94, 115110 (2016)

7. "Electrons at the monkey saddle: A multi- critical lifshitz point "
   A. Shtyk, G. Goldstein, and C. Chamon,
   Phys. Rev. B 95, 035137 (2017)
8. "Coupled spin-1/2 ladders as microscopic models for non-Abelian chiral spin liquids "
   P.-H. Huang, J.-H. Chen, A. E. Feiguin, C. Chamon, and C. Mudry,
   Phys. Rev. B 95, 144413 (2017)

9. "Optimizing varia- tional quantum algorithms using Pontryagin's minimum principle "
   Z.-C. Yang, A. Rahmani, A. Shabani, H. Neven, and C. Chamon,
   Phys. Rev. X 7, 021027 (2017)

10. "d-wave superconductivity in boson+fermion dimer models "

G. Goldstein, C. Chamon, and C. Castelnovo,
Phys. Rev. B 95, 174511 (2017)

11. “Entanglement complexity in quantum many-body dynamics, thermalization, and localization “
Z.-C. Yang, A. Hamma, S. M. Giampaolo, E. R. Mucciolo, and C. Chamon,
Phys. Rev. B 96, 020408 (2017)

12. “Model of chiral spin liquids with Abelian and non-Abelian topological phases “
J.-H. Chen, C. Mudry, C. Chamon, and A. M. Tsvelik,
Phys. Rev. B 96, 224420 (2017)

13. “Dynamic scaling of topological ordering in classical systems “
N. Xu, C. Castelnovo, R. G. Melko, C. Chamon, and A. W. Sandvik,
Phys. Rev. B 97, 024432 (2018)

14. “Tensor network method for reversible classical computation “
Z.-C. Yang, S. Kourtis, C. Chamon, E. R. Mucciolo, and A. E. Ruckenstein,
Phys. Rev. E 97, 033303 (2018)

Methods for Correlated Electronic Materials

Principal Investigator: Garnet Kin-Lic Chan
Division of Chemistry and Chemical Engineering, California Institute of Technology, Pasadena CA 91125

Keywords: density matrix embedding, dynamical mean-field theory, coupled cluster theory, materials spectroscopy, correlated electrons, electronic structure

Project Scope

This project is concerned with the development of new ab initio methods for correlated electronic structure calculations in solids. The work is divided into two main areas: the first focuses on embedding methods, including density matrix embedding theory (DMET) and dynamical mean-field theory (DMFT); the second focuses on diagrammatic methods beyond the GW and GW/BSE approximations to compute materials properties to high precision, using the coupled cluster hierarchy. An important component in both pieces of work is the development of publicly available, open-source software, with production ready implementations of correlated electronic structure methods.

Recent progress

Embedding approaches: applications We have carried out two significant applications of the DMET methodology in the last two years. The first is a detailed application to the 2D Hubbard model in the underdoped region. Here, in collaboration with White, Zhang, Noack, and Corboz, we used DMET to provide a definitive resolution of the ground-state order in the region of the phase diagram where there are many competing phases. We found that the order in this region is a striped phase (as opposed to other charge ordered phases, or superconducting order). The stripes are also very compressible, with near degeneracy between half-filled stripes (found in earlier less converged studies) and fully-filled stripes; fluctuations along this coordinate were also associated with the appearance of pairing order, providing an intriguing hint into the possible channels that generate superconductivity. From a methodological perspective, this study provided a key validation of the accuracy of DMET, with both the energetics and order parameters from larger DMET cluster calculations showing agreement within error bars with the best available estimates from other methods such as DMRG, iPEPS, and CP-AFQMC [1] (Fig. 1).

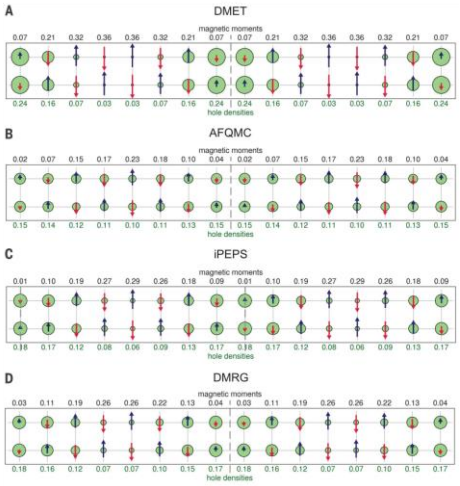

Figure 1 Charge and spin orders from DMET and other methods.

Another important recent application of DMET has been to ab initio calculations. While ab initio DMET was developed in the original works [2, 3], we had not so far applied it much in this setting (although other groups have done so). However, together with other scientists in the Simons Collaboration, we carried out detailed DMET studies on the equation of state of the hydrogen chain [4]. Here, we showed that in smaller basis sets DMET, together with a DMRG solver, provides an accurate estimate for the thermodynamic limit of the equation of state that is only rivaled by TDL extrapolated DMRG data (Fig. 2). In larger basis sets, the DMRG solver in DMET becomes inefficient. Thus, developing improved solvers for ab initio DMET applications has been a recent focus in our work.

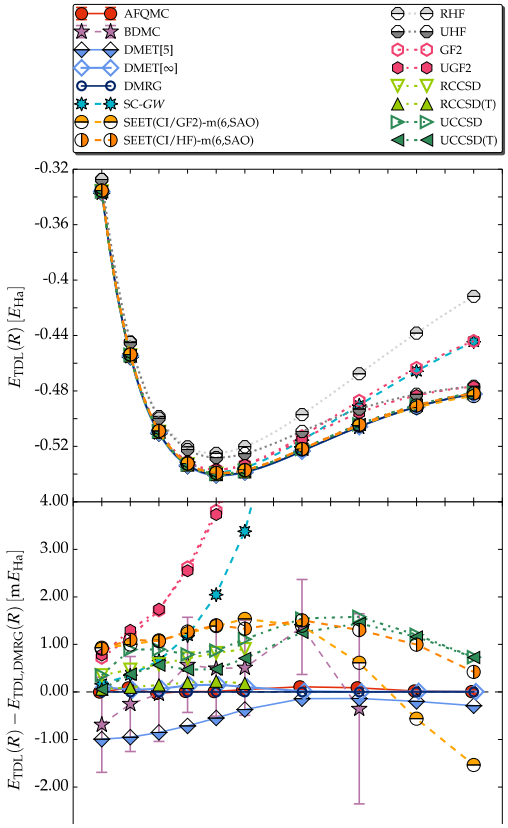

Figure 2 DMET equation of state for hydrogen in the TDL. Note that the DMET (∞) result is almost invisible as the error (relative to DMRG) is almost vanishing.

Embedding approaches: methods We have completed several methodological extensions of DMET, including extensions to finite temperature and to real-time dynamics. In finite temperature DMET, we use an analogy with Krylov space methods for matrix diagonalization to define an extended bath. Combining this with a finite-temperature DMRG solver, we have computed finite temperature paramagnetic phase diagrams for the 1D and 2D Hubbard models exploring the (finite-cluster) metal-insulator phase boundary.

In the extension to real time dynamics, we showed that a very simple formulation of real-time DMET could already yield near exact dynamics for an Anderson impurity problem out of equilibrium; in particular, the embedding approach significantly reduces the finite size effects in the problem, allowing for a more faithful representation of the Kondo peak [5]. The single-impurity real-time DMET is very similar to the time-dependent complete active space self-consistent field method (td-CASSCF) used in chemical physics, and we have recently been exploring the td-CASSCF method for condensed phase dynamical problems. In recent work [6], we used time-dependent CASSCF methods to study atomic scattering off surfaces to explore what happens to the atomic spin in the electronic process. Interestingly, a slow time-scale emerges, related to the exchange energy of the problem, and which can be used to probe the nature of correlations in the atom and the surface in atomic scattering spectroscopies.

Other current work has focused on improving the impurity solver in both DMET and DMFT, and improving the ab initio embedding framework for solids. Some ongoing

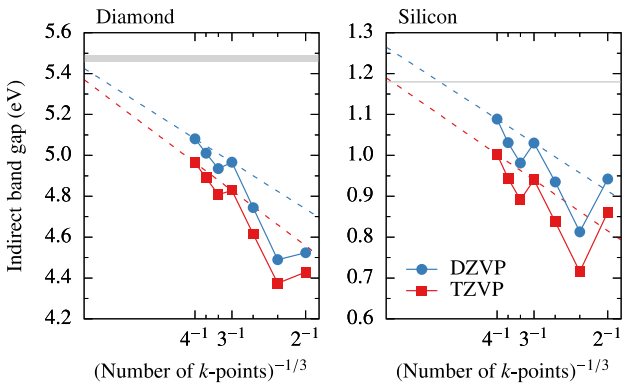

Figure 3 Coupled cluster bandgaps for diamond and silicon demonstrating convergence to the experimental result.

projects include exploring selected configuration interaction solvers; improvements of DMRG to incorporate configuration interaction ideas; and high-order coupled cluster methods. The first project is in collaboration with Cyrus Umrigar. We note also that we have worked to extend the capabilities of the PySCF package for embedding calculations, and the ab initio infrastructure we have developed can be used both for DMET as well as DMFT calculations.

Coupled cluster methods in the condensed phase. We have been building out a full set of coupled cluster (CC) capabilities for calculations in the condensed phase. Our initial work demonstrated that the coupled cluster singles and doubles method gives band structures for simple semiconductors that appear more accurate than those obtained from GW (of course at higher cost) [7] (Fig. 3). The strength of the CC approach, however, lies in its systematic improvability, which avoids the need to make educated guesses about the importance of difference vertex corrections in approaches beyond GW. Since this original study, we have developed the coupled cluster capabilities to treat magnetic systems (unrestricted and general spin-orbital coupled cluster) as well as to compute Green's functions. We have further developed new coupled cluster triples expressions that allow us to capture the remaining correlation error in the band structure, to within an accuracy of a few tenths of an eV. We are currently applying these methods to compute benchmark photoelectron spectra of two-dimensional materials.

In recent theoretical work, we have also developed the finite-temperature extension of coupled cluster theory, by formulating the theory in the time-domain [8]. We have used this work to calculate correlated thermodynamic properties of the finite-temperature uniform electron gas (Fig. 4), and are currently applying our ab initio code

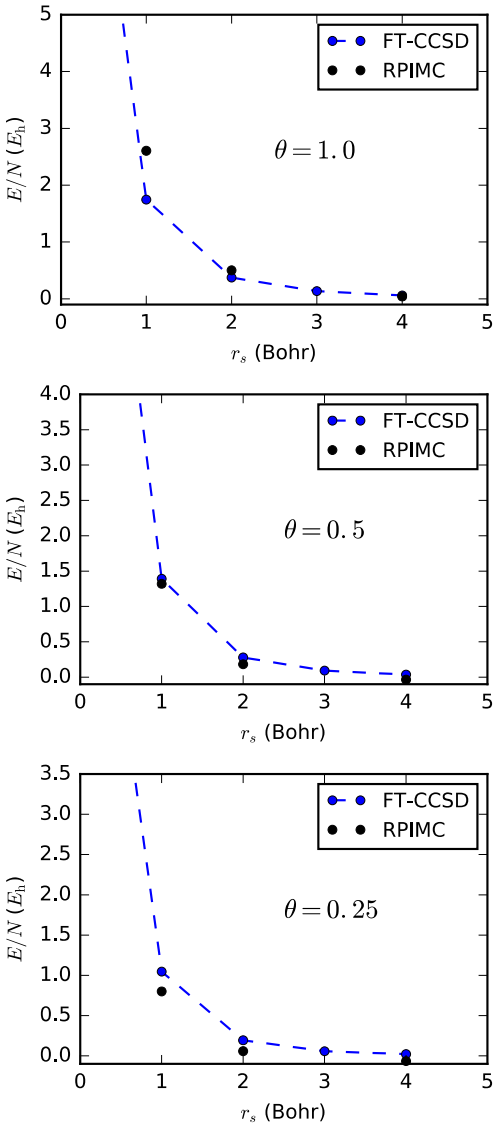

Figure 4 Finite temperature UEG energies from CC and PIQMC; good agreement is seen.

to compute properties of finite-temperature materials. Further, the methods that we have used can be similarly extended onto the Keldysh contour, which then allows for coupled cluster treatments of fully non-equilibrium processes and spectroscopy. Finally, we have also explored the use of coupled cluster theory to study electron-phonon coupling, via the coupled cluster Green's function. These calculations, done in collaboration with Marco Bernardi, provide a first glimpse of the electron-phonon vertex beyond the level of GW theory in real materials, and form a step towards ab initio calculations of superconductivity using diagrammatic methods in moderately correlated materials.

The Python based Simulations of Chemistry Framework All our methodological work is made available via the PySCF program package [9]. This is a feature complete program which has now been widely adopted by research groups in academia and industry; there are over 100 groups currently using or developing methods with the code, making it one of the major electronic structure codes that is primarily developed in the US. In the last year, much effort has been made to make the periodic boundary code in PySCF highly performant as many other research groups (e.g. the QMCPack collaboration) rely on its capabilities. MPI parallelization has recently been added for many of the methods, and in the next year some of the technical improvements we will be focusing on include local correlation methods (e.g. local coupled cluster) as well as reduced scaling implementations of Hartree-Fock exchange in materials.

1. Zheng, Bo-Xiao, et al. "Stripe order in the underdoped region of the two-dimensional Hubbard model." *Science* 358.6367 (2017): 1155-1160.
2. Knizia, Gerald, and Garnet Kin-Lic Chan. "Density matrix embedding: A strong-coupling quantum embedding theory." *Journal of chemical theory and computation* 9.3 (2013): 1428-1432.
3. Wouters, Sebastian, et al. "A practical guide to density matrix embedding theory in quantum chemistry." *Journal of chemical theory and computation* 12.6 (2016): 2706-2719.
4. Motta, Mario, et al. "Towards the solution of the many-electron problem in real materials: equation of state of the hydrogen chain with state-of-the-art many-body methods." *Physical Review X* 7.3 (2017): 031059.
5. Kretchmer, Joshua S., and Garnet Kin-Lic Chan. "A real-time extension of density matrix embedding theory for non-equilibrium electron dynamics." *The Journal of chemical physics* 148.5 (2018): 054108.
6. Kretchmer, Joshua S., and Garnet Kin-Lic Chan. "The fate of atomic spin in atomic scattering off surfaces." *The journal of physical chemistry letters* 9 (2018): 2863-2868.
7. McClain, James, et al. "Gaussian-based coupled-cluster theory for the ground-state and band structure of solids." *Journal of chemical theory and computation* 13.3 (2017): 1209-1218.
8. White, Alec F., and Garnet Chan. "A time-dependent formulation of coupled cluster theory for many-fermion systems at finite temperature." *arXiv preprint arXiv:1807.09961* (2018).
9. Sun, Qiming, et al. "PySCF: the Python-based simulations of chemistry framework." *Wiley Interdisciplinary Reviews: Computational Molecular Science* 8.1 (2018): e1340.

Computational theory applied to nanostructures

James R. Chelikowsky
Center for Computational Materials, Institute of Computational Engineering and Sciences, Departments of Physics and Chemical Engineering, University of Texas at Austin, Austin, TX 78712

Keywords: Computational methods, nanostructures, structural imagining, superconducting and ferromagnetic materials.

Project Scope

This program implements methods for computing and predicting the electronic and structural properties of nano materials. Within the nanoscale size regime, new phenomena can occur that is peculiar to this length scale. At small length scales, quantum confinement can result in altering the properties of a material such that the property of interest resembles neither that of the atomic limit, nor the macroscopic limit. For example, the optical gap of a silicon nanocrystal can become size dependent and tunable. Through size changes alone, silicon can be turned into an optically active material. Such modifications with size can have a direct consequence for understanding and characterizing materials used in electronic, optical, and micro-mechanical applications related to energy sciences and technologies. To capitalize properly on predicting and understanding such phenomena in this nano regime, a deeper understanding of the quantum properties of materials will be required. The work in this project over the past two years has focused on: (1) Orientational dependence of work functions for faceted nanoscale metal clusters. (2) Probe microscopy, centering on atomic force microscopy to understand tip functionalization. (3) Novel properties of recently discovered form of disordered carbon, which purportedly exhibit superhardness, ferromagnetism and high temperature superconductivity.

Recent Progress

*Orientational dependence of work functions for faceted nanoscale metal clusters***.** Work function values measured at different surfaces of a metal are usually different. This raises an interesting question: What is the work function of a nano-size crystal, where differently oriented facets can be adjacent?

Work functions of metallic nanocrystals are also of significant practical interest. The property of accepting or donating electrons is crucial in producing efficient catalysts and is directly related to the electron affinity and work function of a nanoparticle. Since a catalyst needs to be in close contact with the reactants, the *local work function*, which is measured close to the nanocrystal surface, is a controlling property. When molecules are adsorbed on a metal surface or a monolayer is added to it, the formed dipole can modify the work function of the metal. Especially in the case of nanostructured organic/inorganic interfaces, the energy alignment between the molecules and the metal is influenced by the local work function.

The local work function, however, cannot be fully identified with the macroscopic work function measured in photoemission: the variation of the local work function depends more on the electrostatic potential map around the nanocrystal. The difference is

particularly substantial for "real," inhomogeneous interfaces. Also, the local work function is very sensitive to the local chemical environment, e.g., in gold nanoparticles, it is known to be influenced by the surface chemistry of the Si substrate.

Using real space pseudopotentials constructed within density functional theory, the local work function of aluminum and gold nanocrystals, including systems containing over 350 atoms was computed [1]. The real space code used in the computations is ideally suited for such problems as the code was developed to handle confined systems.

The local work function follows the change of the surface plane orientation around multifaceted nanocrystals, and importance of the orbital character near the Fermi level in determining work function differences between facets was confirmed.

Calculations were carried out for two aluminum nanocrystals, which contain the (001), (110), and (111) facets. The electrostatic potential relative to the Fermi level near the (001) facet is about 4.2 eV, 100 meV higher than that of the (111) and (110) facets; at about 1 nm from the nanocrystal, the potential is converged for all facets. These values agree well with work function values from slab calculations and indicate that the local work function of the (001) facet is higher than that of other two facets. The potential anisotropy is also observed in gold nanocrystals, though not as pronounced as in the case of aluminum.

Simulating Atomic Probe Microscopy. Non-contact atomic force microscopy (nc-AFM) with a CO-functionalized tip yields high resolution images of polycyclic aromatic hydrocarbons under many situations. However, the mechanism for producing these enhanced resolution images is not well understood. In order to better understand this mechanism, real-space pseudopotentials constructed using density functional theory were used to simulate nc-AFM images of benzene and dibenzonapthoperylene (DBNP) molecules with selected probe tips, including CO, H_2, N_2, Br and CH_2O. The selected tips provide accurate simulated images, save for the tip functionalized with a Br atom. Contrast inversion was observed with CO and N_2 tips at small tip heights and image distortion with CH_2O tip. Observed distortions in experimental data were attributed to the presence of impurity atoms on the tip probe. This work was featured on the cover of JVSTB (see figure on right.)

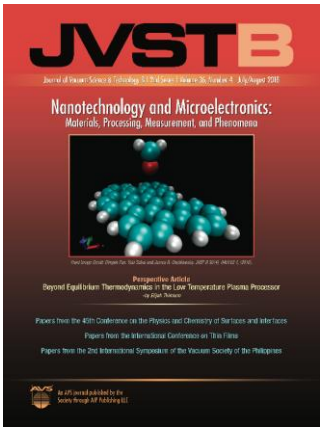

Cover of JVSTB showing a schematic AFM geometry [2].

Disordered Carbon. Experimentalists have claimed that a new form of carbon is a high temperature superconductor, a superhard material and a ferromagnetic material [3]. Can theoretical studies help in exploring these claims, suggesting the underlying mechanisms, and proposing new materials?

Many doped carbon materials are known to be superconductors with relatively low values for T_c. For example, graphite intercalation compounds exhibit superconductivity with alkali- and alkaline-earth metal intercalants with a superconducting transition temperature T_c, up to 11.5 K in the case of CaC_6 under ambient pressure. Alkali-doped fullerene (C_{60}) solids also exhibit superconductivity, e.g., T_c is 33 K in the case of $Cs_xRb_yC_{60}$. In addition to these sp^2 -hybridized carbon materials, boron-doped sp^3 -hybridized diamond is also known to be a superconductor. The highest

T_c experimentally for this material is 11.4 K, although the theoretically predicted highest T_c is approximately 55-80 K.

One obstacle in the realization of a high T_c is the limited amount of boron that can be doped in diamond. Recently, a T_c of 36 K was reported when boron atoms were doped into a new amorphous form of carbon: "Q-carbon" made by quenching supercooled amorphous carbon [3]. The amount of boron doping reported was approximately 17%. The T_c of this boron-doped Q-carbon is comparable to that of MgB_2 (39 K). However, the structural and electronic properties of boron-doped Q-carbon remain largely unknown in spite of its remarkable T_c. Undoped Q-carbon is also measured to be ferromagnetic and superhard.

The effect of boron doping into amorphous carbon was investigated in an attempt to understand Q-carbon and related materials. The structure of Q-carbon was simulated by quenching a random arrangement of carbon atoms for a given density.

Carbon atoms of our simulated amorphous carbon system were replaced by dopant boron atoms one by one. Acceptor states were found to be either shallow or deep depending on the surrounding geometries. Shallow acceptor states, which are important for achieving superconductivity in boron-doped diamond, can be realized when placed in properly chosen substitutional sites. The electron-phonon coupling in boron-doped amorphous carbon was also computed. B shallow acceptor states were found to induce superconductivity as in boron-doped diamond. A T_c of 37 K was calculated at 14 at.% boron with a resulting electron-phonon coupling constant l= 1.1. Even when one completely neglects the electron-phonon coupling of low-frequency vibrational modes, which is often an artifact of a computational simulation, the T_c is 26 K in the 12.5% doping case.

The highest computed T_c of 37 K in the 14% boron doped case achieved is comparable to that observed in boron-doped Q-carbon. Shallow acceptor states were found when doped boron atoms are fourfold-coordinated even when boron dimers are formed. On the other hand, threefold boron atoms are generally not favored since they create deep acceptor states, but interestingly they can increase T_c through an increase in w_{log} in a relatively high doping case.

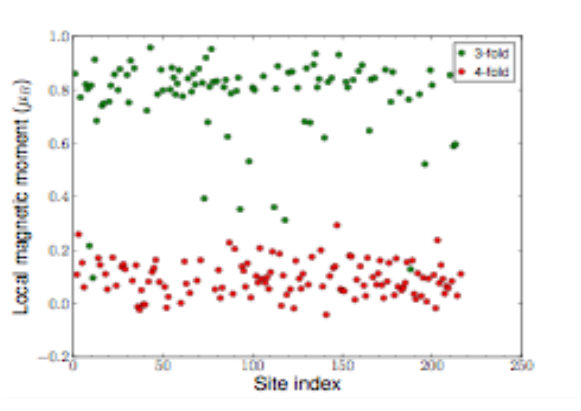

Distribution of local magnetic moments at 216 carbon atomic sites in amorphous carbon (0.4 μ_B/atom and 3.4g/cm^3). Green circles and red circles represent 3-fold and 4-fold coordinated carbon atoms, respectively.

The maximum T_c could be 26 K provided the contribution from low-frequency modes are not included, but it is still sizable.

The present theoretical verification of high T_c in such a covalent light-element amorphous material produced under extreme high temperature and rapid quenching imply that a material under an extreme condition could be a promising superconductor as seen in the recently reported hydrogen sulfide under high pressure.

Ferromagnetism was also investigated in amorphous carbon. Using spin constrained first-principles simulations, amorphous carbon structures can be constructed with the desired

magnetization. The existence of sp^2-like threefold coordinated carbon atoms plays an important role in causing magnetism in amorphous carbon. Detailed geometries of threefold carbon atoms were found to induce the magnetic order in amorphous carbon [5]. In the figure (left), the local magnetic moments are presented for simulated amorphous carbon. The moments for the three-fold sites dominate the magnetic contributions. Whether this is sufficient to explain the experimental observations is problematic.

Future Plans

Work in this project will center on the following three themes: (1) Constructing a practical approach for probe microscopy of nanoscale systems in order to obtain structural information from atomic force microscopy, which can be quantified and correctly interpreted. One objective will be to retain the quantum nature of the probe and sample, while obviating the need for extensive computation. (2) Developing computational methods for predicting the Raman spectra of nanostructures, including complex nanostructures with defects. (3) Predicting the response of complex molecular species, photovoltaic materials and two dimensional materials such as graphene and MoS_2 to external electric or magnetic fields. (4) Continuing the study of doped disordered carbon to estimate a limit for the superconducting transition temperature and to understand magnetic behavior in intrinsic disordered carbon.

References:

1. L. Gao, J. Souto-Casares, J.R. Chelikowsky and A.A. Demkov, "Orientation dependence of the work function: metal nanocrystals," J. Chem. Phys. **147**, 214301 (2017).
2. D. Fan, Y. Sakai and J.R. Chelikowsky, "Real-space pseudopotential calculations for simulating non-contact atomic force microscopy images," J. Vac. Sci. Technol. B **36**, 04H102 (2018).
3. A. Bhaumik, R. Sachan and J. Narayan, "High temperature superconductivity in boron doped Q-carbon," ACS Nano 11, 5351 (2017).
4. Y. Sakai, J.R. Chelikowsky, and M.L. Cohen, "Simulating the effect of boron doping in superconducting carbon," Phys. Rev. B **97**, 054501 (2018).
5. Y. Sakai, J.R. Chelikowsky and M.L. Cohen, "Magnetism in amorphous carbon: a first-principles study," Phys. Rev. Mater. **2**, 074403 (2018).

Publications from August, 2016 to July 2018

1. B.F. Garrett, I. Azuri, L. Kronik and J.R. Chelikowsky, "Real-Space Pseudopotential Method for Computing the Vibrational Stark Effect," J. Chem. Phys. **145**, 174111 (2016).

2. G.D. Nguyen, H.-Zh. Tai, A.A. Omrani, M. Wu, T. Marangoni, D. J. Rizzo1, G. F. Rodgers, R. R. Cloke, Y. Sakai, F. Liou, J.R. Chelikowsky, S. G. Louie, F.R. Fischer, and M. F. Crommie, "Atomically precise graphene nanoribbon heterojunctions from a single molecular precursor," Nat. Nanotechnol. **12**, 1077 (2017).

3. A.J. Lee, Y. Sakai, and J.R. Chelikowsky, "Simulating contrast inversion in atomic force microscopy imaging with real-space pseudopotentials," Phys. Rev. B **95**, 081401(R) (2017).

4. L. Gao, J. Souto-Casares, J.R. Chelikowsky and A.A. Demkov, "Orientation dependence of the work function: metal nanocrystals," J. Chem. Phys. **147**, 214301 (2017).

5. Y. Sakai, J.R. Chelikowsky, and M.L. Cohen, "Simulating the effect of boron doping in superconducting carbon," Phys. Rev. B **97**, 054501 (2018).

6. Y. Sakai, J.R. Chelikowsky and M.L. Cohen, "Magnetism in amorphous carbon: a first-principles study," Phys. Rev. Mater. **2**, 074403 (2018).

7. W. Gao, L. Hung, S. Ogut and J.R. Chelikowsky, "The stability, electronic structure, and optical absorption of boron-nitride diamondoids predicted with first-principles calculations," Phys. Chem. Chem. Phys. **20**, 19188 (2018).

8. D. Fan, Y. Sakai and J.R. Chelikowsky, "Real-space pseudopotential calculations for simulating non-contact atomic force microscopy images," J. Vac. Sci. Technol. B **36**, 04H102 (2018).

9. J.R. Chelikowsky, Handbook of Materials Modeling. Volume 2 Applications: Current and Emerging Materials, Section Editor, Springer, Eds. W. Andreoni and S. Yip (2018, in press).

10. J.R. Chelikowsky, "Emergence of Functionalized Properties in Semiconductor Nanostructures," Handbook of Materials Modeling. Volume 2 Applications: Current and Emerging Materials, Eds. W. Andreoni and S. Yip, Springer (2018, in press).

Computational approach to complex interfaces and junctions

PI: Professor Hai-Ping Cheng[1,2]; SP: Professor James N. Fry[1]
Department of Physics[1] and the Quantum Theory Project[2], University of Florida
Gainesville, FL 32611

Keywords: spin-dependent charge transport, tunneling field-effect, interfaces, 2D systems

Project Scope

This DOE/BES funded project aims to understand fundamental physical processes at interfaces and across nano-molecular-junctions. We focus on spin-dependent charge transport under single and dual gate using first-principles based methods. Systems under investigation include 2D transition-metal metal-phthalocyanines (*M*Pc, *M*=Mn, Fe, Co etc), transition-metal dichalcogenides, (MoS_2, WS_2), topological insulator ($BiSbTeSe_2$), and double and triple barriers made of graphene. Critical to transport behavior in junctions with both vertical and planar configurations are interfacial electronic and magnetic structure and the interplay between structure and properties. Large-scale first-principles simulations allow accurate determination of information at the atomistic level, thus having predicting power. In order to explore multi-physical process, our project also includes theoretical development and algorithm/code implementation of the Green function methods and phonon.

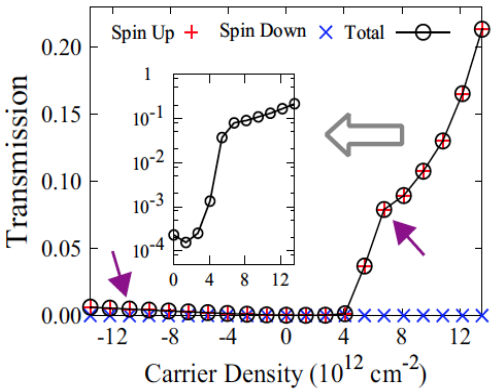

Fig.1 A hetero MPc junction shows spin-dependent transmission switching behavior under a gate voltage.

Recent Progress

1. *Gated spin-dependent transport in magnetic 2D systems.* We studied two-dimensional junctions consisting of transition metal-phthalocyanine (Pc) organic frameworks. In these systems we find a large tunneling magnetoresistance ratio. The transmission functions of such junctions can be tuned using gate voltage by three orders of magnitude. The origin of this dramatic change was thoroughly analyzed, and we found that it comes from orbital alignment and hybridization between the leads and the scattering center electronic states [publication 1]. To further understand the magnetic pattern in these systems, we investigated magnetic phases and phase transitions induced by electrostatic gating of a number of transition MPc systems and found that electrostatic gating can induce phase transitions among homogeneous ferromagnetic and various spin-textured antiferromagnetic states. Wannier function analysis indicates that transition-metal *d*-orbitals and conjugated π-orbitals are hybridized in these organic frameworks. The strong *d*-π hybridization in Mn-containing system leads to partially occupied spin-minority bands, in contrast to compounds containing other transition metal ions, for which electronic structure around the Fermi energy is only slightly spin-split due to weak *d*-π hybridizations, and the magnetic interaction is of the Ruderman-Kittel-Kasuya-Yosida type. We used a double-

exchange model to understand the phase diagram in terms of carrier density and illuminate the complexity and potential to control 2D magnetization [publication 2].

2. *Transport and interface properties of other 2D junctions* [publication 3-7]. In the second part of the previous funding period, which is partially covered by the 2018 DOE PI meeting, we studied a number of gated junctions in vertical and planar configurations. Here, we highlight one system to illustrate the interplay between structure and transport. We studied grapehene-azobenzene-graphene junctions [publication 3], which are related to amazing developments in experiments. The major finding from this study is that the interference of interface states resulting from molecule-graphene interactions at the Fermi energy introduces a dual-peak pattern in the transmission functions and dominates the transport properties of gated junctions, shedding new light on interfacial processes. From our analysis of the difference between *trans* and the *cis* molecules, we concluded that the emerging peak is not the Fano resonance, but contributed by interface molecule-molecule interactions. The resonance peak at the Fermi energy indeed disappears (Fig.2, right panel). We also found that the transport properties are closely related to the configuration and electronic structure of the junction. The enhancement of transmission of the Gr/*cis*/Gr junction at negative energies is due to the tail of the Breit-Wigner resonance through the HOMO. This phenomenon is not found in the *trans* junction, because of the strongly localized HOMO. Azobenezene-containing molecules (ABM) are excellent model systems for studying the interplay among structure, electronic structure, and transport.

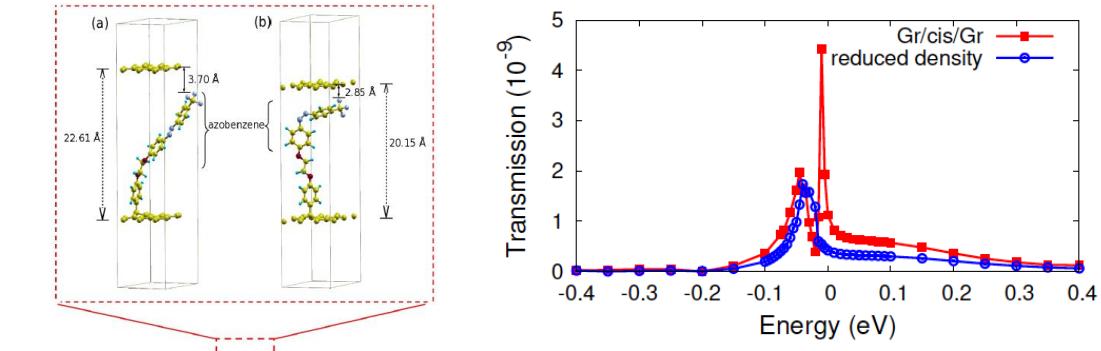

Fig. 2 Left: Schematics of the simulation setup. The insert shows ABM molecules in their *trans* and *cis* configurations. The junction is repeated periodically in the direction into the page. Right: Transmission function of the *cis* ABM at two different densities. Note the disappearance of the sharp peak at the Fermi energy.

Future Plans

1. Topological Insulator Interface and Gate Field Effects We will perform transport calculations on vertical junctions utilizing surface states of topological insulators. Since the beginning of the current funding period (12/1/2018) we have studied the interface between two slabs of topological insulator (TI) $BiSbTeSe_2$ (BSTS). We found that topological interface states

disappear when two TI slabs are close to each other. On the other hand, topological interface states survive when the separation between the TI slabs is larger than 6 Å since the inter-slab interaction is weak. The critical separation is insensitive to the way of stacking between TI slabs.

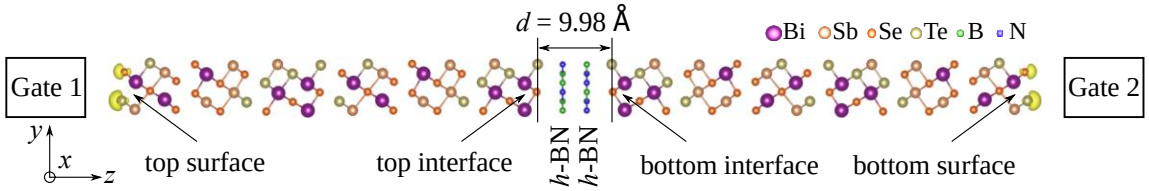

Fig. 3 Atomic structure of the BSTS interface with bilayer *h*-BN under dual gate. The structure is periodic in the □ and □ directions and has finite thickness along the □ direction. The isosurface of excess charge density $\delta\rho = \rho_{Q\neq 0} - \rho_{Q=0}$ is superimposed over the atomic structure colored in yellow, where Q is the net charge of the heterostructure.

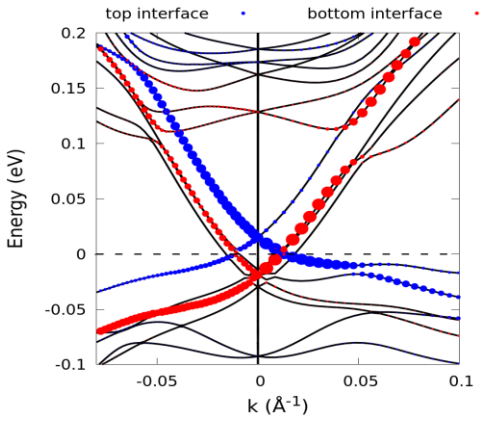

Fig. 4 Fat band structure for the BSTS interface with bilayer *h*-BN. The size of the blue/red circles indicates the localization of a state at the top/bottom surface.

Fig. 4 shows an interface where bilayer *h*-BN is sandwiched between two BSTS slabs. The separation between the BSTS slabs is about 10 Å. Since it is well above 6 Å, topological interface states occur. The band structure of this TI interface is plotted in Fig. 4 where the topological interface states are highlighted by blue and red dots. The blue/red dots are for top/bottom interface states. Topological states reside not only at the interfaces but also at the top and bottom surfaces, which are exposed to vacuum. In our simulations, the hetero-structure is between two gate electrodes, allowing independent control of charge doping and electric field with the aid of the effective screening medium (ESM) method. For the heterostructure doped with 0.05 electrons per unit cell and under zero external electric field, we also plot the distribution of the excess electrons in Fig. 3 The isosurface value of the excess charge density δρ is 5×10^{-5} Bohr^{-3}. It clearly shows that the excess electrons are mainly located at the top and bottom surfaces. In contrast, the interface and the bulk part of the slab are barely doped. As a result, the vertical transport properties weakly depend on doping concentration. However, the bulk part of the slab would be doped in the presence of a finite external electric field, and then the vertical transport properties strongly depend on doping concentration. These findings explain the experimental observations by Yong P. Chen at Purdue University (private communication)

2. Graphene with double-, triple-barriers, and vertical WS_2, and CrI_3 systems We are currently studying spin-dependent electron transport properties in gated graphene double and triple barrier junctions in planar configurations, as well as mono- and bi-layer WS_2 and CrI_3 systems. We obtained preliminary results for all these systems and found some very interesting results with physics rooted in orbital-band interactions. We plan to continue and finish the calculations for

publication. Here, we only highlight results on graphene. These graphene junctions consist of two graphene leads, two (and in one case three) vacuum barriers, and a zigzag graphene nanoribbon (ZGNR) quantum well. Previous studies suggest that zigzag graphene edges are magnetic, which enables the spin-dependent electron transport investigated in our work. We observe resonant electron tunneling, and find that a highly spin-polarized electric current can be obtained in such junctions. Furthermore, spin polarization of the electric current can be controlled by charge doping via a gate voltage. When the vacuum barrier is replaced with monolayer boron nitride, non-resonant electron transmission increases since the barrier height decreases. We also tune the transport properties by changing the width of the quantum well and explore the properties of graphene triple barrier junctions. These double and triple barrier junctions may have potential application as a resonant tunneling diode in low dimensional electronics since they can be fabricated using lithographic techniques. For the WS_2 systems, the inspiration is the interlayer band-to-band transition in bi-layer systems and for CrI_3 is the interplay between stacking and magnetic ordering which can be controlled by gate voltage.

3. *Electron-phonon couplings* As proposed, our intermediate term goal is to include electron-phonon coupling in the transport calculation. We plan to use an alternative approach based on the Bardeen formula [1] that can work with our planewave transport method and go beyond perturbation theory. The current is written as $I = 2\pi/\hbar \int \left[f_{tip}(E) - f_{sample}(E) \right] \rho_{tip}(E) \left| M(E) \right|^2 dE$, where f_{tip} and f_{sample} are the Fermi-Dirac distribution functions for the tip and the sample, respectively, r_{tip} is the electron density of states of the tip, and $M(E)$ is the transition matrix element between the tip and the sample. This approach is the basis of essentially all modern theoretical interpretation and modeling of STM. The idea of interpreting electron transport through a tunneling junction in terms of a transition rate calculated from the Fermi golden rule allowed the formulation of the theory for magnon-assisted spin dependent tunneling in magnetic tunnel junctions. While this theoretical work has demonstrated that the Bardeen approach is better suited for inelastic tunneling, it is limited to single magnon absorption and emission and thus remains in the weak-coupling regime. A recently developed theoretical framework for first-principles modeling of multiphonon transitions in semiconductors [2] is based on the Fermi golden rule just like the Bardeen tunneling formula, and does not require the Born approximation. Implementation of this approach in a quantum transport calculation requires recasting the transport problem within the framework of the Bardeen formula, then deriving the transition matrix element in the context of electron transport. We will work together on the theory, algorithms, and code development. In the renewal period, we aim at theory and algorithms. If time permits, we will implement it in our PWlayer code.

References

1. J. Bardeen, *Tunnelling from a Many-Particle Point of View*, Physical Review Letters **6**, 57 (1961).

2. Georgios D. Barmparis, Yevgeniy S. Puzyrev, X.G. Zhang, and S.T. Pantelides, *Theory of inelastic multiphonon scattering and carrier capture by defects in semiconductors: Application to capture cross sections.* Physical Review B**92**, 214111 (2015).

Publications (August 2016 – July 2018)

1. S.L. Liu, Y.P. Wang, X.G. Li, J.N. Fry, and H.P. Cheng, *Tuning spin transport across two-dimensional organometallic junctions*, Physical Review B97, 035409. (2018).
2. Y.-P. Wang, X.-G. Li, S.-L. Liu, J. N. Fry, and H.-P. Cheng, *Magnetic phase transition induced by electrostatic gating in two-dimensional square metal-organic frameworks*, Physical Review B**97**, 115419 (2018).
3. Y.-P. Wang, J.N. Fry, and H.-P. Cheng, *Multi-Control Over Graphene-Molecule Hetereo-Junctions*, ACS Omega **2**, 5824(2017).
4. G.X. Chen, X.G. Li, Y.P. Wang, J.N. Fry, and H.-P. Cheng, *Two-dimensional lateral GaN/SiC heterostructures: First-principles studies of electronic and magnetic properties*, Physical Review B**95**, 045302 (2017).
5. X.G. Li, Y.P. Wang. J. N. Fry, X.G. Zhang, and H.P. Cheng, *Tunneling field-effect junctions with WS_2 barrier*, J. Phys. Chem. Solids, epub online, 26 Dec. 2017 https://doi.org/10.1016/j.jpcs.2017.12.005
6. Y.-P. Wang, X. -G. Zhang, J.N. Fry, and H.-P. Cheng, *Comparative investigation of electronic transport across three-dimensional nanojunctions*, Physical Review B**95**, 085303 (2017).
7. Y.-P. Wang, X. -G. Li, J.N. Fry, and H.-P. Cheng, *First-principles studies of electric field effects on the electronic structure of trilayer graphene*, Physical Review B**95**, 165428 (2016).

Quantum Dynamics in Complex Magnets: Excitations, Transport, and Disorder

Principal Investigator: Alexander Chernyshev
Institution: Department of Physics and Astronomy, University of California, Irvine

Keywords: quantum magnets, topological bands, dynamical structure factor, disorder, thermal transport

Project Scope

The central objective of this project is the study of quantum effects in complex magnets with a particular focus on their dynamical and transport properties and on the effects of finite temperature and disorder in them. Our interest is driven by advances in experimental studies of new materials and by a broad progress in the spectroscopic techniques that allow for ever more precise analysis of elementary excitations. We have proposed to establish potentially dramatic connections of the effects of disorder with the unexpected thermal transport, of the nonlinear interactions among quasiparticles with the singular spectral features, of the order-by-disorder phenomena with the unconventional order in frustrated magnets, and of the phonon scattering with the quasi-ballistic transport in the gapped spin systems.

Recent Progress

Damped topological magnons in the kagome-lattice ferromagnets.-- The PI together with a graduate student recently demonstrated [1] that an idea of non-interacting topologically nontrivial bands, familiar from fermionic systems, cannot be trivially transplanted to bosonic systems such as ferromagnets on the geometrically frustrated lattices. The key difference is in the particle-non-conserving terms that are generated by the same interactions that are necessary for the sought-after Berry curvature of the bands. These terms, combined with a ubiquitous degeneracy of the two-magnon continuum, produce a substantial broadening of magnon bands precisely in the ranges of **k** and ω that are essential for the topological properties to occur, thus potentially undermining the entire free-band consideration. We provided a detailed account of the effect and proposed further experiments. How the topologically-nontrivial properties of the bands can be defined in the presence of a substantial broadening remains an open question.

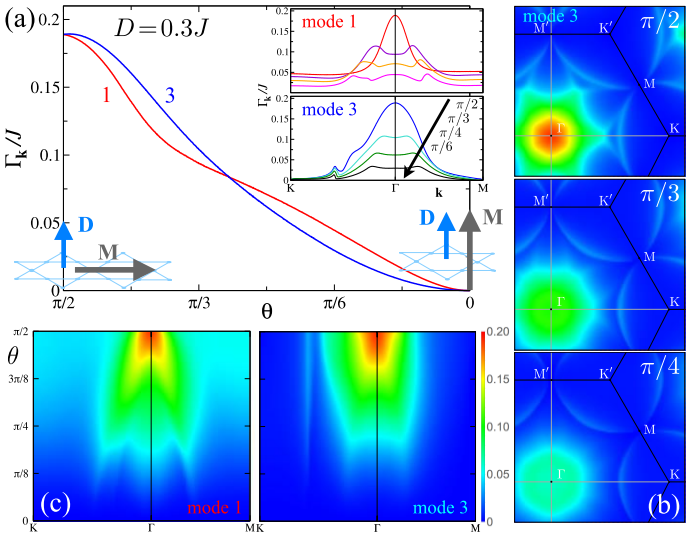

Figure 1. From [1]. Broadening of magnons vs angle θ of magnetization **M** with the DM vector **D**. Insets: same vs **k**; 2D intensity maps (b) vs **k** and, (c) vs **k** and angle θ.

Field-induced decays in XXZ triangular-lattice antiferromagnets.--We have calculated the dynamical structure factor of the XXZ triangular-lattice antiferromagnets in a field, an experimentally observable response function that is highly relevant to several materials that are intensely studied experimentally. We investigated field-induced transformations in the dynamical response of the XXZ model on the triangular lattice that are associated with the anharmonic magnon coupling and decay phenomena. Detailed theoretical predictions were made for a close physical realization of the spin-1/2 XXZ model, $Ba_3CoSb_2O_9$, see Ref. [2]. We have demonstrated that dramatic modifications in magnon spectrum must occur in low out-of-plane fields that are easily achievable for this material. The hallmark of the effect is a coexistence of the well-defined magnon excitations with significantly broadened ones in different regions of the **k**–ω space. The field-induced decays are generic for this class of models and become more prominent at larger anisotropies and in higher fields.

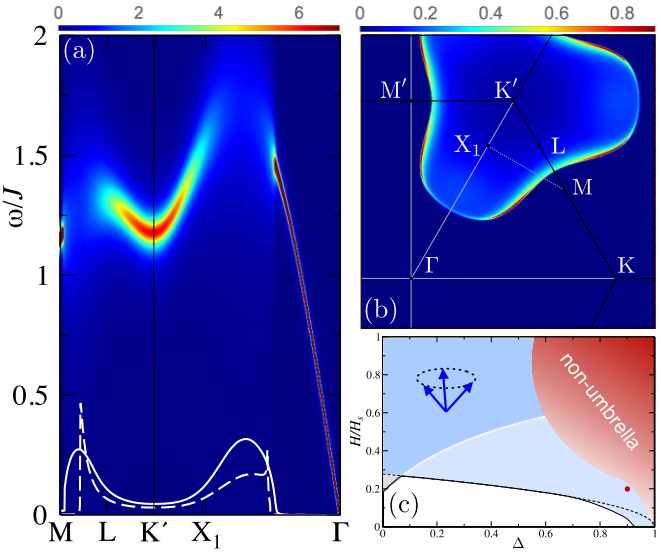

Figure 2. From [2]. (a) Spectral function along the MK' path with for Δ = 0.9 and H=0.2H_s. The dashed and solid lines are broadenings by decays. (b) The 2D intensity plot of damping rate. (c) The H–Δ diagram of the decay thresholds; in shaded regions decays are present.

Novel spin liquid in the anisotropic-exchange antiferromagnet on a triangular lattice.--In a collaboration with the DMRG numerical group of Steven White at UCI, we have provided the most definitive and unbiased study to date of the phase diagram of the most general nearest-neighbor spin model on a triangular lattice [7], the geometry that is iconic to the field of frustrated magnetism. This study is of a direct relevance to a class of new rare-earth-based materials and other systems with strong spin-orbit coupling that yield anisotropic spin-spin interactions. This work provides a much-needed framework to this area of research, clears the path to a consistent interpretation of the current and future experiments, and gives a number of important new insights into the fundamental properties of quantum magnets with spin-orbit-generated low-energy Hamiltonians [7].

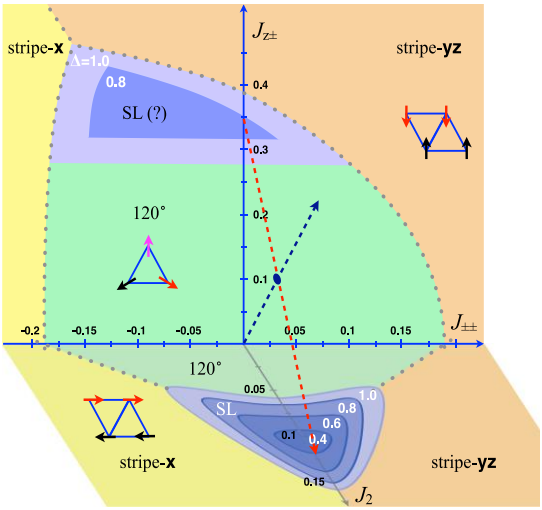

Figure 3. From Ref. 7. Topographic maps of the spin liquid regions of the 3D phase diagrams of the nearest-neighbor and of the J_1–J_2 XXZ model [back and lower panels].

We have also proposed that the recently discovered novel magnetically disordered state in the rare-earth-based materials may be strongly affected by disorder, which destroys an otherwise seemingly robust ordered state. For that, we have proposed a phenomenon of a "mimicry" of a spin-liquid state that should be common in quantum magnets with strong spin-orbit couplings. This scenario is tested for the recently discovered rare-earth-based triangular-lattice antiferromagnet $YbMgGaO_4$ in the experimentally relevant range of parameters. Our work suggests that a randomization of the pseudo-dipolar interaction due to spatially-fluctuating charge environment of the rare-earth ions generates a mimicry of a spin-liquid state in the form of short-range stripe or stripe-superposition domains. This scenario is likely to be relevant to a broad family rare-earth-based quantum magnets [5].

Breakdown of magnons in a strongly spin-orbital coupled magnet.--The description of quantized collective excitations stands as a landmark in the quantum theory of condensed matter. A prominent example occurs in magnets, which support quantized fluctuations of the ordered spins known as magnons. In striking contrast is the recent discovery that strongly spin-orbital-coupled magnets, such as the so-called "proximate Kitaev-material," α-$RuCl_3$, may display a broad excitation continuum inconsistent with conventional magnons. The most discussed explanation refers to a coherent continuum of fractional excitations analogous to the celebrated Kitaev spin liquid. Together with our numerical colleagues at the University of Frankfurt, we have proposed a more general scenario, in which that the unusual, continuum-like dynamical response of the alpha-$RuCl_3$ is due to strongly-anisotropic exchanges that generate strong anharmonic effects in the magnon spectra, which, in turn, lead to significant magnon decays [6]. Our work fully explains the observed dynamical response of α-$RuCl_3$ and suggests a similar scenario for a variety of other systems with anisotropic exchanges. The described phenomenon is the newest member of a class of such effects, with the original theoretical proposal of the effect of magnon decays originating from our group.

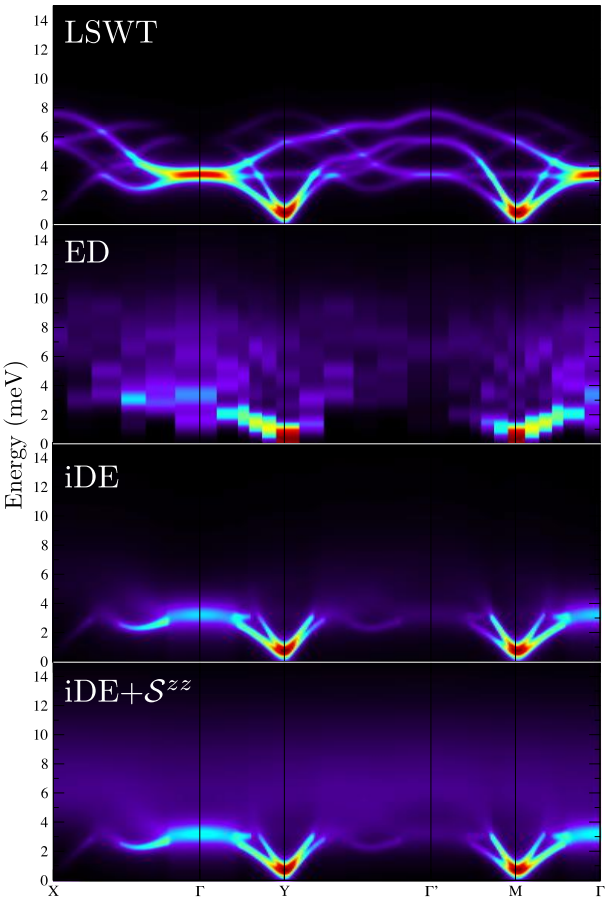

Figure 4. From [6]. Dynamical structure factor $S(\boldsymbol{q},\omega)$ in linear SWT [upper panel], exact diagonalization [2nd upper panel], SWT with the broadening [1st lower panel] and with longitudinal intensity $S^{zz}(\boldsymbol{q},\omega)$ [2nd lower panel].

Future Plans

For the next years, we plan to continue our studies of quantum effects in complex magnets with a focus on their dynamical and transport properties and on the role of disorder in them. Specifically, we have several ongoing projects:

- A deeper study into the enigmatic ground state properties of the rare-earth-based triangular-lattice magnets with strongly anisotropic interaction.
- A study of the longitudinal component of the dynamical response in the honeycomb-lattice Kitaev-Heisenberg magnets, materials of great current interest.
- Effects of impurities, phonons, and external magnetic field on the dynamical and transport properties of complex magnets.

Publications (August 2016 – July 2018)

1. A. L. Chernyshev and P. A. Maksimov, *"Damped Topological Magnons in the Kagome-Lattice Ferromagnets,"* Phys. Rev. Lett. **117**, 187203 (2016).
2. P. A. Maksimov, M. E. Zhitomirsky, and A. L. Chernyshev, *"Field-induced decays in XXZ triangular-lattice antiferromagnets,"* Phys. Rev. B (Rapid Communication) **94**, 140407(R) (2016).
3. J. Oh, M. D. Le, H.-H. Nahm, H. Sim, J. Jeong, T. G. Perring, H. Woo, K. Nakajima, S. Ohira-Kawamura, Z. Yamani, Y. Yoshida, H. Eisaki, S.-W. Cheong, A. L. Chernyshev, and J.-G. Park, "*Spontaneous decays of magneto-elastic excitations in noncollinear antiferromagnet (Y,Lu)MnO_3,"* Nat. Commun. **7**, 13146 (2016).
4. Tao Hong, Y. Qiu, M. Matsumoto, D. A. Tennant, K. Coester, K. P. Schmidt, F. F. Awwadi, M. M. Turnbull, H. Agrawal, A. L. Chernyshev, "*Field-induced spontaneous quasiparticle decay and renormalization of quasiparticle dispersion in a quantum antiferromagnet"*, Nat. Commun. **8**, 15148 (2017).
5. Zhenyue Zhu, P. A. Maksimov, Steven R. White, and A. L. Chernyshev, *"Disorder-Induced Mimicry of a Spin Liquid in $YbMgGaO_4$*," Phys. Rev. Lett. **119**, 157201 (2017).
6. Stephen M. Winter, Kira Riedl, Pavel A. Maksimov, Alexander L. Chernyshev, Andreas Honecker, and Roser Valenti, *"Breakdown of Magnons in a Strongly Spin-Orbital Coupled Magnet*," Nat. Commun. **8**, 1152 (2017).
7. Zhenyue Zhu, P. A. Maksimov, Steven R. White, and A. L. Chernyshev, *"Topography of Spin Liquids on a Triangular Lattice*," Phys. Rev. Lett. **120**, 207203 (2018).

CORRELATED QUANTUM AND THERMAL DYNAMICS OF DISORDERED SUPERCONDUCTING, MAGNETIC, AND LOW-DIMENSIONAL SYSTEMS

DOE/BES Grant No. DE-FG02-93ER45487

Principal Investigator: Dr. Eugene M. Chudnovsky, Distinguished Professor
Department of Physics and Astronomy
Herbert H. Lehman College & CUNY Graduate School
The City University of New York
250 Bedford Park Boulevard West, Bronx, NY 10468-1589
Email: Eugene.Chudnovsky@Lehman.CUNY.edu

Keywords: random fields, topology, skyrmions, quantum tunneling

Project Scope

The work on the DOE/BES grant at CUNY Lehman College and Graduate School, and research planned in the nearest future, covers a number of topics of contemporary condensed-matter theory that include large-scale numerical studies of topology-driven phenomena in magnetic and superconducting systems with quenched randomness, stability of skyrmions in magnetic films, spin-orbit effects and quantum dynamics of magnetic clusters embedded in a superconductor, dynamics of the elastic membrane in application to suspended graphene, and PT-symmetric approach to quantum tunneling with dissipation. Novel "pulse-noise" numerical method has been developed to describe non-equilibrium dynamics of Josephson and spin systems (EPL-2016, PRB-2017, PRE-2017, arXiv-2018). We have demonstrated that one can manipulate the magnetic moment of an atomic cluster by the superconducting current (PRB-2017). Our theory of graphene cantilever under Casimir force provides a powerful tool for the investigation of Casimir effect (PRB-2016, J.Phys.D-2018). This abstract focuses on our most recent work on skyrmions in 2D magnetic systems. By investigating correlations of the topological charge density on 2D lattices containing over one hundred million spins we have shown that quenched randomness transforms ferromagnetic order into skyrmion-antiskyrmion glass (PRL-2018). We also have demonstrated by analytical and numerical methods that skyrmions in magnetic films can be stabilized by static disorder and controlled by the magnetic field (NJP-2018). Theory of quantum collapse of a skyrmion has been developed (arXiv-2018). Future research will focus on computing the rate of thermal decay of skyrmions in various systems and on manipulating quantum spin states by spin-polarized currents.

Recent Progress

Studies of static randomness in field-theory models have a long history. They apply to amorphous magnets and spin glasses, flux lattices in superconductors, magnetic bubble and skyrmion lattices, charge density waves, liquid crystals and polymer physics, and He-3 in aerogel. It has been long understood that the effect of a static random field (RF) on the long-range order is stronger than the effect of thermal fluctuations. Imry and Ma (IM) made a general observation that static randomness, no matter how week, destroys the long-range order in less than $d = 4$ dimensions in systems with continuous-symmetry order parameter. While the

concept of IM domains was widely used by experimentalists in application to various physical systems it was later questioned by theorists who applied renormalization group and replica-symmetry breaking methods to the problem and argued that static randomness must lead to a defect-free Bragg glass characterized by only a power-law decay of correlations. Our large-scale numerical simulations of RF systems (PRL-2014), accompanied by topological argument, have shown that formation of topological defects by the RF is unavoidable. However, the dispute about the nature of the glass state created by static randomness has never been settled.

Most recently we have investigated the borderline case of a three-component spin field in two dimensions that possesses nonsingular topological objects – skyrmions. It has practical importance in application to 2D magnetic systems. Earlier we have shown that in a pure exchange model violation of the scale invariance by the crystal lattice forces skyrmions to collapse (PRB-2012). This changes in the presence of the RF. Interaction of the RF with the skyrmion scales linearly with the RF strength, H_R, forcing sufficiently large skyrmions to blow up rather than collapse [1]. It makes plausible that IM domains in 2D are formed by skyrmions and antiskyrmions of size comparable to the ferromagnetic correlation length R_f. We confirmed this conjecture by studying correlation function of the topological charge density (TCD), q, alongside with the spin-spin correlation function on lattices containing over 100 million spins [2]. Results obtained with collinear initial condition (CIC) for all spins are shown in Fig. 1.

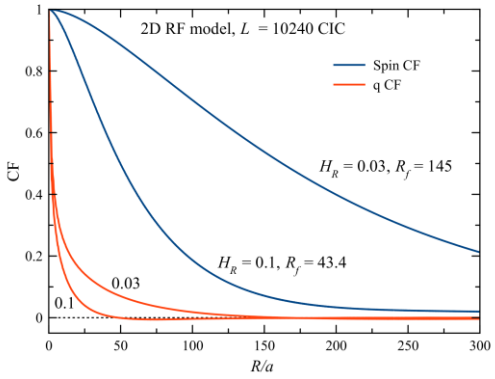

Fig. 1a: Spin-spin and TCG correlation functions.

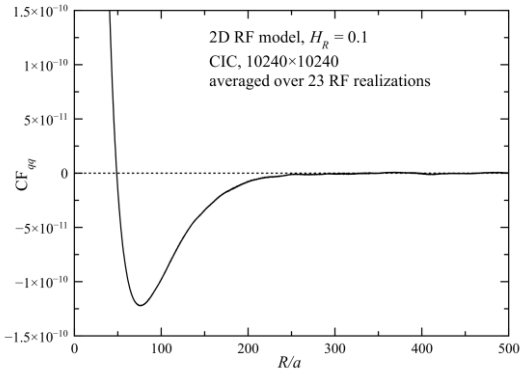

Fig. 1b: Structure of the TCD correlation function.

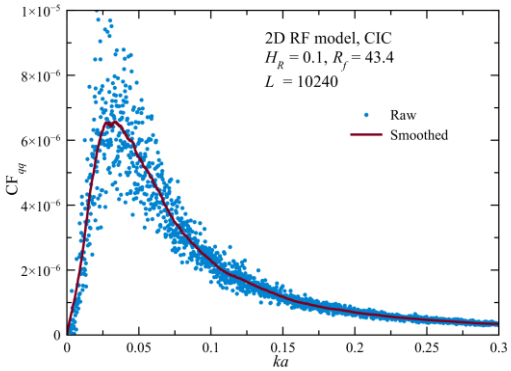

Fig. 2a: Fourier transform of the TCD correlation function.

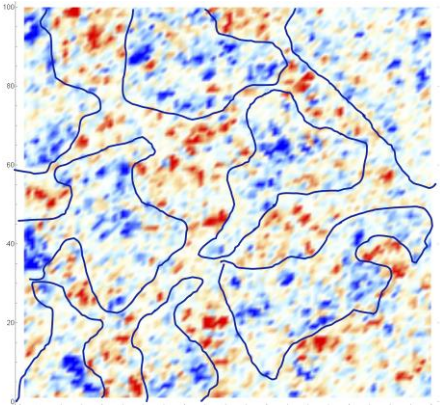

Fig. 2b: Color plot of the TCD.

Even a more clear evidence of the topological structure of IM domains comes from the Fourier

transform of the TCD correlation function that exhibits maximum at $kR_f = 1$, see Fig. 2a. Topological order inside IM domains is also illustrated in Fig. 2b, where colors represent the sign and the amplitude of the TCD. We have found that the absolute value of the topological charge per IM domain is close to Q = 1. These findings [2] shed new light on the fundamental problem of the nature of the glass state in systems with non-trivial topology.

The 2D systems with random anisotropy (RA) exhibit similar properties. One interesting finding of practical importance is that the RA alone (that would be present in disordered films) stabilizes skyrmions [1]. The average skyrmion size is determined by the field, H, and the ratio, D_R/J, of the RA to exchange. On increasing the field, skyrmions shrink from their original size R_f at H = 0, and eventually collapse, see Figs. 3a. Concentration of skyrmions, f_S, is shown in Fig. 3b.

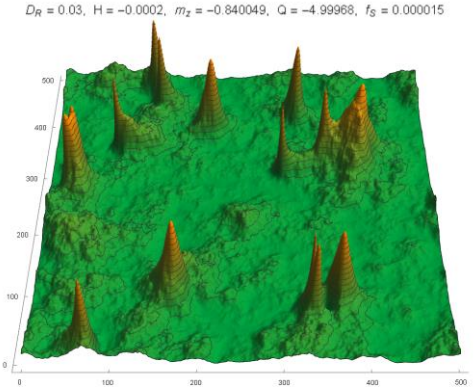

Fig. 3a: Skyrmions in the presence of the field.

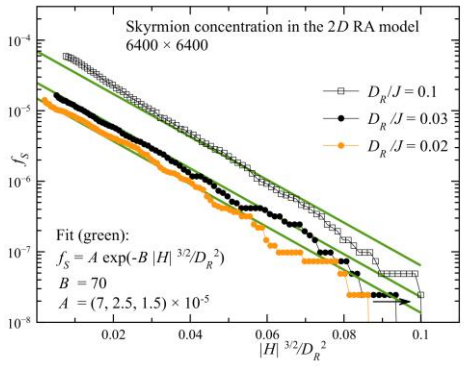

Fig. 3b: Scaling of skyrmion concentration.

The dependence of f_S on parameters has been derived by us analytically and is shown to be in excellent agreement with our numerical experiment [1].

Recent interest to skyrmions is dictated by their potential for topologically protected ultra dense data storage. Can quantum mechanics affect the stability of a small skyrmion? We have developed a theory of quantum collapse of a skyrmion and have shown that this effect may have practical importance. The rate of collapse has been computed as a function of the ratio of the Dzyaloshinskii-Moriya (DMI) interaction, A, to the exchange, J, and the closeness of the

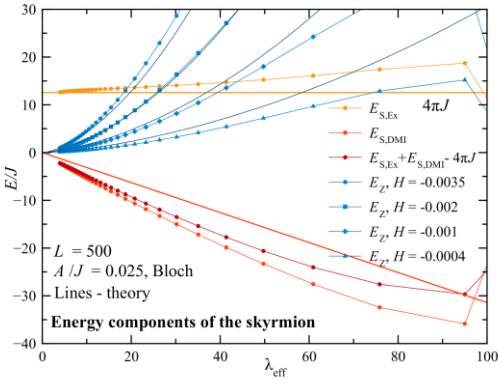

Fig. 4a: Energy components vs size of the skyrmion.

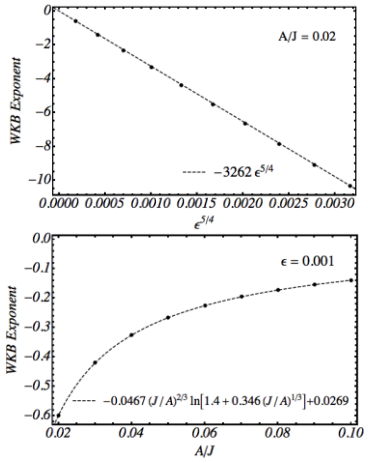

Fig. 4b: WKB exponent vs ε and A/J.

magnetic field to the critical (collapse) field, H_c, described by the parameter $\varepsilon = 1 - H/H_c$. The dependence of the exchange, DMI, and Zeeman energies on the skyrmion size, λ, has been investigated on 500x500 spin lattices and found to be in agreement with analytical results, see Fig. 4a. The Euclidean action corresponding to the underbarrier quantum collapse of a skyrmion via instanton of the equations of motion in imaginary time has been computed, both analytically and numerically, with a good agreement between the two methods, see Fig. 4b.

Future Plans

We are now embarking on a more challenging problem of thermal stability of skyrmions that has paramount importance for utilizing skyrmions as units of topologically protected data storage and processing. Recently Cortes-Ortuno et al. (Nature Commun. 2017) have computed energy barriers for skyrmion collapse and run over the edge of a nanotrack with the help of the NEBM method. No attempt has been made to obtain the decay time. The pulse-noise method recently developed by us and tested on Josephson and spin systems is well suited for that task. We have started with a model that contains exchange, DMI, and Zeeman interaction for which the barrier was computed in our quantum collapse paper. Our initial numerical algorithm considers a small skyrmion in a large square lattice when the effect of the boundary can be ignored. Modes of skyrmion deformation leading to its motion over the barrier and thermal decay are being studied for various types of the DMI. Later we shall study the same problem by placing the skyrmion close to the boundary of the film. As soon as this set of problems is solved we shall include in the algorithm the on-site dipole-dipole interaction and magnetic anisotropy. We shall also consider a multilayered film, hexagonal lattice symmetry, and the field applied at an angle.

Another problem currently under investigation by us is dynamics of quantum spin states induced by a spin-polarized current within PT-symmetric quantum mechanics. Classical counterpart of that problem has been recently studied by Galda and Vinokur (PRB-2016) who obtained instability thresholds corresponding to the magnetization reversal due to the spin-transfer torque. We are asking whether interaction with a short pulse of a spin-polarized current, modeled by a non-hermitian term in the spin Hamiltonian, can provide controlled transitions between quantum spin states. Solution of the Schrodinger equation indicates that such a possibility does exist. The resulting probabilities depend on the amplitude of the current and show bifurcations at certain values of the current. There is also a more subtle problem of the effect of the spin-polarized current on a superposition of quantum states arising from a weak term in the Hamiltonian that does not compute with S_z. To make this problem more realistic and applicable to practical situations we are introducing interaction of the spin with a thermal noise. This set of problems is related to the possibility of manipulation of spin qubits by the electric currents.

References

1. E. M. Chudnovsky and D. A. Garanin, Skyrmion glass in a 2D Heisenberg ferromagnet with quenched disorder, New Journal of Physics **20**, 033006-(9) (2018), cond-mat arXiv:1710.10608.

2. E. M. Chudnovsky and D. A. Garanin, Topological order generated by random field in a 2D exchange model, Physical Review Letters **121**, 017201-(5) (2018), cond-mat arXiv:1803.09117.

3. A. Derras-Chouk, E. M. Chudnovsky, and D. A. Garanin, Quantum collapse of a magnetic skyrmion, cond-mat arXiv:1806.03675 (2018).

Publications (August 2016 – July 2018, DOE/BES support acknowledged)

1. D. A. Garanin and E. M. Chudnovsky, Persistent current in a 2D Josephson junction array wrapped around a cylinder, Europhysics Letters **115**, 27004-(6) (2016).

2. E. M. Chudnovsky and R. Zarzuela, Stability of a suspended graphene under Casimir force, Physical Review B **94**, 085424-(4) (2016).

3. D. A. Garanin and E. M. Chudnovsky, Thermal fluctuations of the Josephson current in a ring of superconducting grains, Physical Review B **95**, 014520-(6) (2017).

4. E. M. Chudnovsky, Manipulating magnetic moments by superconducting currents, Physical Review B **95**, 100503(R)-(4) (2017).

5. D. A. Garanin, Pulse-noise approach for classical spin systems, Physical Review E **95**, 013306-(9) (2017).

6. E. M. Chudnovsky and D. A. Garanin, Skyrmion glass in a 2D Heisenberg ferromagnet with quenched disorder, New Journal of Physics **20**, 033006-(9) (2018).

7. A. Derras-Chouk, E. M. Chudnovsky, D. A. Garanin, and R. Jaafar, Graphene cantilever under Casimir force, Journal of Physics D: Applied Physics **51**, 195301 (2018).

8. E. M. Chudnovsky and D. A. Garanin, Topological order generated by random field in a 2D exchange model, Physical Review Letters **121**, 017201-(5) (2018).

9. D. A. Garanin, Uniform and non-uniform thermal switching of magnetic particles, cond-mat arXiv: 1803.03988 (2018).

10. D. A. Garanin, Effective anisotropy due to surface of magnetic nanoparticles, cond-mat arXiv:1803.10406 (2018).

11. A. Derras-Chouk, E. M. Chudnovsky, and D. A. Garanin, Quantum collapse of a magnetic skyrmion, cond-mat arXiv:1806.03675 (2018).

Spin and orbital physics in Novel Correlated Materials

Piers Coleman, Rutgers University

Keywords: Topological Kondo Insulator, Iron-based Superconductivity.

Project Scope

The research focuses on the role of coupled orbital, spin and geometrically frustrated degrees of freedom as drivers of new kinds of correlated electron behavior, and involves the study of the transformative effects of interactions on strongly correlated topological insulators and semi-metals, the theory of iron-based superconductors and research into the novel phase transitions in frustrated low dimensional magnets and superfluids.

Recent Progress

1. Strongly interacting Topological Materials

Kondo insulators and semi-metals, containing highly localized f-electrons, offer a unique platform to study the interplay of topology, spin-orbit coupling and interactions in quantum materials. In f-electron materials topological effects are encoded in the hybridization between the localized f-states and delocalized conduction electrons. This led us to predict that Kondo insulators will be topological, spuring the discovery of topological behavior in SmB_6[1]. The effects of interactions, crystal symmetry and topological behavior are the focus of this work. We are interested in the manifestation of topological behavior in f-electron systems and the possibility that interactions can can promote new kinds of topological ground-states.

i) Mobius Kondo Insulators

In [**§1]** we argue that the presence of nonsymmorphic crystal symmetries in many heavy fermion materials opens up a new family of topologically protected heavy electron systems. Re-examination of archival resistivity measurements in the nonsymmorphic heavy fermion insulators $Ce_3Bi_4Pt_3$ and CeNiSn reveals the presence of a low-temperature conductivity plateaux, making them candidate members of the new class of material. We developed these ideas with a specific model for CeNiSn, showing how glide symmetries generate surface states with a novel Möbius braiding that can be detected by ARPES or non-local conductivity measurements. One of the interesting effects of strong correlation is the development of partially localization or 'Kondo breakdown' on the surfaces [**§1]**, which transforms Möbius surface states into quasi-one-dimensional conductors, with the potential for novel electronic phase transitions.

ii) Kondo Weyl Semi-metals

Another important crystal symmetry effect is broken inversion symmetry, which can transform a topological insulator into a Weyl Semi-metals (WSM). In [**§2]** we developed a theory of Kondo

Weyl semi-metals, introducing a simple model Hamiltonian in which the driving mechanism WSM is driven by non-centrosymmetric terms in the hybridization. Kondo break-down in Kondo Weyl Semi-metals is predicted to lead to a reconfiguration in the surface Fermi arcs, with a temperature-dependent transformation in the Fermi arcs that can be detected via Shubnikov de-Haas oscillations.

iii) Skyrme Insulators and neutral Fermi surfaces.

The observation of bulk dHvA oscillations and linear specific heat in insulating SmB_6 [2] and YbB_{12} [3], raise the possibility of gapless excitations within the topological bulk. Remarkably, in SmB_6 there are no corresponding Shubnikov de Haas oscillations in the resistivity. These results motivated us to examine the possibility that interactions can transform the bulk of a topological Kondo insulator into a phase with neutral, diamagnetic excitations. dHvA oscillations are a signature of Landau level formation, yet it is difficult to understand how a charged particle can couple selectively to the magnetic field, because microscopically, particles minimally couple to the vector potential $\mathbf{A}(x,y)$, with a kinematic momentum $\boldsymbol{\Pi}=\mathbf{p}-e\mathbf{A}$. Provided gauge invariance holds, such particles cannot respond to the curl ($\mathbf{B}=\nabla \times \mathbf{A}$) , without also responding to the time derivative $\mathbf{E}(t)= -\partial\mathbf{A}/\partial t$, forming a metal.

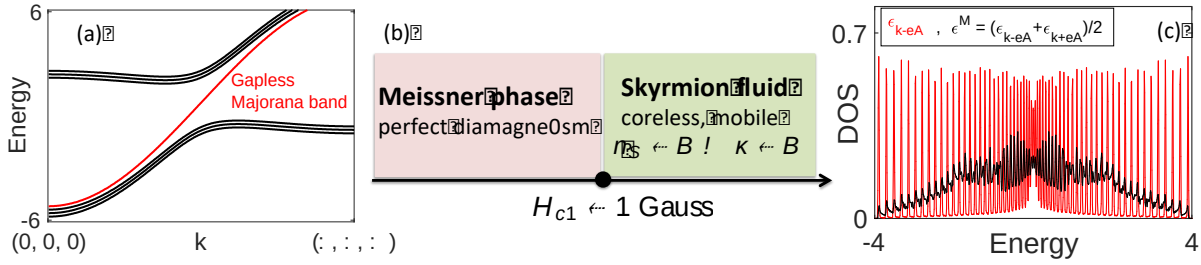

*Fig. 1 Skyrme dielectric showing (a) neutral Fermi surface (b) phase diagram and (c) Landau quantization predicted by [**§3**].*

In **[§3]** we developed the theory of the "Skyrme Dielectric", a kind of failed superconductor with a phase stiffness, but in which the order parameter is unable to sustain a topologically stable circulating supercurrent: this happens if the order parameter manifold G is higher dimensional, permitting vortices to "unravel". (Mathematically, its first homotopy class does not contain the set of integers, $\Pi_1(G) \neq \mathbb{Z}$). We developed a theory in which the local moments of a Kondo lattice fractionalize into neutral Majorana fermions with a Fermi surface, which induce an *odd-frequency* triplet paired state which carries no orbital angular momentum, and thus does not couple to the lattice, giving rise to a higher dimensional order parameter without stable vortices. From the Landau Ginzburg equations, we were able to show that both electric and magnetic fields can penetrate this exotic state, according to the equations:

$$\frac{1}{2\pi}\overline{\hat{n}\cdot(\nabla_i\hat{n}\times\nabla_j\hat{n})} = \frac{2e}{h}\epsilon_{ijk}B_k \quad , \quad \frac{1}{2\pi}\overline{\hat{n}\cdot(\nabla_t\hat{n}\times\nabla_i\hat{n})} = \frac{2e}{h}E_i$$

Skyrme Dielectric

where the overbar denotes a coarse grained average. These equations relate the internal electromagnetic fields to Skyrme textures of the order parameter[**§3]**. At very low fields, the net positive energy of the Skyrmions will cause them to be excluded from the sample, at which point a Meissner effect develops. Experiments have not confirmed this prediction in SmB_6, but this may be because the critical field estimate did not account for the large dielectric constant (ε ~50,000) of SmB_6 . A long version of this theory is in preparation.

2. Iron-based Superconductivity

The family of iron-based superconductors (FeSC) shares a common local electronic structure, with iron atoms contained within tetrahedra of pnictogen or chalgonide atoms. By contrast, the momentum-space electronic structures of the FeSC show great diversity: the sulphide members of this family are even quasi-one dimensional[4]. A recent survey[5] of the family of iron based superconductors found that the ratio $2\Delta/T_c$~7.2 is fixed for all of the bulk iron-based superconductors despite the wide diversity of Fermi surface structure and interaction strengths. These observations, together with the absence of correlation between T_c and the hole/pocket structure of the Fermi surface and their spin fluctuations[5], motivate a change of theoretical perspective. with a renewed focus on the local iron physics and the role of Hund's interactions.

We have recently conducted a study [**§4]** of the quasi one-dimensional(q1D) iron-based superconductor, $FeBa_2S_3$, which shares the same staggered tetrahedral structure as its quasi-two dimensional (q2D) cousins, with a band of delocalized d-electrons forming between Fe^{2+} ions and a two-leg ladder arrangement of the tetrahedral. This system opens up the possibility of analyzing the physics of iron based superconductivity using the powerful tools of one-dimensional renormalization group and bosonization. Using these techniques, we have carried out a renormalization group study of a two-orbital, two-leg ladder model of $FeBa_2S_3$ with Hubbard and Hund's interactions. A key result of our work is the identification of four stable ground-state phases which fan out from a central quantum critical point. Crucially, the Hund's coupling controls which of these four phases is selected and at sufficiently large ratio J/U a fully gapped superconductor develops in which the intraband pairing gaps have signature (+,-,-) on the three pairs of Fermi points. Our theory provides a way to understand the conducting high pressure part of the experimental phase diagram and, by including umklapp scattering, also accounts for the observation of a Mott phase at low pressure.

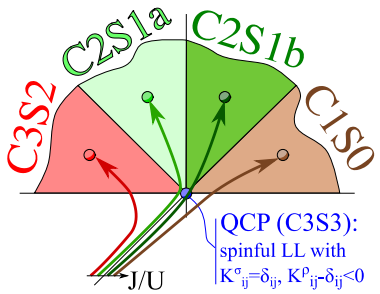

Fig. 2 Fan of phases tuned by Hund's coupling in a q1D model of $FeBa_2S_3$ after [***§4***].

The robustness of iron based superconductivity to a wide variety of Fermi surface topologies, and the common mechanism by which FeSC overcomes the strong Coulomb repulsion at the iron sites is not yet solved. In [**§5]** we discuss this "Coulomb problem" in detail, examining whether

a possible redistribution of the condensate wavefunction between orbitals and Fermi surface can account for the robustness. We conclude, in accordance with [5] that the answer likely resides in a local pairing mechanism, driven by local Coulomb and Hund's interactions.

3. Low dimensional superfluids

Our collaboration with the low-temperature group at Cornell, and University of London, Royal Holloway [**§6]** raises the interesting possibility that a two-dimensional (2D) superfluid in a periodic potential may exhibit *powerlaw supersolidity*. Torsional oscillator measurements [**§6]** show that at certain filling fractions, bilayer 4-He develops a finite superfluid density, but without a Berezinski Kosterlitz Thouless (BKT) transition. Moreover, an anomalous linear temperature dependence of the normal fraction at low temperatures suggest a Goldstone mode at finite wavevectoresting indicative of a zero-energy roton. We proposed [**§6]** that a superfluid with a non-Abelian order parameter manifold offers an explanation: an enlarged symmetry manifold would eliminate the BKT transition, since macroscopic vortices would not be topologically protected, while the emergence of a Goldstone mode at finite wavevector accounts for the enhanced normal fraction at low temperatures T, in contrast with a conventional superfluid, which shows a T^3 behavior.

In [**§7]** we developed a theory for such a non-Abelian supersolid, showing that with certain classes of long-range interaction, it develops a degenerate five dimensional order parameter manifold (S_5) which is unable to develop topologically stable vortices.

Future Plans

1. Strongly interacting Topological Materials

Various new experimental developments, including the discovery of dHvA oscillations in YbB12, together with a bulk thermal conductivity, and the discovery that the d-electron spin resonance in SmB_6 splits into a *doublet* (rather than a triplet) in a field, motivate new research on the idea of a neutral Fermi surface in a Kondo insulator. We plan to (i) extend our Majorana approach to include valence fluctuations, (ii) develop a theory for the spin-exciton of a Skyrme insulator, which as a spinor, rather than a vector may be able to account for the remarkable doublet structure in a field. We are also working with Barry Bradlyn and Jennifer Cano to combine their extensive group theoretical analysis of topological band-structure with interactions.

2. Iron-based Superconductivity

Following the results of our 1D study, we are now developing a model for Hund's driven local pairing. A state of particular interest is the S=1, L=1 state formed from a pair of electrons in the three t_{2g} orbitals of the iron atom.

References

1. Maxim Dzero, Jing Xia, Victor Galitski and Piers Coleman, *Topological Kondo Insulators*, Annual Review of Condensed Matter Physics**,** . **7**:249-280 (2017).

2. M. Hartstein, W. H. Toews, Y.-T. Hsu, B. Zeng, X. Chen, M. Ciomaga Hatnean, Q. R. Zhang, S. Nakamura, A. S. Padgett, G. Rodway-Gant, J. Berk, M. K. Kingston, G. H. Zhang, M. K. Chan, S. Yamashita, T. Sakakibara, Y. Takano, J.-H. Park, L. Balicas, N. Harrison, N. Shitsevalova, G. Balakrishnan, G. G. Lonzarich, R. W. Hill, M. Sutherland, Suchitra E. Sebastian, *Fermi surface in the absence of a Fermi liquid in the Kondo insulator* SmB_6, **14**, 166–172 (2018).

3. Y. Matsuda, Lu Li et al, "Bulk Fermi Surface in a Kondo insulator YbB_{12} Science, in Press (2018); Hsu Liu, Mate Hartstein,Gregory J. Wallace, Alexander J. Davies, Monica Ciomaga Hatnean, Michelle D. Johannes, Natalya Shitsevalova, Geetha Balakrishnan and Suchitra E. Sebastian, *Fermi surfaces in Kondo insulators*, Journal of Physics: Cond. Matt **30**, 16 (2018).

4. H. Takahashi, A. Sugimoto, Y. Nambu, T. Yamauchi, Y. Hirata, T. Kawakami, M. Avdeev, K. Matsubayashi, F. Du, C. Kawashima, H. Soeda, S. Nakano, Y. Uwatoko, Y. Ueda, T. J. Sato, and K. Ohgushi, *Pressure-induced superconductivity in the iron-based ladder material* $BaFe_2S_3$, Nat Mater **14**, 1008 (2015).

5. Tsung-Han Lee, Andrey Chubukov, Hu Miao and Gabriel Kotliar, *On the Superconductivity of Hund's Metals*, arXiv1805.10280, (2018).

Publications (August 2016 – July 2018)

§1 Po-Yao Chang, Onur Erten, Piers Coleman, *Mobius Kondo insulators*, Nature Physics **13**, 794-798 (2017).

§2 Po-Yao Chang and Piers Coleman, *Parity-violating hybridization in heavy Weyl semimetals*, Phys. Rev. B **97**, 155134 (2018).

§3 Onur Erten, Po-Yao Chang, Piers Coleman and Alexei M. Tsvelik, *Skyrme insulators: insulators at the brink of superconductivity*, Phys. Rev. Lett., **119**, 057603 (2017).

§4 Elio J. Konig, Alexei M. Tsvelik and Piers Coleman, *Renormalization group analysis for the quasi-1D superconductor* $BaFe_2S_3$, arXiv:**1802.10580**, (2018)

§5 Elio J. Konig and Piers Coleman, *The Coulomb problem in Iron based superconductors*, arXiv:**1802.10580**, (2018).

§6 Jan Nyeki, Anastasia Phillis, Andrew Ho, Derek Lee, Piers Coleman, Jeevak Parpia, Brian Cowan and John Saunders, *Intertwined superfluid and density wave order in two-dimensional* ^4He, Jan Nyeki, Anastasia Phillis, Andrew Ho, Derek Lee, Piers Coleman, Jeevak Parpia, Brian Cowan and John Saunders, Nature Physics, **13**, 455–459 (2017).

§7 Simon Lieu, Andrew F. Ho, Derek K. K. Lee and Piers Coleman, p-Orbital Superfluid with an S_5 Manifold arXiv:**1803.00970**, (2018).

§8 Piers Coleman, Theory Perspective: SCES 2016 Piers Coleman, Philosophical Magazine, **97**, 36, 3257-3543 (2017).

Materials Theory

Principal Investigator: V. R. Cooper (coopervr@ornl.gov), Oak Ridge National Laboratory

Co-investigators: T. Berlijn, R. S. Fishman, L. R. Lindsay, J. R. Morris, D. S. Parker

Keywords: thermal transport, itinerant magnetism, porous media, superconductors

Project Scope

The overarching goal of this project is to understand and predict atomic-level phenomena to enable the design and discovery of complex and emergent behavior of materials at the macroscale. We aim to understand materials properties such as ferroelectricity, magnetism, and phononic and electronic properties, not only as ground state behaviors, but also in terms of their excitations and transport which ultimately impact functionality. Our effort focuses on the creation and application of first-principles derived, realistic, predictive models of materials properties which enable exploration at increasing length scales, from point defects to interfaces to coupled macroscale interactions. Bridging the gap between local, atomic-level descriptions and their complex macroscopic expressions, this effort will connect fundamental material behavior to their experimental signatures, thereby allowing for direct connections with experiment. In this regard, this project will drive and complement ongoing experimental and theoretical efforts at Oak Ridge National Laboratory.

Recent Progress

Unusual thermal transport from mass variance and disorder

Point defects, dislocations, and dopants/impurities have fundamental and applications-based consequences on materials properties and device design. Both the silicon-based digital revolution and the use of permanent magnets for energy applications depend critically on manipulating impurity states in materials. The ability to intentionally modify materials and manipulate defects provides an avenue for designing novel functionalities.

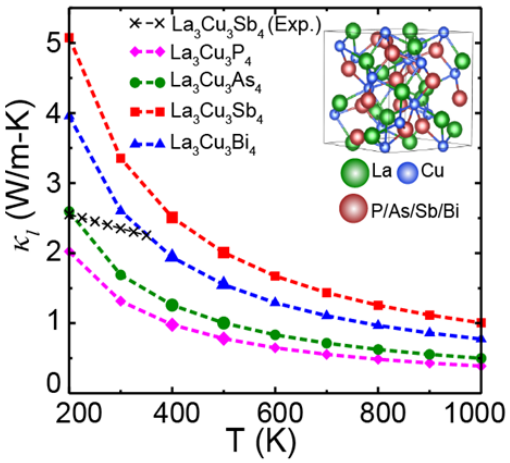

Figure 1 Thermal conductivities of $La_3Cu_3X_4$ (X=P, As, Sb, Bi) illustrating unusual non-monotonic thermal conductivity with increasing mass [1].

To investigate the unusual role that mass differences play in thermal transport, we examined lattice conductivities of complex $La_3Cu_3X_4$ (X=P, As, Sb, Bi) materials, light atom systems LiH/LiF, and functionalized graphene using first principles Peierls-Boltzmann transport methods that include phonon-phonon and phonon-isotope scattering resistance. In all cases, the calculated lattice thermal conductivities (κ) elucidate intriguing transport behaviors governed by mass variance and

disorder, and not described by typical rules of thumb. For instance, in the $La_3Cu_3X_4$ materials, we found that increasing mass (going from *X*=P to Bi) resulted in an unusual increase in lattice conductivity contrary to typical rules (Figure 1) [1]. We understand this in terms of the complex interactions between sound speeds, anharmonicity and scattering phase space. Isotope disorder in LiH and LiF was found to *improve* thermal transport by altering intrinsic phonon-phonon interactions. Lastly, highly unusual, optic phonon-dominated thermal transport was found in $Ge_2Sb_2Te_5$ and functionalized graphene due to highly dispersive optic branches and suppressed acoustic velocities from heavy atoms. These highlight the unusual role that mass differences play in thermal transport; providing new pathways for engineering material behavior.

Solids with ultralow thermal conductivity are of great interest as thermal barrier coatings for insulation or thermoelectrics for energy conversion. However, the theoretical limits of lattice κ are unclear. In typical crystals a phonon picture is valid, whereas low κ values occur in highly disordered materials where this picture fails and heat is carried by random walks among uncorrelated oscillators. Recently, we identified a simple crystal, Tl_3VSe_4, with calculated phonon κ (0.16 W/m-K) half that of the measured κ (0.30 W/m-K) at 300K, approaching disorder κ values although Raman spectra, specific heat and temperature dependence of κ reveal typical phonon characteristics. Adding a transport component based on uncorrelated oscillators explains the measured κ; suggesting that a two-channel model is necessary to explain ultralow κ [2].

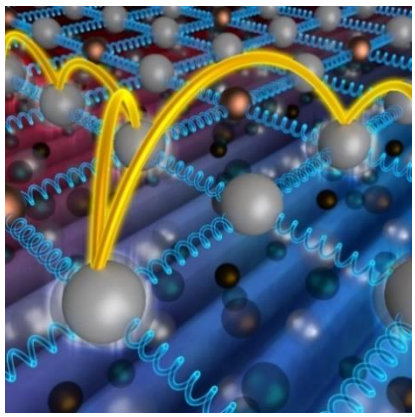

Figure 2 Artist's depiction of the "two-channel" model applied to Tl_3VSe_4. Atoms (Tl:gray and V:red) held together by interatomic forces (shown as springs) transmit heat by random "hopping" (yellow curves) as well as the usual sound wave contribution [2].

Spin-waves and competing interactions in magnetic and multiferroic systems

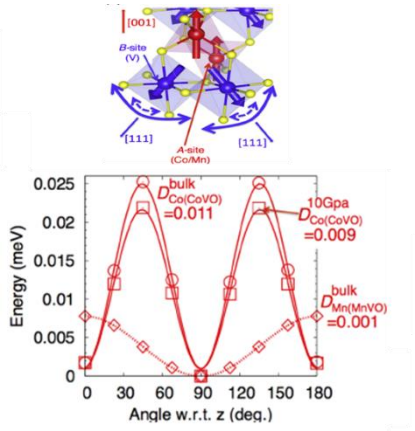

Figure 3 Single-ion anisotropy (SIA) for the S = 1 V^{3+} ions evaluated using DFT for CoV_2O_4. These values are then used in a microscopic model to predict the spin ground state of this compound [3].

Magnetic frustration and competing exchange interactions result in rich phase diagrams, including non-collinear spin arrangements that induce ferroelectricity, allowing for electric field control of magnetizations. To reveal the complex interplay between the magnetic, orbital, and lattice degrees of freedom, neutron scattering measurements, first-principles calculations, and spin models were employed to study the spinel CoV_2O_4. $Mn_{1-x}Co_xV_2O_4$ exhibits an interplay between local, orbitally ordered V moments and itinerant Co electrons. Due to enhanced itinerancy with Co doping, the single-ion anisotropy on the V sites is reduced, which melts the orbitally ordered state and stabilizes a non-collinear spin state in CoV_2O_4 [3]. This transformation was studied by comparing the predictions of DFT and a microscopic

model with neutron-scattering measurements. The interplay between local and itinerant behavior is important for understanding a wide range of technologically important materials.

Recently, we revealed that the observed ferrimagnetism in $Mn_3Si_2Te_6$ arises from closely competing magnetic states and interactions induced by a complex crystal structure, which greatly reduces the ordering temperature despite a large local Mn moment. [4] Employing first principles calculations, we found that the *ferri*-magnetic ground state is stabilized by the interplay between the complex crystal structure, geometric frustration and strong *third*-nearest neighbor antiferromagnetic interactions, despite entirely *anti*-ferromagnetic interactions. Such factors are important in the context of quantum materials.

Signatures of $Ti_{1.5}O_2$ interlayer in electronic structure of superconducting monolayer FeSe

Monolayer FeSe grown on substrates like $SrTiO_3$ have recently been shown to exhibit intriguing superconducting behavior. Most studies report critical temperatures (T_c) for this material to lie within 55-75K which is nearly an order of magnitude larger than for bulk FeSe. Here it is believed that the substrate plays a fundamental role in increasing T_c. One hypothesis is that substrate induced electron doping drives the superconductivity enhancement. Another proposal is that pairing interactions are enhanced by the coupling between the phonons and Fe-*d* electrons in the substrate that is peaked at small momenta. As such, a detailed understanding of the interface is crucial for resolving the microscopic mechanisms of superconductivity in these systems.

In our recent work (under review: Berlijn/Cooper) based on STEM experiments and DFT calculations we have found that $Ti_{1.5}O_2$ forms its own quasi-two-dimensional layer, bonding to both the substrate and the FeSe film by van der Waals interactions (see Fig 4). The presence of this $Ti_{1.5}O_2$ interlayer strongly affects both the electron doping and the interfacial phonons and therefore is crucial to the superconductivity in these systems. Currently in a follow-up study we are characterizing the influence of the $Ti_{1.5}O_2$ interlayer on the electronic structure of monolayer FeSe. Preliminary results show that the interlayer has little effect on the local density of states above the surface as measured by scanning tunneling microscopy. However, given that the interlayer induces significant distortions in the Fe sublattice we expect to see a stronger signature in the momentum dependence of the electronic structure of the Fe-*d* bands as measured by angular resolved photoemission spectroscopy. To further study these effects, we will employ our recently developed band unfolding technique.

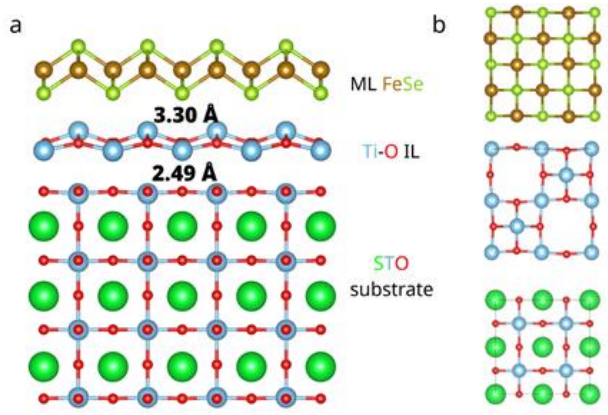

Figure 4 Structure of the FeSe/ $Ti_{1+\delta}O_2$ / $SrTiO_3$ interface, projected along the [100] direction. Atom colors correspond to those of the atom names in the legend.

Continuum model of gas uptake for inhomogeneous fluids

The ability to efficiently simulate the absorption/uptake capacity of gaseous species in porous media is critical to the design and discovery of promising materials for renewable energy generation and greenhouse gas capture. However, approaches such as molecular dynamics simulations and Grand Canonical Monte Carlo simulations can suffer from the lack of accuracy of the underlying atomistic potentials or the inability to simulate for long enough times.

To address this, we have developed an integrated approach that uses adsorption energies determined from density functional theory (using the van der Waals density functional to properly account for the noncovalent dispersion interactions) to generate an equation of state to obtain an initial density distribution [5]. Subsequently, atomistic gas−gas correlations in the inhomogeneous environment are taken into account as perturbations to the bulk fluid gas interactions. The change in calculated density is consequently used to adjust the adsorption density throughout the pore. Recent tests on the adsorption of hydrogen in two metal organic framework materials show tremendous promise for predictions of hydrogen uptake and local densities; thereby, providing a rapid, reasonably accurate approach to predicting uptakes even for systems in which the adsorbent medium has highly variable adsorption strengths.

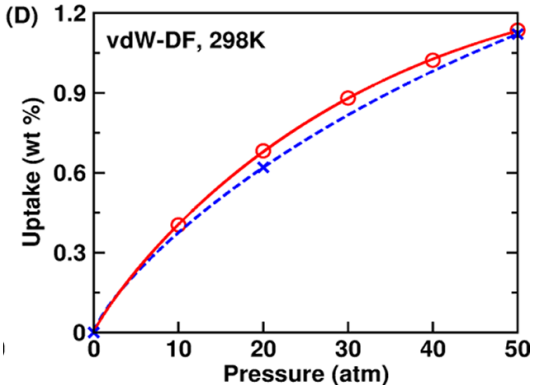

Figure 5 H_2 uptake capacities in $Zn(BDC)(TED)_{0.5}$ using Grand Canonical Monte Carlo simulations (blue dotted line) and the new method (red circles) using the van der Waals density functional for adsorption energies [5].

Future Plans

The future goals of this project will be to extend beyond ground state, first-principles calculations of idealized crystals, to understand how functionality emerges and evolves with realistic descriptions of defects, chemical disorder, and microstructure. This project will emphasize the design and discovery of complex and emergent behavior at the macroscale, using advanced computational and theoretical approaches that allow us to predict how atomic-level phenomena, related to crystal imperfections and chemical disorder, drive material functionality. This will enable predictions of materials with knowledge of defect tolerances and functionality under the conditions which they are utilized. We aim to understand materials properties such as ferroelectricity, magnetism, vibrational and electronic properties in terms of excitations and transport. In this context, this project will focus on the following Specific Aims: (1) Designing defect- and disorder-derived thermal and ionic transport, (2) Unraveling the influence of doping and disorder on magnons and phonons and (3) Interfacial control of emergent phenomena. Ultimately, we will develop and apply first-principles-derived methodologies to create realistic, materials-specific, predictive models of materials properties that link atomic-level interactions with experimentally observable phenomena.

References

1. T. Pandey, C. A. Polanco, L. Lindsay, and D. S. Parker "Lattice thermal transport in $La_3Cu_3X_4$ compounds (X= P, As, Sb, Bi): Interplay of anharmonicity and scattering phase space" *Phys. Rev. B* **95**, 224306 (2017).
2. S. Mukhopadhyay, D.S. Parker, B.C. Sales, A. Puretzky, M.A. McGuire and L. Lindsay "Two-channel model for ultralow thermal conductivity of crystalline Tl_3VSe_4" *Science* **360**, 1455 (2018).
3. J. H. Lee, J. Ma, S. E. Hahn, H. B. Cao, M. Lee, T. Hong, H.-J. Lee, S. Okamoto, H. D. Zhou, M. Matsuda, and R. S. Fishman "Magnetic frustration driven by itinerancy in spinel CoV_2O_4" *Sci. Rep.* **7**, 17129 (2017).
4. A. F. May, S. Liu, S. Calder, D. S. Parker, T. Pandey, E. Cakmak, H. Cao, J. Yan, and M. A. McGuire "Magnetic order and interactions in ferrimagnetic $Mn_3Si_2Te_6$" *Phys. Rev. B* **95**, 174440 (2017).
5. Y. Ihm, V. R. Cooper, L. Vlcek, P. Canepa, T. Thonhauser, J. Hoon Shim, and J. R. Morris "Continuum model of gas uptake for inhomogeneous fluids" *J. Phys Chem. C* **121**, 17625 (2017).

Selected Publications (August 2016 – July 2018)

1. D. W. Tam, T. Berlijn, and T. A. Maier "Stabilization of *s*-wave superconductivity through arsenic *p*-orbital hybridization in electron-doped $BaFe_2As_2$" *Phys. Rev. B*, **98** 24507 (2018)
2. T. Pandey, D. S. Parker, and L. Lindsay "*Ab initio* phonon thermal transport in monolayer InSe, GaSe, GaS and alloys" *Nanotechnology* **28**, 455706 (2017).
3. R. S. Fishman, S. Bordacs, V. Kocsis, I. Kezsmarki, J. Viirok, U. Nagel, T. Room, A. Puri, U. Zietler, Y. Tokunaga, Y. Taguchi, and Y. Tokura "Competing exchange interactions in multiferroic and ferromagnetic $CaBaCo_4O_7$" *Phys. Rev. B* **95**, 024423 (2017).
4. L. Lindsay and Y. Kuang "Effects of functional group mass variance on vibrational properties and thermal transport in graphene" *Phys. Rev. B* **96**, 121404(R) (2017).
5. S. Mukhopadhyay, D. Bansal, O. Delaire, D. Perrodin, E. Bourret-Courchesne, D. J. Singh and L. Lindsay "The curious case of cuprous chloride: Giant thermal resistance and anharmonic quasiparticle spectra driven by dispersion nesting" *Phys. Rev. B* **96**, 100301(R) (2017).
6. R. S. Fishman and S. Okamoto "A spiral spin state with open boundary conditions in a magnetic field" *Phys. Rev. B* **96**, 014439 (2017).
7. M. A. McGuire, J. Yan, P. Lampen-Kelly, A. F. May, V. R. Cooper, L. Lindsay, A. Puretzky, L. Liang, Santosh KC, E. Cakmak, S. Calder, and B. C. Sales "High temperature magneto-structural transition in van der Waals-layered α-$MoCl_3$" *Phys. Rev. Mat.* **1**, 064001 (2017).
8. L. Lindsay "Isotope scattering and phonon thermal conductivity in light atom systems: LiH and LiF" *Phys. Rev. B* **94**, 174304 (2016).
9. K. R. O'Neal, J. H. Lee, M. Kim, J. L. Manson, Z. Liu, R. S. Fishman, and J. L. Musfeldt "Quantum phase transitions in a semiclassical system" *npj Quant. Mater.* **2**, 65 (2017)
10. L. Lindsay "First principles Peierls-Boltzmann thermal transport: A topical review" *Nanos. Microsc. Therm. Eng.* **20**, 67 (2016).

Theoretical Study of Complex Collective Phenomena

Principal investigator: Elbio Dagotto [1,2]. **Co-PIs:** Adriana Moreo [1,2], Satoshi Okamoto [2], Thomas Maier [2].

[1] Department of Physics, University of Tennessee, Knoxville, TN.
[2] Materials Science and Technology Division, Oak Ridge National Lab, Oak Ridge, TN

Keywords: Correlated electrons, superconductivity, computational, interfaces.

Project Scope

Quantum materials, including iron- and copper-based high critical temperature superconductors and correlated oxides such as cobaltites, iridates, manganites, and others, display complex electronic properties that emerge from quantum collective effects, beyond single-particle approximations. Studying these materials is challenging due to phase competition and frustration. Quantum materials often contain dominant crystal substructures with reduced dimensionality, such as layers, ladders, and chains, where correlations effects are amplified. They can also be created artificially as in oxide superlattices.

Our **overarching goal** is the quantitative understanding of the rich phase diagrams of model Hamiltonians for strongly correlated quantum materials where several degrees of freedom (spin, charge, orbital, and/or lattice) are simultaneously active. This is an ambitious goal because the study of correlated electronic systems is conceptually and technically far more difficult than the analysis of materials such as semiconductors where density functional theory provides an excellent description. On the contrary, in quantum materials we employ model Hamiltonians, including Coulomb repulsion, Hund interactions, and spin-orbit coupling. Although naively these models seem simple, complex behavior emerges from local interactions leading to states displaying magnetism, superconductivity, charge and orbital striped patterns, excitonic condensates, and others. To capture these nontrivial states, and their cooperation or competition, the calculations must be accurate. For this purpose our team employs a broad combination of computational and analytical techniques, such as quantum and classical Monte Carlo simulations, density matrix renormalization group (DMRG), dynamical mean field theory, random-phase approximations (RPA), small cluster exact diagonalization, and others.

Recent Progress

Pairing tendencies in ladders and chains. At ambient pressure, the two-leg ladder compound $BaFe_2S_3$, Fig. 1(a), is an insulator with ferromagnetic (FM) spin coupling along rungs and antiferromagnetic along legs. Using a two-orbital Hubbard model studied with DMRG, recently we provided the first steps to understand this intriguing material. The experimentally observed magnetic order at ambient pressure was reproduced and, remarkably, the two-hole binding energy was found to be negative at intermediate U/W coupling, with U the on-site Hubbard repulsion and W the electronic bandwidth, suggesting the formation of Cooper pairs.

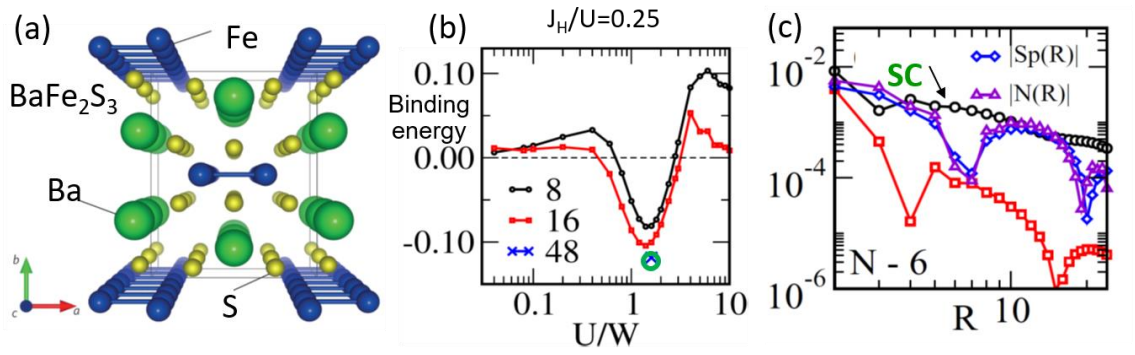

Figure 1. (a) Crystal structure of the two-leg ladder iron superconductor $BaFe_2S_3$. (b) DMRG binding energy vs Hubbard U in bandwidth W units, at various number of sites and a fixed Hund coupling J_H. (c) Pairing correlations decay the slowest on an N=48 site lattice with 6 holes. For details and references see [1].

Because in iron-ladders the rungs are FM, the binding tendencies cannot be the same as in copper-ladders where spin-singlet rungs cause pairing. A new mechanism relying on a combination of spin and orbital degrees of freedom likely operates in $BaFe_2S_3$. Because the precise set of hoppings and geometry used should not be crucial for the qualitative understanding of these pairing tendencies, we simplified the two-orbital model from a ladder to a chain that was then studied with DMRG [1]. The hoppings were reduced to be only intraorbital and between nearest-neighbor sites. The results for the binding energy in Fig. 1(b) are remarkable: it is negative at intermediate coupling and stable with increasing lattice sizes, pointing towards a robust pairing mechanism. Moreover, in some regions of parameter space the spin-singlet pair-pair correlation function decays the slowest, Fig.1(c), suggesting that superconducting tendencies dominate. Note that comparing ladders and chains with two orbitals is reasonable, as a chain with two orbitals is mathematically analogous to a one-orbital two-leg ladder (while with only one orbital, two-leg ladders and chains are fundamentally different).

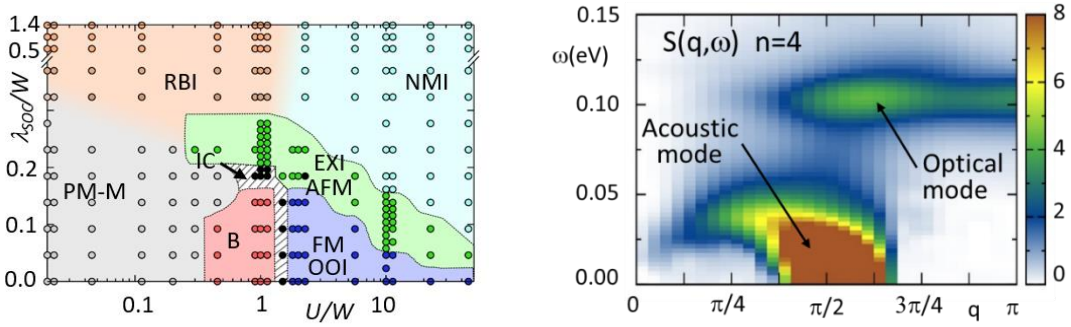

Figure 2. (Left) DMRG phase diagram of a three-orbital Hubbard model with the SOC (Hubbard) coupling in the vertical (horizontal) axis, in bandwidth W units. The many phases are explained in [2]. (Right) Spin dynamical structure factor [3] for the same model in the block B phase (see left panel) uudd (u=spin up, d=spin down).

Multiorbital Hubbard models: influence of spin-orbit coupling and spin dynamics. We have started the analysis of multiorbital Hubbard models including robust spin-orbit coupling (SOC), employing the DMRG technique in one-dimensional systems. Several materials with relevant SOC, see [2], have chains in their structure. Many phases were unveiled, see left panel of Fig. 2

and notation in [2]. In addition, we have also recently started the analysis of spin dynamical structure factors in a three-orbital model in an orbital selective Mott phase [3], see right panel of Fig. 2. Surprises were found such as an acoustic mode with nonzero intensity only for low momenta q and an optical mode at high q. These studies are very challenging computationally and our group is uniquely position to carry out these investigations.

Electronic properties of multi-orbital transition metal oxides. In oxide heterostructures, the *d*-electron density can be controlled by interfacing with other materials from where electrons/holes are transferred. This interfacial electronic movement is usually determined by the work functions of the individual components. However, sometimes special calculations are needed to predict the flow of charge due to interfacial reconstruction. An example are the heterostructures made of $SrIrO_3$ (SIO) and $SrMnO_3$ (SMO) that have similar work functions in principle. Surprisingly, experimental work at ORNL by H.N. Lee et al. showed a robust electron transfer from SIO to SMO. To understand this behavior, we developed a theoretical model based on molecular orbitals at the interface [4]. Because $d(3z^2\text{-}r^2)$ orbitals are extended perpendicular to that interface, they could form interfacial bonding (B) and antibonding (AB) molecular orbitals, and the resulting B level could become lower than the Fermi level, as in Fig. 3. Our calculations [4] indicate that the B molecular orbital has a strong Mn *d* character. Thus, electrons transferred from SIO to this B molecular orbital results in electrons transferring to SMO. This picture predicts a unique strain dependence of the electron transfer.

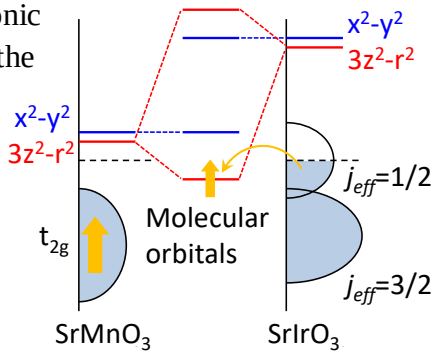

Figure 3. SMO/SIO interface and illustration showing the molecular orbital relevant for charge transfer, see [4].

Spin excitations in heavily doped iron-based superconductors. Heavily electron-doped iron-selenide superconductors have robust critical temperatures despite the absence of hole Fermi pockets at the Brillouin zone's center. This characteristic distinguishes them from their moderately doped counterparts, and challenges the prevailing scenario s± for superconductivity. Inelastic neutron scattering experiments carried out at ORNL on heavily electron-doped $Li_{0.8}Fe_{0.2}$ODFeSe have found nearly ring-shaped magnetic resonant excitations surrounding (π, π) at low energy. With this motivation, we carried out phenomenological calculations [5] based on RPA to study the magnetic excitations of a two-dimensional five-orbital Hubbard model that describes the electronic structure of FeSe with only electron pockets. For a phenomenological *d*-wave gap that changes sign between electron-pockets, these calculations find a low-energy magnetic excitation spectrum below ~40 meV that is broadly consistent with experiments.

Future Plans

Our main lines of future research include: **(1)** We will clarify qualitatively the pairing mechanism of ladder-based iron-based superconductors by continuing our study of multiorbital models. We will explore: (i) What is the full phase diagram of the model were pairing was found varying J_H and the electronic density n? (ii) What is the symmetry of the pair wave function? While the ladder geometry breaks the square-lattice C_4 rotational invariance, and A_{1g} or B_{1g} pairing lose their meaning, in copper-ladders the mean values of the nearest-neighbor-site pairing operators had different signs along legs and rungs, suggesting d-wave-like pairing. A similar analysis in $BaFe_2S_3$ may unveil the approximate symmetry of the pairs, d vs s±. (iii) What is the role of hopping amplitudes, crystal fields, and Hund coupling? Do we need an orbital split, with concomitant doping of just one orbital, or do degenerate orbitals also have pairing? **(2)** We will continue our analysis of heavily doped iron-based superconductors by including the incipient bands below the Fermi level in the formalism. **(3)** We will investigate potentially novel topological effects and phases caused by the influence of spin-orbit coupling on electronic systems with exotic band structures or in reduced dimensionalities. **(4)** We will analyze unusual strain effects and orbital selective Mott phases in materials where different orbitals have different degrees of localization. All our projects will benefit from collaborations with other ORNL-based BES-MSE programs.

References

[1] N. D. Patel, A. Nocera, A. Moreo, and E. Dagotto, *Pairing Tendencies in a Two-orbital Hubbard Model in One Dimension,* Phys. Rev. B **96**, 024520 (2017).

[2] N. Kaushal, J. Herbrych, A. Nocera, G. Alvarez, A. Moreo, F. A. Reboredo, and E. Dagotto, *Density matrix renormalization group study of a three-orbital Hubbard model with spin-orbit coupling in one dimension,* Phys. Rev. B **96**, 155111 (2017).

[3] J. Herbrych, N. Kaushal, A. Nocera, G. Alvarez, A. Moreo, and E. Dagotto, *Spin dynamics of the block orbital-selective Mott phase*, arxiv:1804.01959 (2018).

[4] S. Okamoto, J. Nichols, C. Sohn, S. Y. Kim, T. W. Noh, and H. N. Lee, *Charge Transfer in Iridate-Manganite Superlattices*, Nano Lett. **17**, 2126 (2017).

[5] B. Pan, Y. Shen, D. Hu, Y. Feng, J. T. Park, A. D. Christianson, Q. Wang, Y. Hao, H. Wo, Z. Yin, T. A. Maier, and J. Zhao, *Structure of Spin Excitations in Heavily Electron-Doped $Li_{0.8}Fe_{0.2}ODFeSe$ Superconductors*, Nat. Comms. **8**, 123 (2017).

Publications (August 2016 – July 2018) (see also the five references above).

S. Okamoto, G. Alvarez, E. Dagotto, and T. Tohyama, *Accuracy of the microcanonical Lanczos method to compute real-frequency dynamical spectral functions of quantum models at finite temperatures*, Phys. Rev. E **97**, 043308 (2018).

A. Nocera, Y. Wang, N. D. Patel, G. Alvarez, T. A. Maier, E. Dagotto, and S. Johnston, *Doping evolution of charge and spin excitations in two-leg Hubbard ladders: Comparing DMRG and FLEX results*, Phys. Rev. B **97**, 195156 (2018).

Hanxuan Lin, Hao Liu, Lingfang Lin, Shuai Dong, Hongyan Chen, Yu Bai, Tian Miao, Yang Yu, Weichao Yu, Jing Tang, Yinyan Zhu, Yunfang Kou, Jiebin Niu, Zhaohua Cheng, Jiang Xiao, Wenbin Wang, Elbio Dagotto, Lifeng Yin, and Jian Shen, *Unexpected Intermediate State Photoinduced in the Metal-Insulator Transition of Submicrometer Phase-Separated Manganites*, Phys. Rev. Lett. **120**, 267202 (2018).

J. Sheng, F. Ye, C. Hoffmann, V. R. Cooper, S. Okamoto, J. Terzic, H. Zheng, H. Zhao, and G. Cao, *Anisotropic antiferromagnetic order in the spin-orbit coupled trigonal-lattice $Ca_2Sr_2IrO_6$*, Phys. Rev. B **97**, 235116 (2018).

J. H. Lee, J. Ma, S. E. Hahn, H. B. Cao, M. Lee, T. Hong, H.-J. Lee, M. S. Yeom, S. Okamoto, H. D. Zhou, M. Matsuda, and R. S. Fishman, *Magnetic Frustration Driven by Itinerancy in Spinel CoV_2O_4*, Sci. Rep. **7**, 17129 (2017).

Y. Zhang, L. Lin, J. Zhang, E. Dagotto, and S. Dong, *Pressure-driven phase transition from antiferromagnetic semiconductor to nonmagnetic metal in the two-leg ladders AFe_2X_3 (A=Ba,K; X=S,Se)*, Phys. Rev. B **95**, 115154 (2017).

N. D. Patel, A. Mukherjee, N. Kaushal, A. Moreo, and E. Dagotto, *Non Fermi liquid behavior and continuously tunable resistivity exponents in the Anderson-Hubbard model at finite temperature*, Phys. Rev. Lett. **119**, 086601 (2017).

C. B. Bishop, A. Moreo, and E. Dagotto, *Bicollinear Antiferromagnetic Order, Monoclinic Distortion, and Reversed Resistivity Anisotropy in FeTe as a Result of Spin-Lattice Coupling*, Phys. Rev. Lett. **117**, 117201 (2016).

N. D. Patel, A. Nocera, G. Alvarez, R. Arita, A. Moreo, and E. Dagotto, *Magnetic properties and pairing tendencies of the iron-based superconducting ladder $BaFe_2S_3$: Combined ab initio and density matrix renormalization group study*, Phys. Rev. B **94**, 075119 (2016).

R. Cheng, S. Okamoto, and D. Xiao, *Spin Nernst Effect of Magnons in Collinear Antiferromagnets*, Phys. Rev. Lett. **117**, 217202 (2016).

First-Principles Calculation of Vibrational Mode Lifetimes in Complex Materials

Principal Investigator: Murray S. Daw
Dept of Physics and Astronomy, Clemson University, Clemson, SC 29634
daw@clemson.edu

Keywords: anharmonicity, mode lifetimes, frequency shift

Project Scope

Our goal is to explore the anharmonicity of the vibrational modes of complex materials, as exhibited in their frequencies and lifetimes. Our approach is based on calculating moments of the Liouvillian for the system, which can be used to evaluate frequencies and lifetimes. The first milestone was to develop and apply a program to carry out these calculations based on interatomic potentials. We released the resulting wrapper for LAMMPS ("JazzForLAMMPS") used it to study the anharmonicity of carbon nanotubes, fullerenes, and graphene. The second milestone was to develop a similar driver ("JazzForQE") based on Quantum Espresso, a first-principles electronic structure code (LDA). This has recently been achieved and is being used to study anharmonicity in Si and SnSe. The moments-based method has proven to be a computationally efficient tool for studying anharmonicity in complex materials.

Recent Progress

We review results of our studies of anharmonicity in several materials: carbon nanotubes, fullerenes, graphene, and Si. The first three are based on interatomic potentials (Tersoff, LAMMPS) and the last on first-principles electronic structure (LDA, Quantum Espresso).

Radial Breathing Mode of carbon nanotubes is very anharmonic (Tersoff potential)

We find that the radial modes of the CNT are the least anharmonic, except the Radial Breathing Mode which is the most anharmonic of all modes of the tube. Our calculated frequency shifts are in good agreement with results from Raman spectroscopy.

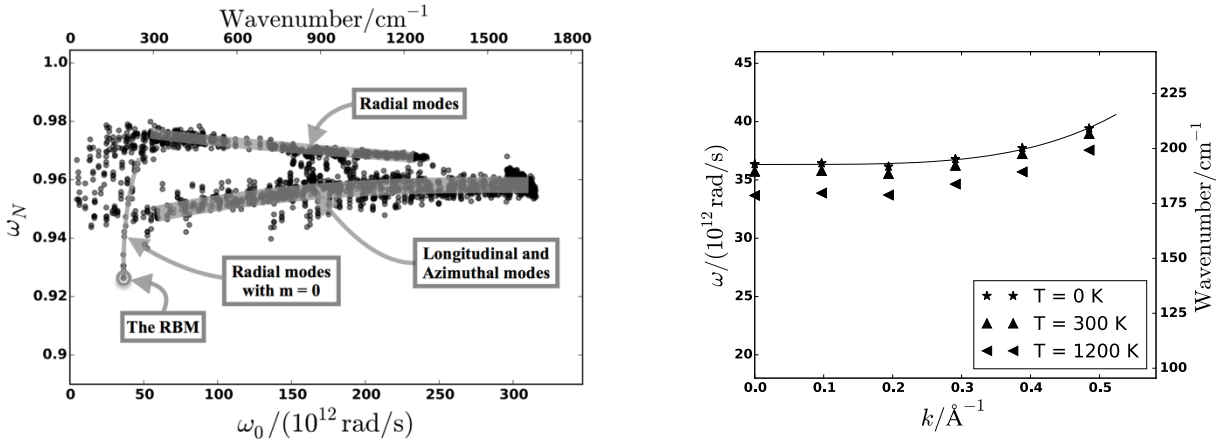

The frequencies of the vibrational modes of a carbon nanotube shift with temperature, revealing their intrinsic anharmonicity. On the left, the frequencies at T=1200K, normalized by their values at T=0K. On the right, the temperature-dependence of modes related to radial breathing mode (RBM).

All modes of fullerenes are uniformly anharmonic (Tersoff potential)

We find that the vibrational modes of fullerenes are uniformly anharmonic. Our results are in good agreement with IR and Raman data.

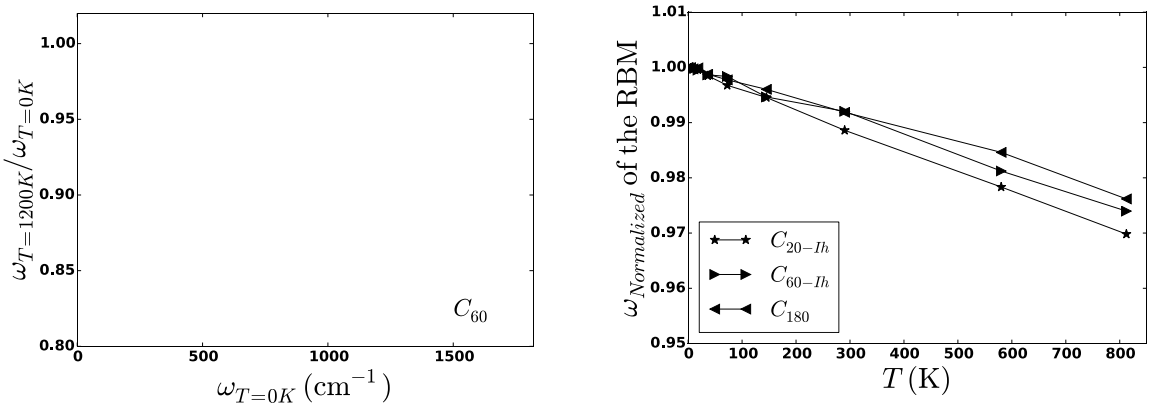

The frequencies of the vibrational modes of fullerenes are uniformly anharmonic. On the left, the frequencies at T=1200K, normalized by their values at T=0K, for a C60 molecule. On the right, the temperature-dependence of the radial breathing mode of several fullerenes.

Anharmonicity renormalizes the dispersion of flexural modes of graphene (Tersoff potential)

We find that the dispersion curves for the flexural modes of graphene are altered by their anharmonic coupling to in-plane modes. At low temperatures the dispersion follows the expected $\omega(k) \propto k^2$, while at higher temperatures the dispersion is renormalized by the anharmonic coupling to $\omega(k) \propto k^{3/2}$. The renormalization of the dispersion has been argued to stabilize flat graphene with respect to wrinkling.

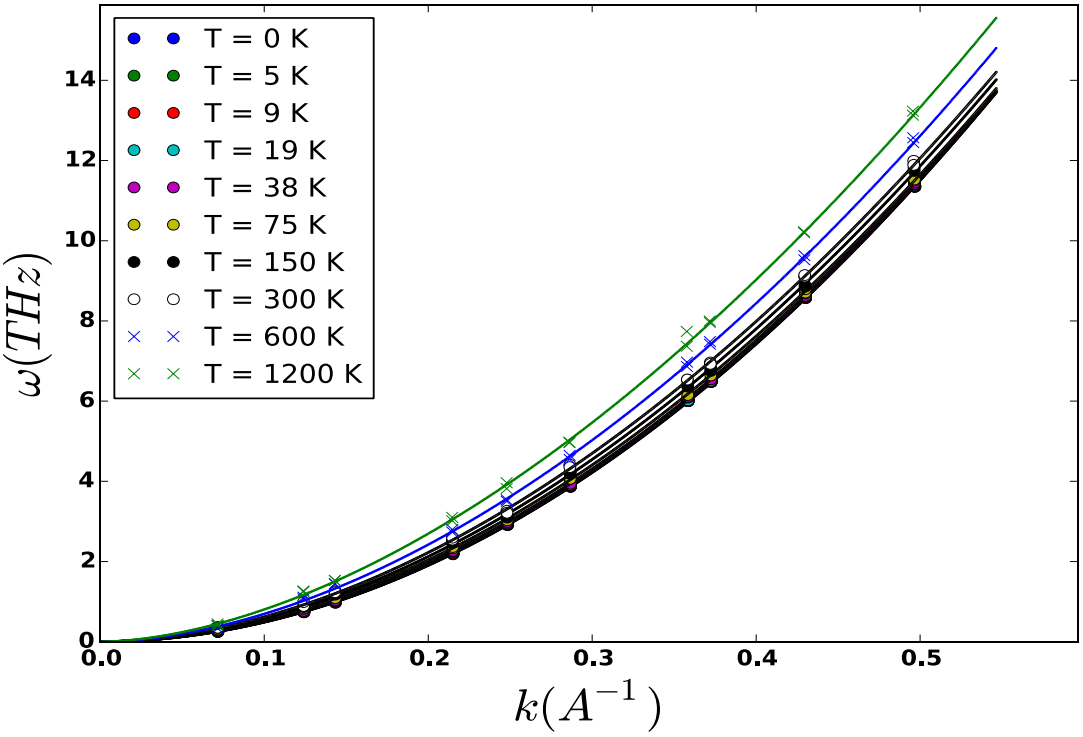

The dispersion w(k) of the flexural mode of graphene is changed in a significant way by its anharmonic coupling to in-plane modes. At low T, the dispersion is quadratic. At high T, the dispersion approaches $\omega(k) \propto k^{3/2}$.

Si is uniformly anharmonic (First principles LDA)

Based on our first-principles calculations, we find that the vibrational modes of Si show a significant shift with temperature, by a factor of at least 7 above what the quasi-harmonic approximation would predict. The modes appear to be uniformly anharmonic, so that the DOS compresses uniformly with temperature. We measure the anharmonicity by the temperature-dependence of the frequency shift: $\alpha = \frac{1}{T}\frac{\omega(T)-\omega(0)}{\omega(0)}$.

The temperature dependence of the mode frequency is a measure of the anharmonicity. We compare our calculated α's to those from a recently INS experiment. The values of α are in 10^(-5)/K.

Mode	LDA	Xpt
TA(X)	-6.8	-6.1
LA/LO(X)	-5.1	-4.9
TO(X)	-5.5	-5.0
O(Γ)	-7.6	-5.0

Future Plans

We are carrying out a modification of the moments method using a more efficient basis function, which we call the Ensemble Eigenstate, which allows a deeper understanding of the anharmonicity. We are continuing the investigation, based on LDA, of the anharmonicity of a series of increasingly more complex materials: Si- and Ge-based clathrates (with and without rattlers), SnSe, PbTe, and several other rocksalts, which generally have been reported experimentally to have enhanced anharmonicity.

References

1. D. Dickel and M. S. Daw, *Improved calculation of vibrational mode lifetimes in anharmonic solids (Part I: Theory)*, Computational Materials Science **47** 698 (2010).

2. D. Dickel and M. S. Daw, *Improved calculation of vibrational mode lifetimes in anharmonic solids (Part II: Numerical Results)*, Computational Materials Science **49** 445 (2010).

3. Y. Gao, D. Dickel, D. Harrison, and M. Daw, *Improved calculation of vibrational mode lifetimes in anharmonic solids (Part III: Extension to Fourth Moment)*, Computational Materials Science **89** 12 (2014).

4. Y. Gao and M. Daw, *Testing the fourth moment approximation of vibrational mode lifetimes in fcc Lennard-Jonesium*, Modeling and Simulation in Materials Science and Engineering **22** 075011 (2014).

5. Y. Gao, H. Wang, and M. Daw, *Calculations of lattice vibrational mode lifetimes using Jazz : a Python wrapper for LAMMPS*, Modeling and Simulation in Materials Science and Engineering **23** 045002 (2015).

Publications (August 2016 – July 2018)

H. Wang and M. Daw, *Anharmonic renormalization of the dispersion of flexural modes in graphene using atomistic calculations*, Phys. Rev. B **94** 155434 (2016).

H. Wang, D. Dickel, and M. Daw, *Theoretical treatment of the anharmonicity of vibrational modes of single-wall carbon nanotubes*, Journal of Raman Spectroscopy **49** 621 (2018).

H. Wang and M. Daw, *Anharmonicity of vibrational modes of fullerenes*, Comp Materials Science **146** 70 (2018).

Theory Institute for Materials and Energy Spectroscopies (TIMES)

T.P. Devereaux, J. J. Rehr, J. E. Moore, B. Moritz, H.-C. Jiang, C.J. Jia, S. C. D. Pemmaraju, F. Vila, and J. J. Kas

Stanford Institute for Materials and Energy Sciences
SLAC National Accelerator Laboratory and Stanford University

Keywords: spectroscopy, x-rays, non-equilibrium, computation

Program Scope

The members of this FWP, also known as TIMES, address cutting-edge problems in materials and energy sciences at next-generation facilities, creating and curating modern codes, developing flexible toolsets, and exploiting applied math methods and algorithm development to enable robust and predictive simulations of spectroscopies. TIMES places a particular emphasis on the science enabled by the west coast light sources: the Linac Coherent Light Source (LCLS) and Stanford Synchrotron Radiation Lightsource (SSRL) at SLAC National Accelerator Laboratory and the Advanced Light Source (ALS) at Lawrence Berkeley National Laboratory (LBNL), with strong synergy to the x-ray scattering/spectroscopy FWP led by T. P. Devereaux, the electronic structure of quantum materials FWP led by Z.-X. Shen, and others in SIMES and beyond.

We will update the following recent progresses at this meeting: i) continued development and implementation of the Corvus workflow tool; ii) extension of the real-time time-dependent density functional theory (RT-TDDFT); iii) development of a perfect hashing algorithm to reduces storage complexity for cluster exact diagonalization wavefunction evaluation; iv) investigating the physics of driven systems in the Floquet regime.

Recent Progress

I. Corvus Workflow Tool

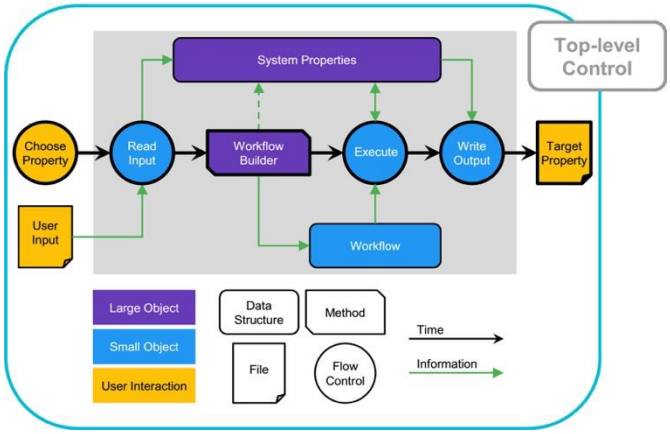

Figure 1: Idealized flowchart for the Corvus workflow tool. Corvus automates most aspects of the standard spectroscopy workflow to create a general purpose, efficient, and end-user friendly experience.

A major thrust of development of our TIMES collaboration has been a python-based package dubbed Corvus, which is designed to facilitate and execute calculations of x-ray spectra using advanced theoretical methods [Story, 2018]. This approach simplifies the development of workflows that combine multiple scientific software packages for various applications. Corvus can be run as an executable script either with a ready-made workflow and input file, or interactively, in order to build custom workflows using a set of Corvus-specific tools. Several prototypical examples have

been developed that link density functional, vibrational, and theoretical spectroscopy codes.

Specialized workflows are needed that exploit the capabilities of multiple codes for evaluation of various spectroscopies. These workflows utilize interchangeable components within the Corvus tool to simplify and control code execution. The input/output capability is provided by Corvus "handlers," which translate the output of one code into the internal Corvus format. Since the internal data format is common, this allows easy linking of various external software packages. Within TIMES, handlers have been developed for FEFF10, NWChem, ORCA, VASP, and ABINIT, allowing users to easily define workflows, e.g., for structural optimization of MD averaged calculations of x-ray spectra.

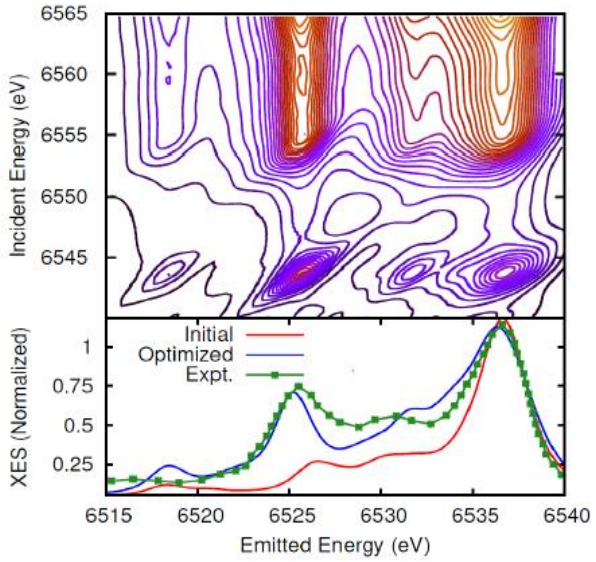

Figure 2: Calculations of RIXS (top) and XAS (bottom) using FEFF with a stucture optimized using ORCA, all integrated within the Corvus workflow tool.

[Story 2018] Corvus: A data-driven framework for interfacing scientific software, S. M. Story, F. D. Vila, J. J. Kas, K. B. Raniga, C. D. Pemmaraju, and J. J. Rehr (U.W. Preprint 2018, submitted to Computer Phys. Communications).

II. Extension of RT-TDDFT

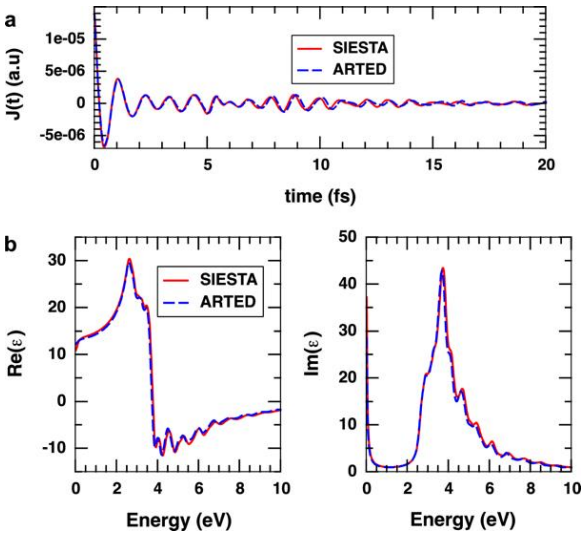

Figure 3: Interaction of a laser pulse and bulk Si in velocity-gauge RT-TDDFT. (a) Magnitude and time-profile of the laser pulse. (b) Time-domain macroscopic current. High-harmonic features show good agreement between the two methods [Pemmaraju2017].

The interaction of laser fields with matter can be modeled efficiently within the velocity-gauge formalism of RT-TDDFT. This approach tends to be more efficient than Green's function methods for large systems, with applicability to non-linear optical response and charge-transfer excitations in x-ray spectra. Our recent work includes the implementation of the velocity-gauge extension of RT-TDDFT within a linear combination of atomic orbitals (LCAO) basis set framework [Pemmaraju2017]. The LCAO framework treats low-energy valence and high-energy core-excitations on an equal footing. Results from this implementation, for both weak and intense laser fields, show excellent agreement with results obtained from established real-space grid and Full-Potential Linearized Augmented Planewave approaches (See Figure 3). Simulations of pump-probe

spectroscopies, utilizing a wide variety of laser pulses from mid-infrared to soft X-ray energies, of particular relevance to LCLS, will be enabled by this extension of RT-TDDFT. The non-perturbative treatment of external laser fields within RT-TDDFT allows for the study of coherent strong-field phenomena, e.g. harmonic generation and light-induced transparency at x-ray frequencies, which allows modeling and interpretation of novel nonlinear x-ray spectroscopies at free electron lasers.

[Pemmaraju2017] Velocity-gauge real-time TDDFT within a numerical atomic orbital basis set, C.D. Pemmaraju, F.D. Vila, J.J. Kas, S.A. Sato, J.J. Rehr, K. Yabana, David Prendergast, Computer Phys. Communications 226, 30-38 (2017).

III. Perfect Hashing Algorithm

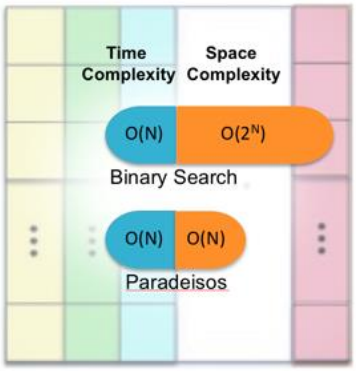

Figure 4: Time and Storage Complexity of the Paradeisos algorithm compared to binary search.

Enumeration of Hilbert space elements can be a time- and memory-consuming process: storing a vector of integer values for the binary occupation number representation of the single-particle basis states for each element of a many-body Hilbert space. Conventional search algorithms, such as binary search, locate the position of an element in this ordered list. However, the memory requirements for storing such an ordered "look-up" list can become a bottleneck. Even large-scale parallelization of the problem still requires storing this vector on each compute node of the simulation. We have designed a perfect hashing algorithm – Paradeisos – which replaces binary search without increasing the computational time complexity, while at the same time leading to substantial savings in aggregate memory usage for distributed parallel computing. The Paradeisos algorithm can be utilized in symmetry-reduced subspaces, and efficiently applied to fermionic, bosonic, and spin quantum many-body systems. These advantages make Paradeisos a promising algorithm to expand the size and dimension of real-space clusters used in the simulation of core-level x-ray spectroscopies, especially in correlated materials [Jia2018].

[Jia2018] C.J. Jia, Y. Wang, C.B. Mendl, B. Moritz, T.P. Devereaux, Paradeisos: A perfect hashing algorithm for many-body eigenvalue problems, Computer Phys. Communications 224, 81 (2018).

IV. The Floquet Regime

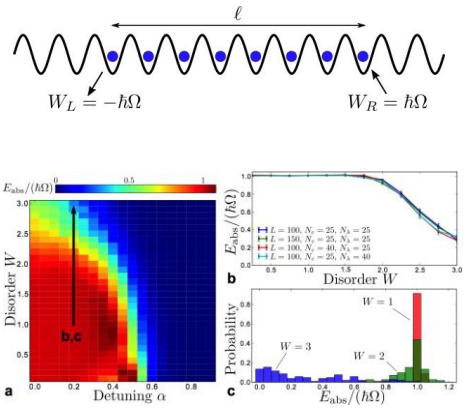

Figure 5: (Top) Schematic of the pumping process. (Bottom) Illustrations of energy quantization that persists even in the presence of relatively large disorder.

Recently, we demonstrated a type of energy pumping in Floquet systems similar to Thouless charge pumping. Under a periodic change of a parameter, a quantized multiple of the electron charge moves from one spatial region to another, e.g. between the ends of a wire, in conventional Thouless

pumping. In [Kolodrubetz2018], we show that a system driven at frequency ω experiences an energy pump at multiples of the energy quantum ħω. This effect should be fairly universal and observable in a variety of systems, easiest at relatively low frequencies in materials with a high degree of microscopic control, such as NV centers in diamond. The ability to pump a specific amount of energy per cycle would lead to a considerably higher degree of control over thermal properties than would be achievable by standard means.

[Kolodrubetz2018] M. H. Kolodrubetz, F. Nathan, S. Gazit, T. Morimoto, and J. E. Moore, Topological Floquet-Thouless energy pump, Phys. Rev. Lett. 120, 150601 (2018).

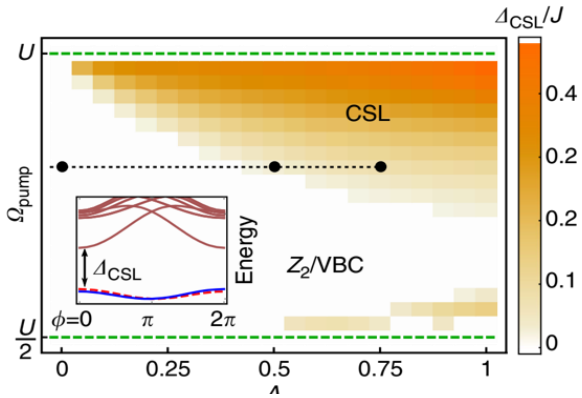

Figure 6: Identification of a photo-induced chiral spin liquid. A putative Z2 spin liquid or valence bond crystal (VBC) transitions into a photo-induced CSL at finite pump strength for frequencies inside the charge gap. Adapted from Ref. [Claassen2017].

Driving a material periodically offers the ability to precisely tailor fundamentally new Hamiltonians, which may stabilize novel phases. Recently, we theoretically demonstrated the use of circularly polarized light to affect these changes and induce a novel chiral spin liquid (CSL) phase [Claassen2017]. The kagome antiferromagnetic materials herbertsmithite, kapellasite, and others display signatures of putative quantum spin liquid (QSL) behavior at low temperatures; and their strong Coulomb repulsion limits absorption and the effects of heating, such that new terms in the Hamiltonian can produce the desired effects. For these models, pumping non-resonantly with circularly polarized light breaks time reversal and promotes a scalar-spin-chirality term in the Hamiltonian, which stabilizes the CSL: a topologically-ordered QSL similar to the bosonic ν=½ fractional quantum Hall state with gapped semion excitations that may form the basis for fault-tolerant quantum computation.

[Claassen2017] M. Claassen, H.-C. Jiang, B. Moritz, and T. P. Devereaux, Dynamical time-reversal symmetry breaking and photo-induced chiral spin liquids in frustrated Mott insulators, Nature Comm. 8, 1192 (2017).

Time-dependent phenomena in correlated materials

Principal Investigator: Adrian Feiguin
Department of Physics, Northeastern University
a.feiguin@northeastern.edu

Project Scope:

Strongly correlated electronic materials, also referred-to as "quantum materials", are systems where several phases compete producing extremely complex many-body states. Although a single phase may dominate the ground state, competing instabilities are often hidden at higher energies, which can be accessible with intense ultrafast pulses of light. Experimentalists can probe the system's dynamics by shaking it with a pulse of light, which allows them to access states that are not accessible via finite-temperature experiments. These types of non thermal states often contain coexisting orders that are not usually present in the standard ground or thermal states, making a remarkable difference in the way the system evolves after photoexcitation.

In addition, manipulating properties of materials via light has opened a realistic and reliable route to study selected emergent states in complex systems such as superconductors, organic charge-transfer solids, Mott and charge density wave insulators, and others. Examples include: photo-induced phase transitions, real-space scanning of molecular orbitals, control over dissociation of molecules, study of ionic and electronic motion, melting of ordered states like in superconductors, as well as the analysis of magnetic and charge order.

The present project aims at studying models and time-dependent processes to understand light-matter interaction in strongly correlated materials, and the interplay between electronic, orbital, vibrational, and spin degrees of freedom. The time-scales involved in the creation and recombination of excitons, or the relaxation of the system after a perturbation, will be dictated by the the way light couples to the different excitations, and how these excitations exchange energy and momentum. Our research will advance our understanding of these processes (related to photochemistry, opto-electronics, and light-harvesting applications), and the interpretation of different equilibrium and time-resolved spectroscopies.

The method of choice to study time-dependent phenomena is the time-dependent density matrix renormalization group (tDMRG), which was co-developed by the PI, and has had a remarkable success expanding our knowledge of correlation effects to the time-domain.

Recent progress:

Finite temperature spectral function of Mott insulating chains: **T**he physics of one-dimensional metals can generally be described in terms of Luttinger liquid(LL) theory: natural excitations are collective density fluctuations that carry either spin ("spinons"), or charge ("holons"). A fermion injected into the system breaks down into excitations carrying different quantum numbers, each with a characteristic energy scale and. Whereas the low-energy physics of the one-dimensional (1d) Hubbard model below half filling is described in terms of LL theory, at half filling (density of particles n = 1, or number of particles N = L) the model has a Mott insulating ground state, with a charge gap but gapless spin excitations. Mott insulators defy conventional paradigms, since the rigid band picture underlying the physics of semiconductors does not apply: in strongly interacting systems, the "bands" change with doping, giving rise to a complex phenomenology that includes

hole pockets, Fermi arcs, and kinks. Our group has focused on investigating the non-equilibrium and finite-temperature properties of this system. In particular, two problems draw our attention: (i) is it possible to independently excite charge and spin via a conveniently designed driving protocol? (ii) What physics emerges at finite temperatures when one of these degrees of freedom is thermalized. Our goal is attack these questions by means of both, state-of-the-art computational methods, and by developing analytical approaches that could shed light on the mechanisms taking place. We have studied the dynamical response of the half-filled one-dimensional Hubbard model for a range of interaction strengths U and temperatures T by a combination of numerical and analytical techniques. Using tDMRG computations we find that the single-particle spectral function undergoes a crossover to a spin-incoherent Luttinger liquid regime at temperatures $T \sim J = 4t^2/U$ for sufficiently large $U > 4t$. At smaller values of U and elevated temperatures the spectral function is found to exhibit two thermally broadened bands of excitations, reminiscent of what is found in the Hubbard-I approximation. The dynamical density-density response function is shown to exhibit a finite-temperature resonance at low frequencies inside the Mott gap, with a physical origin similar to the Villain mode in gapped quantum spin chains. We complement our numerical computations by developing an analytic strong-coupling approach to describe the spin-incoherent regime.

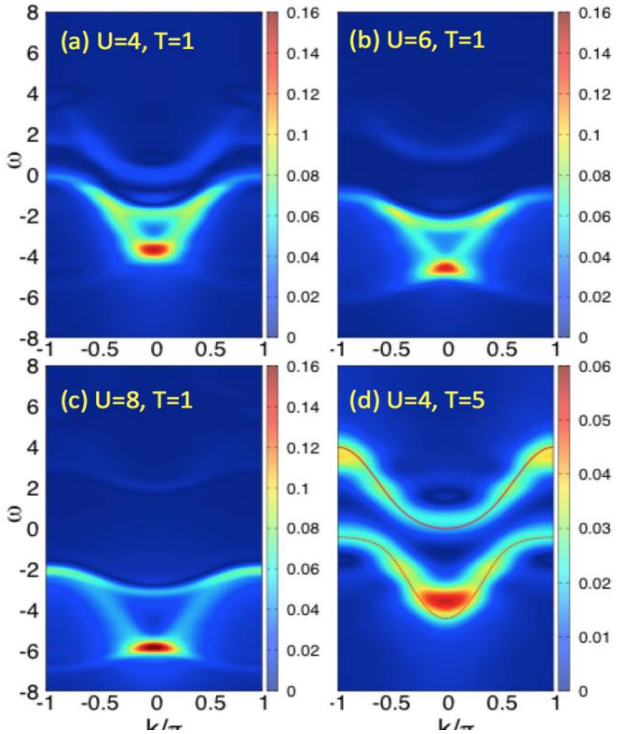

Figure 1 Photoemission spectrum for the 1d Hubbard model with U/t = 4,6,8 and T = 1 calculated with tDMRG. In panel (d) we show results for U = 4 and T = 5. We have included the dispersion obtained from the Hubbard-I approximation.

Unconventional fermionic paired states in a driven Hubbard model: We studied of the one-dimensional attractive fermionic Hubbard model under the influence of periodic driving, demonstrating that the system can be driven into an unconventional paired state with a quasi-condensate with a finite center-of-mass momentum similar to a Fulde-Ferrell state. We show that the momentum of the condensate can be finely tuned by changing the ratio between the amplitude and the frequency of the driving. In particular, by tuning to the value corresponding to suppression of the tunneling, we are able to freeze the condensate. Our work offers the possibility of engineering and controlling unconventional paired states in fermionic condensates.

Efficiency of fermionic quantum distillation: The term distillation refers to the dynamical, spatial separation of singlons and doublons in the sudden expansion of interacting particles in an optical lattice, i.e., the release of a cloud of atoms from a trapping potential. Remarkably, quantum distillation can lead to a contraction of the doublon cloud, resulting in an increased density of the doublons in the core region compared to the initial state. We show that this phenomenon is not limited to Hubbard chains that were previously studied. Interestingly, there are additional

dynamical processes on the two-leg ladder such as density oscillations and self- trapping of defects that lead to a less efficient distillation process.

The breakdown of the Mott insulator: unconventional excitonic condensates and orbital selective superconductivity in multi-orbital systems: It has become more evident that a multi-orbital approach is required in many problems of interest, such as high-temperature superconductivity and transition metal oxides. We studied the photoinduced breakdown of a two-orbital Mott insulator and resulting state. We presented a comprehensive study of a one-dimensional two-orbital model at and below quarter-filling: we find that it realizes an excitonic density wave in which excitons quasi-condense with finite center of mass momentum and an order parameter that changes phase with wave-vector *Q*. In addition, excitons can pair to form bi-excitons in a state that is close to a charge density-wave instability. When pairing dominates over the inter-orbital repulsion, we encounter a regime in which one orbital is metallic, while the other forms a spin gapped superconductor, a genuine orbital selective paired state. By assuming a quasi-classical approximation, we have solved the three-body hole-electron-spinon problem and shown that excitons are held together by forming a bound state with spinons. In order to preserve the antiferromagnetic background, excitons acquire a dispersion that has a minimum away from k=0. The introduction of Hund coupling leads to the creation of doublon-holon pairs. These unconventional "Hund excitons" correspond to bound spin-singlet orbital-triplet doublon-holon pairs. The mechanism responsible for these excitons is the inter-orbital pair-pair interaction which is ignored in many cases.

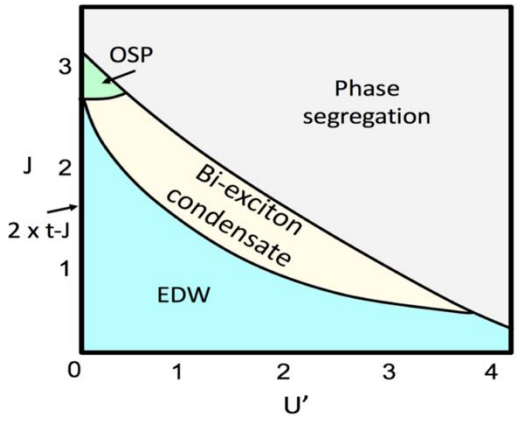

Figure 2 Schematic phase diagram of the two orbital t-J model as a function of U' and J for fixed densities N_1/L = 3/4, N_2/L = 1/4. Along the U' = 0 line the system consists of 2 copies of a t–J chain at different densities. Finite values of U' induce the formation of an exciton density wave (EDW), and increasing J drives an instability toward pairing of excitons (bi-exciton condensate). At small values of U' and large values of J we find the orbital selective paired phase (OSP).

Quantum Magnetism: Using a recently developed completely unbiased and controlled numerical method to solve quantum impurity problems in *d*-dimensional lattices, we studied the competition between indirect exchange and Kondo effect on multiple substrates, including graphene, phosphorene, and topological insulators. We demonstrated the limitations of conventional techniques and put in evidence dramatic non-perturbative many-body effects that defy conventional wisdom. In particular, Kondo effect many times dominates over indirect exchange hindering magnetic order, particularly ferromagnetism. In addition, we have been collaborating with experimental groups in Los Alamos National Lab, Argonne and Brookhaven to understand the rich physics that emerges at high magnetic fields. The interplay between frustrating interactions and high magnetic fields leads to a rich zoo of new phases of quantum origin, with novel excitations. Numerical calculations are aiding experimentalists, helping to identify these phases and to understand their properties.

Planned activities:

Time-resolved tunneling spectroscopy: In a time-resolved experiment one seeks to identify the occupation of each energy eigenstate as a function of time, after the system has been excited

throught a light pump. We propose to carry out a hybrid method combining ideas from the aforementioned setups: after the system has been photoexcited, we allow for electrons to tunnel into an empty parallel wire which has been set at a given gate voltage. Only electrons at a particular energy V can hop. We obtain momentum resolution by simply calculating the occupation of each state, i.e. the momentum distribution function of the probe wire.

Photoexcitation of electronic instabilities in one-dimensional strongly correlated systems: In order to understand the mechanisms behind exciton recombination, we will create excitons by either applying a pump or quenching the interactions, and study the equilibrium and non-equilibrium optical absorption spectrum at half-filling using tDMRG. In addition, we will change the curvature of the Hubbard bands by introducing a second-neighbor hopping, which breaks particle-hole symmetry. This would allow us to quantify the effects of the indirect Auger processes in terms of the relative mass of the doublons and holons. In a separate simulation, we will conduct a real-time study of the excitation propagation and relaxation in real- space, as a function of the interactions (i.e., the Mott gap). In order to enhance phonon-assisted recombination, we will also introduce acoustic phonons, and consider the effects of the Peierls instability. Previously ignored is the effect of impact ionization. Impact-ionization is a three-particle generation process in which an electron (or hole) in the conduction (or valence) band gains its energy by external electric fields and becomes so highly energetic that it can create an electron-hole pair by colliding with an electron in the valence band and exciting it to the conduction band.

Role of the photoexcited electron in RIXS: Typically, in order to simplify the problem, numerical and analytical treatments consider a single band approach in which the core hole acts as an effective potential. In all the theoretical formulations of RIXS, the intermediate dynamics of the excited electron- hole pair is basically ignored. We will study the dynamics of the excitations using time-resolved tunneling to understand the processes in the d band after the excitation is created. The results of these studies will help to unveil the physics of the p electron and its role in the screening mechanism. This is a complex multi-band many-body calculation that will shed light on the relevant processes in X-ray spectroscopies, and help guide theory toward a realistic description of RIXS experiments.

Selected Publications:

DOE Support explicitly acknowledged as "U.S. Department of Energy, Office of Basic Energy Sciences, grant DE-SC0014407" in a total of 14 publications.

1. "Spinon Confinement and a new Longitudinal Mode: Coupled Spin Chains in Yb_2Pt_2Pb"; W. J. Gannon, L. S. Wu, I. A. Zaliznyak, A. E. Feiguin, A. M. Tsvelik, F. Demmel, Y. Qiu, J. R. D. Copley, and M. C. Aronson, Nature Communications (under review).
2. "Excitonic density-waves, biexcitons and orbital-selective pairing in a two-orbital correlated chain"; Chun Yang and A. E. Feiguin. Phys. Rev. B (in press).
3. "Finite temperature dynamics of the Mott insulating Hubbard chain"; A. Nocera, F. H. L. Essler, and A. E. Feiguin, Phys. Rev. B **97** 045146 (2018).
4. "Photoinduced Hund excitons in the breakdown of a two-orbital Mott insulator"; Julian Rincon, E. Dagotto, A. E. Feiguin, Phys. Rev. B. **97**, 235104 (2018).
5. "Efficiency of fermionic quantum distillation"; J. Herbrych, A. E. Feiguin, E. Dagotto, and F. Heidrich-Meisner, Phys. Rev. A **96**, 033617 (2017).

Competing Orders in Correlated Materials: Impact of Disorder and Non-Equilibrium Perturbations

Principal Investigator: Rafael M. Fernandes (rfernand@umn.edu)
School of Physics and Astronomy, University of Minnesota, Minneapolis, MN 55455

Keywords: Competing phases, unconventional superconductivity, non-equilibrium physics, disordered systems, quantum phase transitions

Project Scope

The goal of this project is to explore, understand, and ultimately control the competing electronic ordered states ubiquitously present in correlated materials, with particular emphasis in unconventional superconductors, such as iron-based and copper-based materials. While on the one hand the competition with different types of magnetic, orbital, and charge order limits the transition temperatures of these unconventional superconductors, on the other hand the enlarged ground-state degeneracy associated with these multiple many-body instabilities can give rise to unusual inhomogeneous correlated normal states, such as electronic smectic and nematic phases. To achieve the aforementioned goals, the PI employs a multi-faceted theoretical approach consisting of: (i) The investigation of relatively unexplored regimes with the potential to unveil novel behaviors – in particular, the study of competing phases taken out of equilibrium to determine under which conditions the transition temperatures of iron-based and copper-based materials can be enhanced by optical pulses. (ii) The embracement of realistic features of correlated materials in their microscopic descriptions – in particular, the investigation of the impact that disorder, in its various forms, has on emergent inhomogeneous states present in the phase diagrams of unconventional superconductors. (iii) The promotion of synergy with established and novel experimental probes (with particular emphasis on scanning tunneling microscopy and ultrafast spectroscopy) not only by using data as input of theoretical models, but also by providing concrete guidance for experiments.

Recent Progress

Quantum Monte Carlo simulations of the interplay between anti-ferromagnetism and superconductivity – One of the hallmarks of the phase diagrams of correlated materials is the presence of putative quantum critical points, i.e. second-order phase transitions that are tuned to zero temperature by changes in an external parameter. In many unconventional superconductors, such as cuprates and iron pnictides, the superconducting (SC) dome is often observed near a putative anti-ferromagnetic (AFM) quantum critical point, suggesting a close relationship between these two rather distinct types of electronic order. The theoretical elucidation of this relationship is often hindered by the strong-coupling and non-perturbative nature of the problem, which renders many of the standard theoretical methods questionable at best. To shed new light on this problem, in two works led by former student Dr. X. Wang and in collaboration with the group led by Prof.

E. Berg (Chicago/Weizmann), unbiased Quantum Monte Carlo numerical simulations were performed on an effective low-energy model (called spin-fermion model) in which electrons interact with each other only via the exchange of AFM fluctuations. The key insight was to consider a two-band spin-fermion model, as it does not suffer from the infamous fermionic sign-problem. This allows one not only to perform extensive and systematic simulations down to very low temperatures, but also to compare with different uncontrolled analytical approximations, thus bridging numerics and analytics. In Ref. 8, it was shown that the SC state emerging in the vicinity of the AFM quantum critical point is governed by special regions of the Fermi surface called hot spots, and rather insensitive to global properties of the Fermi surface (such as the density of states). In particular, it was found a rather large transition temperature, of the order of 1% of the bandwidth, that scales as the relative angle between the Fermi velocities of a pair of hot spots. In Ref. 2, the issue of whether charge order (CO) also emerges near the AFM quantum critical point was addressed (see Fig. 1). The results show that the same interactions that promote unconventional SC also promote a "d-wave" type of charge order. By fine-tuning the band structure to half-filling, the simulations revealed a degeneracy between SC and CO, which is a manifestation of an emergent SU(2) symmetry of the Hamiltonian. However, this degeneracy is very fragile: while small deviations from half-filling strongly suppress CO, SC remains rather robust.

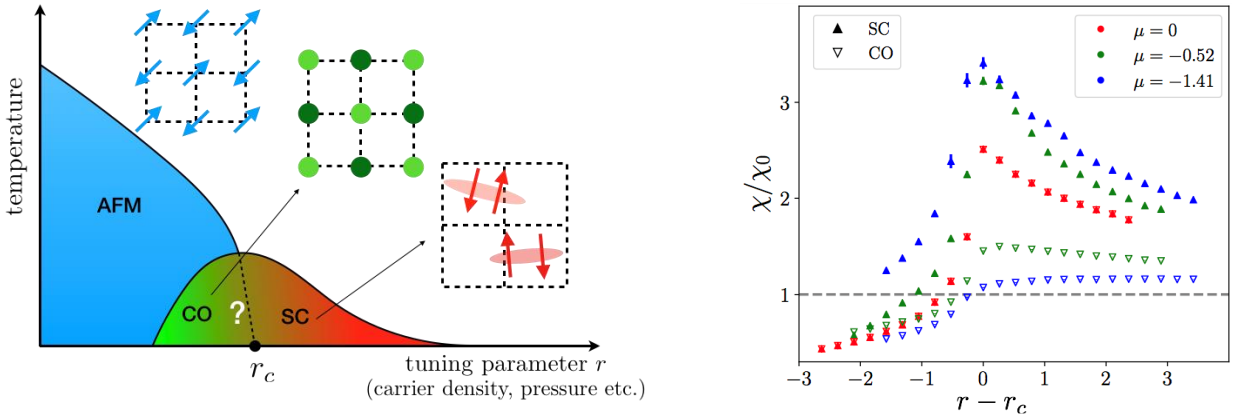

Figure 1: (left) Schematic phase diagram with charge order (CO) and superconductivity (SC) emerging near an anti-ferromagnetic (AFM) quantum critical point. (right) SC and CO susceptibilities extracted from Quantum Monte Carlo simulations of the two-band fermion model for different chemical potential values μ (Ref. 2).

Manipulation of competing orders via non-equilibrium acoustic phonons – The remarkable advances in pump-and-probe ultrafast techniques opened a new route to investigate and manipulate quantum materials. A popular approach consists of the coherently exciting optical phonons by optical pulses to manipulate the electronic properties of the system via the electron-phonon coupling. In Ref. 7, in collaboration with the former postdoc Dr. M. Schuett, Prof. A. Levchenko (Wisconsin), and the former postdoc Prof. P. Orth (Iowa State), the PI proposed a new approach that involves not optical, but acoustic phonons. A non-equilibrium population of acoustic phonons can be excited and controlled by ultrafast manipulation of strain in interfaces and heterostructures, using e.g. shock waves. In contrast to the case of optical phonons, where the transferred energies are larger, heating is expected to be weaker in the case of acoustic phonons. More importantly, it

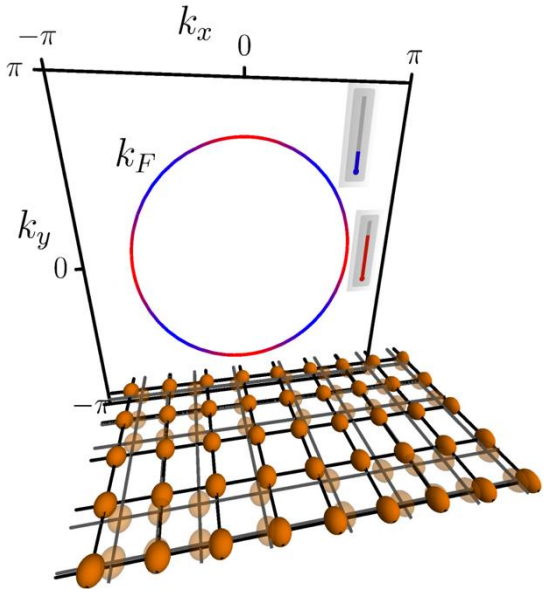

Figure 2: Excitation of non-equilibrium acoustic phonons (bottom panel) leads to an anisotropic redistribution of electronic states at the Fermi surface (top panel), which is manifested as an effective momentum-dependent temperature (red and blue colors). From Ref. 7.

was shown that the anisotropic propagation of the non-equilibrium acoustic phonons leads to an anisotropic redistribution of the low-energy electronic states near the Fermi level. Solution of the Boltzmann equation demonstrated that this redistribution is manifested as an anisotropic effective temperature experienced by the electrons, i.e. an effective temperature that is different in distinct regions of the Fermi surface (see schematic Fig. 2). Therefore, because different types of electronic order are not affected equally by all Fermi-level states, this allows one to selectively melt one among several competing orders. This was shown explicitly by computing, via the Keldysh formalism, the steady-state phase diagram of competing spin-density wave and superconducting orders. The latter was found to be enhanced by selectively melting the former via the excitation of an appropriate non-equilibrium acoustic phonon distribution. Still in what concerns non-equilibrium superconductivity, in Ref. 5, the PI developed, together with the student T. Cui and Prof. P. Orth, a semi-phenomenological model that captures the effects of damping on the gap oscillations of superconductors taken out of equilibrium by strong optical pulses with sub-gap frequencies. This model successfully describes the puzzling time evolution of the gap function of NbN observed experimentally by the group of Prof. J. Wang (Ames Lab).

Impact of disorder on the nematic quantum critical point – Electronic nematic order arising from the partial melting of a density wave, as observed in several quantum materials, is perhaps the most well-known example of vestigial order, i.e. a composite symmetry-breaking order that can condense even when the primary order parameter is uncondensed. Together with Prof. J. Schmalian (Karlsruhe) and Prof. P. Orth (Iowa State), the PI reviewed in Ref. 4 the concept and applications of vestigial order, and also established a firm group-theoretical framework to generalize it beyond

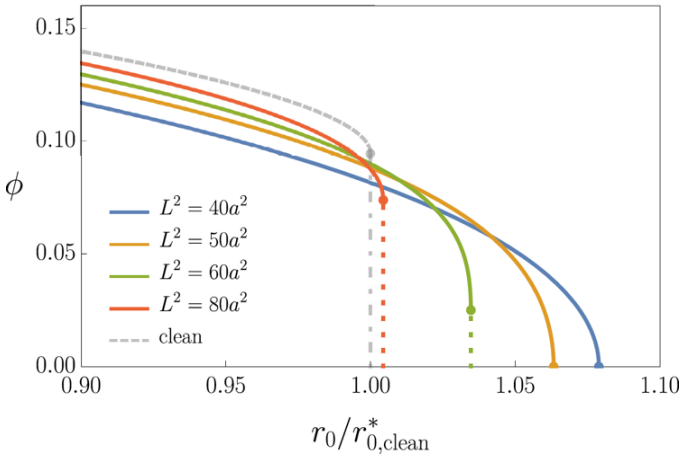

Figure 3: Nematic order parameter inside a finite droplet of linear size *L*, at zero temperature, as function of the distance to the nematic quantum phase transition of the clean system ($r^*_{0,clean}$). From Ref. 6.

nematicity. An important issue that remains little explored is the fate of vestigial nematic order in the presence of disorder, which is always present in the systems where nematicity is observed. In Ref. 6, together with the student T. Cui, the PI addressed the fate of the vestigial nematic quantum phase transition in a disordered system. In the clean case, the quantum transition is known to be first-order and simultaneous to the primary density-wave transition, implying that there is no quantum criticality. The PI found, however, that disorder completely changes this behavior. The reason is because long-range nematic order can be stabilized at finite-size droplets at zero temperature due to the dissipative quantum dynamics, whereas long-range density-wave order cannot. Interestingly, droplets of moderately large sizes order first, even before the bulk system (see Fig. 3). Importantly, nematic order undergoes a second-order transition inside these moderate droplets, in contrast to the first-order transition of the bulk system and of the very large droplets. As a result, the nematic and density-wave quantum transitions split. The outcome is the emergence of an inhomogeneous nematic phase which onsets at a smeared quantum critical point.

Future Plans

Quantum Monte Carlo simulations of purely electronic models – Together with the postdoc Dr. M. Christensen, the Quantum Monte Carlo simulations will be extended beyond the spin-fermion model. In particular, multi-band electronic models will be considered that do not suffer from the sign problem, and in which superconductivity, anti-ferromagnetism, and electronic nematicity, arise from the same interactions. In contrast to the spin-fermion model, in which AFM fluctuations arise from high-energy degrees of freedom, in these purely electronic models the AFM and SC instabilities both arise from the low-energy states. The PI and collaborators will contrast the interplay between AFM and SC in both the regimes of weak and strong interactions, and also establish the relevant properties of the non-interacting band structure that support a high-T_c state.

Non-equilibrium enhancement of superconducting and nematic orders – In collaboration with the student T. Cui and the former postdocs Prof. P. Orth and Dr. M. Schuett, the PI will perform extensive investigations of the dynamics of multi-band superconductors. Particular focuses will be to contrast the gap oscillations of quenched single-band and unconventional multi-band superconductors, as well as the manipulation of gap nodes by ultrafast optical pulses. With the postdoc Dr. M. Christensen and the collaborator Dr. A. Klein, the PI will also study how infrared-active optical phonons can be coherently excited to enhance or even condense nematic order in systems close to a nematic instability.

Intertwined orders in iron-based superconductors – With the postdoc Dr. M. Christensen and former postdoc Dr. J. Kang, the PI will apply the group-theoretical formalism developed in Ref. 4 to the case of iron-based superconductors, taking into account the presence of the glide-plane symmetry and of the sizable spin-orbit coupling. The PI and collaborators will classify all vestigial intertwined orders arising from the magnetic degeneracy of these compounds, which was previously established in Ref. 1. Special attention will be given on the entanglement between spin and orbital degrees of freedom in the different types of $\mathbf{q} = \mathbf{0}$ vestigial orders.

Publications (August 2016 – July 2018)

A list of ten selected publications follows bellow.

1. M. H. Christensen, P. P. Orth, B. M. Andersen, and R. M. Fernandes. *Emergent magnetic degeneracy in iron pnictides due to the interplay between spin-orbit coupling and quantum fluctuations.* arXiv:1712.07188, accepted for publication in Phys. Rev. Lett. (2018).

2. X. Wang, Y. Wang, Y. Schattner, E. Berg, and R. M. Fernandes. *Fragility of charge order near an antiferromagnetic quantum critical point.* Phys. Rev. Lett. **120**, 247002 (2018)

3. J. Kang, R. M. Fernandes, and A. V. Chubukov. *Superconductivity in FeSe: the role of nematic order*. Phys. Rev. Lett. **120**, 267001 (2018).

4. R. M. Fernandes, P. P. Orth, and J. Schmalian. *Intertwined vestigial order in quantum materials: nematicity and beyond*. arXiv:1804.00818, invited review article submitted to the Annual Review of Condensed Matter Physics (2018).

5. T. Cui, X. Yang, C. Vaswani, J. Wang, R. M. Fernandes, and P. P. Orth. *Impact of damping on superconducting gap oscillations induced by ultra-strong Terahertz pulses*. arXiv:1802.09711 (2018).

6. T. Cui and R. M. Fernandes. *Smeared nematic quantum phase transitions due to rare-region effects in inhomogeneous systems.* arXiv:1801.01988 (2018).

7. M. Schütt, P. P. Orth, A. Levchenko, and R. M. Fernandes. *Controlling competing orders via non-equilibrium acoustic phonons: emergence of anisotropic electronic temperature.* Phys. Rev. B **97**, 035135 (2018).

8. X. Wang, Y. Schattner, E. Berg, and R. M. Fernandes. *Superconductivity mediated by quantum critical antiferromagnetic fluctuations: the rise and fall of hot spots.* Phys. Rev. B **95**, 174520 (2017).

9. G. Zhang, J. K. Glasbrenner, R. Flint, I. I. Mazin, and R. M. Fernandes. *Double stage nematic bond-ordering above double stripe magnetism: application to $BaTi_2Sb_2O$.* Phys. Rev. B **95**, 174402 (2017).

10. J. Kang and R. M. Fernandes. *Superconductivity in FeSe thin films driven by the interplay between nematic fluctuations and spin-orbit coupling*. Phys. Rev. Lett. **117**, 217003 (2016).

Thermal and thermoelectric phenomena in novel materials and systems of disordered and interacting electrons

Principal investigator: Professor Alexander Finkel'stein
Department of Physics and Astronomy, Texas A&M University
College Station, TX 77843-4242
finkelstein@physics.tamu.edu

Project Scope

The current DOE sponsored research focuses on the theoretical analysis of thermal transport in systems where the heat transport is special. Of particular interest are electron systems, which exhibit elements of the non-Fermi liquid behavior owing to disorder, and novel systems like Van der Waals heterostructures.

Recent Progress

Below we describe the progress made in the past year in studying physical properties of a graphene layer placed on a disordered substrate. The PI, with his two former PhD students, identified graphene layer on a disordered substrate as a system where Anderson localization of the out of plane vibrations (flexural phonons) could be observed [1]. Flexural phonons (FPs) are a unique addition that Van der Waals heterostructures have brought into microscopic physics. Usually, FPs are considered in the context of the suspended graphene. However, Van der Waals nature of the interaction of the graphene sheet with a substrate provides an interesting possibility to observe the FPs even in *supported* graphene.

In the case of the SiO_2 substrate, for a typical magnitude for corrugations, the graphene layer is partially detached from the substrate. As a result, the layer is suspended between hills of the substrate. In such a *pinned-suspended* flexible layer, flexural phonons (FPs) are scattered by pinning centers induced by a substrate. The main point here is that the pinning centers introduce energy barriers of a finite height for the flexural modes. As a result, a flexural phonon with a small energy cannot enter the area of pinning. Remarkably, the elastic scattering rate of the FPs tends to a finite value for a vanishing wave vector. One may, therefore, expect localization of the FPs, similar to electron localization in two dimensions. We confirmed this idea by calculating statistical properties of the FPs for a model of elastic sheet in the presence of the pinning centers. Finally, we discussed possible manifestations of the FPs, including the *localized* ones, in the thermal conductance. We argued in Ref. 1 that the FPs, and the fact of their localization, might lead to important implications for the thermal transport in graphene on a corrugated substrate.

Flexural Phonons in supported graphene: from pinning to localization

A general question was addressed: If to compare with electrons propagating in a disordered sample, will the statistical properties of the eigenmodes of the pinned elastic layer be the same or

different? The question makes sense because for FPs in a pinned-suspended sheet there is no analogue of the on-site disordered potential *W*. Instead, there is concentration of the pinned sites. Furthermore, the FPs are described by the square of the Laplacian, rather than by the Laplacian in the case of electrons. To understand the general properties of the FPs in the presence of random pinning scatterers, we solved the equation of motion for the out-of-plane displacements for samples with periodic boundary conditions of the size up to 200×200 sites. Eigenmode profiles at two representative energies are shown on Fig. 1:

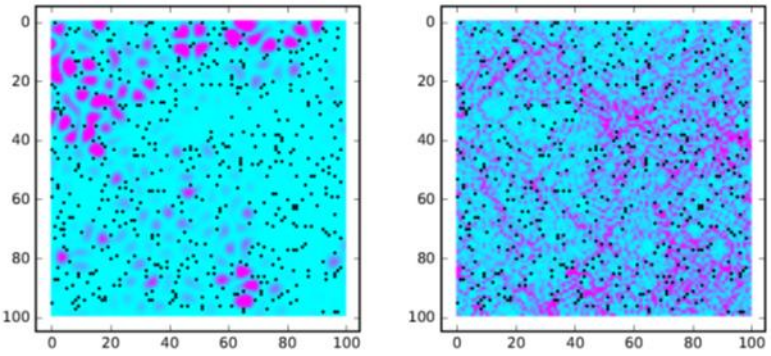

Figure 1: The intensity of the phonon wavefunctions for 5% of the pinned sites at two different energies. Pinned sites are indicated as dots. At a small energy (left panel) the wave function is sparse. At larger energy (right panel) the fractal character of the wave function is clearly seen.

We estimated the energy scale of *strong* localization of the FPs, ω_{loc}^{str}, (that is when the phonon energy is less than the elastic scattering rate, $\omega(k) < \tau^{-1}$) for a graphene layer on the top of the SiO_2 to be a fraction of 1K.

When existence of rather different wave functions was established, the next question aroused is there a transition at a certain energy from localized to delocalized FPs (i.e., the "metal-insulator" transition with the mobility edge), or there is a crossover from strong to weak localization, like for *2d* electrons? To figure this out, we proceeded as follows: We studied the dependence of the Inverse Participation Ratio (IPR) on the sample size *L* for various phonon energies. From the size dependence of the IPR at a given energy, we found an energy-dependent fractal dimension D_2. [For disordered electronic system, the fractal dimension is determined by the conductance $g_{\square}$. In the case of the Gaussian Orthogonal Ensemble (GOE), the size dependence of the IPR is described by the fractal dimension D_2 equal to $D_2 = 2 - 2/\pi g_{\square}$.] For each concentration (%) of the pinned sites we extracted for different energies ω the corresponding value of the *"phonon conductance"*, $g_{ph}(\%, \omega)$, using the expression for the fractal dimension D_2 for electrons. For disordered electrons, the well-developed theory connects the behavior of various physical quantities with the value of the conductance. We calculated numerically the same quantities for the FPs, using the

values g_{ph} extracted from IPR, and found an excellent agreement with the theoretical predictions existing for disordered electrons with $g_{\square} = g_{ph}(\%, \omega)$, see Figs. 2 and 3:

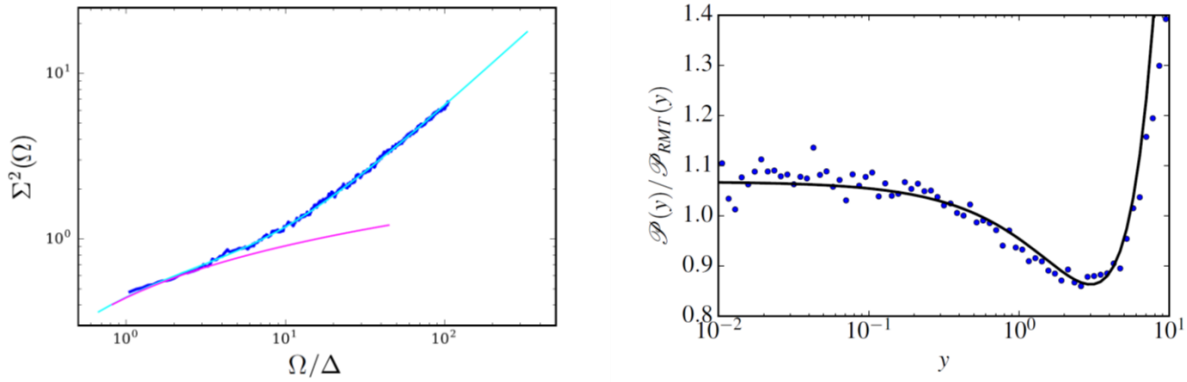

Figure 2 (left): Blue dots: level number variance, $\Sigma^2(\omega, \Omega) = \langle N^2(\Omega)\rangle - \langle N(\Omega)\rangle^2$, in a sample 200×200 with 20% of the pinned sites. The theoretical fit with $g_{\square} = g_{ph} = 1.6$ is plotted by a solid line in cyan. The RMT result is given in magenta. The numerical results presented in Fig. 2 are in full accord with the theoretical expression obtained by the PI and coauthors [1] for disordered electrons in $d = 2$.

Figure 3 (right): Blue dots: the intensity distribution $\mathcal{P}(y)$, i.e., the distribution of the amplitudes of the eigenmodes ψ^2, calibrated with respect to the RMT result, for 10% of the pinned sites. Solid line: fit with the existing theory for disordered electrons with $g_{\square}$ =5.63 and $L/l = 5$.

To summarize, we have calculated numerically a number of quantities characterizing statistical properties of FPs in the pinned flexible layer using the values for g_{ph} extracted from the data for the IPR, and found a very good agreement with the theoretical predictions existing for the disordered electrons in $2d$. Figs. 2 and 3 justify that for the FPs the regime of the weak localization is the same as for the disordered electrons.

Thermal transport in graphene at low temperatures

Graphene layers on top of SiO_2 are expected to play an important role in applications related to thermal transport and for ultrasensitive bolometry. However, the physics of electron overheating in graphene on SiO_2 at low temperatures has not been fully understood, yet. In a number of low temperature measurements (although not always), the heat flux from electrons to the environment (i.e., phonons) has been found to be $\propto T_{el}^3$ (correspondingly, the reversed flux from the phonons to electrons is $\propto T_{ph}^3$). An explanation of the exponent $\delta = 3$ in terms of the interaction of electrons with the acoustic phonons requires using an expression obtained for *unscreened* deformation potential. At concentrations of the electric carriers, electrons or holes, $n \sim 10^{12} cm^{-2}$ and low temperatures, the assumption of the unscreened deformation potential is not realistic. By contrast,

theoretically, the heat flux from electrons to the FPs is known to be $\propto T_{el}^3$. We consider the heat exchange with the FPs as a reasonable explanation of the exponent $\delta = 3$ observed in experiments at low temperatures and *far away* from the neutral point.

Moreover, we believe that the existence of localized FPs may explain the experimental observation of the Caltech group (Phys. Rev. X 3, 041008, 2013) for cooling rate of graphene at temperatures $T < 0.85$K. In this regime, the cooling is dominated by the electron heat diffusion along the sample. However, the Lorenz number $\mathcal{L}$, was found to be 35% above its nominal value $\mathcal{L}_0$ corresponding to the Wiedemann-Franz law. As has been shown in the recent works of the PI [2,3], neither the Fermi liquid nor renormalization-group corrections in disordered $2d$ electron systems can modify the Lorenz number $\mathcal{L}$ to such an extent and, therefore, the result requests for an explanation. We argued in Ref. 1 that the heat exchange of electrons with the localized FPs, δP_{ep}^{loc}, might resolve this problem.

Let us comment upon δP_{ep}^{loc}. First, we recall that interaction of an electron with the FPs is described by the two-phonon processes. Correspondingly, the heat exchange between the electrons and FPs, which is proportional to square of the two-phonon amplitude, contains four powers of the FP-momenta. However, the strongly localized FPs are not Goldstone modes anymore. For localized FPs, the momenta that enter into the matrix elements of the electron-FP interaction should be substituted by the inverse of the localization length. As a result, two powers of frequencies in the expression for the heat flux P saturate at $\omega \simeq \omega_{loc}^{str}$. This, however, leads to a dramatic consequence: in the case of the two-phonon process, the factor describing the dependence on the occupation numbers starts to diverge like ω^{-2}. The diverging integration should be cut-off at an energy typical for the localized FPs. As a result, one gets from the heat exchange of electrons with the localized FPs a contribution to the cooling rate $\delta P_{ep}^{loc} \propto \omega_{loc}^{str} T(T_{el} - T_{ph})$. The discussed term has just the form *imitating* the heat diffusion contribution. Since the estimated energy for strong localization ω_{loc}^{str} is a fraction of 1K, the scale of δP_{ep}^{loc} is in full correspondence with the observed deviation of the Lorenz number $\mathcal{L}$ from its Wiedemann-Franz nominal value.

To summarized, the FPs together with the established fact of their localization may lead to important and non-trivial implications for the thermal transport in graphene.

Publications:

1. W. L. Z. Zhao, K. S. Tikhonov, A. M. Finkel'stein "Flexural phonons in supported graphene: from pinning to localization" https://arxiv.org/pdf/1712.09608.
2. G. Schwiete, A. M. Finkel'stein, "Heat diffusion in the disordered electron gas "Phys. Rev. B 93, 115121 (2016). Comments: 23 pages, 12 figures.
3. G. Schwiete, A. M. Finkel'stein, "Theory of Thermal Conductivity in the Disordered Electron Liquid" JETP, Vol. 122, p.567 (2016). Comments: Special JETP issue dedicated to the 85th birthday of Prof. L. V. Keldysh; 8 pages, 1 figure.

Exotic Kondo Phases: the non-Kramers Doniach phase diagram

Rebecca Flint, Iowa State University

Keywords: Kondo physics

Project Scope

The overarching theme of the project is to discover exotic new phases in heavy fermion materials. In particular, we aim to develop the non-Kramers Doniach phase diagram relevant for Kondo materials based on non-Kramers doublet ground states, as might occur in Pr, Tm or Tb based materials with sufficiently high symmetries. The Kondo effect in non-Kramers doublet materials is naturally the *two-channel* Kondo effect, which requires that any heavy Fermi liquid must break this channel symmetry. This is a channel symmetry breaking heavy Fermi liquid that we call hastatic order [1,2]. It involves a spinorial hybridization that breaks both single and double time-reversal symmetries. The hybridization spinor can order uniformly (ferrohastatic) or in some staggered (antiferrohastatic) order. Alternate ground states are magnetic or quadrupolar orders, superconductivity, and non-Fermi liquid phases. The first part of the project has focused on understanding the nature of hastatic order, both in a simple two-channel Kondo model, and within realistic Anderson models with momentum-dependent spin-orbit coupled hybridization. We have particularly focused on potential experimental signatures and connecting our work to a set of Pr-based materials that with non-Kramers Γ_3 ground states and Kondo physics. Several of these materials (PrV_2Al_{20}[3], $Pr(Ir,Rh)_2Zn_{20}$[4,5]) feature heavy Fermi liquid regions only in intermediate magnetic fields, which can naturally be explained by ferrohastatic order. Future work will study the effect of the non-Kramers doublet on both composite and magnetically mediated superconductivity, the stability of hastatic order, and search for non-Fermi liquids.

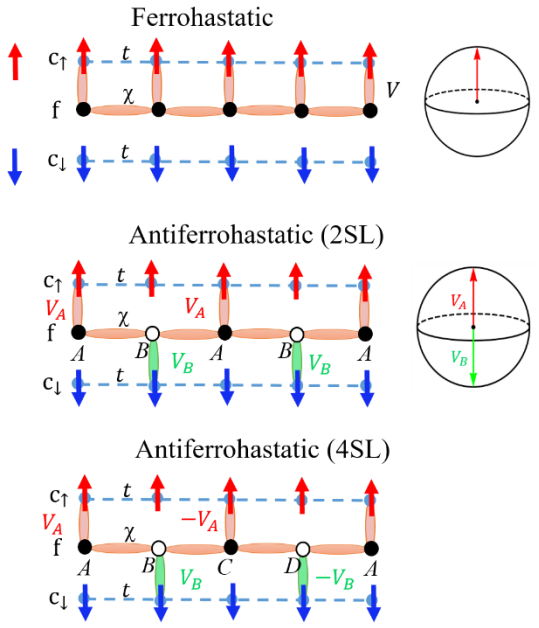

Fig. 1: One dimensional cartoons of hastatic order. In ferrohastatic order (top), only spin-up electrons hybridize and become heavy. In antiferrohastatic order (middle/bottom), both spins hybridize and become heavy. As the hastatic spinor breaks double time-reversal, (T^2 V = -V), there are two types of antiferrohastatic order with identical magnetic moments: a two-sublattice (middle) that breaks time-reversal, and a four-sublattice (bottom) version with a larger unit cell.

Recent Progress

Hastatic order: We have focused on cubic hastatic order based on the Γ_3 ground state, which is purely non-magnetic; here the pseudospin and channel (physical spin) both satisfy

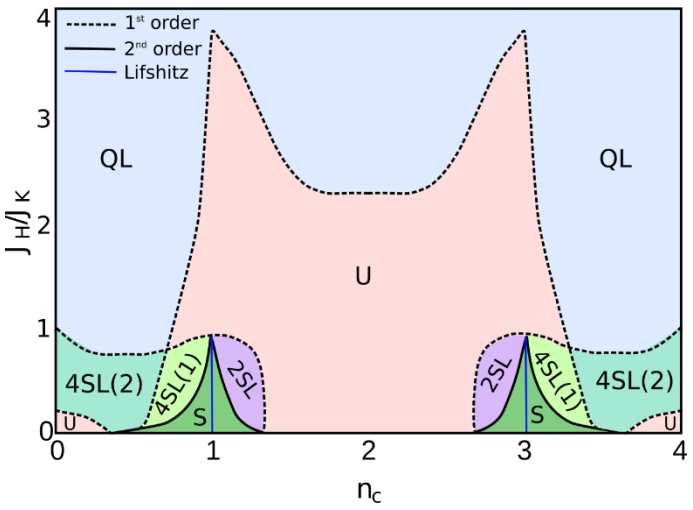

Fig. 2: Ground state phase diagram of the two-channel Kondo-Heisenberg model in two dimensions without full band-degeneracy. The x-axis is the conduction electron filling, while the y-axis is the ratio of the Heisenberg and Kondo coupling terms. Larger J_H favors a quadrupole liquid (QL), which is a proxy for quadrupolar order. Ferrohastatic order (U) is favored near half-filling and for very small filling. There are four kinds of antiferrohastatic order: one without f-electron hopping that breaks no additional symmetries (S) favored near quarter-filling; a two-sublattice (2SL) version that breaks time-reversal; and two four-sublattice (4SL) versions that break inversion [4SL(1)] and rotational [4SL(2)], respectively.

independent SU(2) symmetries, which makes the physics more straightforward than the tetragonal case, where these are interrelated [1]. First, we have used a fermionic SU(N) large-N treatment of the simple two-channel Kondo-Heisenberg model to explore both ferrohastatic and Neel staggered antiferrohastatic states, and their interaction with quadrupolar order (in this fermionic treatment, quadrupolar order takes the form of a quadrupolar version of a spin liquid). These phases are shown in cartoon form in the first figure. Ferrohastatic order involves the local quadrupole moments hybridizing only with the spin-up conduction electron quadrupole moments; essentially, this state forms "half" a heavy Fermi liquid, with heavy spin up electrons, light spin down electrons and half of a hybridization gap.

Antiferrohastatic order is more complicated. One of the key features of hastatic order is the spinorial nature of the hybridization that causes it to break both single and *double* time-reversal symmetry. Our simple model reveals that the antiferrohastatic state can effectively break these in *different* ways. We considered all antiferrohastatic ansatz that have a Neel staggered pattern of the hastatic moments; from the point of view of the magnetic moments, these are all identical. However, while the moments return to themselves under double time-reversal ($T^2 = +1$), the hastatic spinor requires four time-reversal operations to return to itself ($T^2 = -1$); any state that is invariant under time-reversal followed by a lattice transformation must have at least four sublattices (ABCD), as shown in Fig. 1 (bottom), which breaks additional lattice symmetries relative to the two-sublattice version. The two-sublattice version (Fig. 1 middle) actually breaks time-reversal, even though the moments themselves do not. Note that if there is no f-electron hopping, this extra sign can be removed by a gauge transformation and no additional symmetries are broken. In two dimensions, there are two straightforward ways to arrange the four sublattices: either ABCD along a lattice vector, which breaks inversion symmetry, or ABCD around a plaquette, which breaks the four-fold rotational symmetry. These symmetry breakings affect the Kramers degeneracy of the hybridized bands at the Γ point,

allowing these subtle symmetry breakings to be detected via ARPES or potentially quantum oscillations.

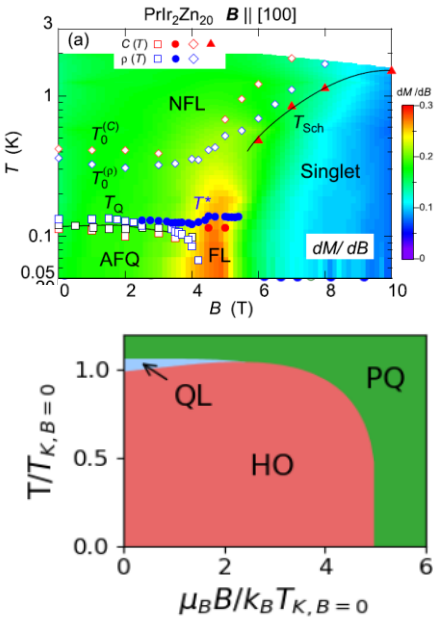

Fig. 3: (Top) Phase diagram of $PrIr_2Zn_{20}$ in magnetic field [4]. Note the in-field heavy Fermi liquid region. (b) A similar theoretical phase diagram showing how ferrohastatic order can be favored over the quadrupolar liquid; note that the quadrupolar liquid (QL) actually enhances hastatic order, while true quadrupolar order would suppress it, so we expect a beyond mean-field theoretical phase diagram to more strongly resemble the experiment.

To obtain a full picture of the physics, we looked not only at the phases themselves, but at the effect of changing the conduction electron filling, band degeneracies and dimensionality, as well as the effect of both channel and pseudospin symmetry breaking fields (here, magnetic and strain fields). We find that both ferro- and antiferrohastatic phases are found in the generic phase diagram, with the ferrohastatic phase favored near half-filling and the antiferrohastatic phase favored near quarter-filling, independent of the details of the conduction electron bandstructure. Magnetic field favors ferrohastatic order, due to its uniform magnetic moment, as seen in Fig. 3 (bottom). Magnetic field also provides the key to differentiate hastatic and quadrupolar orders. Both hastatic and quadrupolar orders will develop significant non-zero rare earth magnetic moments in magnetic field, as the Γ_3 doublet acquires an in-field moment due to mixing with excited crystal field levels. The hastatic moments will always align along the field, with any staggered moments quickly suppressed in field. By contrast, the quadrupolar order moment direction is determined by the order and will be perpendicular to the field for some field directions; additionally, antiferroquadrupolar order leads to significant staggered in-field moments. Hastatic order can further be resolved by optical conductivity or other measurements of the hybridization gaps.

In addition to the simple model, we have developed the appropriate realistic microscopic Anderson model, where the spin-orbit coupled and momentum dependent hybridization is determined with a Slater-Koster approach. Thus far, we have studied the ferrohastatic state, where the spin-orbit coupling leads to new spin textures in momentum space and symmetry breaking hybridization gaps with nodal structures, but no other major changes to the phase diagrams or experimental signatures.

Spin-ice rules in quasicrystalline i-Tb-Cd: In collaboration with Alan Goldman's neutron scattering group at Iowa State, we have modeled the crystal fields magnetic behavior of Tb in the i-Tb-Cd quasicrystal. Tb is a non-Kramers ion, and the nearly icosahedral crystal fields of the Tb site favor a nearly degenerate Ising non-Kramers doublet. These Tb mostly sit on the

vertices of icosahedra and interact via the RKKY effect; these moments freeze into a spin glass at very low temperatures. Above the freezing temperature, the diffuse magnetic scattering is well-described by considering nearest-neighbor antiferromagnetic interactions on the icosahedra alone, which leads to a large degeneracy of ground states that satisfy a version of ice-rules where each triangle on the icosahedra has either two spins pointing "in" to the icosahedra and one pointing "out", or the opposite.

Future Plans

Realistic models for antiferrohastatic order: We are developing the appropriate Anderson model for antiferrohastatic order on the fcc lattice, in order to capture the essential physics of potential hastatic order in PrV_2Al_{20}. We are also searching for potential hastatic topological crystalline Kondo insulators.

Tetragonal hastatic order: Using what we have learned from the cubic models, we are developing a model of tetragonal hastatic order with two d-conduction bands that should capture the physics missing from earlier hastatic models of URu_2Si_2. We may also explore hexagonal hastatic order.

Numerical simulations: We have developed the appropriate finite-U Anderson model with a non-Kramers doublet ground state that can be treated with quantum Monte Carlo techniques (to be done in collaboration with Prof. Bryan Clark at UIUC). These simulations should be capable of finding hastatic, quadrupolar and superconducting phases, as well as non-Fermi liquids, and should give a good idea of the real non-Kramers Doniach phase diagram.

Superconductivity: We will examine the competition and coexistence of superconductivity with hastatic order, treating both composite pair superconductivity and superconductivity mediated by quadrupolar fluctuations. We plan to develop the theory of composite pairing in Γ_3 non-Kramers doublet materials.

References

1. P. Chandra, P. Coleman, and R. Flint, *Hastatic order in URu_2Si_2*, Nature **493**, 621 (2013).
2. P. Chandra, P. Colemna, and R. Flint, *Hybridization with a twist: hastatic order in URu_2Si_2,* Phys. Rev. B **91**, 205103 (2015).
3. A. Sakai and S. Nakatsuji, *Kondo Effects and Multipolar Order in the Cubic $PrTr_2Al_{20}$ (Tr = Ti, V),* J. Phys. Soc. Jpn. **80**, 063701 (2011).
4. T. Onimaru, K. Izawa, K. T. Matsumoto, T. Yoshida,Y. Machida, T. Ikeura, K. Wakiya, K. Umeo, S. Kittaka,K. Araki, T. Sakakibara, and T. Takabatake, *Quadrupole-driven non-Fermi-liquid and magnetic-field-induced heavy fermion states in a non-Kramers doublet system* Physical Review B 94 (2016).
5. T. Yoshida, Y. Machida, K. Izawa, Y. Shimada, N. Nagasawa, T. Onimaru,T. Takabatake, A. Gourgout, A. Pourret, G. Knebel, and J.-P. Brison, *Anisotropic B-T Phase Diagram of Non-Kramers System $PrRh_2Zn_{20}$,* J. Phys. Soc. Jpn. **86,** 044711 (2017).

Publications (August 2016 – July 2018)

1. J. van Dyke, G. Zhang, and R. Flint, *A Realistic Model of Ferrohastatic Order,* arXiv:1802.05752 (2018).

Theory for pump/probe experiments in quantum materials

James K. Freericks, Department of Physics, Georgetown University

Keywords: Nonequilibrium many-body physics, pump/probe experiment, time-resolved ARPES, thermalization

Project Scope

This work is focused on developing theory that is relevant for describing the behavior of quantum materials driven out of equilibrium by large ultrafast light pulses and then examining how they behave as they return to equilibrium. There are two main foci of the work. The first is to develop a new nonequilibrium impurity solver that can be used to solve the nonequilibrium behavior of strongly correlated materials. The second is to develop the theory behind a range of different experimental probes and to employ them to examine how electrons relax in quantum materials after being driven to nonequilibrium.

Recent Progress

We have accomplished much along the project's goals over the past two years. We have collaborated with experimentalists on the electron relaxation problem. Our theory was employed to examine how phonons set one of the timescales for relaxation of high-temperature superconductors and how the evolution of the system varies with pump pulse fluence (See Fig. 1). Our work provided theory for both a tr-ARPES [Rameau, 2016] and an electron diffraction experiment [Konstantinova, et al. 2018]; both experiments were performed at Brookhaven. In addition, we have completed work on the relaxation of electrons in the presence of infinite-heat-capacity [Kemper, et al., 2018] and finite-heat-capacity phonon reservoirs [Abdurazakov, et al. 2018]. One important element of this relaxation work is that we employ exact equations of motion

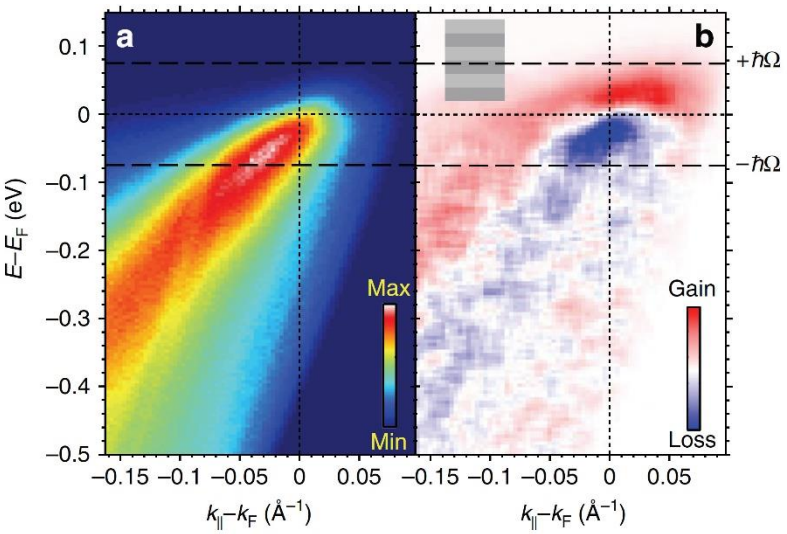

Fig. 1 Time resolved ARPES data from [Rameau, 2016] illustrating the phonon window effect, where electrons within an energy window of the Fermi energy take much longer time to thermalize.

to show how it is the *difference* of the Green's function and self-energy distribution functions that drives the rate of relaxation in these systems.

We have worked out the general theory for how time-resolved electronic Raman scattering works. This is a second-order process, with a complex response function. Fortunately, the B_{1g} symmetry sector can be shown to have no vertex corrections in infinite spatial dimensions, and so the response can be immediately determined. We have examined this for the Falicov-Kimball model [Freericks, et al. 2018, and *in preparation*] and found a number of interesting results (See Fig. 2). We see that when the material is being strongly pumped, the Raman response becomes strongly suppressed, and then recovers quickly when the pump is reduced. The Raman response can be used as an effective thermometer of the system, by invoking the fluctuation dissipation theorem. Curiously, we find that the effective temperatures found from Raman scattering do not immediately agree with those found from tr-ARPES, indicating that the system has not properly thermalized, even if the distribution from ARPES appears to be thermal in shape. This brings to question the validity of the hot electron model and shows the importance of fitting effective temperatures with multiple measurements to ensure they are consistent.

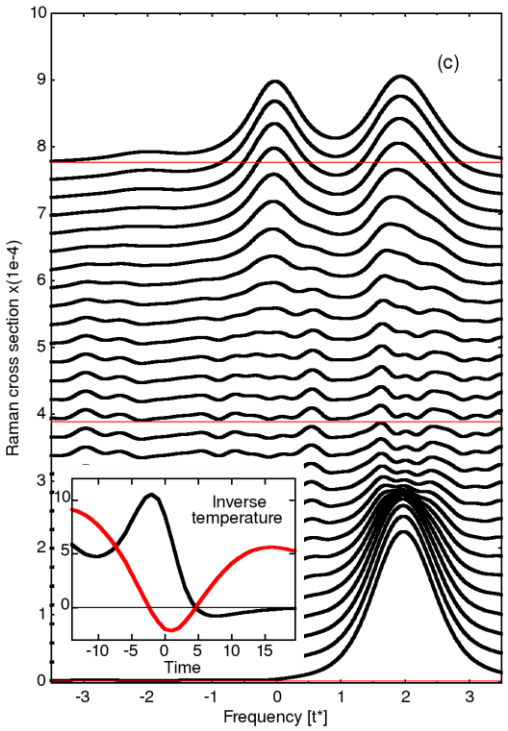

Fig. 2 Time resolved electronic Raman scattering data from [Matveev, 2018] . Note how the Raman response is small when the pump is on (except for some Floquet-like oscillations) an then emerges in a high-temperature state after the pump is off.

We continued early work on the Higgs mechanism and how to observe it in superconductors for d-wave systems [Nozierwiski, 2017] (See Fig. 3) along with two review articles---one on charge density wave systems [Freericks, et al. 2017] and one on superconductors [Kemper et al., 2017]. We also initiated a new line of work in Floquet driven systems. Here, the initial focus was on examining how long a pulse has to be on before a system looks Floquet-like [Kalthoff, et al., 2018]. We are also nearly finished with a paper on the general properties of interacting Floquet systems, including the behavior of the Floquet density of states; in particular, we show that the time-averaged density of states is always nonnegative [*in preparation*]. Finally, we wrote a short paper with an undergraduate on the pseudospin quantum numbers of the attractive Hubbard model, explicitly constructing a wavefunction with nonzero overlap with the ground state that has minimal pseudospin [Boretsky, et al., 2018].

The second main thrust of our work is on developing new computational methods for the nonequilibrium quantum impurity. Solving this problem will have a large impact on dynamical mean-field theory (DMFT) based model of quantum materials driven into nonequilibrium. It is amazing that over a decade since nonequilibrium DMFT was first introduced, that we still rely primarily on perturbative methods to solve for most strongly correlated models (electron-phonon coupling, Hubbard model, periodic Anderson model, etc.). Despite much work on quantum Monte Carlo methods, no working solver for nonequilibrium dynamical mean-field theory is currently available.

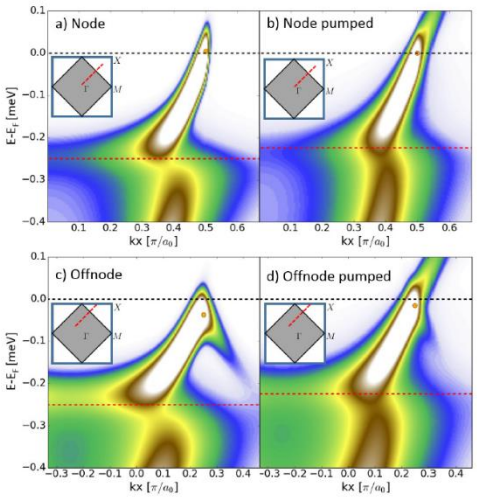

Fig. 3 Time resolved ARPES data for a d-wave superconductor driven to exhibit Higgs oscillations from [Nozierwiski, 2017]. Equilibrium (left) and pumped (right) spectra show the relaxation of the kink and the excitation of electrons, as the system is pumped.

Our strategy is based on generalizing the Wilson approach to the quantum impurity model solution via the numerical renormalization group. We identify a much smaller subspace of the full Hilbert space, where the bath states are active and project the problem into this subspace to make the calculations feasible. The break-up we use is exact, and works on a small Wilson chain, which evolves with time. We do not yet have any significant results in this area, but the postdoctoral fellow working on this problem only started this past March and we are making much progress in the initial problem, which involves solving the equilibrium problem in imaginary time.

Future Plans

We plan to continue working on a number of these different problems. We have an ongoing collaboration with Tom Devereaux's group and have begun examining time-resolved resonant inelastic x-ray scattering (RIXS). We are continuing our collaboration with Andrij Shvaika's group in Ukraine on time-resolved Raman scattering. Our next effort will be on studying the A_{1g} sector, which does require vertex corrections. Fortunately, these vertex corrections can all be evaluated by numerically calculating first-order functional derivatives of the single-particle Green's function. We are working on developing the computer codes to evaluate these problems and then examine their behavior in pump/probe experiments. In addition, we plan to continue our collaborations with Lex Kemper on electron relaxation and work toward developing a more complete understanding of how these strongly pumped systems relax and what determines the relaxation behavior. Finally, we are investing significant effort in developing the new numerical impurity solver, which we hope will become competitive or even surpass the currently available solvers for both equilibrium and nonequilibrium. There are a number of distinct advantages with our approach, but there also are a number of unknowns, particularly with regards to the efficiency

of the numerical algorithms that we have to thoroughly test before we can apply it to these interesting quantum materials problems.

References from Selected Publications (August 2016 – July 2018)

1. [Abdurazakov, et al. 2018] O. Abdurazakov, D. Nevola, A. Rustagi, J. K. Freericks, D. B. Dougherty, A. F. Kemper, *Nonequilibrium Electron Dynamics In Pump-Probe Spectroscopy: Role Of Excited Phonon Populations*, submitted to Phys. Rev. B (arxiv 1807.01323).
2. [Boretsky, et al., 2018] J. Z. Boretsky, J. R. Cohn and J. K. Freericks, *Spin and pseudospin towers of the Hubbard model on a bipartite lattice*, Int. J. Mod. Phys. B **32**, 1840021 (2018).
3. [Freericks, et al. 2017] J. K. Freericks, O. Matveev, Wen Shen, A. M. Shvaika, and T. P. Devereaux, *Theoretical description of pump/probe experiments in electron mediated charge-density-wave insulators*, Physica Scripta **92,** 034007 (2017).
4. [Freericks, et al. 2018] James K. Freericks, Oleh P. Matveev, Andrij M. Shvaika, Thomas Peter Devereaux, *Nonresonant pump/probe electronic Raman scattering within nonequilibrium dynamical mean-field theory*, in Ultrafast Bandgap Photonics III, Michael K. Rafailov, Editors, Proceedings of SPIE Vol. 10638 (SPIE, Bellingham, WA 2018), 1063807.
5. [Kalthoff, et al., 2018] Mona H. Kalthoff, Götz S. Uhrig, and J. K. Freericks, *Emergence of Floquet Behavior for Lattice Fermions Driven by Light Pulses*, to appear in Phys. Rev. B (2018).
6. [Kemper, et al. 2017] A. F. Kemper, M. A. Sentef, B. Moritz, T. P. Devereaux, and J. K. Freericks, *Review of the theoretical description of time-resolved angle-resolved photoemission spectroscopy in electron-phonon mediated superconductors*, Ann. der Phys. **559**, 1600235 (2017).
7. [Kemper, et al. 2018] A. F. Kemper, O. Abdurazakov, and J. K. Freericks, *General principles for the non-equilibrium relaxation of populations in quantum materials*, submitted to Phys. Rev. X (arxiv 1708.05725).
8. [Konstantinova, et al., 2018] T. Konstantinova, J.D. Rameau, A.H. Reid, O. Abdurazakov, L.Wu, R.K. Li, X. Shen, G. Gu, Y. Huan, Laurenz Rettig, Isabella Avigo, Manuel Ligges, James K. Freericks, A. F. Kemper, H.A. Durr,, U. Bovensiepen, P.D. Johnson, X. Wang, and Y. Zhu, *Nonequilibrium electron and lattice dynamics of strongly correlated $Bi_2Sr_2CaCu_2O_{8+\delta}$ single crystals*, Science Adv. **4,** eaap7427 (2018).
9. [Nozierwiski, 2017] B. Nosarzewski, B. Moritz, J. K. Freericks, A. F. Kemper, and T. P. Devereaux, *Amplitude mode oscillations in pump-probe photoemission spectra from a d-wave superconductor*, Phys. Rev. B **96,** 184518 (2017).
10. [Rameau, et al. 2016] J. D. Rameau, S. Freutel, A. F. Kemper, M. A. Sentef, J. K. Freericks, I. Avigo, M. Ligges, L. Rettig, Y. Yoshida, H. Eisaki, J. Schneeloch, R. D. Zhong, Z. J. Xu, G. D. Gu, P. D. Johnson, and U. Bovensiepen, *Energy dissipation from a correlated system driven out of equilibrium*, Nature Commun. **7**, 13761 (2016).

Topological Materials in Quantum Limit:
Quantum Hall Ferroelectricity and Non-Saturating Thermopower

Liang Fu (MIT)

Keywords: thermopower, topological semimetal, ferroelectric quantum Hall states

Project Scope

The current project focuses on theory of novel phases of matter and transport phenomena that appear in topological materials under a quantizing magnetic field. Topological materials possess unconventional electronic spectrum on the surface and in the bulk. For example, topological crystalline insulators have multi-valley Dirac surface states with spin-momentum locking. Topological semimetals have inseparable conduction and valence bands touching each other at singular points or lines in momentum space. Applying a large magnetic field to these topological materials create unconventional Landau level spectrum. This project uncovers new phases of matter and transport phenomena in topological materials in the quantum limit.

Recent Progress

Ferroelectric quantum Hall states

Surface states of the topological crystalline insulator SnTe or bismuth hosts multiple Dirac valleys located away from time-reversal-invariant momenta. These Dirac pockets are highly anisotropic, and their principal axis point in different symmetry-related directions. Landau levels of these multi-valley Dirac electrons were recently observed in scanning tunneling microscopy experiments on (001) surface of $Pb_{1-x}Sn_xSe$ [Madhavan, Fu et al, Science, 2013] and on (111) surface of bismuth [Yazdani, MacDonald et al, Science, 2016]. Remarkably, in the case of bismuth, splitting of Landau levels was observed when they cross Fermi energy at low temperature and attributed to valley degeneracy lifting.

We study spontaneous quantum Hall valley degeneracy breaking at integer fillings, driven by Coulomb interaction between these Dirac electrons. Due to the Fermi surface anisotropy that imprints itself on the shape of Landau orbitals (see Fig.1), at even-integer fillings pairs of valleys at opposite momenta are simultaneously occupied, leading to a nematic quantum Hall state. More interestingly, we find that at odd-integer fillings the quantum Hall ground state is fully valley polarized and breaks all rotational symmetry. This state possesses an in-plane electric polarization, which grows rapidly with the magnetic field and characterizes the underlying Fermi surface geometry. Therefore we call this state a “quantum Hall ferroelectric” [1], where topological order arises from symmetry breaking driven by electron correlation.

Following our prediction, Yazdani’s group has found evidence of this ferroelectric quantum Hall states in bismuth [Yazdani, MacDonald et al, Nature Physics 2018]. New Landau level splittings

at Fermi energy were observed at odd-integer fillings, which shows the completely removal of valley degeneracy. Moreover, spatial imaging of impurity bound states of this odd-integer quantum Hall state shows the absence of quasiparticle interference between different valleys. This reveals the single-valley nature of the quantum Hall ground state, i.e., the formation of a quantum Hall ferroelectric.

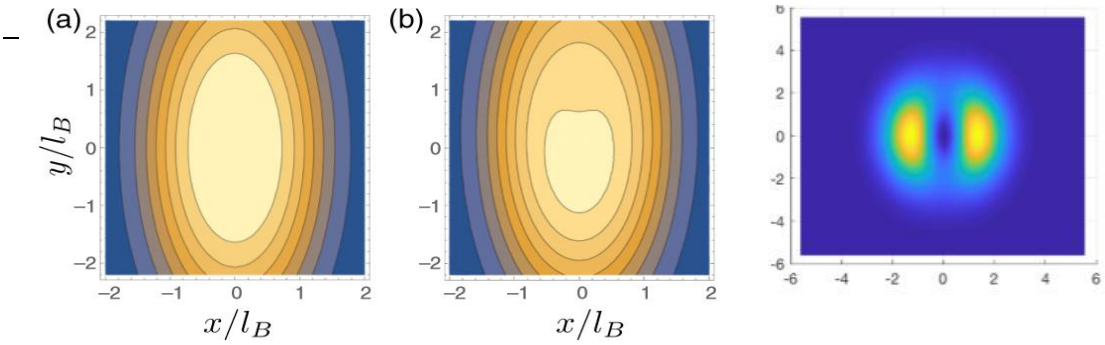

Landau orbitals associated with an elliptical Fermi surface (a) and a teardrop shaped Fermi surface (b). The latter lacks inversion symmetry and carries a built-in electric dipole, leading to a quantum Hall ferroelectric. The rightmost panel shows spatial profile of a localized exciton in multi-valley quantum Hall system.

Large, non-saturating thermopower under magnetic field

Motivated by a recent experiment on the topological crystalline insulator $Pb_{1-x}Sn_xSe$, we theoretically studied thermoelectric effects in narrow/zero gap semiconductors under a quantizing magnetic field. We show that when the Hall resistivity is dominant, thermoelectric transport is essentially determined by thermodynamics. In particular, the thermopower (i.e., the Seebeck coefficient) is simply given by the ratio of entropy density and net charge density, independent of transport coefficients at zero field.

It is well-known that at zero magnetic field electrons and holes contribute oppositely to thermopower. In contrast, we find that at a quantizing magnetic field electrons and holes contribute *additively* to thermopower, due to the Hall motion driven by Lorenz force (see Fig.2). Furthermore, in the quantum limit, the entropy of electron and hole carriers increases linearly with the magnetic field due to the increasing Landau level degeneracy, even though the net charge density is fixed by dopant density. Therefore we show that the thermopower increases linearly with the magnetic field without saturation [2]! Our result agrees excellently with the measured thermopower in the quantum limit of $Pb_{1-x}Sn_xSe$, whose origin and significance has been unknown before.

There is currently great demand for thermoelectric materials, which can convert waste heat into electricity and consume electrical energy for cooling. However, improving the efficiency of thermoelectric materials has been a challenge, as the "figure of merit" *ZT* depends on electrical and thermal conductivity, in addition to thermopower. Typically, these factors are interrelated and

cannot be independently optimized. Our work offers a new possibility of boosting thermoelectric efficiency by applying a magnetic field to the small-gap semiconductors.

Future Plans

We are currently studying localized excitations in ferroelectric quantum Hall states. Depending on the strength of impurity potential, we find either localized electrons or excitons can be induced as in-gap states (see Fig.1). We are studying the spatial profile of these excitations which serve as a probe of the electric dipole moment and can be directly imaged in STM experiments.

We are also carrying out a systematic study of thermoelectric transport in topological semimetals/insulators in both strong and weak field regime. We shall study both Seebeck and Nernst coefficient as a function of magnetic field, carrier density, and temperature. The effect of phonon-drag on thermopower in the dissipative transport regime will also be studied.

The field-induced large thermopower by itself does not guarantee good thermoelectric performance. The other two factors, electrical and thermal conductivity, are also important. We plan to study electrical conductivity in high field limit, taking into account potential positive or negative magnetoresistance effects. The ultimate goal of this study is to find the optimum condition for record-high thermoelectric performance that enable practical applications.

References

1. I. Sodemann, Z. Zhu, L. Fu, *Quantum Hall Ferroelectrics and Nematics in Multivalley Systems*. Phys Rev X. **7**, 041068 (2017).

2. B. Skinner, L. Fu, *Large, nonsaturating thermopower in a quantizing magnetic field*. Science Advances **4**, eaat2621 (2018).

Publications (August 2016 – July 2018)

1. S. Vijay, J. Haah, L. Fu, *Fracton Topological Order, Generalized Lattice Gauge Theory and Duality*. Phys. Rev. B **94**, 235157 (2016).

2. J. Ruhman, V. Kozii, L. Fu, *Odd-parity superconductivity near inversion breaking quantum critical point in one dimension*. Phys. Rev. Lett. 118, 227001 (2017).

3. J. Liu, Y. Qi, Z. Meng, L. Fu, *Self-Learning Monte Carlo Method*. Phys. Rev. B 95, 041101 (2017).

4. I. Sodemann, Z. Zhu, L. Fu, *Quantum Hall Ferroelectrics and Nematics in Multivalley Systems*. Phys Rev X. **7**, 041068 (2017).

5. Y. Wang, L. Fu, *Topological phase transitions in multi-component superconductors*. Phys. Rev. Lett. 119, 187003 (2017).

6. B. Skinner, L. Fu, *Large, nonsaturating thermopower in a quantizing magnetic field*. Science Advances **4**, eaat2621 (2018).

7. H. Shen, B. Zhen, L. Fu, *Topological Band Theory for Non-Hermitian Hamiltonians.* Phys. Rev. Lett. 120, 146402 (2018).

8. C. Fang, L. Fu, *Rotation Anomaly and Topological Crystalline Insulators*. *arXiv:1709.01929*

9. H. Shen, L. Fu, *Quantum Oscillation from In-gap States and non-Hermitian Landau Level Problem.* Phys. Rev. Lett. 121, 026403 (2018).

10. D. Wang, L. Kong, P. Fan, H. Chen, S. Zhu, W. Liu, L. Cao, Y. Sun, S. Du, J. Schneeloch, R. Zhong, G. Gu, L. Fu, H. Ding, H. Gao, *Evidence for Majorana bound states in an iron-based superconductor*. Science (in the press)

Theory of Fluctuations in Strongly-Correlated Materials

Principal investigator: Victor Galitski
PI Institution: Joint Quantum, Institute, University of Maryland
E-mail: galitski@umd.edu

Keywords: heavy-fermion materials, superconductivity, heterostructures, topological insulators, fluctuations

Project Scope

The main general focus of the project is to explore the interplay between fluctuation phenomena and strong correlations in quantum materials, including superconductors. The specific goals of the projects are the following:
1. To develop a theory of heterostructures involving topological insulators and magnetic materials.
2. To extend the theory of topological Kondo insulators to strongly fluctuating regimes, where the mean field theory breaks down, and to guide experiments that would probe and exploit the interplay between strong correlations and topological physics in heavy-fermion compounds.
3. To develop a non-perturbative theory of quantum fluctuations in superconductors, with the focus on the interplay between Aslamazov-Larkin-type fluctuations and phase fluctuations (including solitons) of the order parameter.

Recent Progress

- In Ref. [1], an experiment was performed, following PI's suggestion, to probe Klein tunneling paradox in a proximity induced superconducting state in the topological Kondo insulator – samarium hexaboride. A perfect quantization of Andreev reflection was detected, which is a hallmark of the predicted effect.

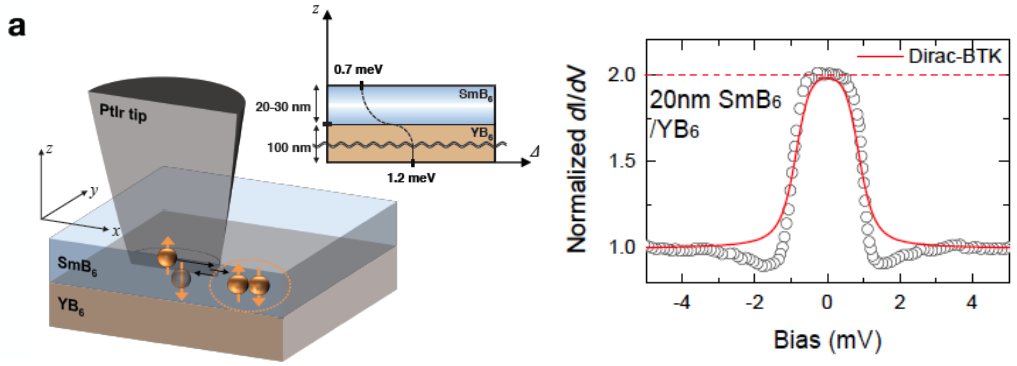

Figure 1: (a) Schematic of point contact Andreev reflection (PCAR) measurement on SmB6/YB6 heterostructures. Electrons with momentum parallel to the plane of the surface states of SmB6 dominantly contribute to the measured conductance. The inset shows variation of the superconducting pair potential (Δ) in SmB6 (20-30 nm)/YB6 heterostructure. The curve on the right shows measured differential conductance (along with theory fit), which exhibit perfect Andreev reflection due to Klein paradox.

- In Ref. [2], PI's experimental colleagues, Jing Xia and Zach Fisk and their group in Irvine, implemented PI's suggestion to use strain in order to increase the hybridization gap. Unexpectedly, a small tensile strain of a few percent led to an enhancement of the Kondo

topological state up to nearly room temperature.

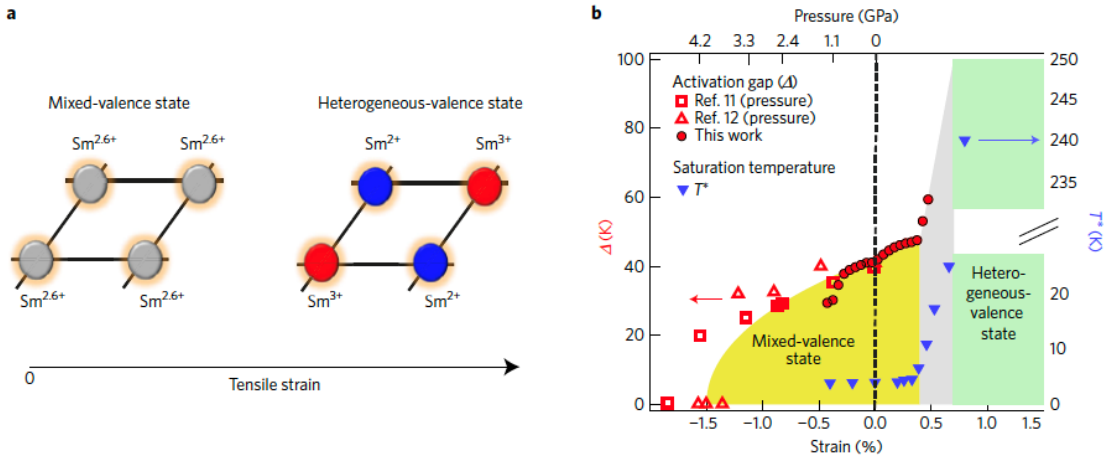

Figure 2: Temperature–strain phase diagram. (a) A schematic illustration of strain-induced transition from temporal fluctuating mixed-valence state to spatially heterogeneous-valence state. (b) A reconstructed phase diagram of SmB6 under strain with data from this paper as well as pressure data obtained in previous work.

- In Ref. [3], the PI and his posdtocs suggested that one can realize a non-Fermi liquid phase in topological heterostructures, and that the system may be unstable against the Amperean pairing instability.
- In Ref. [4], the PI and his postdoc, Efimkin, proposed an explanation of an experimental anomaly in drag resistivity in bilayers, by invoking the ionization-recombination crossover between the electron-hole plasma and exciton gas.
- In Ref. [5], Ganeshan, Gorshkov, Gurarie, and the PI proposed a way to realize so-called "genons" using spin degree of freedom. Originally proposed in a series of papers by PI's colleague Barkeshli et al., they represent a way to achieve non-Abelian excitations out of Abelian topologically-ordered states, by "gluing" two layers in a certain way – in effect implementing higher-genus surfaces. The actual physical gluing is unrealistic, but it might be possible to effectively implement it by replacing the layer index with spin components, and effectively "gluing" them with spin-dependent local terms.

Future work

Below is a brief description of specific researches to be pursued by the PI in the near future:

- The PI will consider an experimental platform to realize a non-Fermi liquid phase in heterostructures involving a fluctuating magnet coupled to a spin-orbit-coupled interface, where magnetic fluctuations act similarly to a dynamical gauge field.
    - Theory of transport in the non-Fermi liquid will be developed to enable its detailed experimental investigations.
    - Motivated by PI's theoretical and experiment-theory collaborative works on superconductivity in ferromagnetic heterostructures, the PI will develop a theory of Amperean superconductor - a novel strongly-correlated phase of matter possible in such systems.

    - A platform to realize a tunable "synthetic" spin-fluctuation model will be considered, where a spin-fluctuation pairing glue and the electron degrees of freedom can be disentangled.
- Motivated by puzzling experiments on topological Kondo insulator (TKI), samarium hexaboride, a theory of strong correlations beyond mean-field for this class of material will be developed.
    - The experimental mystery of quantum oscillations coming from TKI's insulating bulk (as observed by the Sebastian group in Cambridge) will be examined in conjunction with experiment by Fisk-Xia group in Irvine, first proposed by the PI, which observed an enhancement of the Kondo insulating behavior from 4 K to nearly room temperature under strain [2].
    - Strong-correlation effects on TKI's surface will be studied with an eye on the possibility of proximity-induced topological order *vs.* magnetic ordering, relevant to recent experiments of the Paglione group in Maryland.
- The PI proposes to study observable signatures of chaos in disordered quantum materials: from weakly-interacting normal metals to strongly-correlated hydrodynamic "bad metals."
    - A particularly interesting new phenomenon involves Lyapunov corrections to interference effects and instabilities, that rely on the presence of counter-propagating trajectories. Classical chaos implies the loops can not be identical in a disordered system. This may lead to breakdown of Anderson theorem - a basic result in the theory of superconductivity.
    - The PI proposes to study the fundamental problem of connecting single-particle Lyapunov effects and many-body quantum chaos. The former imply individual chaotic scatterings of electrons off of impurities, while the latter involves interaction-dominated scatterings. The PI's specific proposal is to start with a better-understood single-particle chaos and attempt a controlled cross-over into a hydrodynamic description (*e.g.,* in a fluctuating, quantum-critical system).

References:

[1] Seunghun Lee et al., https://arxiv.org/abs/1806.09765, submitted to *Nature,* "Observation of perfect Andreev reflection due to Klein paradox in a topological superconducting state."
[2] A. Stern, M. Dzero, V. Galitski, Z. Fisk, and J. Xia, *Nature Materials* **16**, 708 (2017), "Surface-dominated conduction up to 240 K in the Kondo insulator, samarium hexaboride, under strain."
[3] M. Kargarian, D. Efimkin, and V. Galitski, *Phys. Rev. Lett.* **117**, 076806 (2016), "Amperian pairing at the surface of topological insulators."
[4] D. Efimkin and V. Galitski, Phys. Rev. Lett. **116**, 046801 (2016), "Anomalous Coulomb Drag in Electron-Hole Bilayers due to the Formation of Excitons."
[5] S. Ganeshan, A. V. Gorshkov, V. Gurarie, and V. M. Galitski, Editors' Suggestion in Phys. Rev. B **95**, 045309 (2017), "Exactly soluble model of boundary degeneracy."

Selected publications

1. M. Kargarian, D. Efimkin, and V. Galitski, "Amperean Pairing at the Surface of Topological Insulators," *Phys. Rev. Lett.* **117**, 076806 (2016)

2. X. Gong, M. Kargarian, A. Stern, D. Yue, H. Zhou, X. Jin, V. Galitski, V. Yakovenko, and J. Xia, "Time-Reversal-Symmetry-Breaking Superconductivity in Epitaxial Bismuth/Nickel Bilayers," *Science Advances* **3**, e1602579 (2017)
3. A. Stern, M. Dzero, V. Galitski, Z. Fisk, and J. Xia, "Kondo insulator SmB6 under strain: surface dominated conduction near room temperature," *Nature Materials* **16**, 708 (2017)
4. S. Ganeshan, A. V. Gorshkov, V. Gurarie, and V. M. Galitski. "Exactly soluble model of boundary degeneracy," Editors' Suggestion in *Phys. Rev. B* **95**, 04530 (2017)
5. T. A. Sedrakyan, V. M. Galitski, and A. Kamenev, "Topological spin ordering via Chern-Simons superconductivity," *Phys. Rev. B* **95**, 094511 (2017)
6. D. Efimkin and V. Galitski, "Anomalous Coulomb Drag in Electron-Hole Bilayers due to the Formation of Excitons," *Phys. Rev. Lett.* **116**, 046801 (2016)
7. H. M. Hurst, D. K. Efimkin, and V. Galitski, "Transport of Dirac electrons in a random magnetic field in topological heterostructures," *Phys. Rev. B* 93, 245111 (2016)
8. Z. M. Raines and V. M. Galitski, "Enriched axial anomaly in Weyl materials," Rapid Communication in Phys. Rev. B 96, 161115(R) (2017)
9. M. Kayyalha, M. Kargarian, A. Kazakov, I. Miotkowski, V. M. Galitski, V. M. Yakovenko, L. P. Rokhinson, and Y. P. Chen, "Anomalous low-temperature enhancement of supercurrent in topological-insulator nanoribbon Josephson junctions: evidence for low-energy Andreev bound states," submitted to *Phys. Rev. Lett*., https://arxiv.org/abs/1712.02748
10. S. Kim, O. Tchernyshyov, V. Galitski, and Y. Tserkovnyak, "Magnon-induced non-Markovian friction of a domain wall in a ferromagnet," *Phys. Rev. B* **97**, 174433 (2018)
11. A. A. Allocca, D. K. Efimkin, and V.M. Galitski, "Fingerprints of Berry phases in the bulk exciton spectrum of a topological insulator," submitted to *Phys. Rev. B,* https://arxiv.org/abs/1801.01559
12. Seunghun Lee, Valentin Stanev, Xiaohang Zhang, Drew Stasak, Jack Flowers, Joshua S. Higgins, Sheng Dai, Thomas Blum, Xiaoqing Pan, Victor Yakovenko, Johnpierre Paglione, Richard L. Greene, Victor Galitski, and Ichiro Takeuchi, "Observation of perfect Andreev reflection due to Klein paradox in a topological superconducting state," submitted to *Nature* in June, 2018
13. Jonathan B. Curtis, Zachary M. Raines, Andrew A. Allocca, Mohammad Hafezi, Victor M. Galitski, "Cavity Quantum Eliashberg Enhancement of Superconductivity," submitted to *Physical Review Letters*, https://arxiv.org/pdf/1805.01482.pdf
14. Victor Galitski, Mehdi Kargarian, and Sergey Syzranov**,** "Dynamo Effect and Turbulence in Hydrodynamic Weyl Metals," submitted to *Physical Review Letters*, https://arxiv.org/pdf/1804.09339.pdf

SEMICONDUCTOR NANOSTRUCTURES BY SCIENTIFIC DESIGN

PI: Giulia Galli, University of Chicago & Argonne National Laboratory
gagalli@uchicago.edu

Keywords: DFT, MBPT, electronic transport, semiconductor nanostructures

Project Scope

The overarching goal of this project is the **development and application of first principles methods** to predict the **charge transport properties of nanostructured semiconductors.** We study materials for energy conversion, with main focus on group IV, and IV-VI compounds.

Functional nanostructured systems have long been recognized as a promising platform for the development of materials with target properties and they are an active area of theoretical and experimental research. While much progress has been made in recent years to predict structural and electronic properties of functional materials for energy conversion applications, robust, ab initio methods for the description and optimization of transport properties are not yet available, although several, useful codes based on various models for electron and ionic transport have been developed. In this project we are developing methods and algorithms for the prediction of electron and hole transport in materials with complex morphology from first principles, as summarized in Fig.1.

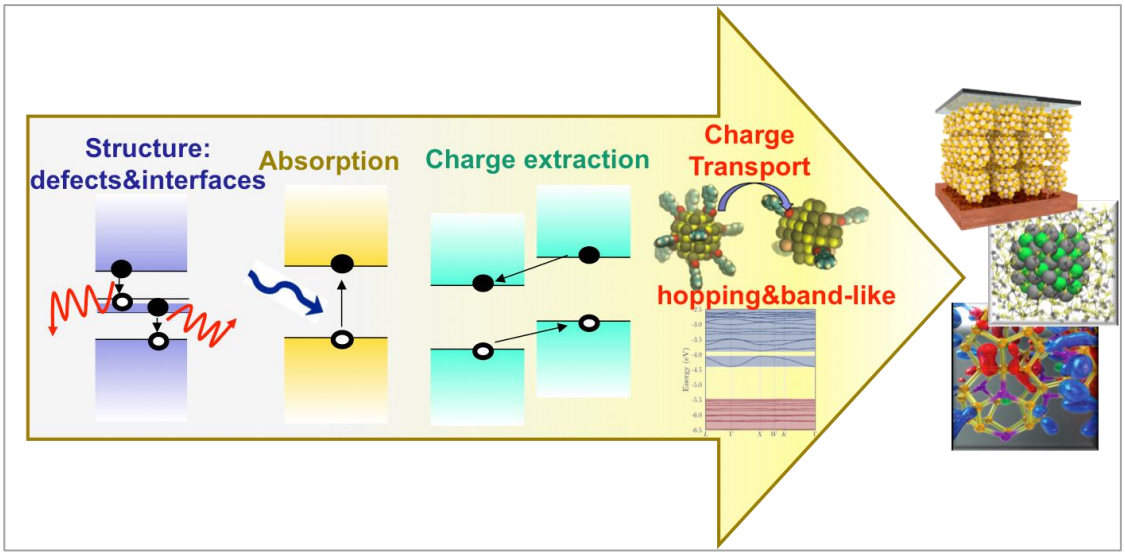

Figure 1 *Schematic representation of the physical processes and systems investigated in this project. We are developing and applying first principles methods to predict charge (electron and hole) transport in nanostructured semiconductors, including ensembles of nanoparticles (NPs), embedded NPs and inorganics clathrates and perovskites (icons on right hand side). Structural and electronic properties (absorption, photoemission and band offsets) are obtained from calculations based on density functional and many body perturbation theory.*

Main questions and recent progress

The main questions we seek to answer are the following:

- **What is the main mechanism (or are there competing mechanisms) of electronic and hole transport in inorganic nanostructured solar cells** composed of semiconducting nanoparticles, as a

function of nanoparticle (NP) size, ligands capping the NPs and interfaces with leads utilized in experimental devices?

Using constrained Density Functional Theory (DFT) methodologies inclusive of the effect of leads, we have carried out charge transport calculations for Si clusters [1] and work is in progress to investigate transport in PbSe NP solids, for which extensive calculations of electronic properties have been carried out and compared to experiments [2,3]. A notable finding on Si NP regards the impact on transport properties of defects, which, at least for dangling bonds, appear to be qualitatively different at the nanoscale, than in the bulk.

- **What is the main mechanism (or are there competing mechanisms) of electronic and hole transport in perovskite solar cells and how is transport affected by the presence of substitutional halogens and (Schottky) defects**? Using ab initio calculations we have investigated the coexistence of free and localized carriers in these materials, arising from polaron formation. We found that polarons will form in both $CH_3NH_3PbBr_3$ and $CH_3NH_3PbI_3$ crystals, but that they are more pronounced in $CH_3NH_3PbBr_3$ and we used our findings to rationalize recent experiments [4]. Our combined experimental and theoretical study indicates that single-crystal $CH_3NH_3PbBr_3$ could represent the key to understanding the impact of polarons on perovskite transport.

- How is charge transport affected by the arrangements (e.g. **superlattices) of nanoparticles and nanoplatelets into solids?** Work is in progress to study solids of nanostructures at low and high pressure (e.g. diamondoinds [5]), including nanoplatelets of chalcogenides [6].

[1] Charge Transport in Nanostructured Materials: Implementation and Verification of Constrained Density Functional Theory, Matthew Goldey, Nicholas Brawand, Márton Vörös, and Giulia Galli J. Chem. Theory Comput. 13 (6), 2581-2590 (2017)

[2] Optical Absorbance Enhancement in PbS QD/Cinnamate Ligand Complexes, Daniel Kroupa, Márton, Vörös, Nicholas Brawand, Noah Bronstein, Brett McNichols, Chloe Castaneda, Arthur Nozik, Alan Sellinger, Giulia Galli and Matthew Beard, J. Phys. Chem. Lett., 9(12), 3425-3433 (2018).

[3] Enhanced Multiple Exciton Generation in PbS|CdS Janus-like Heterostructured Nanocrystals Daniel M. Kroupa, Gregory F. Pach, Márton Vörös, Federico Giberti, Boris D. Chernomordik, Ryan W. Crisp, Arthur J. Nozik, Justin C. Johnson, Rohan Singh,Victor I. Klimov, Giulia Galli, and Matthew C. Beard, ACS Nano 2018 (under review).

[4] Excitations Partition into Two Distinct Populations in Bulk Perovskites, Lili Wang, Nicholas P. Brawand, Márton Vörös, Peter D. Dahlberg, John P. Otto, Nicholas E. Williams, David M. Tiede, Giulia Galli, and Gregory S. Engel, Advanced Optical Materials, 1700975 (2018).

[5] Sterically controlled mechanochemistry under hydrostatic pressure, Hao Yan, Fan Yang, Ding Pan, Yu Lin, Fei Hua Li, J. Nathan Hohman, Diego Solis-Ibarra, Jeremy E. P. Dahl, Robert M. K. Carlson, Boryslav A. Tkachenko, Andrey A. Fokin, Peter R. Schreiner, Giulia Galli, Wendy L. Mao, Zhi-Xun Shen and Nicholas A. Melosh, Nature, 554, 505-510 (2018).

[6] Colloidal Synthesis of Six-Monolayer-Thick CdSe Nanoplatelets, Wooje Cho, Siyoung Kim, Igor Coropceanu,Vishwas Srivastava, Benjamin T. Diroll, Abhijit Hazarika, Igor Fedin, Giulia Galli, Richard D. Schaller, and Dmitri V. Talapin, Chem. Materials 2018 (under review).

Non-Equilibrium Effects in Conventional and Topological Superconducting Nanostructures

Leonid Glazman, Department of Physics, Yale University, leonid.glazman@yale.edu
Alex Kamenev, Department of Physics, University of Minnesota, kamen002@umn.edu

Keywords: Andreev reflection, quasiparticles, proximity effect, Majorana fermions, conductance

Project Scope

In this program, we concentrate on quantum kinetic phenomena in conventional and topological superconducting nanostructures. A special focus is placed on the quasiparticles kinetics and its effect on the coherent dynamics of the superconducting order parameter. Understanding the kinetics is important for a broad array of basic and applied problems of superconductivity emerging in the development of devices of the future quantum information technology. The two major directions in developing the superconducting qubits aim, respectively, at perfecting the conventional-superconductor qubits, and building devices carrying Majorana states. The non-equilibrium quasiparticles limit the coherence times of the conventional superconducting qubits, which raises the problem of quasiparticles trapping. Advancing the diffusion and trapping theory is a part of current effort. The electron transport spectroscopy of Majorana states in engineered p-wave superconducting structures relies on the understanding of quasiparticles tunneling, which is another major part of the current theoretical effort.

Recent Progress

1. Conductance of quantum dots proximitized by a superconducting or normal metal.

The recently developed semiconductor quantum dots proximitized by a normal [1] or superconducting [2] metal combine high density of energy levels with controllable quantum point contacts connecting dots to leads and carrying no more than a few quantum modes. Large, proximitized by a superconductor dots may become an elemental base for topologically-protected qubits. This promise has led to experimental studies of the dots' conductance across the putative topological transition [3] and generated the need for appropriate theory. We built such quantitative theory in the series of four papers. The first one was published in June of 2016, see Ref. [4]. It was followed by **publications** [1-3] which appeared since August 2016.

The case of weakly-transparent contacts, allowing for a detailed comparison with experiments was considered in Ref**.** [4]; **publications** [1-3] dealt mostly with the case of strong tunneling. We uncovered two main features of the weak-tunneling regime: upon the increase of magnetic field $\boldsymbol{B}$, the height of the Coulomb blockade peaks in conductance drops (and each peak splits in two) once the trivial superconducting gap is suppressed below the charging energy $\boldsymbol{E_C}$. The conductance drop associated with the peak splitting is a manifestation of a well-known quasiparticle poisoning effect that blocks the two-electron tunneling (i.e., Andreev reflection)

across the dot. This effect is a clear signature of a non-topological nature of superconductivity in the dot; our theory explains the observed conductance [2,3] quantitatively in the proper parameters domain. At higher field, upon the topological transition, the peak conductance $G_M(T,B)$ should increase, reaching the unitary limit at low temperatures T. We found the full dependence of the peak conductance $G_M(T,B)$ on temperature and system parameters. In the topological phase, $G_M(T,B)$ is parametrically larger than the $B=0$ conductance $G(T)$; if the contacts to leads are symmetric and weak (junction conductances $\tau_L=\tau_R=\tau<<1$), then, for single-channel junctions, the ratio $G_M(T,B)/G(T)\sim 1/\tau$ is large. On the contrary, the observed [3] ratio was $G_M(T,B)/G(T)<1$, casting a doubt in the accepted in [3] interpretation of the data. We demonstrated in out **publication** [3] that the difference in $G(T)$ between the conventional and topological superconducting states is further enhanced in the strong-tunneling regime: the electron transport in the trivial state is suppressed at low temperatures due to the developing asymmetric two-channel Kondo effect, while in the topological phase Majorana states facilitate resonant tunneling.

Technically simpler experiments with quantum dots proximitized by a normal metal allowed the group of F. Pierre to investigate in great detail the suppression of Coulomb blockade by quantum charge fluctuations. The finite-temperature ($T>E_C$) theory of "weak" Coulomb blockade in a dot with almost-ideal single-channel junctions was still lacking. We developed it, and worked together with the experimental group to provide a detailed comparison of the measurements with the theory, see Fig. 1. Special attention was paid to the pre-exponential factor of the thermally-activated behavior. Finding the dependence of the pre-exponential factor on the junctions conductances τ_L , τ_R was the main technical difficulty which we overcame in our **publication** [4].

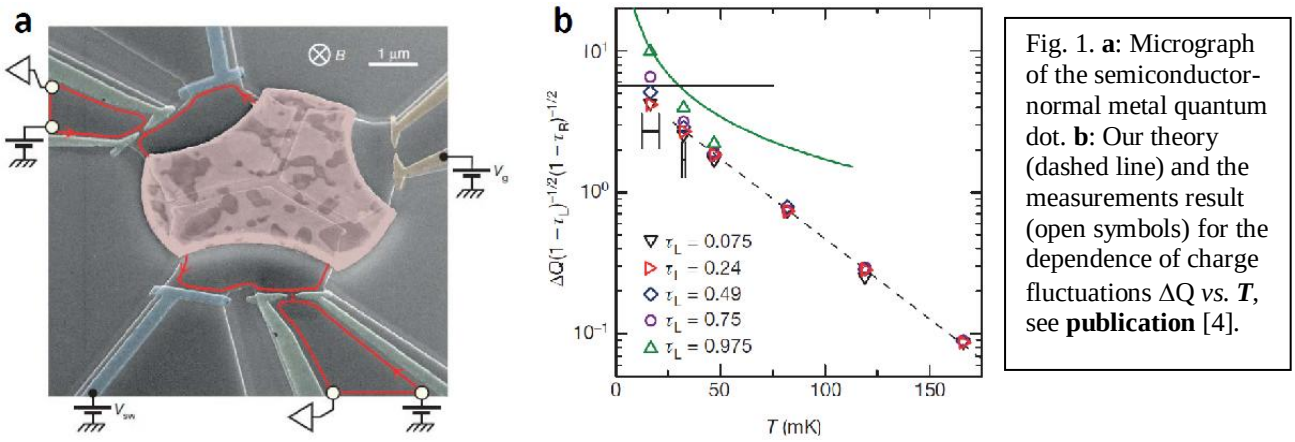

Fig. 1. **a**: Micrograph of the semiconductor-normal metal quantum dot. **b**: Our theory (dashed line) and the measurements result (open symbols) for the dependence of charge fluctuations ΔQ *vs.* T, see **publication** [4].

2. Relaxation and trapping of quasiparticles in inhomogeneous superconductors.

Evacuation of non-equilibrium quasiparticles is crucial for increasing the coherence time scales of superconducting quantum devices. One of the practical ways of mitigating the adverse effect of quasiparticles is to trap them and thus keep away from the active parts of a device.

Remarkably, the normal cores of stray vortices may trap quasiparticles [5]. Trapping of a quasiparticle occurs due to its inelastic scattering involving emission of a phonon or creation of a particle-hole pair inside the vortex core. In our recent **publication** [5] we developed a microscopic theory of quasiparticle trapping in a vortex facilitated by phonon emission. One may characterize this effect by the trapping power $P = \int d^2 r/t_{tr}(\boldsymbol{r})$ which has the units of diffusion coefficient; here $1/t_{tr}(\boldsymbol{r})$ is the local trapping rate. Modeling the vortex core by a normal-state cylinder of radius r_c , we found

$$P=[D(p_F\,\xi)^2\Delta^4/10\pi\rho_m v_t^5](r_c/\xi)^2$$

at $\boldsymbol{T}\ll\boldsymbol{\Delta}$. Here $\boldsymbol{\Delta}$ is the electron diffusion coefficient in the normal state, $\boldsymbol{p_F}$ is the Fermi momentum, $\boldsymbol{\xi}$ is the superconducting coherence length, $\boldsymbol{\rho_m}$ is the material mass density, and $\boldsymbol{v_t}$ is the speed of the transverse sound mode. The derivation accounts for the electro-neutrality condition, allowing us to exclude the electron-phonon interaction constant as an independent parameter from the result. Using the standard characteristics of an Al film and assuming $r_c \sim\boldsymbol{\xi}$, we find $\boldsymbol{P}$ by a factor of $\boldsymbol{10^2}$ smaller than the measured [5] value, so the high measured trapping power remains a puzzle. To find the formula for $\boldsymbol{P}$ with all the coefficients, we had to derive the quasiparticle-phonon collision integral for a ``dirty" superconductor in the absence of time-reversal symmetry. This is the most important result of **publication** [5].

Normal-metal traps are by far more effective than vortices, as their area may greatly exceed that of a vortex core. The contact between a trap and Al superconducting structure occurs usually through a tunnel barrier created by the aluminum oxide. It prevents the suppression of the gap in superconductor by the proximity effect and preserves the divergence of the quasiparticle density of states at energy $\boldsymbol{E=\Delta}$. Therefore the rate of escape of a trapped quasiparticle back into superconductor increases with $\boldsymbol{E}$ approaching $\boldsymbol{\Delta}$. It makes the effective trapping rate temperature-dependent. We developed this consideration into a quantitative microscopic theory in **publications** [6-8] and explained the measured dependence of the decay rate of injected quasiparticles on temperature and trap size, see Fig. 2.

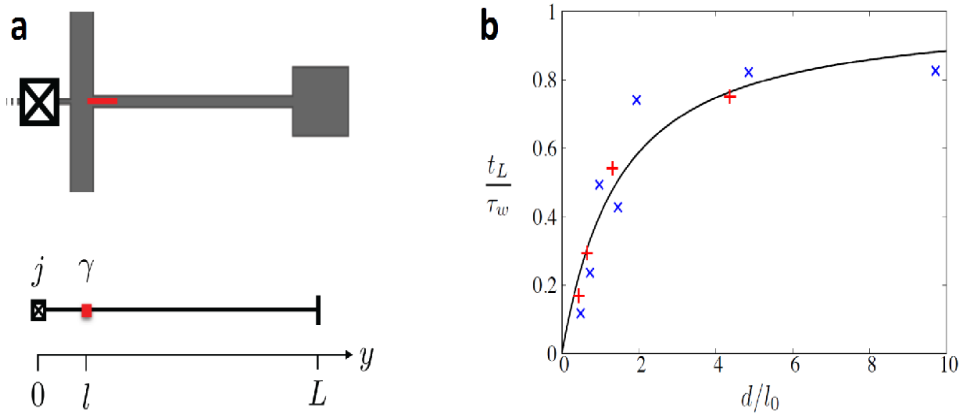

Fig. 2. **a**: A part of transmon device and its one-dimensional model used in calculations (upper and lower parts of the panel, respectively); trap is shown in red. **b**: The decay rate of the excess quasiparticle density $\boldsymbol{1/\tau_w}$ as a function of the trap size $\boldsymbol{d}$. The dimensionless variables use quasiparticle diffusion rate $\boldsymbol{1/t_L}$ across the device, and length $\boldsymbol{l_0}$ characterizing the temperature-dependent trapping rate. The data taken at T=13mK (x) and T=50mK (+) collapse on a single theory curve, see **publication** [7].

Future Plans

1. Develop a comprehensive theory of microwave properties of long one-dimensional arrays of small Josephson junctions, in order to elucidate the dynamics of weakly-pinned charge density waves.

2. Find the signature changes in multiple Andreev reflection, Josephson plasma oscillations, Shapiro steps, and the Coulomb blockade effect associated with the transition to a topological state in proximitized semiconductor nanowires. The peculiarity of the state emerging right after the transition is in the coexistence of trivial sub-system having a nascent energy gap with a sub-system carrying a fully-developed topological order.

3. Address the dissipative transport across superconducting (topological as well as trivial) quantum point contacts, including finding analogues of the well-known for the normal-state conductors Mott formula for thermopower and Landauer formula for dissipative conductance.

References

1. F. D. Parmentier, A. Anthore, S. Jezouin, H. le Sueur, U. Gennser, A. Cavanna, D. Mailly and F. Pierre, *Strong back-action of a linear circuit on a single electronic quantum channel*, Nat. Phys. **7**, 935 (2011).

2. A. P. Higginbotham, S. M. Albrecht, G. Kirsanskas, W. Chang, F. Kuemmeth, P. Krogstrup, T. S. Jespersen, J.Nygard, K. Flensberg, and C. M. Marcus, *Parity lifetime of bound states in a proximitized semiconductor nanowire*, Nat. Phys. **11**, 1017 (2015).

3. S. M. Albrecht, A. P. Higginbotham, M. Madsen, F. Kuemmeth, T. S. Jespersen, J. Nygard, P. Krogstrup, and C.M. Marcus, *Exponential protection of zero modes in Majorana islands*, Nature **531**, 206 (2016).

4. B. van Heck, R. M. Lutchyn, and L. I. Glazman, *Conductance of a proximitized nanowire in the Coulomb blockade regime*, Phys. Rev. B **93**, 235431 (2016).

5. C. Wang, Y. Y. Gao, I. M. Pop, U. Vool, C. Axline, T. Brecht, R. W. Heeres, L. Frunzio,, M. H. Devoret, G.Catelani, L. I. Glazman, and R. J. Schoelkopf, *Measurement and Control of Quasiparticle Dynamics in a Superconducting Qubit*, Nat. Comm. **5**, 5836 (2014).

Publications (August 2016 – July 2018)

1. R. M. Lutchyn, K. Flensberg, and L. I. Glazman, *Quantum charge fluctuations of a proximitized nanowire*, Phys. Rev. B **94**, 125407 (2016).

2. R. M. Lutchyn and L. I. Glazman, *Transport through a Majorana island in the strong tunneling regime*, Phys. Rev. Lett. **119**, 057002 (2017).

3. M. Pustilnik, B. van Heck, R. M. Lutchyn, and L. I. Glazman, *Quantum criticality in resonant Andreev conduction*, Phys. Rev. Lett. **119**, 116802 (2017).

4. S. Jezouin, Z. Iftikhar, A. Anthore, F.D. Parmentier, U. Gennser, A. Cavanna, A. Ouerghi, I.P. Levkivskyi, E.Idrisov, E.V. Sukhorukov, L.I. Glazman, and F. Pierre, *Controlling charge quantization with quantum fluctuations*, Nature **536**, 58 (2016).

5. Y. Savich, L. Glazman, and A. Kamenev, *Quasiparticle relaxation in superconducting nanostructures*, Phys. Rev. B **96**, 104510 (2017).

6. R.-P. Riwar, A. Hosseinkhani, L. D. Burkhart, Y. Y. Gao, R. J. Schoelkopf, L. I. Glazman, and G. Catelani, *Normal-metal quasiparticle traps for superconducting qubits*, Phys. Rev. B **94**, 104516 (2016).

7. A. Hosseinkhani, R.-P. Riwar, R. J. Schoelkopf, L. I. Glazman, and G. Catelani, *Optimal configurations for normal-metal traps in transmon qubits*, Phys. Rev. Applied **8**, 064028 (2017).

8. R.-P. Riwar, L. I. Glazman, and G. Catelani, *Dissipation by normal-metal traps in transmon qubits*, Phys. Rev. B **98**, 024502 (2018).

Simulation of Correlated Lattice and Impurity Systems out of Equilibrium

PI: Emanuel Gull, University of Michigan, Ann Arbor
Keywords: Dynamics of quantum impurities, time-dependent dynamical mean field theory, continuous-time quantum Monte Carlo, quantum transport, non-equilibrium quenches and steady state

Project Scope

Correlated quantum systems out of equilibrium exhibit a wealth of intriguing and unexpected quantum phenomena: Quantum dots at low temperature show Kondo behavior when a bias voltage is applied. Femto- and atto-second pump-probe spectroscopy experiments on Mott-insulating transition-metal compounds reveal a radical change of the nature of the many-body wave-function after a rapid change of interaction parameters, exposing a collapse and reestablishment of insulating behavior. Similarly, the dielectric breakdown of Mott-insulating materials to which a large voltage is applied leads to surprisingly long-lived quasi-static intermediate states. Our theoretical understanding of these phenomena lags far behind our experimental capabilities, as it requires a precise and unbiased solution of the quantum mechanical equations of motion. This project develops and applies numerically exact methods for correlated quantum impurity and lattice models out of equilibrium.

Recent Progress

Much of the development over the recent years focused on algorithms for quantum impurities. With controlled quantum Monte Carlo methods, results could be obtained for the time-dependence of Anderson impurity models in difficult regimes. For example, the picture on the right shows the real-time dependence of the population of a quantum impurity that, at time zero, is in one of the atomic states indicated. As time progresses, a time-dependent magnetic field leads to oscillation and relaxation. Steady-state is reached almost immediately for the empty and occupied states, whereas the periodic field drives the singly occupied states to a steady state faster than would happen without the applied field (for parameters and description see Phys. Rev. Lett. 112, 146802 (2014))

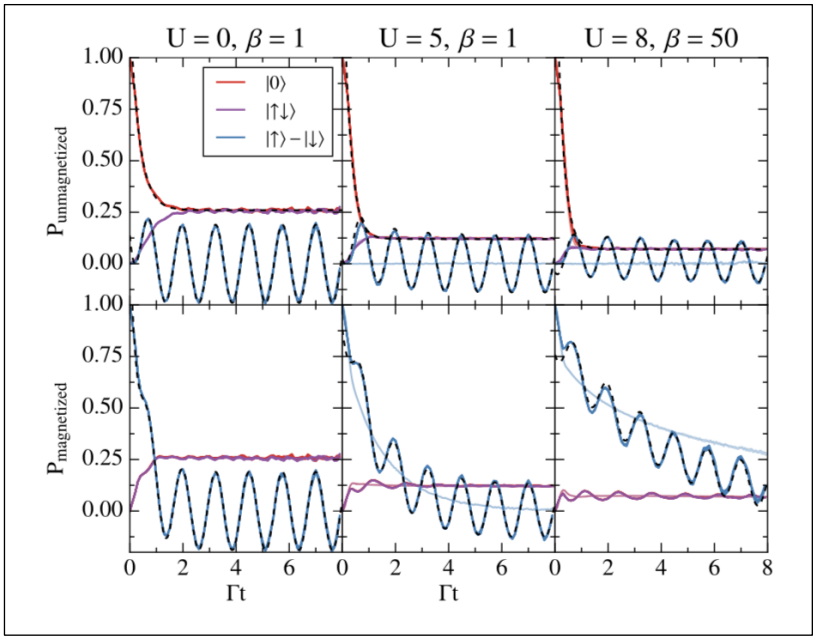

Populations are comparatively easy to compute in Monte Carlo methods. However, for most applications, currents and spectral functions are needed. Our development of a current formalism for impurity model and its implementation (Phys. Rev. B 95, 085144 (2017)) lead to figures such

as the one plotted on the right (for detailed parameters see publication), where the evolution of a current after an interaction quench is shown. Also shown are results from the frequently used 'crossing' approximation methods. As is evident, the semi-analytic non-crossing and one-crossing approximations are accurate for very short times but converge to the wrong steady state and transient behavior. In contrast, the quantum Monte Carlo methods converge as their diagram order is increased (order, in this case, corresponds to the number of crossings). Results such as these allow to obtain numerically exact results for intermediate transients and steady-state currents for strongly interacting impurity systems.

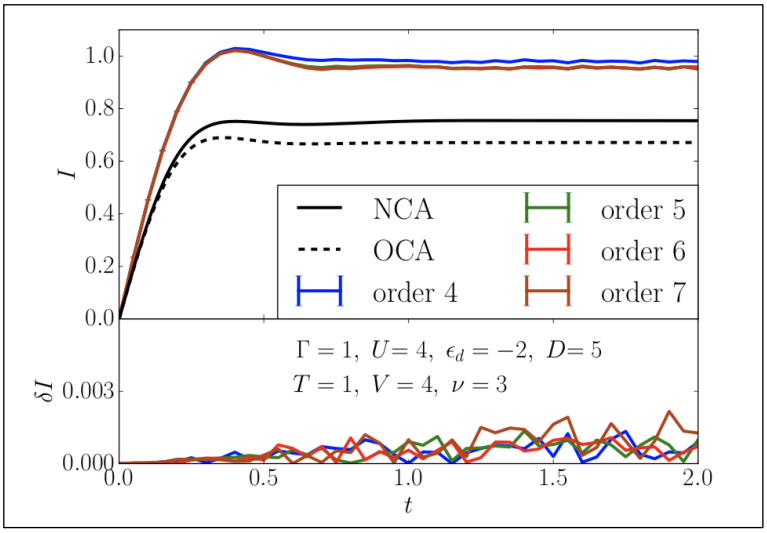

With the same formalism that allowed to compute currents, we can obtain single-particle excitation spectra ('spectral functions') for non-equilibrium systems. This is illustrated in the left panel, where an auxiliary lead formalism was used to study the old problem of the 'voltage splitting of the Kondo peak': as a quantum impurity is exposed to a large symmetric bias field, its resonance peak at zero chemical potential is expected to be suppressed. (For parameters see Phys. Rev. Lett. 112, 146802 (2014)). Some (but not all) theoretical methods predict an additional splitting of the peak. With numerically exact calculations that do not contain the additional approximations needed for analytical progress, we were able to show that the voltage splitting of the Kondo peak is real (the error bars displayed on the plot contain all stochastic and systematic errors) and, thereby, pave a way for obtaining spectral functions and time-dependent Green's functions of strongly correlated quantum impurities.

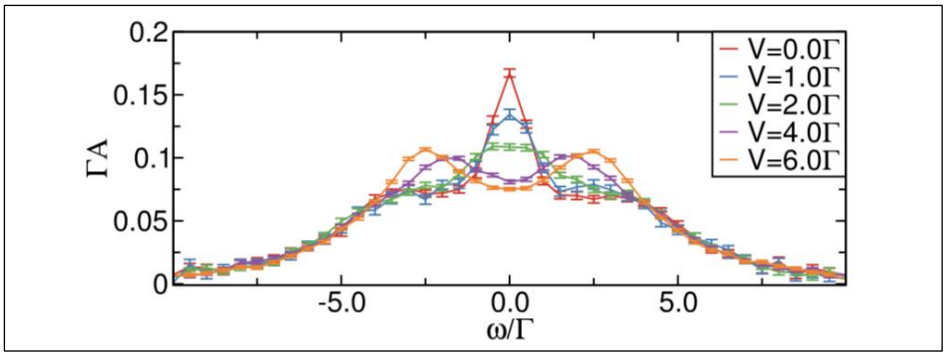

Later progress allowed to consider the effect of thermal initial ensembles (rather than diagonal density matrices, see below for a spectral function obtained for parameters corresponding to the mixed valence regime of a quantum impurity and its convergence as a function of diagram order), paving the way for applications to non-equilibrium dynamical mean field theory (see results in Phys. Rev. B 96, 155126 (2017)).

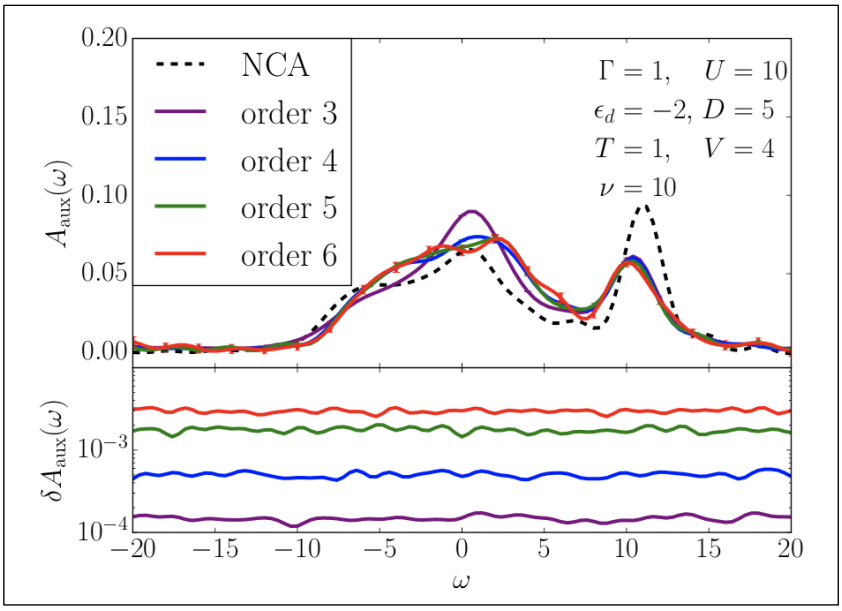

At the same time, we have been able to obtain to gather information about noise statistics and, in particular, we could for the first time compute the Full Counting Statistics (FCS) in interacting models (see below for a first passage time distribution in an interacting out-of-equilibrium model, for detailed parameters see Phys. Rev. B 97, 115109 (2018)).

This progress would have been impossible without the development of powerful new numerically exact quantum Monte Carlo algorithms. In particular, the development of bold-line Monte Carlo methods and, as of 2016, the development of the inchworm Monte Carlo method, allowed to reach numerically exact results for unprecedentedly long times and low temperatures. Progress in many-body theory allowed to compute diagrams exponentially faster; to overcome the dynamical sign problem; to compute fewer of these diagrams for the same exact answer; and to gain access new types of observables and new physics. The numerical implementation of these solvers similarly came a long way, with the first implementations based on MPI and able to scale only to hundreds of cores, whereas present implementations are based on modern asynchronous runtime systems and scale to thousands of cores with minimal overhead.

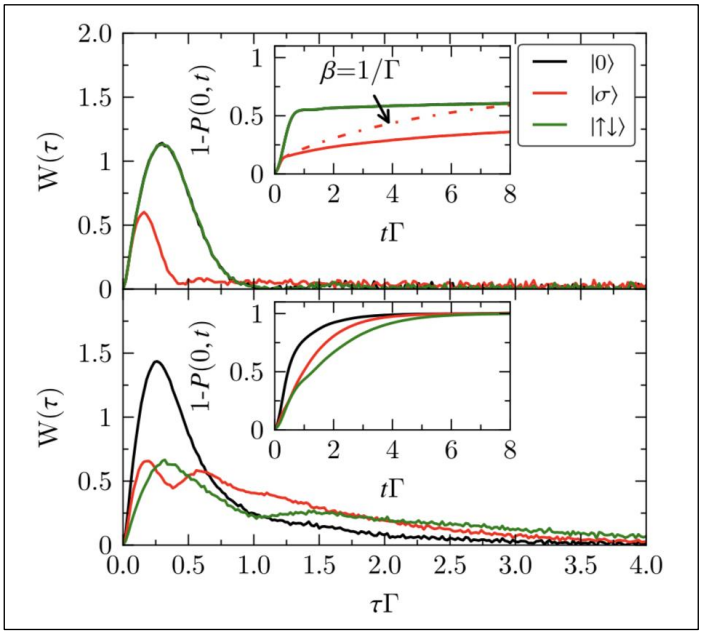

Future Plans

Now that the algorithms needed to perform non-equilibrium dynamical mean field calculations in practice are in place, the near-term future will focus on exploring quenches and periodic drives in time-dependent dynamical mean-field theory. Algorithms that properly capture finite temperature physics, the correct short time physics and the relaxation rates, while being able to converge to the correct long-term steady-state behavior are needed, and there are currently no alternatives to our diagrammatic Monte Carlo methods available that satisfy all of these points.

Publications

1. Green's functions from real-time bold-line Monte Carlo: spectral properties of the nonequilibrium Anderson impurity model, Guy Cohen, Emanuel Gull, David R. Reichman, Andrew J. Millis, Phys. Rev. Lett. 112, 146802 (2014)
2. Green's functions from real-time bold-line Monte Carlo, Guy Cohen, David R. Reichman, Andrew J. Millis, Emanuel Gull, Phys. Rev. B 89, 115139, (2014)
3. Solutions of the Two Dimensional Hubbard Model: Benchmarks and Results from a Wide Range of Numerical Algorithms, J. P. F. LeBlanc, Andrey E. Antipov, Federico Becca, Ireneusz W. Bulik, Garnet Kin-Lic Chan, Chia-Min Chung, Youjin Deng, Michel Ferrero, Thomas M. Henderson, Carlos A. Jiménez-Hoyos, E. Kozik, Xuan-Wen Liu, Andrew J. Millis, N. V. Prokof'ev, Mingpu Qin, Gustavo E. Scuseria, Hao Shi, B. V. Svistunov, Luca F. Tocchio, I. S. Tupitsyn, Steven R. White, Shiwei Zhang, Bo-Xiao Zheng, Zhenyue Zhu, Emanuel Gull, Phys. Rev. X 5, 041041 (2015)
4. Taming the dynamical sign problem in real-time evolution of quantum many-body problems, Guy Cohen, Emanuel Gull, David. R. Reichman, Andrew J. Millis, Phys. Rev. Lett. 115, 266802 (2015)
5. Voltage quench dynamics of a Kondo system, Andrey E. Antipov, Qiaoyuan Dong, Emanuel Gull, Phys. Rev. Lett. 116, 036801 (2016)
6. Updated Core Libraries of the ALPS Project, A. Gaenko, A. E. Antipov, G. Carcassi, T. Chen, X. Chen, Q. Dong, L. Gamper, J. Gukelberger, R. Igarashi, S. Iskakov, M. Könz, J. P. F. LeBlanc, R. Levy, P. N. Ma, J. E. Paki, H. Shinaoka, S. Todo, M. Troyer, E. Gull, Comput. Phys. Comm. 213 (2017) 235-251
7. Currents and Green's functions of impurities out of equilibrium -- results from inchworm Quantum Monte Carlo, Andrey E. Antipov, Qiaoyuan Dong, Joseph Kleinhenz, Guy Cohen, Emanuel Gull, Phys. Rev. B 95, 085144 (2017)
8. Quantum Monte Carlo solution of the dynamical mean field equations in real time, Qiaoyuan Dong, Igor Krivenko, Joseph Kleinhenz, Andrey E. Antipov, Guy Cohen, Emanuel Gull, Phys. Rev. B 96, 155126 (2017)
9. Numerically exact full counting statistics of the nonequilibrium Anderson impurity model, Michael Ridley, Viveka Nand Singh, Emanuel Gull, Guy Cohen, Phys. Rev. B 97, 115109 (2018)
10. Inclusion-Exclusion Principle for Many-Body Diagrammatics, Aviel Boag, Emanuel Gull, Guy Cohen, currently under review at Physical Review B.

Disordered Quantum Impurity Systems

Principal Investigators: Stephan Haas and Hubert Saleur, Department of Physics and Astronomy, University of Southern California, CA 90089

Keywords: quantum many-body systems, non-equilibrium physics, disordered systems, many-body localization, quantum entanglement

Project Scope

Impurities - small quantum systems coupled to various types of baths - are a crucial component of quantum-many body physics. Not only are they ubiquitous, they also provide many ways to probe, both theoretically and experimentally, the properties of a large variety of systems. The study of impurities in interacting systems has a long history, with hallmark results such as the observation of fractionally charged excitations in tunneling Luttinger liquids experiments. In this project, we explore the physics, in particular the dynamics, of quantum impurity systems in the presence of strong disorder and/or strong fluctuations. We concentrate on the multi-channel Kondo problem and its variants, e.g. resonant levels and quantum dot problems, in strongly disordered quantum spin chains, in equilibrium, after quenching, and under steady-state driving. We investigate in parallel the dynamics of these same systems coupled to various types of dissipation. Furthermore, we extend our studies to higher dimensions. Specific points of interest are (i) new unconventional fixed points and associated scaling functions, (ii) the effects of disorder on transport through quantum dots, and (iii) out-of-equilibrium steady-state crossovers and phase transitions induced by dissipation. We achieve our goal by combining analytical approaches based on integrability, conformal field theory and the real space renormalization group, and by developing numerical techniques based on matrix product algorithms and the kernel polynomial method.

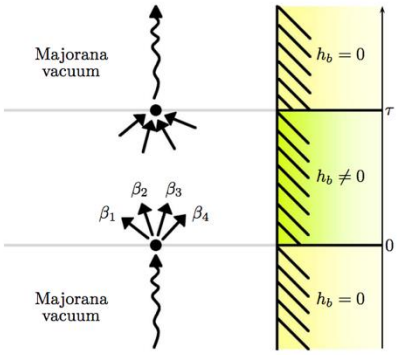

The Loschmidt echo in the resonant level model can be thought of as a partition in the Ising model with alternating vanishing and finite boundary magnetic fields h_b. A quantum quench then effectively creates an arbitrary number of fermionic excitations in the system. τ is the imaginary time.

Recent Progress

Healing of Defects in Random Antiferromagnetic Spin Chains - In recent work, we focused on the effects of a weakened link in random antiferromagnetic spin chains. [1] Here, we showed how universal healing occurs, and that homogeneity is restored at low energy, in a way that is qualitatively similar to the fate of impurities in clean ferromagnetic spin chains, or in Luttinger liquids with attractive interactions. We found that healing in the random case occurs even without interactions and is characteristic of the random singlet phase. Using real space renormalization group and exact diagonalization methods, we characterized this universal healing

crossover by studying the entanglement across the weak link. Specifically, we identified a characteristic crossover healing length l^* that separates a regime where the system is cut in half by the weak link from a fixed point where the spin chain is healed.

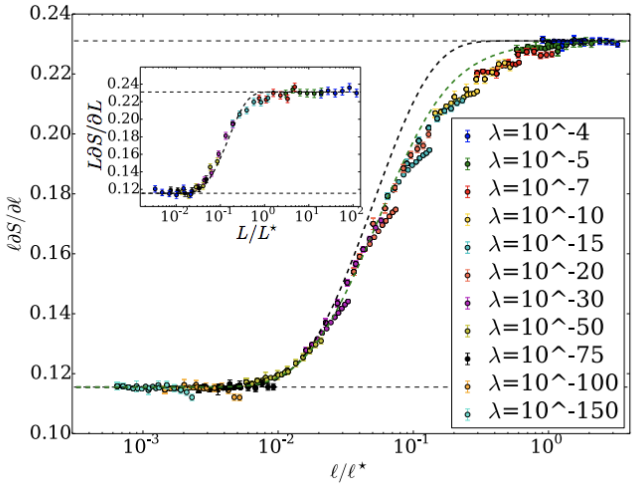

Universal crossover function obtained from numerical renormalization group calculation of the entanglement entropy in an interval l with a weak link of strength λ, introducing a crossover scale $l^* \sim (\ln(\lambda))^2$. The observed universal crossover behavior connects the high-energy regime ($l<l^*$) of two effectively disconnected chains with the low-energy regime ($l>l^*$) of a single healed chain. This implies that at sufficiently long length scales, the effects of the impurity are screened away. The dashed curve following the numerical data is an approximate analytical function we were able to derive. [1]

Remarkably, as seen in this figure, in the case of disordered antiferromagnetic chains healing occurs even without interactions (XX limit), and is associated with a rich crossover physics. The existence of this healing flow is compatible with the results of Ref. [2] where it was found that the ground state of the chain with $\lambda = 1$ and the chain with $0 < \lambda < 1$ are not orthogonal, and that there is no Anderson catastrophe. The same would be observed in a clean XXZ chain in the attractive regime. Since the repulsive or attractive nature of the interactions is so crucial for determining the fate of weak links in clean Luttinger liquids, it will be interesting to also investigate the effect of weak perturbations in random ferromagnetic chains to determine whether they also heal at low energy.

Topological Protection of Coherence in a Dissipative Environment - One dimensional topological insulators are characterized by edge states with exponentially small energies. According to one generalization of topological phases to non-Hermitian systems, finite systems in a non-trivial topological phase display surface states with exponentially long life times. In recent work [3], we explored the possibility of exploiting such non-Hermitian topological phases to enhance the quantum coherence of a fiducial qubit embedded in a dissipative environment. Here, we showed that a network of qubits interacting with lossy cavities can be represented, in a suitable super-one-particle sector, by a non-Hermitian "Hamiltonian" of the desired form. We then studied, both analytically and numerically, one-dimensional geometries with up to three sites per unit cell, and up to a topological winding number W=2. For finite-size systems we found that the number of edge modes is a complicated function of W and the system size N. Furthermore, we observed that there are precisely W modes localized at one end of the chain. In such topological phases the quibt's coherence lifetime is exponentially large in the system size. We verified that, for W>1, at large times, the Lindbladian evolution is approximately a non-trivial unitary. For W=2 this results in Rabi-like oscillations of the qubit's coherence measure.

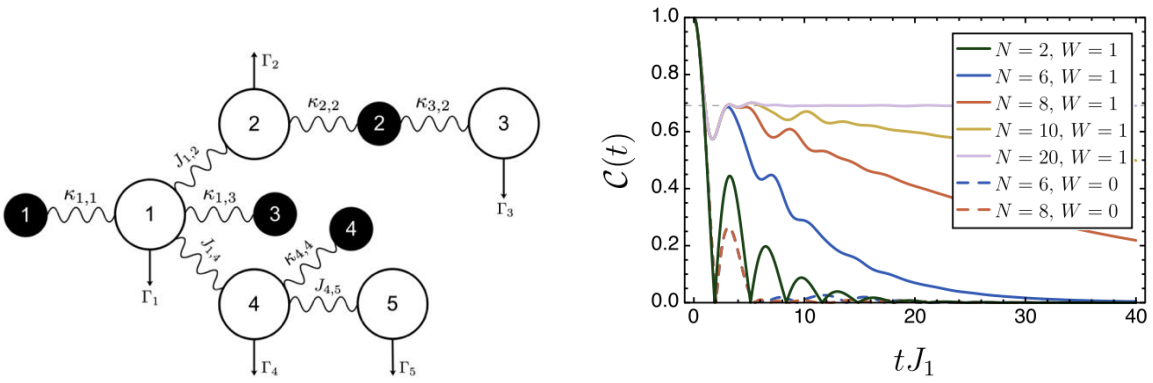

Left: A general network of qubits interacting with lossy cavities. Wavy lines indicate coherent hopping and straight arrows incoherent decay. White dots represent (leaky) cavities, whereas black dots are (long-lived) two-level systems. **Right**: Behavior of a coherence measure in the non-Hermitian generalization of the Schrieffer-Su-Heeger model with an even number of sites. Continuous lines are results in the topological non-trivial phase (W=1). Increasing the number of sites N has the effect of exponentially increasing the coherence time scale, beyond which the approximate dark state in these systems starts decaying. Dashed lines are for the topological trivial phase (W=0). We observed that the lattice of cavities with W=1 vastly improves the lifetime of coherence.

Non-Hermitian topological phases in a finite system permit the construction of states whose decay time is either infinite or exponentially large in the system size. This feature is extremely appealing from the point of view of creating long-lived quantum bits. In our recent work we have shown that networks of qubits interacting with lossy cavities may be configured to possess nontrivial topological structure. For networks with a simple linear geometry, we found that localization and long-livedness of the topological edge modes both concur to dramatically increase the coherence of a qubit sitting at the end of the chain. Specifically, a nonzero topological winding number W results in an exponentially long-lived qubit. Although at finite size the exact number of edge modes is a complicated function of W and N, there are always W edge modes localized at one end of the chain. For W = 2 we found that the long-time dissipative, Lindbladian evolution becomes approximately unitary, and the coherence of the qubit displays long-lived Rabi oscillations. In general, such long-lived, topological edge modes are not legitimate quantum states but rather they are off-diagonal elements of quantum states, or coherences. The possibility of using such long-lived coherences for quantum computation is an interesting and challenging objective for our future studies.

Disordered Quantum Spin Chains with Long-Range Antiferromagnetic Interactions – Furthermore, we investigated the magnetic susceptibility $\chi(T)$ of quantum spin chains with power-law long-range antiferromagnetic couplings as a function of their spatial decay exponent α and cutoff length ξ [4]. The calculations were based on the strong disorder renormalization method which was used to obtain the temperature dependence of $\chi(T)$ and distribution functions of couplings at each renormalization step. For the case with only algebraic decay ($\xi = \infty$) we found a crossover at $\alpha* = 1.066$ between a phase with a divergent low-temperature susceptibility $\chi(T \to 0)$ for $\alpha > \alpha*$ to a phase with a vanishing $\chi(T \to 0)$ for $\alpha < \alpha*$. For finite cutoff lengths ξ, this crossover was observed to occur at a smaller $\alpha*(\xi)$. Additionally, we studied the localization of spin excitations for $\xi = \infty$ by evaluating the distribution function of excitation energies and we found a delocalization transition that coincides with the opening of the pseudo-gap at $\alpha_c = \alpha*$.

Future Plans

Moving forward, we will address the problem of how to characterize criticality in open quantum systems. To tackle this, we will develop a generalized scaling theory of critical phenomena for out-of-equilibrium quantum systems, described by master equations, including driving and dissipative terms. This generalization of scaling theory for closed systems is non-trivial: it is based on a multi-gap hypothesis, whereby in open systems criticality can occur both due to a divergence of the spatial correlation length and/or the components of the complex relaxation time.

Critical properties of physical observables, such as generalized susceptibilities, will be computed, using the non-equilibrium steady state solutions, ρ_{NESS}, of the master equations. Universal scaling functions will be derived, connecting the finite-size and finite-time scaling at criticality with off-critical regimes. We will also determine the underlying renormalization group equations based on a path integral formulation of the problem, akin to those for equilibrium phase transitions. Furthermore, we will derive generalized scaling and hyper-scaling relations between critical exponents in the out-of-equilibrium context and formulate generalized conformal field theories for open quantum systems.

The multi-gap scaling paradigm will be explicitly applied to interacting lattice models, using finite-size scaling analysis to extract their critical properties. Specifically, we will analyze and characterize out-of-equilibrium quantum phase transitions in (i) integrable quadratic Lindbladians, (ii) Davies-Lindblad generators and their respective Hamiltonian systems with Hamiltonian bath, and (iii) driven-dissipative generalizations of the Bose-Hubbard model.

References

1. Healing of Defects in Random Antiferromagnetic Spin Chains, R. Vasseur, A. Roshani, S. Haas, and H. Saleur, Europhys. Lett. 119, 50004 (2017).

2. Multifractal orthogonality catastrophe in one-dimensional random quantum critical points, R. Vasseur and J. E. Moore, Phys. Rev. B 92, 054203 (2015).

3. Topological Protection of Coherence in a Dissipative Environment, L. Campos Venuti, Z. Ma, H. Saleur, S. Haas, Phys. Rev. A 96, 053858 (2017).

4. Disordered Quantum Spin Chains with Long-Range Antiferromagnetic Interactions, N. Moure, H.-Y. Lee, S. Haas, R. N. Bhatt, S. Kettemann, Phys. Rev. B 97, 014206 (2018).

5. Many Body Localization Transition in Random Quantum Spin Chains with Long-Range Interactions, N. Moure, S. Haas, S. Kettemann, Eur. Phys. Lett 111, 27003 (2015).

Publications

A list of selected publications follows below.

1. Plasmonic Superconductivity in Layered Materials, M. Rösner, R. E. Groenewald, G. Schönhoff, J. Berges, S. Haas, T. O. Wehling, submitted to Nature Communications (2018).

2. Disordered Quantum Spin Chains with Long-Range Antiferromagnetic Interactions, N. Moure, H.-Y. Lee, S. Haas, R. N. Bhatt, S. Kettemann, Phys. Rev. B 97, 014206 (2018).

3. Healing of Defects in Random Antiferromagnetic Spin Chains, R. Vasseur, A. Roshani, S. Haas, and H. Saleur, Europhys. Lett. 119, 50004 (2017).

4. Topological Protection of Coherence in a Dissipative Environment, L. Campos Venuti, Z. Ma, H. Saleur, S. Haas, Phys. Rev. A 96, 053858 (2017).

5. Probing Gap Plasmons Down to Sub-Nanometer Scales Using Collapsible Nano-Fingers, B. Song, Y. Yao, R. E. Groenewald, Y.Wang, H. Liu, Y. Li, S. Cronin, A. Schwartzberg, S. Cabrini, S. Haas, and W. Wu, ACS Nano 10.1021/acsnano.7b01468 (2017).

6. Universal entanglement dynamics following a local quench, R. Vasseur, H. Saleur, 10.21468/SciPostPhys.3.1.001 (2017).

7. Interplay of screening and superconductivity in low-dimensional materials, G. Schönhoff, M. Rösner, R. Groenewald, S. Haas, T. O. Wehling, Phys. Rev. B 94, 134504 (2016).

8. Valley Plasmonics in the Dichalcogenides, R.E. Groenewald, M.R. Rösner, G. Schönhoff, S. Haas, T.O. Wehling, Phys. Rev. B 93, 205145 (2016).

Symmetry in Correlated Quantum Matter

Principal investigator: Michael Hermele
Department of Physics, University of Colorado Boulder, Boulder, CO 80309
michael.hermele@colorado.edu

Keywords: topological phases of matter, strongly correlated materials, fractons

Project Scope

The goal of this project is to characterize, classify and elucidate the properties of highly entangled forms of quantum matter, in which symmetry or the geometry of the crystalline lattice plays a key role. Current efforts are focused on two families of quantum states of matter, crystalline symmetry protected topological (cSPT) phases, and fractonic states of matter, *i.e.* those supporting fracton excitations and other excitations with restricted mobility. In cSPT phases, both the symmetries and the discrete geometry of crystal lattices play a key role. In fractonic states, the geometry of the crystal lattice enters via sub-dimensional excitations that are constrained to move on certain lattice planes or axes. Current work on cSPT phases is based on an approach we developed to classify these states, and focuses on applying this approach in more realistic settings, with the goal of identifying new examples of cSPT phases in materials or realistic models, and understanding the physical properties of these states. Current work on fractonic matter is multi-faceted, reflecting the plethora of open questions pertaining to these states, and includes efforts both to understand theoretical questions pertinent to fractonic matter, and to identify systems where fractonic states may be realized.

Recent Progress

Classifying crystalline topological phases – In Refs. 4 and 7, and together with Liang Fu in Ref. 4, we developed an approach to classify crystalline symmetry protected topological (cSPT) phases in arbitrary spatial dimension and for arbitrary symmetry, with no assumptions needed about the strength of interactions. Our approach, which is based on a kind of dimensional reduction, leads to the conclusion that cSPT phases can be viewed as "topological crystals," *i.e.* they can be realized as stacks and arrays of lower-dimensional topological phases (Fig. 1). This means that each entry in the topological classification table corresponds to a concrete pattern of lower-dimensional states in real space, that can be used as a starting point for understanding physical properties, and even points a way toward possible realizations.

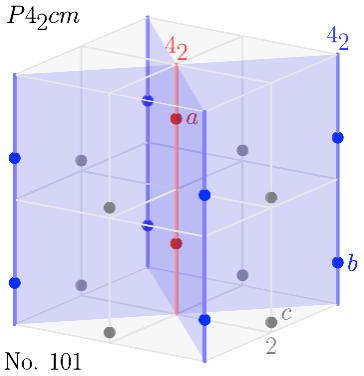

Figure 1. Unit cell of a topological crystal state for space group $P4_2cm$. Colored points, lines and planes represent lower-dimensional topological states. (Image from online material of Ref. 7.)

Surface field theories of point group SPT phases – An important step toward understanding surface phenomena of interacting SPT phases is to identify surface field theories, or other tractable descriptions of the surface physics. In Ref. 8, we employed our dimensional reduction approach (Refs. 4 and 7) at surfaces of three-dimensional bosonic SPT phases protected by point group symmetry, to identify candidate surface field theories for these states. For instance, with mirror symmetry, the idea is to inhomogeneously gap out a field theory away from the mirror axis, reducing it to an effective one-dimensional problem, which can be identified with the edge of a lower-dimensional topological state on the mirror plane. In this way, the anomaly of the field theory can be identified, in the sense that this determines the SPT phase for which it can be a surface theory. We identified three different classes of field theories that describe surfaces of many different SPT phases.

Coupled-layer constructions of fractonic states of matter – One reason models for fractonic states of matter are mysterious is that it has often not been obvious how or whether their ground states are related to more familiar quantum phases of matter. In collaboration with Ethan Lake and Xie Chen, we showed that some fracton phases can be obtained via coupled layers of two-dimensional topological phases (Ref. 6). The coupling mechanism is a condensation of "*p*-strings" where the point-particle excitations of the two-dimensional layers arrange into string-like objects (Fig. 2), that then condense. Among other results, we described the already-known X-cube fracton model in terms of coupled toric code layers, and constructed new fracton models. More recently, in arXiv:1806.04687 (to be submitted), we used similar ideas to construct and study models for fracton phases supporting non-Abelian excitations with restricted mobility.

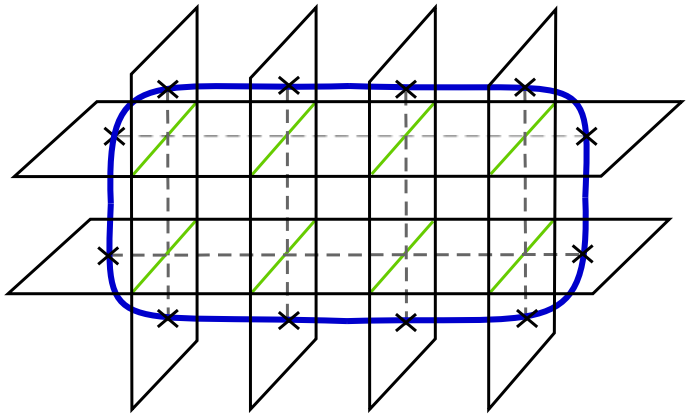

Figure 2. Depiction of a p-string (blue line) formed out of flux excitations (crosses) in a system of coupled toric code layers. Upon condensing p-strings, the X-cube fracton phase results. (From Ref. 6.)

Non-local entanglement entropy in fractonic states of matter – Topological entanglement entropy has become an important tool to characterize topological phases in two and three dimensions. It is natural to ask whether there are analogs of topological entanglement entropy for fractonic matter that capture the non-local entanglement in these states. In collaboration with Sid Parameswaran and Rahul Nandkishore (Ref. 9), we answered this question in the affirmative, computing several different measures of non-local entanglement entropy in the X-cube and cubic

code fracton models. The most striking result is the presence of a term linear in the size of the subregion.

Relating tensor gauge theories to gapped fractonic states of matter – Fracton states of matter have generally been studied either via exactly solvable model Hamiltonians, which support fully gapped states, or via lattice tensor gauge theories, which describe states with gapless photon-like excitations. The relationship between these two different theoretical descriptions, and two different types of fracton topological phases of matter, was elucidated in a collaboration with Xie Chen (Ref. 10), where we explored the states resulting from Higgs and confinement transitions in tensor gauge theories.

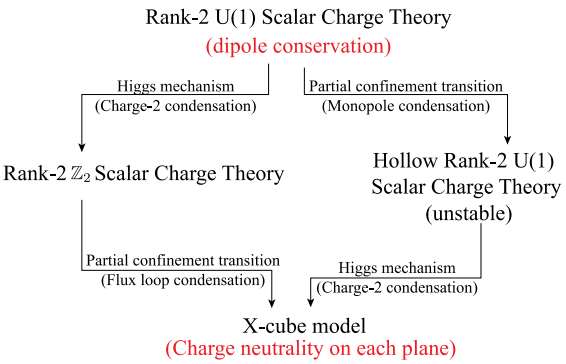

Figure 3. Diagram illustrating two routes from a U(1) tensor gauge theory (the rank-2 scalar charge theory) to the X-cube model. (From Ref. 10.)

Future Plans

Real space classifications of free fermion crystalline topological phases. While free-fermion topological phases, including those with crystalline symmetry, can in principle be classified using K-theory, there is a paucity of concrete results available for three-dimensional systems with space group symmetry. In particular, results for the physically important case of electronic insulators with time reversal symmetry and significant spin-orbit coupling (class AII) are not available. We are using our dimensional reduction approach to classify such free-fermion crystalline topological phases, and thus developing an alternative to K-theory. Our approach allows for interactions to be easily included, and is physically transparent as it is connected to concrete real-space constructions.

Generalizing fusion and statistics of anyons to fracton topological phases. An important characterization of two-dimensional topological phases is in terms of the fusion and braiding statistics properties of their anyon excitations. For fracton topological phases, so far such sharp characterizations have largely been missing. We are currently developing a generalization of the fusion theory of Abelian anyons to fracton topological phases, and using this theory to provide a description of novel statistical processes.

Publications (August 2016 – July 2018)

A list of ten selected publications follows below.

1. S. B. Lee, M. Hermele and S. A. Parameswaran, *Fractionalizing glide reflections in two-dimensional Z_2 topologically ordered phases*, Phys. Rev. B **94**, 125122 (2016).

2. X. Chen and M. Hermele, *Flux-Fusion Anomaly Test and Bosonic Topological Crystalline Insulators*, Phys. Rev. X **6**, 041006 (2016).

3. X. Chen and M. Hermele, *Symmetry fractionalization and anomaly detection in three-dimensional topological phases*, Phys. Rev. B **94**, 195120 (2016).

4. H. Song, S.-J. Huang, L. Fu and M. Hermele, *Topological phases protected by point group symmetry*, Phys. Rev. X **7**, 011020 (2017).

5. Y.-P. Huang and M. Hermele, *Theory of quantum kagome ice and vison zero modes*, Phys. Rev. B **95**, 075130 (2017).

6. H. Ma, E. Lake, X. Chen and M. Hermele, *Fracton topological order via coupled layers*, Phys. Rev. B **95** (2017).

7. S.-J. Huang, H. Song, Y.-P. Huang and M. Hermele, *Building crystalline topological phases from lower-dimensional states*, Phys. Rev. B **96**, 205106 (2017). Editors' suggestion.

8. S.-J. Huang and M. Hermele, *Surface field theories of point group symmetry protected topological phases*, Phys. Rev. B **97**, 075145 (2018).

9. H. Ma, A. T. Schmitz, S. A. Parameswaran, M. Hermele, and R. M. Nandkishore, *Topological entanglement entropy of fracton stabilizer codes*, Phys. Rev. B **97**, 125101 (2018).

10. H. Ma, M. Hermele and X. Chen, *Fracton topological order from the Higgs and partial-confinement mechanisms of rank-two gauge theory*, Phys. Rev. B **98** 035111 (2018).

High-throughput and data-driven materials discovery tools with application to thermoelectric materials design

Lead Investigator: Anubhav Jain, Energy Storage & Distributed Resources Division, Lawrence Berkeley National Laboratory. Email: ajain@lbl.gov
Keywords: "thermoelectrics", "high-throughput density functional theory", "open source software", "feature extraction"

Project Scope

This project aims to build software and methodological tools for data-driven materials design and apply those tools towards the design of new thermoelectric materials. The software being developed encompasses implementation and automation of existing methodologies as well as development of new methodologies in the areas of calculation automation and feature extraction for large data set analysis. The approach to thermoelectrics materials discovery includes both high-throughput screening with density functional theory and data mining methods. Success is measured by software and methodological impact as well as progress in the research and discovery of novel thermoelectric formulations.

This project creates and applies software tools to generate theoretical data on a large scale, i.e., via millions of simulations executed over a variety of supercomputing resources. It also develops software tools for the analysis of large data sets, specifically implementing feature extraction methods relevant to the materials science domain. By generating large data sets as well as transforming those data sets to make the best use of existing machine learning methods, this project aims to accelerate and change the way in which materials design is done.

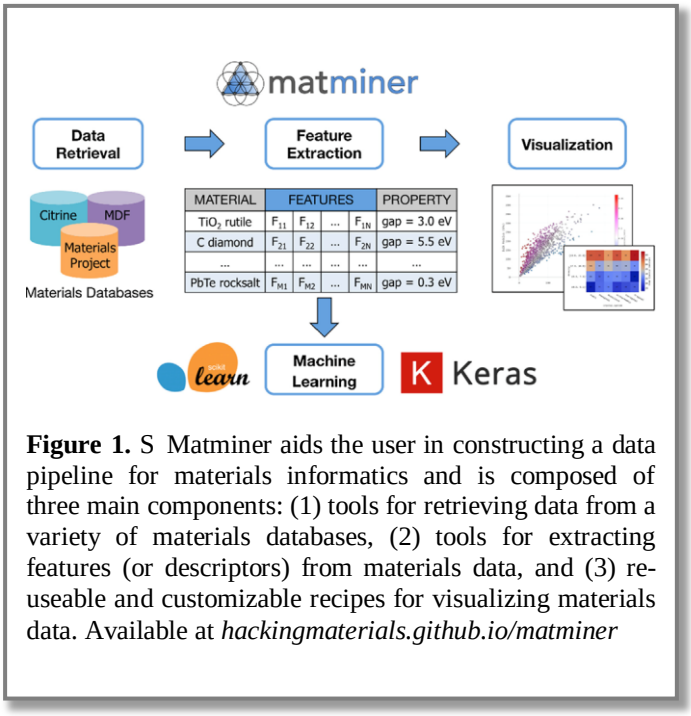

Figure 1. S Matminer aids the user in constructing a data pipeline for materials informatics and is composed of three main components: (1) tools for retrieving data from a variety of materials databases, (2) tools for extracting features (or descriptors) from materials data, and (3) re-useable and customizable recipes for visualizing materials data. Available at *hackingmaterials.github.io/matminer*

Recent Progress

To demonstrate the applicability of this framework, we are collaborating with the experimental groups of Snyder (Northwestern) and White (Dalhousie University) as well the theory group of Hautier (U. Catholique Louvain) to discover and experimentally realize new classes of thermoelectric materials. We have also used our software tools in collaboration with the Pei group (Tongji University) to better understand band convergence in new thermoelectric formulations, including a GeTe derivative with extremely high figure of merit[1] (zT ~ 2.4, device zT ~1.5) – see Figure 2.

We have developed and released two software libraries as a result of this award:

- **Atomate** – software to simplify the process of generating data with theoretical methods[2]. Atomate implements common workflows for determining over a dozen materials properties (e.g., band structure, elastic tensor, dielectric constants, etc.) and allows those workflows to be automated at large supercomputing centers. Atomate has been adopted by several research groups worldwide and is

now the production software infrastructure for data generation for the Materials Project. Atomate is available at *hackingmaterials.github.io/atomate*

- **Matminer** – software to retrieve and analyze large materials data sets (Figure 1). Matminer can retrieve data by interfacing with the APIs of several large database providers (Materials Project, Citrine Informatics, Materials Data Facility, MPDS) or load a user's internal data sets. It then assists the user with feature extraction – i.e., the process of converting raw data such as composition, crystal structure, or band structure into a series of physically relevant numbers that can be used to determine patterns in the data. Matminer has implemented 20 different featurization patterns, many of methods developed in the literature but with no open-source implementation, and is capable of generating many thousands of materials descriptors. Matminer also includes a built-in visualization package and interfaces to standard Python-based libraries for machine learning. Thus, matminer serves as a bridge between the materials community and the data science community. Matminer is available at *hackingmaterials.github.io/matminer*

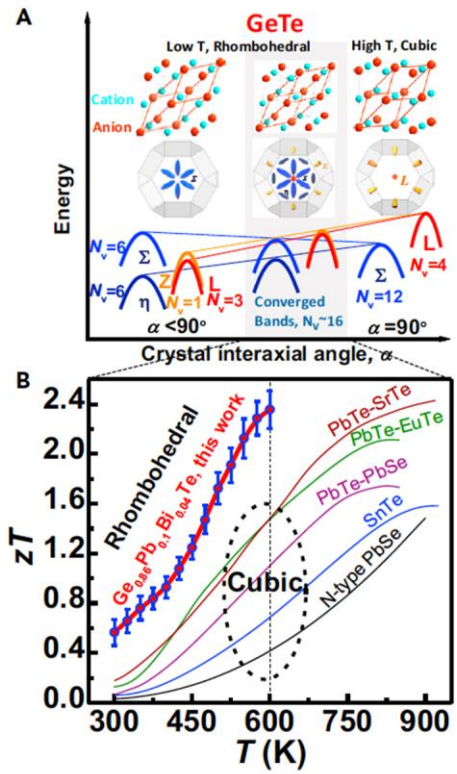

Figure 2. Band convergence achieved by slightly lowering the symmetry leads to highly converged bands (Nv ~ 16) and extremely high measured thermoelectric properties.

Apart from software development, we have:

- Generated a large data set of electron transport properties under the constant relaxation time approximation for >45,000 compounds and published the data as open access[3] (downloadable through Dryad at *https://doi.org/10.5061/dryad.gn001*). A dedicated "app" for exploring this data through the Materials Project web site is in development.
- Used the data set above to screen for new thermoelectric materials. Three materials from the screening were experimentally synthesized and tested by colleagues. The first of these, $TmAgTe_2$, reached a figure of merit (zT) of 0.35, with further improvement limited by achievable doping[4]. A second, $YCuTe_2$, reached a zT of 0.75, to our knowledge the highest zT for a computationally designed material in a new structure class[5]. A third quarternary compound was synthesized, but demonstrated low performance due to inability to dope; a report is forthcoming.
- We have assessed the accuracy of various high-throughput methods to the accuracy of thermoelectrics screening[6]. For example, we found that Seebeck coefficients are better reproduced than the power factor under the constant relaxation time approximation (as expected), but underestimation of the band gap for typical DFT functionals can be problematic for both properties. We have also compiled reports on the thermoelectric potential for less-studied chemistries such as phosphides[7].
- We continued development of the AMSET method for modeling electron properties ("high-throughput" implementation of electron scattering models). The method is now being re-tested on several semiconductors with known experimental data and showing good accuracy.

- We continued development of the "rocketsled" (previously TurboWorks) code for performing adaptive simulations with the FireWorks workflow package. The rocketsled code enables one to use supercomputing centers to perform automatic inverse searches (via optimization techniques such as Gaussian process or machine learning surrogate models) when a forward solution can be computed. For example, we plan to use rocketsled to let the computer "guide" which thermoelectric materials should be screened rather than screening researcher-generated lists of compounds.

All the software and data developed by this project is being provided openly. The software is hosted online at Github (all projects listed at: *https://www.github.com/hackingmaterials*) under a Berkeley Software Distribution open source license. A large data set on electron transport properties has been shared through the Dryad repository (*https://doi.org/10.5061/dryad.gn001*).

Future Plans

Future plans are currently concentrated on development of new crystal structure descriptors for materials data mining as well as improved electron transport models (over a constant relaxation time approximation) that balance accuracy and automation. These developments will be used to continue the search for new thermoelectric materials. We have also been extending our data set of computations to compounds with partial occupancies.

This project has demonstrated that new and unconventional thermoelectric compositions with moderate zTs can be uncovered through a computational approach. One of the major limitations in achieving even higher zT has been difficulties in estimating achievable doping levels, which has a large effect on the observed experimental properties but cannot be easily determined from calculations. Better methods are needed to estimate the extent to which a material can be doped n- or p-type and may be the subject of future work.

References / Publications

1. Li, J., Zhang, X., Chen, Z., Lin, S., Li, W., Shen, J., Witting, I. T., Faghaninia, A., Chen, Y., Jain, A., Chen, L., Snyder, G. J. & Pei, Y. Low-Symmetry Rhombohedral GeTe Thermoelectrics. Joule 1–12 (2018). doi:10.1016/j.joule.2018.02.016
2. Ward, L., Dunn, A., Faghaninia, A., Zimmermann, N. E. R., Bajaj, S., Wang, Q., Montoya, J., Chen, J., Bystrom, K., Dylla, M., Chard, K., Asta, M., Persson, K. A., Snyder, G. J., Foster, I. & Jain, A. Matminer: An open source toolkit for materials data mining. Comput. Mater. Sci. 152, 60–69 (2018).
3. Mathew, K., Montoya, J. H., Faghaninia, A., Dwarakanath, S., Aykol, M., Tang, H., Chu, I., Smidt, T., Bocklund, B., Horton, M., Dagdelen, J., Wood, B., Liu, Z.-K., Neaton, J., Ong, S. P., Persson, K., et al. Atomate: A high-level interface to generate, execute, and analyze computational materials science workflows. Comput. Mater. Sci. 139, 140–152 (2017).
4. Ricci, F., Chen, W., Aydemir, U., Snyder, G. J., Rignanese, G.-M., Jain, A. & Hautier, G. An ab initio electronic transport database for inorganic materials. Sci. Data 4, 170085 (2017).
5. Zhu, H., Hautier, G., Aydemir, U., Gibbs, Z. M., Li, G., Bajaj, S., Pöhls, J.-H., Broberg, D., Chen, W., Jain, A., White, M. A., Asta, M., Snyder, G. J., Persson, K. & Ceder, G. Computational and experimental investigation of TmAgTe 2 and XYZ 2 compounds, a new group of thermoelectric materials identified by first-principles high-throughput screening. J. Mater. Chem. C 3, 10554–10565 (2015).
6. Aydemir, U., Pöhls, J.-H., Zhu, H., Hautier, G., Bajaj, S., Gibbs, Z. M., Chen, W., Li, G., Ohno, S., Broberg, D., Kang, S. D., Asta, M., Ceder, G., White, M. A., Persson, K., Jain, A., et al. YCuTe2 : a member of a new class of thermoelectric materials with CuTe 4 -based layered structure. J. Mater. Chem. A 4, 2461–2472 (2016).
7. Chen, W., Pöhls, J.-H., Hautier, G., Broberg, D., Bajaj, S., Aydemir, U., Gibbs, Z. M., Zhu, H., Asta, M., Snyder, G. J., Meredig, B., White, M. A., Persson, K. & Jain, A. Understanding thermoelectric properties

from high-throughput calculations: trends, insights, and comparisons with experiment. J. Mater. Chem. C 4, 4414–4426 (2016).
8. Pöhls, J.-H., Faghaninia, A., Petretto, G., Aydemir, U., Ricci, F., Li, G., Wood, M., Ohno, S., Hautier, G., Snyder, G. J., Rignanese, G.-M., Jain, A. & White, M. A. Metal phosphides as potential thermoelectric materials. J. Mater. Chem. C 5, (2017).
9. Faghaninia, A., Yu, G., Aydemir, U., Wood, M., Chen, W., Rignanese, G.-M. G.-M., Jeffrey, S., Hautier, G., Jain, A., Snyder, G. J., Hautier, G., Jain, A., A., F., G., Y., U., A., M., W., et al. A computational assessment of the electronic, thermoelectric, and defect properties of bournonite (CuPbSbS3) and related substitutions. Phys. Chem. Chem. Phys. 19, 6743–6756 (2017).
10. Chu, I.-H., Roychowdhury, S., Han, D., Jain, A. & Ong, S. P. Predicting the volumes of crystals. Comput. Mater. Sci. 146, (2018).

Quantitative Studies of the Fractional Quantum Hall Effect

Principal investigator: Jainendra Jain
Department of Physics, 104 Davey Lab, Penn State University, University Park, PA 16802
jkj2@psu.edu

Keywords: fractional quantum Hall effect; composite fermions; topological states; diffusion Monte Carlo; density functional theory

Project Scope: The fractional quantum Hall effect (FQHE) is a rare example of a nontrivial, strongly-correlated condensed-matter system that one can hope to understand in a quantum chemistry sense. To be sure, one can write effective field theories that capture the topological content of the phenomenon as well as its low-energy, long-distance properties. But one can also construct, within the composite fermion theory, microscopic wave functions that represent directly the actual wave functions of electrons. Furthermore, comparisons with computer experiments tell us that this theory should allow calculations of "non-topological" quantities with a few % accuracy. Comparisons with laboratory experiments, although decent, are not accurate to the level of a few percent. The reason is that the experimental numbers are affected by Landau level (LL) mixing, finite thickness corrections and disorder, all of which are set to zero in computer comparisons[1].

Given the paradigmatic status of the FQHE, we believe it is worthwhile to push theory to its limits and to obtain as accurate a quantitative understanding as possible. Such an understanding will not only be satisfying and give us further confidence in our understanding, but significant quantitative deviations from experiments may also reveal new puzzles. For this purpose, we have employed the "fixed phase diffusion Monte Carlo (DMC)" method to treat LL mixing. We have also developed a density functional theory (DFT) of the FQHE to deal with systems of non-homogeneous densities, occurring, for example, at the edge of a FQHE state. We have tackled several additional puzzles presented by experiments.

Recent Progress:

All publications supported by DOE during the period 2016-2018 are listed at the end. We highlight some of the prominent results here.

Spin phase transitions [Ref. 3]: Transitions between differently spin-polarized states have been observed as a function of the Zeeman energy. Earlier calculations obtained qualitative agreement with experiments, but could not resolve quantitative discrepancies. We have asked how LL mixing affects spin phase transitions. A convenient measure of the

[1] Interestingly, we have a better quantitative understanding of the non-trivial part of the physics, namely the FQHE, than of the extraneous effects coming from finite width and LL mixing.

strength of LL mixing is the ratio of interaction energy to cyclotron energy $\kappa = (\frac{e^2}{\epsilon l})/(\hbar\omega_c)$. Because κ is not small ($\kappa = 1 - 2$ in typical n-doped GaAs systems and 5-10 in p-doped GaAs systems), a non-perturbative approach is desirable. We have employed the so-called fixed phase DMC method for this purpose developed in 1990s by Ortiz, Ceperley and Martin. In this approach, one uses an initial "trial" wave function to fix the phase sector, and defines a Schrodinger equation for the amplitude of the wave function, with the gradient of the fixed phase playing the role of a vector potential. The DMC method then iteratively projects this state into the ground state within this phase sector. The final result is as good as the choice of the phase. We fix the phase using the accurate wave functions within the lowest LL.

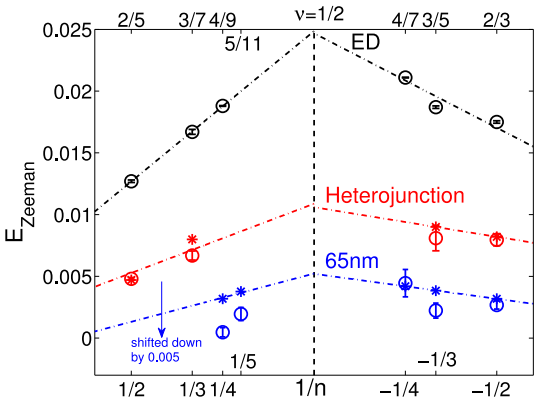

In Ref. [3] we have applied this method to spin phase transitions in the FQHE. Experiments measure the critical Zeeman energies, which are a direct measure of the Coulomb energy differences between the two competing states with different spin polarizations. In the accompanying figure the experimental results are shown by red and blue stars for a heterojunction sample and a quantum well of width 65 nm; black circles show the prediction of ideal theory neglecting finite thickness and LL mixing; and red and blue circles show results including both finite width and LL mixing. The last are in excellent agreement with experiments. It is remarkable that we are able to predict the energy difference, which itself is a few percent of the energy, with this accuracy.

Density functional theory of the FQHE [Ref. 6]: In paper [6] we developed a density function theory (DFT) for fractional quantum Hall effect, to treat systems in the presence of a non-uniform external potential. A previous DFT approach by Ferconi, Geller and Vignale naturally produced an integer filling at very low temperatures, and required thermal averaging to yield a fractional filling. Our new angle here was to formulate the problem in terms of composite fermions, because integer fillings of composite fermions correspond to fractional fillings of electrons. We constructed an exchange correlation functional for composite fermions and obtained self-consistent solutions in an iterative scheme within a local density approximation. We studied the nature of "edge reconstruction" as a function of T. The figure below shows the density profile for the ½ Fermi sea when exposed to a periodic potential from a crystal in a nearby layer (for different lattice constants).

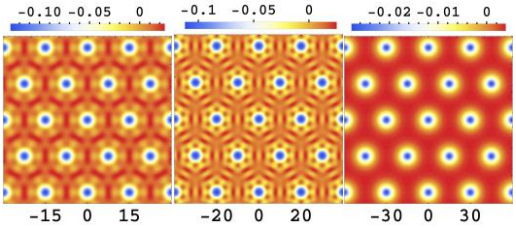

Phase diagram for the 2D crystal in high magnetic fields [Ref. 9]: The nature and the phase digram of the crystal is of fundamental interest, especially in the FQHE regime where an interplay between the strongly correlated liquid and solid leads to several re-entrant phase transitions. Experiments have indicated that LL mixing induces a crystal. In paper [9] we apply the fixed phase DMC method to determine the phase diagram of the crystal. The calculated phase diagrams (above) show that the crystal phase depends very sensitively on both the filling factor and the LL mixing parameter κ. For example, while the FQHE states at 1/3 and 2/5 are very robust to LL mixing, a crystal appears at intermediate fillings at relatively low LL mixing. This explains the fact that in p-doped samples an insulating phase, presumably a pinned crystal appears in the vicinity of 1/3 state. Interestingly, we find that the crystal phase in the vicinity of 1/5 is a strongly correlated crystal of composite fermions, not of electrons.

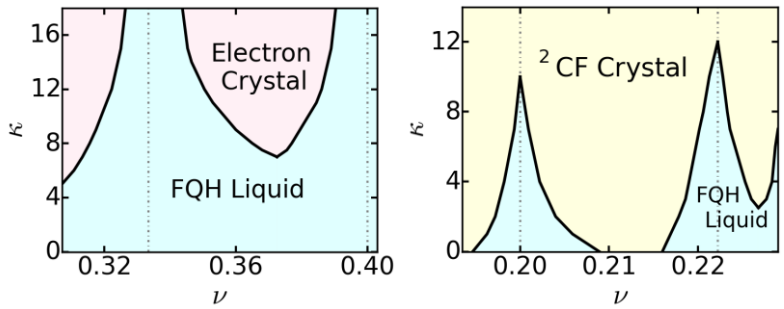

Beyond composite fermions - parton theory of FQHE [Ref. 11]: One of the persistent puzzles in FQHE has been the remarkably different behaviors in the lowest and second LLs. For example, a FQHE is seen at $\nu = 5/2$ but a Fermi sea at $\nu = 1/2$. In paper [11], we have proposed that the FQHE states in the second LL arise from a new mechanism, namely the parton paradigm, which includes the composite fermion states but also states beyond. In the parton construction, one first breaks electrons into fictitious particles, called partons; then places each species of partons into an integral QHE state; and finally fuses the partons back into physical electrons to produce an ansatz wave function for an incompressible FQHE state. It was recently shown by Balram, Barkeshli and Rudner (PRB, in press) that the anti-Pfaffian phase for the 5/2 FQHE can be described in terms of a parton wave function. Further pursuing that line, we have argued that a sequence of parton wave functions reproduces many prominent fractions seen in the second LL. In particular, we have explained how the FQHE at 2+6/13, first observed in 2010, can appear naturally as a strong fraction. We have proposed experimental quantities that can reveal the parton structure of this state and also verify its remarkably different topological structure than that of the 6/13 FQHE state in the lowest LL.

Future Plans

Here I list some of the problems that we are currently investigating.

Kohn Sham equations for FQHE: We are developing the Kohn-Sham equations for the FQHE. In 1990s, Heinon had obtained physically meaningful results by solving the KS

equations via an ensemble density functional method. We will formulate the Kohn-Sham equations for composite fermions. We have already made substantial progress on issue, and currently my student is in the process of studying screening of an external charge.

The effect of correlations on the transverse wave function: It is customary to calculate the transverse wave function at zero magnetic field and use it even in the FQHE regime. This cannot be the whole story, as experiments show in the same sample a single layer behavior for certain fractions and a bilayer behavior at others. The fixed phase DMC enables us to determine how the transverse wave function depends on the correlations in two dimensions, and, in particular, how the transition from a single layer to a bilayer as a function of the quantum well width depends on the filling factor. A student has made good progress on this issue.

Additionally, we will investigate whether the parton construction sheds new light on the nature of excitations of the second LL FQHE states.

Publications supported by DOE during 2016-2018

1. "Robustness of topological surface states against strong disorder observed in Bi_2Te_3 nanotubes," Renzhong Du et al., Phys. Rev. B 93, 195402 (2016) [10 pages].

2. "Topological phases of two-component bosons in species-dependent artificial gauge potentials," Ying-Hai Wu and Tao Shi, Phys. Rev. B 94, 075103 (2016).

3. "Landau level mixing and particle hole symmetry breaking for spin transitions in fractional quantum Hall effect," Y. Zhang, A. Wojs and J. K. Jain, Phys. Rev. Lett. 117, 116803 (2016).

4. "Observation of the quantum-anomalous-Hall insulator to Anderson insulator quantum phase transition and its scaling behavior," Cui-Zu Chang, Weiwei Zhao, Jian Li, J. K. Jain, Chaoxing Liu, Jagadeesh S. Moodera, Moses H. W. Chan, Phys. Rev. Lett. 117, 126802 (2016). [Editor's Suggestion]

5. "Tunnel transport and interlayer excitons in bilayer fractional quantum Hall systems," Yuhe Zhang, J.K. Jain, and J. P. Eisenstein, Phys. Rev. B 95, 195105 (2017). [Editor's Suggestion]

6. "Density-Functional Theory of the Fractional Quantum Hall Effect," Jianyun Zhao, M. Thakurathi, M. Jain, D. Sen, J. K. Jain, Phys. Rev. Lett. 118, 196802 (2017). [Editor's Suggestion]

7. "Surprising robustness of particle-hole symmetry for composite-fermion liquids," G. J. Sreejith, Y. Zhang and J. K. Jain, Phys. Rev. B 96, 125149 (2017).

8. "Inter-Landau level Andreev reflection at the Dirac point in graphene quantum Hall state coupled to an $NbSe_2$ superconductor," Manas Ranjan Sahu, Xin Liu, Arup Kumar Paul, Sourin Das, Pratap Raychaudhuri, J. K. Jain and Anindya Das, submitted to Phys. Rev. Lett.

9. "Landau level mixing induced crystallization in the fractional quantum Hall regime," Jianyun Zhao, Yuhe Zhang, J.K. Jain, submitted to Phys. Rev. Lett.

10. "Evidence for a new non-Abelian even-denominator fractional quantum Hall state in graphene," Youngwook Kim, Ajit C. Balram, Takashi Taniguchi, Kenji Watanabe, Jainendra K. Jain, Jurgen H. Smet, submitted to Nature Physics.

11. "Fractional Quantum Hall Effect at $\nu = 2 + \frac{6}{13}$: The Parton Paradigm for the Second Landau Level," A. C. Balram, S. Mukherjee, K. Park, M. Barkeshli, M. S. Rudner, and J. K. Jain, submitted to Phys. Rev. Lett.

12. "Topological Superconductivity in Landau Levels," G.-S. Jeon, J. K. Jain, and C.-X. Liu, submitted to Phys. Rev. Lett.

Mapping & Manipulating Materials Phase Transformation Pathways

PI: Duane Johnson, Ames Lab

Keywords: Materials Theory, Computational Materials, Novel Algorithms

Project Scope: To predict energy-relevant, complex multicomponent materials and tailor their functionality, guide synthesis and characterization, we will develop and apply unique electronic-structure-based thermodynamic techniques to predict stability by mapping *global solid-solid transformations* and *local structural instabilities* (e.g., short-range order). We will advance thermodynamic linear-response theory to predict chemical ordering involving coupled electronic, chemical, magnetic, and displacive fluctuations in multicomponent systems for discovery and design of useful properties and for direct comparison to experiment. We will map solid-solid transformation pathways (enthalpies & transition barriers) between states via new methods, including a proper *solid-state nudged-elastic band* method that incorporates non-conserved order parameters (e.g., magneto-volume effects) and disorder. Jointly, these methods *uniquely assess global and local materials stability between competing structures and synthesis routes*, revealing opportunities to manipulate properties. Applications will be on novel and responsive materials, e.g., multicomponent magnets and high-entropy alloys, iron-arsenide superconductors, and caloric and topological materials.

Recent Progress

- **Discovery & Design:** We advanced electronic-structure thermodynamic linear-response theory, code, and calculations of short-range order in arbitrary (N-component) multiple principal element alloys (a.k.a. high-entropy alloys).
  Identified Electronic Origins and Tailor Properties:
  - We associate thermodynamic and mechanical properties to competing electronic effects in high-temperature refractory systems (e.g., increased 2000K modulus in TiZrTaMoW over commercial materials) for direct discovery and design, **e.g., see pubs. [1], [2], & [10]**.
  - Via dispersion-engineering, thermodynamic and thermoelectric properties in a series of refractory metal systems were investigated and then tailored, increasing, for example, the thermoelectric figure of merit ZT by 10× factor for *high-temperature waste-heat recovery materials*. It is unpublished while we await experimental confirmation for IP purposes.

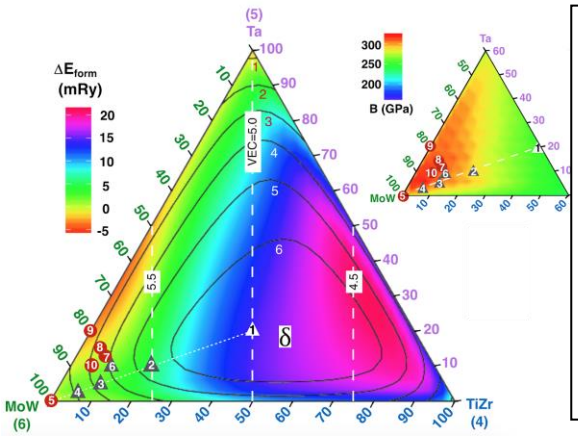

High-throughput calculations in full Gibbs' design space (a 2-D cut through 5-D composition space): **formation enthalpy (mRy)** and **bulk modulus (GPa) vs. (x,y) for $(MoW)_xTa_y(TiZr)_{1-x-y}$**, which contains the equiatomic high-entropy alloy (#1). Optimal alloy is in line perpendicular to (#10). Plot indicates vertical (dashed) lines of *valence-electron count* (VEC), and contours of *size mismatch* (δ). Short-range order (SRO) for segregation (triangles) or ordering (circles) indicate where Fermi surface effect alters stability, ordering, and needed moduli.

- **Thermodynamic Linear-Response in General Crystal Lattices**: Completed theory and implemented for chemical short-range order in multi-sublattice crystal structures. Tested and passed 6 out 7 validation criteria using homogeneous solid-solution as reference (***to be published***). Started from generalized theory, reported in last TCMP PI meeting.
- **Forces and Phonons:** In collaboration (LSU/Ames), code/algorithms have been developed to calculate full densities and forces in KKR using proposed embedding and Dyson's equation iteration schema (***to be published – test results shown in triennial review proposal***).
- **Alternative Synthesis Routes:** We have recently addressed transformation pathways for materials under application of general stress tensor, e.g., non-hydrostatic stresses, such as Si I → Si II, where uniaxial stress can produce transformation with 20× lower than hydrostatic pressures, producing novel materials via new synthetic pathways (***submitted***).
- **Topological and Superconducting Materials:** Over the past ~2 years we have been collaborating with Paul Canfield's FWP to help theoretically identify or predict specific electronic features that lead to unusual topological behavior, see publications, including control of type-II Weyl states, identification of Dirac node arcs, and topological boundaries controlled by spin-orbit coupling and atomic sizes (chemical pressure).

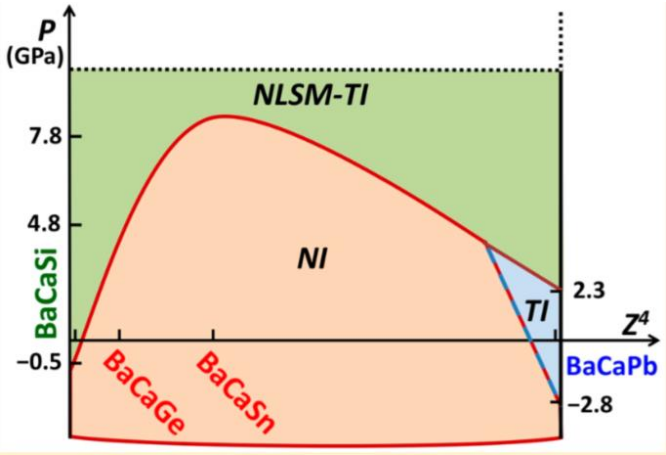

Topological transitions in BaCaX (X=group V) systems due to alloying, spin-orbit coupling and pressure effects. **Multiple topological states can be supported in the same crystal structure.** Boundaries vs alloying are desired.

Future Plans

Triennial review proposal was submitted in May 2018 and details the major directions proposed. In short, we propose to extend the thermodynamic linear-response methods to **arbitrary complex multicomponent systems**, such as those with partial order, as exhibited in most iron-arsenides or magnetic superconductors, including linear-response for magnetic SRO at high temperatures or spin waves at low temperatures, extending design capabilities, e.g., in complex alloys (see **[1], [2], & [10]**), quantum materials (see **[3], [4], [7], & [8]**), and new sythnetic routs (e.g., see **[9]**). We also propose to extend the KKR Green's function methods to incorporate forces, spin-order coupling, electron-correlation, etc., using mathematical embedding to incorporate the key physics and iterating Dyson's equation to include in electronic structure and thermodynamics (a factor of 10× faster than direct solve). These direct include or determine the underlying electronic origin for behavior (**e.g., [2]**). Having completed generalizing the solid-state nudged elastic band for correct coupling of degrees of freedom (used worldwide now) and

for *non-conserved order* parameters to address, e.g., magneto-volume collapse during transformations, we will focus on the ability to address partially disordered systems – to enable mapping of transition states in arbitrary chemical and magnetic systems using the KKR with embedding. Novel topological materials exhibiting various levels of disordered (e.g., alloying and synthesis vacancies as found in off-stoichiometric systems, like $(Ca\text{-}Sr)Co_{2-y}As_2$, $(Ba\text{-}K)Fe_2As_2$, or other systems, with Lifshitz and quantum critical points that control quantum response will be directly addressed. **Examples include publications include [3], [4], [7], & [8]**. The unique algorithms, codes, and applications will provide quantitative predictive and design capabilities that are unique worldwide. We have made some of the codes available as open-source, e.g., all the solid-state nudged elastic band codes, including extensions. With generalization of KKR-CPA codes, we plan to make these open source, depending on software development.

Publications (August 2016 – July 2018, *10 out of 24 – top relevant*)

1. Prashant Singh, A. Sharma, A. V. Smirnov, M.S. Diallo, P. Ray, G. Balasubramanian, and Duane D. Johnson, "Design of high-strength refractory complex solid-solution alloys," *npj* Computational Materials **4**:16 (2018). 10.1038/s41524-018-0072-0
2. Prashant Singh, A.V. Smirnov, and Duane D. Johnson, "TaNbMoW refractory high-entropy alloys: anomalous ordering behavior and its intriguing electronic origin," Phys. Rev. Materials **2**, 055004-6 (2018). 10.1103/PhysRevMaterials.2.055004
3. Lin-Lin Wang, A. Kaminski, P. Canfield, and Duane D. Johnson, "Different topological quantum states in ternary Zintl compounds: BaCaX (X=Si, Ge, Sn, and Pb)," J. Phys. Chem. C **122**, 705-13 (2018). 10.1021/acs.jpcc.7b11111
4. Lin-Lin Wang, N. H. Jo, Y. Wu, Quansheng Wu, A. Kaminski, P. C. Canfield, and Duane D. Johnson, "Phonon-induced topological transition to a type-II Weyl semimetal," Phys. Rev. B **95**, 165114-7 (2017). 10.1103/PhysRevB.95.165114
5. Yuchen Pei; Zhiyuan Qi; Tian Wei Goh; Lin-Lin Wang; Raghu V. Maligal-Ganesh; Chaoxian Xiao; Xinle Li; Shiran Zhang; Franklin (Feng) Tao; Duane D. Johnson, and Wenyu Huang, "Intermetallic structures with atomic precision for selective hydrogenation of nitroarenes," J. of Catalysis **395**, 307-314 (2017). 10.1016/j.jcat.2017.10.011
6. Prashant Singh, Manoj K. Harbola, and Duane D. Johnson, "Better band gaps for wide-gap semiconductors from a locally corrected exchange-correlation potential that nearly eliminates self-interaction errors," J. Phys.: Condens. Matter **29**, 424001 (2017). 10.1088/1361-648X/aa837b
7. Daixiang Mou, Tai Kong, William R. Meier, Felix Lochner, Lin-Lin Wang, Qisheng Lin, Yun Wu, S. L. Bud'ko, Ilya Eremin, D.D. Johnson, P.C. Canfield, and A. Kaminski, "Enhancement of the superconducting gap by nesting in $CaKFe_4As_4$ – a new high-temperature superconductor," *Phys. Rev. Lett.* **117**, 277001 (2016). 10.1103/PhysRevLett.117.277001
8. Yun Wu, Tai Long, Lin-Lin Wang, D.D. Johnson, Daixiang Mou, Lunan Huang, Benjamin Schrunk, S. L. Bud'ko, P.C. Canfield, and Adam Kaminski, "Asymmetric Mass Acquisition in LaBi: Topological semimetal candidate," *Phys. Rev. B* **94**, *081108-4 (**Rapid**)* (2016). 10.1103/PhysRevB.94.081108
9. Lin-Lin Wang, A. Herwadkar, J. M. Reich, Duane D. Johnson, S. D. House, P. Peña-Martin, A. Rockett, I. M. Robertson, S. Gupta, and V. K. Pecharsky, "Towards Direct Synthesis of Alane: A Predicted Defect-Mediated Pathway Confirmed Experimentally," *Chem. Sus. Chem.* **9**, 2358-2364 (2016). 10.1002/cssc.201600338
10. Aayush Sharma, Prashant Singh, Duane D. Johnson, Peter K. Liaw, and Ganesh Balasubramanian, "Atomistic clustering-ordering and high-strain deformation of $Al_{0.1}CrCoFeNi$ high-entropy alloys," *Scientific Reports* **6**, 31028 (2016). 10.1038/srep31028

Thermoelectric Energy Harvesting and Heat Management with Quantum Heterostructures

Principle Investigator: Andrew N. Jordan
Department of Physics and Astronomy, University of Rochester, Rochester, NY 14627
jordan@pas.rochester.edu

Keywords: Thermoelectricity, nanoengines, quantum measurement, mesoscopic transport

Project Scope

Thermoelectric effects in solid state systems manifest the conversion of temperature differences into electrical currents (the Seebeck effect), as well as the conversion of voltage differences into heat currents (the Peltier effect). The field has attracted much interest in recent years because of the possibility of converting heat from the environment into electrical work, also known as energy harvesting. This form of energy harvesting has many possible applications, such as in electric circuits on computer chips that produce large amounts of heat. The heat production is now so great in these chips that it limits further transistor density, requiring cooling in order not to overheat. One can use the harvested energy from a primary circuit to run auxiliary circuits such as autonomous sensors. Alternatively, one can use these heat engines in reverse to actively cool the circuits as an electrical refrigerator. Our overarching goal is to develop thermoelectric devices with a detailed microscopic theory of the physics, operating in particular on quantum principles. The research program is focused on specific research tasks and objectives: **O1)** *Extend three terminal thermoelectric devices to the superconducting domain*. We will investigate power generation in superconducting systems based on Josephson junction devices and interactions with microwave photons, making use of temperature differences in the extended system and the intrinsic nonlinearities of the Josephson junctions. The physics of different geometries will be optimized to maximize power or efficiency at maximum power. **O2)** *Develop a thermoelectric transistor.* The proposed device is based on three-terminal structures, and works by delivering a large heat current between two (different temperature) terminals from a small temperature and/or voltage change on the third terminal. We will explore quantum dot geometries as well as quantum Hall edge state geometries to manage the flow of heat from one region to another. **O3)** *Investigate the interplay between quantum measurement and the generation of charge currents.* Local hot spots on a potential well are known to generate particle currents under some circumstances because of the spatially changing diffusion. Quantum measurement leads to intrinsic disturbance noise that is a purely quantum mechanical analog of thermal noise. Measurements should also create this rectification effect, giving a new kind of thermodynamic resource to be investigated. Feedback will also be incorporated.

Recent Progress

Quantum measurement powered engines **–** Together with my postdoc, Cyril Elouard, we have invented quantum engines powered entirely by a position-resolving measurement performed on a quantum particle, published in Pub. 1. These engines produce work by moving the quantum particle against a force. Unlike classical information-driven engines (e.g., Maxwell's demon), the energy is not extracted from a thermal hot source but directly from the observation process via a

partial wave-function collapse of the particle. We have calculated the work done and the efficiency for different values of the engine parameters. Feedback is required for optimal performance. We find that unit efficiency can be approached when one measurement outcome prepares the initial state of the next engine cycle, while the other outcomes leave the original state nearly unchanged.

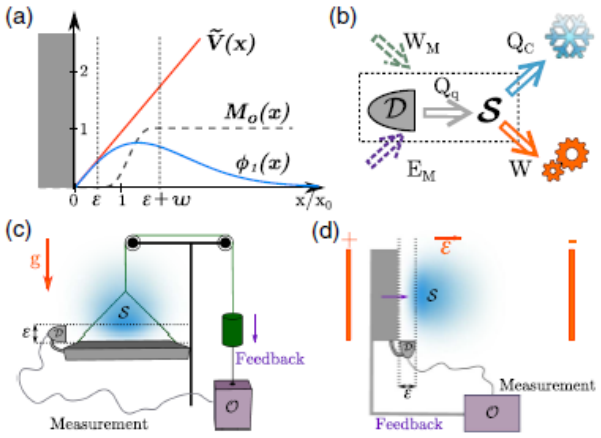

Fig. 1. (a) Situation under investigation. The particle's initial wave function (blue solid line) is the ground state which is confined between the tilted scaled potential (depicted as a solid red line) and the wall (in gray). The generalized measurement is characterized by the dotted line, able to tell that, for sure, the particle is outside a spatial region. (b) Energy exchanges occurring during the engine cycle: The measurement provides the "quantum heat", which is split between useful work and the heat dissipated in the cold bath (c),(d) Two possible implementations: The atom elevator and the single electron battery.

The engine consists of the system (a single particle), a detector, and a controller to either move a wall's position or keep it in place, see Fig. 1. The object of the engine is to convert energy given by the measurement process into useful work. The three strokes of the engine cycle are as follows: (1) Measurement.—A generalized measurement of the particle's position occurs, resulting in the stochastic result i (inside) or o (outside) of a spatial region. Generally, the new (disturbed) state of the particle is no longer in its ground state and therefore has a greater internal energy, regardless of which outcome occurs. The energy gained by the particle during this step must be provided by
the measurement, because total energy is conserved. We refer to the average energy gain over both outcomes, as "quantum heat" because of its stochastic nature, (2) Feedback.—If outcome i was found (the particle is close to the wall), then the engine controller does nothing.
If outcome o is found (the particle must be a distance larger than ε from the wall), then the controller suddenly moves the wall to the right this same distance. This costs no work, in principle, because the wave function's value is 0. (3) Reset.—Whatever the outcome, we let the particle relax in contact with a bath of temperature cold with respect to the energy splitting. For a relaxation time long enough, the particle is in its ground state, possibly with an advanced wall. As the particle is in a known pure state after the measurement, this step can, in principle, be replaced with a coherent energy extraction step mapping the post-measurement states to the ground state(s), such that no thermal bath is required.

We stress that a simple transfer of energy is not sufficient to make a working engine. The energy must be transferred in such a way that it can be efficiently extracted. To this end, our three-stroke engine is near optimal, because one outcome produces nearly the correct ground state of the system in the next cycle, while the other outcomes leaves the state nearly the same as before. The ability to advance our wall with no work expended allows efficient conversion of kinetic to potential energy to make the particle do work against an opposing force, provided by the measurement process. In spite of the stochastic nature of the measurement process, we are able to attain efficiencies approaching unity. This result clearly illustrates the differences with conventional quantum thermal engines.

Resonant tunneling quantum dot thermoelectric engine **–** In collaboration with theorists Björn Sothmann (Universität Duisburg-Essen), Rafael Sánchez (Universidad Autónoma de Madrid), and the experimental group of Charles Smith (Cambridge University), we have recently demonstrated a nanoscale energy harvester that utilizes the physics of resonant tunneling quantum dots, see Fig. 2. This work is based on our theoretical proposal of Ref. 1. Gate defined quantum dots on GaAs/AlGaAs high-electron-mobility transistors are placed on either side of a hot electron reservoir. The discrete energy levels of the quantum dots are tuned to be aligned with low energy electrons on one side and high energy electrons on the other side of the hot reservoir. The quantum dots thus act as energy filters and allow a rectification of electrical current and production of electrical power. This energy harvester device, measured at 120mK in Helium dilution refrigerator, can generate a thermal power of 0.12fW when the temperature difference beside two dots is about 1.65 K. Different AC Joule heating currents are applied near the hot reservoir to gain different temperature profiles in the cavity. The experiments and theoretical analysis have been carried out, and the manuscript is nearing completion.

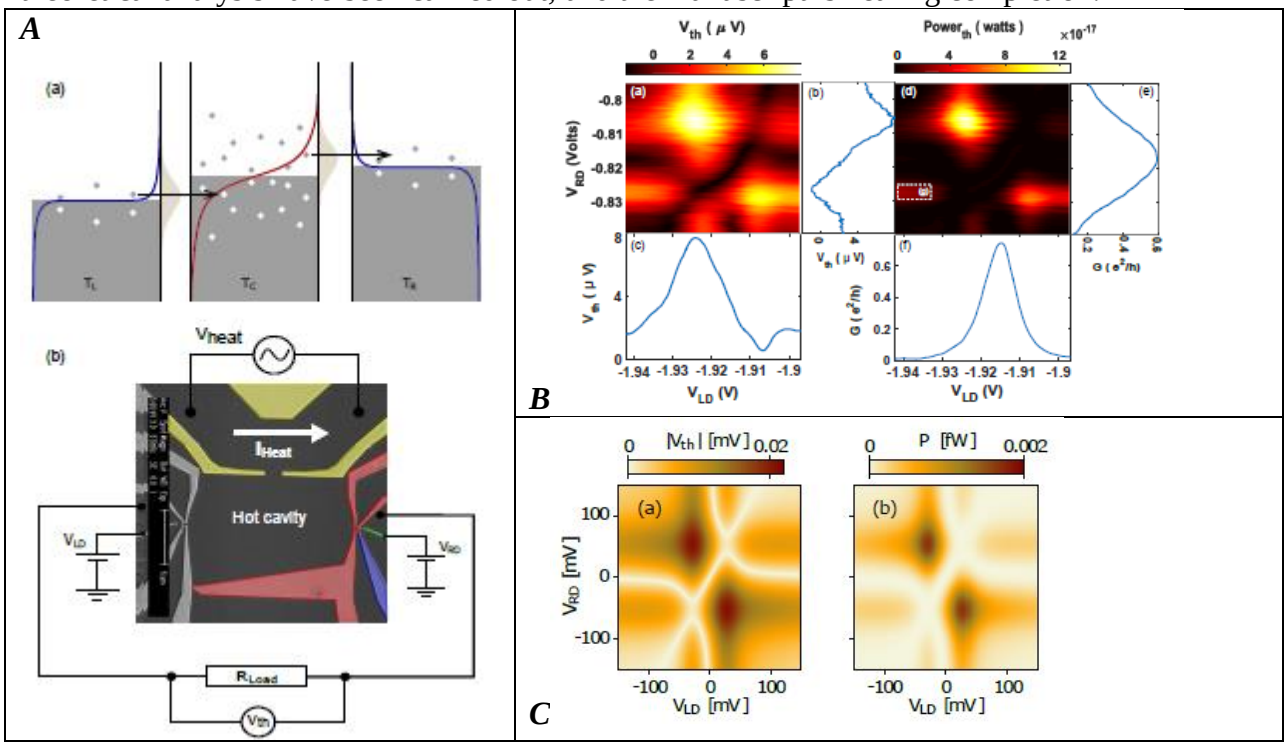

Fig. 2. ***A*** (a) Energy diagram of the nanoscale heat engine. Resonant tunneling quantum dots divide the sample into three spatial regions at temperatures TL; TC; TR, and serve as energy filters (transmission functions are indicated in the quantum dot regions). (b) False color SEM image of the device with the electrical circuit used for the thermopower measurement. ***B*** Experimental data: The thermal voltage Vth, across the device, is plotted as a function of left and right plunger gates measured whilst an AC current, is applied to the heating channel. ***C*** Theoretical simulation of the data is shown in panel ***B***.

Fluctuation theorems for continuous quantum measurement **-** Fluctuation theorems are relations constraining the out-of-equilibrium fluctuations of thermodynamic quantities like the entropy production that were initially introduced for classical or quantum systems in contact with a thermal bath, Ref. 2. Together with PhD student Sreenath Manikandan and postdoc Cyril Elouard, we have demonstrated that in the absence of thermal bath, the dynamics of continuously

measured quantum systems can also be described by an analogous fluctuation theorem, expressed in terms of a recently introduced arrow of time measure. This theorem captures the emergence of irreversible behavior from microscopic reversibility in continuous quantum measurements. From this relation, we demonstrated that measurement-induced wave-function collapse exhibits absolute irreversibility (like the free expansion of a gas in a thermodynamic system), such that Jarzynski, Ref. 3, and Crooks-like equalities, Ref. 4, are violated. We apply our results to different continuous measurement schemes on a qubit: dispersive measurement, homodyne and heterodyne detection of a qubit's fluorescence. The manuscript is complete, and will be available as a preprint at the DOE meeting.

Future Plans

From 2018-05-29 to 2018-07-20, I am a coordinator of the Kavli Institute for Theoretical Physics (KITP) program "Thermodynamics of quantum systems: Measurement, engines, and control". This program has brought many leading experts from around the globe to work together in an intense environment, focused on the most pressing and important problems in the fields of quantum thermodynamics. The outcome of this meeting has generated a huge number of new ideas for the PI, closely connected with the proposed topics of this grant. I intend to work on the following projects:

Heat transistor utilizing quantum dot and quantum point contact - By coupling a quantum point contact to a quantum dot hosting electrons that tunnel in an out of a thermal reservoir, we will be able to realize the heat transistor mentioned in the project description of this abstract. In collaboration with Björn Sothmann (Universität Duisburg-Essen), Rafael Sánchez (Universidad Autónoma de Madrid), and Janine Splettstoesser (Chalmers), we will optimize the properties of the quantum point contact and the coupling energy to obtain a nonlinear electrical current response when a small temperature is applied to the bath. This may also be used for precision thermometry.

Cyclic superconducting refrigerator – Together with Francesco Giazotto (Scuola Normale Superiore, Pisa), we have begun developing a new kind of superconducting refrigerator. By coupling to both another superconductor and normal metal, and driving an oscillating magnetic field, we believe that a high-power fridge can be built.

Extension of the quantum measurement engine to many particles on a lattice. – By extending our ideas with Cyril Elouard to a many-particle system on the lattice, we will carry our research on the scaling up of our quantum measurement engine. This work will be carried out in collaboration with Rafael Sánchez (Universidad Autónoma de Madrid).

Joint nonlocal quantum measurement refrigerator. – Building off of recent work by Michele Campisi and coworkers, Ref. 5, we will adapt their cooling method to be implemented in circuit QED systems, with heat transfer via photons through a coaxial cable, separating qubits in different cavities. The goal is to cool one blackbody radiator. This work will be carried out with Benjamin Huard (ENS Lyon), Michele Campisi (Pisa), and Géraldine Haack (Univ. Geneva).

References

1. A. N. Jordan, B. Sothmann, R. Sánchez, and M. Büttiker, *Powerful and efficient energy harvester with resonant-tunneling quantum dots*, Phys. Rev. B **87**, 075312 (2013).
2. U. Seifert, *Stochastic thermodynamics, fluctuation theorems, and molecular machines,* Rep. Prog. Phys. 75, 126001 (2012).
3. C. Jarzynski, *Nonequilibrium Equality for Free Energy Differences*, Phys. Rev. Lett. **78**, 2690 (1997).
4. G. Crooks, *Entropy production fluctuation theorem and the nonequilibrium work relation for free energy differences*, Phys. Rev. E **60**, 2721 (1999).
5. L. Buffoni, A. Solfanelli, P. Verrucchi, A. Cuccoli, M. Campisi, *Quantum Measurement Cooling*, arXiv:1806.07814

Publications (August 2016 – July 2018)

1. C. Elouard, and A. N. Jordan, *Efficient Quantum Measurement Engines*, Phys. Rev. Lett. **120**, 260601 (2018).
2. J. Monsel, C. Elouard, A. Auffèves, *An autonomous quantum machine to measure the thermodynamic arrow of time*, arXiv:1804.02296
3. Cyril Elouard, H. Mohammady, *Work, heat and entropy production along quantum trajectories*, arXiv:1805.08305
4. Cyril Elouard, Alexia Auffèves, Géraldine Haack, *Energetic witnesses of entanglement genesis in a half-parity measurement setup*, arXiv:1807.02487

SELF-HEALING CERAMICS AND MECHANICAL METAMATERIALS

Rajiv K. Kalia, Aiichiro Nakano, Priya Vashishta
University of Southern California

PROGRAM SCOPE

We perform massively parallel reactive molecular dynamics (RMD) simulations to investigate crack healing in ceramics operating at high temperatures. Self-healing of defects and cracks can dramatically increase the reliability and lifetime of ceramics, thus reducing maintenance costs for a broad range of energy technologies from ceramic turbine blades to solid-oxide fuel cells.[9-10]

We are also performing large-scale molecular dynamics (MD) simulations to investigate thermo-mechanical behavior of mechanical metamaterials. In recent years, we have witnessed significant developments in the design of mechanical metamaterials with negative Poisson's ratio, negligible shear modulus, and negative compressibility. These unusual properties of mechanical metamaterials have been exploited to design beautiful, intricate, robust and scalable three-dimensional structures consisting of ultrathin and extraordinarily flexible ceramic sheets and hollow ceramic tubes. These flexible structures have a wide range of applications in energy generation and storage (e.g., batteries, solar panels), flexible electronics and spintronics, self-actuated systems and stimuli-responsive sensing devices, and nanorobotics.

RECENT PROGRESS

Recent experiments have demonstrated crack healing in Al_2O_3 by SiC nanoparticles (n-SiC).[15-16] Ando *et al*. have measured the bending strength of sintered Al_2O_3/SiC composites [1-4]. They introduce indentation cracks on Al_2O_3 surfaces and observe crack healing by n-SiC in the temperature range of 900° C and 1,300° C. Ando *et al*. have suggested a two-step process of crack healing: First, n-SiC is oxidized by atmospheric oxygen and a 2-4 nm thick amorphous silica layer is formed around n-SiC; second, heat generated by oxidation and associated volume expansion produce molten silica which diffuses into cracks and heals them.

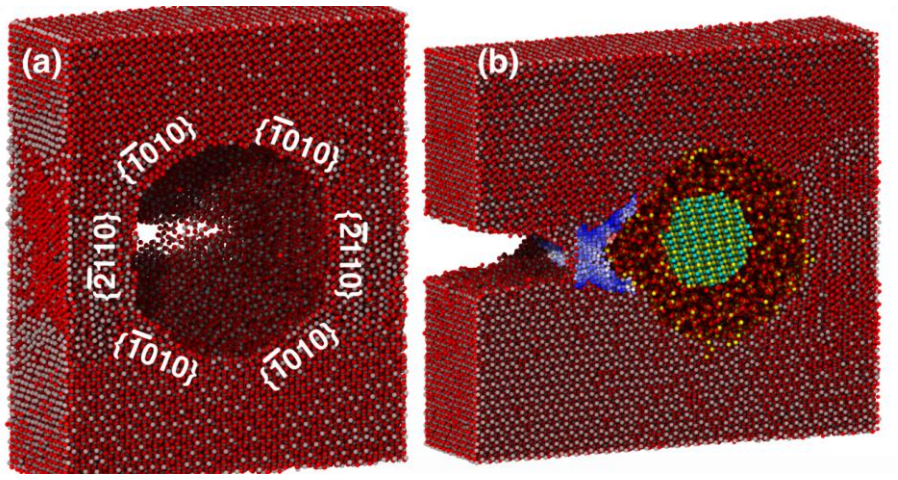

Figure 1: Faceting of an Al_2O_3 cavity around a SiC/SiO_2 nanoparticle at 3.4% strain. (a) Al_2O_3 cavity further away from the pre-crack changes to hexagonal shape while (b) Al_2O_3 cavity near the pre-crack changes from spherical to pentagonal shape.

We have examined atomistic mechanisms of crack healing in Al_2O_3 by oxidized n-SiC and also grain nucleation and grain growth due to the presence of n-SiC in Al_2O_3. Prior to this work, we performed RMD simulation to study oxidation of n-SiC [5]. Nanoparticles were cut out of cubic SiC crystal and placed in an oxygen rich environment. The chemical reaction, $SiC(s) + \frac{3}{2}O_2(g) \rightarrow SiO_2(s) + CO(g)$, led to the formation of silica layers around n-SiC. The first few layers formed rapidly but the growth slowed down due to limited diffusion of reactants to the n-SiC/SiO_2 interface. The thickness of the silica shell around n-SiC ranged between 2 and 4 nm, depending on the pressure and temperature of the oxygen environment. This is in good agreement with experiments of Osada *et al.* [4].

The initial configuration of an RMD simulation consists of pre-cracked α-Al_2O_3 crystal containing oxidized n-SiC inside spherical cavities of radii between 4 nm and 7 nm. Shapes of cavities in Al_2O_3 change dramatically under strain at 1,426° C. Figure 1(a) shows a snapshot of an atomic

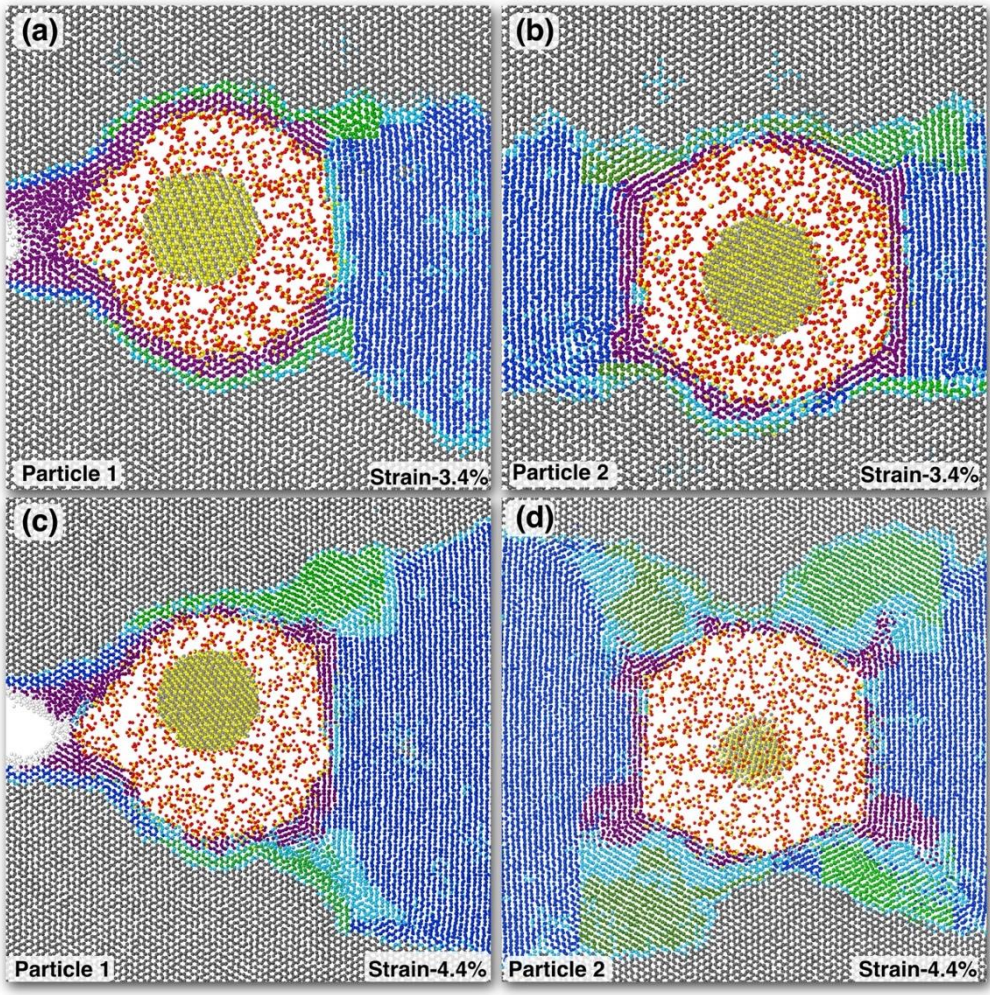

Figure 2: Nucleation and growth of multiple secondary grains at the interface of Al_2O_3 and n-SiC/SiO_2. Here the Al_2O_3 matrix contains two rows of n-SiC/SiO_2. Secondary grains form above 3% strain and facets of the Al_2O_3 cavity act as nucleation sites for these grains. Particle 1 in the figure is in row 1 which is closer to the crack than particle 2 in row 2.

configuration of a cavity containing a n-SiC/SiO_2 nanoparticle (NP). The cavity is no longer spherical. It has facets parallel to prismatic (A) $\{\bar{2}110\}$ and prismatic (M) $\{\bar{1}010\}$ planes of crystalline α-Al_2O_{33}. These results agree with transmission electron microcopy (TEM) studies of faceting of internal cavities in α-Al_2O_3 [6]. Analyzing the equilibrium Wulff shapes of cavities annealed at 1,600° C, experiments reveal well-developed facets in cavities smaller than 100 nm.

Cavities near the crack facet differently from cavities farther away from the crack. This is due to the stress field of the crack. When the applied strain increases and the crack advances towards nearby cavities, the facets of cavities closest to the crack front first shrink in size and then merge to change the cavity shape from hexagonal to pentagonal; see Fig. 1(b). These faceting transitions are caused by surface diffusion of Al and O atoms. Our calculations show that surface diffusion coefficients of Al and O are 4×10^{-7} and 2×10^{-7} cm^2/s, respectively.

Crack healing begins with the diffusion of molten silica through the pinched-off region of alumina cavities (see Fig. 1(b)). At the onset of crack healing, silica diffuses through nanopores that open up between the crack and the nearest alumina cavities. Unlike bulk, molten silica which consists of SiO_4 tetrahedra, silica in the cavities of alumina at 1,426° C consists of various SiO_x fragments (x = 0, 1, 2 and 3). Some of the crack-healing features we observe are similar to those seen in fluorescent imaging of a crack in a silica film evaporated on PMMA containing polymer coated CdSe/ZnS nanoparticles [7].

The presence of nanoparticles in faceted cavities gives rise to grain nucleation and grain growth in the strained alumina matrix. Snapshots in Fig. 2(a)-(d) show nucleation of grains (blue) on facets normal to the direction of crack propagation. These grains are nucleated by the rotation of n-SiC inside the cavities. Inside the grains are under coordinated Al (5-fold) and O (3-fold) atoms due to broken Al-O bonds. Grains between neighboring n-SiC grow with an increase in the applied strain and coalesce at a strain of 4.4%. Grain boundaries are amorphous and contain nanoscale pores at small strains. At higher strains, pores coalesce to form secondary cracks which are also healed by silica diffusion from cavities.

FUTURE PLANS

Origami has become a powerful practical tool to design mechanical metamaterials. We will perform large-scale RMD simulations based on quantum-mechanically informed force fields to investigate thermo-mechanical behavior of robust origami structures of atomically-thin layered materials and MXenes. We will study self-healing of defects such as surface cavities and cracks in MAX-phase ceramics Ti_2AlC and Ti_2AlN. We will examine the kinetics of oxidation and growth of aluminum oxide in surface cracks, and time scale for mass transport in thermal diffusion as a function of temperature in healing defects such as surface cavities and crack surfaces in Ti_2AlC and Ti_2AlN. The study of thermal diffusion and oxidation kinetics in defect structures will provide valuable information about self-healing of MAX-phase ceramics.

REFERENCES

1. Ando, K.; Kim, B. S.; Chu, M. C.; Saito, S.; Takahashi, K., *Fatigue Fract. Eng. Mater. Struct.* **2004,** *27*, 533-541.
2. Nakao, W.; Ono, M.; Lee, S.-K.; Takahashi, K.; Ando, K., *J. Eur. Ceram. Soc.* **2005,** *25*, 3649-3655.
3. Osada, T.; Nakao, W.; Takahashi, K.; Ando, K.; Saito, S., *J. Eur. Ceram. Soc.* **2007,** *27*, 3261-3267.
4. Osada, T.; Nakao, W.; Takahashi, K.; Ando, K., *J. Am. Ceram. Soc.* **2009,** *92*, 864-869.
5. Nomura, K.; Kalia, R. K.; Li, Y.; Nakano, A.; Rajak, P.; Sheng, C.; Shimamura, K.; Shimojo, F.; Vashishta, P., *Sci. Rep.* **2016,** *6*, 24109.
6. Choi *et al.*, *J. Am. Ceram. Soc.* **80**, 62 (1997).
7. Gupta et al., *Nat. Mater.* 5, 229 (2006).

PUBLICATIONS

- *Faceting, Grain Growth, and Crack Healing in Alumina*
  Pankaj Rajak, Rajiv K. Kalia, Aiichiro Nakano, and Priya Vashishta
  ACS Nano under review.
- *Structure and Dynamics of Water Confined in Nanoporous Carbon*
  Yuzi He, Ken-ichi Nomura, Rajiv K. Kalia, Aiichiro Nakano, and Priya Vashishta
  Phys. Rev. Mater. under review.
- *Direct Atomic Simulations of Facet Formation and Equilibrium Shapes of SiC Nanoparticles*
  Anders Hafreager, Henrik A. Sveinsson, Anders Malthe-Sørensson, Aiichiro Nakano, Rajiv K. Kalia, Priya Vashishta
  Under preparation, to be submitted to *Nature Mater*.

Center for Predictive Simulation of Functional Materials

Paul R. C. Kent (PI, ORNL), Anouar Benali (ANL), P. Ganesh (ORNL), Jaron T. Krogel (ORNL), Ho Nyung Lee (ORNL), Lubos Mitas (NCSU), Eric Neuscamman (UC Berkeley), Miguel A. Morales-Silva (LLNL), Luke Shulenburger (SNL).

Keywords: Quantum Monte Carlo, Electronic Structure, Correlated Materials

Website: https://cpsfm.ornl.gov

Project Scope

The strong coupling between charge, spin, orbital, and lattice degrees of freedom that results in desired functionalities in functional materials such as transition metal oxides also challenges established modeling approaches. For example, functionals for density functional theory calculations are used empirically in practice, while extant quantum many-body approaches do not offer the capabilities, accuracy, and general applicability that is desired. Our ability design, understand, and interpret the physics hosted by these materials is therefore hindered. The goal of the *Center for Predictive Simulation of Functional Materials is the development, application, validation, and dissemination of parameter-free methods and open source codes to predict and explain the properties of functional materials for energy applications*. The ability to quantitatively predict, analyze, and therefore design functional materials with tailored properties aims to accelerate new materials development and bring truly enabling and essential clarity to our modeling and understanding of functional materials.

Recent Progress

The Center is focused on the development and application of Quantum Monte Carlo (QMC) methods, as implemented in the open source QMCPACK code (https://www.qmcpack.org). In the first two years of the Center we have made a number of essential improvements to the methodology while also applying these and existing techniques to prototypical transition metal oxides. Selected progress is detailed below:

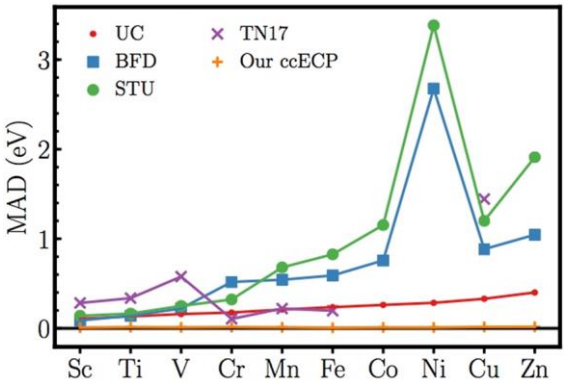

Figure 1. Mean absolute errors of various 3d element pseudopotentials for a broad range of excitations. Our ccECPs [7] and unpublished, have small errors and (not shown here) relatively constant error vs bond length in dimer tests.

New generation of pseudopotentials: While QMC calculations can be run with all electrons in the valence, for materials of interest the use of pseudopotentials is essential. We have developed a new generation of effective core potentials (pseudopotentials) optimized for many-body

methods. These aim to reproduce the properties of the all electron Hamiltonian, are fit and tested using only high-accuracy many-body methods such as coupled-cluster, and use a simple Gaussian form suitable for QMC or quantum chemical evaluation. Potentials from H to Zn have been generated. For the 3d row (Fig. 1), they are a significant improvement over previous widely used potentials. To distribute these potentials we have developed an open community website https://www.pseudopotentiallibrary.org, for state of the art potentials, including those contributed by other groups, in formats suitable for common electronic structure and quantum chemical codes.

New formulation and implementation of auxiliary field QMC: Besides the longer-established real space QMC methods, we are also developing AFQMC methods due to their greater initial accuracy with simple trial wave functions and easier access to many properties. We have released an initial AFQMC implementation as part of QMCPACK, and are developing a new formulation with greatly reduced memory demands that will soon be released. This will enable studies of more complex materials and/or use of larger basis sets for greater convergence. AFQMC can be applied directly, but we also plan to perform cross validation studies using both methods and thereby more convincingly predict correlated phenomena in transition metal oxides. This is illustrated in Fig. 2, which demonstrates a convergence test in the primitive cell of carbon diamond. The nodal surface in real-space diffusion Monte Carlo is converged using an optimized perturbatively generated wavefunction and displays modest basis set dependence. AFQMC shows a strong basis set dependence. Both methods are converged to exact results (100% of the correlation energy) for the Hamiltonian.

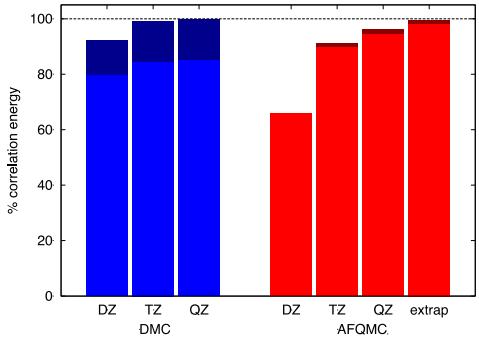

Figure 2: Correlation energy recovered for a calculation of a diamond primitive cell using either CIPSI-DMC or AFQMC. **100% correlation energy corresponds to exact results and identical energies**. Light bars indicate single determinant trial wavefunctions, dark bars use large multiple determinant trial wavefunctions. DZ, TZ, QZ and extrap refer to the size of the basis used to construct the trial wavefunction. DMC (blue) has a small basis set dependence, but gains a significant amount of correlation energy from improving the trial wavefunction. AFQMC (red,) shows a stronger basis set dependence, but a lower sensitivity to the quality of the trial wavefunction.

Accurate band gap calculations in real space QMC: The band gap and related optical properties of materials are fundamental to materials characterization, but accurate calculations of these properties are a major challenge for QMC methods. The methods are primarily ground state methods and do not intrinsically produce spectra. Access to the lowest excited state of each symmetry has traditionally been obtained by performing individual many-body calculations for the ground and excited states, but overall accuracy has been limited due to lower accuracy wavefunctions for excited states. To overcome this, we have developed an optimization algorithm for excited states and multideterminant wavefunctions and applied this method to solids for the first time. Initial application to a range of solids Si, C, LiH, ZnO and LiF finds a mean absolute error of just 3.5% at the variational Monte Carlo level.

Applications: We have performed bulk and defect studies of NiO [5] and VO_2,[6] and bulk studies of HfO_2 and ZrO_2 to validate the accuracy of standard QMC methodologies. Using a combination of QMC, density functional theory, and pressure writing experiments in VO_2 [1], we propose a mechanism for vacancy mediated control of the metal-insulator transition. We have also studied the momentum distribution (Fig. 3), which is a property which requires a full many-body method to access. Experimental measurements show strong qualitative discrepancies from DFT results. Unlike previously studied conventional materials, e.g. sodium metal, the momentum distribution in VO_2 lacks a strong discontinuity at the Fermi energy, suggesting non-Fermi liquid behavior.

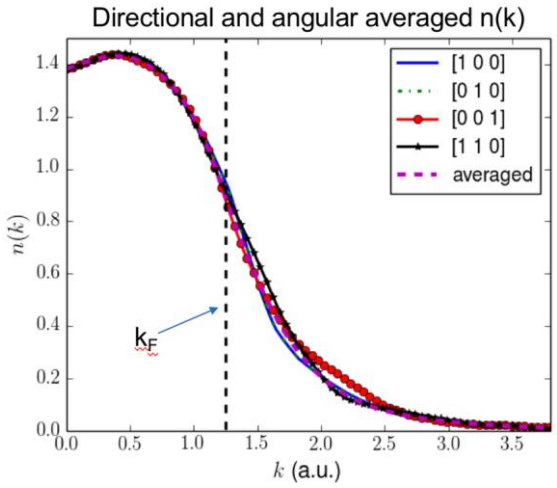

Figure 3. Momentum distributions of rutile VO_2 computed by QMC. The lack of a strong discontinuity at k_F indicates non-Fermi liquid behavior in this material and requires a many-body method to access.

QMCPACK releases and data: A major activity of the Center is the development of the open source QMCPACK code. The citation paper for QMCPACK [4] was published, which gives a thorough overview of the design, features, and performance of the current code. We have made 8 code releases so far and are developing all the techniques mentioned above to levels suitable for wider use. i.e. With tests, documentation and sufficient examples to perform research calculations. Data from the Center projects is published via the Materials Data Facility. E.g. The results of [6] can be fully reproduced and reanalyzed via the data hosted at https://doi.org/10.18126/M2NS7Q, or used to help design studies on related systems.

Future Plans

To help increase the accessibility and use of QMC methods and QMCPACK, in the next 12 months we will co-organize an introductory QMC school and the Telluride Stochastic Methods in Electronic Structure workshop, and an advanced QMCPACK tutorial and user meeting. We will develop the documentation and publish video tutorials for common calculations for those unable to attend the QMC training.

We have developed a several new techniques or methods, e.g. band gap prediction and AFQMC, with initial demonstration to simple bulk materials. These will be applied and extended to transition metal oxides and from bulk to defective systems, where their use is most needed to address uncertainties in current electronic structure methods.

Pseudopotentiallibrary.org will be extended to include data formats for more electronic structure codes, including formats with projectors needed for Kleinman-Bylander evaluation. For scalability

and reproducibility, we will add an automated testing system to provide test data for all contributed potentials on the website. Our goal is to enable pseudopotentials to be rationally chosen and quantitively compared, as has recently been achieved in density functional theory.

Publications (August 2016 – July 2018)

See https://cpsfm.ornl.gov/pubs.html for full list of published, accepted and submitted papers.

1. Y. Sharma, J. Balachandran, C. Sohn, J. T. Krogel, P. Ganesh, L.Collins, Q. Li, N. Balke, S. Kalinin, O. Heinonen, and H. N. Lee. "Nanoscale Control of Metal-Insulator Transition in Epitaxial Vanadium Dioxides," ACS Nano (2018). https://doi.org/10.1021/acsnano.8b03031 Data https://doi.org/10.18126/M2TD16
2. A. Benali, Y. Luo, H. Shin, D. Pahls, and O. Heinonen. "Quantum Monte Carlo Calculations of catalytic energy barriers in a metallorganic framework with transition-metal functionalized nodes", J. Phys. Chem. C. (2018). https://doi.org/10.1021/acs.jpcc.8b02368
3. Suhwan Song, Min-Cheol Kim, Eunji Sim, Anouar Benali, Olle Heinonen, and Kieron Burke. "Benchmarks and reliable DFT results for Spin Gaps of Small Ligand Fe (II) Complexes," J. Chem. Theory Comput. **14** 2304 (2018). https://doi.org/10.1021/acs.jctc.7b01196 Data https://doi.org/doi:10.18126/M20923
4. Jeongnim Kim, Andrew Baczewski, Todd D. Beaudet, Anouar Benali, M Chandler Bennett, Mark A Berrill, Nick S Blunt, Edgar Josue Landinez Borda, Michele Casula, David M Ceperley, Simone Chiesa, Bryan K Clark, Raymond C Clay III, Kris T Delaney, Mark Dewing, Kenneth P Esler, Hongxia Hao, Olle Heinonen, Paul R C Kent, Jaron T Krogel, Ilkka Kylanpaa, Ying Wai Li, M Graham Lopez, Ye Luo, Fionn D. Malone, Richard M Martin, Amrita Mathuriya, Jeremy McMinis, Cody A Melton, Lubos Mitas, Miguel A Morales, Eric Neuscamman, William D Parker, Sergio D Pineda Flores, Nichols A Romero, Brenda M Rubenstein, Jacqueline A R Shea, Hyeondeok Shin, Luke Shulenburger, Andreas Tillack, Joshua P Townsend, Norm M. Tubman, Brett Van Der Goetz, Jordan E Vincent, D. ChangMo Yang, Yubo Yang, Shuai Zhang, Luning Zhao. "QMCPACK : An open source ab initio Quantum Monte Carlo package for the electronic structure of atoms, molecules, and solids" J. Phys: Cond. Mat. **30** 195901 (2018). https://doi.org/10.1088/1361-648X/aab9c3
5. H. Shin, Y. Luo, P. Ganesh, J. Balachandran, J. T. Krogel, P. R. C. Kent, A. Benali, and O. Heinonen. "Electronic Properties of doped and defective NiO: A quantum Monte Carlo study", Physical Review Materials **1** 073603 (2017). https://doi.org/10.1103/PhysRevMaterials.1.073603 Data https://doi.org/10.18126/M2HW64
6. Ilkka Kylanpaa , Janakiraman Balachandran, Panchapakesan Ganesh , Olle Heinonen, Paul R. C. Kent, and Jaron T. Krogel. "Accuracy of ab initio electron correlation and electron densities in vanadium dioxide," Phys. Rev. Materials **1** 065408 (2017). https://doi.org/10.1103/PhysRevMaterials.1.065408 Data https://doi.org/10.18126/M2NS7Q
7. M. Chandler Bennett, Cody A. Melton, Abdulgani Annaberdiyev, Guangming Wang, Luke Shulenburger, and Lubos Mitas. "A New Generation of Effective Core Potentials for Correlated Calculations," J. Chem. Phys. **147** 224106 (2017) (2017). https://doi.org/10.1063/1.4995643. Data https://doi.org/10.18126/M2DK97
8. Jacqueline A. R. Shea and Eric Neuscamman. "Size consistent excited states via algorithmic transformations between variational principles," J. Chem. Theory Comput. **13** 6078 (2017) http://doi.org/10.1021/acs.jctc.7b00923 Data https://doi.org/10.18126/M2J63D
9. T. McDaniel, E. F. D'Azevedo, Y. W. Li, K. Wong, and P. R. C. Kent. "Delayed Slater determinant update algorithms for high efficiency quantum Monte Carlo" J. Chem. Phys. **147** 174017 (2017). https://doi.org/10.1063/1.4998616 . Data https://doi.org/10.18126/M24328
10. Luning Zhao and Eric Neuscamman "A Blocked Linear Method for Optimizing Large Parameter Sets in Variational Monte Carlo" J. Chem. Theory Comput. **13** 2604 (2017). http://dx.doi.org/10.1021/acs.jctc.7b00119 Data https://doi.org/10.18126/M2S59H .

Emergence of High Tc Superconductivity out of Charge and Spin Ordered Phases

Principal Investigator: Dr. Eun-Ah Kim
Department of Physics, Cornell University, Ithaca, NY 14853
Eun-ah.kim@cornell.edu

Project Scope

The scope of this project was to investigate the mechanisms and roles of charge/spin orders in high Tc superconductors. From the beginning of the EARLY CAREER AWARD in 7/13/2013, the PI have been applying symmetry and quantum field theory based perspective to experimental data and using the results as input to microscopic model studies. During last two years of the project, the PI has successfully extended the synergetic approach to using machine learning.

Recent Progress

Machine Learning States of Matter [1-3]: The application of machine learning to central questions in the theory of quantum matter is a rapidly developing field [R1]. The PI entered the field from a unique perspective emphasizing human-artificial neural network (ANN) synergy, which was highlighted in a physics view point article [R2] featuring the PI's work. In particular, the PI introduced the process that interfaces traditional theoretical understanding with a neural network, dubbed quantum loop topography [1-2]. Quantum loop topography is a procedure of pre-processing the quantum state of the system by evaluating two-point operators that form loops at independent Monte Carlo steps (see Fig 1). The use of the quantum loop topography is critical for detecting phases without order parameters. When available, order parameters allow for classical descriptions of phases; order parameter configurations can be readily fed into ANNs with the usual image recognition abilities [R3]. However, when the order parameter is absent or numerically inaccessible, detecting the relevant quantum phase had been challenging [R3]. Quantum loop topography is a versatile strategy for designing and selecting input data guided by the key physical property of the target phase (such as the topological response [1] (or quasi-particle statistics [2]). With the quantum loop topography, we were able to obtain quantum phase diagrams with a fractional Chern insulator [1] and Z_2 quantum spin liquid [2] using a simple, locally built ANN with a single hidden layer. We obtained quantum phase diagrams at orders of magnitude faster pace, benefitting from the ANNs recognition abilities and by-passing Monte Carlo updates.

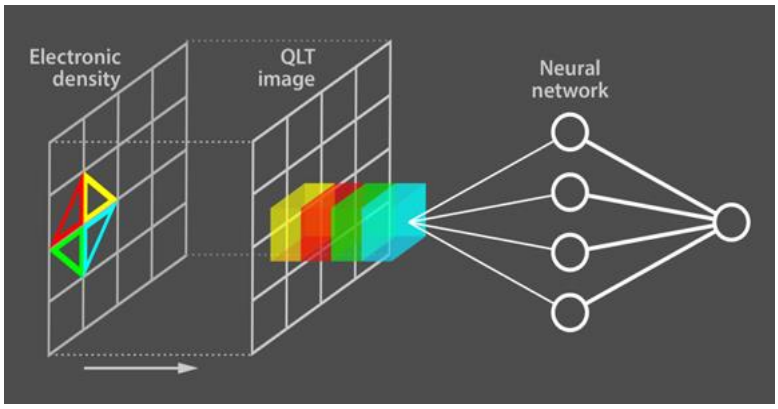

Fig. 1 Adapted from [1] by APS/Alan Stonebraker. Quantum loop topography is a preprocessing layer that selects and organizes input guided by physical properties of the target phase, such as characteristic response.

Out of equilibrium phases form another prime example of physics beyond order parameters. Ref. [R4] first established that entanglement spectra of individual eigenstates could be used as inputs to detect many-body localization (MBL) transition in a disordered quantum spin chain. Nevertheless, instances of machine learning offering new insights have been rare up to now. In [3] the PI showed that a single feed-forward neural network can decode the defining structures of two distinct MBL phases and a thermalizing phase, using entanglement spectra obtained from individual eigenstates. For this, the PI introduced a simplicial geometry-based method for extracting multipartite phase boundaries. The PI found that this method outperforms conventional metrics for identifying MBL phase transitions, revealing a sharper phase boundary and shedding new insight on the topology of the phase diagram (see Fig 2). Furthermore, the phase diagram we acquire from a single disorder configuration confirms that the machine-learning-based approach we establish here can enable speedy exploration of large phase spaces that can assist with the discovery of new MBL phases. To our knowledge, [3] represents the first example of a standard machine learning approach revealing new information on phase transitions [R5].

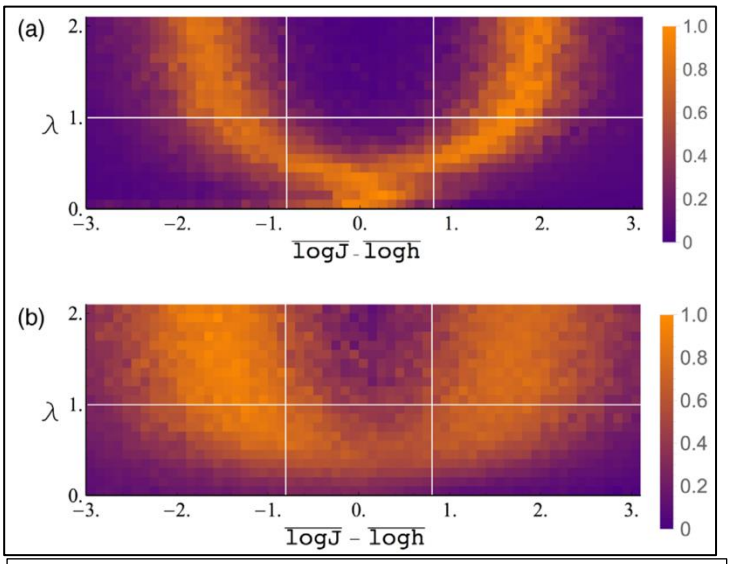

Fig. 2 The contrast between the phase boundaries extracted using (a) our machine learning measure and (b) the standard measure of average standard deviation of the entanglement entropy.

Non-Fermi liquid and Quantum Criticality [4-7]:

A mysterious incoherent metallic normal state with T-linear resistivity is ubiquitous among strongly correlated superconductors. Recent progress with microscopic models exhibiting incoherent metal transport has presented the opportunity for us to study new models that exhibit direct transitions into a superconducting state out of incoherent metal states within the framework of connected Sachdev-Ye-Kitaev (SYK) "quantum dots" in [4]. Here local SYK interactions within a dot produce incoherent metal transport in the normal state, while local attractive interactions drive superconductivity. Through explicit calculations, we found two features of superconductivity arising from an incoherent metal normal state: First, despite the absence of quasiparticles in the normal state, the superconducting state still exhibits coherent superfluid transport. Second, the non-quasiparticle nature of the incoherent metal Green's functions produces a large enhancement in the gap ratio $2\Delta/T_c$ with respect to its BCS value of 3.53.

For further insight into the stability of non-Fermi liquids, the PI has been studying half-filled Landau levels using quantum Field theory [5] and numerics [6] focusing on the role and

mechanism of nematic instability. Nematicity in quantum Hall systems has been experimentally well established at excited Landau levels. The mechanism of the symmetry breaking, however, is still unknown. Pomeranchuk instability of Fermi liquid parameter $F_l \leq -1$ in the angular momentum l=2 channel has been argued to be the relevant mechanism, yet there are no definitive theoretical proofs. In [6] we calculated, using the variational Monte Carlo technique, Fermi liquid parameters F_l of the composite fermion Fermi liquid with a finite layer width. We considered F_l in different Landau levels n=0,1,2 as a function of layer width parameter η. We found that unlike the lowest Landau level, which shows no sign of Pomeranchuk instability, higher Landau levels show nematic instability below critical values of η (see Fig 3). Furthermore the critical value η_c is higher for the n=2 Landau level, which is consistent with observation of nematic order in ambient conditions only in the n=2 Landau levels. The picture emerging from [6] is that approaching the true 2D limit brings half-filled higher Landau level systems to the brink of nematic Pomeranchuk instability.

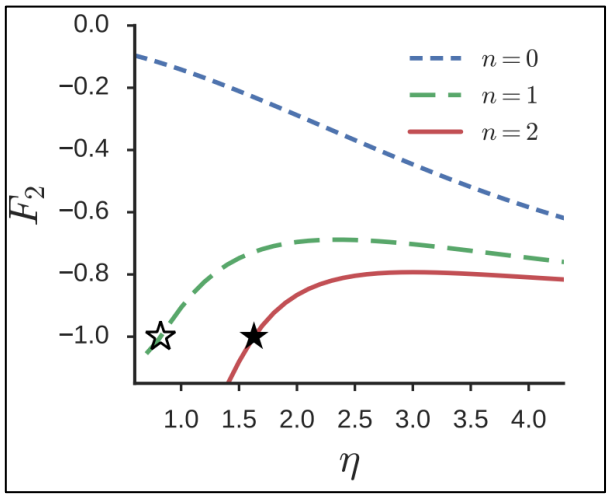

Fig. 3 The contrast between the phase boundaries extracted using (a) our machine learning measure and (b) the standard measure of average standard deviation of the entanglement entropy.

The PI and collaborators have applied the new understanding of duality to address the long-standing puzzle of superuniversality among different quantum Hall inter-plateaux transitions. Previous theoretical studies of these transitions within the framework of Abelian Chern-Simons theory coupled to matter found critical exponents that appear to directly depend on the change of the Hall conductivity across a specific phase transition, in contrast to what is observed experimentally. In [7] we used non-Abelian bosonization and modular transformations to investigate theoretically the phenomenon of superuniversality. Specifically, we introduced a new effective theory that has an emergent U(N) gauge symmetry with N>1 for a quantum phase transition between an integer quantum Hall state and an insulator. We then used modular transformations to generate from this theory new effective descriptions for transitions between a large class of fractional quantum Hall states whose quasiparticle excitations have Abelian statistics. In the 't Hooft large N limit, the correlation length and dynamical critical exponents are independent of the particular transition, hence superuniversal. We argued that this superuniversality survives away from the large N limit using recent duality conjectures.

Future Plan

The award period for the EARLY CAREER AWARD discussed here ended on July 13, 2018. However the machine learning efforts the PI initiated will continue on with the new DOE project. The new

project will focus on interpreting what the neural network learned and on learning physical insight from experimental data.

References

[R1] L. Zdeborová, "Machine learning: New tool in the box", Nature Physics **13**, 420 (2017).

[R2] https://physics.aps.org/articles/v10/56

[R3] J. Carrasquilla and R. G. Melko, "Machine learning phases of matter", Nat Phys **13**, 431 (2017).

[R4] E. P. L. van Nieuwenburg, Y.-H. Liu, and S. D. Huber, "Learning phase transitions by confusion", Nat Phys **13**, 435 (2017). http://dx.doi.org/10.1038/nphys4037.

[R5] https://physicsworld.com/a/machine-learning-reveals-quantum-phases-of-matter/

List of Publications

[1] *Quantum Loop Topography for Machine Learning*, Yi Zhang and Eun-Ah Kim, Phys. Rev. Lett. **118**, 216401 (2017).

[2] *Machine learning Z2 quantum spin liquids with quasiparticle statistics*, Yi Zhang, Roger G. Melko, and Eun-Ah Kim, Phys. Rev. B **97**, 079904 (2018).

[3] *Machine Learning Out-of-Equilibrium Phases of Matter*, Jordan Venderley, Vedika Khemani, and Eun-Ah Kim, Phys. Rev. Lett., **120**, 257204 (2018).

[4] *Coherent superconductivity with large gap ratio from incoherent metals*, AA Patel, MJ Lawler, EA Kim, arXiv preprint arXiv:1805.11098, under review with Phys. Rev. Lett.

[5] *Nematic fluctuations balancing the zoo of phases in half-filled quantum Hall systems,* Andrej Mesaros, Michael J. Lawler, and Eun-Ah Kim, Phys. Rev. B **95**, 125127 (2017).

[6] *Pomeranchuk instability of composite Fermi liquid*, Kyungmin Lee, Junping Shao, Eun-Ah Kim, F. D. M. Haldane, and Edward H. Rezayi, arXiv preprint arXiv:1802.08261, under review with Phys. Rev. Lett.

[7] *Non-Abelian fermionization and fractional quantum Hall transitions,* Aaron Hui, Michael Mulligan, and Eun-Ah Kim, Phys. Rev. B **97**, 085112 (2018).

[8] *Non-Abelian bosonization and modular transformation approach to superuniversality*, arXiv preprint arXiv:1712.04942, under review with Phys. Rev. Lett.

Correlation effects and Magnetism in Actinides: Elements and Compounds

Principal Investigator: Gabriel Kotliar

Department of Physics and Astronomy, Rutgers University, Piscataway, New Jersey 08854, USA.

Condensed Matter Physics and Materials Science Department, Brookhaven National Laboratory, Upton, New York 11973, USA.

Keywords: actnides, orbital differentiation, superconductivity.

Project Scope

First principles description of actinide materials pose many challenging issues, because of relativistic effects, strong multiplet effects and hybridization. It also poses qualitative questions which are unique to this series, and its theory is essential for the interpretation of experiments as shown in the recent neutron scattering experiments [1] (Figure 1).

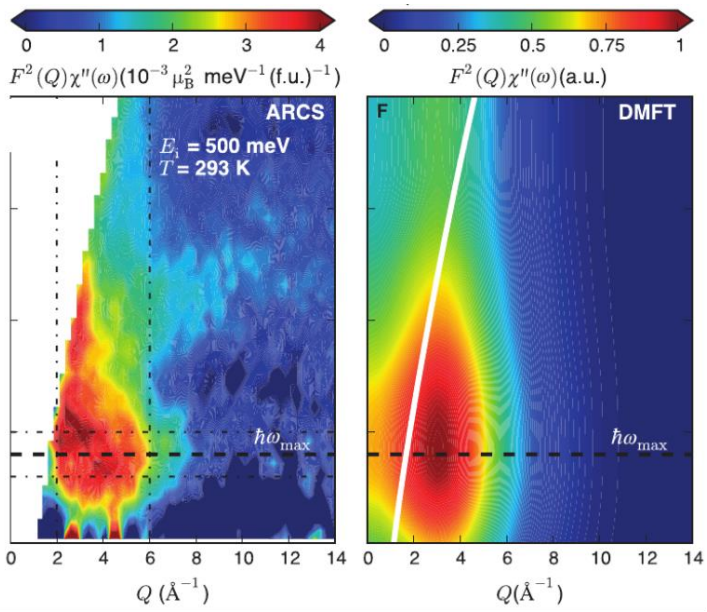

Figure 1:Experimental(left) and theoretical (right) neutron spectroscopy of δ-Pu [1].

Grant US DOE BES DE-FG02-99ER45761 addresses this challenge using a combination of realistic electronic structure methods to treat correlated electron materials.

Recent Progress

This poster will focus on an important example, of Pu-based compounds, $PuCoGa_5$ which has attracted major interest as an analog of δ-Pu, and because it develops superconductivity at Tc = 18.5 K, which is the record transition temperature among the family of heavy fermion superconductors.

We investigate the orbital differentiation of $PuCoGa_5$ normal state within DFT+DMFT using the continuous time quantum Monte Carlo (CTQMC) and the vertex-corrected one-crossing approximation (OCA) as the impurity solvers.

According to our results [2] there is a strong tendency of the Pu-5f orbitals to differentiate at low temperatures. In particular, within CTQMC we find that $5f_{5/2}$ states exhibit a Fermi-liquid behavior whereas one electron in the $5f_{7/2}$ states is at the edge of a Mott localization at low temperatures. We corroborate these findings on orbital differentiation with DFT+DMFT(OCA) calculations, which in turn demonstrate that $5f_{5/2}$ electrons have a much larger Kondo scale than the $5f_{7/2}$. These results are very intriguing in the light of the conjectured [3] connection between superconductivity and orbital differentiation.

Future Plans

The surprising discovery of orbital differentiation reported above opens several research avenues. The consequences for the spin dynamics has to be explored, by resolving the contribution of each orbital to the spin susceptibility. A second fundamental question is how the level of orbital differentiation, varies in the different phases of elemental Pu, and in other compounds. Finally, the differences and similarities between Pu 115 and elemental Pu , and in particular the origin of superconductivity needs further investigation. RPA treatments [5] suggest nodal $s^{\pm}$, further technical advances will enable LDA+DMFT which can refine the investigations of the spin fluctuations and which can be compared with experiments.

References

1. M. Janoschek, P. Das, B. Chakrabarti, D. L. Abernathy, M. D. Lumsden, J. M. Lawrence, J. D. Thompson, G. H. Lander, J. N. Mitchell, S. Richmond, M. Ramos, F. Trouw,

2. J.-X. Zhu, K. Haule, G. Kotliar, and E. D. Bauer,*The valence-fluctuating ground state of plutonium*, Sci. Adv. **1**, e1500188 (2015).

3. W. H. Brito, S. Choi, Y. X. Yao, and G. Kotliar, *Orbital-dependent correlations in $PuCoGa_5$*, Phys. Rev. B **98**, 035143 (2018).

4. Luca de' Medici, H*und's Induced Fermi-liquid instabilities and enhanced quasiparticle interactions*, Phys. Rev. Lett. **118**, 167003 (2017).

5. T. Das, J.-X. Zhu, and M. J. Graf, *Theory of nodal $s^{\pm}$ -wave pairing symmetry in the Pu-based 115 superconductor family*, Sci. Rep. **5**, 8632 (2015).

Publications

1. S. S. Galley, A. A. Arico, T.-H. Lee, Y.-X. Yao, X. Deng, J. S. Storbeck, V. Dobrosavljevic, T. E. Albrecht-Schmitt, N. Kaltsoyannis, N. Lanatà, *Uncovering the Origin of Divergence in the CsM(CrO4)2 (M=La, Pr, Nd, Sm, Eu; Am) Family through Examination of the Chemical Bonding in a Molecular Cluster and by Band Structure Analysis*, JACS **140**, 1674 (2018).

2. T. Ayral and G. Kotliar, *Dynamical Mean Field Theory, Density-Matrix Embedding Theory and Rotationally Invariant Slave Bosons: a Unified Perspective*, Phys. Rev. B **96**, 235139 (2017).

3. W. H. Brito, S. Choi, Y. X. Yao, and G. Kotliar, *Orbital-dependent correlations in $PuCoGa_5$*, Phys. Rev. B **98**, 035143 (2018).

Non-collinear magnetism and dynamic effects in Dzyaloshinskii-Moriya magnets

Principal investigator: Professor Alexey Kovalev
Department of Physics and Astronomy, University of Nebraska-Lincoln
alexey.kovalev@unl.edu

Keywords: Skyrmion lattice, Dzyaloshinskii-Moriya interaction, boundary magnetization twist, magnetization dynamics, Weyl magnons

Project Scope

The primary goal of this proposal is to obtain a general understanding of effects related to spin-orbit interactions in the context of equilibrium and nonequilibrium thermodynamics in mesoscale and nanoscale magnetic systems with ferromagnetic, antiferromagnetic, and non-collinear ordering. To this end, we will advance our fundamental knowledge about magnetism and phase transitions in systems with Dzyaloshinskii-Moriya interactions (DMI) that are driven out of equilibrium by applying temperature gradients, microwave fields, and/or electric and magnetic fields. Pure spin and energy currents mediated by magnons can then be induced in such systems where low dissipation (ideally non-dissipative) transport without generation of Oersted fields becomes possible. The proposed research program has three major objectives: (1) understand effects of DMI on spin and energy transport phenomena and magnetic order parameter dynamics in systems with and without magnetic textures such as domain walls, skyrmions, and magnetic vortices by developing a hydrodynamic description of such systems combined with diagrammatic and linear response approaches; (2) understand dynamic effects in the context of novel emergent phases in magnets with DMI; (3) assess the feasibility of novel ultra-low-power spintronic devices that combine logic and memory functionalities by employing theoretical descriptions of spin and energy currents and their interplay with magnetic order parameter dynamics.

Recent Progress

Boundary twists, instabilities, and (anti)skyrmion creation – the PI, in collaboration with Aldo Raeliarijaona (postdoc), Rabindra Nepal (graduate student), have formulated and studied the general boundary conditions dictating the magnetization profile near an interface between magnets with dissimilar properties. Boundary twists near an edge due to DMI have been first discussed in [Wilson et al., Phys. Rev. B 88, 214420 (2013)] and in [Rohart and Thiaville, Phys. Rev. B 88, 184422 (2013)]. A recent work

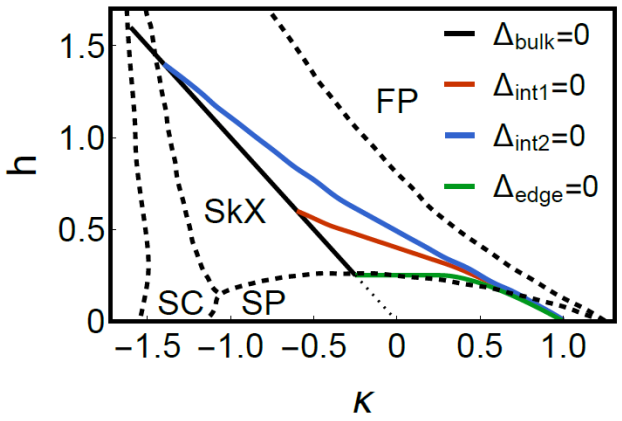

Figure 1 The dashed lines represent thermodynamic phase boundaries between the polarized state (FP), the hexagonal skyrmion lattice (SkX), the square skyrmion lattice (SC), and the chiral soliton lattice (SP). The black line corresponds to vanishing gap of bulk magnons. The bold colored lines correspond to vanishing gap of magnons localized at an interface between two chiral magnets with dissimilar DMI.

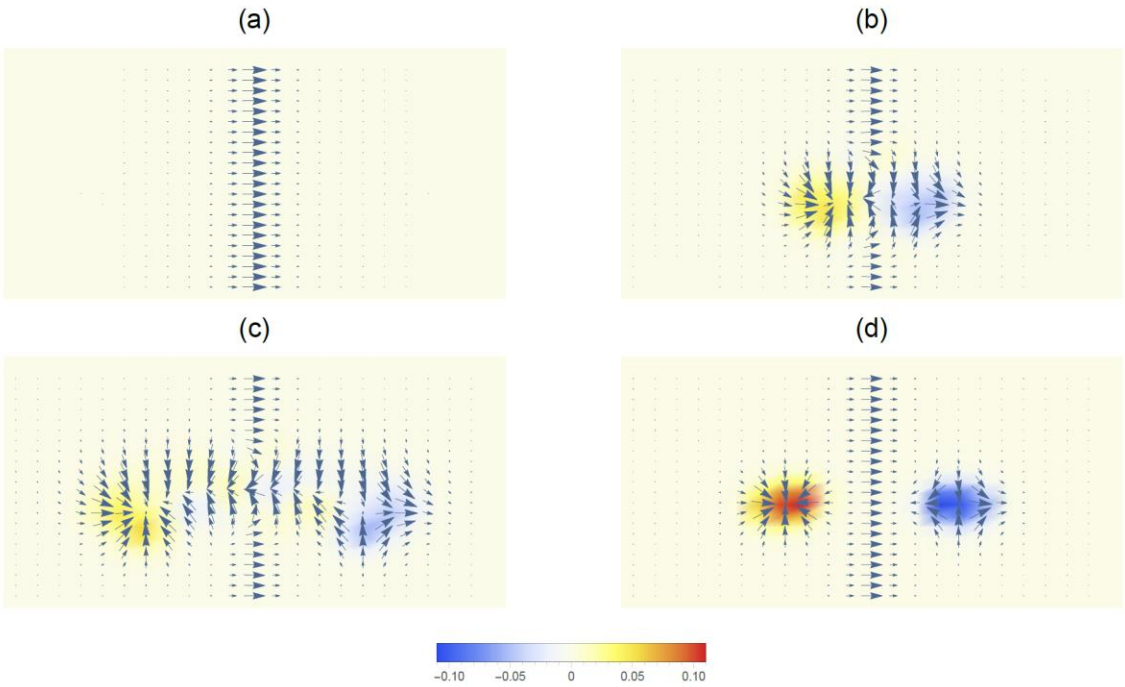

Figure 2 Snapshots of skyrmion-antiskyrmion pair creation process in a system with an interface separating the Rashba- and Dresselhaus-like DMI. The plots show the in-plane magnetization (arrows) and the topological charge density (color coding is shown in the lower part of the plot).

[K. M. D. Hals and K. Everschor-Sitte, Phys. Rev. Lett. 119, 127203 (2017)] has shown that boundary conditions at the edge of a chiral magnet require the consideration of the full rank-3 Dzyaloshinskii-Moriya tensor. We have shown that the rank-3 Dzyaloshinskii-Moriya tensor is necessary to describe the behavior of magnetization near an interface separating materials with dissimilar properties. We have shown that in general case the boundary conditions lead to the magnetization profile interpolating between the Neel- and Bloch-type twists. We have studied various scenarios how skyrmions and antiskyrmions can be created from interface magnetization twists due to local instabilities originating in the closing of magnon gap (see Figure 1). We conclude that a judicious choice of Dzyaloshinskii-Moriya tensor (hence a carefully designed material) can lead to local instabilities generating certain types of skyrmions or antiskyrmions. The local instabilities have been shown to appear in solutions of the Bogoliubov-de-Gennes equations describing ellipticity of magnon modes bound to interfaces (see Figure 1). In one scenario, a skyrmion-antiskyrmion pair can be created due to such local instabilities at an interface between materials with properly engineered DMI (see Figure 2). The paper has been submitted to Physical Review X.

Spin Hall and Nernst effects of Weyl magnons – the PI, in collaboration with Vladimir Zyuzin (former postdoc) have continued to study various Berry phase related effects of magnons associated with DMI. We have designed a simple model of a three-dimensional insulating magnetic structure which represents a magnonic analog of the layered electronic system described by A. A. Burkov and L. Balents [Phys. Rev. Lett. 107, 127205 (2011)]. Our model realizes Weyl magnons as well as surface states with a Dirac spectrum. In this model, DMI is responsible for the separation of opposite Weyl points in momentum space (see Figure 3). We have calculated the intrinsic (due to the Berry curvature) transport properties of Weyl and so-called anomalous Hall effect magnons. The results are compared with

fermionic analogs. In the future, we are planning to use this model for realizations of various transport phenomena related to the chiral anomaly with magnons. The paper has been published in Physical Review B.

Magnetic skyrmion bubble motion driven by surface acoustic waves – the PI, in collaboration with Utkan Gungordu (former postdoc), Rabindra Nepal (graduate student) have studied the dynamical control of a magnetic skyrmion bubble by using counter-propagating surface acoustic waves (SAWs) in a ferromagnet. We have determined the effect of magnetic bubble mass and derived the force equations due to SAWs acting on a magnetic bubble using Thiele's method. We have found that the force that pushes the bubble is proportional to the strain gradient for the major strain components. We have studied the dynamical pinning and motion of magnetic bubbles by SAWs in a nanowire. In a disk geometry, we have studied a SAWs-driven skyrmion bubble oscillator with two resonant frequencies. The paper has been published in Applied Physics Letters.

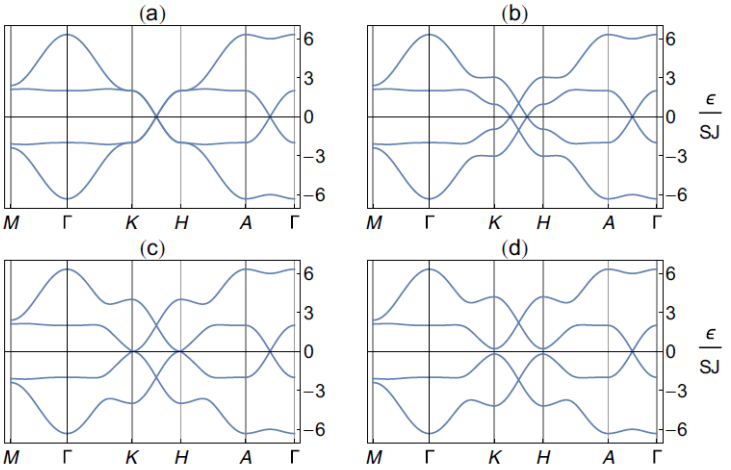

Figure 3 Spectrum of magnons. (a) Vanishing DMI, results in the formation of the Dirac node between the K and H points in the Brillouin zone. (b) Finite DMI splits the Dirac node into two Weyl points where the splitting is proportional to the strength of DMI. (c) and (d) The Weyl points annihilate at larger DMI which leads to the formation of the AHE magnon phase.

Chiral topological insulator of magnons – the PI, in collaboration with Bo Li (graduate student) have proposed a magnon realization of 3D topological insulator in the AIII (chiral symmetry) topological class. So far only magnon analog of the Chern insulator and a magnon analog of the quantum spin Hall effect comprised of two copies of magnon Chern insulators have been proposed. In the proposed system the topological magnon gap opens due to the presence of DMI. The existence of the topological invariant has been established by calculating the bulk winding number of the system. Within our model, the surface magnon Dirac cone is protected by the sublattice chiral symmetry. By analyzing the magnon surface modes, we have confirmed that the backscattering is prohibited. By weakly breaking the chiral symmetry, we have observed the magnon Hall response on the surface due to opening of the gap. Finally, we have shown that by changing certain parameters, the system can be tuned between the chiral topological insulator, three-dimensional magnon anomalous Hall, and Weyl magnon phases. The paper has been published in Physical Review B.

Future Plans

Investigation of the chiral anomaly of magnons in thermal and spin transport – the PI will study magnon-mediated spin and energy transport phenomena associated with the Weyl magnons and the chiral anomaly. As DMI can play an important role in formation of the Weyl nodes we will consider various systems (e.g. systems with pyrochlore lattice) in

which such interactions are present. We will formulate experimental signatures of the chiral anomaly and propose experimental verifications.

Thermal torques and Onsager reciprocity in insulating antiferromagnets – the PI will study how Neel order dynamics can be affected by energy and magnon currents in insulating antiferromagnets. We will build on our recent studies of magnon-mediated spin torques in Dzyaloshinskii-Moriya ferromagnets. Here the Berry phase corrections should play an important role. We will also study the Onsager reciprocal effect by which energy can be pumped by the dynamics of the Neel order parameter. We will explore possible experimental signatures in magnetoelectric Cr2O3.

Collective and nonlinear phenomena in skyrmion lattices – the PI will study skyrmion and antiskyrmion lattices. We will study various transport phenomena through such lattices and explore the interplay between the collective skyrmion dynamics and transport. We will pay attention to the role of defects and skyrmion pinning. This study might find applications in recent proposals of reservoir computing.

Develop new concepts for memory, logic, and neuromorphic devices – the PI will study non-linear effects of skyrmion-like elements and their networks. We will employ a combination of phenomenological and ab initio treatment to study possible realizations of the memory and logic functionalities. To this end we will study the transport and dynamic properties of networks of skyrmion-like elements and design possible realizations of devices with novel functionalities. We will also explore antiskyrmions and other unconventional skyrmion-like structures and try to identify their advantages compared to skyrmions.

Publications (published since 9/1/2016)

1. K. D. Belashchenko, A. A. Kovalev, M. van Schilfgaarde, "Theory of spin loss at metallic interfaces", Phys. Rev. Lett. **117**, 207204 (2016).
2. V. Zyuzin, A. A. Kovalev, "Magnon spin Nernst effect in antiferromagnets", Phys. Rev. Lett. **117**, 217203 (2016).
3. A. A. Kovalev, V. Zyuzin, B. Li, "Pumping of magnons in a Dzyaloshinskii-Moriya ferromagnet", Phys. Rev. B **95**, 165106 (2017).
4. A. Raeliarijaona, R. Nepal, A. A. Kovalev, "Boundary twists, instabilities, and (anti)skyrmion creation," under review for Physical Review X.
5. V. A. Zyuzin, A. A. Kovalev, "Spin Hall and Nernst effects of Weyl magnons," Phys. Rev. B **97**, 174407 (2018).
6. R. Nepal, U. Gungordu, A. A. Kovalev, "Magnetic skyrmion bubble motion driven by surface acoustic waves," Appl. Phys. Lett. **112**, 112404 (2018).
7. B. Li, A. A. Kovalev, "Chiral topological insulator of magnons", Phys. Rev. B **97**, 174413 (2018).
8. U. Gungordu, R. Nepal, A. A. Kovalev, "Stabilization and control of Majorana bound states with elongated skyrmions", Phys. Rev. B **97**, 115136 (2018).
9. A. A. Kovalev, "Skyrmions and antiskyrmions in quasi-two-dimensional magnets", under review for Frontiers in Physics.

Beyond RPA screening in GW: applications to d- and f-electron systems, including localized defects.

Walter R. L. Lambrecht, Department of Physics, Case Western Reserve University

Keywords: GW method, lattice dynamics, point defects, semiconductors, halide perovskites

Project Scope

The quasiparticle self-consistent (QS) *GW* method provides a great improvement over semilocal density functional approximations to obtain the electronic energy band structure for many materials. However, for strongly ionic materials and strongly correlated oxides, it tends to overestimate the gaps significantly. One goal of this project is to determine whether this is mainly because of approximations in the screening of *W*, such as the lack of inclusion of electron-hole effects or due to electron-phonon coupling and to include such effects. A second aim of the project is to understand lattice distortion couplings on the band structure of halide perovskites and the structural stability of that family of compounds. An overarching goal is to improve the accuracy and applicability of the QS*GW* approach, in particular for defects and large systems.

Recent Progress

Corrections to RPA-GW. In highly ionic solids such as MgO, NaCl, the band gap calculated in the QS*GW* approach is overestimated by more than 1 eV. In literature, this has been attributed to either the random phase approximation (RPA) used in calculating the screened Coulomb interaction *W*,[1,2] or to electron-phonon effects. [3,4] In particular, it was proposed by Botti and Marques[3] (BM) to include the lattice-polarization contribution to the screening of *W* in the long-wavelength limit. Several questions however remained unclear: how does one implement the screening only in the $q \rightarrow 0$ limit, over what range of q should the effect be applied, and how does this fit into the overall theory of electron-phonon coupling? We made progress in resolving these questions in recent work.[5,6] First, the screened Coulomb interaction $W(q,\omega=0)$ has an integrable divergence of the form $1/\varepsilon q^2$ which is treated by the offset-Γ method, which already involves the macroscopic dielectric constant ε. We may thus replace the latter by the static value including the lattice polarization effect by using the generalized Lyddane-Sachs-Teller (LST) relation. However, this breaks the balance of the offset-Γ method between the $q=0$ term treated analytically, and the discrete summation over $q\neq 0$ points. Thus the result would become mesh size dependent. We thus need to choose the strength of the $q=0$ term by choosing the length scale of the q-box it represents so as to optimally include the lattice polarization effect. At first, we tried to determine this by studying the q-dependence of the lattice polarization contribution to the screening by using a direct method. Namely we apply a cosine shaped external perturbation in a supercell with a given wave vector q and determine its screening by carrying out self-consistent

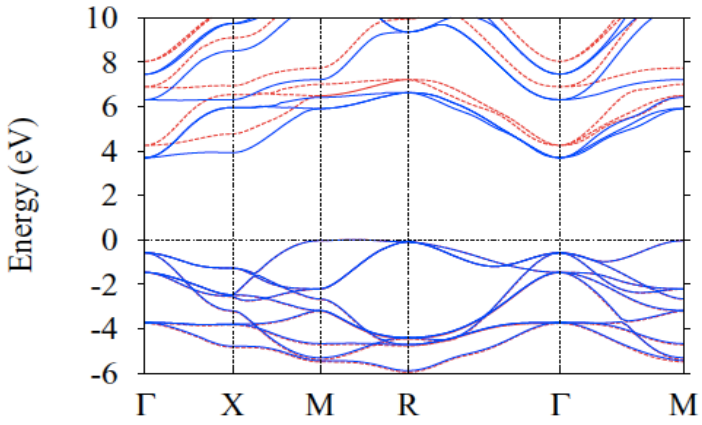

Figure 1: Band structure of $SrTiO_3$ with (blue) and without (red) lattice-polarization correction.

calculations of the screened potential including the lattice relaxation. Thereby we were trying to extend the LST relation to finite *q*. However, inspired by recent work on the Fröhlich contribution [7] to the electron-phonon coupling we realized the proper length scale is the polaron length scale, which depends not only on the LO phonon frequency but also the electron or hole effective mass. Using this insight, we were able to obtain good agreement between the BM approach with an appropriate *q* cut-off and the direct polaron shift approach of Ref. 7 and found that the effect in ionic solids is typically only of order 5 % of the GW gap correction. We were also able to clarify thereby that the BM approach thus implemented corresponds precisely to the long-range Fröhlich part of the electron-phonon coupling self-energy. Furthermore, analyzing the literature results of Refs. 1,2 we found that the inclusion of electron-hole effects on the screening by means of an exchange-correlation kernel amounts to about a 20 % correction of the GW-LDA gap correction. This justifies a commonly used approach of including only 80 % of the self-energy $\Delta\Sigma=\Sigma-v_{xc}$, labeled the 0.8Σ approximation. We extended the approach to cases with several phonons and applied it to $SrTiO_3$, (Fig. 1) which we considered as a typical example of a complex d-band oxide. We found again that both electron-phonon and electron-hole effects on the screening are required to correct the *GW* self-energy correction of the gap.

Stability of halide perovskites: In a second subproject,[8] we studied the stability and distortion modes of halide perovskites ABX_3, with A={Cs, Rb}, B={Pb, Sn, Ge, Si}, and X={I, Br, Cl}. Two distinct distortion modes are known in perovskites: octahedral rotations and ferroelectric displacements of the B atom inside its surrounding X octahedron. Octahedral rotations about different axes indicate a Goldschmidt tolerance factor t<1 and may ultimately lead to formation of different phases than the 3D perovskite structure. The latter are found to strongly distort the band structures, thereby spoiling the favorable features of the halide perovskites for photovoltaic applications, such as the strong direct optical absorption.[9,10] On the other hand, ferroelectric distortions were found to lead to only minor changes in the band structure.[11] We found that while Pb and Sn based halide perovskites favor the rotation distortion mode, the Ge and Si based ones favored the ferroelectric distortion (Fig.2). While the Goldschmidt factor clearly plays a role in the rotation behavior, the ferroelectric distortion was shown to be related to lone pair behavior of the *s* electrons in these atoms when they are required to behave as divalent ions. We were able to show that the rotations increase the density, while the ferroelectric distortion reduces the density. Furthermore, we analyzed quantitatively trends in the angular rotation with

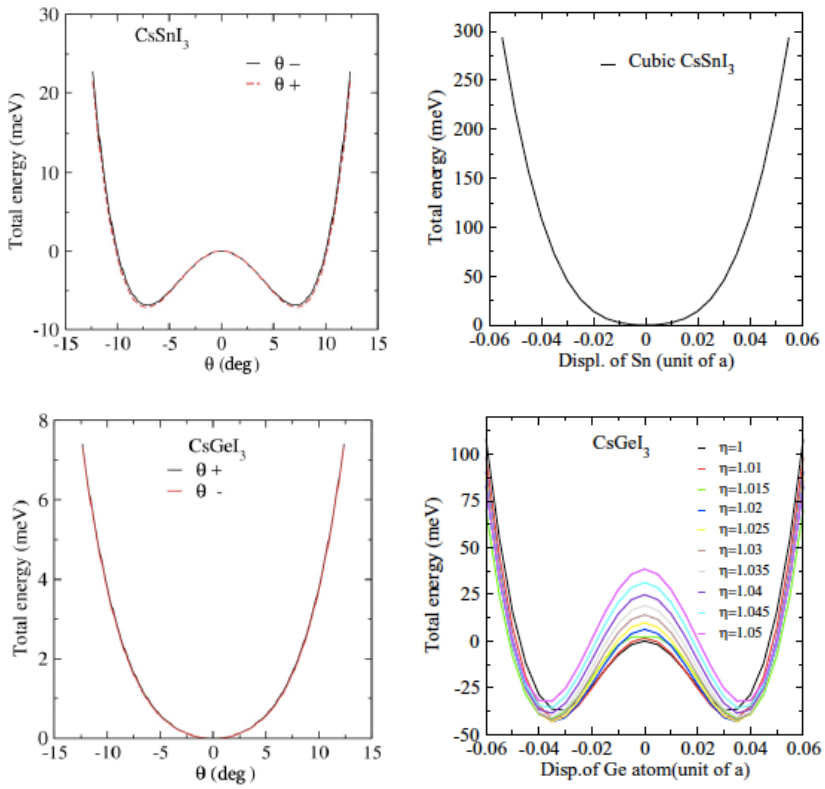

Figure 2: Energy as function of octahedron rotation (left) and B atom off-centering (right) in $CsSnI_3$ (top) and$CsGeI_3$ (bottom)

X-anion and found that upon lattice expansion, the rotation angle is reduced. Above some critical expansion, the rotation type distortion disappears and even Sn and Pb based materials were shown to distort via the ferroelectric off-centering. This unexpected symmetry breaking effect at high temperatures has recently been found in other materials such as Pb-VI compounds where it has been called "emphanisis" and was shown to be related to lone pair physics related to the deep valence *s* electrons. We show here that surprisingly this effect is even stronger for Ge and Si. The ferroelectric inversion symmetry breaking distortion is also shown to lead to sizable non-linear optical effects in the Ge-based halide perovskites, for which we also calculated the phonon modes and Raman spectra.[12]

Future Plans

Recently, electron hole interaction effects were included in the QS*GW* (questaal.org) code we are using. We are now in the process of applying this approach to V_2O_5, a layered material, for which the above combination of 0.8Σ and lattice polarization corrections still failed to correct the extremely large QS*GW* overestimate of the gap. We will also explore if d-d transitions contributing to the dielectric function in V_2O_{5-x} could explain the additional screening and thus attribute the extreme gap overestimate to extrinsic effects.

In the halide perovskite subproject, we want to explore if the lone pair physics can explain the related monoclinic structures[13] and further study the potential stability and electronic structure of the Si-based perovskites and determine their gaps more accurately within QS*GW*.

Finally, we continue to work on the self-energy editor approach for QSGW calculations of defects that we reported on in the last PI meeting or 2016. In particular, we are trying to explore

how to use the total energies of the QS*GW* approach. The latter provides a non-local exchange correlation potential in the Kohn-Sham Schrödinger equation which leads to eigenvalues that correspond to quasiparticle excitation energies, but on the other hand, the density functional theory connection of this exchange correlation potential change to the corresponding total energy is then lost. Nonetheless, we believe that improving the occupied one-electron energies should improve the total energy even if it is only included in the sum of one electron energies. This aspect of QS*GW* needs further investigation. We also want to explore the self-energy editor cut-and-paste approach for hybrid functionals, where the link to total energies is maintained. The method provides an approximate way to construct the self-energy (or exact exchange) for a large defect system from that of the host and a smaller defect system.

References

[1] M. Shishkin, M. Marsman, and G. Kresse, Phys. Rev. Lett. **99**, 246403 (2007).
[2] W. Chen and A. Pasquarello, Phys. Rev. B **92**, 041115 (2015).
[3] S. Botti and M. A. L. Marques, Phys. Rev. Lett. **110**, 226404(2013).
[4] G. Antonius, S. Poncé, E. Lantagne-Hurtubise, G. Auclair, X.Gonze, and M. Côté, Phys. Rev. B **92**, 085137 (2015).
[5] W. R. L. Lambrecht, C. Bhandari, and M. van Schilfgaarde, Phys. Rev. Mater. **1**, 043802 (2017).
[6] C. Bhandari, M. van Schilfgaarde, T. Kotani, and W. R. L. Lambrecht, Phys. Rev. Materials **2**, 013807 (2018)
[7] J. P. Nery and P. B. Allen, Phys. Rev. B **94**, 115135 (2016).
[8] S. Kumar Radha, C. Bandhari and W. R. L. Lambrecht, Phys. Rev. Materials **2**, 063605 (2018).
[9] L.-y. Huang and W. R. L. Lambrecht, Phys. Rev. B **88**, 165203 (2013).
[10] L.-y. Huang and W. R. L. Lambrecht, Phys. Rev. Materials **1**, 024601 (2017).
[11] L.-y. Huang and W. R. L. Lambrecht, Phys. Rev. B **93**, 195211 (2016).
[12] L.-y. Huang and W. R. L. Lambrecht, Phys. Rev. B **94**, 115202 (2016).
[13] L.-y. Huang and W. R. L. Lambrecht, Phys. Rev. B **91**, 075206 (2015).

Publications

Refs. 5,6,8,10, 11,12,13 above

Strongly Correlated Electronic Systems: Local Moments and Conduction Electrons

Principal Investigator: Patrick Lee, Physics department, MIT.

Keywords: Spin liquid, Mott insulator, superconductivity, random singlet.

Project Scope

This project focuses on the study of strong correlation physics, where the strong repulsion between electrons in solids lead to novel properties which emerge at low temperatures in ways which are both unexpected and profound. Examples include superconductivity, magnetism and more recently, exotic phenomena such as fractional charge and fractional statistics in the quantum Hall effect, spin charge separation in quantum spin liquids etc. An important new theme is the importance of topology in controlling the electronic structure of matter. By paying close attention to experiments, we develop theory which explains observations and predict new phenomena. In the past two years we have made progress on several fronts. We studied the transport and optical properties of a class of materials called Weyl semimetals. We also re-opened the problem of superconductivity at very low electron density, and applied our ideas to newly discovered examples such as Bismuth and a potential class of topological superconductors with strong spin orbit coupling. Below we will focus on our recent work on a third topic, the cluster Mott insulator and a related problem of randomly distributed local moments.

Recent Progress

1. Frustrated magnets, Quantum spin liquids and cluster Mott insulators.

Frustration in an antiferromagnet due to lattice geometry such as the Kagome structure can lead to the quantum spin liquid. Another route is the proximity of a Mott insulator to the metal insulator transition, as demonstrated in the organics. Recently there have been several examples of what we call cluster Mott insulator, where the unit cell is enlarged due to clustering and flat bands emerge, resulting in a correlation driven Mott insulator. Examples include the charge density wave state in 1T-TaS_2 and the recently discovered twisted bi-layer graphene. We carried out numerical DMRG studies on a triangular lattice to demonstrate the appearance of a spinon Fermi surface spin liquid state. In the presence of randomness, another state, the random singlet state, may appear. We find that local moments are common in many spin liquid candidates and these may dominate the low temperature thermodynamic properties. We found that the low temperature specific heat in the presence of a magnetic field satisfy scaling and data collapse, and that the Dzyaloshinskii-Moriya

(DM) term which has not been treated up to now, plays an important role in determining the classification of the scaling function.

A. **Spinon Fermi surface in the cluster Mott insulator 1T-TaS_2. [P7]**

1T-TaS_2 is a well-studied charge density wave material for over 40 years and we have proposed that it may be a quantum spin liquid that has escaped attention for all this time. [1] Remarkably this suggestion was recently confirmed experimentally when Matsuda's group reported the observation of a linear T term in the thermal conductivity. [2] This is usually taken as strong evidence for a spinon Fermi surface, because there is no other known way that an insulator can conduct heat like a metal and has been seen only once before, in the organic spin liquid. This opens up an exciting prospect because unlike the organics, relatively large single crystals are available and neutron scattering can be performed. 1T-TaS_2 is unique among 2D charge density wave compounds in that it has an insulator ground state. The lattice deforms to form clusters of 13 atoms, forming a star of David pattern, as shown in Fig 1b and 1c. Each Ta atom contains a single spin ½ electron, but 12 of these are paired in a cluster, leaving a single electron on each star of David cluster. As shown in Fig 1a, band calculations find a very narrow band after zone folding. While the undistorted TaS_2 is weakly correlated, a weak repulsion is sufficient to drive this into a Mott insulator. A Mott insulator is expected to have local moments which in most cases form an anti-ferromagnetic ground state. Surprising, there is no sign of a local moment per cluster. Instead the magnetic susceptibility drops at the transition at 180K and stays constant below that. A quantum spin liquid with a spinon Fermi surface will explain this behavior, as well as the linear T thermal conductivity. We are led to consider a model of triangular lattice of star of David clusters with nearest neighbor exchange J between the spin on each cluster, and a ring exchange term K. We expect a large K/J ratio for a weak Mott insulator, ie a state just on the insulator side of the Mott transition. We study this model using DMRG, [P7] extending an earlier study of 2 and 4 wide wires. [3] By going to 6 and 8 wide systems we find that a spin liquid state is stabilized for K/J exceeding a critical value. Beyond this point we find peaks in the spin-spin correlation structure factor S(k) (Fig 1d). These peak positions lie on rings corresponding to a radius of $2k_F$ (and rings that are related by Umklapp scattering) as expected for a spinon Fermi surface. In addition, we find a constant spin susceptibility. These results are the strongest evidence we have to date for the existence of a quantum spin liquid with a spinon Fermi surface in a triangular lattice near the Mott transition.

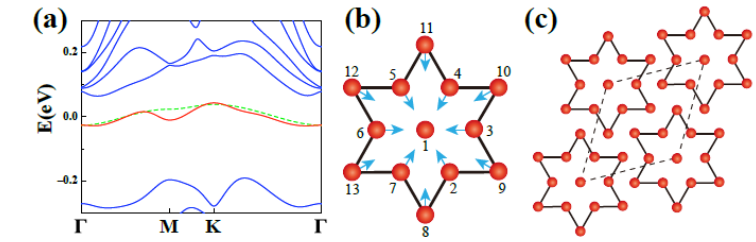

(d)

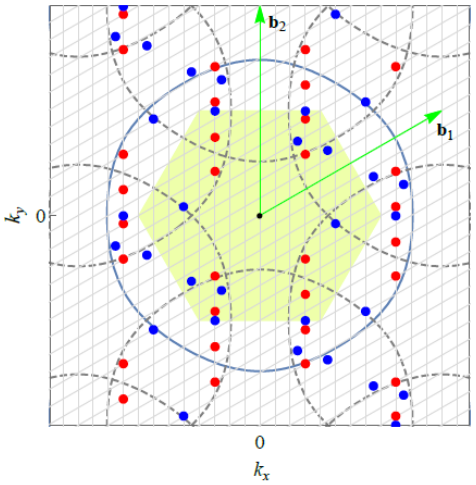

Fig 1. Taken from ref. [P7] : (a) The flat band found by LDA calculations including spin orbit coupling (shown in red) that emerges in the reduced BZ formed by the star of David cluster shown in (b) and (c) These clusters form a triangular lattice with 13 Ta per unit cell. (d) Results of our DMRG calculation on the cluster model. The peak in the spin structure factors are marked by the dots. Red and blue dots are from the 6 and 8 wide systems respectively. The solid circle marks the 2k_F positions and the dashed circles mark the Umklapp replica's. The green hexagon marks the BZ. The observation that the dots fall on or near these circles strongly support the conclusion that a quantum spin liquid with a spinon Fermi surface is the ground state.

B. Scaling of the specific heat in the random singlet model. [P6]

A number of frustrated spin systems are known to exhibit low temperature specific heat which is linear or quadratic in temperature, with a coefficient that decreases with increasing magnetic field. [4.5] This is sometimes considered as evidence for exotic ground state such as quantum spin liquid. We show instead that this is a consequence of a general phenomenon of local moments pairing into random singlet states.[6]. We generalize the previous model to include spin-orbit coupling and point out the importance of the anti-symmetric exchange term, also known as the Dzyaloshinskii-Moriya (DM) term. [P16] We find that specific heat data C(H, T) collapse into scaling form $C(H, T) \sim H^{-\gamma} F_q(T/H)$ where $F_q(x) \sim x^p$ and p take the value 0, 1 or 2 , depending on the importance and the symmetry of the DM term. These cases correspond to linear, quadratic or cubic temperature dependence of the specific heat. We demonstrate the data collapse for the cluster Mott insulator $LiZn_2Mo_3O_8$, [P6] the Kitaev model candidate $H_3Li\ Ir_2O_6$ [5] and the spin liquid Kagome compound $ZnCu_3(OH)_6Cl_2$. [6]

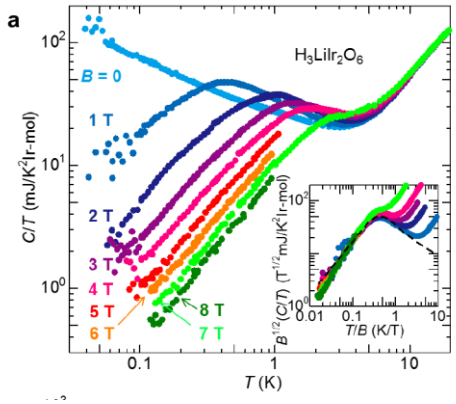

Fig 2. Taken from ref [5} showing heat capacity data and the data collapse shown in the inset. This is a candidate material proposed to realize the spin liquid state of the Kitaev model on the honeycomb lattice. In ref [5] the scaling was taken as evidence for a spin liquid state, but we show that the scaling can be explained by a random singlet model in the presence of Dzyaloshinskii-Moriya coupling, as predicted by our theory. [P7}

Future Plan

Cluster Mott insulators and the appearance of superconductivity with doping.

Recently we have encountered two exciting new examples of cluster Mott insulators, where electrons are localized on a cluster of sites resulting in a flat band. In addition to 1T-TaS_2. We have the twisted bi-layer graphene (TBG), where the moire pattern creates a large unit cell. At or near certain magic angles, a flat band emerges. [7,8] These two systems share a number of common features and a lot of differences as well and both are rich grounds for further studies. In TaS_2 there is now strong evidence for a quantum spin liquid with a spinon Fermi surface. [2] In TBG a correlation driven insulator appears at half-filling. [7,8] The excitement about TBG is that superconductivity appears upon doping, with a high ratio of T_c to the Fermi temperature. Starting from the HiTc Cuprates, it has long been suspected that superconductivity is a competitive ground state when a Mott insulator is doped, especially if one is close to the Mott transition. [9,10] Another well known example is the quasi-two dimensional organic ET salts, where superconductivity of relatively high temperature appears on either doping [11] or driving the system toward a metal by pressure. For a review, see [12]. The TBG offers the possibility of a new example. It is also encouraging that recent experiments show that mono-layer 1T- $TaSe_2$ [13] and 1T- $NbSe_2$ [14] are Mott insulators as well, even though the bulk crystals are metallic. This has led us to propose in our recent paper [P7] that these systems are prime candidate for high temperature superconductivity if they can be doped by gating. Compared with TBG, these materials have the advantage that the energy scale is much larger, and a higher temperature superconductor may be expected.

On the theoretical front, we will extend our DMRG study to the Hubbard model on the triangular lattice and study the effect of doping. It is interesting that moire based cluster Mott system has been proposed for other transition metal dichalcogenides as well [15].

References

1. K. T. Law and P. A. Lee *"1T-TaS_2 as a quantum spin liquid"* PNAS **114** (27) 6996-7000. (2017).
2. H. Murayama, Y. Sato, X. Z. Xing, T. Taniguchi, S. Kasahara, Y. Kasahara, M. Yoshida, Y. Iwasa, and Y. Matsuda, *"Coexisting localized and itinerant gapless excitations in a quantum spin liquid candidate 1T-TaS_2"* arXiv:1803.06100 (2018).
3. M. S. Block, D. N. Sheng, O. I. Motrunich and M. P. A. Fisher, *"Spin Bose metal and valence bond solid phases in a spin ½ model with ring exchanges on a 4-leg triangular ladder."* Physical Review Letters **106**, 157202 (2011).
4. K. Kitagawa, T. Takayama, Y. Matsumoto, A. Kato, R. Takano, Y. Kishimoto, S. Bette, R. Dinnebier, G. Jackeli and H. Takagi, *"A spin-orbit entangled quantum liquid on a honeycomb lattice"* Nature **554**, 341 (2018).
5. J. S. Helton, K. Matan, M. P. Shores, E. A. Nytko, B. M. Bartlett, Y. Yoshida, Y. Takano, A. Suslov, Y. Qiu, J.-H. Chung, D. G. Nocera, and Y. S. Lee, *"Spin Dynamics of the Spin*-1/2 *Kagome Lattice Antiferromagnet* $ZnCu_3(OH)_6Cl_2$" Phys. Rev. Lett. **98**, 107204 (2007).
6. R. N. Bhatt and P. A. Lee, *"Scaling Studies of Highly Disordered Spin-½ Antiferromagnetic Systems"* Phys. Rev. Lett. **48**, 344 (1982).
7. Y. Cao, V. Fatemi, A. Demir, S. Fang, S. L. Tomarken, J. Y. Luo, J. D. Sanchez-Yamagishi, K. Watanabe, T. Taniguchi, E. Kaxiras, R. C. Ashoori, and P. Jarillo-Herrero, *"Correlated Insulator Behaviour at half-filling in magic angle graphene superlattices"* Nature **556**, 80–84 (2018).
8. Y. Cao, V. Fatemi, S. Fang, K. Watanabe, T. Taniguchi, E. Kaxiras, and P. Jarillo-Herrero, *"Magic-angle graphene superlattices: a new platform for unconventional superconductivity"* Nature **556**, 43–50 (2018).
9. P. W. Anderson, *"The Resonating Valence Bond State in La2CuO4 and Superconductivity"* Science **235**, 1196 (1987).
10. P. A. Lee, N. Nagaosa, and X.G. Wen, *"Doping a Mott insulator: Physics of high-temperature superconductivity"* Rev. Mod. Phys. **78**, 17 (2006).
11. H. Oike, K. Miyagawa, H. Taniguchi, and K. Kanoda, *"Pressure-Induced Mott Transition in an Organic Superconductor with a Finite Doping Level"* Phys Rev. Lett **114**, 067002 (2015).
12. Y. Zhou, K. Kanoda, and T.-K. Ng, *"Quantum spin liquid states"* Rev. Mod. Phys. **89**, 025003 (2017).
13. Y. Nakata, T. Yoshizawa, K. Sugawara, Y. Umemoto, T. Takahashi, and T. Sato, *"Selective Fabrication of Mott-Insulating and Metallic Monolayer $TaSe_2$" ACS Appl. Nano Mater.*,1456-1460 *(* 2018).
14. Y.Nakata, K. Sugawara, R. Shimizu, Y. Okada, P. Han, T. Hitosugi, K. Ueno, T.Sato, and T. Takahashi, *"Monolayer 1T-$NbSe_2$ as a Mott insulator", NPG Asia* Materials **8**, 157-1-5 (2016).
15. F. Wu, T. Lovorn, E. Tutuc, and A. H. MacDonald, *"Hubbard Model Physics in Transition Metal Dichalcogenide Moiré Bands"* arXiv 1804.03151 (2018).

Publications (August 2016 – July 2018)

P1. C.K. Chan, N. Linder, G. Refael and P.A. Lee, *"Photocurrents in Weyl semimetals"* Phys. Rev. B **95**, 041104 (R) (2017).

P2. C.-K. Chan and P. A. Lee, *"Emergence of gapped bulk and metallic side walls in the zeroth Landau level in Dirac and Weyl semimetals."*Phys. Rev. B **96**, 195143 (2017).

P3. J. Ruhman and P. A. Lee, *"Pairing from dynamically screened Coulomb repulsion in bismuth"* Phys. Rev. B **96**, 235107 (2017).

P4. L. Savary, J. Ruhman, J.W.F. Venderbos, L. Fu, and P.A. Lee*," Superconductivity in three-dimensional spin-orbit coupled semimetals."* Phys. Rev. B **96**, 214514 (2017).

P5. J. W. F. Venderbos, L, Savary, J. Ruhman, L. Fu, and P. A. Lee *"Paiiring states of spin 3/2 fermions: symmetry-enhforced topological gap functions."* Phys. Rev X **8**, 011029 (2018).

P6. I. Kimchi, J. P. Sheckelton, T. M. McQueen, P. A. Lee, *"Heat capacity from local moments in frustrated disordered quantum spin systems: scaling and data collapse"* arXiv:1803.00013 (2018).

P7. W.-Yu He, X. Y. Xu, G. Chen, K. T. Law, and P. A. Lee, *"Spinon Fermi surface in a cluster Mott insulator model on a triangular lattice and possible application to 1T-TaS_2"* arXiv 1803.00999 (2018), Physical Review Letters, to appear.

P8. X. Y. Xu, K. T. Law, and P. A. Lee, *"Kekulé valence bond order in an extended Hubbard model on the honeycomb lattice, with possible applications to twisted bilayer graphene"* arXiv:1805.00478 (2018).

P9. D. Chowdhury, B. Skinner, and P. A. Lee, *" Effect of magnetization on the tunneling anomaly in compressible quantum Hall states"* arXiv:1709.06091 (2017), Physical Review Letters, to appear.

P10. D. Chowdhury, B. Skinner, and P. A. Lee, *"Semiclassical theory of the tunneling anomaly in partially spin-polarized compressible quantum Hall states"* Phys. Rev. B 97, 195114 (2018).

Theory of Materials Program at the Lawrence Berkeley National Laboratory

Principal Investigator:
Steven G. Louie – Physics Department, UC Berkeley, and Materials Sciences Division, LBNL, Berkeley, CA 94720 (sglouie@berkeley.edu)
Co-Principal Investigators:
Marvin L. Cohen – Physics Department, UC Berkeley, and Materials Sciences Division, LBNL, Berkeley, CA 94720 (mlcohen@berkeley.edu)
Dung-Hai Lee – Physics Department, UC Berkeley, and Materials Sciences Division, LBNL, Berkeley, CA 94720 (dhlee@berkeley.edu)
Jeffrey B. Neaton – Physics Department, UC Berkeley, and The Molecular Foundry, LBNL, Berkeley, CA 94720 (jbneaton@lbl.gov)
Lin-Wang Wang – Materials Sciences Division, LBNL, Berkeley, CA 94720 (lwwang@lbl.gov)

Keywords: novel materials; reduced-dimensional systems; topological phases; first-principles calculations; new methods.

Project Scope

The goal of this project is to understand and compute material properties and behaviors, covering a range of systems that include complex materials, nanostructures, superconductors, reduced-dimensional materials, and strongly correlated electron systems. Novel materials and new concepts are explored. The major objectives include studies on: superconductivity and mechanisms; excited states in novel materials and nanostructures; methodology developments; symmetry and topological phases of matter; and transport phenomena. A variety of theoretical techniques are employed, ranging from first-principles electronic structure methods and many-body perturbation theory approaches to new conceptual and computational frameworks suitable for complex materials/nanostructures and strongly interacting systems. One emphasis is to investigate realistic systems employing microscopic first-principles approaches, including many-body effects. Model systems are also examined. Close collaboration with experimentalists is maintained. Another emphasis is to push theory beyond the Landau paradigm toward a framework suitable for very strongly correlated systems and novel topological phases. New phenomena, new phases, and new organization principles may be discovered. Equally important is the development of computational methods suitable for increasingly complex materials, reduced dimensional systems, and strongly correlated materials.

Recent Progress

Activities since the last PI Meeting in 2016 covered advances on atomically thin two-dimensional (2D) crystals, topological phases, molecular junctions, nanostructures, superconductors, photovoltaics, strongly correlated systems, and new theoretical and computational methods. Since August 2016, fifty-two (52) papers have been published

acknowledging this Program including publications in journals such as *Science*, *Nature "family" (Nat. Materials, Nat. Nanotechn., Nat. Commun., etc.), Phys. Rev. Letters, Nano Letters, J. Am. Chem. Soc*., *ACS Nano, J. Phys. Chem. C, Phys. Chem. Chem. Phys.*, among others. The work has led to formulation of new concepts, prediction of novel phenomena, and explanation of experiments for a range of materials. Some selected results are:

- Ab initio theory on environmental screening effects in 2D materials: renormalization of the bandgap, electronic Structure, and optical spectra
- Magnetic brightening and control of dark excitons in monolayer WSe2
- Predictions of the structure-properties relations of 2D materials: few-layer black phosphorous
- Large bulk photovoltaic effect and spontaneous polarization of single-layer monochalcogenides
- Theory of symmetry rules shaping spin-orbital textures in surface states
- Prediction of TiRhAs as a Dirac nodal line semimetal and new class of half-metallic ferromagnets via first-principles calculations

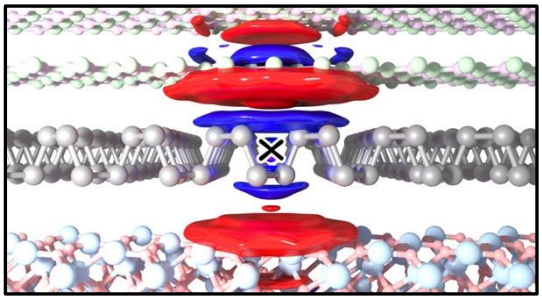

Fig 1. Calculated induced screening charge to a point charge in monolayer phosphorene due to substrate (sapphire) and encapturation (BN), illustrating the importance of nonlocal environmental screening to the electronic and optical properties of atomically thin 2D materials.

- New method for automated construction of maximally localized Wannier functions for bands with nontrivial topology.
- Ab initio electronic relaxation times and transport in noble metals.
- Ab initio studies of halide perovskites – electronic structures, optical properties, and their influence on photovoltaic applications
- Ab initio studies of transport through single-molecule junctions: molecule-electrode coupling, energy level alignment, and mapping of transmission function
- Elucidation of role of potential disorder and electron-electron interaction in the effective mass in bilayer graphene at low carrier densities
- Holographic theory of fermionic topological phase transitions -- our previous holographic theory for phase transition between bosonic symmetry protected topological states is extended to the fermions.
- Testing the Wannier Koopmans method (WKM) for band gap calculations of different materials (alkali halide, 2D material, organic crystal and band alignment)
- GPU implementation of the linear scaling three-dimensional fragment code for large system calculations.
- Development of a Green-Kubo formalism to calculate thermal conductivity based ab initio method
- Application of real-time time-dependent density functional method to different physical problems

- Development of neural-network force field based on ab initio calculations
- Demonstration that anti-ferromagnetism can enables electron-phonon coupling in iron-based superconductors
- Studies of alternate structures of TiO2 and Si suggest new paths for making photovoltaics
- Simulated effects of boron doping in amorphous carbon and their possible connection to superconductivity in Q-carbon

Future Plans

Planned activities are focused in: 1) reduced-dimensional systems, in particular quasi 1D and 2D materials; 2) excited-state properties of novel materials; 3) theoretical and methodological developments; 4) symmetry and topological phases; and 5) transport phenomena. Areas 1 & 4 concern with understanding and/or discovery of new phases and new classes of materials with novel properties. Areas 2 & 5 concern with excited-state (spectroscopic) and transport properties of materials and nanostructures. Area 3 concerns with developments of theoretical and computational methods that would allow accurate and predictive studies. Some selected projects include:

- Theory of topological phases and phase transitions in materials
- Photophysics & excitons in materials with nontrivial band topology
- Optoelectronic phenomena in quasi 2D materials and those with defects
- Controlling plasmons in metallic transition metal dichalcogenides layers and related quasi-2D materials.
- Electronic and transport phenomena of novel energy and topological materials
- Methods for and applications of tunneling-based transport phenomena through nanoscale heterogeneous interfaces
- Further development of the neural network force field methodology for more complex systems
- Study of carrier dynamics in nanosystems using nonadiabatic molecular dynamics method
- Magnetism and superconductivity in amorphous carbon
- Electron structure and electron-phonon couplings in FeSe

Selected 10 Publications (Out of a total of 52 publications during August 2016 – July 2018)

1. J. I. Mustafa, M. Bernardi, J. B. Neaton, and S. G. Louie, “Ab initio electronic relaxation times and transport in noble metals,” Phys. Rev. B 94, 155105 (2016).
2. C. S. Ong, S. Coh, M. L. Cohen, and S. G. Louie, “Real-space study of the optical absorption in alternative phases of silicon,” Phys. Rev. Mat. 1, 075408 (2017).

3. D. Y. Qiu, F. H. da Jornada, and S. G. Louie, “Environmental screening effects in 2D materials: Renormalization of the bandgap, electronic structure, and optical spectra, of few-layer black phosphorus,” Nano Lett. 17, 4706 (2017).
4. X. X. Zhang, T. Cao, Z. G. Lu, Y. C. Lin, F. Zhang, Y. Wang, Z. Q. Li, J. C. Hone, J. A. Robinson, D. Smirnov, S. G. Louie, and T. F. Heinz, “Magnetic brightening and control of dark excitons in monolayer WSe2,” Nat. Nanotechnol. 12, 9 (2017).
5. T. Rangel, B. M. Fregoso, B. S. Mendoza, T. Morimoto, J. E. Moore, and J. B. Neaton, "Large bulk photovoltaic effect and spontaneous polarization of single-layer monochalcogenides," Phys. Rev. Lett. 119, 067402 (2017)
6. Z. Q. Fan, X. W. Jiang, J. Luo, L. Y. Jiao, R. Huang, S. S. Li, and L. W. Wang, "In-plane Schottky-Barrier field-effect transistors based on 1T/2H heterojunctions of transition-metal dichalcogenides," Phys. Rev. B 96, 165402 (2017).
7. M. Weng, S. Li, J. Zheng, F. Pan, and L.W. Wang, “Wannier Koopmans Method Calculations of 2D Material Band Gaps,” J. Phys. Chem. Lett. 9, 281 (2017).
8. L. Tsui, Y-T Huang, H-C Jiang, and D-H Lee, “The phase transitions between Zn x Zn bosonic topological phases in 1+1 D, and a constraint on the central charge for the critical points between bosonic symmetry protected topological phases,” Nuclear Physics B 919,470 (2017)
9. Y. Sakai, J. R. Chelikowsky, and M. L. Cohen, “Magnetism in amorphous carbon,” Phys. Rev. Materials 2, 074403 (2018).
10. Z. Li, T. Cao, and S. G. Louie, “Two-dimensional ferromagnetism in few-layer van der Waals crystals: Renormalized spin-wave theory and calculations,” J. of Mag. and Mag. Mat., 463, 28-35 (2018).

CHARGE CARRIER HOLES CORRELATIONS AND NON-ABELIAN PHYSICS IN NANOSTRUCTURES, QUANTUM HALL EFFECT AND HYBRID SUPERCONDUCTOR/SEMICONDUCTOR STRUCTURES.

Principal Investigator: Yuli Lyanda-Geller, yuli@purdue.edu
Department of Physics and Astronomy, Purdue University West Lafayette IN 47907

Project Scope.

The project goal is to uncover new non-Abelian effects and states with non-Abelian statistics in charge carrier holes systems. We investigate Integer and Fractional Quantum Hall states at and around crossings in spectra of single-particle holes states arising due to strong angular momentum-orbital interactions of Luttinger holes. The key to understanding Quantum Hall charge carrier holes systems at the crossings, where polarization of holes states changes, is modeling domain walls in quantum Hall ferromagnets. In order to find realizations of Majorana Fermions and parafermions, we develop methods of modeling of states in domain walls in quantum Hall ferromagnets in the presence of superconducting proximity effect.

Recent Progress

Magnetic field spectral crossings of Luttinger holes in gated quantum wells.

Our previous consideration of holes in rectangular quantum wells lead to finding numerous crossings in holes spectra in spin 3/2 degenerate valence band in a magnetic field. In order to develop Majorana and parafermion settings in quantum Hall holes systems, one needs to develop systems, in which two counter-propagating edge states with opposite spin polarization of holes will form a domain wall. Holes systems offer an opportunity to create such counter-propagating edge states by using electrostatic gating of a single quantum well. Recently, we developed theory of gated quantum wells in charge carrier holes system, calculating the dependence of holes parameters on the gate voltage. In particular, we calculated the Rashba and other spin-orbit constants [1], g-factor and orbital splitting of states, taking into account mutual transformation of heavy and light holes states at the hetero-boundaries.

When the single-particle 2D holes spectrum in magnetic field is close to crossing in the absence of gate voltage, different gate voltages result in different ground states, and in the case of different gating of two adjacent areas of the 2D holes gas, a domain wall emerges between the two different ground states. In the proximity of a superconductor, a topological superconducting state and Majorana bound states emerge at the boundaries between normal and topological superconductor.

In order to obtain a parafermion setting, three problems must be resolved:

- Modeling hole-hole interactions in the fractional quantum Hall effect (FQHE)
- Modeling spectral crossings and domain walls in the fractional quantum Hall setting
- Modeling superconducting proximity for small number of particles in FQHE.

Fractional quantum Hall effect in charge carrier holes systems [2].

We have advanced our understanding of fractional quantum Hall effect in holes systems by investigating entanglement properties of the ground state. Results for topological entanglement entropy support earlier conclusions made by analysis of the overlap of the wavefunctions for small system sizes with Moore-Read trial wave functions and overlaps of wavefunctions of excitations with wavefunctions of excitations of the ideal Pfaffian state. In particular, we obtained substantial and convincing body of evidence supporting the non-Abelian nature of hole FQHE state at a filling factor ν=1/2 of the ground state of holes [2].

We have calculated the topological entanglement entropy for this system using two different methods, which demonstrate non-Abelian correlations. We have extended our exact diagonalization studies from N=8 and N=10, where N is the number of particles, to N=14,16. For cases, in which the many-body Hilbert space becomes too large, we now apply density matrix renormalization group (DMRG) in a spherical shell geometry.

Modeling of Fractional Hall effect in the presence of in-plane electric fields.

In order to further develop theory of the Fractional Hall Effect in Valence Band Hole Liquid and understand non-Abelian holes matter, it is important to understand how electric fields can shift the balance between different many-body states. It is important to understand various configurations in which the effects of electric field can be studied.

Even without application of gate voltage to the structure, electric fields emerge naturally in quantum Hall systems in the process of measurement, which requires an application of voltage. This small voltage difference across a sample applied in experiments to probe the system is often ignored in theoretical studies due to the Galilean invariance in the thermodynamic limit.
No experimental sample, however, is Galilean invariant. To understand this phenomenon, we first turned our attention to exploration of the effects of the probe electric fields in a disk geometry in electron systems with finite thickness at a filling factor ν=5/2 [3]. At this filling factor, both non-Abelian Moore-Read state and stripe states are possible. We have found that weak probe fields enhance the Moore-Read Pfaffian state but sufficiently strong electric fields destroy the incompressible state. We observe that in a disk geometry, the behavior of the system depends on the polarity of the applied radial field, which can potentially be observed in experiments using in a Corbino disc configuration. Our simulation also shows that the application of such a field enhances the coherence length of quasi-holes propagating through the edge channels.

To explore the effects of these electric fields, we performed exact diagonalization calculations in a disk geometry with a finite sample thickness for n=8, 10 and 12 particles. We have explored the phase diagram of the system as the strength of the applied electric field U, the Landau level mixing strength $\kappa = (e^2/\varepsilon l_m)/\hbar\omega_c$, and interactions with the neutralizing background are varied. Here l_m is the magnetic length and ω_c is the cyclotron frequency. We have found regions where the total angular momentum makes the Pfaffian state plausible, and confirm its existence using overlap integrals with the known Pfaffian wavefunction. The in-plane fields can be used to fine-tune the ground state and improve the edge properties of the non-Abelian states. Recently

we also analyzed how the transition between the Pfaffian and stripe/nematic state occurs due to application of barometric strain [4].

Theory of Majorana Fermions in integer quantum Hall ferromagnets [5].

In order to be able to analyze emergence of Majorana Fermions in domain walls between two hole states with different spin polarization in gated quantum Hall systems, we first modeled a related electronic system of a single CdTe quantum well doped with Mn magnetic impurities, in which domain walls emerge as a result of crossing of electron states due to compensation of cyclotron energy difference between the ground and the first excited Landau levels, positive energy spin splitting due to electron magnetization caused by their exchange interaction with Mn ions, and negative Zeeman splitting. In the case of non-uniform Mn doping along the growth axis of the structure, two different gate voltages applied to neighboring areas of the 2D gas result in two different magnetizations and two different ground states in these areas, realizing a domain wall in a quantum Hall ferromagnet.

The experimentally observed spectrum of such domain wall shows avoided crossing rather than crossing of spin states. Indeed our calculation shows that owing to Rashba spin-orbit interactions, the domain wall becomes gapped. In this case, impurities play a considerable role in transport through domain walls, and are crucial for generating Majorana modes when gapped integer quantum Hall ferromagnet domain wall is coupled to an s-type superconductor. In order to address topological superconductivity and transport through domain walls in this system, we have developed theory of electron states in the presence of short-range impurities as well as model electron states for smooth random potential in spin-orbit coupled Landau levels. We demonstrate that robust Majorana modes emerge for both of these types of random potential [5].

Theory of parafermions in fractional quantum Hall ferromagnets [6].

Topological quantum computation can be performed with Majorana fermions, but such qubits are not computationally universal. Parafermions, higher order non-Abelian excitations, are predicted to have denser rotation group and their braiding enables two-qubit entangling gates. A two-dimensional array of parafermions can serve as a building block for a system which supports Fibonacci anyons with universal braiding statistics, a holy grail of topological quantum computing. We propose that domain walls formed at spin phase transitions in the FQHE regime have the prerequisite helical structure to support parafermion excitations when coupled to an s-wave superconductor.

Conducting channels at the boundaries between two incompressible polarized and un-polarized $\nu = 2/3$ states, which are formed from two counter-propagating $\nu = 1/3$ states with opposite spin orientation, constitute fractional helical domain walls. Local control of polarization by electrostatic gates allows formation of a reconfigurable network of these domain walls with fractionalized charge excitations and, potentially, parafermion manipulation and braiding.

We performed exact diagonalization numerical studies of fractional helical domain walls [6], and more recently studied such domain walls coupled to a superconductor. To simulate edge states we use the disk geometry Fig. 4. Long-range Coulomb interactions between electrons are introduced using Haldane pseudopotentials. A neutralizing background and a confinement potential are used to hold electrons inside the disk. As is evident from experiments, spin transition can be controlled

by modulation of either Coulomb or Zeeman energies interchangeably. In our modeling we use spatially-dependent Zeeman splitting to control spin polarization of the 2DEG. The central region of the disk is characterized by a high Zeeman energy, while Zeemann splitting is neglected in the outer region. Between these areas the Zeeman term varies smoothly resulting in a smooth variation of wavefunctions across the disk.

We included up to 12 electrons in the exact diagonalization calculation for a fully spin-polarized states and 8 electrons for unpolarized states or coexisting polarized and unpolarized states at ν = 2/3. Energies and wavefunctions for the ground state and edge states, their density and spin density distributions for the disk geometry have been calculated. The ground state for 8 particles has the total angular momentum projection L_z = 46, in agreement with the composite fermion theory. The ground state is spin polarized in the interior part of the disk and spin unpolarized in the exterior area, as expected. The lowest excited states have angular momenta L_z = 45 and 47. These states are the current carrying states defining the domain wall. The difference in spin polarizations between these two states in shown in Fig. 4, it smoothly changes sign across the domain wall. The two edge states with different Lz on the disk have different angular velocities. When mapped onto a plane, these two states will have different linear velocities, i.e. their velocities will have counter-propagating components. Combined with the different spin polarization these states have a finite overlap with Cooper pair wavefunctions in a proximity s-wave superconductor, as has been shown for domain walls in integer quantum Hall ferromagnets.

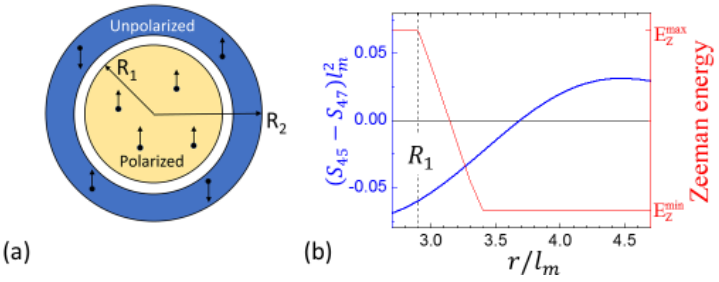

(a) Disk geometry. (b) The blue curve is the difference between spin densities for the modes with angular momentum L_z = 45 and 47, the excited states on the two sides of the domain wall formed near R_1. The profile of the spatially-dependent Zeeman interaction used to form the domain wall is shown in red.

In order to model proximity superconductivity, we introduce one more electron and a hole into our 8-electron domain wall system, and numerically solve the Bogoliubov-DeGennes equation, by using electrostatic constraint term that leads to the ground state with L_z = 46. The resulting spectrum of the system at L_z = 46 has in-gap state with almost zero energy ("almost" is presumably due to small size finite system), which we attribute to parafermions.

Future Work. We will extend the developed methods of calculating domain walls in quantum Hall ferromagnets in electron integer and fractional quantum Hall states to charge carrier holes systems. We will study interacting holes at ν = 2/3 and explore the conditions needed for degeneracy resulting in a parafermion defects without the need for proximity superconductor in a fractional quantum Hall liquid of holes in a wide quantum well. We also will investigate parafermions in holes systems in the presence of proximity superconductor.

Publication list

[1] J. Liang and Y. Lyanda-Geller, "Charge Carrier Holes and Majorana Fermions", *Phys. Rev. B (Rapid Communications)* 95, 201404 (2017).

[2] G.E. Simion and Y.B. Lyanda-Geller, Non-Abelian ν=1/2 quantum Hall state in Γ_8 Valence Band Hole Liquid", *Phys. Rev. B (Rapid Communications)*, 95, 161111 (2017).

[3] A. Tylan-Tyler and Y. Lyanda-Geller, "In-plane Electric Fields and the ν=5/2 Fractional Quantum Hall Effect in Disc Geometry", *Phys. Rev. B (Rapid Communications)*, 95 121302 (2017).

[4]) K.A. Schreiber, N. Samkharadze, G.C. Gardner,Y. Lyanda-Geller, M.J. Manfra, L.N. Pfeiffer, K.W. West, and G.A. Csathy, Universality of the Paired-to-Nematic Quantum Phase Transition in the Two-Dimensional Electron Gas, Nature Communications, 9 2400 (2018).

[5]) G. Simion, A. Kazakov, L. P. Rokhinson, T. Wojtowicz, and Y. B. Lyanda-Geller, Impurity-generated non-Abelions, Phys. Rev. B 97, 245107 (2018)

[6] T. Wu, A. Kazakov, G. Simion, Z. Wan, J. Liang, K. West, K. Baldwin, L. N. Pfeiffer, Y. Lyanda-Geller, and L. P. Rokhinson, Formation of helical domain walls in the fractional quantum Hall regime as a step toward realization of high-order non-Abelian excitations, Phys. Rev. B 97, 245304 (2018)

.

Transport and Spontaneous Electronic Order

Allan MacDonald and Qian Niu, The University of Texas at Austin

Keywords: Berry phase, valleytronics, Moiré patterns, quantum Hall, two-dimensional materials

We have completed theoretical studies of geometric, topological, and correlation effects on electronic properties, including the interplay between transport and ordering, mainly in 2D materials but also in other systems. Our research can be roughly classified into the following 5 categories: 1) Berry phase effects on magneto-electronic properties; 2) Berry phase and disorder effects in transport; 3) Valley physics in 2D semiconductors; 4) Exotic properties in graphene systems; and 5) Correlated phases in other 2D electron systems.

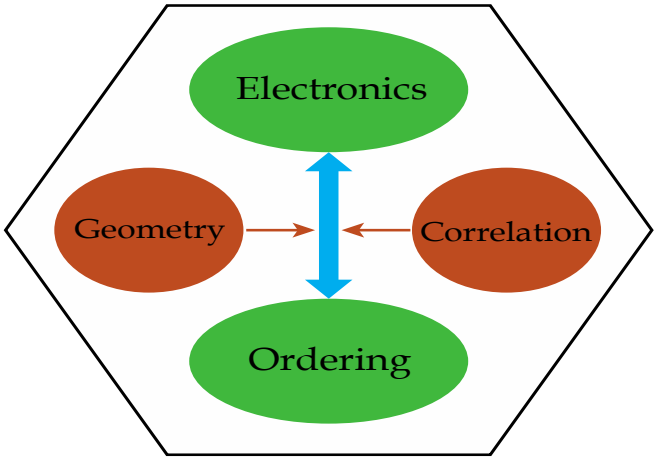

Interplay of electronics and ordering
through geometric and correlation effects in 2D systems

1) Berry phase effects on magneto-electronic properties: In systems in which time reversal symmetry has been broken, either spontaneously or by an external magnetic field, Berry phase and curvature in the electronic states plays an important role in thermodynamic, transport and magnetic properties.

We have formulated a semiclassical theory of electronic effects on magnetization dynamics to give a systematic yet transparent account of various mechanisms [1]. In addition, we followed up on our discovery of anomalous Hall and magneto-optical Kerr effects in non-collinear antiferromagnets, to address a large orbital magnetization that is crucial in understanding their magnetic field manipulation [2].

We have derived an accurate semiclassical quantization rule for Landau levels, by establishing a link with the theory of magnetization and susceptibility in the weak

field limit [3]. Our semiclassical theory has also been applied to the problem of magnetoconductivity [4, 5], to address some general issues in magneto transport studies of Weyl and other semimetals.

2) Berry phase and disorder effects in transport: Taking disorder and Berry curvature effects into account simultaneously is a complicated task in transport theory. Building upon previous success with the anomalous Hall effect, we have renewed our efforts trying to extend the theory to other phenomena such as the chiral anomaly and spin-orbit torques.

One approach is based on a kinetic equation for the density matrix, in which inter band coherence induced by the electric field and disorder can be systematically taken into account [6, 7]. We have also developed a semiclassical approach, in which inter band coherence manifests as dressing of the Bloch states due to field and disorder induced inter band coupling [8]. This latter approach has recently been rigorously justified by careful comparison with the Luttinger theory, and will be adopted as an important component in our proposed semiclassical theoretical framework for spintronics research. We have also studied disorder effect on spin-orbit torques beyond the Boltzmann limit, i.e. in the regime with disorder strength greater than spin-orbit coupling [9].

3) Valley physics in 2D semiconductors: Hexagonal lattices such as graphene and transition metal dichalcogenides have a pair of pockets of low energy electronic states at the corners of the Brillouin zone that are time-reversal partners. Very interesting electronic, optical, and phononic properties have been found in association with such valleys.

We have done new work on achieving topological phases by tuning valley dependent boundary state coupling [10], and investigated valley dependent magnetoresistance in two dimensional semiconductors [11]. In addition, we have collaborated with experimental colleagues at UT Austin on exciton valley coherence [12] and on tuning the Γ-K valley populations in hole-doped trilayer WSe2 [13].

4) Correlation effects in graphene systems: Pristine monolayer and double layer graphene has been made routinely in experiments, and its properties can be tuned in a variety of manners by Coulomb interaction and by external modulation.

We have extensively investigated the appearance and the properties of different possible phases associated with quadratic band touching in pristine double layer graphene [14], and have investigated phonon-mediated superconductivity in twisted bilayer graphene [15]. We have also studied moiré-induced electronic band structures in graphene on hexagonal boron nitride [16], and investigated layer pseudospin skyrmions and topological moiré states in twisted homobilayers [17]. We have also developed a helical network model for twisted bilayer graphene [18].

5) Correlated phases in other 2D electron systems: Because of the reduced dimensionality, interaction effects in two-dimensional materials are much stronger than in their three-dimensional counterpart. We have been interested in finding correlated phases in a variety of two dimensional electronic systems.

We have investigated possible orbital and spin ordering in 2d electrons defined at oxide interface [19], time-reversal symmetry broken nematic insulators near quantum spin Hall phase transition [20], non-local transport due to spin-superfluidity in a ferromagnetic thin film [21], and Hubbard model physics in transition metal dichalcogenide morie' bands [22]. We have also collaborated with experimentalists on spin-Seebeck effect due to spin-orbit locking of topological surface states [23], and on ferroelectric quantum Hall phase by visualizing Landau level wave function interference [24].

Publications

[1] Xiong, B., Chen, H., Li, X., and Niu, Q., "Electronic contribution to the geometric dynamics of magnetization," Phys. Rev. B **98**, 035123 (2018).
[2] Chen, H., Wang, T.-C., Xiao, D., Guo, G.-Y., Niu, Q., and MacDonald, A. H., "Manipulating anomalous Hall antiferromagnets with magnetic fields," arXiv:1802.03044 (2018).
[3] Gao, Y., and Niu, Q., "Zero-field magnetic response functions in Landau levels," Proceedings of the National Academy of Sciences **114**, 7295 (2017).
[4] Gao, Y., Yang, S. A., and Niu, Q., "Intrinsic relative magnetoconductivity of nonmagnetic metals," Phys. Rev. B **95**, 165135 (2017).
[5] Chen, H., Gao, Y., Xiao, D., MacDonald, A. H., and Niu, Q., "Semiclassical theory of linear magnetoresistance in crystalline conductors with broken time-reversal symmetry," arXiv:1511.02557 (2015).
[6] Sekine, A., Culcer, D., and MacDonald, A.H., "Quantum kinetic theory of the chiral anomaly," Phys. Rev. B **96**, 235134 (2017).
[7] Culcer, D., Sekine, A., and MacDonald, A. H., "Interband coherence response to electric fields in crystals: Berry-phase contributions and disorder effects," Phys. Rev. B **96**, 035106 (2017).
[8] Xiao, C., and Niu, Q., "Semiclassical theory of spin-orbit torques in disordered multiband electron systems," Phys. Rev. B **96**, 045428 (2017).
[9] Xiao, C., and Niu, Q., "Rashba torque beyond the Boltzmann regime," Phys. Rev. B **96**, 035423 (2017).
[10] Li, X., and Niu, Q., "Topological phase transitions in thin films by tuning multivalley boundary-state couplings," Phys. Rev. B **95**, 241411(R) (2017).
[11] Sekine, A., and MacDonald, A. H., "Valley-dependent magnetoresistance in two-dimensional semiconductors," Phys. Rev. B **97**, 201301(R) (2018).
[12] Hao, K., Xu, L., Wu, F., Nagler, P., Tran, K., Ma, X., Schüller, C., Korn, T., MacDonald, A. H., Moody, G., and Li, X., "Trion valley coherence in monolayer

semiconductors," 2D Materials **4**, 025105 (2017).
[13] Movva, H. C. P., Lovorn, T., Fallahazad, B., Larentis, S., Kim, K., Taniguchi, T., Watanabe, K., Banerjee, S., MacDonald, A. H., and Tutuc, E., "Tunable Γ − K valley populations in hole-doped trilayer WSe2," Phys. Rev. Lett. **120**, 107703 (2018).
[14 Su, J. J., and MacDonald, A. H., "Spatially-indirect exciton condensate phases in double bilayer graphene," Phys. Rev. B **95**, 045416 (2017).
[15] Wu, F., MacDonald, A., H., and Martin, I., "Theory of phonon-mediated superconductivity in twisted bilayer graphene," arXiv1805.08735v1 (2018).
[16] Jung, J., Laksono, E., DaSilva, A. M., and MacDonald, A. H., Mucha-Kruczynski, M., and Adam, S., "Moiré band model and band gaps of graphene on hexagonal boron nitride. Phys. Rev. B **96**, 085442 (2017).
[17] Wu, F., Lovorn, T., Tutuc, E., Martin, I., and MacDonald, A. H., "Layer pseudospin skyrmions and topological moiré bands in twisted homobilayers," arXiv.1807.03311v1 (2018).
[18] Efimkin, D. K., and MacDonald, A. H., "Helical network model for twisted bilayer graphene," Phys. Rev. B **98**, 035404 (2018).
[19] Tolsma, J. R., Polini, M., and MacDonald, A. H., "Orbital and spin order in oxide two-dimensional electron gases," Phys. Rev. B **95**, 205101 (2017).
[20] Xue, F., and MacDonald, A. H., "Time-reversal symmetry broken nematic insulators near quantum spin Hall phase transitions," Phys. Rev. Lett. **120**, 186802 (2018).
[21] Chen, H., and MacDonald, A. H., in *Universal Themes of Bose-Einstein Condensation*, Cambridge University Press (2017).
[22] Wu, F., Lovorn, T., Tutuc, E., and MacDonald, A. H., "Hubbard model physics in transition metal dichalcogenide moiré bands," Phys. Rev. Lett. **121**, 026402 (2018).
[23] Okuma, N., Masir, M. R., and MacDonald, A. H., "Theory of the topological spin-Seebeck effect at a topological-insulator/ferromagnetic-insulator interface," Phys. Rev. B **95**, 165418 (2017).
[24] Randeria, M. T., Feldman, B. E., Wu, F., Ding, H., Gyenis, A., Ji, H., Cava, R. J., MacDonald, A. H., and Yazdani, A., "Ferroelectric quantum Hall phase revealed by visualizing Landau level wave function interference," Nat. Phys. **14**, 796-800 (2018).

Computational Framework for Unbiased Studies of Correlated Electron Systems

Principal Investigator: Thomas A. Maier (Oak Ridge National Laboratory)
Co-PIs: Douglas Scalapino (University of California, Santa Barbara), Steven Johnston (University of Tennessee, Knoxville), Satoshi Okamoto, Gonzalo Alvarez, Tom Berlijn, Ying Wai Li (Oak Ridge National Laboratory)

Keywords: Strong correlations, superconductivity, spin liquids, numerical many-body theory

Project Scope

This project seeks to understand, predict, and ultimately control the effects of correlations in quantum materials such as unconventional superconductors, quantum spin liquids, and other strongly correlated systems through the application of high-end computational science, and thus help guide the design of new materials with optimized properties. This goal will be reached by developing a computational framework for controlled and unbiased studies of strongly interacting electron systems comprised of a diverse suite of complementary quantum many-body techniques, with implementations that scale and perform efficiently on current petascale and future exascale computing architectures. Three specific aims guide this research: (1) Development of improved and accelerated algorithms and efficient implementations based on state-of-the-art numerical methods to enable controlled and reliable studies of realistic but reduced models of correlated electron systems. (2) Applications of these algorithms to study and understand the mechanisms leading to the complex phases and physical behavior observed in unconventional superconductors and quantum spin liquids. And, (3) Development of improved procedures for accurately computing dynamical properties of a system, enabling experimental verification and validation of the theoretical predictions and scenarios emerging from the simulations through probes such as neutron scattering.

Recent Progress

Below are some highlights of progress made in the initial year of this project discussing the development of new algorithms as well as numerical calculations of correlated electron systems.

Pairfield fluctuations of the 2D Hubbard model – Pairfield fluctuations at temperatures above the superconducting transition temperature provide information on the nature of the phase out of which superconductivity emerges. These fluctuations can be characterized in tunneling experiments where the current between a superconductor and a non-superconducting material is measured. In the traditional low T_c superconductors, the fluctuating pair-field is well described by time-dependent Ginzburg-Landau (GL) theory with parameters set by the lattice phonon spectrum and

the Fermi liquid out of which the superconducting state emerges. In the case of the high-T_c cuprates, however, the materials are quasi two-dimensional and depending upon the doping, the superconducting phase can emerge from a non-Fermi liquid pseudogap phase or a non-pseudogap phase. Here we have used dynamic cluster quantum Monte Carlo DCA(QMC) calculations to study the bulk spin susceptibility $\chi_s(q=0,T)$ and the d-wave pairfield susceptibility $\chi_d(T) \sim [1-\lambda_d(T)]^{-1}$ of a 2D Hubbard model for various dopings (see Fig. 1). These calculations show that the temperature dependence of $\lambda_d(T) \sim \ln\frac{T}{T_c}$ at large doping, where there is no pseudogap, is consistent with Ginzburg-Landau amplitude fluctuations of the pairfield. At smaller dopings, where the superconducting state emerges from a pseudogap phase, we find linear behavior, $\lambda_d(T) \sim T - 1.8T_{KT}$, providing evidence for Emergy-Kivelson phase fluctuations of the pairfield which merge into Kosterlitz Thouless fluctuations with $\lambda_d(T) \sim \exp(-\frac{k}{\sqrt{|T-T_{KT}|}})$ as the transition is approached. Thus, we find evidence that the pseudogap provides an environment where the carrier density is low and thus the phase stiffness is weakened leading to phase fluctuations.

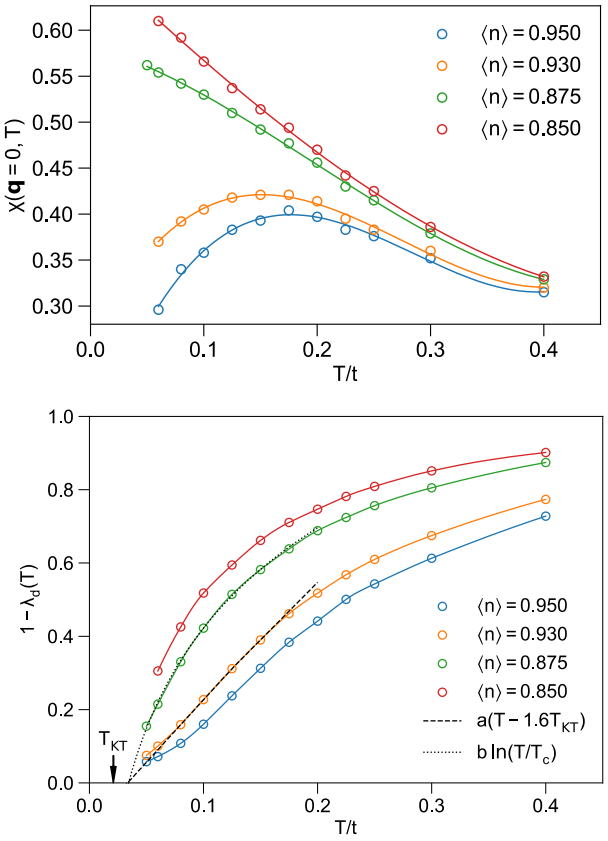

Figure 1: Top panel: The bulk spin susceptibility $\chi_s(q=0,T)$ of a 2D Hubbard model for different electron densitites $\langle n\rangle$ versus temperature T. For the underdoped $\langle n\rangle = 0.95$ and 0.93 systems, the downturn of $\chi_s(q=0,T)$ below a temperature T^* indicates the opening of a pseudogap. Bottom panel: The temperature dependence of $1-\lambda_d(T)$, where $\lambda_d(T)$ is the d-wave eigenvalue of the fully renormalized gap equation. When the effective carrier density is suppressed by the pseudogap, the effects of phase fluctuations and Kosterlitz-Thouless behavior change the characteristic temperature dependence of $\lambda_d(T)$.

Orbital selective behavior in multi-orbital Hubbard-Holstein models – The discovery of the iron-based superconductors (FeSC) has spurred widespread interest in multi-orbital systems. Our previous research effort has led to the formulation of several new concepts including the orbital-selective Mott phase (OSMP) and a Hund's metal, both of which arise due to the interplay between orbital degrees of freedom and strong electron correlations. But despite these advancements, very little is known about how competing interactions like the ubiquitous electron-phonon (e-ph) interaction influences these phases. In this project, we have begun mapping the phase diagrams of several multi-orbital Hubbard-Holstein models using dynamical mean field theory (DMFT) and determinant quantum Monte Carlo (DQMC) as a function of the Hubbard U and the e-p coupling strength λ for both infinite and one-dimensional (1D) models [1]. In the infinite dimensional case, we find that the e-ph interaction, even at weak couplings, significantly modifies

the phase diagram and introduces an orbital-selective Peierls insulating phase (OSPI) that is analogous to the widely studied OSMP. At small e-e and e-ph couplings, we find a competition between the OSMP and the OSPI, while the Mott and charge-density-wave (CDW) insulating phases compete at large couplings. The phase diagram for the 1D case is very similar (see Fig. 2). For weak e-e and e-ph interactions, we observe a competition between an OSMP and a (multicomponent) CDW insulating phase, with an intermediate metallic phase in between. For large e-e and e-ph couplings, the OSMP and CDW phases persist, while the metallic phase develops short-range orbital correlations and becomes insulating when both interactions are large but comparable. Our results have broad implications for the FeSCs, where many studies have neglected the e-ph interaction in theoretical models. This treatment is motivated mainly by an initial ab initio calculation showing that the dimensionless coupling strength $\lambda = 0.2$ in these materials. Our results indicate that e-ph couplings of this magnitude can redraw the phase boundaries of these multiorbital models. In light of recent evidence for correlation-enhanced e-ph interactions in the FeSC, it is becoming clear that the lattice may play a subtler role in these compounds than initially expected, and additional research in this area is needed.

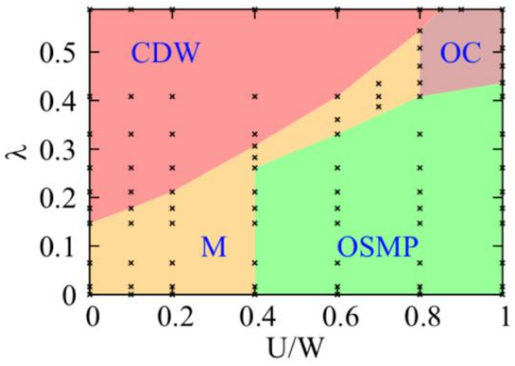

Figure 2: The low-temperature phase diagram of a one-dimensional three-orbital Hubbard-Holstein model. Several phases are present including a metallic (M) phase, and orbital-selective Mott phase (OSMP), an insulating charge-density-wave (CDW), and an insulating state with short-range orbital correlations (OC).

Thermal Pure Quantum State Microcanonical Lanczos Method (TPQ-MCLM) to study dynamics of quantum spin models – The finite temperature Lanczos method (FTLM) provides a tool to calculate dynamical spectral functions of interacting quantum systems at finite temperature. However, since this method is based on the canonical ensemble, energy eigenvalues and eigenstates of the model system have to be obtained by diagonalizing the Hamiltonian matrix multiple times. The microcanonical Lanczos method (MCLM) is an alternative approach that is based on the microcanonical ensemble. In this method, static and dynamical quantities are computed using a small number of excited states with the energy eigenvalue corresponding to the internal energy E of the system at temperature T. In contrast to the FTLM, the Hamiltonian matrix has to be diagonalized only once or a few times. Therefore, the computational cost of MCLM is much cheaper than that of FTLM, but the internal energy E has to be provided as an input parameter. Here, we have proposed to use the recently developed thermal pure quantum (TPQ) state method to compute the internal energy E as a function of T. Since TPQ states are generated iteratively without diagonalizing the Hamiltonian matrix, this method is extremely efficient. We have tested the accuracy of our combined TPQ-MCLM approach by comparing results with the standard FTLM for a 1D antiferromagnetic Heisenberg model with spin $S = 1/2$. Fig. 3 shows the computed spin dynamical structure factor $S(q, \omega)$ of a 24-site Heisenberg chain at $T = J$ (left) and $T = 0.5J$ (right). At high temperature $T = J$, TPQ-MCLM and FTLM give nearly identical results. At lower temperatures, the discreteness of energy eigenvalues creates spiky features in $S(q, \omega)$ for both the TPQ-

MCLM and FTLM near $q = \pi$. Nevertheless, the TPQ-MCLM shows weaker features than the FTLM at $T = 0.5J$, indicating that our method is more suitable than the FTLM to calculate the dynamical properties of an interacting quantum model in the thermodynamic limit in a wider range of temperatures. Moreover, we find that the overall temperature dependence is consistent with previous reports from quantum Monte-Carlo (QMC) calculations as well as finite-temperature density-matrix renormalization group (DMRG) calculations. In contrast to QMC, however, the TPQ-MCLM can be applied to frustrated systems. Furthermore, the TPQ-MCLM can be applied to 2-dimensional or 3-dimensional systems within the usual limitation of the system size.

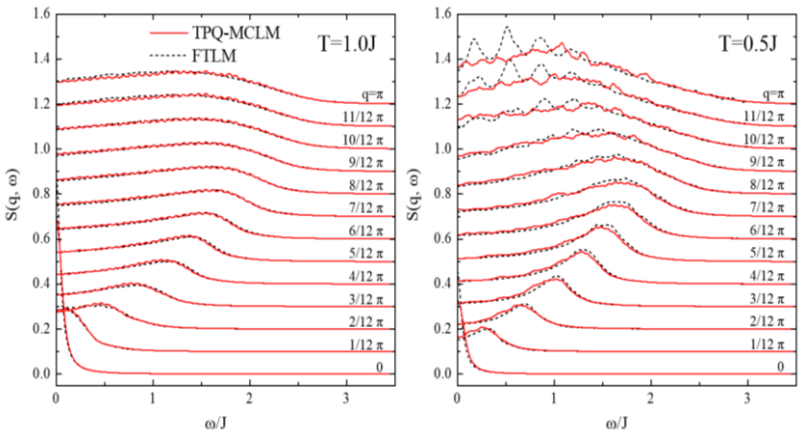

Figure 3: Spin dynamical structure factor $S(q, \omega)$ of a 24-site Heisenberg chain at $q = n\pi/12$ with $n = 0$~12 at the temperatures indicated. Solid and dashed lines are the TPQ-MCLM results and the FTLM results, respectively.

Future Plans

Unconventional superconductors – We aim to carry out DCA and DQMC calculations of the full momentum and frequency dependence of the 4-point scattering vertex in Hubbard models of superconductors. The goal is to understand the interplay between spin, charge orbital and pairing correlations. Combined with calculations of the dynamical properties, this will provide the deepest insight into the underlying mechanisms that give rise to these correlations and phases. We will also apply these techniques to more complex models, including the 3-band Hubbard model of the cuprates, multi-orbital models of the iron-based superconductors as well as Hubbard models with additional lattice degrees of freedom.

Quantum spin liquids – We plan to apply our TPQ-MCLM method as well as finite temperature DMRG to generalized Kitaev models for Na_2IrO_3 and α-$RuCl_3$ to investigate the thermodynamic and dynamical signatures of the Kitaev spin liquid phase. We also plan to develop a TPQ-DMRG method by replacing the exact diagonalization by DMRG to enable access to larger system sizes.

References

1. S. Li, Y. Tang, T. A. Maier, and S. Johnston, *Phase Competition in a One-Dimensional Three-Orbital Hubbard-Holstein Model*, Phys. Rev. B **97**, 195116 (2018).
2. S. Okamoto, G. Alvarez, E. Dagotto, and T. Tohyama, *Accuracy of the Microcanonical Lanczos Method to Compute Real-Frequency Dynamical Spectral Functions of Quantum Models at Finite Temperatures*, Phys. Rev. E **97**, 043308 (2018).

Publications (October 2017 – July 2018)

1. I. Esterlis, B. Nosarzewski, E. W. Huang, B. Moritz, T. P. Devereaux, D. J. Scalapino, and S. A. Kivelson, *Breakdown of the Migdal-Eliashberg Theory: a Determinant Quantum Monte Carlo Study*, Phys. Rev. B **97**, 140501 (2018).
2. A. Nocera, Y. Wang, N. D. Patel, G. Alvarez, T. A. Maier, E. Dagotto, and S. Johnston, *Doping Evolution of Charge and Spin Excitations in Two-Leg Hubbard Ladders: Comparing DMRG and FLEX Results*, Phys. Rev. B **97**, 195156 (2018).
3. M. Jiang, U. R. Hähner, T. C. Schulthess, and T. A. Maier, *d-Wave Superconductivity in the Presence of Nearest-Neighbor Coulomb Repulsion*, Phys. Rev. B **97**, 184507 (2018).
4. S. Li, Y. Tang, T. A. Maier, and S. Johnston, *Phase Competition in a One-Dimensional Three-Orbital Hubbard-Holstein Model*, Phys. Rev. B **97**, 195116 (2018).
5. S. Okamoto, G. Alvarez, E. Dagotto, and T. Tohyama, *Accuracy of the Microcanonical Lanczos Method to Compute Real-Frequency Dynamical Spectral Functions of Quantum Models at Finite Temperatures*, Phys. Rev. E **97**, 043308 (2018).
6. T. Dahm and D. J. Scalapino, *Dependence of Tc on the Q-Ω Structure of the Spin-Fluctuation Spectrum*, Phys. Rev. B **97**, 184504 (2018).

A New Approach to the Interacting Phonon Problem

Chris A. Marianetti

Columbia University, Department of Applied Physics and Applied Mathematics, New York, NY 10011

Keywords: Phonon interactions, strongly correlated materials, phase transitions.

Project Scope

The goal of this proposal is two-fold. First, we are developing a formalism to reliably, efficiently, and reproducibly compute phonons and their interactions from first principles. While computing phonons from first-principles is largely considered a solved problem, practical shortcomings of existing methods still preclude their use under a broad range of conditions. Alternatively, computing phonon interactions from first-principles is still a rapidly evolving field, and the basic form of phonon interactions is not well known even in classic materials systems. Our *Hierarchical Finite Difference* approach brings the full force of group theory to the interacting phonon problem, yielding the most efficient finite difference algorithm allowed by group theory for a function defined over a crystal lattice. Furthermore, our approach produces only the irreducible derivatives of the Born-Oppenheimer surface; which will be crucial to assessing, disseminating, and storing our results. The phonons and their interactions can then be used to predict a myriad of materials properties in a variety of different approximations.

The second goal of our proposal is to develop an efficient and accurate approach for computing the thermodynamics of the interacting phonon problem. We are developing a new approach to the many-body problem: Entropy Functional Theory. Our approach involves the construction of the entropy as a functional of a subspace of the density matrix; and we are developing a generic approximation to this formal construction which could be applied to any quantum mechanical problem with non-commuting operators. Preliminary results on the infinite dimensional one band Hubbard model show remarkable agreement with the exact solution.

Recent Progress

Phonons and Phonon Interactions **-** Efficiently extracting a high resolution Taylor series expansion of the Born-Oppeheimer surface from an arbitrary first-principles approach is of great importance. We have developed an optimal formalism to compute phonons and their interactions at arbitrary order and crystal dimension on a regular grid using finite difference; exploiting symmetry to the fullest. Building on a key theorem we derive, our approach ensures that a given derivative can always obtained from the smallest possible supercell dictated by the translation group, in addition to the smallest number of first-principles calculations dictated by space group and permutation symmetry. Our approach maximally exploits any derivatives the first-principles approach can efficiently deliver perturbatively (e.g. Hellman-Feynman forces,

etc) to obtain higher order derivatives. We prove that our approach is superior to any single-supercell finite difference approach. Applications have been executed for graphene, computing and tabulating the irreducible derivatives up to 4th order. Sample measurements of irreducible derivatives are shown in Figure 1, right panel.

No matter what formalism is used to compute the Taylor series of the Born-Oppenheimer surface, one needs some clear criteria to assess the quality of the results. A critical test is to compute the volume derivatives of the phonons, where the n-th derivative probes the n+2-th order force constants to infinite range. The first volume derivative of the phonons is the main ingredient of the Gruneisen parameters, and our cubic interactions successfully converge to the direct measurements (see Figure 1, left panel).

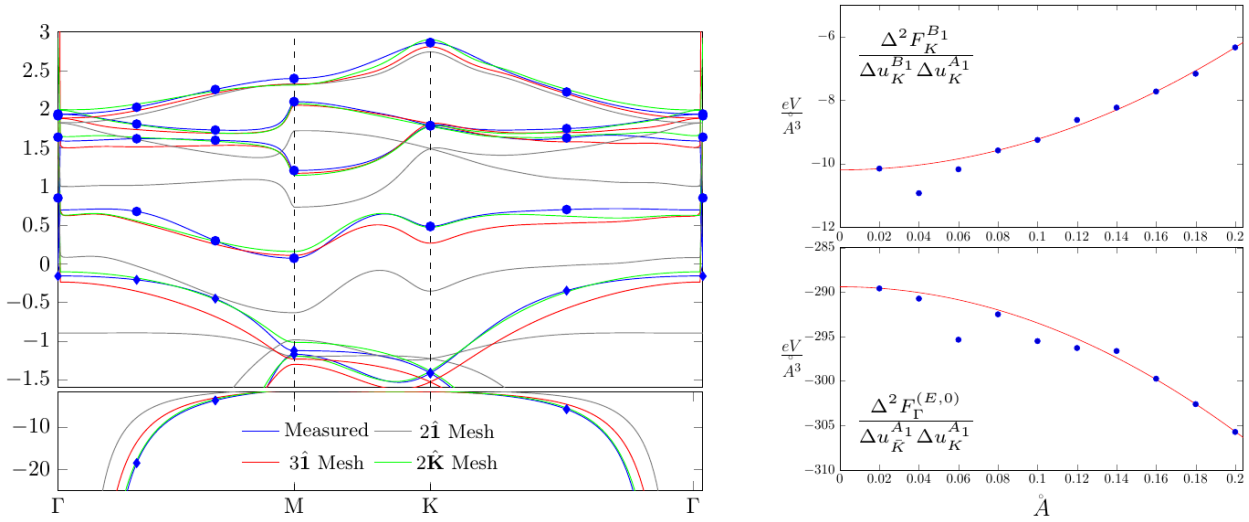

Figure 1: (Left Panel) The Gruneisen parameters plotted on path through the irreducible Brillouin zone. The blue points/lines are directly measured via derivatives of the phonons, while the other lines are predictions based on 3rd order phonon interactions on increasingly dense meshes. (Right Panel) Finite difference measurements of irreducible derivatives; the quadratic error tail allows for extrapolation to the discretization free solution.

Entropy Functional Theory - Having succeeded in generating an approach to compute phonons and their interactions, we will need an efficient formalism to solve these models. More generally, interacting lattice models, both Fermionic and Bosonic, embody some of the most basic aspects of condensed matter and materials physics, and therefore reliable and efficient solutions are critical. Here we introduce Entropy Functional Theory (EFT), which is a formalism that delivers all thermodynamic properties, and is highly amenable to reliable approximations. The entropy functional (EF) depends upon the single particle density matrix (SPDM) and the local reduced density matrix (LRDM), and can be formally constructed via the Legendre transform of the free energy functional or a constrained search. The latter perspective motivates a geometric representation of EF on the SPDM+LRDM manifold which formally may be constructed as a sum of entropy from the individual SPDM and LRDM spaces for an

appropriately chosen coordinate transformation. We propose a general approximation to construct the EF using only perturbation theory from various limits.

We provide a test of theory on the single band Hubbard mode in infinite dimensions, where the dynamical mean-field theory in conjunction with quantum Monte-Carlo yields the numerically exact solution (See Figure 2). We demonstrate that the double occupancy, quasiparticle weight, and charge gap are all predicted with remarkable accuracy for arbitrary values of the on site interaction; performing far better than the well known Gutzwiller approach, or any other efficient theory. Furthermore, EFT can also accurately capture the double occupancy as a function of temperature. Given that our approach is precise and it has a negligible computational cost, EFT will have broad applications in model Hamiltonians and materials physics.

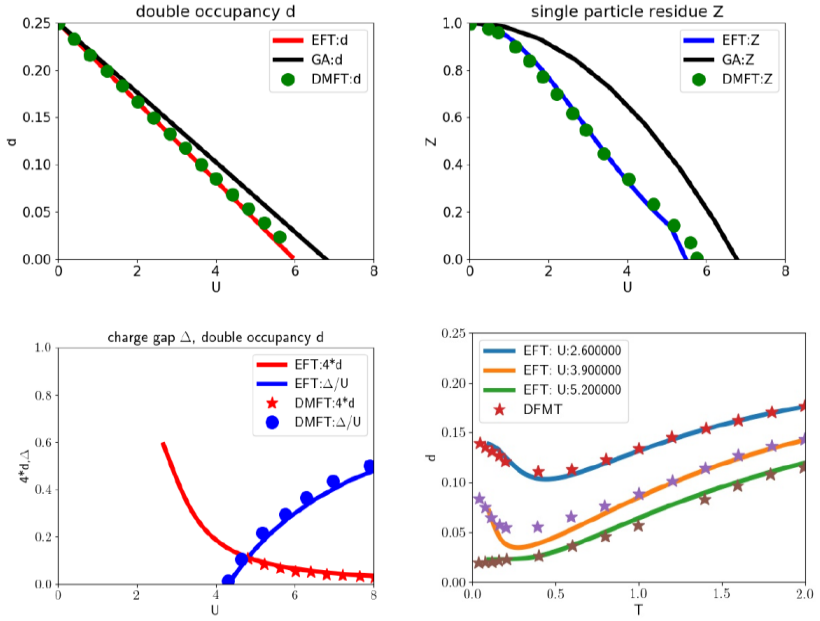

Figure 2: All panels are for the Hubbard model on the Bethe lattice in infinite dimensions; EFT is compared to DMFT, and Gutzwiller where indicated. (upper left) The double occupancy as a function of the Hubbard U. (upper right) The quasiparticle weight Z. (left panel) A plot of both the charge gap and the double occupancy. (right panel) The double occupancy as a function of temperature for different values of U; spanning the metallic and insulating regime.

Re-based double perovskites - Re-based double perovskites have garnered substantial attention due to their high Curie temperatures and display of complex interplay of structural and metal-insulator transitions (MIT). We were drawn to the Ca_2FeReO_6 system by a first-order, isostructural metal-insulator transition, which will serve as a critical testbed for our formalism for interacting phonons. However, the origin of the structural transition was completely unknown, leading us to study the family A_2BReO_6 (A=Sr,Ca and B=Cr, Fe); which share a common low energy Hamiltonian. We have predicted that C-type Re orbital ordering is driving the structural and metal-insulator transition (See Figure 3), which is consistent with all known experiments, but still awaiting direct confirmation. It should be noted that our DFT+U calculations were successful in capturing the experimentally observed metallic state in Sr2FeReO6, while producing the experimentally observed insulating states in all other cases; with the use of the same U in all materials.

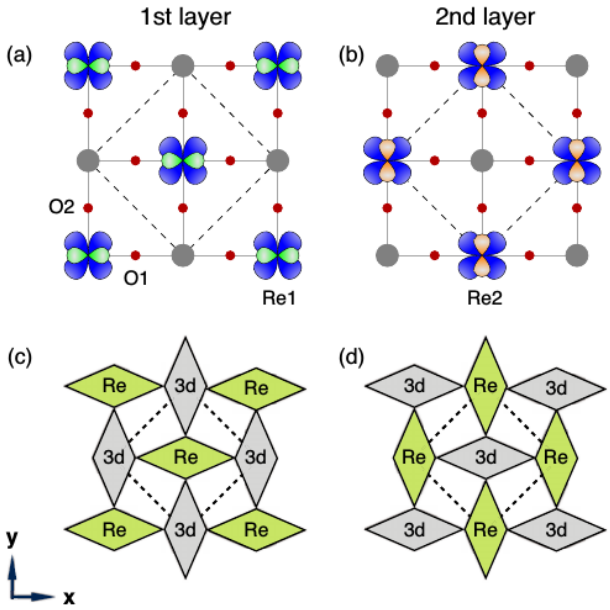

Figure 3: Schematic diagrams of the C-type orbital ordering in A_2BReO_6 for the 1st and 2nd layer along the c-axis of the conventional cubic cell, shown in panels (a) and (b), respectively. Red dots correspond to oxygen atoms while grey dots correspond to B atoms (ie. Cr or Fe). The pictured t2g orbitals are located on Re sites (dxy is blue, dxz is green, dyz is orange). Panels (c) and (d) depict a schematic of the C-type octahedral distortion, whereby each local octahedron is distorted in a positive or negative Eg distortion.

Future Plans

Phonon interactions **-** Having finished developing our hierarchical framework for computing phonons and interactions, we will apply our approach to a variety of systems. First, we will compute the phonons of alpha plutonium for the first time. Despite the fact that the phonons were measured experimentally roughly a decade ago, no predictions have been made yet; in part due to the computational expense of existing approaches. In addition to the phonons, we will also compute the cubic interactions, which will allow us to predict the coefficient of thermal expansion; addressing one of the more mysterious properties of plutonium.

A second major application is the rare-earth nickelates, for which we identified the so-called site-selective Mott transition that is accompanied with a concomitant bond disproportionation transition. Furthermore, our previous work proved that the finite temperature phase transition is basically an interacting phonon problem. The experimental phase diagram of the disproportionation phase transition as a function of temperature, pressure, and rare-earth cation has been long known, but never predicted from first-principles. Our hierarchical finite difference approach will be used to compute the phonon interactions and predict the phase transition. Along these same lines, we will compute the phonons and phonon interactions in the Re-based double perovskites and predict the structural phase transition in Ca_2FeReO_6.

Entropy Functional Theory **-** Our entropy functional theory will be extended to systems with more than one orbital (or polarization) per lattice site; allowing us to study interacting phonon models. Calculations will be performed for the multi-orbital Hubbard model in infinite dimensions, where numerically exact solutions are known. Additionally, we will apply EFT to interacting phonon models of phonon interactions, focusing on graphene where we now have accurate irreducible phonon interactions. The latter results will be directly compared to classical and quantum Monte-Carlo calculations.

Publications (August 2016 – July 2018)

1. T. Lee and C.A. Marianetti, *Structural and metal-insulator transitions in rhenium based double perovskites via orbital ordering*, Phys. Rev. B 97, 045102 (2018)

Structure and Electronic Properties of Dirac Materials

Principal investigator: Eugene Mele
Department of Physics and Astronomy, University of Pennsylvania, Philadelphia PA 19104
mele@physics.upenn.edu

Personnel (*=DOE supported): Z. Addison* (Penn GS), A.B. Li*(Penn GS), J. Venderbos (PD), C.L. Kane, A.M.Rappe
External Collaborators: Ch. Bruder, F. Kusmartsev, T. Low, F. Guinea, D. Basov, M. Fogler, H. Min

Project Scope

This project explores electronic phenomena in Dirac materials focusing on new responses induced by layer-layer interactions, stacking order and laterally confined electronic states. The work uses a combination of analytical model model building and symmetry analysis augmented by atomistic computations. We explore the electronic physics near grain boundaries in 2D bonded networks and the effects of stacking order on transport, electrodynamics, optical and infrared response in layered materials. The calculations are carried out on representative prototypical materials (graphene, transition metal dichalcogenides, metal silicides and three dimensional Dirac materials) with focus on generic properties that can be realized in a wide family of materials. Specific problems addressed are (a) electronic transport through confined modes in one dimensional domain walls, (b) structurally induced optical gyrotropy, (c) infrared electrodynamics (d) anomalous transport phenomena from momentum-space geometry. These phenomena enable potential applications of controlled transport of charge, spin, orbital angular momentum and energy.

Project Highlights

1.1 Quantum transport at edges and interfaces of 2D Materials

Single layer graphenes host one dimensional domain walls that can arise in several different contexts. They exist as extended lattice defects in CVD-grown material (e.g. as twin boundaries), they can be written by electrostatic doping (e.g. in p-n junctions) and they can be induced by orbital quantization in a spatially varying perpendicular magnetic field (e.g. snake states). We studied confined electronic states that occur in each of these situations with the goal of understanding their uses as configurable transport channels for charge and spin. In collaboration with the Crommie group at Berkeley we recently discovered that closely related spectral signatures appear in spatially resolved scanning tunneling spectroscopy at edges and grain boundaries for the Quantum Spin Hall state in single layer 1T'-WSe_2.

Highlights of our work are the discoveries: (1) that interfacial states on zero-angle grain boundaries are topologically protected zero modes that are protected by a novel *nonlocal* chiral symmetry of the graphene Hamiltonian near its charge neutrality point **[Ref. 1]** (to our knowledge the significance of this nonlocality was developed for the first time in our work (2) the spectra for laterally confined states at p-n junctions and snake states for modulated B-fields with uniform chemical potential are gauge equivalent representations of the same problem (i.e. when expressed in a Nambu particle-hole doubled representation the two problems can be formally interconverted by a position-dependent particle-hole transformation **[Ref. 2]** and (3) ballistic transport through a gate defined p-n junction can be configured as a gate-tunable valley filter **[Ref**

3]. This latter approach has been extended to study transport channels in configurable grain boundaries in graphene **[Ref. 4]** and in 2D WSe2 prepared in a Quantum Spin Hall state **[Ref. 5]**.

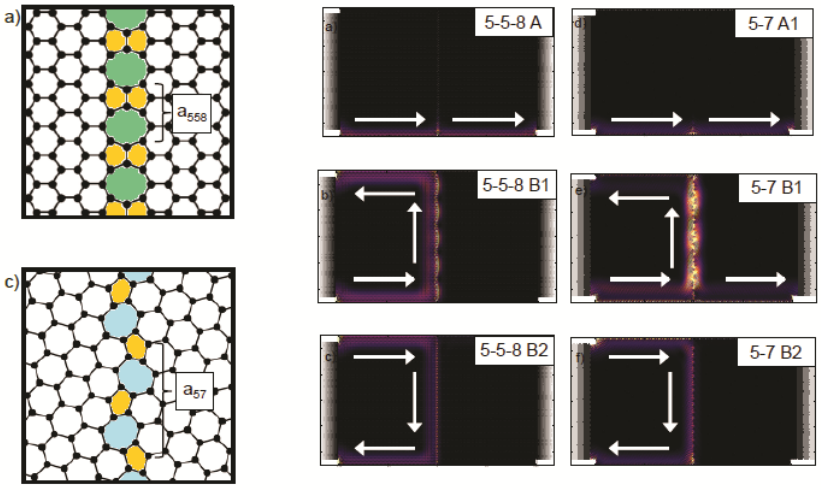

Figure 1 Twin grain boundaries (a,c) in the graphene lattice are domain walls that laterally confine electronic states. When the bulk is gapped by a quantizing magnetic field quantum transport channels for charge and spin is mediated through topologically protected modes on the outer edges (right, top) and confined interfacial modes (right center and bottom) that connect opposite edges. Transport through the domain wall channels and switching from the edge to the interior inter-edge pathways can be controlled by an electrostatic gate **[from Ref. 4].**

1.2 Stacking order and near field electrodynamics in multilayer graphenes

It is generally appreciated that the low energy electronic physics of bilayer and multilayer graphenes are exquisitely sensitive to their atomic-scale stacking arrangement. *Spatially varying* stacking patterns are encountered in many experimental settings, among these are stacking discommensurations where the AB and BA arrangements are joined, twisted graphenes bilayers where the symmetry axes of neighboring layers are rotationally misaligned and even more complex stacking patterns containing networks of these domain walls. In earlier work we studied the effects of domain walls in the interlayer registry on the electronic properties and found that their valley projected spectra host pairs of laterally confined propagating interfacial states **[Ref. 6]**. We collaborated with an experimental group (D. Basov, UCSD/Columbia) who use near field plasmon reflection microscopy (s-SNOM) for imaging and spectroscopy of these linear stacking domain walls (Figure 2). We find that the experimental signatures in SNOM of plasmon backscattering from stacking domain walls are *different for different wall orientations* and are quantitatively understood by a registry-dependent local modification of the band structure *within the walls* **[Ref. 7]**. This produces contrast in the local conductivity and thereby a voltage-tunable boundary condition on in-plane electrodynamics. Importantly we discovered that this generally occurs with almost no scalar electrostatic contribution, i.e. the conductivity contrast does not arise from a local charge accumulation or depletion in the wall and instead it can be unfolded to probe the interlayer hybridization of electronic states within the wall. These results also highlight a powerful use of s-SNOM for providing spectroscopic information on surface features at the sub 10-nm scale.

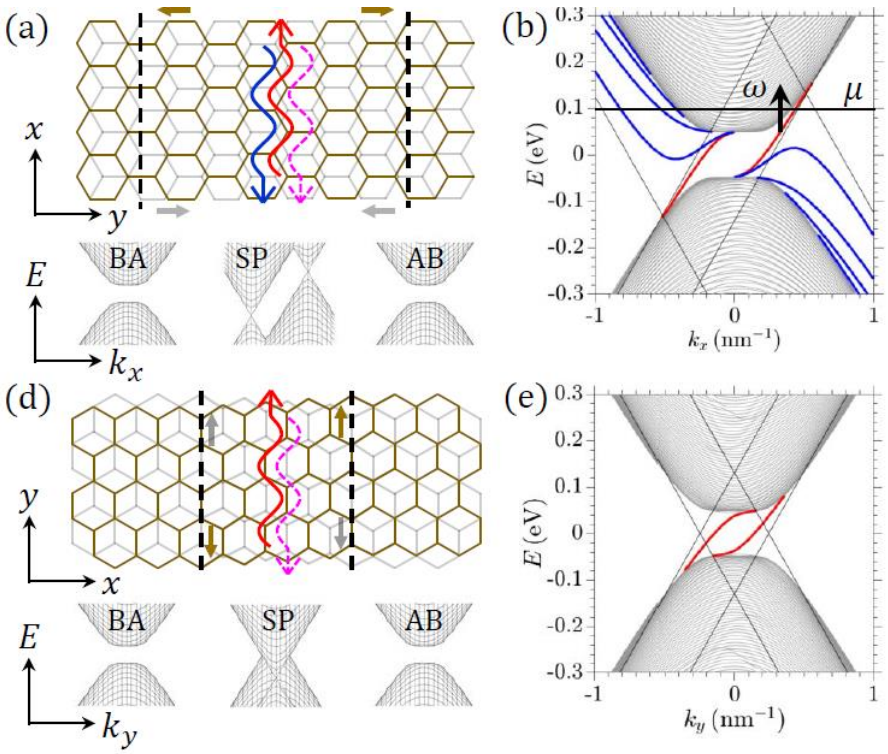

Figure 2 Stacking domain walls in bilayer graphene fission the BLG quadratic point degeneracy to form two linear Weyl points that are offset in both energy and momentum (left panel) depending on the orientation of the wall. With an interlayer bias, the gapped ground states of the valley projected Hamiltonians have a topological order that protects two chiral branches per valley in the domain (right, red lines). The variation of the stacking order in the domain wall locally changes the band structure, laterally confining additional "nontopological" modes which contribute to the local electrodynamic impedance of the wall. This efficiently scatters propagating surface plasmon polaritons (TM modes). The scattering amplitude is measured by studying the standing wave patterns produced in near field plasmon reflection imaging (s-SNOM) and is quantitativey described by this theoretical model. **(from Ref. 7)**

1.3 Novel Circular Photogalvanic Phenomena

The circular photogalvanic effect (CPGE) is a nonlinear response whereby a steady state charge current is produced by second order downconversion of a *circularly polarized optical field*. The signature is an optically induced charge current whose direction is selected by the sense of circular polarization of the light. It is of fundamental interest as a demonstration of optical injection of angular momentum and as an incisive probe of (sometimes subtle) symmetry breaking in various condensed phases. We studied this effect in three different materials platforms: (a) We discovered a new type of shape-induced and voltage-controlled circular photogalvanic effect (CPGE) at the surfaces of Si nanowires. The results are noteworthy because the bulk lattice structure of Si has mirror symmetries that forbid an intrinsic bulk CPGE. Furthermore the spin-orbit interaction in Si is negligibly weak for our experiments at optical wavelengths effectively excluding the possibility of any significant surface CPGE from a Rashba type coupling to spins on the boundaries. We found that the CPGE in Si nanowires arises instead as an orbital effect produced by the atomic arrangement on the boundary of a semiconducting nanowire which, in combination with a gate electrode, can (tunably) break all mirror symmetries and enable CPGE **[Ref. 8]**. (b) We discovered a new form of CPGE in the Weyl semimetals $MoTe_2$ and $Mo_{0.9}W_{0.1}Te_2$ alloys which is greatly enhanced in their low temperature Weyl phases. Here the CPGE is manifest by a charge current that circulates *around* the waist of a finite-size circularly-polarized optical field. Our theoretical analysis found that this is a new type of CPGE, which we named the

spatially dispersive, i.e. **q**-dependent *s-CPGE,* whereby the spatial variation of the amplitude of the driving field effectively eliminates a bulk material symmetry at linear order in **q** enabling the response **[Ref. 9]**. (c) We discovered that 2D metal silicides (e.g. Cu_2Si) realize a purely orbitally-induced topological texture in their band structures that can be coherently manipulated optically using circularly polarized light producing an optically controlled anomalous Hall response "on demand".

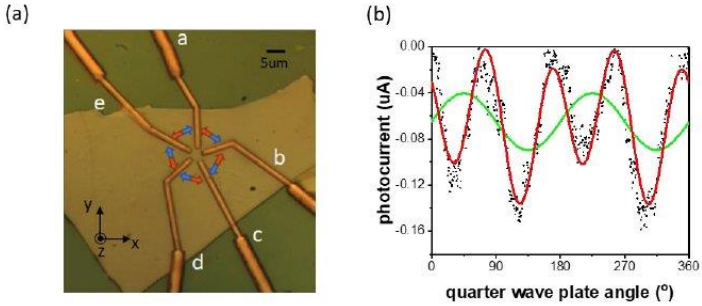

Figure 3. s-CPGE is a spatially dispersive variant of the circular photogalvanic effect where a charge current circulates around the waist of a finite-size beam of a circularly polarized optical driving field (left). The effect was discovered in the Weyl semimetal phase of $MoTe_2$ where its signature is a circulating charge current where its magnitude and direction are selected by the ellipticity of the optical field (right). **[from Ref. 9]**

DOE Supported Publications

1. M. Phillips and E.J. Mele "Zero Modes on Zero Angle Grain Boundaries in Graphene" *Physical Review B* 91, 125404 (2015)

2. Y Liu, RP Tiwari, M Brada, C Bruder, FV Kusmartsev, EJ Mele "Snake states and their symmetries in graphene" *Physical Review B* 92 (23), 235438 (2015)

3. T Sekera, C Bruder, EJ Mele, RP Tiwari "Switchable valley filter based on a graphene p– n junction in a magnetic field" *Physical Review B* 95 (20), 205431 (2017)

4. M Phillips, EJ Mele "Charge and spin transport on graphene grain boundaries in a quantizing magnetic field" *Physical Review B* 96 (4), 041403 (2017)

5. Zahra Pedramrazi, Charlotte Herbig, Madeleine Philips, Dillon Wong, Yi Chen, Hsin-Zon Tsai, Shujie Tang, Hyejin Ryu, Artem Pulkin, Zahid Hussain, Sung-Kwan Mo, Zhi-Xun Shen, Oleg Yazyev, Eugene Mele, Michael Crommie "Exploring the Electonic Properties of Strain-induced Grain Boundaries in the 2D Quantum Spin Hall State in 1T'-WSe_2" (to be published, paper presented at 2018 APS March Meeting Abstract, *Bull. Am. Phys. Soc*. (2018))

6. F Zhang, AH MacDonald, EJ Mele "Valley Chern numbers and boundary modes in gapped bilayer graphene" *Proceedings of the National Academy of Sciences* 110 (26), 10546-10551 (2013)

7. Bor-Yuan Jiang, Guang-Xin Ni, Zachariah Addison, Jing K. Shi, Xiaomeng Liu, Shu Yang Frank Zhao, Philip Kim, Eugene J. Mele, Dimitri N. Basov, and Michael M. Fogler "Plasmon Reflections by Topological Electronic Boundaries in Bilayer Graphene" *Nano Letters 17* (11), 7080-7085 (2017)
DOI: 10.1021/acs.nanolett.7b03816

8. S Dhara, EJ Mele, R Agarwal "Voltage-tunable circular photogalvanic effect in silicon nanowires" *Science* 349 (6249), 726-729 (2015)

9. Z Ji, G Liu, Z Addison, W Liu, P Yu, H Gao, Z Liu, AM Rappe, CL Kane, E.J. Mele and R. Agarwal. "Spatially dispersive circular photogalvanic effect in a Weyl semimetal"(in review, arXiv:1802.04387)

Disorder, interactions, and their interplay in novel narrow-gap Dirac materials and Weyl semimetals

Principal Investigator: Dr. Eugene Mishchenko
Department of Physics, University of Utah
Salt Lake City, UT 84112
mishch@physics.utah.edu

Keywords: Dirac materials, Coulomb interaction, transport, optics, disorder

Project scope

Progress of the modern day condensed matter physics is to a large extent driven by the synthesis of new materials, advances in their experimental characterization and theoretical description. Recent discoveries of novel gapless Weyl semimetals, in which magnetic dopants essentially suppress the gap, have added to the family of graphene and topological insulators actively investigated over the past decade. With the field of novel semimetals rapidly maturing, its focus necessarily shifts from demonstrations of the feasibility of such materials to their quantitative characterization. While the transport and optical properties of graphene and topological insulators are well captured within a picture of free non-interacting electrons, gapless 3D Weyl semimetals and narrow-gap 2D semiconductors with Dirac spectrum are known to be extremely susceptible to disorder and electron-electron interactions.

In theory, the effects of disorder and interactions cannot be taken into account neither on perturbative nor on the mean-field level. The major goal of the project is a development of the approaches to description of disordered Dirac fermions, interacting Dirac fermions, and, finally, the impact of interplay of disorder and interactions on the properties of Dirac fermions. Particular projects to be addressed are: 1) optical conductivity of 3D gapless Dirac fermions in the presence of smooth disorder, 2) interplay of disorder and Coulomb interactions in the spectral properties of such fermions, 3) formation and structure of the impurity band with Coulomb supercritical clusters, 4) Coulomb interaction-driven renormalization of the electron spectrum and of the transport response in the presence of strong magnetic field, 5) instanton approach to the disorder-induced fluctuation states in zero-gap 3D materials, and 6) the role of disorder in quantum anomalous Hall effect.

Recent progress

The main objective of the proposed research is the effects of disorder and interactions and their interplay in the Dirac materials. In essence, this issue boils down to incorporation of disorder and interactions into the systems whose bare spectrum is described by the matrix Hamiltonian. From this perspective, the research conducted during the first year can be viewed as developing the tools and intuition for attacking the more challenging problems pertaining to disorder and interactions in topological insulators and Weyl semimetals. More specifically, we studied the models in which the effects of disorder and interactions in matrix Hamiltonians are tractable. Nonetheless, the outcome of the first year also includes the concrete predictions for the observable quantities.

Depolarization effect in quasi-1D Dirac materials

Namely, in our paper “Breakdown of classical electrostatics in the depolarization of quantum wires and nanotubes” (L. Shan, E. G. Mishchenko) the Hamiltonian studied was the 1D Dirac Hamiltonian. It captures the properties of gapful and gapless carbon nanotubes. The peculiarity of electron-electron interactions in these systems stems from the “easiness” of creation of electron-hole pairs. For the first time, we have identified the importance of two types of Coulomb interaction: a conventional forward scattering (without the change of the angular momentum) and a novel dipolar interaction occurring with the change of the angular momentum of electrons. The role of this interaction in Dirac spectrum quantum wires has not been appreciated in the existing literature. We demonstrate how this interaction naturally appears as a result of the geometry of the system and shows in its optical response to a transverse ac electric field. In particular, we have developed non-perturbative theory of the absorption spectrum and showed how the traditional textbook electrostatics treatment of the depolarization effect, which relies on the effective dielectric permittivity approximation, breaks down for quasi-one-dimensional Dirac materials. We have developed a novel hybrid many-body approach that combines the method of bosonization with the diagram technique to account for the two parts of the electron-electron interaction. This approach will be used when we consider combined effects of interactions and disorder during the next stage of this project.

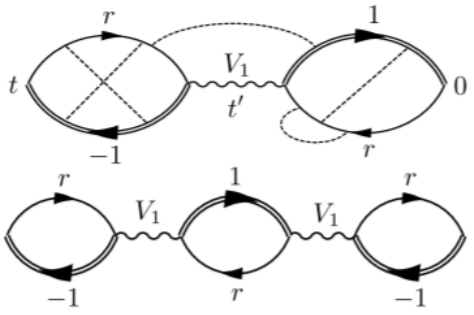

FIG. 1. Processes that describe the many-body depolarization response of a metallic carbon nanotube to the transverse electric field. Shown are the first- and second-order corrections to the polarization function χ(ω) in the interaction V_1 (wavy line), which facilitates electron-electron scattering processes with the change in the circumferential angular momentum. The interaction V_0 (dashed line), which describes processes without a change in the angular momentum, is accounted to all orders, including interactions between different loops (not shown in the second-order diagram). The diagrams providing the leading contributions are shown. Massive gapped electrons m = ±1 are indicated with a double line; gapless states with a single line.

Interaction between resonant impurities in graphene

In our paper “Potential and spin-exchange interaction between Anderson impurities in graphene” (M. Agarwal, E. G. Mishchenko), the interaction effects were studied for a 2D Dirac Hamiltonian, which yields a perfect description of the properties of graphene. We studied the interaction of impurities in this system. Again, the peculiarity of this interaction originates from high polarizability of graphene. We have addressed a basic question pertaining to disorder in Dirac materials. In particular, we have considered the interaction of realistic impurities, such as hydrogen adatoms, with the Dirac electrons, and an effective coupling between impurities mediated by these electrons. The effective interaction consists of a potential (spin-independent) part and a spin-spin

exchange coupling. Hydrogen atoms are well described by the Anderson model and may display resonant behavior, depending on the geometry of the system, such as depending on whether the impurities reside on the same or opposite sublattices. This fact determines the sign and the strength of the interaction, both its potential and spin-spin contributions. The most significant effect occurs when the two-impurity energy level crosses the Dirac point, resulting in the dramatic enhancement of the interaction of the impurities with conduction electrons. This effect has not been recognized in the Weyl and Dirac fermion literature, which typically treats disorder in the smooth or short-range approximations. This novel aspect of disorder in Dirac materials is expected to be crucial when formation of realistic impurity bands in Dirac materials is considered during the next stage of this project.

Landau-Zener transitions in a system with Dirac spectrum and noise

Our paper “Suppression of the Landau-Zener transition probability by a weak classical noise” (Rajesh K. Malla, E. G. Mishchenko, M. E. Raikh), as well as the next two papers, emerged in the course of our study of the effects of disorder on 1D Dirac systems. The spectrum of such system has the form $E = \sqrt{\Delta^2 + v^2k^2}$, where Δ is the gap, v is the velocity, and k is the wave vector. We focused on the case of the “transverse” disorder, which amounts to a random spatial modulation of Δ. To better understand the properties of this Hamiltonian, we noticed that, when the wave vector is replaced by time, the spectrum $E = \sqrt{\Delta^2 + v^2k^2}$, describes the adiabatic levels in the Landau-Zener transition. With Δ changing with time, the problem maps on the Landau-Zener transition in the presence of noise. It should be emphasized, that the problem of suppression of the adiabaticity of the transition by the environment is central to the field of information storage and readout in qubits. In this way, our study of the effects of *static* disorder in 1D Dirac systems allowed us to obtain original analytic results in the field of driven qubits. Inspired by this success, we realized that our results for Dirac systems with two sub-bands offer an insight into the physics of multilevel Landau-Zener transition. Multilevel Landau-Zener transition is a much harder problem than the ordinary Landau-Zener transition. Our findings broadened significantly the class of models for which this problem can be solved analytically.

Excitons in metallic carbon nanotubes

In our paper “Binding energy and lifetime of excitons in metallic carbon nanotubes” (L. Shan, M. Agarwal, and E. G. Mishchenko), we addressed formation of excitons in a quasi-1D metallic Dirac system. The difficulty of describing excitons in semiconducting SWNTs analytically lies with the fact that excitons can neither be considered strictly 1D nor 2D objects. However, the situation changes in the case of metallic nanotubes where, by virtue of screening from gapless metallic subbands, the radius of the exciton becomes much larger than the radius of the nanotube. Taking advantage of this, we develop the theory of excitons in metallic nanotubes, determining that their binding energy is about 0.08v/R, in agreement with the existing experimental data. Additionally, because of the presence of the gapless subbands, there are processes where bound excitons are scattered into unbound electron-hole pairs belonging to the gapless subbands. Such processes lead to a finite exciton lifetime and the broadening of its spectral function. We

calculate the corresponding decay rate of the excitons.

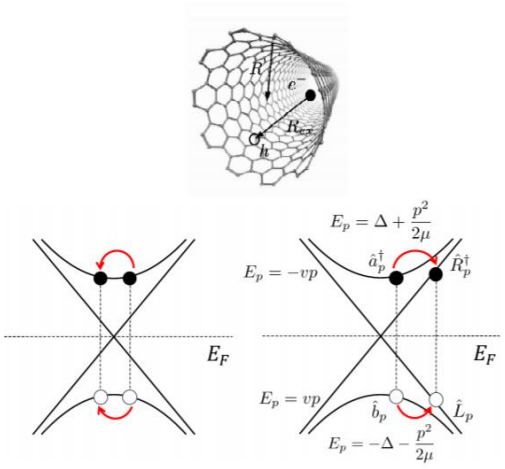

FIG. 2. (Upper) Exciton in a metallic carbon nanotube is characterized by a radius that significantly exceeds the radius of the nanotube, making the exciton a quasi-1D object. (Left) Exciton state emerges due to the final state interaction of electron and hole with energy below the parabolic subband. (Right) Scattering processes indicated between the massive and massless subbands that are responsible for a final lifetime of the excitons.

Planned activities (2018-2019)

We plan to focus on the optical conductivity of 3D gapless Dirac fermions in the presence of smooth disorder and the effects of disorder and interactions in Dirac materials that exhibit quantum anomalous Hall (QAH) effect. This effect accompanies the ferromagnetic transition in the system of magnetic dopants. Experimentally, the QAH transition manifests itself as a jump in the dependence of longitudinal resistivity on a weak external magnetic field. Microscopically, this jump originates from the emergence of a chiral edge mode on one side of the ferromagnetic transition. Specifics of the disorder in these materials is that has a *magnetic* origin and stems from the spatial fluctuations in the density of dopants. In theory, magnetic disorder distinguishes itself by the fact that the Hamiltonian of interaction of electrons with disorder has a *matrix form*. This suggests that non-perturbative approaches to the effects of disorder and interaction should be modified.

Recent publications

1. L. Shan, M. Agarwal, and E. G. Mishchenko, *Binding energy and lifetime of excitions in carbon metallic nanotubes,* arXiv:1807.03962, submitted to Phys. Rev. B.

2. M. Agarwal and E. G. Mishchenko, *Potential and spin-exchange interaction between Anderson impurities in graphene*, arXiv:1802.06171, submitted to Phys. Rev. B.

3. R. Malla and M. Raikh, *Landau-Zener transition in a two-level system coupled to a single highly-excited oscillator*, Phys. Rev. B **97**, 035428 (2018).

4. L. Shan and E.G. Mishchenko, *Breakdown of classical electrostatics in the depolarization of quantum wires and nanotubes*, Phys. Rev. B 96, 195441 (2017).

5. R. Malla and M. Raikh, *Loss of adiabaticity with increasing tunneling gap in non-integrable multistate Landau-Zener models*, Phys. Rev. B 96, 115437 (2017).

6. R. Malla, E.G. Mishchenko, and M. Raikh, *Loss of adiabaticity with increasing tunneling gap in non-integrable multistate Landau-Zener models*, Phys. Rev. B 96, 075419 (2017).

Simple metals at high pressures and impact of spin-orbit in 5d atom compounds by electronic structure quantum Monte Carlo methods

Principal investigator: Lubos Mitas
Department of Physics, North Carolina State University, Raleigh, NC 27695-8202,
lmitas@ncsu.edu

Keywords: quantum Monte Carlo, electronic structure, many-body methods, fixed-node, spin-orbit

Project Scope:
The key goal of this project is to expand applicability of quantum Monte Carlo (QMC) methods in real space for many-body electronic structure calculations of strongly correlated quantum systems including full quantum treatment of spin and increasing the accuracy of fixed-phase/node calculations [1-8]. We report on expansion of QMC for treating spins as quantum variables that enable us to describe arbitrary phases (eg, noncollinear spin states) in many-body framework. In addition, this enables to reformulate the commonly used QMC fixed-node formalism into the fixed-phase framework that opens new avenues for further developments. For example, this form generically guarantees an ergodic sampling for any state and makes it amenable to release-node/phase techniques for overcoming the fixed node/phase constraints.

Recent Progress:
Electronic structure quantum Monte Carlo (QMC) calculations are routinely done with particle spins being assigned as fixed labels, up or down. Since spins commute with Hamiltonians without explicit spin terms, the problem simplifies to spatial-only solution of the stationary Schrodinger equation. We have succeeded in overcoming this limitation and our new approach [3-6] represents, for the first time, an independent method that is able to recover ~ 95% of the correlations with explicitly many-body, spinor-based, wave functions that directly compares with traditional basis set approaches such as Configuration Interaction, while it is applicable to significantly larger systems. In the following we briefly describe the key aspects of this new method that is further elaborated in Refs. [3-6]. Furthermore, we have demonstrated the equivalency of the fixed-phase and fixed-node methods for real wave functions, ie, showing that the spinor-based QMC can be consider as a general and more powerful method for QMC calculations. Very recently, we started to explore the methodology for released-phase/node calculations for decreasing the impact of the constraint biases on calculated quantities. Brief description of the methodology and future plans follows.

Fixed-phase as a generalization of the fixed-node for complex wave functions and its upper bound property. Let us first consider a many-electron Hamiltonian $H = T + V$, where V denotes electronic, ionic (local) and possibly other interactions while T is the total kinetic energy. When the desired eigenstate is real the stochastic methods of solutions are well-known and are mostly based on the familiar fixed-node approximation as have been described in many QMC reviews. This time, our focus is on cases with inherently complex wave functions so that we write any eigenstate as $\Psi = \rho\, exp(i\Phi)$, where $\rho(\mathbf{R}) \geq 0$ is a non-negative amplitude and $\Phi(\mathbf{R})$ is a phase. Here by $\mathbf{R} = (\mathbf{r}_1, ..., \mathbf{r}_N)$ we denote a set of spatial coordinates of N fermionic particles. If we substitute Ψ into the imaginary-time Schrödinger equation we get the following real and imaginary components

$$-\partial_\tau \rho = \left[T + V + \frac{1}{2}(\nabla \Phi)^2\right]\rho$$

and

$$-\partial_\tau \Phi = [T\Phi - \rho^{-1}\nabla\rho \cdot \nabla\Phi]$$

The imaginary part describes a conservation of the phase flow. The real part is the relation that provides the eigenvalue, ie, its solution converges to the desired eigenstate amplitude in the limit $lim\ \tau \to \infty\ \rho(\tau)$. The generalization of the fixed-node for the complex wave functions is the so-called *fixed-phase approximation*. This is given by replacing the exact phase by the trial phase $\phi \to \phi_T$ where the trial function is written as $\Psi_T = \rho_T \exp(i\Phi_T)$. The fixed-phase and fixed-node methods are closely related. In particular, the fixed-node is the special case of the fixed-phase as has been shown before (see for example, Refs. [3-6] and references therein). In general, they also provide similar accuracy in most cases as our very recent study shows [3]. Note that the fixed-node is variational for arbitrary non-negative and symmetric amplitude $\rho(\boldsymbol{R})$. The fixed-phase method is actually commonly used by QMC practitioners in another setting, for example, in sampling the Brillouin zone of periodic systems by twist-averaging.

Overcomplete spin representation. The treatment of spins as quantum variables in QMC is done in two-component spinor formalism. The determinantal part of the wave function is written as an anti-symmetric product of one-particle spinors that are given as

$$\chi(r,s) = \phi^{\uparrow}(r)\chi^{\uparrow}(s) + \phi^{\downarrow}(r)\chi^{\downarrow}(s)$$

where $\chi^{\uparrow,\downarrow}(s)$ are corresponding spin functions. The spin s is treated as continuous (periodic) variable in the interval $(0, 2\pi)$ and the spin functions are chosen as $\chi^{\uparrow}(s) = \exp(+is)$, $\chi^{\downarrow}(s) = \exp(-is)$. Note that this implies an overcomplete representation [3-6] that enables us to use continuous sampling of spins similarly to the ordinary spatial variables.

Trial wave functions. The trial function with variable spins is a generalization of the widely used product of Jastrow factor and linear combination of Slater determinants with the distinction that these are determinants of single-particle spinors

$$\Psi_T(\boldsymbol{R},\boldsymbol{S}) = \sum_k c_k \det{}_k\left[\{\chi_j(\boldsymbol{r}_i, s_i)\}\right] \exp[U(\boldsymbol{R})]$$

where $\boldsymbol{R} = (\boldsymbol{r}_1, \boldsymbol{r}_2, \ldots)$ and $\boldsymbol{S} = (s_1, s_2, \ldots)$ are spatial and spin coordinates, respectively.

FPSODMC as a general method for electronic structure QMC. The developed method had a number of properties that make it attractive and more general for wide use. We call this approach fixed-phase spinor/spin-orbit diffusion Monte Carlo, or FPSODMC, in short. Let us briefly list its basic properties:

• the sampled amplitude ρ (from $\Psi = \rho e^{i\varphi}$) is *nonnegative everywhere* and its zero locus is of codimension 2 (eg, such as points in 3D space, unlike for the fixed-node approach where the node has codimension 1, ie, it divides the space into domains);

• therefore the ”basis set” of random paths is complete and sampling is generically ergodic from the outset for any state, ground or excited;

• it is variational and the well-known fixed-node approximation is its special case;

• within the fixed-phase approximation the method recovers correlations of all orders;

• the fixed-phase approximation has a clear form of an effective potential with one-to-one correspondence to the calculated state and with constructive possibilities for improvements;

• it naturally enables to treat spins as quantum variables and spin-related interactions.

Figure 1. (Left panel) The ground and lowest excited states of the WO molecule calculated by QMC with two levels of treatment of spin-orbit effects [2]: AREP (averaged spin-orbit) and REP (explicit spin-orbit and spinors). Note significant recovery of low-lying excitation in explicit spin-orbit calculation. (Right panel) Ordinary fixed-node calculation (FNDMC) and subsequent released-node/phase calculation within spinor formalism (RNSODMC) for a few-electron system. Note rapid recovery of nearly exact energy without major increase of fluctuations and correspondingly mild loss of efficiency.

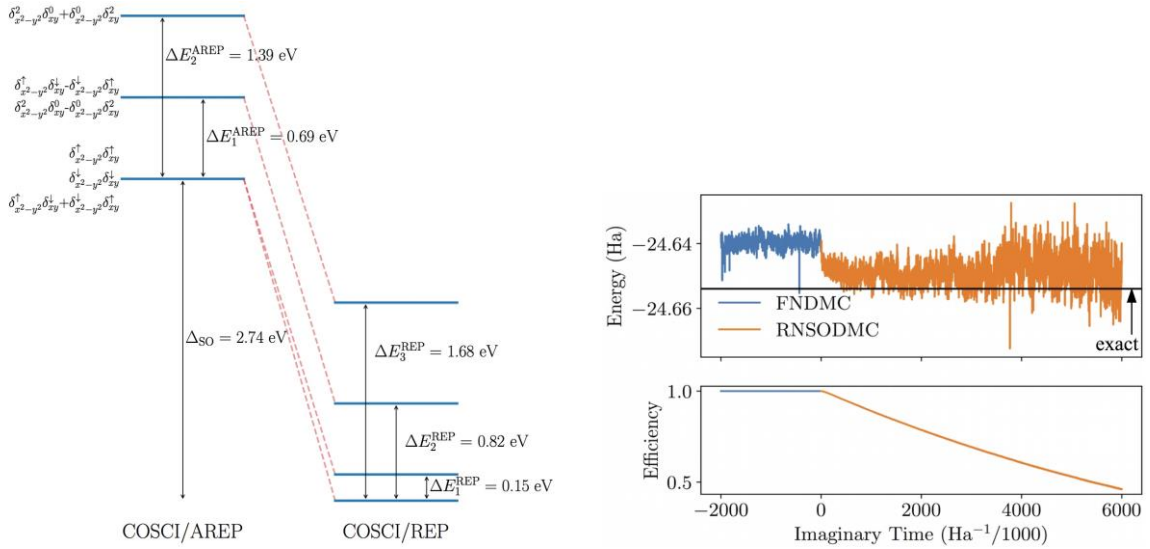

Spin-orbit calculations and fixed-node vs fixed-phase equivalency tests. We tested the developed FPSODMC methodology on a number of cases [2-7], see also Fig. 1 (Left panel). The calculations showed the reliability of the method and also surprising impact of spin-orbit, for example, in a case if seemingly “simple” molecule of Sn_2, where already for elements such as tin (4^{th} row), the spin-orbit impact on the binding of this molecule is changed by almost 0.5 eV (!), in excellent agreement with experiment Fig. 2 [4]. Corrections by 1 eV or more in the 5^{th} row are common [3,5]. In addition, we tested the correspondence of fixed-phase and fixed-node methods for nominally real wave functions cases (where the spinor fixed-phase should provide the fied-node result) and we found excellent agreement [3]. This provided important illustration of the universality of the FPSODMC method.

Finally, we mention study of fixed-node biases in Li systems (atom, molecule, cluster, solid) [8] and comparisons of fixed-node and fixed-phase biases [4], as well as a vision note that is a part of larger vision paper on data for materials design and calculations [1].

Future plans:

The key focus of our future effort can be summarized as follows:

a) Exploring the potential of the fixed-phase spinor diffusion Monte Carlo (FPSODMC) method for nearly-exact calculations that would suppress the systematic biases to ≈ 1% of the correlation energy. We intend to devise this using favorable properties of FPSODMC framework such as positivity of the sampled quantum amplitude, completeness of the sampling paths, smooth behavior of local energy with overcomplete spin representation and others advantages as elaborated later. These features will be exploited for ”softening” of the fixed node/phase constraints while keeping the significant reach of the diffusion Monte Carlo method intact.

b) Another area is to expand the many-body electronic structure QMC calculations to quantum systems at low and ambient temperatures. Calculations of many-body thermal density matrices is a significant leap forward and we intend to focus on advances that are realistic and feasible within the project timeframe. In particular, we plan to explore variational Monte Carlo to build the thermal density matrices by constructing and sampling part of the states relevant for the low/ambient temperature window. In an alternative direction we plan to couple Density Functional Theory (DFT) with subsequent or simultaneous QMC corrections using correlated sampling techniques. This will enable many-body calculations of quantities such as electron-phonon couplings or impact of temperature on excitations.

c) These developments will be applied to obtains insights into quantum effects in two classes of materials. One such area is the many-body physics of 2D materials with 5d elements such tungsten dichalcogenides that exhibit an unusual richness of quantum effects and therefore shows promising potential as a new class of technological materials. The second class of materials with technological relevance extends from our current effort to study impacts of spin-orbit in 5d periodic materials such as iridate compounds.

Publications (2015-2018):

1. M.B. Nardelli and L. Mitas, Data generation beyond standard DFT for high-throughput applications, *in* “The 2018 Materials by Design Roadmap" by K. Alberi et al, in press, J. Phys. D, Appl. Phys., (2018).

2. C. A. Melton, M. C. Bennett, and L. Mitas, Projector quantum Monte Carlo with averaged vs explicit spin-orbit effects: Applications to tungsten molecular systems, J. Phys. Chem. Solids, XX, YYYY, (2018), in press, https://doi.org/10.1016/j.jpcs.2017.12.033

3. C. Melton, and L. Mitas, Quantum Monte Carlo with variable spins: Fixed-phase and fixed-node approximations, Phys. Rev. E **96**, 043305 (2017)

4. C. A. Melton, L. Mitas, Fixed-node and fixed-phase approximations and their relationship to variable spins in quantum Monte Carlo, arXiv: 1605.03813, in *Recent Progress in quantum Monte Carlo*, edited by S. Tanaka, P.-N. Roy and L. Mitas, ACS, (2016), Vol. 1234, p.1-12, Am. Chem. Soc. (peer rev.); DOI: 10.1021/bk-2016-1234.ch001

5. C. A. Melton, M. C. Bennett, L. Mitas, Quantum Monte Carlo with variable spins, J. Chem. Phys. **144**, 244113 (2016)

6. C. A. Melton, M. Zhu, S. Guo, A. Ambrosetti, F. Pederiva, L. Mitas, Spin-orbit interaction in electronic structure quantum Monte Carlo, Phys. Rev. A **93**, 042502 (2016)

7. A. Ambrosetti, P. L. Silvestrelli, F. Pederiva, L. Mitas, and F. Toigo, Repulsive Atomic Fermi Gas with Rashba Spin-Orbit Coupling: a Quantum Monte Carlo Study, Phys. Rev. A **91**, 053622 (2015)

8. K. M. Rasch, L. Mitas, Fixed-node diffusion Monte Carlo method for lithium systems, Phys. Rev. B **92**, 045122 (2015)

Nonequilibrium phenomena in Topological Insulators

Principal investigator: Professor Aditi Mitra
Center for Quantum Phenomena, Department of Physics,
New York University, New York, NY 10003
aditi.mitra@nyu.edu

Project Scope

The primary goal of this program is to explore nonequilibrium phenomena in topological insulators (TIs). Within this broad topic, the current focus is to understand Floquet topological insulators (FTIs). These are systems that show topological properties on the application of a time-periodic driving, and host a richer phase diagram than their static counterparts.

Recent Progress:
We have been pursuing the following three directions. One is to understand FTIs through their entanglement properties. Since these systems are manifestly out of equilibrium, and therefore have no ground-state to speak of, we have been studying how the topological properties appear in the entanglement statistics of a state. This could be a unitarily evolved state, or a many body exact eigenstate of the FTI. The second aspect has been to collaborate with an experimentalist at NYU (Javad Shabani) to explore the possibility of achieving a FTI that hosts Majorana fermions. Thirdly, we have been studying the role of interactions, and whether the combined effect of periodic driving and interactions can lead to novel correlated states.

Below we give more details based on results published in the last 2 years.

Dynamical generation of superconducting order of different symmetries in hexagonal lattices [1]: Usually in discussing superconductivity, especially out of equilibrium, only one kind of superconducting order is assumed. But in a realistic system, there are many different competing superconducting phases. Can a nonequilibrium environment be used to tune the symmetry of the superconducting phase? We answered this question affirmatively by studying doped graphene subjected to a high frequency laser and where the attractive interactions are switched on rapidly, as in a quantum quench. In the absence of interaction, the non-interacting system, to a good approximation, is equivalent to the Haldane model of a Chern insulator. We found that broken time-reversal symmetry favors d+id (or chiral d-wave) superconductivity when the interaction quench is of small amplitude. For larger quench amplitudes on the other hand, the system favors s-wave superconductivity. The reason has to do with the fact that for small interaction quench amplitudes, the physics in the vicinity of the Fermi-surface is relevant, and this favors the equilibrium intuition of d+id superconductivity. On the other hand as the quench amplitude increases, quasiparticles everywhere in momentum space are active in the dynamics. This effectively dephases the d-wave order-parameter and favors an s-wave. Figure 1 was the phase diagram obtained which shows how the superconducting phase changes as the interaction quench amplitude increases.

Long-range Kitaev Chains via Planar Josephson Junctions [2]: Despite the activity in studying FTIs, the experimental realizations of it are not that many. We therefore turned our attention to collaborating with an experimental group at NYU (lead by Javad Shabani) to explore the possibility of realizing FTIs. The set-up is shown in the top panel of Figure 2. As a first step, we characterized the static system as a rather exotic version of the Kitaev chain with long range hopping and pairing terms (lower panel of Figure 2), whose properties can be tuned by myriad experimental knobs such as gate voltage, in plane magnetic field, parameters of the Josephson junction etc. We also extracted the topological properties using a novel real space invariant based on the Clifford pseudospectrum. While this approach is well known among mathematicians, it is less used among physicists. It is a very helpful tool when there is disorder, and usual momentum space topological invariants cannot be used.

Entanglement properties of the time periodic Kitaev Chain [3]:
The Kitaev chain is the simplest example of a 1D topological insulator. When periodically driven, the system shows a rich phase diagram, with a topological invariant of Z0xZpi. The two integers refer to the number of Majorana zero modes and Majorana Pi modes respectively. In Ref. 3 we studied how these two kinds of Majorana modes manifest in the entanglement statistics. We found that this depended on the state. For example, for the many body exact eigenstate of the half-filled system with the lowest entanglement, coined the Floquet ground state (FGS), the Majorana zero and Pi modes appear qualitatively differently than in the quasi energy spectrum. Figure 3 shows their behavior. The Majorana fermions are sensitive to Floquet micro-motion. Thus at most times they hybridize with each other, reducing the invariant to Z2. At only two special times during the drive cycle, corresponding to the time-reversal symmetric (TRS) points, do the Majorana fermions decouple. At one TRS point, the number of Majorana modes in the entanglement spectrum is |Z0+Zpi|, while at the other their number is |Z0-Zpi|. In Ref. 3 we also studied the fate of these two kinds of Majorana modes on a unitarily evolved state.

Central charge of critical Floquet states in 1d [4]:
Nonequilibrium systems are usually complicated and strongly dependent on microscopic details. Thus to come up with a universal description is challenging, and once found, very rewarding. We raised the question, do critical Floquet chains support a universal description? We affirmatively answered this question by showing that the lowest entangled exact eigenstate of the half-filled chain shows a logarithmic scaling of the entanglement entropy at the critical point (Figure 4). The prefactor of the logarithm can be interpreted as a central charge, where this charge knows about both the Majorana zero and Pi modes on either side of the critical point. We also found that Floquet micro-motion does not affect the value of the central charge. In particular the micro-motion gives rise to time-dependent behavior in the sub-leading terms of the entanglement entropy at the critical point.

Future plans:
Superconducting instabilities in periodically driven systems–
In continuation of Ref. [1], we plan to explore superconducting instabilities in periodically driven 2D systems, but now studying the limit of low frequency driving where the possibility of more unusual phases is greatly increased.
Interacting Floquet topological phases in one dimension-
In continuation of our work in Refs. [3, 4] we plan to study entanglement statistics of Floquet systems with interactions.
Realistic experimental systems to realize Floquet Majorana zero and Pi modes-
Continuing on our work in Ref. [2], we plan to expand the phase diagram of the set-up shown in Figure 2 to the case of periodic driving.

Publications
[1]. Hossein Dehghani and Aditi Mitra, Phys. Rev. B 96, 195110 (2017).
[2]. Dillon Liu, Javad Shabani, and Aditi Mitra, Phys. Rev. B 97, 235114 (2018).
[3]. Daniel Yates and Aditi Mitra, Phys. Rev. B 96, 115108 (2017).
[4]. Daniel Yates, Yonah Lemonik, and Aditi Mitra, arxiv: 1805.00573, PRL (in review).

Figure 1: Haldane model with pairing interactions (J) that has been switched on rapidly in time. The dominant superconducting phase can be tuned from d+id (or chiral d-wave) to s wave, by changing the magnitude of the interaction quench amplitude.

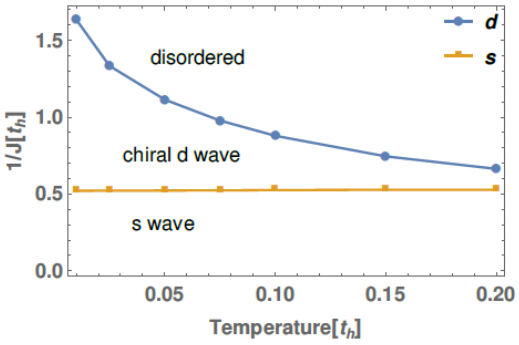

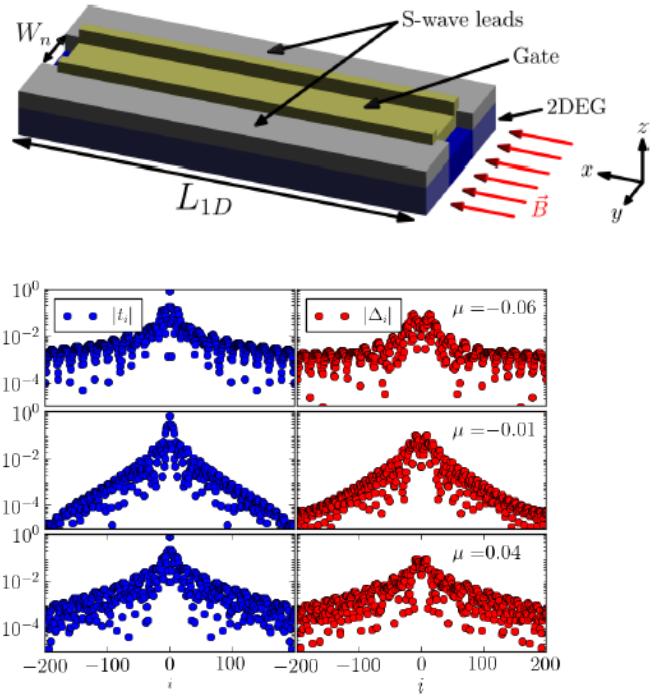

Figure 2: The device (top panel) consisting of a Josephson junction arising from a s-wave superconductor proximitized to a spin orbit coupled 2DEG. This device can host Majorana fermions (Shabani lab, NYU). We showed that this experimental platform is equivalent to an effective 1d Kitaev chain with long range and tunable couplings (lower panel).

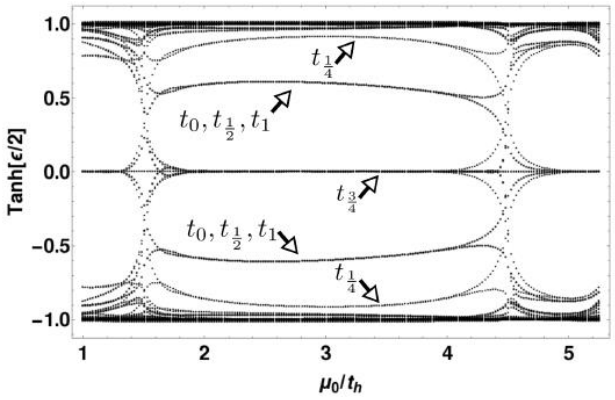

Figure 3: Majorana zero and Pi modes in the entanglement spectrum of the Floquet ground state. The Floquet micro-motion causes the Majorana modes to hybridize at times away from the special time-reversal symmetric (TRS) points. At the two TRS points the number of Majorana zero modes is |Z0+Zpi| and |Z0-Zpi|

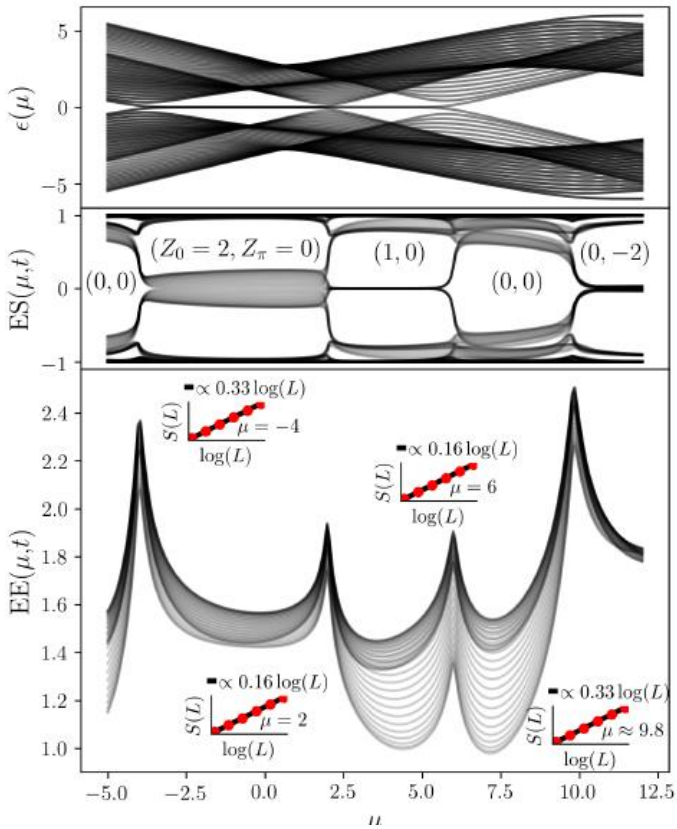

Figure 4: Top panel: Quasi-energy spectrum of a periodically driven Kitaev chain showing Majorana zero and Pi modes. Middle-panel: Entanglement spectrum (ES) at several different times during the drive cycle. Lower-panel: Entanglement entropy (EE) and its scaling. The leading behavior is captured by a central charge that accounts for the change in the number of Majorana zero and Pi modes on either side of the critical point.

Non-Equilibrium Physics at the Nanoscale

Principal investigator: Dirk K. Morr
Department of Physics, University of Illinois at Chicago, IL 60607
dkmorr@uic.edu

Project Scope

The goal of this program is to discover and understand novel non-equilibrium phenomena at the nanoscale. The PI investigates the form of non-equilibrium charge, spin and energy transport in a wide range of materials, including unconventional superconductors, topological insulators and superconductors, quantum critical materials, and hybrid perovskites. Exploring the properties of these systems out-of-equilibrium provides unprecedented opportunities to gain insight into the effects of strong correlations and the nature of topological phases. The complexity of these systems allows for the emergence of novel transport functionalities, such as the creation of spin-diodes, or the formation of states with a topologically protected quantized conductance. In turn, the discovery of such novel out-of-equilibrium properties provide new markers for the detection of strongly correlated and topological quantum systems.

Recent Progress

Below is a selection of four examples, highlighting the accomplishments of the PI's research program over the last year.

Majorana Fermions in Magnetic-Superconductor Hybrid Structures

Majorana modes in topological superconductors hold unprecedented potential as a novel platform for quantum computing. In collaboration with the experimental scanning tunneling spectroscopy (STS) group of R. Wiesendanger (Hamburg University), the PI

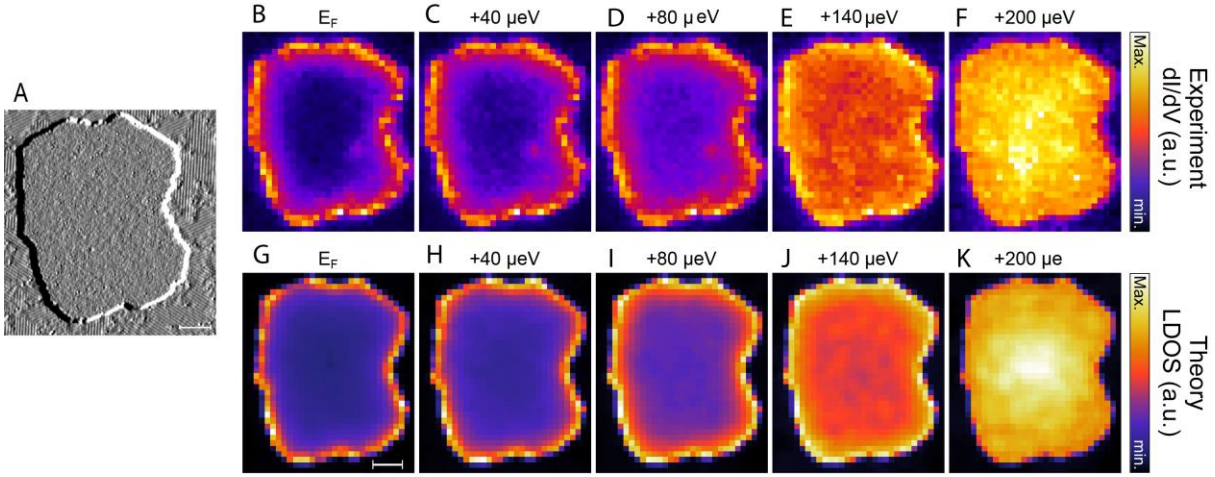

Figure 1: A Fe magnetic island deposited on a Re-O(2x1) surface**.** Energy evolution of the spatially resolved experimental dI/dV (**B-F**) and of the theoretically computed LDOS (**G-K**).

recently reported the observation of topological Majorana edge modes in two-dimensional magnetic-superconductor hybrid structures [1]. By depositing magnetic Fe islands on an

Re-O(2x1) surface – Re being an s-wave superconductor – (see Fig.1A), the Wiesendanger group observed a large enhancement of the spatially resolved differential conductance, dI/dV, at the Fermi energy, E_F, (Fig. 1B), and a characteristic evolution of dI/dV with increasing energy (Figs.1C-F). By using a realistic band-structure model, the PI demonstrated that this hybrid system realizes a topological superconductor with Chern number $C = 20$. The good agreement between the energy evolution of the theoretically computed local density of states (Figs.1G-K) and the experimentally observed dI/dV (Figs. 1B-F) provides strong evidence for the existence of a topological Majorana edge mode. The PI also showed that the robustness of the zero energy Majorana mode against edge disorder provides further support for their topological nature. Finally, the PI demonstrated that by removing the O(2x1) layer, the hybrid system can be tuned into a trivial phase, in agreement with the experimental observations. These results present not only the first observation of Majorana edge modes in two-dimensional topological superconductors, but also open a new path for tuning such hybrid systems between topological and trivial phases through quantum engineering of surface layers..

Josephson Scanning Tunneling Spectroscopy in $d_{x^2-y^2}$-wave Superconductors

The development of Josephson Scanning Tunneling Spectroscopy (JSTS) has opened unique possibilities to gain insight into the spatial nature of unconventional $d_{x^2-y^2}$-wave superconductors. The PI recently showed [2] that the spatial variations in the experimentally measured Josephson current I_c images those of the superconducting order parameter (SCOP), thus providing a crucial missing link for the interpretation of JSTS experiments (Fig.2). The good agreement between the spatial form of theoretically computed I_c and the SCOP does not only hold around defects [Figs. 2(a),(b)], but also in the magnetic field induced Fulde-Ferrell-Larkin-Ovchinnikov state [Figs. 2(c),(d)]. The PI also showed that JSTS can probe for the nature of the pseudo-gap region in the cuprate superconductors. These results establish that JSTS provides direct insight into the spatial form of the SCOP, which is of great importance for the exploration of unconventional cuprate, iron based and heavy fermion superconductors.

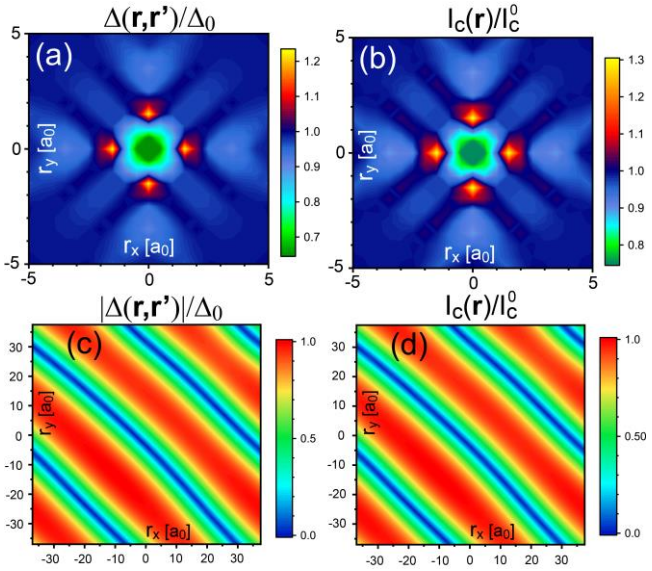

Figure 2: Spatial variations of (a),(c) the superconducting order parameters, and (b),(d) I_c around a non-magnetic defect (a),(b) and in the FFLO phase (c),(d).

Quantum Design of Majorana Fermions

The use of Majorana fermions for topological quantum computing requires the ability to create and manipulate them at the atomic scale. In collaboration with S. Rachel (University of Melbourne), the PI recently demonstrated the possibility for dimensional tuning of Majorana fermion between one and two dimensions in magnetic-superconductor (MSC)

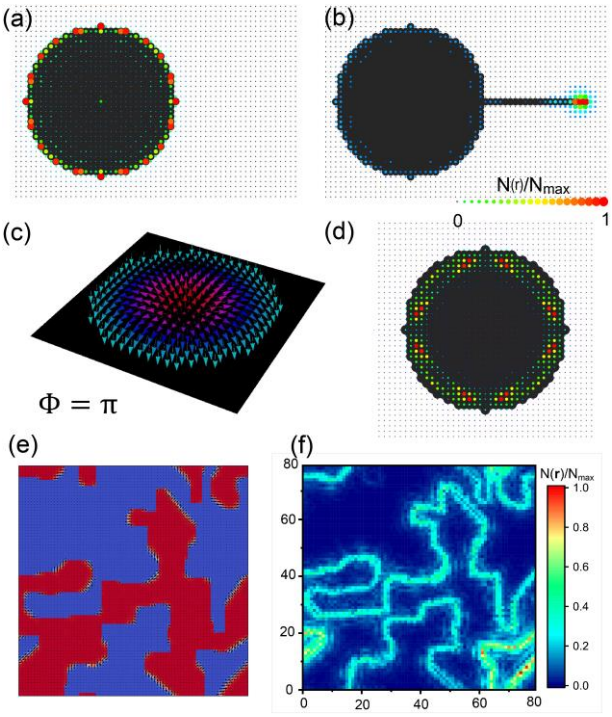

Figure 3: (a),(b) Zero-energy LDOS reflecting Majorana fermions. (c) Skyrmion, and (d) resulting Majorana edge mode. (e) Magnetic domains and (f) LDOS showing Majorana modes at domain walls.

hybrid structures [3]. The PI showed that by attaching a 1D chain of magnetic atoms to a 2D magnetic island, it is possible to tune between Majorana modes delocalized along the edge of the island [Fig.3(a)] and a Majorana fermion localized at the end of the chain [Fig.3(b)]. The MSC system can thus be tuned from a 2D [Fig.3(a)] to a 1D [Fig.3(b)] topological superconductor. Moreover, by attaching multiple chains to a topological island, it is possible to extract the Chern number of the system from the real space structure of the LDOS. The PI also demonstrated that by imposing a skyrmion magnetic structure [Fig.3(c)] on a trivial MSC system, one can create a topological superconductors with well defined Majorana edge modes [Fig.3(d)]. Finally, the PI showed that Majorana modes of arbitrary shape can be created in topological superconductors by generating magnetic domains [Fig.3(e)], with Majorana modes being located along the domain walls. These results present new approaches to creating Majorana fermions at the atomic scale.

Imaging Emergent Heavy Dirac Fermions in a Topological Kondo Insulator

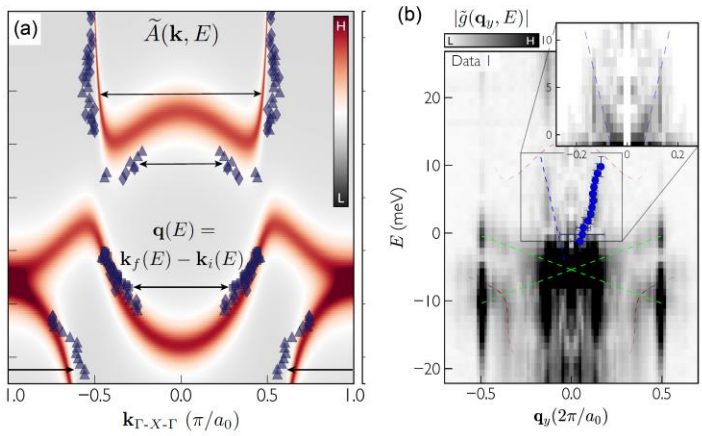

Figure 4: (a) QPI spectrum of hybridized bulk heavy magnetic and light conductions bands in SmB6. (b) QPI spectrum of 2 Dirac cones at the surface.

Kondo insulators are primary candidates in the search for strongly correlated quantum phases which may host topological order, fractionalization and non-Abelian statistics. Their hybridization gap is predicted to encode a non-trivial topological invariant and to possess emergent heavy Dirac fermion surface modes. In collaboration with the STS group of J. Hoffman (Harvard), the PI recently reported the observation of such Dirac surface modes in the Kondo insulator SmB_6 [4]. By extending a previously developed theory for QPI spectroscopy in heavy fermion materials, the PI showed that the experimental QPI spectrum did not only reflect the hybridization between two heavy magnetic bands and a light conduction band [Fig.4(a)], but also encoded two emergent heavy Dirac surface cones [Fig.4(b)] within the bulk hybridization gap. These results taken

together provide strong evidence for the topological nature of this strongly correlated Kondo insulator.

Future Plans

The planned activities for the next year will extend in several directions. First, the PI will extend his work to investigate the emergence of topological superconductivity on the surface of $FeSe_{1-x}Te_x$, as evidenced by recent observations of zero-energy states inside vortex cores. In addition to developing a microscopic theory for such a state, the PI intends to study how JSTS can image (a) the emergence of superconducting triplet correlations near vortex cores, and (b) the phase-winding of the superconducting order parameters around vortices. Second, the PI plans to study JSTS spectroscopy in the iron-based superconductors. In particular, the PI intends to investigate whether the multi-band structure of these materials still allow one to correlate the spatial structure of the Josephson current with that of the multi-band SCOP. Third, the PI plans to study how the interplay of strong interactions and disorder determine the local flow of charges and the global transport properties of strongly correlated materials. Of particular interest is here the question to what extent strongly correlated materials possess a unique signature in scanning tunneling shot-noise spectroscopy. Fourth, the PI intends to identify universal spectroscopic and transport signatures of topological Majorana modes, in addition to the quantized tunneling conductance previously discovered by the PI.

Publications (2017 -2018)

1. "Real-Space Visualization of Majorana Edge Modes in a two-dimensional Nanoscale Magnet-Superconductor Hybrid System", A. Palacio-Morales, E. Mascot, S. Cocklin, H. Kim, S. Rachel, D. K. Morr, and R. Wiesendanger, submitted to Science.
2. "Josephson Scanning Tunneling Spectroscopy in $d_{x^2-y^2}$ -wave superconductors: a probe for the nature of the pseudo-gap in the cuprate superconductors", M. Graham and D.K. Morr, submitted to Phys. Rev. Lett.
3. "Quantum Design of Majorana Fermions", E. Mascot, S. Cocklin, S. Rachel, and D.K. Morr, in preparation.
4. "Imaging emergent heavy Dirac fermions of a topological Kondo insulator", H. Pirie, A. Soumyanarayanan, Y. Liu, P. Chen, M.M. Yee, Y. He, P.F.S. Rosa, J.D. Thompson, D.-J. Kim, Z. Fisk, X. Wang, J. Paglione, D. K. Morr, J. E. Hoffman, and M. H. Hamidian, submitted to Science.
5. "Orbital superconductivity, defects, and pinned nematic fluctuations in the doped iron chalcogenide $FeSe_{0.45}Te_{0.55}$, S.Sarkar, J. Van Dyke, P. Sprau, F. Massee, U. Welp, W.-K. Kwok, J.C.Davis, and D. K. Morr, Phys. Rev. B **96**, 060504 (2017) (Rapid Communication).
6. "Quantized charge transport in chiral Majorana edge modes", S. Rachel, E. Mascot, S. Cocklin, M. Vojta, and D.K. Morr, Phys. Rev. B **96**, 195162 (2017); Editor's suggestion.
7. "Scanning Tunneling Potentiometry, Charge Transport and Landauer's Resistivity Dipole from the Quantum to the Classical Transport Regime", D. K. Morr, Phys. Rev. B **95**, 195162 (2017).
8. "Imaging the Spatial Form of a Superconducting Order Parameter via Josephson Scanning Tunneling Spectroscopy}, M. Graham and D.K. Morr, Phys. Rev. B **96**, 184501 (2017).

Design of Functional Materials Based on New Principles of Disorder

Principal Investigator: Sidney R. Nagel

The University of Chicago; Chicago, IL 60637

Keywords: Allostery, Auxetic materials, Networks, Jamming, Pruning for functionality

Project Scope

This project addresses the question: How does disorder provide new potentialities for the behavior of a material that would be absent in a crystalline material of the same composition? In order to elaborate on novel ideas about bond-level independence of properties in disordered materials, this work addresses the possibility of creating new classes of mechanical meta-materials which have applications everywhere from microscopic biological molecules (that is, allosteric interactions) to large scale architectural disordered networks in which functional elements can be included. Examples of a global property would making an auxetic material for which the Poisson's ratio is negative. While most common materials have a positive Poisson's ratio (so that uniaxial compression along one axis would lead to expansion in the other two perpendicular axes) it is very rare to find a commonly occurring material where the Poisson's ratio is negative (so that compression along one axis leads to compression along all the axes and a change in volume).

Previous work has established that jamming is one extreme pole of rigid matter. This understanding allows a new way of investigating materials that cannot be easily classified as crystals or glasses. The project will use these ideas to address the mechanical properties of materials with different kinds of disorder.

The issue of memory formation raises another set of questions at the heart of how the energy landscape is organized and how it can be manipulated to store information in a solid. The project seeks to understand the degree to which multiple memories can be stored in a single system and create a holistic understanding of how inputs can be used to create a desired response.

Recent Progress

Instabilities in jammed packings and the density of vibrational states

Disordered solids inhabit an extremely high-dimensional rugged energy landscape with a vast number of metastable minima. Dealing with such a complex topography poses challenges for understanding how the system moves among metastable basins as a result of thermal excitations or external perturbations such as compression or shear. We focused on instabilities induced in zero-temperature systems by applied compression or shear as a first step in understanding how a disordered solid traverses its landscape. We considered the contribution to the density of vibrational states and the distribution of energy barrier heights of incipient

instabilities in a glass modeled by a jammed packing of spheres. On approaching an instability, the frequency of a normal mode and the height of the energy barrier to cross into a new ground state both vanish. These instabilities produce a contribution to the density of vibrational states that scales as ω^3 at low frequencies ω, and a contribution to the distribution of energy barriers ΔH that scales as $\Delta H^{-1/3}$ at low barrier heights.

Designing function into a network:

The modulus of a rigid network of harmonic springs depends on the sum of the energies in each of the bonds due to the applied distortion: compression in the case of the bulk modulus, B, or shear in the case of the shear modulus, G. The distortion need not be global and we introduce a local modulus, Li, associated with changing the equilibrium length of a single bond, i, in the network. We show that Li is useful for understanding many aspects of the mechanical response of the entire system. For example, it allows an understanding, and efficient computation, of how each bond in a network contributes to global properties such as B and G and sheds light on how a particular bond's contribution to one modulus is, or is not, correlated with its contribution to another.

We explored the range over which the elasticity of disordered spring networks can be manipulated by the removal of selected bonds. By taking into account the local response of a bond, we demonstrated that the effectiveness of pruning can be improved so that auxetic (i.e., negative Poisson's ratio) materials can be designed without the formation of cracks even while maintaining the global isotropy of the network. This is shown in Fig. 1. When G/B > 1 (in 2D) or 3/2 (in 3D), the Poisson's ratio is negative. The bulk modulus and shear modulus scale with the number of bonds removed and we have gotten a good estimate of the exponents characterizing these power laws. We also found that there are spatial correlation lengths in the change of bulk modulus and shear modulus upon removing different bonds that diverge as the network approaches the isostatic limit where the excess coordination number ($Z-Z_C$) approaches 0.

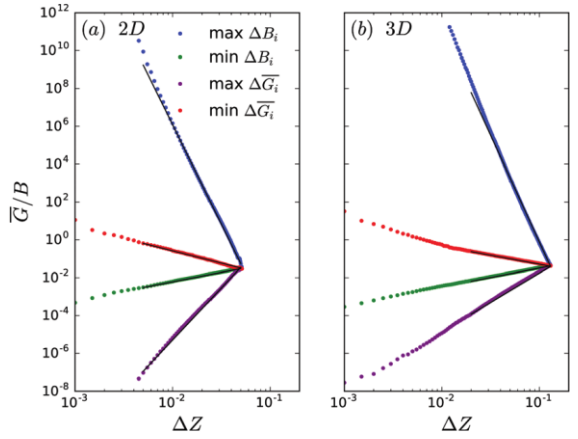

FIg. 1 The evolution of G /B as a function of ΔZ (a) in two dimensions and (b) in three dimensions. As discussed in the text, ΔZ signifies the number of bonds removed. As the ratio becomes very large, the network becomes auxetic with a negative Poisson's ratio.

Recent advances in designing metamaterials have demonstrated that global mechanical properties of disordered spring networks can be tuned by selectively modifying only a small subset of bonds. Using a computationally efficient approach, we extended this idea to tune more general properties of networks. With nearly complete success, we were able to produce a strain between any two target nodes in a network in response to an applied source strain on any other pair of nodes by removing only ~1% of the bonds. An example is shown in Fig. 2. The target pair of nodes can be either opened or closed in phase with a perturbation at the source sites. We also were able to control multiple pairs of target nodes, each with a different individual response, from a single source, and to tune multiple independent source/target responses simultaneously

into a network. We have fabricated physical networks in macroscopic 2D and 3D systems that exhibit these responses. This work is inspired by the long-range coupled conformational changes that constitute allosteric function in pro- teins. The fact that allostery is a common means for regulation in biological molecules suggests that it is a relatively easy property to develop through evolution. In analogy, our results show that long-range coupled mechanical responses are

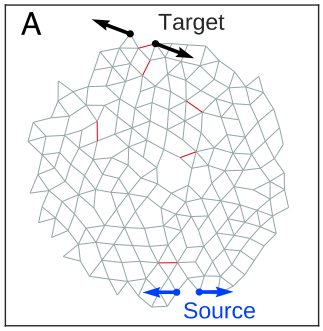

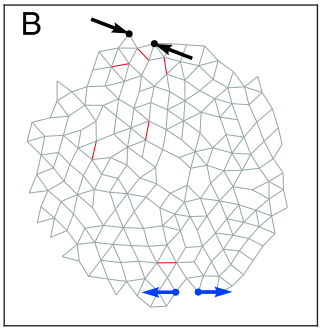

Fig. 2 Network with 194 nodes, and 407 bonds at $\Delta Z = 0.19$ tuned to exhibit (*A*) expanding ($\eta = +1$) and (*B*) contracting ($\eta = -1$) responses to within 1% of the desired response. Source nodes are shown in blue, and target nodes are shown in black. Arrows indicate the sign and magnitude of the extensions of the source and target. The removed bonds are shown as red lines.

similarly easy to achieve in disordered networks.

Nature is rife with networks that are functionally optimized to propagate inputs in order to perform specific tasks. Whether via genetic evolution or dynamic adaptation, many networks create functionality by locally tuning interactions between nodes. We explore this behavior in two contexts: strain propagation in mechanical networks and pressure redistribution in flow networks. By adding and removing links, we were able to optimize both types of networks to perform specific functions. We defined a single function as a tuned response of a single “target" link when another, predetermined part of the network was activated. Using network structures generated via such optimization, we investigated how many simultaneous functions such networks could be programmed to fulfill. We found that both flow and mechanical networks display qualitatively similar phase transitions in the number of targets that could be tuned, along with the same robust finite-size scaling behavior. These properties can be understood in the context of a new class of constraint-satisfaction problems.

Stretched-exponential relaxation

Relaxation in structural glasses is often approximated by a stretched-exponential form: $f(t) = A \exp[-(t/\tau)^{\beta}]$. We have shown that the relaxation in a model of sheared non- Brownian suspensions can be well approximated by a stretched exponential with an exponent β that depends on γ, the strain amplitude: $0.25 < \beta < 1$. In a one-

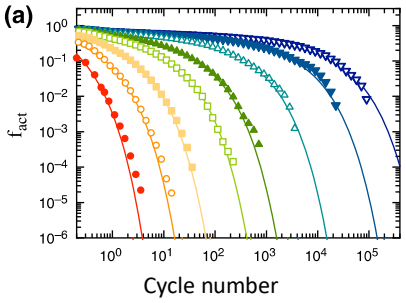

Fig. 3 Collapse of relaxation curves in the purely-repulsive 1D model for cyclically driven non-Brownian suspension. **a** f_{act} versus time for a wide range of γ from 0.1 to 0.97. Solid lines are an approximation to a stretched exponential function. **b** The data collapse onto a master curve when the axes are rescaled.

dimensional version of the model, we showed how the relaxation originates from density fluctuations in the initial particle configurations. As shown in Fig. 3, our analysis is in good agreement with numerical simulations and reveals a functional form for the relaxation that is distinct from, but well approximated by, a stretched-exponential function.

Memory formation in cyclically driven systems

Athermal disordered systems can exhibit a remarkable response to an applied oscillatory shear: After a relatively few shearing cycles, the system falls into a configuration that had already been visited in a previous cycle as shown in Fig. 4. After this point the system repeats its dynamics periodically despite undergoing many particle rearrangements during each cycle. We studied the behavior of orbits as one approaches the jamming point in simulations of jammed particles subject to oscillatory shear at fixed pressure and zero temperature. As the pressure is lowered, we found that it becomes more common for the system to find periodic states where it takes multiple cycles before returning to a previously visited state. Thus, there is a proliferation of longer periods as the jamming point is approached.

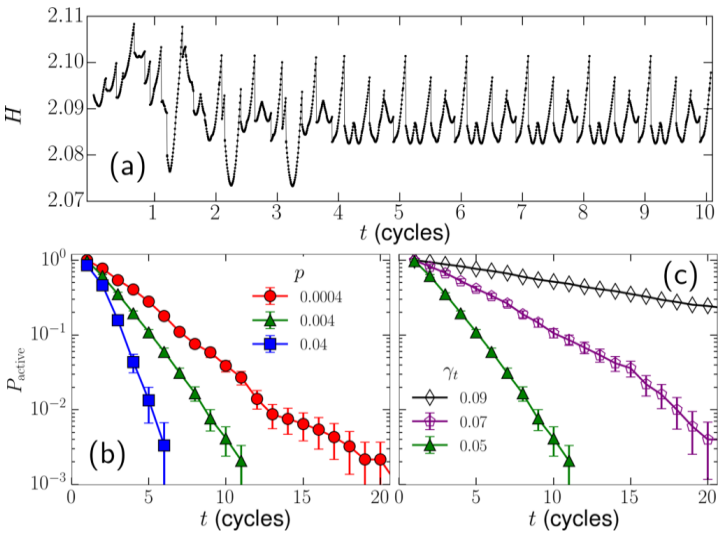

Fig. 4. (a) The enthalpy H as a function of number of shear cycles applied to a jammed system of particles. An oscillatory strain with amplitude, $\gamma_t = 0.15$ is applied quasistatically to a system of N = 64 particles. (b), (c) The probability P_{active} of a system to still be "active" and not in a periodic cycle *vs.* the number of applied shear cycles t, for a fixed $\gamma_t = 0.05$ in (b) and for a fixed pressure $p \approx 0.004$ in (c). The system very rapidly finds a state after which the motion is periodic.

Future Plans

In the coming year, we plan to continue to investigate to what degree materials can be designed to have unique response. In particular, the question arises whether the material can learn how to alter its own structure by manipulation of the inputs. For example, in the case of memory formation discussed above, the material learns relatively quickly, simply by shearing in a cyclic manner, to find a ground state where it is in a periodic cycle. This is an example of how memory can be used to train materials to have unique properties. In the shearing model we will investigate the number of different inputs that can be read out from a trained system.

We are continuing to study how complex a task can be (that is, how many functions can be independently specified) before the material is saturated and can no longer satisfy all of the requirements simultaneously. This builds on preliminary results that indicate that there is a transition between satisfied and unsatisfied behavior of these networks.

Publications (August 2016 – July 2018)

1. Justin C. Burton and S. R. Nagel, "Echoes from Anharmonic Normal Modes in Model Glasses," *Phys. Rev. E* **93**, 032905 1-10 (2016). DOI: 10.1103/PhysRevE.93.032905

2. Michelle M. Driscoll, Bryan Gin–ge Chen, Thomas H. Beuman, Stephan Ulrich, S. R. Nagel, and Vincenzo Vitelli, "The role of rigidity in controlling material failure," *PNAS* **113**, 10813-10817 (2016). doi: 10.1073/pnas.1501169113 arXiv:1501.04227

3. Jason W. Rocks, Nidhi Pashine, Irmgard Bischofberger, Carl P. Goodrich, Andrea J. Liu, and S. R. Nagel, "Designing allostery-inspired response in mechanical networks," *PNAS* **114,** 2520–2525 (2017). doi:10.1073/pnas.1612139114 arXiv:1607.08562

4. Marco Baity-Jesi, Carl P. Goodrich, Andrea J. Liu, S. R. Nagel, and James P. Sethna, "Emergent *SO(3)* Symmetry of the Frictionless Shear Jamming Transition," *J. Stat. Phys.* **167**, 735-748 (2017). DOI: 10.1007/s10955-016-1703-9 arXiv:1609.00280

5. Joseph D. Paulsen, S. R. Nagel, "A model for approximately stretched-exponential relaxation with continuously varying stretching exponents," *J. Stat. Phys.* **167**, 749-762 (2017). DOI: 10.1007/s10955-017-1723-0 arXiv:1611.07344

6. Maxim O. Lavrentovich, Andrea J. Liu, S. R. Nagel, "Period proliferation in periodic states in cyclically sheared jammed solids," *Phys. Rev. E* **96**, 020101(R) (2017). arXiv:1705.08368.

7. Ning Xu, Andrea J. Liu, and S. R. Nagel, "Instabilities of jammed packings of frictionless spheres under load," *Phys. Rev. Lett.* **119**, 215502 (2017). arXiv:1704.00900

8. Daniel Hexner, Andrea J. Liu, and S. R. Nagel, "Role of local response in manipulating the elastic properties of disordered solids by bond removal," *Soft Matter* **14**, 312-318 (2018). DOI: 10.1039/c7sm01727h ArXiv:1708.07207

9. Daniel R. Reid, Nidhi Pashine, Justin M. Wozniak, Heinrich M. Jaeger, Andrea J. Liu, S. R. Nagel, Juan J. de Pablo, "Auxetic metamaterials from disordered networks," *PNAS* **115**, E1384-E1390 (2018). arXiv: 1710.02493

10. Daniel Hexner, Andrea J. Liu, and S. R. Nagel, "Linking microscopic and macroscopic response in disordered solids," *Phys. Rev. E* **97**, 063001 (2018). arXiv:1706.06153

Condensed Matter Theory

Lead PI – Mike Norman
Co-PIs – Olle Heinonen, Alex Koshelev, Peter Littlewood, Ivar Martin,
Kostya Matveev, Andrew Millis, Hyowon Park
Materials Science Division, Argonne National Laboratory, Argonne, IL 60439

Project Scope

This program covers the areas of strongly correlated transition metal oxides and related materials, low dimensional systems, and topological matter. Specifically, the understanding of novel phenomena and electronic phases in transition metal oxides and related materials, including the influence of spin-orbit, defects, chemical doping, and interfaces, topological properties and dynamics of magnets, artificial spin ices, spin liquids, spin chains, and superconductors, including driven systems, and electrical and thermal transport in quantum wires and low carrier density semimetals.

Recent Progress

Topological Hall effect in diffuse ferromagnetic thin films with spin-flip scattering. Topological magnetic textures in thin films, such as skyrmions, give rise to a contribution to the Hall effect (the topological Hall effect). This comes from an emergent magnetic field generated by the magnetic texture that acts on itinerant electrons in addition to the external magnetic field. The contribution to the Hall effect is usually estimated to be proportional to the flux density of the skyrmions. We showed that when spin-flip scattering is present, the contribution to the Hall effect is reduced, and the reduction depends on the ratio of the spin diffusion length to the skyrmion radius. This result can help interpret experiments on the electrical detection of skyrmions based on the Hall effect, and would become particularly important when the size of the skyrmions is further reduced to tens of nanometers.

Topological frequency conversion in strongly driven quantum systems. We have demonstrated how quasiperiodic driving can be used to realize complex lattice models in a higher dimensional frequency/time space. The simplest example is a single spin-1/2 particle exposed to two elliptically polarized periodic waves, which can realize the chiral Bernevig-Hughes-Zhang model of a topological insulator (Figure 1). The signature of temporal topological phenomena arising from incommensurate drives is *energy pumping between drives, with quantized power*. This general principle may be of practical importance, as it could be used to convert photons between distinct photonic modes in optical cavities when coupled by a small magnetic particle. The energy pumping rate between modes can be as large as 1 MW for a 1 mm sized magnetic particle.

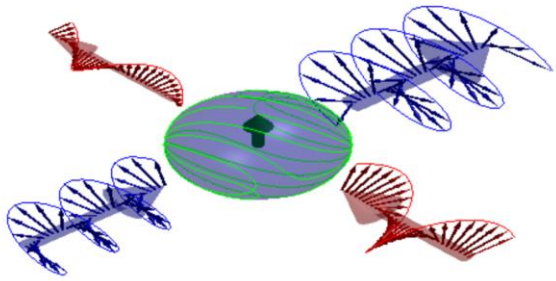

Figure 1: Using a 2D topological insulator band structure as a guide to engineer the quantized energy pumping between different frequency modes: a spin 1/2 driven by two sources with incommensurate frequencies. In the topological phase, the spin trajectory (green line) fully covers the Bloch sphere (blue). The intermode coupling induced by the spin dynamics pumps energy from one drive (red) to the other (blue) at a quantized rate.

Phonon-Mediated Superconductivity in Twisted Bilayer Graphene. Recently, interaction-induced insulating states surrounded by nearby phases of strong-coupling two-dimensional superconductivity have been discovered in bilayer graphene when a relative twist of layers leads to a long period moiré superlattice. The superconducting pairing mechanism

of twisted bilayer graphene has not yet been established, and a variety of possibilities are currently being explored. We have constructed a theory of magic angle superconductivity in twisted bilayer graphene in which the attractive interaction is mediated by the phonon modes of the individual two-dimensional graphene sheets. We find that this mechanism generates attraction in both s and d wave channels, and is strong enough to account for the superconducting transition temperatures observed experimentally.

One-dimensional systems: Second sound. At low temperatures, the relaxation of one-dimensional systems proceeds in two steps. First, the elementary excitations relax and form a gas that can move with respect to the center of mass of the system. The eventual equilibration of the gas of excitations with the rest of the system occurs after an exponentially long time. As a result, in a very broad range of frequencies, the system behaves as two coupled fluids. In this regime, the behavior of the system is very similar to that of superfluid ^{4}He. In particular, the system supports two sound modes instead of one. For systems with spin, one of the sound modes is a wave of density, whereas the other is a wave of entropy. In contrast, in a spinless one-dimensional system, each of the sound modes is a wave of both density and entropy. The hybrid nature of these sound modes results in a very unusual evolution of density perturbations in the system. For example, a density pulse created at one point splits into two pulses after traveling a long enough distance from the source.

Averievite, a new copper oxide spin liquid. We have predicted that the copper oxide mineral averievite, which has copper kagome layers sandwiched by copper-vanadium honeycomb layers, should exhibit spin liquid behavior upon substitution of the honeycomb coppers by zinc. This has been verified by Mitchell's group who synthesized both the pure and zinc-substituted versions, showing the absence of magnetism in the latter. In addition, we predict that upon titanium substitution for vanadium, one can dope this oxide, leading to a highly two dimensional kagome dispersion with potential topological and unconventional superconducting properties.

Nickelates as cuprate analogs. In collaboration with Mitchell's group, we have shown via an analysis of x-ray absorption and the electronic structure that an oxygen reduced Ruddlesen-Popper phase of nickelates, metallic $Pr_4Ni_3O_8$, behaves like an overdoped cuprate, with a partially filled 3d x^2-y^2 orbital. We have theoretically explored doping the rare earth site by a 4+ ion like cerium, and found that in the limit of a d^9 configuration for nickel, one obtains a magnetic charge transfer insulator as in cuprates. This implies that this class of materials should in principle exhibit high temperature superconductivity for intermediate values of the doping.

Nature of the metal-insulator transition in nickelate films. Via a combined experimental and theoretical study, we showed that oxygen vacancies play a critical role in the nature of the metal-insulator transition and 3d orbital polarization in few unit cell thick films of correlated oxide materials. We provided the first dynamical mean field theory (DMFT) calculations of properties of films with different surface terminations and provided a comparison to x-ray absorption experiments. We are currently studying the effects of antiferromagnetism and charge transfer on the ultra-thin films due to oxygen vacancies using DFT+DMFT.

Unconventional slowing down of charge dynamics in ferrites. In collaboration with Haidan Wen and Anand Bhattacharya, we studied the energy landscape for the competing magnetic order of charge-ordered ferrites as a function of the Fe-O bond length using first-principles calculations, revealing the intriguing nature of coupled electron-lattice relaxation that results in critical slowing down near the charge ordering temperature, as revealed by ultra-fast spectroscopy.

Future Plans

Weyl semimetals. We are investigating the possibility of a large, controllable inverse Edelstein effect in Weyl semimetals (WSMs), in which a spin accumulation at the interface of a normal metal and a WSM gives rise to a charge current. The inverse Edelstein effect in WSMs may be large and can potentially be controlled in a number of ways, for example by changing the Fermi energy in the WSM, by applying external strain or magnetic field, or by changing the direction of injected spins in the WSMs.

Anomalous Hall effect in transition metal sulfides. Recently, a strong anomalous Hall response was demonstrated in the absence of a magnetic field or any notable magnetization in $CoNb_3S_6$. In collaboration with our experimental colleagues at Argonne, we will work to decipher the (antiferro) magnetic state that is the cause of this effect.

Sound in quantum wires. We plan to study the attenuation of sound modes in quantum wires. This will require a detailed theory of both the viscosity and thermal conductivity of the system. Understanding attenuation of sound will enable us to determine precisely the conditions for the observation of both first and second sound modes. In addition, we expect to be able to develop a full description of the crossover from two sound modes at higher frequencies to the ordinary single sound behavior for lower frequencies.

4d and 5d oxide cuprate analogs. Building on our success with nickelates, we will explore other cuprate analogs by considering transition metal ions besides nickel. We have preliminary results on palladium that are promising in regards to a hypothetical $La_4Pd_3O_8$ material (an oxygen reduced n=3 Ruddlesen-Popper phase). In particular, this palladate is predicted to have a Fermi surface similar to that observed in cuprates. We plan to extend these endeavors to other potentially relevant transition metal ions such as silver, gold, and platinum.

Elastic interactions in transition metal oxides. We will combine our successful approach to modelling long range elastic interactions in oxides to understand the trends in phase transitions, together with DMFT calculations of local energies in correlated oxides. The goal is to develop a practical code to describe dynamical fluctuations in solids, by incorporating accurate quantum mechanics at a local site together with realistic nonlinear elastic couplings to describe long-range correlations. This will be compared to x-ray and neutron pdf studies of correlated oxides of interest, beginning with nickelates.

Exploring layered nickelates. Motivated by the extensive results from Mitchell's group, we will study tri-layer nickelates using DFT+DMFT to address not only the observed metal-insulator transition, but also how the Fermi surface in the metallic phase changes under the influence of doping, pressure, and the presence of apical oxygens vacancies. We will also investigate the oxygen reduced version of higher-order Ruddelsen-Popper phases besides n=3 (n=4 and higher) which have the promise of being more easily doped into a high temperature superconducting phase.

Quantum FFLO state in clean layered superconductors. Highly-anisotropic layered superconductors are considered plausible candidates for the realization of the Fulde-Ferrell-Larkin-Ovchinnikov [FFLO] state in a magnetic field directed along the layers due to reduced orbital effects. On the other hand, nothing unusual is anticipated in the case of a magnetic field oriented *perpendicular* to the layers. We will investigate the influence of Landau quantization on the superconducting instability for this geometry. Preliminary results suggest that the quantization correction to the Cooper-pairing kernel with a finite Zeeman spin splitting promotes the formation of a non-uniform FFLO state in which the order parameter is periodically modulated along the magnetic field, i.e., between the layers.

Select Publications (2017-2018)

1. Direct Observation of the Skyrmion Hall Effect, W. Jiang, X. Zhang, G. Yu, W. Zhang, M. B. Jungfleisch, J. E. Pearson, O. Heinonen, K. L. Wang, Y. Zhou, A. Hoffmann and S. G. E. te Velthuis, Nature Physics **13**, 162 (2017).
2. Topological phase transformations and intrinsic size effects in ferroelectric nanoparticles, J. Mangeri, Y. Espinal, A.M. Jokisaari, S.P. Alpay, S. Nakhmanson and O. Heinonen, Nanoscale **9**, 1616 (2017).
3. Tailoring Magnetic Skyrmions by Geometric Confinement of Magnetic Structures, Steven S.-L. Zhang, C. Phatak, A. K. Petford-Long and O. Heinonen, Applied Physics Letters **111**, 242405 (2017).
4. Topological Hall effect in diffuse ferromagnetic thin films with spin-flip scattering, Steven S.-L. Zhang and Olle Heinonen, Phys. Rev. B **97**, 134401 (2018).
5. Interplay between orbital-quantization effects and the Fulde-Ferrell-Larkin-Ovchinnikov instability in multiple-band layered superconductors, Kok Wee Song and Alexei E. Koshelev, Phys. Rev. B **97**, 224520 (2018).
6. Nematic and chiral superconductivity induced by odd-parity fluctuations, Fengcheng Wu and Ivar Martin, Physical Review B **96**, 144504 (2017).
7. Topological frequency conversion in strongly driven quantum systems, Ivar Martin, Gil Refael and Bertrand Halperin, Physical Review X **7**, 041008 (2017).
8. Hubbard Model Physics in Transition Metal Dichalcogenide Moire Bands, Fengcheng Wu, Timothy Lovorn, Emanuel Tutuc and A. H. MacDonald, Phys. Rev. Lett. **121**, 026402 (2018).
9. Viscous Dissipation in One-Dimensional Quantum Liquids, K. A. Matveev and M. Pustilnik, Phys. Rev. Lett. **119**, 036801 (2017).
10. Second Sound in Systems of One-Dimensional Fermions, K. A. Matveev and A. V. Andreev, Phys. Rev. Lett. **119**, 266801 (2017).
11. Viscosity of a multichannel one-dimensional Fermi gas, W. DeGottardi and K. A. Matveev, Phys. Rev. B **97**, 045135 (2018).
12. Hybrid Sound Modes in One-Dimensional Quantum Liquids, K. A. Matveev and A. V. Andreev, Phys. Rev. Lett. **121**, 026803 (2018).
13. Nature of the tensor order in $Cd_2Re_2O_7$, S. Di Matteo and M. R. Norman, Phys. Rev. B **96**, 115156 (2017).
14. Electron doped layered nickelates: Spanning the phase diagram of the cuprates, A. S. Botana, V. Pardo and M. R. Norman, Phys. Rev. Materials **1**, 021801(R) (2017).
15. Large orbital polarization in a metallic square-planar nickelate, J. Zhang, A. S. Botana, J. W. Freeland, D. Phelan, H. Zheng, V. Pardo, M. R. Norman and J. F. Mitchell, Nature Physics **13**, 864 (2017).
16. Symmetry-enforced line nodes in unconventional superconductors, T. Micklitz and M. R. Norman, Phys. Rev. Lett. **118**, 207001 (2017).
17. Unconventional slowing down of electronic recovery in photoexcited charge-ordered $La_{1/3}Sr_{2/3}FeO_3$, Yi Zhu, Jason Hoffman, Clare E. Rowland, Hyowon Park, Donald A. Walko, John W. Freeland, Phillip J. Ryan, Richard D. Schaller, Anand Bhattacharya and Haidan Wen, Nature Communications **9**, 1799 (2018).
18. Random Electric Field Instabilities of Relaxor Ferroelectrics, J. R. Arce-Gamboa and G. G. Guzman-Verri, npj Quantum Materials **2**, 28 (2017).
19. Twelve Inequivalent Dirac Cones in Two-Dimensional ZrB_2, A. Lopez-Bezanilla, Phys. Rev. Materials **2**, 011002(R) (2018).
20. Landau theory and giant room-temperature barocaloric effect in MF_3 metal trifluorides, A. Corrales-Salazar, R. T. Brierley, P. B. Littlewood and G. G. Guzman-Verri, Phys. Rev. Materials **1**, 053601 (2017).

FRACTIONALIZED EXCITATIONS IN TOPOLOGICAL STRONGLY CORRELATED MATTER

PI Natalia Perkins
Co-PI Ioannis Rousochazakis

University of Minnesota

Keywords: Quantum spin liquid, fractionalization, dynamical response

Project scope

The main focus of this proposal is on theoretical understanding of quantum materials with strong spin-orbit coupling, non-trivial topology and correlations. These materials are fertile grounds for exotic magnetic states and, in particular, for quantum spin liquid (QSL) phases of matter. Such phases host a remarkable set of emergent phenomena, such as long-range entanglement, topological degeneracy and fractionalized excitations. The overarching goal of this research proposal is to advance our understanding of these novel states of matter and provide accurate theoretical predictions for their experimental detection.

We are particularly interested in materials with 2D and 3D tri-coordinated lattices, where the interplay of the strong spin-orbit coupling and electronic correlations gives rise to dominant highly anisotropic Ising-like interactions between effective moments. The motivation behind this interest is the possibility of realizing the Kitaev quantum spin liquid. The presence of the exact solution of the Kitaev model on the honeycomb lattice and its 3D generalizations makes Kitaev spin liquids especially appealing for theoretical studies and experimental realizations, since by studying them a lot can be learn about generic behavior of other QSLs, which are much more difficult to describe.

The projects are divided roughly into two areas: The study of phases realized in Kitaev materials, and study of the signatures of topological QSL phases of matter in dynamical scattering probes, such as the inelastic neutron scattering, Raman and Resonant X-ray scattering.

Recent progress

Quantum spin liquid in the semiclassical regime [4]: According to received wisdom, QSLs can arise in frustrated magnets with low spin S, where strong quantum fluctuations act to destabilize conventional, magnetically ordered states. However, this is not always the case. In our study we found a Z_2 QSL ground state that appears already in the semiclassical, large-S limit. This state has both topological and symmetry-related ground-state degeneracy, and two types of gaps, a “magnetic flux” gap that scales linearly with S

and an “electric charge” gap that drops exponentially in S. The magnet is the spin-S version of the spin-1/2 Kitaev honeycomb model, which has been the subject of intense studies in correlated electron systems with strong spin-orbit coupling, and in optical lattice realizations with ultracold atoms. In particular, we have shown that the low-energy sector of the large-S Kitaev honeycomb model is described by a Toric code on a honeycomb superlattice (see Fig.1). The magnetic (plaquette) and electric (vertex) flux terms of the effective description arise respectively from the zero-point energy of spin waves and quantum mechanical tunneling between different orientations of frozen dimers (Fig.1 (b)). This work was done with Yuriy Sizyuk and Ioannis Rousochatzakis.

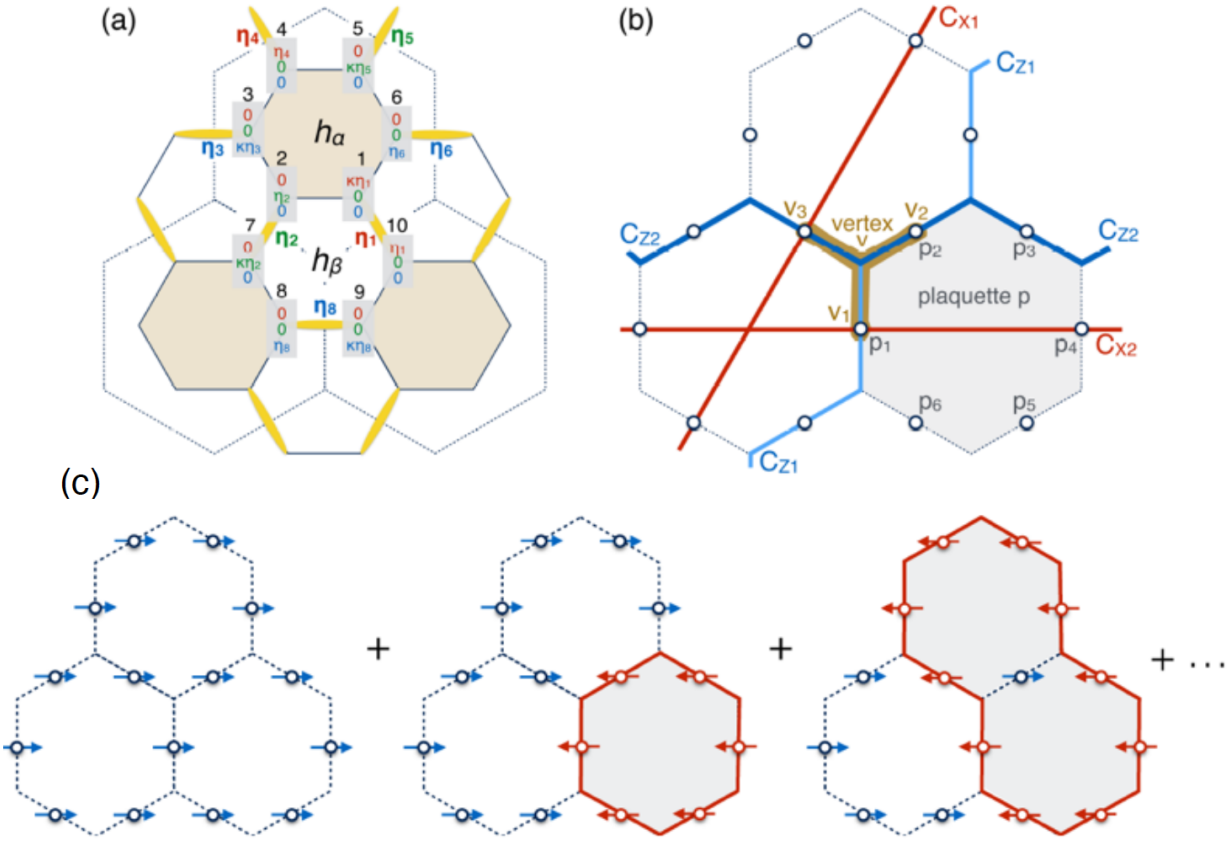

Fig.1: The mapping to a Toric code on a honeycomb superlattice. (a) Star dimer pattern selected from spin waves. The η’s describe the orientation of the two spins per dimer. They sit at the middle of the bonds of a honeycomb superlattice (dashed). (b) The resulting Toric code description on the honeycomb superlattice. Both plaquette and vertex terms, connecting six and three sites are shown. For the torus geometry, CX1 and CX2 (similarly for CZ1 and CZ2) are non-contractible loops that wrap the system in different directions. (c) The quantum spin liquid ground states of the Toric code correspond to massive, equal-amplitude superpositions of all possible loops of spins (red solid lines) pointing along -x (red arrows), on top of a FM background of spins pointing along +x (blue arrows).

Evolution of intertwined orders in the Kitaev magnet beta-Li_2IrO_3 [1,2]:

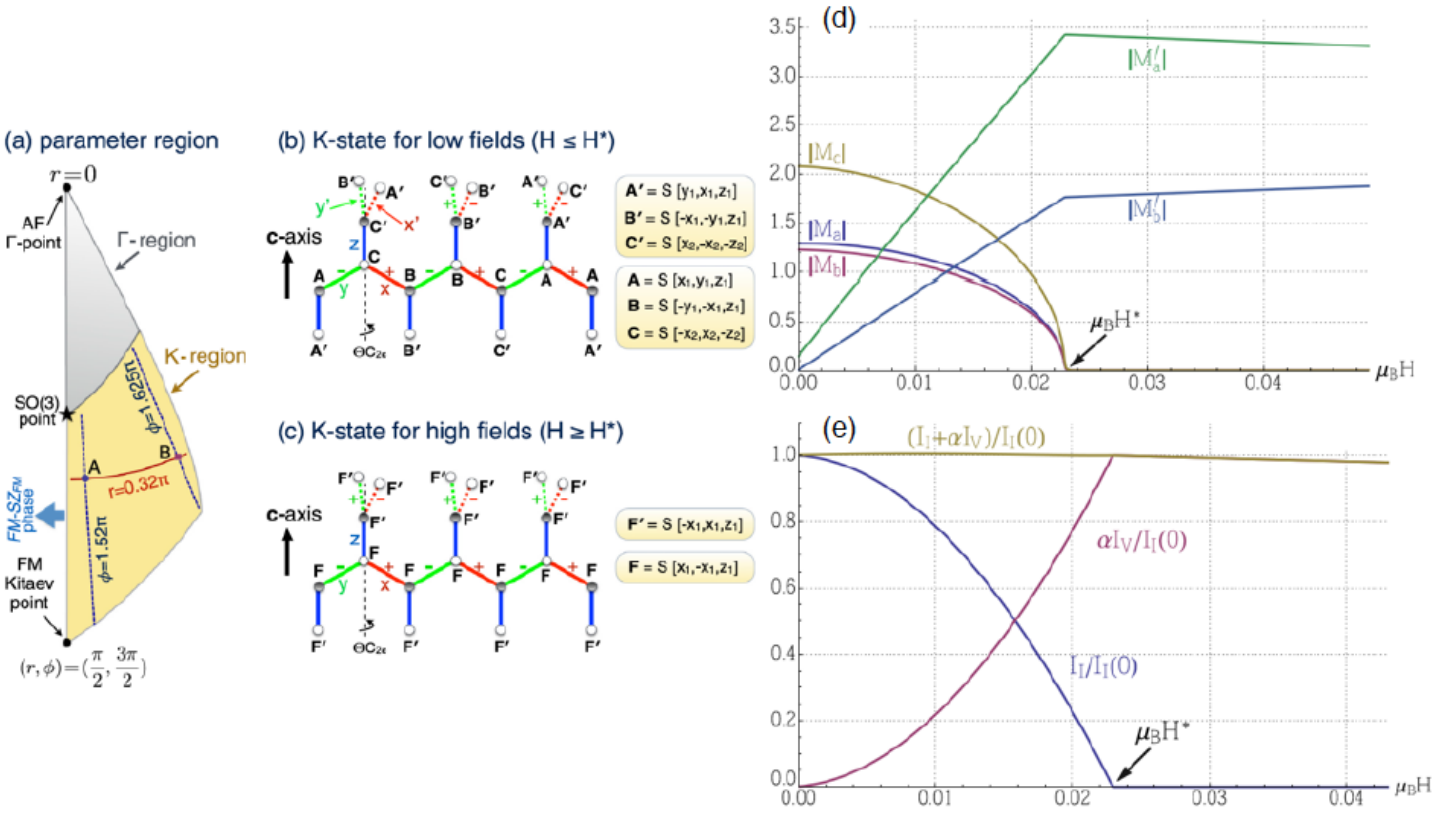

Fig.2 (a) The relevant parameter space where K-dominat state realizes. (b),(c) The structure of the K state at low and high fields. The solid (dashed) green and red bonds depict the xy (x'y') chains running along **a**+**b** (**a**-**b**). The blue vertical segments point along the **c** axis and depict the **z** bonds. The Cartesian components of the spins are shown in the side panels.(d) Evolution of the various Fourier components of the static structure factor of the K state with a magnetic field H along **b**. The intensity sum rule: evolution of the combinations I_1, I_V, and I_{tot} with a magnetic field H along **b**.

We performed a theoretical study of the static and dynamical properties of the three-dimensional, hyper-honeycomb Kitaev magnet *beta-Li_2IrO_3* in the presence of external magnetic field (Fig.2). At zero field this magnet is known to develop (below 37 K) a counter-rotating incommensurate spiral. In our work we showed that this incommensurate order can be understood in terms of a long-wavelength twisting of a nearby commensurate period-3 state, which has the same key qualitatively features as the experimentally observed on. This order is very fragile against a magnetic field along the crystallographic b-axis and disappears completely at a characteristic field H* (Fig.2(d)). At small fields, the system develops a significant uniform zigzag component along a-axis (superimposing the magnetization along b-axis). The zigzag component grows linearly with field until it shows a kink at H*, but is otherwise

undetectable at zero field. In our study we showed that the zigzag order is not emerging from its linear coupling to the field (via a staggered, off-diagonal element of the g-tensor), but from its intertwining with the incommensurate order and the longitudinal magnetization. The emerging picture explains all qualitative experimental findings at zero and finite fields, including the rapid decline of the incommensurate order with field and the so-called intensity sum rule (Fig.2(e)). The latter are shown to be independent signatures of the smallness of the Heisenberg exchange J, compared to the Kitaev coupling K and the off-diagonal anisotropy Gamma. Remarkably, in the regime of interest, the field H* at which the incommensurate component vanishes, depends essentially only on J, which allows to extract an estimate of J<4K from reported measurements of H*. This work was done in collaboration with Samuel Ducatman and Ioannis Rousochatzakis.

Publications

1. Ioannis Rousochatzakis and Natalia B. Perkins, *Magnetic field induced evolution of intertwined orders in the Kitaev magnet beta-Li2IrO3*, Phys. Rev. B 97, 174423 (2018).
2. Jianlong Fu, Johannes Knolle and Natalia B. Perkins, *Majorana representations of spin and an alternative solution of the Kitaev honeycomb model*, Phys. Rev. B 97, 115142 (2018).
3. Samuel Ducatman, Ioannis Rousochatzakis and Natalia B. Perkins, *Magnetic structure and excitation spectrum of the hyperhoneycomb Kitaev magnet beta-Li2IrO3*, Phys. Rev. B 97, 125125 (2018).
4. Ioannis Rousochatzakis, Yuriy Sizyuk and Natalia B. Perkins, *Quantum spin liquid in the semiclassical regime*, Nature communications 9, 1575 (2018).
5. Natalia B. Perkins, *Kitaev physics crystalized*, Nature Physics (News and Views) 13, 1041 (2017).
6. Gabor B. Halasz, Brent Perreault and Natalia B. Perkins, *Probing spinon nodal structures in three-dimensional Kitaev spin liquids*, Phys. Rev. Lett. 119, 097202 (2017).
7. Jianlong Fu, Jeffrey G. Rau, Michel J. P. Gingras, and Natalia B. Perkins, *Fingerprints of quantum spin ice in Raman scattering*, Phys. Rev. B 96, 035136 (2017).
8. Gabor B. Halasz, Natalia B. Perkins, and Jeroen van den Brink, *Resonant Inelastic X-Ray Scattering Response of the Kitaev Honeycomb Model*, Phys. Rev. Lett.117, 127203 (2016).
9. Brent Perreault, Johannes Knolle, Natalia B Perkins, and F. J. Burnell, *Resonant Raman scattering theory for Kitaev models and their Majorana fermion boundary modes*, Phys. Rev. B 94, 104427 (2016).

The Materials Project

Kristin Persson (Energy Technologies Division, LBNL), Gerbrand Ceder (Materials Sciences Division, LBNL), Anubhav Jain (Energy Technologies Division, LBNL), Jeffrey Neaton (Materials Sciences Division, LBNL), Shyue Ping (Ong UC San Diego), Daniel Gunter (Computing Research Division, LBNL), Mark Asta (Materials Sciences Division, LBNL), Daryl Chrzan (Materials Sciences Division, LBNL), Lane Martin (Materials Sciences Division, LBNL), Geoffroy Hautier (U Louvain la Neuve, Belgium), Peter Khalifah (Brookhaven National Laboratory)

Keywords: Materials Design, Density Functional Theory, Materials Property Database

Project Scope

Materials discovery and development is a key innovation driver for new technologies and markets, and an essential part of the drive to a renewable energy future. The goal of the Materials Project (online at http://www.materialsproject.org) is to accelerate materials discovery and education through advanced scientific computing and innovative design tools. The proposed work will significantly impact the scientific community, computer science research, and education by providing unprecedented data and materials design tools as well as comprehensive capabilities for scientists to share their processes and results. **High-throughput calculations, state-of-the-art electronic structure methods as well as novel datamining algorithms for surface, defect, electronic and finite temperature property predictions will be combined with existing capabilities at the Materials Project for tens of thousands of materials to yield an unparalleled materials design environment**. We envision a fundamentally networked and data-intensive model of scientific discovery where computation and simulation can be leveraged at a massive scale, where many of the mundane details of recording and saving work are handled by online services, where results can be immediately validated against high order methodologies and experimental results, and where the process of scientific discovery can leverage the accumulated knowledge of Nature with something akin to a Google search – "find the electrochemical properties and crystal structure for compound X".

Recent Progress

The Materials Project efforts can be categorized into three primary scientific thrusts: Data Generation, Data Dissemination, and Design; along with the supporting thrust of Scientific Software Development.

We continue to expand the database of unique structure-property relationships available in the Materials Project. This last year we have continued to compute new materials from structures in the Pauling Files, orderings of disordered ICSD compounds, and new compounds added to the ICSD since 2015. This has yielded over 10,000 new materials. Our database of elastic constants is also growing at a rapid pace with over 5,000 new elastic constants, doubling the size of our complete elastic tensor dataset. We continue to develop new capabilities such as extending the continuum elasticity formalism to higher order elastic tensors[1] which will enable predictions of thermal conductivity and fracture behaviour. In addition, we have developed a formalism to construct convex hulls with our Pourbaix infrastructure and calculate metastability energies for

compounds as a function of pH and voltage.[2] A new area of exploration for Materials Project lies in the area of computed characterization methodologies where we have already computed over 500,000 K-edge x-ray absorption near edge structure (XANES) spectra.[3] Additional over 1,500 precise phonon band structures have been computed and disseminated with detailed thermodynamic properties including vibrational entropy.[4]

Disseminating data and tools in a useful manner is key to our impact on the materials science community. MP accomplishes this in a variety of ways ranging from our existing website infrastructure that is designed to be easily navigable to our API that allows full access to our data. Recently, we've been challenging these assumptions, as they are based on positive feedback only, by performing our own usability testing with undergraduate students at UC Berkeley. Students with varying degrees of materials science understanding are asked to perform routine to complex tasks while being recorded to understand where we can improve the interface. This has yielded a number of insights on aspects of MP to improve, from the complexity of querying language to the overall structure of the website, to increase our impact.

In line with this theme is our MP workshop which is a key dissemination platform for detailed usage of our python based software infrastructure. This two and half day course focuses on using the Materials Project infrastructure from searching the website to querying for data to implementing automated high throughput workflows on DOE supercomputers. This workshop is taught in a hands-on manner with lesson plans following the Software Carpentry model to actively engage attendees and ensure they learn by listening, following, and actually performing the analysis and automation themselves.

Understanding synthesis pathways and predicting the synthesizability of materials continues to be a key bottleneck in the design of materials. Recently, MP developed a method to determine if a material was in absolute not synthesizable based on the metastability of the material vs its compositional amorphous energy.[5] This method provides a chemically independent and highly specific cut off for synthesizability that characterizes the wide variety of metastability limits seen in modern materials ranging from the relatively high amorphous limits in nitrides and carbon to the very limited amorphous limit in boron-oxide.

Software infrastructure is key to every aspect of MP, from the workflow tools to data pipelines to the website architecture. The significant growth in properties that MP computes is currently pushing our ability to rapidly develop new dissemination vehicles. We've begun to remedy this by breaking apart monolithic software tools into a modular architecture that isolates calculation management from data analysis pipelines to the website system such that they can be developed and operate independently of each other. This will allow for more developers of varying degrees of expertise to integrate into our development platform without compromising code and toolchain quality.

Future Plans

The Materials Project continues to grow at a rapid pace. Our goals for the following year are to add interface and defect properties: particularly grain boundary structures and energies as well as intrinsic defect formation energies. We also plan on adding new design tools including one based on text-mining abstracts to build knowledge networks of compounds. This network is similar in nature to the connection of terms and websites employed by Google, but in this case, connects

generic search criteria to compounds and structures. Additionally, our efforts at building similarity metrics will be connected to this framework and allow for a more natural material science exploration of materials for targeted applications. We continue to develop new software to support these lofty goals including a new website architecture that should provide modular development, which should enable a faster timeline from calculations to final dissemination vehicle via a website application.

References

1. S. Winter, J. Montoya, K. A. Persson, and D. C. Chrzan, Ab initio calculation of thermal expansion with application to understanding Invar behavior in gum metal, Phys. Rev. Materials **2**, 7 (2018)
2. A.K. Singh, L. Zhou, A. Shinde, S.. K. Suram, J.H. Montoya, D. Winston, J.M. Gregoire, and K.A. Persson, Electrochemical Stability of Metastable Materials, Chemistry of Materials **29**, 23 (2017)
3. K. Mathew, C. Zheng, D. Winston, C. Chen, A. Dozier, J.J. Rehr, S.P. Ong, and K.A. Persson, High-throughput computational X-ray absorption spectroscopy, Scientific Data **5**, 180151 (2018)
4. G. Petretto, S. Dwaraknath, H. PC Miranda, D. Winston, M. Giantomassi, M. J. Van Setten, X. Gonze, K. A. Persson, G. Hautier, and G. Rignanese. "High-throughput density-functional perturbation theory phonons for inorganic materials." Scientific data **5**, 180065, (2018)
5. M. Aykol, S. Dwaraknath, W. Sun, and K.A. Persson, Thermodynamic limit for synthesis of metastable inorganic materials, Science Advances **4**, 4 (2018)

Publications (August 2016 – July 2018)

If more than 10 publications, list only the 10 most relevant.

1. K. Latimer, S. Dwaraknath, K. Mathew, D. Winston, and K.A. Persson, Evaluation of thermodynamic equations of state across chemistry and structure in the materials project, npj Computational Materials **4** ,1 (2018)
2. I. S. Winter, J. Montoya, K. A. Persson, and D. C. Chrzan, Ab initio calculation of thermal expansion with application to understanding Invar behavior in gum metal, Phys. Rev. Materials **2**, 7 (2018)
3. L. Ward, A. Dunn, A. Faghaninia, N.E.R. Zimmermann, S. Bajaj, Q. Wang, J. Montoya, J. Chen, K. Bystrom, M. Dylla, K. Chard, M. Asta, K.A. Persson, J. Snyder, I, Foster, and A, Jain, Matminer: An open source toolkit for materials data mining, Computational Material Science **152**, 60 (2018)
4. D.P. Tabor, L.M. Roch, S.K. Saikin, C. Kreisbeck, D. Sheberla, J.H. Montoya, S. Dwaraknath, M. Aykol, C. Ortiz, H. Tribukait, C. Amador-Bedolla, C.J. Brabec, B. Maruyama, K.A. Persson, and A. Aspuru-Guzik. Accelerating the discovery of materials for clean energy in the era of smart automation, Nature Reviews Materials **3**, 5 (2018)
5. M. Aykol, S. Dwaraknath, W. Sun, and K.A. Persson, Thermodynamic limit for synthesis of metastable inorganic materials, Science Advances **4**, 4 (2018)

6. N.E.R. Zimmermann, D.C. Hannah, Z. Rong, M. Liu, G. Ceder, M. Haranczyk, and K.A. Persson, Electrostatic Estimation of Intercalant Jump-Diffusion Barriers Using Finite-Size Ion Models, The Journal of Physical Chemistry Letters **9**, 3 (2018)
7. M. Aykol and K.A. Persson, Oxidation Protection with Amorphous Surface Oxides: Thermodynamic Insights from Ab Initio Simulations on Aluminum, ACS Applied Materials and Interfaces **10**, 3 (2018)
8. J. Dagdelen, J. Montoya, M. de Jong, and K. Persson, Computational prediction of new auxetic materials, Nature Communications **8**, 1 (2017)
9. K. Mathew, J.H. Montoya, A. Faghaninia, S. Dwarakanath, M. Aykol, H. Tang, I. Chu, T. Smidt, B. Bocklund, M. Horton, J. Dagdelen, B. Wood, Z. Liu, J. Neaton, S.P. Ong, K. Persson, and A. Jain, Computational Materails Science **139**, 140 (2017)
10. J.H. Montoya and K.A. Persson, A high-throughput framework for determining adsorption energies on solid surfaces, npj Computational Materials **3**, 1 (2017)

Symmetry, Correlation, Spin-Orbit Coupling, and their Interplay

PI: Warren E. Pickett, Physics Dept., University of California Davis

Keywords: topological phases, spin-orbit coupling, symmetry-breaking, nanotechnology

Project Scope and Historical Perspective

Recent work, due to our group and others, has demonstrated that delicate interplay between strong correlations, large spin-orbit coupling (SOC), and opportunities due to symmetry breaking, can lead to new physical phases with unusual properties. Some with topological character of the electronic state are among the most current, while others such as charge ordering (or lack of it) provide new insight into long standing issues. In a few contexts we have found that the effect of even rather weak SOC can be magnified by strong interactions. In our several studies of (001) interfaces and thin film overlayers of perovskite transition metal oxides (viz. $LaAlO_3$ on a $SrTiO_3$ substrate), broken charge and spin symmetry phases were common but SOC was never a factor. The suggestion that buckled bilayer honeycomb lattices of open-shell 3d ions, produced by (111) layer growth of *5d*-based perovskites, provides a new vista for strong interaction -- large SOC-broken symmetry interplay, has led us to turn our attention to such systems. Several of these findings have been reported. Symmetry in itself is emerging as a central consideration, as it has in many other contexts. Although sometimes couched in terms of global (space group; magnetic order) terms, it seems that sometimes it is the local symmetry of an open-shell ion that is crucial: large Hubbard U encourages (Jahn-Teller) distortions, lowering symmetry; SOC produces large orbital moments, leading to huge magnetocrystalline anisotropy, bootstrapping effects of SOC. A distinct, honeycomb lattice system that contains a Chern phase in its generalized phase diagram has been evident in two systems reported as nearly complete in the previous report.

This project addresses a number of DOE/BES priorities. Electronic correlations are addressed specifically: most of the applications are to strongly correlated materials, but there are several other characteristics that modulate the effects of strong interactions. We address materials design (MGI), not in a high throughput manner such as several groups are doing well, but in making applications to atomic layer-by-layer grown materials that experimentalists are gaining experience with. Several competing energy scales make the systems we study less amenable to high throughput approaches. One aspect of our design vision during this period was to replace oxides with nitrides, for hole transport reasons: holes in oxides almost never conduct. Phenomena studied include magnetism, quantum phase transitions, and thermoelectric behavior, occasionally having superconducting possibilities in mind. Topological characters of Hamiltonians (of real materials) are being given priority in this project. Design/prediction of topological insulators, semimetals, and now metals is an active area for us, and understanding their origins in real materials is the real focus.

Historical perspective. Degeneracies were studied by von Neumann and Wigner [1] early on, establishing that two parameters in a real Hamiltonian are sufficient to adjust the system to an accidental degeneracy; a complex Hamiltonian requires three parameters. Conyers Herring (1937) [2] discovered that loops of degeneracies – nodal loops (NLs) -- could occur in crystals and should not be rare. R. R. Haering (not Herring!) in 1958 [3] discovered a nodal loop in rhombohedral graphite, see Fig. 1. Studies of such nodal loops seemingly lay dormant until the

modern era, when Phil Allen in 2007 [4] discovered such loops in common aluminum, moreover he pursued the consequences of spin-orbit coupling (SOC) on the Berry phase associated with a contour that encircles the loop. The paper of Balents and coworkers in 2011 [5] brought this peculiar phenomenon of nodal loop semimetals to the fore of topological material research, although it was not until 2015 that an exponential explosion of NL papers appeared.

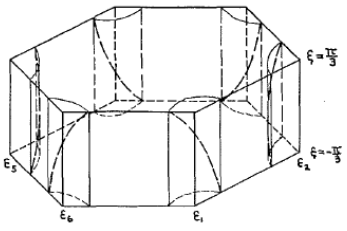

FIG. 3. Lines along which the two π-bands touch. The lines lie on cylinders $\sigma = \beta$, whose axes are the edges ϵ_i. (The drawing is not to scale.)

Figure 1. The illustration from R. R. Haering [3] of the nodal loop surrounding the point K in rhombohedral graphite, likely the first identification of a nodal loop in an actual crystalline material.

Recent Progress: summaries of two projects

Coexistence of Triple Nodal Points, Nodal Lines, and Flat Bands.

The Cu_3Au structured intermetallic $PbPd_3$, known for 3 decades in the context of applications, was explored with density functional methods; here DFT is fine for accounting for correlation effects. A prominent feature is the remarkably flat bands along the Γ-X directions very close to the Fermi level E_F. This band is the top of the Pd *4d* complex, leaving a 2D-like step in the density of states N(E). Two topological aspects of much current interest were found as well, which we first consider neglecting SOC. Three symmetry related loops of degeneracies (nodal loops) surrounding the zone corner R point were discovered, interconnected along the R-M lines [Fig. 2(c)]. Such loops are known to lead to "drumhead surface states" within the projection of the loops onto the surface zone; in $PbPd_3$ they do not however cross E_F. Finally, triple nodal points (TNP) -- in practice, the crossing of a doubly degenerate band with another band -- were discovered near E_F. Like Weyl points, these lead to "Fermi arcs" (not quite at E_F in $PbPd_3$) in the surface spectrum.

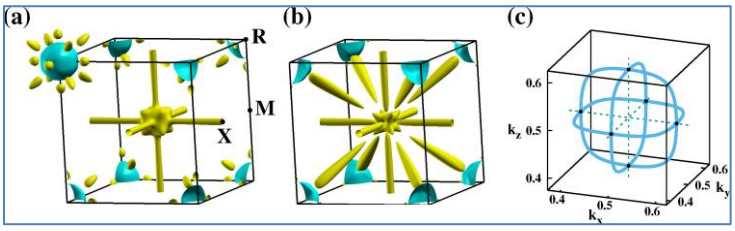

Figure 2. Delicate Fermi surfaces of (a) $PbPd_3$ and (b) $SnPd_3$, including SOC. Panel (c) provides the intersecting nodal loops surrounding the R point in $PbPd_3$.

Spin-orbit coupling (SOC) affects strongly and in different ways this unusual coexistence of unconventional features. For the flat bands, SOC drives them to 7 meV above E_F, with merely 3 meV dispersion. SOC-derived hybridization with a crossing band near displaces bands and leaves delicate Fermi surface features. Theo Siegrist (NHMFL & FSU) has grown single crystals and obtained Shubnikov-de Haas oscillations that will provide a close connection to our calculations. As known, SOC lifts the degeneracy of the nodal loop, so – no nodal loop, no (precise) drumhead states. That is not the end of the story. Phil Allen (in ground-breaking work not deemed at the time to justify an independent publication) demonstrated [4] that the non-analytic character and associated Berry phase can be followed as SOC is 'turned on', and the nodal loop (which does not actually exist!) can nevertheless be located by theoretical spectroscopy. The Berry phase of π is reduced in magnitude and dependent on the circuit of integration around the degeneracy, but it remains: the smile of the Cheshire Cat. As for the TNPs: SOC removes part of the degeneracy leaving 3D Dirac points, again not exactly at E_F since, $PbPd_3$ being a metal, there is no global constraint on the energy position of band features.

Materials Design: <111>-oriented Oxide and Nitride Nanolayers. In the previous 2-year abstract we reported the computational design of Chern insulator phases in <111> bilayers of $LaRuO_3$ and $LaOsO_3$ embedded in $LaAlO_3$. We currently have a collaboration with the NSF MIP PARADIM to synthesize the Ru member (work ongoing). One project during this period has been to extend the design of <111>-oriented nanostructures to nitrides, building on the knowledge that semiconducting III-V nitrides have been synthesized for optoelectronic applications for decades. Two 2-carrier (electron + hole) systems resulted. One is a nitride-oxide <111> heterostructure, ScN embedded in insulating MgO. Beyond a critical thickness of five ScN layers, this nanoslab hosts spatially separated conducting Sc *3d* electrons and N *2p* holes, each confined to two atomic layers, with ScN providing both conducting layers. A guiding concept is that the N^{3-} anion should promote robust two carrier 2D hole conduction compared to that of O^{2-}; metal mononitrides are mostly metallic and even superconducting while most metal monoxides are insulating. Our results, including calculation of Hall coefficient and thermopower for each conducting layer separately, provide guidance for further exploration, both experimental and theoretical, on nitride-based conducting gases that could promote study of long sought exotic states viz. new excitonic phases and distinct, nanoscale parallel superconducting nanolayers.

This line of thought was extended to CrN <111> layers encased in MgO. Due to the ferromagnetic alignment of the Cr t_{2g} spins, both electron and hole 2D gases are provided by the magnetic Cr ion: spin-up holes in the t_{2g} bands, spin-down electrons in the e_g bands, on opposite sides of the CrN slab. Bloch-Boltzmann transport calculations revealed that large thermopowers can be engineered in each of the 2D gases. Procedures had to be generalized somewhat to carry out these calculations. Finally, we designed a nanoscale thermoelectric device (repeated slabs) that could produce roughly a 1 V potential difference across a 100 nm nanostructure, given a temperature difference of 50K.

Future Plans.

- Analyze the character of the recently reported double perovskite magnet Sr_2SrOsO_6, which orders at 1000K, for possibilities of a Chern insulating phase and to analyze its magnetocrystalline anisotropy.
- Continue the collaboration with the NSF MIP PARADIM experimentalists. to verify good <111> growth and compare with our designed Chern phases in bilayer $LaRuO_3$.
- Extend our design to untouched <111> *trilayers*, which form the promising "dice lattice;" with a tight-binding s orbital it harbors a flat band and Chern insulating phases.

References

[1] J. von Neumann and E. P. Wigner, On the behavior of eigenvalues in adiabatic processes, Physik. Z. **30**, 467 (1929). Translated in R. S. Knox and A. Gold, Symmetry in the Solid State (Benjamin, New York, 1964), p. 167.

[2] W. C. Herring, Accidental Degeneracy in the Energy Bands of Crystals, Phys. Rev. **52**, 365 (1937); see also his PhD thesis (Princeton, 1937).

[3] R. R. Haering, Can. J. Phys. **36**, 352 (1958).

[4] P. B. Allen, What happens to geometric phase when spin-orbit interactions lift band degeneracies? arXiv:0709.1457 (2007) [unpublished]. P. B. Allen and W. E. Pickett, Physica C **549**, 102 (2018).

[5]A. A. Burkov, M. D. Hook, and L. Balents, Topological nodal semimetals, Phys. Rev. B 84, 235126 (2011)

Selected Supported Publications from 2016-2018

C.-T. Kuo and 17 coauthors, Atomic-layer-resolved composition and electronic structure of the cuprate $Bi_2Sr_2CaCu_2O_{8+\square}$ from soft x-ray standing-wave photoemission, (submitted, 2018).

K.-H. Ahn, W.E. Pickett, and K.-W. Lee, Coexistence of Triple Nodal Point, Nodal Lines, and Unusual Flat Band in intermetallic $PbPd_3$, Phys. Rev. B (2018, in press).

P. B. Allen and W. E. Pickett, Accidental Degeneracy in k-space, Geometrical Phase, and the Perturbation of □ by Spin-orbit Interactions, Physica C **549**, 102 (2018).

H. Guo, S. Gangopadhyay, R. Pentcheva, and W. E. Pickett, Wide Gap Chern Mott Insulating Phases achieved by Design, npj Quantum Materials **2**, 4 (2017).

H. Li, X. Zhou, T. Nummy, J. Zhang, V. Pardo, W. E. Pickett, J. Mitchell, and D. Dessau, Fermiology and Electron Dynamics of Trilayer Nickelate $La_4Ni_3O_{10}$, Nat. Commun. **8**, 704 (2017).

H.-M. Guo, T. Mendes, W.E. Pickett, and R.T. Scalettar, Magnetic Order-Disorder Transitions on a 1/3-Depleted Square Lattice, Phys. Rev. B **95**, 045131 (2017).

A. S. Botana, W. E. Pickett, and V. Pardo, All *3d* electron-hole bilayers in CrN/ScN(111) multilayers for thermoelectric applications Phys. Rev. Applied **7**, 024002 (2017).

A. S. Botana, W. E. Pickett, and V. Pardo, Nitride Multilayers as a Platform for Parallel Two-Dimensional Electron-Hole Gases: MgO/ScN(111), Phys. Rev. B **93**, 085125 (2016).

S. Gangopadhyay and W. E. Pickett, Interplay between spin-orbit coupling and strong correlation effects: Comparison of the three osmate double perovskites Ba_2AOsO_6 (A=Na, Ca, Y), Phys. Rev. B **93**, 155126 (2016).

A. S. Botana, V. Pardo, W. E. Pickett, and M. R. Norman, Charge ordering in Ni^{1+}/Ni^{2+} nickelates: $La_4Ni_3O_8$ and $La_3Ni_2O_6$, Phys. Rev. B **94**, 081105(R) (2016).

Complex (anti)ferroic oxides: statics and dynamics at finite temperatures

Inna Ponomareva, University of South Florida

Keywords: phase competition, ferroics, dynamics, nanostructures, computational methodology

Project Scope

Complex oxides that exhibit ferroic, antiferroic or multiferroic properties are of extreme fundamental and technological importance. Fundamentally such materials are very attractive because they exhibit delicate energy competitions which result in appearance of some spontaneous property (magnetization, electric polarization or strain) or particular type of ordering. Technologically they are in the heart of numerous applications. A few examples include memory applications, pyroelectric sensors, pressure sensors, capacitors, optical communications, ultrasonic motors, phase-array radars, ultrasound imaging and actuators, thermistors, filters, light detectors, high-power microwave devices, and many others. However, despite of their special role in both fundamental and applied sciences, many such materials and their properties remain rather poorly understood. Some examples include statics and dynamics of antiferroelectrics and relaxors, exotic energy conversion mechanisms in (anti)ferroics, fundamental intrinsic dynamics of such materials, and (anti)ferroic phenomena at the nanoscale. Such lack of understanding critically hinders both scientific and technological progress, especially as it applies to the nanoscale. *The ultimate goal of this project is to achieve a fundamental understanding of statics and dynamics of complex oxides that exhibit ferroic, antiferroic, multiferroic or relaxor properties at both macro- and nano-scales through state-of-the-art computer simulations.* To reach this goal we define the following objectives:

Objective 1. To develop a set of computational tools that allows accurate modeling of static and dynamical properties of some ferroics, antiferroics, and relaxors at finite temperatures. The set will feature the following (i) accurate first-principles-based potentials; (ii) capability to simulate both static and dynamical properties; (iii) capability to simulate both bulk and nanoscale materials.

Objective 2. To explore, predict and understand at an atomistic level the fundamental static and energy converting properties of (anti)ferroics and relaxors using such new simulator.

Objective 3. To explore, predict and understand at an atomistic level the fundamental dynamical properties of (anti)ferroics and relaxors at microwave and infrared frequencies using such new simulator.

Recent Progress

The untold story of soft mode dynamics in ferroelectric nanostructures. Many ferroelectric phase transitions are of displacive type. They are governed by the polar optical mode that softens as the Curie temperature is approached. As a result the dynamics of the soft mode is critical for the understanding ferroelectric phase transitions at the fundamental level. In ferroelectrics the soft mode is very sensitive to the mechanical boundary conditions such as pressure, stress or strain. In fact, this sensitivity is utilized for determining mechanical stresses and strains in experimental settings. Consequently, for macroscopic ferroelectrics the soft mode dynamics is a subject of intense investigation. In a surprising contrast, very little is known about the soft mode dynamics in ferroelectric nanostructures, which are in the frontier of both fundamental and applied research. Is this dynamics similar to the one in bulk or is there a dynamical "fingerprint" associated with the reduced dimensionality? What story could the soft mode dynamics tell about the fundamentals of the phase transitions in nanosrtuctures?

When it comes to the boundary conditions, they play far more complex and important role in ferroelectric nanostructures than in bulk ferroelectrics. For example, the electrical boundary conditions, such as surface charge compensation, are capable of complete transformation of ferroelectricity at the nanoscale. Formation of locally polar nanostripes, nanoscale domain-closure patters, vortexes and other exotic typologies are just a few instances [1-3]. Many of these patterns are further enriched through the contributions from mechanical boundary conditions which are ubiquitous at the nanoscale. Motivated to fill this gap in understanding of phase transitions in ferroelectric nanostructures we developed and carried out first-principles-based finite-temperature atomistic simulations to investigate both equilibrium phases and soft mode dynamics in ultrathin ferroelectric $PbTiO_3$ nanowires with poor surface charge compensation subjected to a wide range of mechanical boundary conditions. In our study we (i) reveal an unexpected drastic hardening of some soft modes in ferroelectric nanowires and discuss its implications for the phase transitions at the nanoscale; (ii) predict the dynamical fingerprint for the famous domain-closure pattern at the nanoscale; (iii) establish how exactly the soft mode dynamics is influenced by both electrical and mechanical boundary conditions, and (iv) propose a way to identify such boundary conditions by the change in the soft mode dynamics.

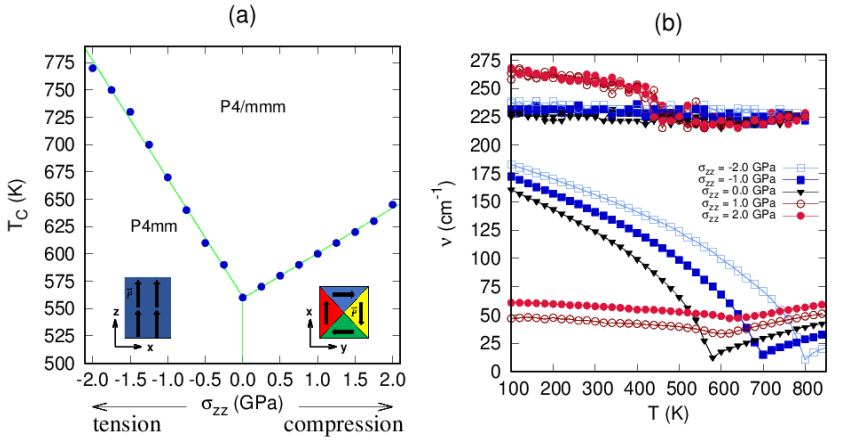

Fig.1. Dependence of the Curie temperature in $PbTiO_3$ nanowire on the uniaxial stress applied along the axial direction (a); the temperature evolution of soft mode frequencies in the presence of stress.

Figure 1(a) shows the temperature stress phase diagram for the $PbTiO_3$ nanowire with the lateral size of 4.8 nm under axial stress. The temperature evolution of the soft mode frequencies is given in Fig.1(b). One surprising finding is the presence of hard high-frequency mode above 200 cm^{-1} that does not exist in the bulk. The significance of this mode is that it forbids phase transition associated with the onset of net spontaneous polarization along the direction of the depolarizing field.

Another interesting finding is the presence of two different phases in the phase diagram below the Curie temperature. In particular, for stress-free nanowire we observe a polar phase with the polarization confined to the axial direction, while under uniaxial compression we find macroscopically nonpolar flux-closure phase in the cross section of the nanowire [see schematization in Fig.1(a)]. Does this finding imply the possibility to switch between the polar and nonpolar phases by the external stress which could open a way to all-mechanical polarization control and unprecedented electromechanical coupling?

Unveiling the electromechanical potential of ferroelectric nanowires. Electromechanical coupling is in the heart of the nanogenerator – a device that harvests and converts mechanical energy at the nanoscale. Successful nanogenerators have been demonstrated experimentally in several piezoelectric nanowires and their arrays[4]. However, the roadblock on the way to practical applications is actually rather small output electrical power produced by the nanogenerator. To overcome this roadblock a drastic improvement in the electromechanical coupling is critically needed. Such a drastic improvement is more likely to be achieved through discoveries of some unconventional forms of coupling rather than through improvement of the conventional piezoelectric coefficients. The possibility to switch the polarization by the application of stress to ferroelectric nanowires may hold the potential to such unconventional form of the electromechanical coupling. To investigate into the possibility to achieve all-mechanical polarization control in unusual electromechanical coupling in ferroelectric nanowires we carried out finite-temperature first-principles-based simulations for the ultrathin nanowires under uniaxial compression applied either quasi-statically or dynamically.

Figure 2 illustrates some of our key findings. Panels (a) and (b) show the response of the polarization and strain to the uniaxial stress application and removal. They demonstrate that for the temperature of practical importance the macroscopic polarization and spontaneous strain can be reversibly switched off by the uniaxial stress. Panel (c) shows schematically the dipole pattern in the cross section of the nanowire for the macroscopically nonpolar phase. The nearly discontinuous changes in the polarization and strain lead to the anomalous values of piezoelectric and elastic coefficients which are given in panels (d) and (f). We find that piezoelectric coefficient d_{33} can reach the value of 5400 pC/N which far exceeds the best performing ceramics value of 3200 pC/N. The critical stress needed to achieve phase switching shows a strong temperature dependence which is given in Fig.2(f). As the Curie temperature approaches the critical stresses first merge together and then decrease. We carried out Molecular Dynamics simulations to demonstrate that the reversible polarization control by mechanical stress persist up

to gigahertz frequencies. The origin of the effect is traced to the delicate competition between the electrostatic and electromechanical energies which is unique to the nanowire geometry. The all-mechanical polarization control is, therefore, a shape effect and is expected to occur in different types of the ferroelectric nanowires as well as in their arrays. The associated electromechanical coupling has the potential to outperform the current state-of-the-art one.

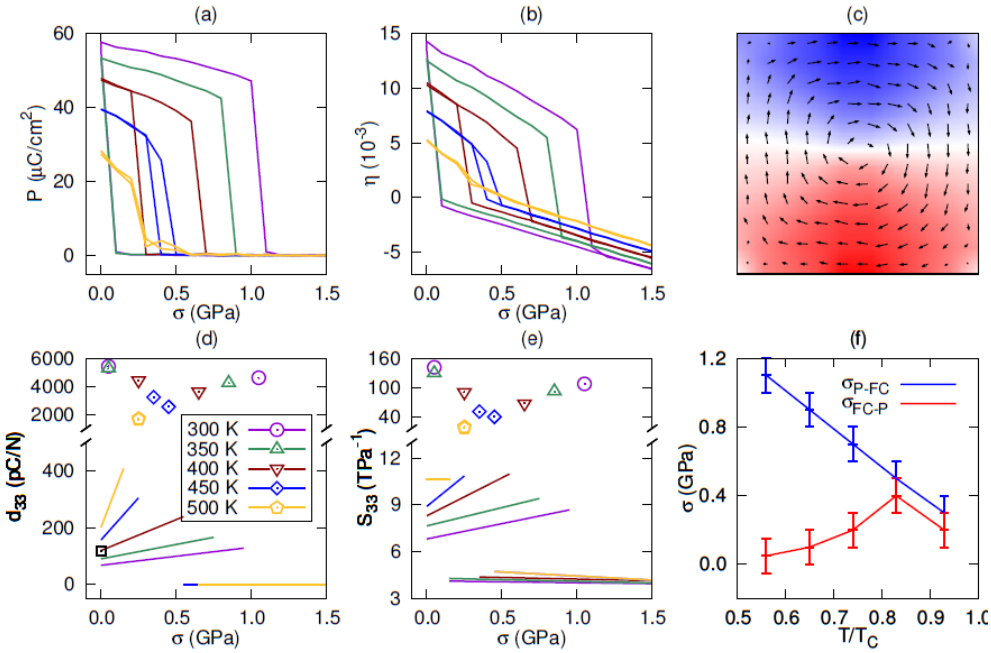

Fig.2. Dependence of the polarization (a), strain component (b), piezoelectric coefficient d_{33} (d) and elastic constant s_{33} (e), on stress applied in quasi-static regime. (c) Schematic visualization of the dipole pattern in the nanowire's cross section for 2.0 GPa stress. (f) Dependence of the critical stresses on the fractional temperature. The error bar indicates the stress step used in simulations.

Future Plans

Our studies this far illustrate the potential of ferroics with energy and, consequently, phase competitions to exhibit unusual properties that could lead to advances in energy usage and conversion. The next step is to further promote such phase competitions through alloying materials with different equilibrium phases. Some examples are ferroelectric-antiferroelectric phase competition in lead titanate zirconate alloys, or ferroelectric-paraelectric phase competition in barium zirconate titanate alloys. Our studies on the advancement of fundamental understanding of phase transitions in ferroics also reveal a critical need for extending the work to the class of ferroics with order-disorder phase transitions, which so far remain far less

understood, especially at the nanoscale. As many emergent ferroelectrics exhibit such type of the phase transition timely addressing this question becomes of paramount importance.

References

1. D. D. Fong, G. B. Stephenson, S. K. Streiffer, J. A. Eastman, O. Auciello, P. H. Fuoss, and C. Thompson, *Ferroelectricity in Ultrathin Perovskite Films*, Science **304**, 1650 (2004)

2. I. I. Naumov, L. Bellaiche, and H. Fu, *Unusual phase transitions in ferroelectric nanodisks and nanorods*, Nature **432**, 737 (2004).

3. S. Matzen, G. Nesterov, O. Rispens, J. A. Heuver, M. Biegalski, H. M. Christen, and B. Noheda, S*uper switching and control of in-plane ferroelectric nanodomains in strained thin films*, Nat. Comm. **5**, 4415 (2014).

4. Z. L. Wang and J. Song, *Piezoelectric Nanogenerators Based on Zinc Oxide Nanowire Arrays*, Science **312**, 242 (2006).

Publications (August 2016 – July 2018)

1. R. Herchig and I. Ponomareva, *Unusual soft mode dynamics in ferroelectric $PbTiO_3$ nanowire under different mechanical boundary conditions*, J. Appl. Phys. **122**, 214103 (2017).

2. Z. Fthenakis and I. Ponomareva, *Dynamics of antiferroelectric phase transition in $PbZrO_3$*, Phys. Rev. B **96**, 184110 (2017).

3. R. Herchig, *Complex Electric-Field Induced Phenomena in Ferroelectric/Antiferroelectric Nanowires*, PhD thesis, University of South Florida (2017).

4. D. Pappas, Z. G. Fthenakis and I. Ponomareva, *All-mechanical polarization control and anomalous (electro)mechanical responses in ferroelectric nanowires*, submitted (2018).

5. Z. Fthenakis and I. Ponomareva, Intrinsic dynamics of the electric-field-induced phase switching in antiferroelectric $PbZrO_3$ ultrathin films, submitted (2018).

Emergent properties of highly correlated electron materials

Principal Investigator: Srinivas Raghu

Department of Physics, Stanford University, Photon Sciences, SLAC National Laboratory, Stanford, CA 94305

Keywords: Unconventional Superconductivity, Quantum criticality, compressible quantum Hall states, statistical mechanics of quenched disorder and interactions.

Project Scope

The primary goal of this program has been to explore robust low energy properties of correlated electron materials in the context of effective model systems. These effective models involve far fewer microscopic degrees of freedom than are present in an actual system. This allows us to identify well-controlled solutions to the theory in various limits and to extract the qualitative, robust features that may carry over to real materials. In certain cases, the models can be solved using exact non-perturbative techniques. Specific issues that have been addressed in this project in the past two years include: 1) effects of quenched disorder and strong interactions on gapless two dimensional quantum matter[P4, P5], 2) physics of compressible states near half-filled Landau levels[P3, P6, P7, P9], 3) superconductivity near a metallic quantum critical point[P2], 4) collaboration with experimental colleagues on correlated materials and interface phenomena[P1, P8].

Recent Progress

Exact boson-fermion duality on 3D Euclidean lattice –

The idea of statistical transmutation plays a crucial role in descriptions of the fractional quantum Hall effect. However, a conjectured duality[R1] between a critical boson and a massless 2-component Dirac fermion extends this notion to gapless systems. This duality sheds light on highly non-trivial problems such as the half-filled Landau level, the superconductor-insulator transition, and surface states of strongly coupled topological insulators. Although this boson-fermion duality has undergone many consistency checks, it had remained unproven. In [P6], the PI, in collaboration with a postdoc Jing-Yuan Chen, and the PI's student Jun Ho Son, constructed the duality in a non-perturbative fashion using an exact UV mapping of partition functions on 3D Euclidean lattice. The work is analogous to earlier lattice constructions of a duality between the 3D XY model and an abelian gauge theory [R2]. The PI has been working on non-relativistic extensions of this duality to make contact with realistic condensed matter systems. The PI has also been studying the effects of quenched disorder using such lattice duality constructions, where one side of the duality is trivially solvable and sheds light on a strongly interacting theory in the presence of quenched disorder[P5].

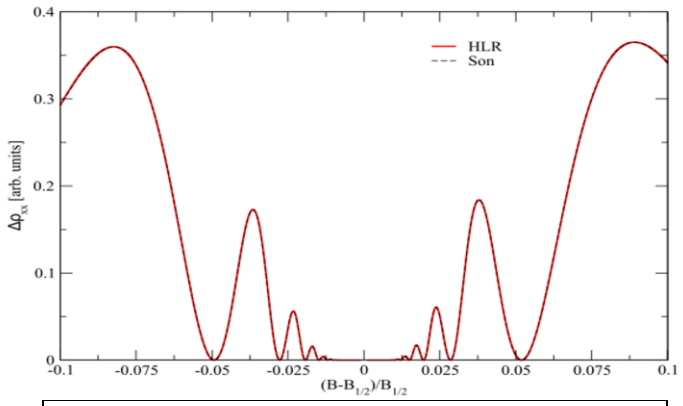

Figure 1: Results for Weiss oscillations in the non-relativistic HLR theory[R2] overlayed with results for Son's theory of Dirac composite fermions[R3].

Magnetoquantum oscillations in the half-filled Landau level –

The gapless ground state near a half-filled Lowest Landau level is one of the best examples of a non-Fermi liquid metal. In [P3], the PI, in collaboration with his student Alfred Cheung and Prof. Michael Mulligan (former postdoc) studied conductance oscillations in the Half-filled Landau level, in the presence of static electric fields, known as Weiss oscillations. Using composite fermion mean-field theory, we found surprisingly that two candidate theories of composite fermions - a non-relativistic theory of Halperin Lee and Read (HLR)[R3], and a theory by D. Son involving Dirac composite fermions[R4] - made identical predictions for Weiss Oscillations.

In a second paper[P7], the PI, with his student Prashant Kumar and Michael Mulligan studied dc transport in the half-filled Landau level using these composite fermion theories. Both lattice models and continuum models were studied and a fully quantum mechanical transport calculation was undertaken, extending previous studies[R5]. We found agreement between HLR and Son's theories, in keeping with a symmetry known as particle-hole symmetry. While the particle-hole symmetry is manifest in Son's Dirac theory, it appears to be explicitly broken in the HLR theory.

In a third paper with Prashant Kumar and Michael Mulligan[P9], we set out to explain these unexpected similarities by showing that with disorder present, both the HLR and Dirac theories sit at a quantum critical point between integer quantum Hall and insulating phases of composite fermions. The quantum critical point exhibits an emergent particle-hole symmetry, which explained the similarities between these two theories. Additionally, the properties of the HLR theory at the critical point can be solved treating disorder *non-perturbatively*, due to a special feature known as supersymmetric quantum mechanics[P9]. This feature enabled us to find a mapping between the HLR and the Dirac theory, valid at least in the disorder-dominated regime. We are currently probing the effect of gauge fluctuations on this equivalence between the two theories.

Effects of quenched disorder on 2D gapless quantum spin liquids –

Spin liquids are exotic materials whose ground states cannot be simply understood as weakly entangled product states of electrons. Several candidate spin liquid materials consist of emergent fermion fields (spinons) that are electromagnetically neutral, but which couple to emergent U(1) gauge fields that arise from strong underlying interactions. In some cases the

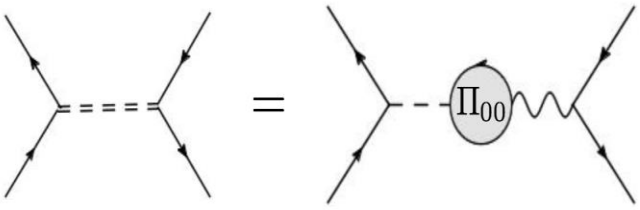

Figure 2: In a Dirac spin liquid, emergent gauge field fluctuations act to screen disorder. Potential disorder is screened by electric gauge fluctuations making the system stable to weak disorder.

spinons are gapless, having a Dirac band structure and at low energies, realizes the problem of 2+1 dimensional quantum electrodynamics, a strongly coupled effective field theory. In [P4], the PI, in collaboration with Pallab Goswami and a former undergrad student Hart Goldman (now grad student at UIUC), studied the effect of quenched disorder in such systems. We found that strong gauge fluctuations lead to spectacularly different behavior in the presence of disorder. For instance, in the presence of weak potential disorder, such systems *do not* undergo Anderson localization, because gauge fluctuations act to screen the disorder. We also found similar conclusions for flux disorder. In the case of a random Dirac mass, the spinons realize a novel finite disorder and finite gauge coupling fixed point corresponding to an interacting dirty metallic phase. We have obtained these results from perturbative renormalization group studies. More recently, we have extended our analysis in the strong coupling limit and obtained non-perturbative results using duality[P5]. In this study, we found that such Dirac spin liquid states realize *perfect* conductors, in which disorder flows to zero in the long wavelength limit. We are extending our conclusions to consider candidate spin liquids having a spinon Fermi surface.

Eliashberg theory versus the renormalization group -

The study of mechanisms of superconductivity in quantum materials, often involves either Eliashberg theory, or the Renormalization group (RG). The former constitute a set of integral equations for the superconducting gap functions and self-energies, whereas the latter are a set of differential equations governing attractive BCS couplings. While clearly the two methods must produce the same physics, they appear to be distinct and often, only one method is preferred. In [P2], we showed exactly how to map the Eliashberg equations for the BCS gap to RG flow equations for the BCS couplings. As an application, we reproduced the classic Macmillan formula for T_c using the RG for the electron-phonon problem, and we studied the problem of superconductivity near a metallic quantum critical point, where recent work by the PI uncovered a quantum critical point with finite, scale-invariant BCS couplings (corresponding to a failed superconductor).

Future Plans

The PI, in collaboration with his student Alfred Cheung, is studying thermal and thermoelectric transport near a 2D magnetic field tuned superconductor-insulator transition, using a recent theory the PI constructed, which exhibits the phenomenon of self-duality at the transition. The goal is to obtain predictions for thermoelectric transport coefficients within the framework of this model.

The PI, in collaboration with his students Alfred Cheung and Yue Yu, is constructing a theory of Strontium Ruthenate, an unconventional triplet superconductor, in the presence of strain. The goal is to study the effects of inhomogeneous strain, as well as competing phases and fluctuation effects.

The PI, in collaboration with his student Jun Ho Son, is studying a recently described web of dualities, in 2 spatial dimensions. The goal is to obtain such dualities in a non-perturbative fashion using lattice construction in conjunction with numerics.

The PI in collaboration with his student Prashant Kumar, is studying network models of quantum Hall plateau transitions. Traditionally, such models are specified in electron coordinates. However, the PI is studying `dual' network models descried in the language of composite fermions. The aim of the project is to see whether critical exponents obtained in such composite fermion network models are closer to those measured in experiment.

References

R1. W. Chen, M.P.A. Fisher, Y.-S. Wu, *Mott transition in an anyon gas*, Phys. Rev. B **48**, 13749 (1993).

R2. C. Dasgupta, B. Halperin, *Phase transition in a lattice model of superconductivity*, Phys. Rev. Lett. **47**, 1556 (1981).

R3. B. Halperin, P.A. Lee, N. Read, *Theory of the half-filled Landau level*, Phys. Rev. B **47**, 7312 (1993).

R4. D.T. Son, *Is the composite fermion a Dirac particle?* Phys. Rev. X **5**, 031027 (2015).

R5. C. Wang, N. R. Cooper, B.I. Halperin, A. Stern, *Particle-hole symmetry in the fermion-Chern-Simons and Dirac descriptions of a half-filled Landau level*, Phys. Rev. X **7**, 031029 (2017).

Relevant Publications (August 2016 – July 2018)

P1. A. G. Swarz, H. Inoue, T. A. Merz, Y. Hikita, S. Raghu, T. P. Deveraux, S. Johnston, H. Y. Hwang, *Polaronic behavior in a weak-coupling superconductor*, PNAS 115, 1475 (2018).

P2. H. Wang, S. Raghu, G. Torroba, *Non-Fermi liquid superconductivity: Eliashberg approach versus the renormalization group*, Phys. Rev. B **95**, 165137 (2017).

P3. A. K. Cheung, S. Raghu, M. Mulligan, *Weiss Oscillations and particle-hole symmetry at the half-filled Landau level*, Phys. Rev. B 95, 235424 (2017).

P4. P. Goswami, H. Goldman, S. Raghu, *Metallic phases from disordered (2+1)-dimensional quantum electrodynamics*, Phys. Rev. B 95, 235145 (2017).

P5. H. Goldman, M. Mulligan, S. Raghu, G. Torroba, M. Zimet, *Two-dimensional conductors with interactions and disorder from particle-vortex duality*, Phys. Rev. B 96, 245140 (2017).

P6. J.-Y. Chen, J. Son, C. Wang, S. Raghu, *Exact boson-fermion duality on a 3D Euclidean lattice*, Phys. Rev. Lett. 120, 016602 (2018).

P7. P. Kumar, S. Raghu, M. Mulligan, *Composite fermion Hall conductivity and the half-filled Landau level*, arXiv:1803.07767 (2018).

P8. A.G. Swarz, A. Cheung, H. Yoon, Z. Chen, Y. Hikita, S. Raghu, H. Hwang, *Superconducting tunneling spectroscopy of spin-orbit coupling and orbital depairing in Nb:$SrTiO_3$*, arXiv:1805:00047 (2018).

P9. P. Kumar, M. Mulligan, S. Raghu, *Why is the HLR theory particle-hole symmetric?* arXiv:1805.06462 (2018).

Ultrafast charge and spin dynamics in functional materials: electron correlations at play

Principal Investigator: Talat S Rahman
Department of Physics, University of Central Florida, Orlando, FL 32816

Keywords: electron correlations, ultrafast charge dynamics, dynamical mean field theory, time dependent density functional theory, demagnetization

Project Scope

Our work focuses on understanding, explaining, and eventually predicting factors that control some striking magnetic, electronic, structural and optical properties of functional nanomaterials both in equilibrium and out of equilibrium, in response to external fields. Since electron correlations may play a role, we also develop and apply reliable and efficient *ab initio* techniques that allow inclusion of such effects. With these beyond density functional theory (DFT) methods, calculations of the ground state and the excitation spectra (*equilibrium* properties) already reveal characteristics distinct from weakly correlated materials. And deeper insights are obtained from calculations in the *non-equilibrium* regime, in their response to ultrafast probes. Comparison with available experimental data provides further grounds for evaluating the contributions of non-adiabatic (memory) effects, which may turn out to be significant. Furthermore, to ensure dynamically stability and to evaluate the role of phonons, we determine system vibrational dynamics and electron-phonon coupling parameters. The research stages include determination of some or all of the following: 1) the lowest energy geometric and electronic structure using reliable schemes (e.g. genetic algorithm); 2) phonon dispersion through density functional perturbation theory (DFPT); 3) magnetic properties via our nano-DFT+DMFT (dynamical mean field theory) code[1]; 5) optical response, using our density matrix based time dependent density functional theory (DM-TDDFT) code[2]; 6) ultrafast charge and spin dynamics with our TDDFT+DMFT[3]. Some examples of recent work include: ultrafast demagnetization of Ni; optical response of pure and transition metal doped arrays of noble metal atom nanochains; optical excitations in mono and few layer transition metal dichalcogenides; and ultrafast charge dynamics in vanadium oxides (VO_2 and V_2O_3).

Recent Progress

Further developments in techniques beyond DFT: Exchange-correlation (XC) kernels such as screened long-range, Slater and bootstrap have been incorporated in the DM-TDDFT code as they are found to work the best for a variety of semiconductors. We have also implemented an efficient algorithm for calculating the absorption and emission spectra of nanomaterials. Furthermore calculation of the four-wave mixing spectra and response to multiple-pulse excitations is now possible, enabling analysis of interaction of multiple excited states. At the same time, in the nano-DFT+DMFT code, the approximate Multi-Orbital Iterative Perturbation Theory (MO-IPT) solver, in which the expression for the single-electron self-energy is a generalization of the expression for the second order in the local Coulomb repulsion parameter self-energy and chosen such that the resulting self-energy satisfies known limiting cases (such as the high-frequency and large-Coulomb repulsion limits), has been supplemented by the exact one based on the Continuous-Time Quantum Monte Carlo (CT-QMC) as implemented in the Abinit code. Finally, the above progress in the DMFT code has enabled extraction of reliable XC kernels for our TDDFT+DMFT approach. We are pursuing extraction of analytical forms for this

exchange correlation functional which would be suitable for broad applications. Some highlights of recent results on charge and spin dynamics in correlated materials is summarized below.

Ultrafast demagnetization dynamics in bulk Ni: While Ni is not known as a material with strong electron correlations, experimental observations of its ultrafast demagnetization (loses about 57% of magnetization within 50 femto second) has remained a puzzle, as theoretical techniques have so far not been able to account for it, other than through disconnected phenomenological models. Through application of the TDDFT+DMFT formulation, we show that proper inclusion of electron correlations and non-adiabatic (time dependence of electron interaction) effects leads to demagnetization (34%) at the femto second time scale, in reasonable agreement with experimental observations (see Fig. 1c). Note that DFT and even adiabatic TDLDA fail badly. Furthermore, we trace this ultrafast demagnetization to spin-flip transitions from occupied to unoccupied orbitals implying a dynamical reduction of exchange splitting. These conclusions are found to be valid for a large range of laser pulse parameters: amplitude, energy, and duration.

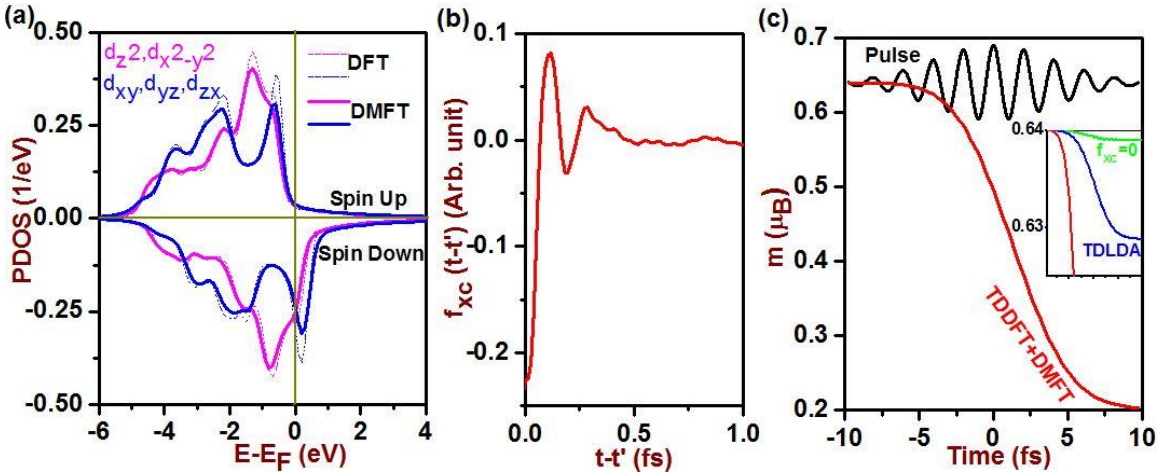

Fig.1. **(a)** The DFT (dashed lines) and DFT+DMFT (continuous lines, T=216K) spin-orbital resolved density of states of bulk Ni. **(b)** Time dependence of the DMFT XC kernel for Ni. **(c)** The demagnetization dynamics obtained for the uncorrelated DFT (green), adiabatic LDA (blue) and non-adiabatic TDDFT+DMFT (red) with the laser pulse (black curve) amplitude 0.05V/Å, duration 7.2fs and energy 2eV.

Spatially-resolved metallization in VO_2: For the perennial Mott insulator VO_2 we have applied TDDFT+DMFT to isolate effects of electron correlations and memory and their consequences for the observed spatially-resolved metallization. Interestingly, the DFT revealed V dimerization along the c_R direction and the presence of two nonequivalent O (see Fig.2a) plays an important role in the observed spatially-nonhomogeneous dynamics. The DFT+DMFT results, obtained for an effective five d-band (V) and three p-band (O) Hubbard model with the on-site Coulomb repulsion U=4eV, and exchange energy J=0.64eV on V atoms, and the inter-site (same-orbital same-spin) interaction within the V dimmers, V=1eV, yield the experimentally observed gap 0.67eV (Fig.2a). TDDFT results show that relaxation to the metallic state takes place at ~50fs, in agreement with experimental data.[4] Time-dependencies of the electron (and hole) chemical potential (Fig.2b), show that non-adiabatic effects slow down the relaxation processes and that the nonadiabatic solution is closer to the experimentally estimated relaxation times, suggesting importance of memory effects. Fig. 2b shows that U "accelerates" the initial growth of metallic domain as a result of enhanced scattering effects. The anisotropic growth of the metallic bubbles and conductivity can be traced to differences in the effective hopping parameters along and perpendicular to the V chains. Nonequivalence of the two sets of O leads to unusual anti-ferroelectric charge ordering (induced potential, Fig. 2c) in good agreement with experimental

data.[5] In particular, strong modification of the potential takes place on atoms close to the V-dimers, as a result of the weaker hybridization with V states. Surprisingly, there is also large charge density redistribution (potential change) in the inter-dimer region after the excitation, implying V-chain-type metallization (anisotropic conductivity) in agreement with data (Fig. 2c).

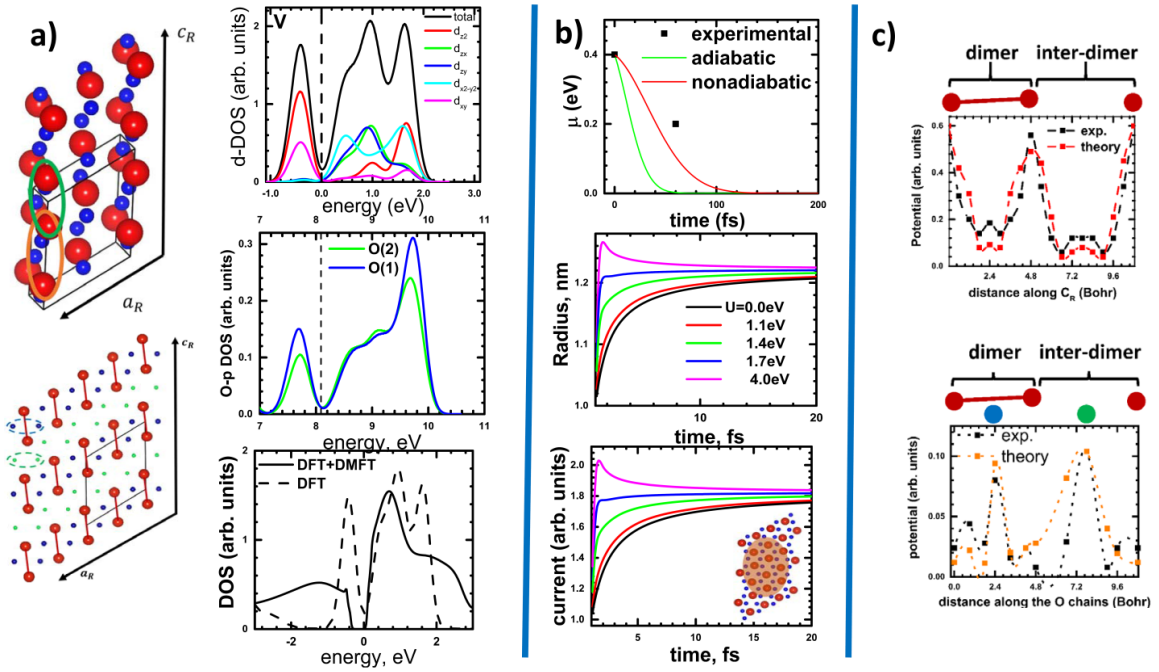

Fig. 2(a) Top left: The VO_2 (M_1) unit cell with V (red) and O (blue): V-dimer along the c_R axis encircled in green and the two unpaired V in orange; Bottom left: V-dimer (red balls and sticks) and two nonequivalent O atoms (blue – close to a dimer, green – close to a non-dimerized V pair). Right: DFT total and projected V d-orbital DOS (top), DFT total p-orbital DOS for the two non-equivalent O (middle), DFT and DFT+DMFT (U=4eV, J=0.65eV, V=1eV) d-orbital DOS for VO_2. The Fermi energy is either at zero or at the dashed line. (b) Top: calculated time evolution of the chemical potential (μ) for a 0.82fs excitation pulse (field E=1eV/Bohr). The non-adiabatic results is in good agreement with experimental data.[4] Middle and bottom: temporal evolution of metallic domain radius and conductivity (along c_R) for $E = 2\frac{eV}{nm}$ (pulse duration 1fs). Bottom insert: metallic bubble schematics elongated ~50% in the direction of V chains. (c) Calculated and experimental[5] pulse-induced modification of the static potential along V chains (top) and along the oxygen atoms (bottom).

Femto second charge dynamics in V_2O_3: Motivated by recent time resolved optical measurements of a fast (ps) increase in conductivity and possible spatially non-homogeneous metallization, we have carried out a TDDFT+DMFT study of the ultrafast charge dynamics to address the following questions: what orbitals are involved in the metallization process, what are the times of the inter-orbital charge transfer accompanying the metallization, what is the role of the memory effects in the fs dynamics? The DMFT calculations performed using MO-IPT with U=5eV, J=1eV obtained the gap ~0.6eV in agreement with experimental data. Furthermore, the low-energy excitation spectrum is found to corresponds to inter-layer transitions between the d-states of V occupying two sub-layers. As shown in Fig. 3c, the excited charge density and the resulting charge conductivity have a power-like time-dependency and their decay depends very much on the local Coulomb repulsion and electron correlations (scattering). Similarly, we find that the size of the excited metallic domains grows power-like at 10fs time scale. The results summarized in the Fig. 3 may help shed light on details of the spatially-resolved ultrafast metallization in V_2O_3 and also provide a test for the inter-layer dimer scenario for the breakdown

of the insulating phase and consequent metallic domain growth in future ultrafast experiments on conductivity and emission in V_2O_3.

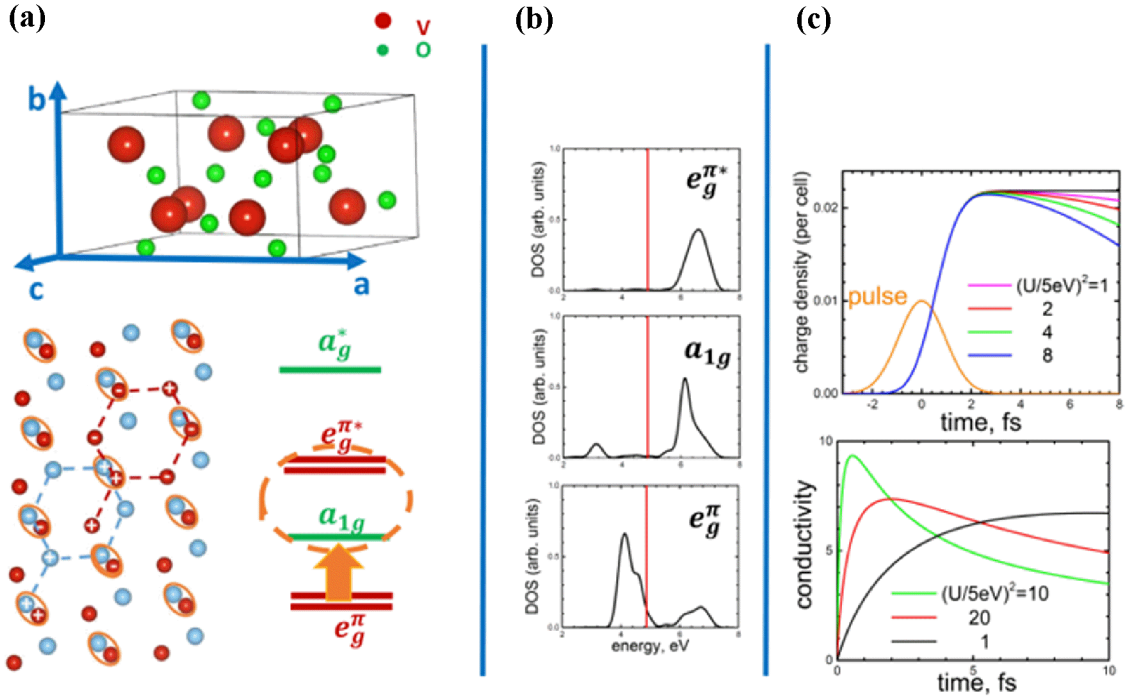

Fig. 3 **(a)** Top: the V_2O_3 unit cell; Bottom: the corresponding double-layer vanadium lattice and sublattices with spin up (+) and spin down (-) electrons; the schematics of the low-energy transitions are also shown. **(b)** The projected density of the d-electron states involved in the low-energy transitions depicted in A. **(c)** Time-resolved excited charge density (top) and conductivity (bottom) at different values of the local Coulomb repulsion U. The laser pulse is shown in orange.

Future Plans

We will extend TDDFT+DMFT to include: 1) the nonlinear regime in which we will use the XC potential instead of the XC kernel. Here, the Sham-Schluter equation will be used to express XC potential in terms of the electron self-energy; 2) spatial fluctuations, i.e. inclusion of momentum-dependence in electron self-energy and charge susceptibility. This will be done using the so-called Dynamical Vertex Approximation, successfully developed in the framework of DMFT. Two new directions will be also pursued for DM-TDDFT: 1) search for accurate and universal (for excitonic effects) XC kernel by analyzing solution of the Bethe-Saltpeter equation for susceptibility and 2) expression for simple yet accurate XC potential to describe strongly-perturbed systems (as starting point several long-range kernels already proposed in the literature will be tested). We will also continue to examine the optical (and magnetic properties) of a number of systems (as proposed by us) with attention to the role of electron-phonon coupling.

References

1. A. Kabir, V. Turkowski, and T.S. Rahman, J. Phys. Condens. Matt. 27, 125601 (2015).
2. A. Ramirez-Torres, V.Turkowski, and T. S. Rahman, Phys. Rev. B 90, 085419 (2014).
3. V. Turkowski and T.S. Rahman, Journal of Physics: Condensed Matter 29, 455601 (2017).
4. D. Wegkamp, M. Herzog, L. Xian, M. Gatti, P. Cudazzo, C.L. McGahan, R.E. Marvel, R.F. Haglund, Jr., A. Rubio, M. Wolf, and J. Stähler, Phys. Rev. Lett. **113**, 216401 (2014).
5. A. Pashkin, C. Kübler, H. Ehrke, R. Lopez, A. Halabica, R. F. Haglund, Jr., R. Huber, and A. Leitenstorfer Phys. Rev. B **83**, 195120 (2011).

Selected Publications (2016-2018)

PI: Talat Rahman

Grant Acknowledged: DOE DE-FG02-07ER46354

1. W. Keune, S. Hong, M.Y. Hu, J. Zhao, T.S. Toellner, E.E. Alp, W. Sturhahn, T.S. Rahman, and B. Roldan Cuenya, "Influence of interfaces on the phonon density of states of nanoscale metallic multilayers: Phonon confinement and localization," Physical Review B **98**, 024308 (2018). DOI:10.1103/PhysRevB.98.024308
2. K. Kuhnke, V. Turkowski, A. Kabakchiev, T. Lutz, T.S. Rahman, and K. Kern, "Pentacene Excitons in Strong Electric Fields," Chemphyschem **19**, 277-283 (2018). DOI:10.1002/cphc.201701174
3. J. Paul, C.E. Stevens, H. Zhang, P. Dey, D. McGinty, S.A. McGill, R.P. Smith, J.L. Reno, V. Turkowski, I.E. Perakis, D.J. Hilton, and D. Karaiskaj, "Coulomb-interaction induced coupling of Landau levels in intrinsic and modulation-doped quantum wells," Physical Review B **95**, 245314 (2017). DOI:10.1103/PhysRevB.95.245314
4. V. Turkowski, N.U. Din, and T.S. Rahman, "Time-Dependent Density-Functional Theory and Excitons in Bulk and Two-Dimensional Semiconductors," Computation **5**, 39 (2017). DOI:10.3390/computation5030039
5. V. Turkowski and T.S. Rahman, "Nonadiabatic exchange-correlation kernel for strongly correlated materials," Journal of Physics: Condensed Matter **29**, 455601 (2017). DOI:10.1088/1361-648X/aa8ac1
6. S. Acharya, V. Turkowski, and T.S. Rahman, "Towards TDDFT for Strongly Correlated Materials," Computation **4**, 34 (2016). DOI:10.3390/computation4030034
7. C.J. Páez, K. DeLello, D. Le, A.L.C. Pereira, and E.R. Mucciolo, "Disorder effect on the anisotropic resistivity of phosphorene determined by a tight-binding model," Physical Review B **94**, 165419 (2016). DOI:10.1103/PhysRevB.94.165419
8. P. Patoka, G. Ulrich, A.E. Nguyen, L. Bartels, P.A. Dowben, V. Turkowski, T.S. Rahman, P. Hermann, B. Kästner, A. Hoehl, G. Ulm, and E. Rühl, "Nanoscale plasmonic phenomena in CVD-grown MoS_2 monolayer revealed by ultra-broadband synchrotron radiation based nano-FTIR spectroscopy and near-field microscopy," Optics Express **24**, 1154-1164 (2016). DOI:10.1364/OE.24.001154
9. J. Paul, C.E. Stevens, C. Liu, P. Dey, C. McIntyre, V. Turkowski, J.L. Reno, D.J. Hilton, and D. Karaiskaj, "Strong Quantum Coherence between Fermi Liquid Mahan Excitons," Physical Review Letters **116**, 157401 (2016). DOI:10.1103/PhysRevLett.116.157401
10. S.R. Acharya, V. Turkowski, and T.S. Rahman, "Ultrafast demagnetization dynamics in bulk Ni: a non-adiabatic TDDFT+DMFT study," Preprint available. https://physics.ucf.edu/~talat/preprints/Acharya-2017-Ni.pdf

Physical Analysis of the Bulk Photovoltaic Effect for Solar Harvesting Materials

Principal investigator: Professor Andrew M. Rappe

Department of Chemistry, University of Pennsylvania

rappe@sas.upenn.edu

Keywords: Bulk photovoltaic effect, Ferroelectric, Solar materials

Project Scope

The primary goal of this program is to understand and design bulk photovoltaic effect (BPVE) materials by developing and using theoretical approaches based on density functional theory. The most attractive feature of the BPVE is the generation of above-band gap photovoltages, which offers a route to overcome the Shockley−Queisser limit of the p−n junction PV technology, where the open-circuit voltage is limited by the fundamental band gap of bulk semiconductors.

In this project, we propose to expand our BPVE research along two aspects. One emphasis is to study new physics of BPVE, including the ballistic current mechanism, temperature effect and phonon influence on shift current, as well as exciton effect on shift current. Better understanding of their effects influence on BPVE can extend our knowledge of how to design the next-generation ferroelectric solar cell. The other emphasis is exploring new material classes for solar harvesting based on BPVE. We propose to study many narrow band-gap ferroelectric semiconductors, including organic and hybrid materials, layered two dimensional materials, and low dimensional polar organic materials.

Recent Progress

Below, we highlight progress made in the last two-year award period (August 2016 – July 2018). Progress has been made in finding novel strategies for enhancing photovoltaic effects [1-3], better understanding of photovoltaic materials, including effects of temperature[4], dopants[5] and improper ferroelectricity induced by frustrated magnetism[6], and methodological development supporting these efforts [7].

Novel strategies for enhancing photovoltaic effects

We have revealed novel strategies for enhancing photovoltaic effects, including spin-orbit coupling [1], dimensional reduction [2] and polar order engineering [3].

1) *Spin-orbit enhanced carrier lifetimes in noncentrosymmetric semiconductors.* We showed that strong spin-orbit coupling enhances the photovoltaic properties of some noncentrosymmetric semiconductors, by inducing a spin splitting of frontier orbitals and modifying their carrier lifetimes. We performed a large-scale density functional theory (DFT) screening study to identify candidate materials that display this effect. We find transition

dipole moment enhancement factors of up to three orders of magnitude, reflecting the physical impact of spin-orbit coupling on the carrier lifetime.

As a result of this study, we devised materials design rules for systems displaying this mechanism. We propose that materials with heavy atoms in low-coordinated environments are likely to display this mechanism. In particular, 3-fold and 4-fold coordination numbers are particularly favorable, as they break local inversion symmetry, leading to Rashba-type spin splitting of bands. On the other hand, we find that the bulk polarization is inconsequential. This paper provides a route to discovering new materials with large photovoltaic effects, and suggests that further explorations of the spin-orbit coupling and lattice symmetry could prove to be useful for manipulating the photophysics of materials.

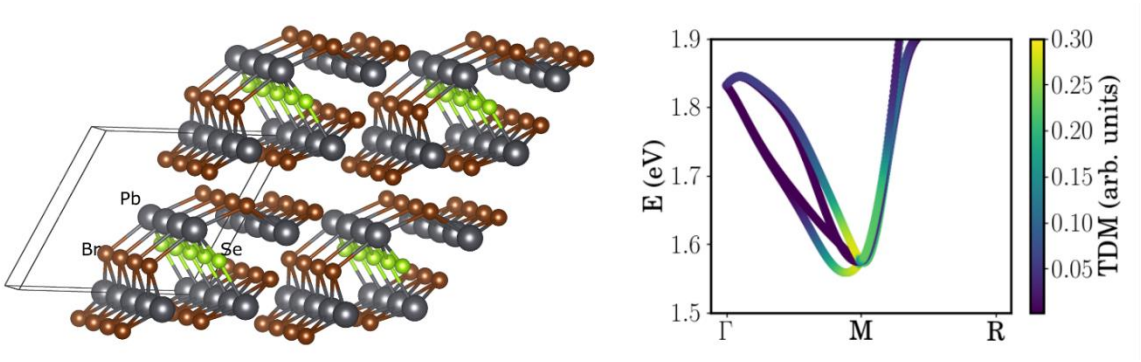

Figure 1: Crystal structure of Pb_4SeBr_6 (left), and transition dipole moments of the four lowest-energy transitions between valence and conduction bands (right), with color representing the magnitude of transition dipole moments, showing spin-orbit suppressed and enhanced transitions. Adapted from *J. Phys. Chem. Solids* ASAP (2018)

2) *Bulk photovoltaic effect enhanced in low-dimensional polar organic materials*. With a strategy designed to break the inversion symmetry along the polymer chain, we demonstrate that conjugated vinylene-linked hybrid heterocyclic polymers can produce a strong bulk photovoltaic response to light, outperforming benchmark inorganic materials. The high current density results from the delocalized wave functions, composed mainly of carbon p orbitals. The great structural and electronic flexibility of polymers offers a robust paradigm to enhance the shift current response through chemical and physical modifications. This work suggests that the development of polymer blends with polymers of different band gap is a way to use the whole visible light spectrum for energy conversion.
3) *Enhancing ferroelectric photovoltaic effect by polar order engineering*. Another strategy for enhancing photovoltaic effects that we have developed is the use of polar order engineering. While ferroelectric materials for photovoltaics have sparked great interest because of their switchable photoelectric responses and above-bandgap photovoltages, it is still not known if conventional strategies that focus mainly on narrowing the bandgap to better match the solar spectrum would be the best way to improve their performance. Thus far, the fundamental connection between polar order and photovoltaic effect has been largely overlooked. In this work, we report large photovoltaic enhancement by *A*-site substitutions in a model ferroelectric photovoltaic material, $BiFeO_3$. As revealed by theoretical calculations and optical measurements, the enhancement is accompanied by the chemically driven rotational

instability of the polarization, which, in turn, affects the charge transfer at the band edges and drives a direct-to-indirect bandgap transition, highlighting the strong coupling between polarization, lattice, and orbital order parameters in ferroelectrics. Polar order engineering thus provides an additional degree of freedom to further boost photovoltaic efficiency in ferroelectrics and related materials.

Better understanding the polar photovoltaic materials.

4) *Phonon influence on bulk photovoltaic effect.* We explore the changes of shift current response induced by phonon vibrations in the prototypical ferroelectric GeTe, which have a large shift current response due to its intrinsic narrow band gap and high covalency. We found that the shift current response in GeTe is about 5 times larger than that of multiferroic $BiFeO_3$, whose strong ferroelectricity favors the large shift current response while the relatively large band gap suppresses it. Through the representative phonon vibration modes, including phonon vibrations at the Γ point, and the antiferroelectric mode at the finite phonon wave vector, we explore the phonon influence on the shift current response.

   Furthermore, we demonstrate the temperature dependence of the shift current response by averaging the phonon vibration influence in the Brillouin zone. Our investigation provides an explicit experimental prediction about the temperature dependence of BPVE and can be extended to other classes of noncentrosymmetric materials.

5) *Accurate Electronic Band Structure Calculations for Doped $BiFeO_3$.* In past award period, we demonstrate $BiFeO_3$ as a photovoltaic, highlighting it as a viable candidate for ferroelectric-based photovoltaic devices. In order to guide the numerous research efforts in photovoltaic application, we investigate the influence of many dopants onto the electronic structure of $BiFeO_3$. By comparing the conventional DFT results for alkali and alkaline-earth metal doping with more accurate hybrid-DFT calculations, we show that the problems of standard DFT go beyond a simple systematic error. Conventional DFT shows bad transferability and the more reliable hybrid-DFT has to be chosen for a qualitatively correct prediction of doping induced changes in the electronic structure of $BiFeO_3$. Our findings could guide higher accuracy predictions of photovoltaic properties of $BiFeO_3$ under the dopants influence.
6) *Improper magnetic ferroelectricity in helicoidal spiral $CaMn_7O_{12}$.* Helicoidal magnetic order breaks inversion symmetry in quadruple perovskite $CaMn_7O_{12}$, generating one of the largest spin-induced ferroelectric polarizations measured to date. We explore the microscopic orgin of the polarization including exchange interaction, coupling to the spin helicity, and charge density redistribution via first principle calculation. Berry phase computed polarization (P = 2169 $\mu C/m^2$) exhibits nearly pure electronic behavior, with negligible Mn displacements (≈ 0.7 mA). Persistent electronic polarization induced by helical spin order in the nearly inversion-symmetric ionic crystal lattice suggests opportunities for ultrafast magnetoelectric response and potential bulk photovoltaic application in multiferroic.

Methodological development - hybrid functional pseudopotentials

7) The results outlined in this section, are made possible by advances in computational methodology. The methodological component of this research program in photovoltaics aims

to improve the accuracy of electronic structure calculations, which will lead to more reliable predictions of photovoltaic phenomena. This particular work improves hybrid functional calculations, which are one of the few methods thought to be able to calculate band gaps reliably. However, routine hybrid density functional calculations at present are not fully self-consistent, relying on generalized gradient approximation pseudopotentials due to the lack of hybrid functional pseudopotentials. We presented a scheme for generating hybrid functional pseudopotentials, and analyzed the importance of pseudopotential density functional consistency for hybrid functionals. For the PBE0 hybrid functional, we benchmarked our pseudopotentials for structural parameters and fundamental electronic gaps of the Gaussian-2 (G2) molecular dataset and some simple solids. Our results show that using our PBE0 pseudopotentials in PBE0 calculations improves agreement with respect to all-electron calculations, and enables higher accuracy predictions of photovoltaic properties.

Future Plans

Other mechanisms contributed to the BPVE

In the past award period, we have demonstrated the shift current as the primary mechanism of the BPVE in $BaTiO_3$ and $PbTiO_3$. Ballistic current mechanism was also considered as a primary contribution, e.g. the BPVE in GaAs. Such processes rely on the generation of an asymmetric distribution of nonthermalized carriers, in contrast to the coherent evolution in the shift current mechanism. Up to date, no first-principles methodology has been developed in calculation of ballistic photocurrent. In doing so, we will obtain the theoretical framework of ballistic current with consideration of electron-phonon scattering.

We also plan to optimize our calculation of shift current by considering many effects, such as temperature effects and many-body effects. Building upon our work on phonon influence on shift current in GeTe, we will continue our investigation into the shift current repose of the temperature effect. We propose to study the shift current of GeTe and SbSI including the lattice expansion effect caused by temperature and the band-structure renormalization induced by electron-phonon interaction. To understanding the many-body effect influence on shift current, we propose to investigate the shift current of three-dimensional and two-dimensional ferroelectric with considering the *GW* correction and Bethe-Salpeter equation for exciton effect influence.

New classes of materials for BPVE

Based on our earlier work on the BPVE response of the polar compounds $LiAsS_2$ and $LiAsSe_2$, we propose to study similar structure materials: group-IV monochalcogenides. This class of material represented by few layer SnTe has been confirmed as the two-dimensional room-temperature ferroelectric in experiment. We expect their high spontaneous polarization and narrow band gap will enhance the BPVE performance. The study of BPVE in these materials will help us understand the relationship between the structure and the shift current response from a more fundamental point of view, providing more explicit materials design principles for higher BPVE performance in polar materials.

Most Relevant Publications (2017-2018)

1. Liang Z. Tan, and Andrew M. Rappe. *Spin-orbit enhanced carrier lifetimes in noncentrosymmetric semiconductors*. Journal of Physics and Chemistry of Solids (2018).
2. Shi Liu, Fan Zheng, and Andrew M. Rappe. *Giant bulk photovoltaic effect in vinylene-linked hybrid heterocyclic polymer*. The Journal of Physical Chemistry C **121**, 6500-6507 (2017).
3. L. You, F. Zheng, L. Fang, Y. Zhou, L. Z. Tan, Z. Zhang, G. Ma, D. Schmidt, A. Rusydi, L. Wang, L. Chang, Andrew. M. Rappe, and Junling Wong. *Enhancing ferroelectric photovoltaic effect by polar order engineering*. Science advances, **4**, eaat3438 (2018).
4. S. Gong, F. Zheng, and Andrew M. Rappe. *Phonon Influence on Bulk Photovoltaic Effect in the Ferroelectric Semiconductor GeTe*. Physical Review Letters **121**, 017402 (2018).
5. Julian Gebhardt, and Andrew M. Rappe. *Accuracy and Transferability of Ab Initio Electronic Band Structure Calculations for Doped BiFeO3*. Journal of Physics: Conference Series. **921**, 012009 (2017).
6. Jin Soo Lim, Saldana-Greco Diomedes, and Andrew M. Rappe. Improper magnetic ferroelectricity of nearly pure electronic nature in helicoidal spiral $CaMn_7O_{12}$. Physical Review B **97**, 045115 (2018).
7. Jing Yang, Liang Z. Tan, and Andrew M. Rappe. *Hybrid functional pseudopotentials*. Physical Review B **97**, 085130 (2018).

Extending the Reach of Computational-Theoretical Methods to Materials at the Energy Frontier

PI Fernando A. Reboredo, Co PIs Mao-Hua Du, Markus Eisenbach, Jaron T. Krogel
Materials Science and Technology Division, Oak Ridge National Laboratory

Keywords: many-body, magnetism, defects, disorder, computing

Project Scope

This program is designed to overcome challenges that are both at the frontier of basic-energy-relevant materials research and address problems beyond current theoretical and computational capabilities. Many properties of correlated oxides, magnetic materials, interfaces and reduced dimensionality systems are currently beyond the accuracy of standard Density Functional Theory (DFT). Our goal is to significantly improve our description and understanding of electronic correlations, magnetic interactions, and quantum phenomena modified by defects, disorder and dimensional reduction in an *ab initio* framework. We are: 1) improving diffusion Monte Carlo (DMC) methods and applying them to strongly correlated transition metal oxides, oxide interfaces, and defect phenomena, 2) Developing first principles multiple scattering methods to understand the statistical physics of magnetic materials, disorder and alloys, and 3) Designing and controlling reduced dimensional systems and composite nanostructured solids. This program includes both accurate *ab initio* approaches and method development on model systems, allowing rapid testing and subsequent extension to real materials. Our priority is to develop and apply new theories going well beyond current approaches to exploit high-performance computers (HPC). We thus focus on stochastic DMC and Wang-Landau (WL) methods because of both accuracy and scalability in HPC. Accordingly, we aim to improve the state of the art using highly accurate DMC or including temperature in DFT approximations with WL. We will quantify errors in ubiquitous DFT approximations. We will describe correlation, disorder, interfaces and 2D materials with potential energy applications with accuracy comparable to experimental needs in large physically-relevant systems.

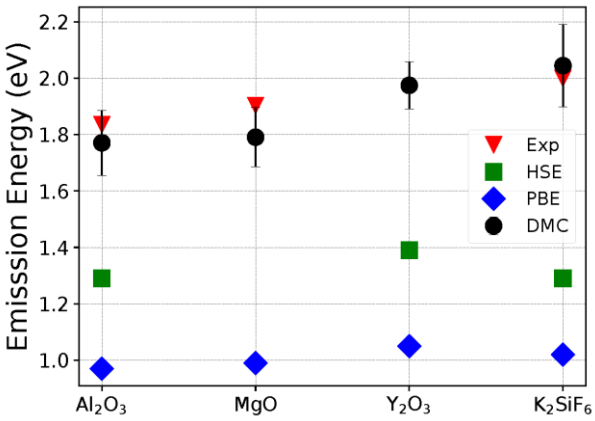

Figure 1: Excitations of a Mn impurity in different oxides calculated with DMC and two approximations of DFT (HSE and PBE) compared with available experimental data. [1]

Recent Progress

Excitation energies of localized correlated defects via many-body ab initio diffusion quantum Monte Carlo: Defects, dopants, and interfaces dominate the optical properties of insulators and

semiconductors. Using Mn4+-doped solids as our test case, we show [1] that DMC is able to predict phosphorescence emission energies within statistical error. We also identify a new material with an emission energy 1.97(8) eV which is close, within the error bar, to the optimum of 2.03 eV, for a red emitting phosphor. To our knowledge, our work is the first report on studying a transition metal impurity using an ab initio many-body electronic structure method. DMC presents a significant improvement over density functional theory (DFT). Semi-local and hybrid DFT largely underestimates and fails to reproduce the trends in the emission energies. Our work underscores the importance of an accurate account of exchange, correlation and excitonic effects for localized excitations in defective solids.

Magnetic Anisotropy in FePt Nano-Particles: The theoretical description of magnetic devices requires knowledge of the magneto-crystalline anisotropy energy (MAE) at a local level, which cannot easily be accessed experimentally. Thus, there exists a need for calculations of the MAE at the device level for real materials beyond idealized crystal structures to explain experimental observations. We have demonstrated that we can understand theoretically the magnetic properties of a real FePt nano-particles [2], based on the atomic positions and chemical composition of a real FePt particle that was described experimentally with atomic resolution. We calculated the spatially resolved spin and orbital magnetic moments as well as the magneto-crystalline anisotropy of this particle, taking into account the deviation from the ideal FePt crystal structure. Thus, our calculations account for local anti-site defects, anti-phase boundaries and, most importantly, the contribution of L10 and L12 grain boundaries to the MAE, see Figure 2. The calculations were performed using our fully-relativistic LSMS code that solves the Dirac equation for electrons in solid state systems within a DFT framework. This work demonstrates the utility of combining first principles calculations for large systems with experimental characterization. This can be applied to a variety of systems with scientific interest.

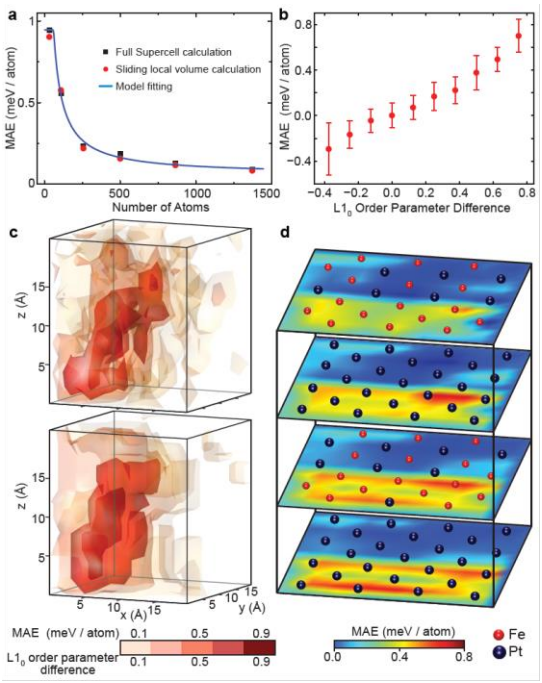

Figure 2 Local MAEs calculated for (a) various volumes sizes cut from the FePt nano-particle and compared to a model of L10 inside a L21 matrix. (b) and (c) calculated local MAE (c top) compared to the experimentally measured L10 order

Electronic structure, defects, and impurities in hybrid organic-inorganic and inorganic halide perovskites: $CH_3NH_3PbI_3$ and related halide perovskites have recently been investigated for a wide range of applications, including photovoltaics light-emitting diodes lasers and radiation detection. The understanding and prediction of the electronic properties of defects is this large

class of materials is critically important but is still rather limited. We have made important contribution to the understanding of the role of ns2 cations (the cations with outer electron configuration of ns2, such as Pb2+, Sn2+, Ge2+, Bi3+) in the electronic structure, the properties of native defects, defect complexes, and impurities, ion migration and the related current-voltage hysteresis in solar cells, the growth mechanisms and the chemical stability of halide perovskites as well as the physical properties of Ge- and Bi-based halides, chalcohalides, and oxyhalides. In order to understand transport and trapping, we have systematically studied charge transition levels for native defects and defect complexes in $CH_3NH_3PbI_3$. [3]

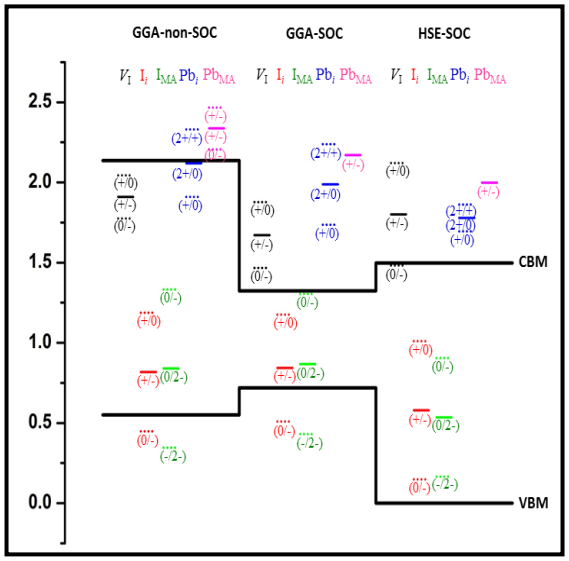

Figure 3: Charge transition levels of V_I, I_i, I_{MA}, Pb_i, and Pb_{MA} in $CH_3NH_3PbI_3$ calculated using GGA-non-SOC, GGA-SOC, and HSE-SOC calculations.

Strong correlation, interfaces, and defects in ferrite superlattices:

Though correlations, interfaces, and defects have each been a significant challenge for ab-initio theories, we showed for the first time that they can be handled simultaneously in a DMC calculation. [4] This is now possible thanks to (1) continuous improvement in methods, codes, and pseudopotentials and (2) their testing in simpler systems done both by us and colleagues in the field. Highly accurate Diffusion Monte Carlo calculations were performed for oxygen vacancies in a $SrFeO_3$/$(LaFeO_3)2$ superlattice (see Figure 4). Oxygen dynamics is key in fuel cells and oxygen concentration is a factor determining the critical temperature of superconducting cuprates. Interfaces are known to change the natural properties of bulk materials. Using high performance computers we can predict with DMC how defects, interfaces and correlations interplay in novel artificial functional materials. In this case, interfaces can be used to control the direction of oxygen transport. This study was preceded by benchmark DMC calculations on the formation energies and migration energy barriers of oxygen vacancies on the parent compounds ($SrFeO_3$ and $LaFeO_3$), [5] where there was experimental information available that allowed us to establish the

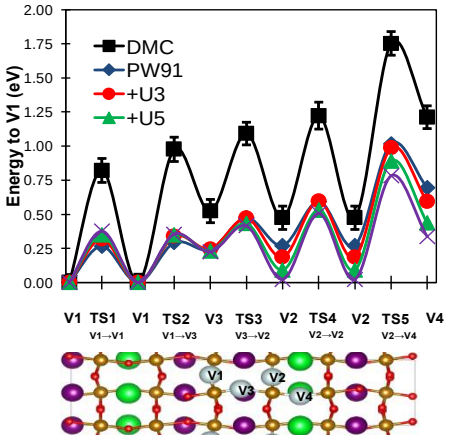

Figure 4 Formation energy and transition energy barriers of an oxygen vacancy at different minima in a $(SrFeO_3)_1/(LaFeO_3)_2$ superlattice. Highly accurate DMC results are compared with approximations of density functional theory [4,5].

validity of our approach before studying the superlattice case. The differences in density profile induced by oxygen dopants calculated on the parent compounds with DMC and several approximations of DFT illuminate the corrections that should be made in DFT methods.

Future Plans

Strongly correlated transition-metal oxide perovskites, interfaces between oxides superlattices and interfaces: We have reached the maturity and confidence required to address problems of immediate interest for the material's experimental program at ORNL. In the area of DMC, our program has been gradually changing emphasis from fundamental theoretical development to the construction of the building blocks for calculations of real materials. That next stage included, for example, the development and testing of pseudopotentials. The following step was to test our pseudopotentials on simple transition metal oxides (TMOs. After our theoretical methods were compared with experiments in some examples of perovskites involving transition metals, and other binary oxides involving two transition metals. We established the accuracy of our DMC approach by direct comparison calorimetric data. We are now in position to address more complex problems. The possibility to calculate artificial materials and nanostructures is currently taking most of our attention. We have already performed a proof of principle of what can be done with DMC for the case of the ferrite superlattices mentioned above. While future studies will require similar prior validation and benchmark steps, we can now claim that calculations of other superlattices and interfaces are within reach.

Develop first principles multiple scattering methods to understand the statistical physics of magnetic materials, disorder and alloys: We will advance the understanding of the behavior of disordered materials, multi-component alloys and magnetic materials at zero and finite temperatures from first principles. We will achieve this, by applying O(N) multiple-scattering theory, Wang-Landau Monte-Carlo and combined spin and molecular dynamics simulations in conjunction with DMC methods to evaluate the quality of the DFT approximations underlying our calculations.

Design and control reduced dimensional systems and composite nanostructured solids: Optoelectronic and luminescent properties in novel energy materials based on complex multinary compounds and low-dimensional nanostructures are strongly modified by defects, dopants, and excitons. However, the accurate theoretical treatment of excited-state properties, electron correlation at transition/rare-earth metal dopants, and charge trapping at defects in these materials remains challenging. We will develop methodologies to provide descriptions of exciton excitation/emission, excited-state relaxation, optical transitions at transition/rare-earth metal dopants.

References

1. K. Saritas, W. Ming, M.-H. Du, and . A. Reboredo, *Excitation energies of localized correlated defects via many-body ab initio diffusion quantum Monte Carlo*, (submitted to Nat. Comm. Phys).
2. Y. Yang, C.-C. Chen, M. C. Scott, C. Ophus, R. Xu, A. Pryor, Jr., L. Wu, F. Sun, W. Theis, J. Zhou, M. Eisenbach, P. R. C. Kent, R. F. Sabirianov, H. Zeng, P. Ercius, and J. Miao, *Deciphering chemical order/disorder and material properties at the single-atom level*, Nature, **542,** 75 (2017).
3. W. Ming, D. Yang, T. Li, L. Zhang, and M. H. Du, *Formation and diffusion of metal impurities in perovskite solar material CH3NH3PbI3: Implications on solar cell degradation and choice of electrode*, Adv. Sci., Adv. Sci. **5**, 1700662 (2018); and references there in.
4. J. A. Santana, R. Mishra, J. T. Krogel, A. Borisevich, P. R. C. Kent, S. T. Pantelides, and F. A. Reboredo, *Quantum many-body effects in defective transition-metal-oxide superlattices*, J. Chem. Theory Comput. **13,** 5604 (2017).
5. J. A. Santana, J. T. Krogel, P. R. C. Kent, F. A. Reboredo, *Diffusion quantum Monte Carlo calculations of SrFeO3 and LaFeO3*, J. Chem. Phys. **147,** (3) 034701, (2017).

Ten Most Recent Intellectually Lead Publications:

1 Wenmei Ming, Dongwen Yang, Tianshu Li, Lijun Zhang, and Mao-Hua Du, *"Formation and diffusion of metal impurities in perovskite solar material $CH_3NH_3PbI_3$: Implications on solar cell degradation and choice of electrode," Adv. Sci.* **5**, 1700662 (2018). Pub ID 75007

2 Jaron T. Kroger and Fernando A. Reboredo, *"Kinetic energy classification and smoothing for compact B-spline basis sets in quantum Monte Carlo," J. Chem. Phys*. **148,** 044110 (2018). Pub ID 103110

3 Xianglin Liu, Yang Wang, Markus Eisenbach, and G. Malcolm Stocks, *"Fully-relativistic full-potential multiple scattering theory: A pathology-free scheme," Comput. Phys. Commun*. **224** (2018). Pub ID 74399

4 Wenmei Ming, Hongliang Shi, and Mao-Hua Du, *"Doping Y2O3 with Mn4+ for Energy-Efficient Lighting"* Journal of Materials Chemistry C, 6, 4171 (2018). Pub ID 108350

5 A. L. Dzubak, C. Mitra, M. Chance, S. Kuhn, G. E. Jellison, A. S. Sefat, J. T. Krogel, and F. A. Reboredo, *$MnNiO_3$ revisited with modern theoretical and experimental methods*, *J. Chem. Phys.* **147**, 174701 (2017).

6 J. A. Santana, R. Mishra, J. T. Krogel, A. Y. Borisevich, P. R. C. Kent, S. T. Pantelides, and F. A. Reboredo, *Quantum many-body effects in defective transition-metal-oxide superlattices*, *J. Chem. Theory Comput.* **13**, 5604 (2017).

7 A. Dzubak, J. T. Krogel, F. A. Reboredo, *Quantitative estimation of localization errors of 3d transition metal pseudopotentials in diffusion Monte Carlo*, *J. Chem. Phys.* **147** (2) 024102, (2017).

8 J. A. Santana, J. T. Krogel, P. R. C. Kent, F. A. Reboredo, *Diffusion quantum Monte Carlo calculations of $SrFeO_3$ and $LaFeO_3$*, *J. Chem. Phys*. **147**, (3) 034701, (2017).

9 V. Sharma, A. Herklotz, T. Z. Ward, F. A. Reboredo, *Designing functionality in perovskite thin films using ion implantation techniques: Assessment and insights from first-principles calculations*, *Sci. Rpt*. **7**, 11166, (2017).

10 M.-H. Du, *Hybrid organic-inorganic halide perovskites: Electronic structure, dielectric properties, native defects, and the role of ns^2 ions, in Theoretical Modeling of Organohalide Perovskites for Photovoltaic Applications*, Edited by Giacomo Giogi and Koichi Yamashita, CRC Press, Boca Raton, FL, (2017).

New Dimensions in the Theory of Excited States and X-ray Spectra

Principal investigator: John J. Rehr, Dept. of Physics, University of Washington, Seattle, WA 98195-1560, jjr@uw.edu

Keywords: x-ray, cumulant Green's function, GW, exchange-correlation, finite temperature

Project scope

Next-generation x-ray sources have the potential for investigations of materials with unprecedented precision over multiple length, time, and temperature scales. However, current theoretical techniques are inadequate to take full advantage of these opportunities. A complete understanding involves many aspects of condensed matter theory, and in particular, the treatment of many-body correlation effects over several dimensions including real-space, time-dependence and finite-temperature. Thus our project aims to develop quantitative theories for calculating excited states and spectra of materials in all of these regimes. These developments are crucial for interpretations of experimental spectra. Much of our current research is based on cumulant-Green's function methods that go beyond independent particle methods to treat many-body effects. We also aim to make these developments available in advanced software that can be used by investigators in university, industrial, and government laboratories. Besides contributing to fundamental understanding of condensed matter physics, our research will enable many quantitative investigations of complex materials of broad scientific and technological interest.

Recent Progress

Finite temperature cumulant Green's function approach − Understanding matter in extreme conditions is an important challenge in many fields, ranging from plasma- and astrophysics to inertial confinement fusion and x-ray spectroscopy with XFEL sources. A significant advance from our research has been the development of a finite-temperature (FT) extension of the retarded cumulant Green's function approach. This permits calculations of both excited-state and thermodynamic properties of electronic systems [1], and has become a major focus of our current research. Such excited state effects are generally inaccessible to conventional zero temperature density functional theory (DFT) or even quantum Monte Carlo (QMC) methods. Briefly, this approach uses an exponential representation of the Green's function in the time-domain $G(t)=G_0(t)e^{C(t)}$, and has been found to be advantageous compared e.g., to the GW approximation, a standard method for going beyond DFT. Our method incorporates a cumulant $C(t)$ linear in the RPA

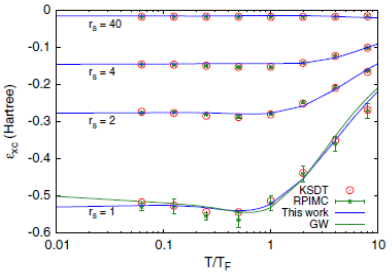

Figure 1. FT exchange-correlation energy ε_{xc} vs T/T_F and density r_s,: cumulant (blue), GW (green), path integral Monte-Carlo (crosses) and FT DFT (circles)

screened Coulomb interaction W and is no more difficult to calculate than the GW self-energy. Results for the homogeneous electron gas are obtained for a wide range of densities and temperatures T, from cool to the warm dense matter regime. Remarkably, exchange-correlation energies ε_{xc} and potentials v_{xc} , which are calculated using the Galitskii-Migdal-Koltun (GMK) sum-rule, are found to be in good agreement (typically within a few percent) of existing theories such as path integral Monte-Carlo and fits to finite-temperature DFT functionals (Fig. 1). The theory also permits a physical interpretation of these exchange-correlation contributions. Among the novel effects at finite T, we find that electronic correlation effects remain strong at high T while ε_{xc} becomes small.

Coulomb-hole and screened-exchange at finite temperature – In a follow-up study we developed a finite temperature generalization of the static COHSEX approximation for the quasi-particle self-energy. The study yields explicit comparisons of the static and dynamically screened exchange (SEX) and coulomb hole (COH) contributions for the homogeneous electron gas [2]. Consistent with $T=0$ behavior, we find that the static SEX approximation agrees well with the fully dynamic results at all temperatures and densities. In contrast, dynamic corrections to the COH approximation are always significant, especially for unoccupied states well above the Fermi level. Notably, the COHSEX self-energy, which is real at $T=0$, is found to be complex-valued at finite-T**.** Overall, we find that the static COHSEX approximation is much faster to calculate than the fully dynamic theory but only accurate to about 10% at best.

Exchange and correlation in finite-temperature TDDFT – In an initial effort to apply these advances to spectra, we developed a FT generalization of time-dependent density functional theory (TDDFT) [3]. FT-TDDFT is analogous to that at $T=0$ in many respects. For example, in the local density approximation, we showed that the FT-TDDFT exchange-correlation kernel $f_{xc}(T,n)$ can be expressed as a density derivative of the exchange correlation potential $v_{xc}(T,n)$, i.e., $f_{xc}(T,n) = \partial v_{xc}(T,n)/\partial n$, where $n=N/V$ is the electron number density. An approximation for the kernel is obtained from the FT generalization of the retarded cumulant expansion. Results for $f_{xc}(T,n)$ and for the loss function are obtained for a wide range of temperatures and densities including the warm dense matter regime (Fig. 2).

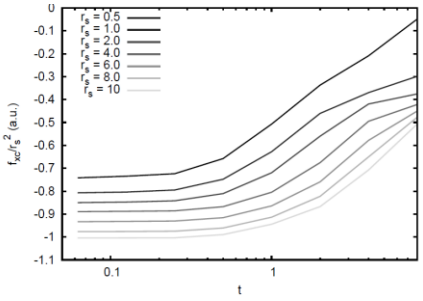

Figure 2. FT exchange-correlation kernel f_{xc} vs $t = T/T_F$ and density r_s, from the FT cumulant approach.

Excited states and x-ray spectra – A significant product of our research is the application of our theoretical techniques to calculations of excited states and x-ray spectra. An example is the extension of the retarded cumulant approach to treat plasmon-satellites in Na [4], in collaboration with the Paris group. Another is the development of a velocity gauge generalization of real-time TDDFT [5], in collaboration with colleagues in the TIMES theory institute at SLAC. Other examples are discussed in several of our Publications [1, 2, 5, 7, and 9]. Notably, the x-ray

spectroscopy code FEFF developed by our group has been adopted for automated calculations of x-ray absorption spectra for the Materials Project at LBNL [see Publication 7].

Future Plans

Finite-temperature Cumulant Green's function **–** One of our primary future objectives is the development of several extensions of the finite-*T* cumulant Green's function approach. In particular, we have begun to calculate a broad set of thermodynamic properties, starting with those of the interacting homogeneous electron gas and including spin-polarization. These include total energy, chemical potential, Helmholtz free energy, and electronic equation of state over a wide range of densities and temperatures from $(T < T_F)$ to the warm-dense matter regime ($T \approx T_F$), where T_F is the Fermi temperature. All of these properties can be partitioned into independent particle and exchange-correlation parts. Since the former are known exactly, we plan to focus on the exchange-correlation contributions. For example, this will elucidate the cross-over from exchange- to correlation-dominated behavior with increasing temperature. The special case of $T \approx 0$ is of particular interest, where our approach based on the GMK sum rule can be compared with the predictions of Fermi liquid theory. A related goal is to incorporate these finite-temperature capabilities into our x-ray spectroscopy code FEFF. This can be accomplished by substituting existing $T=0$ routines with our finite-*T* exchange-correlation potentials, self-energies, and Debye-Waller factors. This effort will enable calculations of spectra in realistic systems over a broad range of temperatures. An important application is the development of a two-temperature model for simulations of pump-probe experiments, which is needed to interpret spectra e.g., from ultra-high-intensity XFEL sources such as the LCLS.

Real-time approach for x-ray spectra – Another future topic aims to extend our real-time approaches for x-ray spectra, especially for treating inelastic losses beyond the quasi-particle approximation. With the advent of ultra-high intensity pulsed x-ray sources, theoretical treatments of real-time response and complementary theoretical software tools are called for, both for prediction and interpretation of experiment. We plan to carry out extensions of our time-dependent codes to include time-dependence of the x-ray probe, and other perturbations. An important goal is the treatment of charge-transfer (CT) excitations. One of the successes of our previous grant was an efficient real-time cumulant approach for such excitations. We now plan to carry out a more extensive series of investigations, including applications to various *d*- and *f*-electron systems. These developments will permit a better understanding of dynamic response in the x-ray regime, and help to develop improved codes for modeling the response in general materials.

Excited states and inelastic losses in x-ray spectra **–** Although the cumulant Green's function approach has been very successful in understanding inelastic losses, plasmon satellites and corrections to the GW approximation, many improvements are possible. For example, we plan to investigate ways to include self-consistency and alternative treatments of screening. We also plan to investigate off-diagonal contributions to the particle-hole Green's function, as this will enable a unified description of intrinsic, extrinsic, and interference effects. These additions will enable a simultaneous treatment of both localized and extended electronic excitations in order to obtain an improved treatment of excited states and spectra in correlated systems.

Spin-dependence and Correlated Systems – One of the drawbacks of many approaches for x-ray spectra is the neglect of, or simplistic approximations for spin- and multiplet effects However, a number of improved methods have recently been developed, and we plan address this topic by combining several of our theoretical approaches (i.e., real-time, cumulant, RSGF, etc, with approaches that explicitly treat correlated local electronic and spin structure such as charge transfer multiplet models.

References

1. J. J. Kas and J. J. Rehr, *Finite temperature Green's function approach for excited state and thermodynamic properties of cool to warm dense matter*, Phys. Rev. Lett. **119**, 176403 (10/2017).

2. Tun S. Tan, J. J. Kas, and J. J. Rehr, *Coulomb-hole and screened-exchange in the electron-self energy at finite temperature*, UW Preprint, submitted to Phys. Rev. B (04/2018).

3. J. J. Rehr and J. J. Kas, *Exchange and correlation in finite-temperature TDDFT*, Eur. Phys. J. B **91**, 153 (07/2018).

4. J. S. Zhou, M. Gatti, J. J. Kas, J. J. Rehr, and L. Reining, *Cumulant Green's function calculations of plasmon satellites in bulk sodium: Influence of screening and the crystal environment*, Phys. Rev. B **97**, 035137 (01/2018).

5. F. D. Vila, J.J. Kas, S. A. Sato, J. J. Rehr, C. D. Pemmaraju, F. D. Vila, J. J. FD; K. Yabana, and D. Prendergast, *Velocity-gauge real-time TDDFT within a numerical atomic orbital basis set*, Comp. Phys. Comp. **226**, 38 (05/2018).

Publications

A list of ten selected publications follows below.

1. E. Klevak, F. D. Vila, J. J. Kas, J. J. Rehr, and G. T. Seidler. *Finite temperature calculations of the Compton profile of Be, Li, and Si*, Phys. Rev. B **94**, 214201, (12/2016).

2. F. Fossard, G. Hug, K. Gilmore, J. J. Kas, J. J. Rehr, F. D. Vila, and E. L. Shirley, *Quantitative first-principles calculations of valence and core excitation spectra of solid C_{60}*, Phys. Rev. B **95**, 115112, (03/2017).

3. Z. Zhou, J. J. Kas, J. J. Rehr, and W. C. Ermler, *Relativistic Dirac-Fock atom properties for Z=121 to Z=138*. At. Data Nuc. Data Tab. **114**, 262, (03/2017).

4. J. J. Kas and J. J. Rehr, *Finite temperature Green's function approach for excited state and thermodynamic properties of cool to warm dense matter*, Phys. Rev. Lett. **119**, 176403 (10/2017).

5. B. Ravel, M Newville, J. J. Kas, and J. J. Rehr, *The effect of self-consistent potentials on EXAFS analysis*, J. Synchrotron Rad, **24,** 1173 (11/2017).

6. J. S. Zhou, M. Gatti, J. J. Kas, J. J. Rehr, and L. Reining, *Cumulant Green's function calculations of plasmon satellites in bulk sodium: Influence of screening and the crystal environment*, Phys. Rev. B **97**, 035137 (01/2018).

7. C. Zheng, K. Mathew, C. Chen, Y. Chen, H. Tang, A. Dozier, J. J. Kas, F. D. Vila, J. J. Rehr, L. F. J. Piper, K.A. Persson, and S.P. Ong, *Automated generation and ensemble-learned matching of X-ray absorption spectra*, NJP Computational Materials **4**, 1 (03/2018).

8. Tun S. Tan, J. J. Kas, and J. J. Rehr, *Coulomb-hole and screened-exchange in the electron-self energy at finite temperature*, UW Preprint; submitted to Phys. Rev. B. (04/2018).

9. F. D. Vila, J.J. Kas, S. A. Sato, J. J. Rehr, C. D. Pemmaraju, F. D. Vila, J. J. FD; K. Yabana, and D. Prendergast, *Velocity-gauge real-time TDDFT within a numerical atomic orbital basis set*, Comp. Phys. Comp. **226**, 38 (05/2018).

10. S., Vimolchalao, W. H. Liang, F. D. Vila, J. J. Kas, F. Farges, and J. J. Rehr, *Bethe-Salpeter Equation Calculations of Color Center Defects in Diamond*, J. Chem. Phys. Sol. **122**, 87 (07/2018).

Emerging phenomena in the strong spin-orbit coupled perovskite oxides

Principal Investigator: Sashi Satpathy
Department of Physics, University of Missouri, Columbia, MO 65211
satpathys@missouri.edu

Project Scope

The overall goal of this project is to understand and develop a theoretical description of the emerging phenomena in complex oxides and their interfaces, where competing interactions including strong correlation, spin-orbit coupling (SOC), electron-lattice interactions, charge-orbital order, etc. determine the rich behavior observed in these systems. We describe here our studies on the strong spin-orbit coupled oxides such as the iridates, which are of considerable current interest. We focus on two related topics undertaken during the past two years, viz., (i) The prediction of a spin-orbital entangled two-dimensional electron gas (2DEG) at the polar interface between $LaAlO_3$ (LAO) and Sr_2IrO_4 (SIO) and (ii) The anomalous Hall effect at the strong spin-orbit coupled oxides. Other major topics of our research will be briefly mentioned.

Recent Progress

1) **Spin-orbital entangled 2DEG at the iridate interfaces –** In this work, using density-functional theory (DFT) calculations, we showed that a spin-orbital entangled 2DEG forms at the (001) LAO/SIO polar interface between an ordinary band insulator and a spin-orbit coupled Mott insulator, aided by the combination of the spin-orbit coupling, Coulomb interaction, and polar catastrophe. What is special about this 2DEG is that it is not only localized on a single 2D layer, but also that the electron states are spin-orbital entangled, resulting in a novel 2DEG system, the only such example to our knowledge.

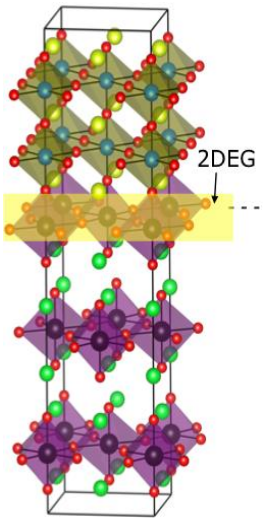

Fig. 1: Structure of the LAO/SIO (001) polar interface, indicating the formation of a spin-orbital coupled 2DEG, sharply localized at the interface [From Ref. 1].

In a seminal paper, Ohtomo and Hwang reported the observation of a conducting layer of 2DEG at the interface between two 3d transition metal oxides, $LaAlO_3$ and $SrTiO_3$ (STO), that led to an explosion of research ion the oxide interfaces and the discovery of a number of exotic phenomena such as the giant negative magneto-resistance, interfacial magnetism, tunable Rashba spin-orbit interaction, and the coexistence of magnetism and superconductivity. It has also been suggested that the interface may be a candidate material for Majorana fermions and may even host the ever-elusive Fulde-Ferrel-Larkin-Ovchinikov superconducting state formed due to the Rashba spin-orbit interaction. In these interfaces, the conducting layers extend to several monolayers and consist of multiple subbands, making them complicated quasi-2D materials and furthermore, the SOC is weak. On the other hand, in the last few years, there has been a considerable interest on the 5d materials such as Sr_2IrO_4 and other iridates, because of a large SOC that controls their electronic behavior, and recently interfaces between 3d and 5d oxides, such as LAO and SIO, are beginning to be grown.

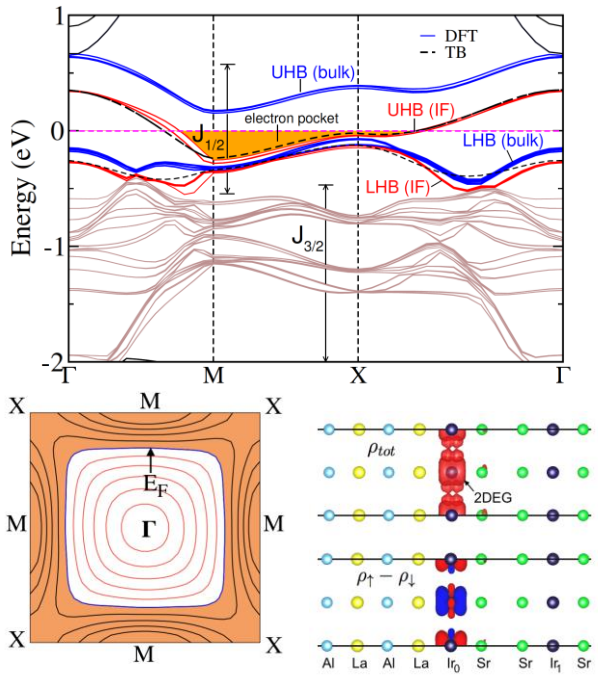

Fig. 2: DFT band structure indicating the electron pocket in the interface-localized upper Hubbard band [UHB (IF)] (top), the 2D Fermi surface (bottom left), and the charge and the spin densities indicating the spin-orbital entanglement and the localization of the 2DEG on a single IrO_2 layer [From Ref. 1].

In this work, based on density-functional theory (DFT) calculations, we predicted a sharply localized 2DEG at a prototypical 3d-5d interface, viz., the (001) LAO/SIO interface, with properties fundamentally different from those of the 3d interfaces, in the sense that: (i) The 2DEG is spin-orbital entangled due to the strong SOC, (ii) The interface electronic structure consists of a single half-filled band, leading to a simple model system for the spin-orbital entangled electron gas, and (iii) The 2DEG is sharply localized on a single IrO_2 interface layer.

The interface is polar, and a 2DEG forms with ½ electron per interface Ir due to the electronic reconstruction driven by polar catastrophe, the same physics that is well known from the 3d interfaces. Fig. 2 summarizes the basic results obtained from DFT calculations performed with the full-potential linear muffin-tin orbitals (FP-LMTO) method with the LSDA+SO+U functional, which included SOC and the Hubbard U correction. As seen from the band structure, the electron gas occupies the J_{eff} = ½ upper Hubbard band (UHB) in the interface layer, which becomes half-filled with a simple square-like Fermi surface. Quite remarkably, the 2DEG is localized on a single IrO_2 layer (Fig. 2 bottom), unlike other polar interfaces such as the LAO/STO interface, where the 2DEG is several monolayers thick. If experimentally confirmed, this would be the first candidate material to host the spin-orbital entangled 2DEG with a strong spin-orbit interaction and may start a significant new area of research.

2) **Anomalous Hall effect (AHE) in the oxide structures** – In this work, we evaluated the anomalous Hall effect in a typical, large SOC oxide material, in particular in the $SrMnO_3/SrIrO_3$ (SMO/SIO) interface, for which there is considerable experimental interest including the measurement of the AHE. In our future research plan, we are working to predict for the first time that the AHE can be controlled by an external electric field, which apart from the beautiful science can have potential device applications such as in sensors.

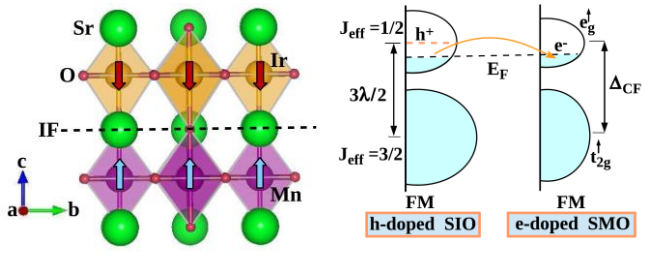

Fig. 3: The $(SMO)_1/(SIO)_1$ (100) heterostructure considered for the study of the AHE. Right part shows the charge transfer across the interface, an important ingredient in driving the magnetic state as well as the AHE. [From Ref. 2].

In ferromagnetic materials, the Hall resistivity R_H has an anomalous contribution R_s in addition to the ordinary one R_0, the latter arising due to the Lorentz force acting on the electrons in an external magnetic field. The anomalous contribution is proportional to the magnetization of the material in contrast to the ordinary contribution, which is proportional to the external

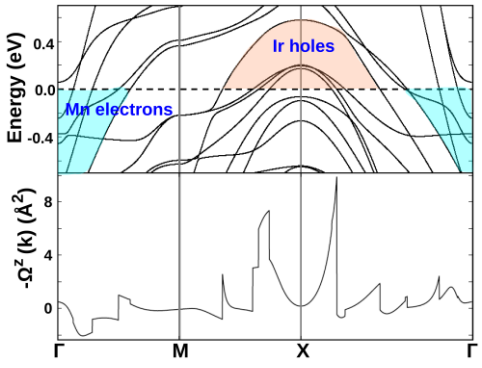

Fig. 4: DFT band structure for the $(SMO)_1/(SIO)_1$ superlattice (top) and the computed Berry curvature summed over the filled bands along the specified line of k points in the Brillouin zone (bottom). [Bhowal and SS, unpublished, Ref. 3]

magnetic field, and it is usually an order of magnitude larger than the latter. Although the AHE was recognized by Hall himself, the effect was not understood until seventy years later, when Karplus and Luttinger showed that it can be understood by considering the effect of SOC on the spin-polarized electrons. The left-right asymmetry introduced by SOC deflects the spin up and down electrons in the opposite directions and in a ferromagnet, this leads to the AHE. The effect was later reformulated in terms of the Berry curvature by Niu and coworkers.

In this work, we studied the AHE for the $SrMnO_3/SrIrO_3$ interface in order to understand the origin of the AHE in this system. This was selected for detail study as a prototype system because of the current interest and existing experimental data. The insight we gained from this study allows us to propose a tunable AHE for the first time (ongoing work).

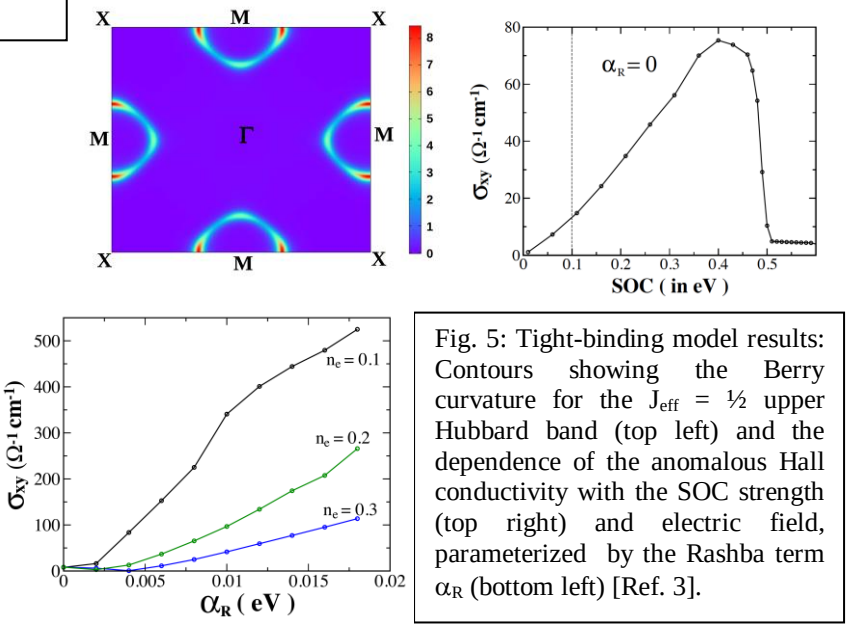

Fig. 5: Tight-binding model results: Contours showing the Berry curvature for the J_{eff} = ½ upper Hubbard band (top left) and the dependence of the anomalous Hall conductivity with the SOC strength (top right) and electric field, parameterized by the Rashba term α_R (bottom left) [Ref. 3].

The AHE was studied using DFT and a tight-binding (TB) model Hamiltonian was used to understand the results. The Hamiltonian included the d orbitals, exchange splitting J_{exc}, the SOC term λ, and the electric field term that produces the Rashba interaction α_R, viz.,

$$H = -\sum_{i\mu,j\nu} t_{ij}^{\mu\nu} c_{i\mu\sigma}^{\dagger} c_{j\nu\sigma} + J_{ex} \sum_{i\mu,\sigma,\sigma'} c_{i\mu\sigma}^{\dagger} \sigma_{\sigma\sigma'}^{z} c_{i\mu\sigma'} + \frac{\lambda}{2} \sum_{\mu\sigma,\nu\sigma'} c_{i\mu\sigma}^{\dagger} \vec{L}_{\mu\nu} \cdot \vec{\sigma}_{\sigma\sigma'} c_{i\nu\sigma'} + \alpha_R \sum_{i\mu,j\nu} c_{i\mu}^{\dagger} [\hat{\sigma} \times \vec{d}_{ij}^{\mu\nu} \cdot \hat{z}] c_{j\nu},$$

with familiar symbols. From the band structure, the Berry curvature was calculated using a standard perturbative expression, the summation of which over the occupied states produces the anomalous Hall conductivity σ_{xy}. The central results are shown in Figs. 4 and 5. The DFT computed anomalous Hall conductivity of 26 Ω^{-1} cm^{-1} agrees quite well with the experimental value (20 Ω^{-1} cm^{-1}). The model calculations indicate a strong electric-field dependence (via the symmetry breaking Rashba interaction term), leading to the possibility of the tuning of the AHE by an applied electric field (Fig. 5, bottom left).

3) **Other Works:** Some of the other notable works in the past two years where the SOC plays a central role consisted of (i) The origin of the Dzyaloshinskii-Moriya interaction (DMI) in MnSi, a prototypical material for skyrmion state (Ref. 4) and in a model spin-polarized electron gas (Ref. 5), (ii) Magnetic anisotropy and spin wave gap in the osmates (Refs. 6-8), and (iii) Magnetic instability in electron doped iridates (Ref. 9).

Future Plans

1) Tunable Anomalous Hall Effect in the strong spin-orbit coupled structures: This will follow our work on the Anomalous Hall effect described above. Our model studies using a tight-binding Hamiltonian indicate a strong electric-field dependence via the Rashba spin-orbit interaction, present in a broken inversion symmetry system, such as a system with an applied electric field or a surface. The strength of the Rashba interaction increases with the electric field, but in a solid may be significantly reduced due to screening. Although the electric field dependence is quite strong from the model studies, full DFT studies will be needed to establish the magnitude of the effect. Initially, we will study the $(LMO)_1/(SIO)_1$ interface, discussed above already, for which we have obtained encouraging preliminary results. It will then be extended to surfaces as well. For example, in one of our earlier works [Shanavas and SS, Phys. Rev. Letts. 112, 086802 (2014)], we had shown that the Rashba effect can be field tuned on the surface of a strong SOC material, using the (001) $KTaO_3$ surface as an example.

2) Spin-orbital and Fermi surface instability in doped iridates – In our work (Ref. 9), we studied the instability of the anti-ferromagnetic (AFM) state in the electron-doped iridates, and contrary to the expectation from the Nagaoka Theorem, where a single doped carrier is expected to destroy the AFM state in the half-filled Hubbard model, we found the AFM state to be stable up to a critical doping concentration in agreement with existing experiments on the doped iridates. This was studied within the J_{eff} = ½ sector, and the spiral spin-wave state was found to be the ground state, once the instability occurs. For intermediate strength of the SOC, the J_{eff} = 1/2 and 3/2 sectors mix and the possibility of a complex spin and orbital instability exists. Furthermore, the classic Pomeranchuk instability for the spinless Fermi surface might lead to new types of instabilities in the presence of a strong SOC. This will be studied by computing the susceptibility of an appropriate model Hamiltonian to spin/orbital fluctuations and by examining if the susceptibility is large enough to lead to instabilities.

Selected Publications

1. C. Bhandari and S. Satpathy, "Spin-orbital entangled 2DEG at the $LaAlO_3/Sr_2IrO_4$ interface," Phys. Rev. B (RC) (In Press) (2018).
2. S. Bhowal and S. Satpathy, "Emergent Magnetism at the 3d-5d Interface: $SrIrO_3/SrMnO_3$, AIP Conf. Proc., ArXiv:1804.06381 (2018).
3. S. Bhowal and S. Satpathy, "Intrinsic Anomalous Hall Effect at the 3d-5d oxide Interface: $SrIrO_3/SrMnO_3$, In preparation (2018).
4. K. V. Shanavas and S. Satpathy, "Electronic structure and the Dzyaloshinskii-Moriya interaction in MnSi," Phys. Rev. B 93, 195101 (2016).
5. M. Valizadeh and S. Satpathy, "Dzyaloshinskii-Moriya interaction in the presence of Rashba and Dresselhaus spin-orbit coupling," Phys. Rev. B 97, 094419 (2018).
6. C. Bhandari and S. Satpathy, "Effect of epitaxial strain on the optical properties of $NaOsO_3$," J. Phys. Chem. Solids (2017, In Press).
7. S. Mohapatra, C. Bhandari, S. Satpathy, and A. Singh, "Effects of the structural distortion on the electronic band structure of $NaOsO_3$ studied within density functional theory and a three-orbital model," Phys. Rev. B 97, 155 154 (2018).
8. A. Singh, S. Mohapatra, C. Bhandari, and S. Satpathy, "Spin-orbit coupling induced magnetic anisotropy and large spin wave gap in NaOsO3," (2018, submitted to New J. Physics).
9. S. Bhowal, J. Moradi Kurdestany, and S. Satpathy, "Stability of the Antiferromagnetic State in the Electron Doped Iridates," J. Phys: Condensed Matter 30, 235601 (2018).

Quantum Monte Carlo Studies of Multiband Hubbard Models

Principal Investigator: Richard Scalettar
Department of Physics, University of California, Davis, CA 95616
scalettar@physics.ucdavis.edu

Keywords: Quantum simulations, Magnetic Phase Transitions, Novel Superconducting Phases

Project Scope

This project involves the physics of multiband Hubbard models and, in addition to that global goal, has three more specific objectives: (i) the exploration of how electrons behave at the interface between different materials, for example, how magnetism in one might penetrate into another; (ii) the development of an understanding of the 'Knight shift anomaly', a phenomenon which occurs at low temperatures in a class of solids known as heavy fermion materials, in which the response of the electrons to the nuclear spin is no longer proportional to the magnetic susceptibility; and (iii) the study of solids represented by 'depleted lattices' in which a regular array of sites is removed.

Recent Progress

Compressible Ferrimagnetism in the depleted Periodic Anderson Model[1]*:* Tight-binding Hamiltonians with single and multiple orbitals exhibit an intriguing array of magnetic phase transitions. In most cases the spin ordered phases are insulating, while the disordered phases may be either metallic or insulating. We reported a Determinant Quantum Monte Carlo study of interacting electrons in a geometry which can be regarded as a two-dimensional Periodic Anderson Model (PAM) with depleted interacting (f) orbitals. For a single depletion, we observed an enhancement of antiferromagnetic correlations and formation of localized states. (See Figure 1). For half of the f-orbitals regularly depleted, the system exhibits a ferrimagnetic ground state (See Figure 2). We obtained a quantitative determination of the nature of magnetic order, which we discussed in the context of Tsunetsugu's theorem, showing that, although the dc conductivity indicates insulating behavior

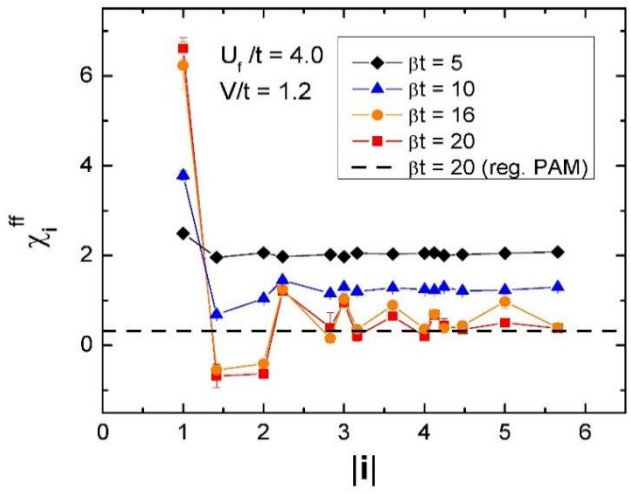

Figure 1: Local susceptibility of f-orbitals as a function of distance |i| from an ion defect. The dashed black line is the value of the magnetic susceptibility in the undepleted PAM at temperature T equal to one-twentieth of the intersite hopping t.

at half-filling, the compressibility remains finite.

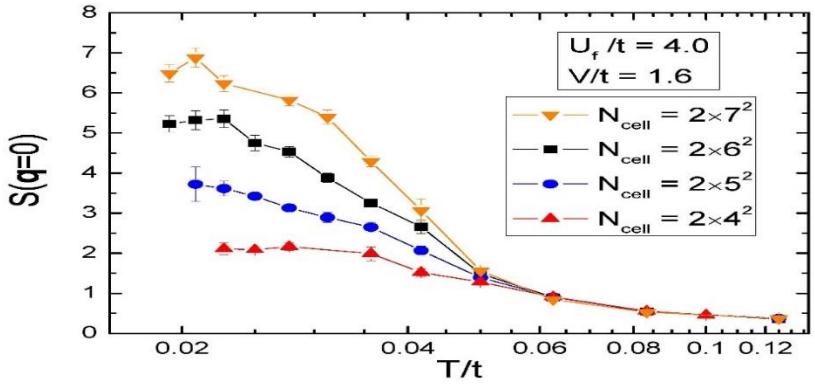

Figure 2: Homogeneous spin structure factor S(q=0) versus temperature for a ratio of conduction electron-local orbital hybridization V to conduction electron hybridization t of V/t=1.6. The on site repulsion on the local orbitals U=4t.

Phonon dispersion and the competition between pairing and charge order[2]*:* The Holstein Model (HM) describes the interaction between fermions and a collection of local (dispersionless) phonon modes. In the dilute limit, the phonon degrees of freedom dress the fermions, giving rise to polaron and bipolaron formation. At higher densities, the phonons mediate collective superconducting (SC) and charge density wave (CDW) phases. Quantum Monte Carlo (QMC) simulations have considered both these limits, but have not yet focused on the physics of more general phonon spectra. We undertook QMC studies of the role of phonon dispersion (Figure 3) on SC and CDW order in such models. We quantified the effect of finite phonon bandwidth and curvature on the critical temperature Tcdw for CDW order, and also uncovered several novel features of diagonal long range order in the phase diagram, including a competition between charge patterns at momenta q=(π,π) and q=(0,π) which lent insight into the relationship between Fermi surface nesting and the wavevector at which charge order occurs (Figure 4). We also demonstrated SC order at half-filling in situations where nonzero bandwidth sufficiently suppresses Tcdw (Figure 5).

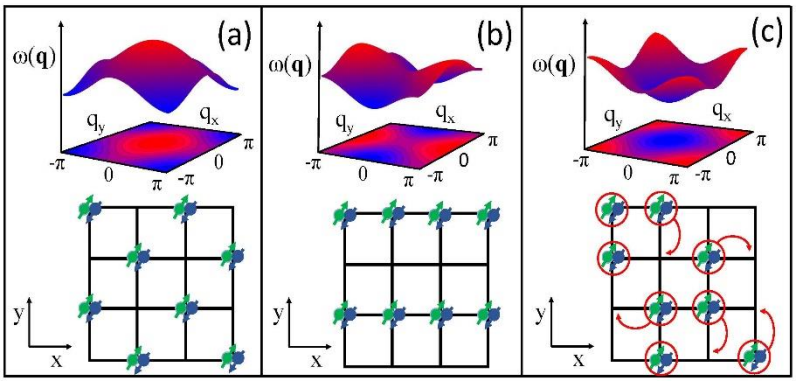

Figure 3: Sketch of bare phonon dispersion (top) and its resulting charge ordering (bottom) for (a) downward curvature, (b) mixed curvature (saddle point at the origin), and (c) upward curvature cases. The arrows on the latter correspond to hopping to any available sites and emphasize the possibility of mobile pairs.

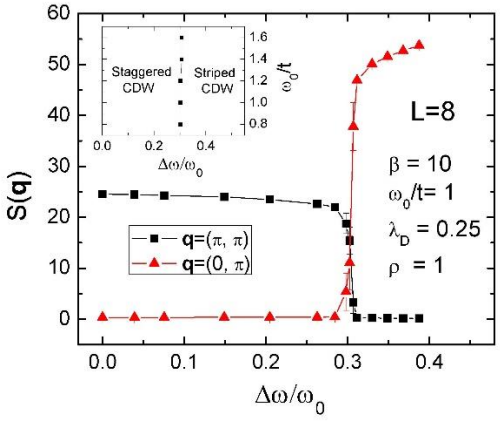

Figure 4: The CDW-SC transition at half-filling: As the phonon dispersion increases, the CDW structure factor S(π,π) is strongly suppressed, while the pairing susceptibility Ps is enhanced. Circles, triangles and diamonds correspond to linear system sizes L=6, 8 and 10, respectively.

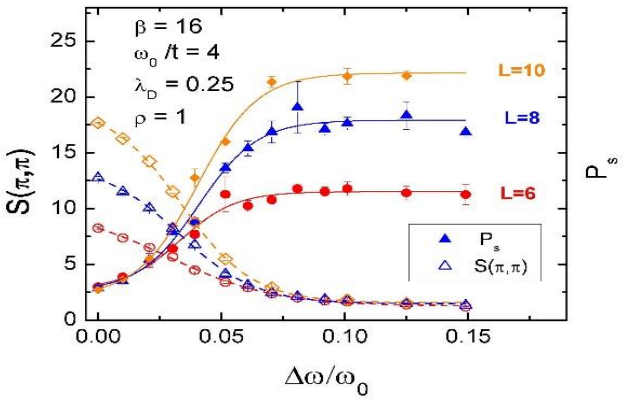

Figure 5: Schematic picture of our twisted bilayer graphene superlattice with AA and AB/BA regions. (b) The effective lattice which results from treating each AA region as an effective 'site' connected by modulated hopping amplitudes. Three elementary vectors e1,e2,e3 are indicated. (c) The band structure of the effective model in the first Brillouin zone. (d) The density of states corresponding to the band shown in (c). In (d) we also show the density of states of the limiting cases of the triangular (t'=t) lattice and hexagonal (t'=0) lattice. In (c) and (d), the anisotropic factor t'/t=0.3.

Pairing symmetry of interacting fermions on twisted bilayer graphene superlattice[3]*:* We examined the pairing symmetry of an effective Hamiltonian for interacting fermions on a twisted bilayer graphene superlattice with the determinant quantum Monte Carlo method. Our model (Figure 6) had the symmetry of a triangle lattice and a nearly-flat low energy band, features which underlie the magic-angle twisted bilayer graphene superlattice. This was realized via a Hubbard Hamiltonian on a triangular lattice with modulated hopping: We began with a honeycomb geometry and hopping t, then added sites at the center of each hexagon with hopping t'. We showed that the low temperature phase is insulating at half-filling, even for relatively weak interactions. The natures of the spin and pairing correlations upon doping were determined, and exhibit an electron-hole asymmetry

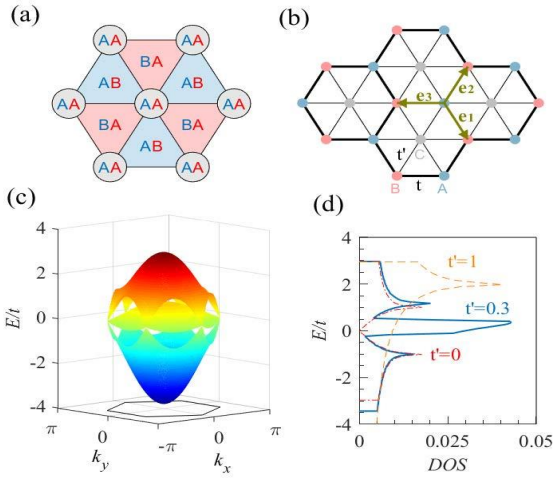

Figure 6: Schematic picture of our twisted bilayer graphene superlattice with AA and AB/BA regions. (b) The effective lattice which results from treating each AA region as an effective 'site' connected by modulated hopping amplitudes. Three elementary vectors e1,e2,e3 are indicated. (c) The band structure of the effective model in the first Brillouin zone. (d) The density of states corresponding to the band shown in (c). In (d) we also show the density of states of the limiting cases of the triangular (t'=t) lattice and hexagonal (t'=0) lattice. In (c) and (d), the anisotropic factor t'/t=0.3.

consistent with experiment. Among the pairing symmetries allowed, we demonstrated that the dominating channels are d-wave, opening the possibility of condensation into an unconventional d(x2-y2)+id(xy) phase, which is characterized by an integer topological invariant and gapless edge states.

Future Plans

A renewal DOE proposal entitled "Quantum Simulations of Strong Correlation Effects at Interfaces" has been funded. Under that grant, we propose to use quantum simulation techniques to study three different condensed matter systems.

Interfaces between charge density wave (CDW) and metallic materials: Here our planned focus will be on a quantitative description of how the charge correlations manifest in a CDW material penetrate an interface into a metallic region. We will begin with simulations of a layered syatem consisting of a Holstein model with strong electron-phonon coupling, and hence a CDW low temperature phase, coupled to several layers of free electrons. After understanding the half-filled system, we intend to investigate what happens when the CDW is doped, and superconducting correlations are enhanced.

Magnetic domains and local nuclear magnetic resonance response in heavy fermion systems: We will continue our study of the structures of magnetic domains which form as a result of chemical substitution in heavy fermion systems, and how quantum simulations can help interpret the local nuclear magnetic resonance response around different types of impurities.

Effect of disorder on unconventional pairing of Dirac fermions: We have recently performed several investigations of the nature of superconductivity of Dirac fermions. We intend to use quantum monte carlo to understand the effect of disorder in this situation, similar to early work we did on the role of randomness on s-wave and d-wave pairing with conventional electron dispersion relations. Our specific models will be the Hubbard model on honeycomb and π-flux phase lattices.

References

1. N.C. Costa, M.V.M. Araujo, J.P. Lima, T. Paiva, R.R. dos Santos, and R.T. Scalettar, *Compressible Ferrimagnetism in the depleted Periodic Anderson Model*, Phys. Rev. **B97**, 085123 (2018).
2. N.C. Costa, T. Blommel. W.-T. Chiu, G.G. Batrouni, and R.T. Scalettar, *Phonon dispersion and the competition between pairing and charge order*, Phys. Rev. Lett. **120**, 187003 (2018).
3. Huaiming Guo, Xingchuan Zhu, Shiping Feng, and Richard T. Scalettar, *Pairing symmetry of interacting fermions on twisted bilayer graphene superlattice*, Phys. Rev. **B97**, 235453 (2018).

Publications (August 2016 – July 2018)

1. W. Hu, R.T. Scalettar, E.W. Huang, and B. Moritz, *Effect of an Additional Conduction Band on Singlet-Antiferromagnet Competition in the Periodic Anderson Model*, Phys. Rev. **B95**, 235122 (2017).
2. Natanael C. Costa, Wenjian Hu, Z.J. Bai, Richard T. Scalettar, and Rajiv R.P. Singh, *Principal component analysis for fermionic critical points*, Phys. Rev. **B96**, 195138 (2017).

3. G.G. Batrouni and R.T. Scalettar, *Interaction-Induced Gradients Across a Confined Fermion Lattice*, Phys. Rev. **A96**, 033632 (2017).
4. H.-M. Guo, Lei Wang, and R.T. Scalettar, *Quantum phase transitions of multi-species Dirac fermions*, Phys. Rev. **B97**, 235152 (2018).
5. Huaiming Guo, Ehsan Khatami, Yao Wang, T.P. Devereaux, R.R.P. Singh, and R.T. Scalettar, *Unconventional pairing symmetry of interacting Dirac fermions on a pi-flux lattice*", Phys. Rev. **B97**, 155146 (2018)
6. Wenjian Hu, *Exploring Phase Transitions Using Conventional Monte Carlo Simulations and Machine Learning Techniques* Ph.D. thesis, (2018).
7. N.C. Costa, M.V.M. Araujo, J.P. Lima, T. Paiva, R.R. dos Santos, and R.T. Scalettar, *Compressible Ferrimagnetism in the depleted Periodic Anderson Model*, Phys. Rev. **B97**, 085123 (2018).
8. N.C. Costa, T. Blommel. W.-T. Chiu, G.G. Batrouni, and R.T. Scalettar, *Phonon dispersion and the competition between pairing and charge order*, Phys. Rev. Lett. **120**, 187003 (2018).
9. Chuang Chen, Xiao Yan Xu, Junwei Liu, George Batrouni, Richard Scalettar and Zi Yang Meng, *Symmetry Enforced Self-Learning Monte Carlo Method Applied to the Holstein Model*, Phys. Rev. **B98** 041102(R) (2018).
10. Huaiming Guo, Xingchuan Zhu, Shiping Feng, and Richard T. Scalettar, *Pairing symmetry of interacting fermions on twisted bilayer graphene superlattice*, Phys. Rev. **B97**, 235453 (2018).

First-Principles Understanding of Optical Excitations within Low-Dimensional Materials

PI: Sahar Sharifzadeh

Department of Electrical & Computer Engineering, Boston University, Boston, MA 02215

Keywords: two-dimensional materials; excitons; defects in two-dimensional semiconductors

Project Scope

The objective of this project is to utilize first-principles computational approaches to understand optical excitations within two-dimensional monolayers and heterostructures, with the ultimate goal of designing new materials by modifying the chemical and physical structure on the nanoscale. In 2D heterostructures, the nature and movement of the exciton is determined to a large extent by the electron-electron and electron-phonon strengths within individual monolayers, as well as the coupling between layers, all of which in turn depend on chemistry, solid-state screening properties, and quantum confinement. Controlling the nature and migration properties of excitons requires an understanding of the complex relationship between electrons, phonons, defects, disorder, and dynamics. The aim of this project is to determine, by analysis of highly accurate density functional theory (DFT) and many-body perturbation theory (MBPT) calculations, how these complexities can be decomposed into simple, tunable parameters.

The specific goals of this project are to 1) understand electron conductivity, absorption and transparency of monolayer semiconductors and metals; 2) develop a theory of excitons near defects in low dimensions; and 3) understand the influence of inter-layer interactions in heterostructures.

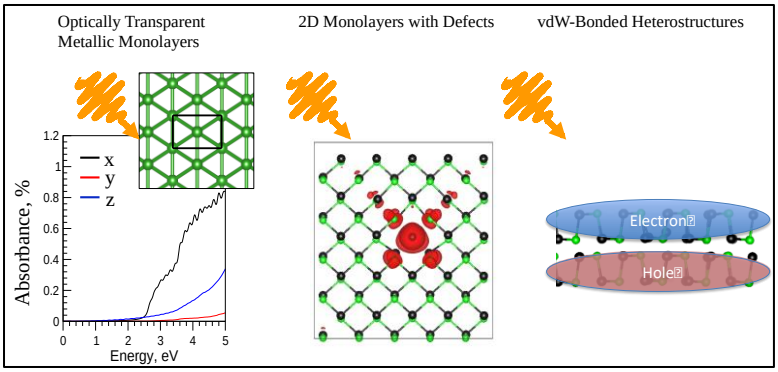

Figure 1: A schematic of the Project Scope. Left: electron-phonon and electron-electron interactions within monolayer boron; approximated structure (right) and calculated absorption (left) are shown. Center: excitonic effects in the presence of defects; an excited state within monolayer semiconductor GeSe with the introduction of a single Se vacancy is shown. Right: Intralayer interactions and charge-transfer excitations within 2D heterostructures.

I. Understanding the optoelectronic properties of borophene relative to graphene

2D boron, or borophene, is a monolayer metal, and has been considered as a possible replacement for graphene. It has been predicted that the freestanding form of borophene has a metallic density of states, high mobility and high optical transparency [1]. Currently, freestanding borophene has not been fabricated; however, monolayer boron on metal substrates has been recently synthesized [2].

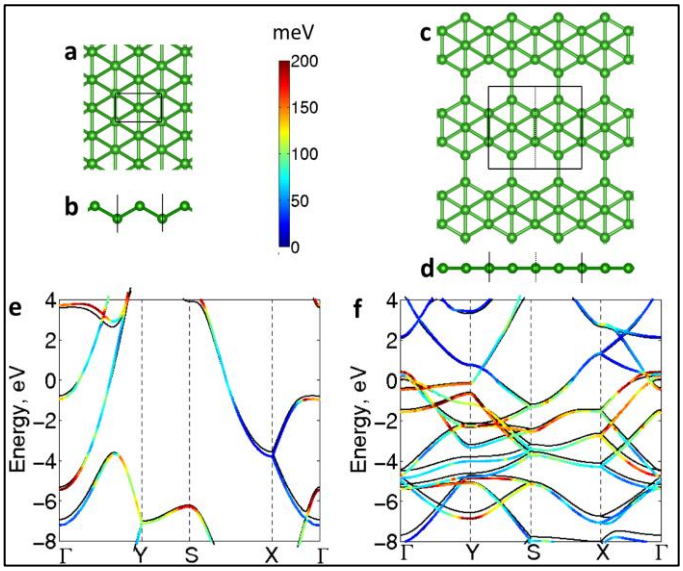

Figure 2: a-d) The structure of two allotropes of borophene with e) and f) showing the band structure of each calculated via the GW approximation. The isosurface colors show the strength of electron-phonon coupling calculated using the EPW package. There is a strong geometrical structure-dependence of the electronic structure and electron-phonon coupling strength. Figure from Ref. 6.

We utilized the MBPT formalism within the GW/BSE approximation to understand the electronic and optical properties of the experimentally-realized and theoretically-predicted borophene structure [6]. By including electron-electron, electron-phonon and electron-hole interactions at the order of first-order perturbation theory, we studied the electron conductivity and excitonic properties within two allotropes of borophene and revealed the influence of strain on the optoelectronic properties. As shown in Figure 2, the GW bandstructure, computed using the Quantum Espresso and BerkeleyGW packages, suggests that the electronic structure of the monolayer strongly depends on the crystal structure. Additionally, we utilized the electron-phonon wannier (EPW) software to describe the electron-phonon self-energies within first-order perturbation theory. We predicted that while the density of available electrons at the Fermi energy is large, the electron-phonon scattering is also large (Figure 2) and limits the conductivity of borophene such that it is a poorer conductor than graphene. By numerical electromagnetics simulations in combination with first-principles theory, we elucidated the optical transparency range of borophene, determining that the borophene monolayer is transmitting in the visible range if the finite thickness is considered. This is because of internal reflections due to the small thickness, and verifies that the often-applied semi-infinite limit should not be applied to 2D systems [6]. Lastly, we showed that strain can be used to modify the electronic and optical properties of borophene [7]. In particular, with application of uniaxial tensile and compressive strains, we demonstrate that the response of borophene to light is highly dependent on the polarization direction of incoming light, an anisotropy that can be tuned via strain.

II. Theory of excitons near point defects in low dimensions

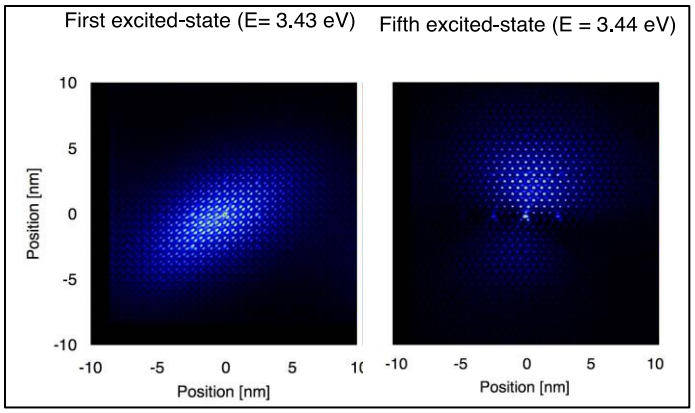

Figure 3: A plot of the electron-hole correlation function for two low-energy excitations in bulk GaN containing a +1 charge N-vacancy. The hole is localized near the defect site. The figure on the left shows a bulk-like character while the figure on the right shows localized defect-like character.

We have utilized MBPT to study excitons near point defects in bulk GaN as a first step to describing excitons in defective two-dimensional materials [8]. GaN is a well-studied wide gap material, with applications to power electronics and blue light emitting diodes. In a prior study, we had utilized the GW approximation to show that introduction of the N^{+1} vacancy (V_N^{+1}) results in shallow states near the band-edge of GaN [3].

Our initial GW/BSE calculations suggest that there are both defect-like and bulk-like low-energy excitations present (see Figure 3). We are currently studying the convergence of the optical absorption spectrum and exciton wavefunction with common computational parameters that are specific to defects, including electrostatic corrections that must be applied due to the presence of charged defects within periodic boundary conditions [8].

Lastly, we performed studies of excitons near point defects within monolayer GeSe, a promising optoelectronic material. Studies suggest that the presence of deep defects in this material leads to efficient water splitting in the presence of light, indicating localized excitons near defects [4**]**. We calculated the bandstructure and excitonic properties associated with one charged Se vacancy in the monolayer and determined that for this system, there are deep in-gap defect states that may dominate the optoelectronic properties [9]. Currently, we are exploring the likelihood of formation of a series of defects, and have started collaboration with Dr. Alexander Weber-Bargioni at Lawrence Berkeley National Laboratory to study the optical properties of single defects using a near-field optical scanning-probe [5]. Additionally, because defect complexes, rather than point defects, may form we have initiated molecular dynamics studies of GeSe, simulating the defect formation in the presence of a strong light pulse. Our goal is to determine what are the defect complexes that arise naturally in this system in order to have a better understanding of how our simulations compare to experiment [10].

Future Plans

We plan to continue to develop an understanding of excitons near point defects. For the GaN crystal, we will determine the appropriate computational methods for describing excitons near point defects, and we will then apply this understanding to the studies of defects in monolayer

GeSe. For GeSe, we plan to determine the likely defect structures that will arise in experiment, calculate the excitonic properties associated with these defects, including the role of exciton-phonon interactions, and compare calculated and measured optical spectra. The role of exciton-phonon interactions will be very important but is difficult to compute due to computational complexity and may require method development. Based on these calculations, we will develop an effective mass model of the exciton by determining the form of the electron-hole kernel computed within BSE and electron-phonon interactions by analysis of Huang-Rhys factors.

In addition, we will begin studies of the interfacial properties of borophene with GeSe. The main focus of this work will be to understand how optical transparency in the metal and absorption in the semiconductor are modified by interfacial geometry, charge transfer, and intra-layer phonons. This study will be extended to donor-acceptor heterointerfaces in the longer term.

References

1. M.H. Evans, J.D. Joannopoulos, and S.T. Pantelides, "Electronic and mechanical properties of planar and tubular boron structures" Phys. Rev. B 72, 1 (2005).

2. A. J. Mannix, X.-F. Zhou, B. Kiraly, J.D. Wood, D. Alducin, B.D. Myers, X. Liu, B.L. Fisher, U. Santiago, J.R. Guest, M.J. Yacaman, A. Ponce, A.R. Oganov, M.C. Hersam, and N.P. Guisinger, "Synthesis of borophenes: Anisotropic, two-dimensional boron polymorphs" Science 350, 1513–1516 (2015).

3. D. K. Lewis, M. Matsubara, E. Bellotti, and S. Sharifzadeh, "Quasiparticle and Hybrid Density Functional Methods in Defect Studies: An Application to the Nitrogen Vacancy in GaN," Physical Review B 96, 235203 (2017).

4. D. D. Vaughn, R.J. Patel, M.A. Hickner, and R.E. Schaak, "Single-Crystal Colloidal Nanosheets of GeS and GeSe" J. Am. Chem. Soc. 132, 15170 (2010).

5. C. Kastl, R. Koch, C. Chen, J. Eichhorn, B. Schuler, T. Kuykendall, S. Moser, A. Bostwick, C. Jowiak, S. Aloni, A. Weber-Bargioni, E. Rotenberg, and A.M. Schwartzberg, "2D Materials under the Microscope(s): Connecting Material Properties and Electronic Structure to Many-Body Excitonic Phenomena in Monolayer WS2 Proceedings of 2D Photonic Materials and Devices Volume 10534, 1053404 (2018).

Publications (August 2017 – July 2018)

6. L. Adamska, S. Sadasivam, J.J. Foley IV, P. Darancet, and S. Sharifzadeh, "First-Principles Investigation of Borophene as a Monolayer Transparent Conductor," Journal of Physical Chemistry C, 122 4037 (2018).

7. L. Adamska and S. Sharifzadeh, "Fine-Tuning the Optoelectronic Properties of Freestanding Borophene by Strain," ACS Omega 2, 8290 (2017).

8. D.K. Lewis and S. Sharifzadeh, "Excitonic Effects Near Point the Nitrogen Vacancy Defect in GaN", in preparation.

9. D.K. Lewis and S. Sharifzadeh, "Strong Excitonic Effects Near Point Defects in GeSe," in preparation.

10. M. Alaghemandi, D.K. Lewis, S. Sharifzadeh, "Defect Formation in Ge Monochalcogenides: a Molecular Dynamics Study," in preparation.

Theoretical Studies in Very Strongly Correlated Matter

B Sriram Shastry, University of California Santa Cruz, Santa Cruz, CA 95064; sriram@physics.ucsc.edu

Keywords: Very Strong correlations, Non-perturbative Techniques, Beyond Fermi Liquids, Transport studies, Photoemission spectra,.

Project Scope

This project is focussed on a set of problems in very strongly correlated matter arising in condensed matter physics. Reliable and systematic calculation of physical properties measured by experiments with ever increasing resolution is a pressing problem in the field. While successful numerical techniques are becoming available, thanks to impressive technical progress achieved in dynamical mean field theory and the density matrix renormalization group, corresponding progress in analytical methods has been lacking. The chief bottleneck is the inability to treat large correlations, where the Hubbard interaction scale U is as large or greater than the bare band width W . A similar inability applies to the further idealized case of *extreme correlations*, i.e. with $U \to \infty$. In the extreme correlations regime one can study the *t-J* model, where Gutzwiller projected electrons move on the lattice, and interact via the super-exchange interaction with scale J. This model has been proposed as the effective Hamiltonian to describe physics on the lowest energy scales, i.e. within the lower Hubbard band. It is convenient since the large scale U is not explicitly present in the model, however now, the Gutzwiller projection creates formidable hurdles to developing an analytical theory. In the recent past the PI has found an effective machinery to treat these extreme correlations, by adapting the Schwinger techniques originally developed for quantum electrodynamics, and adding insights from sum rules as well as the Luttinger-Ward theorem of an invariant Fermi volume. The resulting *extremely correlated Fermi liquid* theory is formulated exactly, and holds considerable promise in overcoming the mentioned barriers. The proposal outlines projects designed to test the ECFL theory against other established techniques, in overlapping regimes. The proposal outlines collaborative efforts with experimentalists to understand a large body of data from ARPES, as well as conductivity and other transport techniques.

Recent Progress

Resistivity and Hall constant studies. In Ref. (1), the PI and his group together with Professor Antoine Georges (Paris, New York) have studied the high T behavior of resistivity in infinite dimensions, by combining a variety of techniques to establish some important results. One of the findings is that the resistivity is linear in T, which is expected, but the origin is in the 1/T shrinking of the f-sumrule for a single band model. This is different from the 1/T dependence of a relaxation time, as found in other calculations

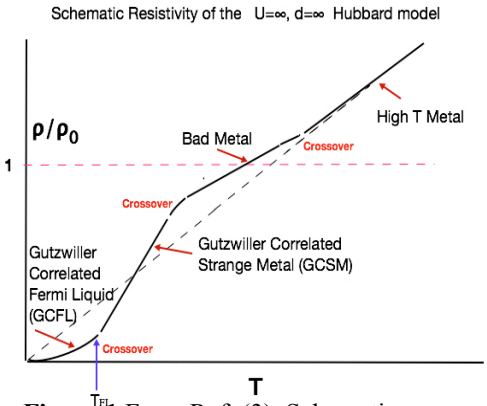

Figure.1 From Ref. (3). Schematics of T dependent resistivity. Gutzwiller correlations alone produce this rich variety in d=∞ , U=∞.

employing string theory techniques. An unexpected finding is that the density dependence of the conductivity at high T is simply (linearly) dependent on 1-n rather than n. It is then found that the scattering rate is independent of the density! In Ref. (3,5) the PI's group, together with Professor R. Zitko (Ljubljana) has computed from ECFL and DMFT techniques the resistivity, Hall constant and optical conductivity for the infinite dimensional case, at low and the strange metal regime, i.e. an intermediate T region which are of experimental interest. The varieties of T dependence of the resistivity, arising purely from the infinite U constraint are surprisingly many. These are schematically shown in Fig. (1).

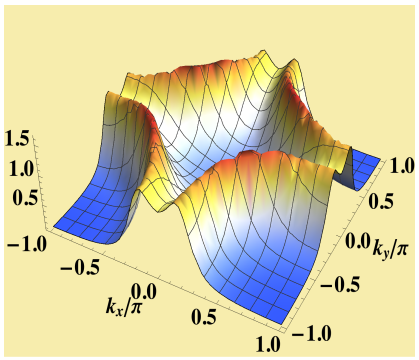

Figure. 2 The spectral function from Ref. (6) at t'=-.4,n=.85. T=63K above and T=210K below. Note the sharp drop in intensity for the relatively small T change.

2-d t-t'-J model ECFL results. In Ref. (4.) the PI and graduate student Mai have applied the $O(\lambda^2)$ ECFL equations, previously tested against DMFT in d= ∞, to the physically important case of 2 dimensions. The model used is the t-t'-J model, where the second neighbor hop t'>0 describes electron doping and t'<= 0 the hole doped models, with their associated physical systems. This work finds that the hole doping and t'/t play a very important role in determining the quasiparticle weight Z, which is generally very small ~<.1 for the cases relevant to cuprate materials. A significant result is that the *effective Fermi temperature* is about two orders of magnitude lower than the bare value obtained from band structure, and is further very sensitive to hole doping and t'/t. As a result the spectral functions are extraordinarily sensitive to T, on a very low T scale as seen in Fig. (2). Secondly the resistivity in Fig. (3) shows a crossover from T^2 to a linear T behavior at a very low effective Fermi scale which is as low as 50K in some cases, and t'/t controls the magnitude and sign of the curvature of the resistivity.

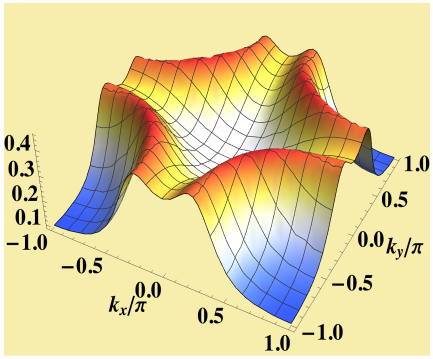

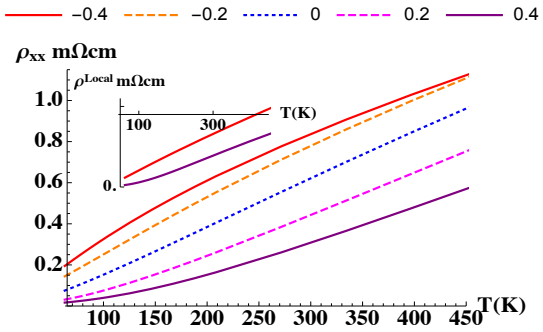

Figure. 3 The 2-d t-t'-J model normal state resistivity Ref. (4) with n=0.85, t'/t in the top legend. Note the very low Ferm scale and the change in curvature with t'/t from concave-up t'>0 (electron doped) to concave-down t'<0 (hole doped). The inset shows a local resistivity without the t'/t factors inherent in the bare vertex.

Photoemission and Raman scattering studies. A remarkable features of photoemission derived E(k) vs. k dispersion relations is the narrowness of the band relative to the DFT calculations, and the various kink features. The low energy kink at ~70 meV has been viewed as a consequence of the scattering of quasiparticles by either a phonon, or a charge/spin related bosonic mode in several studies. In Ref. (2) our group has highlighted the fact that purely correlation driven physics is also capable of producing such a low energy kink. Further it is shown that the EDC kink spectrum can be deduced from the MDC spectrum using the ECFL theory. The

comparison between theory and experiments in optimally doped BISSCO (A. Kaminski *et. al.* PRL **86**, 1070 (2001)) are shown in Fig. (4) Further the many distinctions between the EDC and MDC spectra from the correlation model and the bosonic model are clarified. In Ref (7) The non-resonant Raman scattering intensity, susceptibility and the so called Raman resistivity in all polarization geometries are calculated from the two dimensional ECFL results of Ref. (4). Fig. (5) displays the results for the electron doped cuprates, where the calculations agree well with experiments (A. Koitzsch et. al PR **B67**, 184522 (2003)) done (only) in the B_{2g} geometry. Our calculations also give detailed predictions for the (as yet unmeasured) A_{1g} and B_{1g} geometries for the same parameters, which should make an interesting comparison.

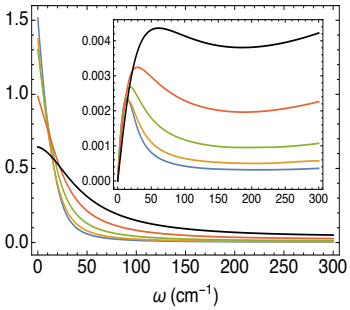

Figure. 5 B2g Raman intensity and susceptibility (inset) from Ref. (7).

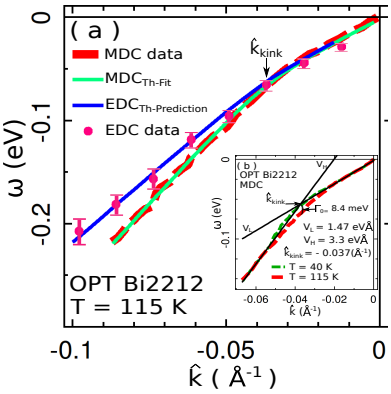

Figure. 4 The measured EDC spectrum (magenta dots) compared to theory (blue line) from Ref. (2).

1-dimensional models using DMRG and ECFL. In Ref. (6), together with Prof Steven White at UC Irvine, we have studied the 1-dimensional t-t'-J model, using two different techniques. On the one hand recent progress in density matrix renormalization group (DMRG) leads to almost exact spectral functions using the numerical methods. On the other hand the analytical ECFL equations that have been tested in high dimensions, can also be applied to this limit. Ref. (6) shows that the two techniques indeed give very similar results. One of the interesting outcomes of this collaboration is the elucidation of the momentum dependence of the Dyson self-energy in 1-dimension. This is an interesting problem since the k-dependence is expected to be very strong in this limit. Our results, shown in Fig. (6) display a ridge structure in the self-energy from both techniques. This study also confirms that the same ECFL equations yield an accurate description of the physics in as diverse situations as the d= ∞ limit and the d=1 case.

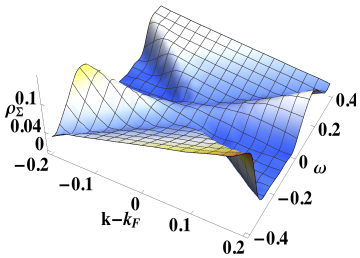

Figure. 6 Imaginary self energy from Ref. (6). DMRG (top) and ECFL (below) show similar ridges in the k-space

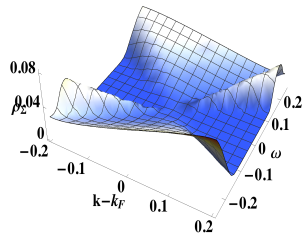

Luttinger-Ward sumrule: Very recently in Ref. (10), the PI has found a new non-perturbative proof of an extended version of the Luttinger-Ward sumrule for Fermions in interacting systems. The extension covers Fermi liquids, Tomonaga-Luttinger models in 1-dimension, non-canonical (Gutzwiller projected) electrons and gapped superconductors. An interesting result relates to an effective carrierdensity directly found from a weighted first moment of the experimental spectral density from photoemission. This can be compared to contemporary theories, and should yield interesting insights into the underlying T scales.

Future Plans

Fermi surface studies The PI and his group are currently working on several experimentally relevant features of the Fermi surface in 2-dimensional t-t'-J model. The spectral peak intensities are sensitively dependent on three main variables, temperature T, density n and the ration t'/t, and by varying these one can expect to understand a large set of materials in the strongly correlated category. We are pushing the ECFL technique in several directions, to have the sensitivity to extract relevant results. One of the new objects of interest is from Ref. (10), the Tdependent effective number of electrons . We are trying to calculate this accurately and to correlate it with the thermal evolution of the Fermi surface.

Raman, Photoemission and Density fluctuations studies Our group is in contact with several experimentalists working in these techniques. The ECFL theory in 2-dimensions has started to yield interesting results in non-resonant Raman scattering, as reported in Ref. (7). The Raman resistivities are obtainable from the low ω intensities, and the different polarization geometries probe different combinations of t and t', which can then be extracted from such studies. In photoemission studies, our group is in touch with the newly formed experimental ARPES group at UC Davis of Professor Inna Vishik, to test several predicted features of kinks. Our group is also working on introducing long-ranged Coulomb interactions into ECFL. The motivation is to understand recent work on momentum resolved electron diffractions.

High order Schwinger diagram studies and other theoretical imrpvements: Our group is working on higher order expansion, going beyond the $O(\lambda^2)$ ECFL equations used so far. We already have brute force results for 3^{rd} and 4^{th} order in $d=\infty$, and are using these to test the Monte Carlo codes that are being developed. When the testing is done satisfactorily, we expect to have a clear idea of the rate of convergence of the λ expansion in variour regimes of density and temperature.

Broken symmetry solutions: The PI and his group are developing solutions in the broken symmetry regimes. The magnetic and superconducting phases of the t-t'-J model are expected to be approachable within ECFL after a more thorough understanding of the theory in the liquid state, which now seems close at hand.

Publications (August 2016 – July 2018)

A list of ten selected publications follows below.

1. Edward Perepelitsky, Andrew Galatas, Jernej Mravlje, Rok Zitko, Ehsan Khatami, B Sriram Shastry, and Antoine Georges, *Transport and Optical Conductivity in the Hubbard Model: A High-Temperature Expansion Perspective*, Phys. Rev. **B 94**, 235115 (2016).
2. Kazue Matsuyama, Edward Perepelitsky and B Sriram Shastry, *Origin of Kinks in Energy Dispersion of Strongly Correlated Matter*, arXiv:1610.08079, Phys. Rev. **B 95**, 165435 (2017).
3. Wenxin Ding, Rok Zitko, Peizhi Mai, Edward Perepelitsky and B. Sriram Shastry, *A Strange Metal from Gutzwiller correlations in infinite dimensions*, arXiv:1703.02206v2, Phys. Rev. **B 96**, 054114 (2017
4. B Sriram Shastry and Peizhi Mai, *Extremely Correlated Fermi Liquid theory of the t-J model in 2 dimensions: Low energy properties*, arXiv:1703.08142, New Jour. Phys. **20** 013027 (2018).
5. Wenxin Ding, Rok Zitko, and B. Sriram Shastry, *A Strange Metal from Gutzwiller correlations in infinite dimensions II: Transverse Transport, Optical Response and Rise of Two Relaxation Rates*, arXiv:1705.01914, Phys. Rev **B96**, 115153 (2017).
6. Peizhi Mai, Steven R White and B Sriram Shastry, *The t-t'-J model in one dimension using extremely correlated Fermi liquid theory and time dependent density matrix renormalization group,* arXiv:1712.05396, Phys. Rev. **B98**, 035108 (2018).
7. Peizhi Mai and B Sriram Shastry, *Non-resonant Raman Scattering in Extremely Correlated Fermi Liquids*, arXiv:1805. 09935 (Submitted for publication.)
8. Edward Perepelitsky and B. Sriram Shastry, *Band-edge quasiparticles from electron phonon coupling and resistivity saturation*, arXiv:1806.1127. (Submitted for publication.)
9. Rok Zitko, H. R. Krishnamurthy and B. Sriram Shastry, *Reversal of particle-hole scattering-rate asymmetry in Anderson impurity mode*l, arXiv:1807.11343. (Submitted for publication.)
10. B. Sriram Shastry, *Fermi Surface Volume of Interacting Systems*, arXiv:1808.00405 (Submitted for publication.)

Novel Fractional Quantum Hall Effect and New Topological Phase in Interacting Systems

Principle investigator: Dr. Donna N. Sheng

California State University Northridge

Northridge, CA 91330

donna.sheng@csun.edu

Project Scope

The project involves theoretical (numerical) study of the topological physics in strongly interacting systems. We aim to make significant contribution in solving strongly correlated systems and provide fundamental understanding for emerging topological physics in such systems. By developing the state of art density matrix renormalization group (DMRG) based numerical method for such systems, we search and discovery non-Abelian states in fractional quantum Hall systems and other correlated systems without Landau levels. Our work is aiming to provide answers for the nature of new quantum phases of interacting topological systems, explain experimental results, and predict new experimental findings. We have made important progress in the following areas: (i) Identify and characterize multi-component FQHE states and other strongly correlated topological phases; (ii) Identifying different quantum phase diagrams for spontaneous time reversal symmetry breaking, quantum anomalous Hall effect (QAHE), and nontrivial current carrying topological state; (iii) Numerical development, studying dynamic structure factor for chiral spin liquid, and quantum phase transitions; (iv) Obtaining initial progress in understanding the nontrivial role of disorder for non-Abelian FQHE system.

Recent Progress

Identify and characterize multi-component FQHE states and other topological phases:

In the work of studying the multi-component FQHE of interacting particles in topological bands, we demonstrate that a class of SU(N) FQHE states can emerge at fractional filling factors N/(N + 1)

(N/(2N + 1)) for bosons (fermions) in the lowest Chern band, characterized by the nontrivial fractional Hall responses and the fractional charge pumping. Based on our numerical simulations of Chern number matrix for multi-component systems, we establish robust FQHE states with diagonal elements for K-matrix, K_{jj}=2 (3), and the off-diagonal elements K_{j,j'}=1 (2) for general N for boson (fermion) case with suitable repulsive interactions. Both of K matrices are related to the Cartan matrix of the Lie algebra SU(N) by a special linear group SL(N,Z) transformation, indicating that these FQHE states exhibit an SU(N) Kac-Moody symmetry at level one. The beautiful connections between

mathematics and topological ordering in realistic system is demonstrated here. Figure 1 illustrates energy spectrum, topological degeneracy, and how to obtain Chern number matrix from Berry phases for a SU(4) FQHE state.

We further explore the possibility of realizing robust non-Abelian topological chiral spin liquid phase in the two-dimensional Kitaev honeycomb model subject to a magnetic field. By combining DMRG and exact diagonalization, we study the energy spectra, entanglement, topological degeneracy, and expectation values of Wilson loop operators, allowing for robust characterization. While the ferromagnetic (FM) Kitaev spin liquid was known to be destroyed by a weak magnetic field, the antiferromagnetic (AFM) Kitaev spin liquid remains robust up to a critical magnetic field that is an order of magnitude larger than the FM case. Such a phase is an example of non-Abelian FQHE for bosons, demonstrating quantized thermal Hall effect. Interestingly, for larger fields, an intermediate gapless phase is observed, before a second transition to the high-field partially-polarized paramagnet. We attribute this rich phase diagram, and the remarkable stability of the non-Abelian chiral topological phase in the AFM Kitaev model, to the interplay of strong spin-orbit coupling and frustration enhanced by the magnetic field. Our findings suggest relevance to recent experiments on RuCl3 under magnetic fields.

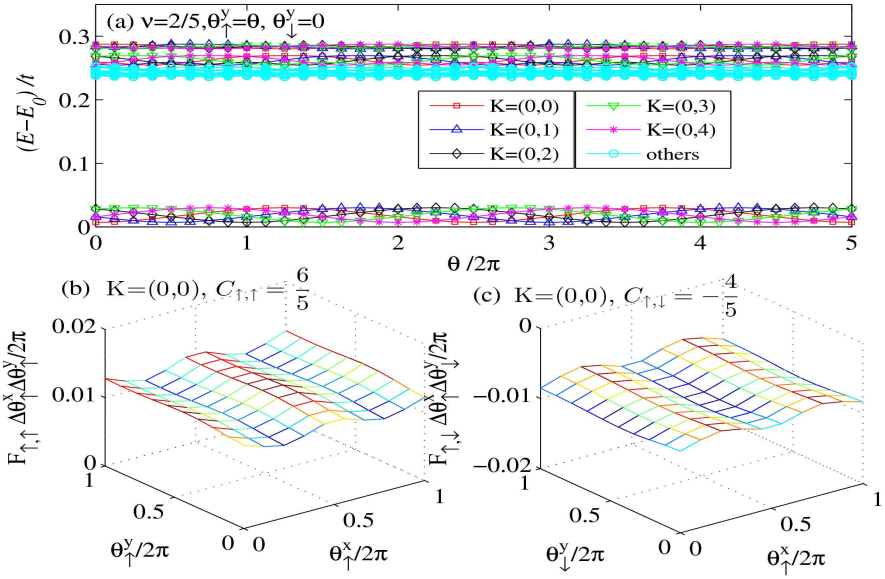

Caption for Figure 1: (a) Energy spectrum, which establishes topological degeneracy for a SU(4) FQHE. (b-c) The diagonal and off-diagonal elements of Chern number matrix are obtained based on inserting different twisted boundary phases (fluxes).

We also explore the quantum phase transitions in quantum Hall bilayer systems with total filing nu=1 of the lowest LL. In our calculations, we obtain three distinct phases, including an exciton superfluid phase with spontaneous interlayer coherence at small d, a composite Fermi liquid at large d, and an intermediate phase for 1.1<d<1.8 (in units of the magnetic length). By following different physical quantities, we identify two transitions through (i) a dramatic change in the Berry curvature of the ground state under twisted boundary conditions on the two layers; (ii) an energy level crossing of the first excited state; (iii) exciton superfluid stiffness. The intermediate phase is identified to show an even-odd effect in pseudospin (layer transfer) excitation gap, which possibly extrapolates to a finite value in the thermodynamic limit, indicating the enhanced intralayer correlation. Our identification of an intermediate phase and its distinctive features shed new light on the theoretical understanding of the quantum Hall bilayer system at total filling nu=1.

Spontaneous time reversal symmetry breaking, Dirac gap opening and closing, and nontrivial current carrying states

In recent years, the possibility of realizing novel interaction-driven topological phase has attracted a lot of research activities, which may significantly extend the classes of topological states of matter. In a series of work, we identify spontaneous interaction-driven nonzero Berry phase and QAHE emerging in extended fermion-Hubbard models on kagome and checkerboard lattices where the noninteracting systems are semimetals with quadratic band crossings. By means of the state-of-the-art DMRG, we expose universal properties of the QAHE including time-reversal symmetry spontaneous breaking and quantized Hall conductance. For kagome lattice model with frustrated nearest neighbor hopping (t>0), we demonstrate that weak second nearest neighbor interaction will promote a robustly gapped QAHE. For checkerboard model as illustrated in Figure 2, we demonstrate the instability of the quadratic band touching towards an interaction-driven QAHE. For strong interactions, the system breaks the rotational symmetry realizing a nematic charge-density-wave phase. Interestingly, for intermediate interactions we discover a symmetry-broken bond-ordered critical phase sandwiched in between the QAHE and CDW phases, which splits the QBT into two Dirac points driven by interaction. Our identification of an intermediate phase shed new light on the theoretical understanding of the interaction-driven phases in quadratic band touching systems. Besides the QAHE, we also identify interaction-driven fractionalized topological state emerging in an extended Bose-Hubbard model on kagome lattice, where the non-interacting band structure is topological trivial. Our work paves a way of finding interaction induced topological phase at the phase boundary of conventionally ordered solid phases.

By studying a doped Mott insulator on square lattice described by the t-J model based DMRG and exact diagonalization calculations, we identify persistent spin currents in the ground state, which are concomitant with a nonzero total momentum or angular momentum associated with the doped hole. By further making superpositions of the degenerate ground states with zero or unidirectional spin currents, we show that different patterns of spatial charge and spin modulations will emerge. We provide a theoretical understanding of the spin current based on a many-body Berry-like phase and mutual statistics between doped holes and spins.

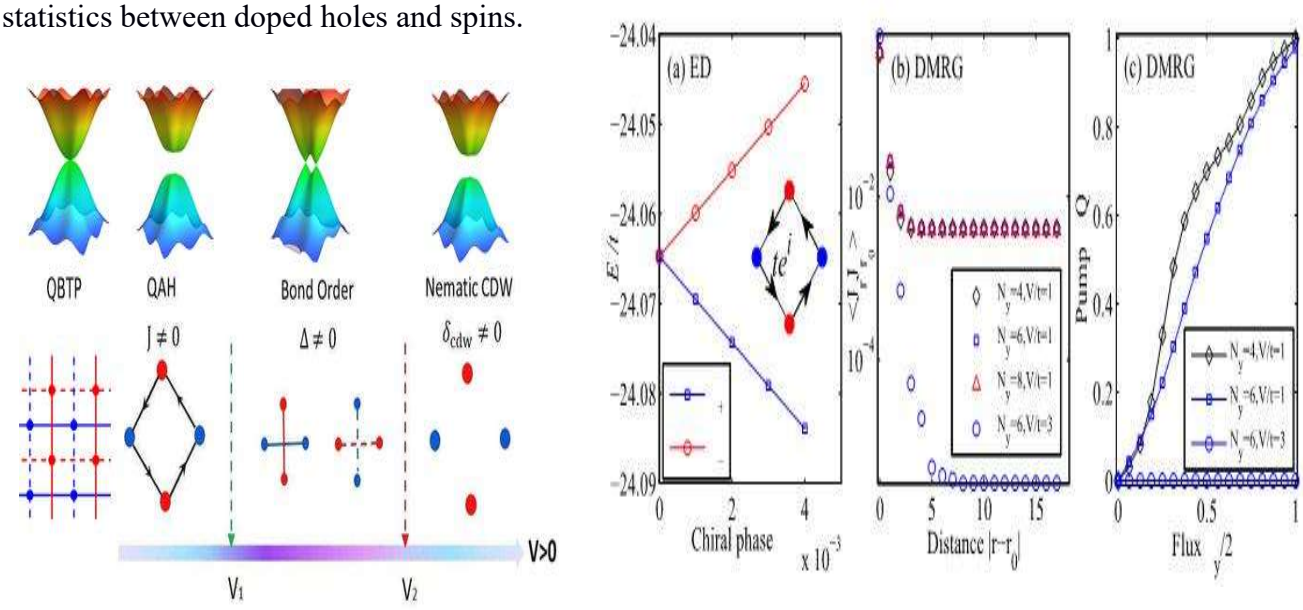

Caption for Figure 2. Left panel: Illustrating phase diagram for checkerboard semi-metal system with quadratic band touching and interactions. Right panel: Spontaneous current and charge pump are illustrated.

Dynamic structure factor and quantum phase transitions

We study dynamical spin structure factor (DSSF) of S = 1/2 Heisenberg model on the kagome lattice by means of DMRG. The chiral spin liquid phase and nearby magnetic ordered state, as well as a time-reversal invariant (TRI) spin liquid state show distinct dynamical response behavior. First of all, the DSSF of the TRI spin liquid displays important spectral intensity predominantly at low frequency region around Q = M point in momentum space, and shows a broad spectral distribution at high frequency region for momenta along the boundary of the extended Brillouin zone. Secondly, spinon excitation spectrum is identified from momentum and energy resolved DSSF, which shows critical behavior with much reduced spectrum intensity comparing to the neighboring chiral spin liquid. By adding a weak Dzyaloshinkii-Moriya interaction, the DSSF demonstrates a strong sensitivity to the boundary conditions more consistent with a gapless spin liquid. These results capture the main observations in the inelastic neutron scattering measurements of herbertsmithite, and indicate the spin liquid nature of the ground state with fractionalized spinon excitations. By following the DSSF crossing the quantum phase transition between the chiral spin liquid and the magnetical ordered phase, we identify the spinon condensation driving the quantum phase transition.

Future direction: We will search and discover different non-Abelian states in fractional quantum Hall and other interacting systems. Furthermore, we will further develop numerical methods to target properties of excited states and dynamic response functions in strongly correlated systems. At last, we will also develop numerical algorithms to characterize the topological order in disordered correlated systems.

Publications

1. Tian-sheng Zeng, W. Zhu, D. N. Sheng, *Tunning topological phase and quantum anomalous Hall effect by interaction in quadratic band touching systems*, arXiv:1805.01101.

2. Yafei Ren, T.-S. Zeng, W. Zhu, D. N. Sheng, *Quantum Anomalous Hall Phase Stabilized via Realistic Interactions on a Kagome Lattice*, arXiv:1806.11094.

3. Zheng Zhu, Itamar Kimchi, D. N. Sheng, Liang Fu, *Robust non-Abelian phase in antiferromagnetic Kitaev model under magnetic field*, Phys. Rev. B 97, 241110 (2018).

4. Tian-Sheng Zeng, D. N. Sheng, *SU(N) fractional quantum Hall effects in topological flat bands*,

Phys. Rev. B 97, 035151 (2018).

5. Zheng Zhu, Liang Fu, D. N. Sheng, *Numerical Study of Quantum Hall Bilayers at Total Filling nu_T=1: A New Phase at Intermediate Layer Distances*, Phys. Rev. Lett. 119, 177601 (2017).

6. Zheng Zhu, Inti Sodemann, D. N. Sheng, Liang Fu, *Anisotropy Driven Transition from Moore-Read State to Quantum Hall Stripes*, Phys. Rev. B 95, 201116(R) (2017).

7. Tian-Sheng Zeng, W. Zhu, and D. N. Sheng, *Two-component quantum Hall effects in topological flat bands*, Phys. Rev. B 95, 125134 (2017).

8. W. Y. Deng, Y. J. Ren, Z. X. Lin, L. Sheng, D. N. Sheng, D. Y. Xing, *Analytical theory and possible detection of the ac quantum spin Hall effect*, Scientific Reports 7, 5078 (2017).

9. W. Zhu, Zhao Liu, F. D. M. Haldane, and D. N. Sheng, *Fractional quantum Hall bilayers at half filling: Tunneling-driven non-Abelian phase*, Phys. Rev. B 94, 245147 (2016).

10. W. Zhu, Shou-Shu Gong, Tian-Sheng Zeng, Liang Fu, and D. N. Sheng, *Interaction-Driven Spontaneous Quantum Hall Effect on a Kagome Lattice*, Phys. Rev. Lett. 117, 096402 (2016).

Electron Correlations, Bad-Metal Behavior and Unconventional Superconductivity

Principal Investigator: Qimiao Si, Rice University; Qmsi@rice.edu

Keywords: Correlated electrons, unconventional superconductivity, bad metals, orbital selective Mott, quantum phase transitions

Project Scope

This project aims to deepen our understanding of electron correlations, bad-metal behavior, and their connections with magnetism and unconventional superconductivity. The premise is that the electron correlations lead to bad metallicity in the normal state and often generate an antiferromagnetic (AF) order, and the proximity to both promotes unconventional superconductivity. This notion connects well with the experimental observations in the iron-based superconductors (FeSCs), where superconductivity develops in strongly-correlated bad-metal normal state near an AF order. A main focus is to understand the multi-orbital correlations and superconductivity in the FeSCs. Wherever possible, unifying themes that may pertain to other strongly correlated materials will be sought for. As such, related systems will also be examined. The research directions include: a) orbital-selective correlations in the FeSCs; b) understanding orbital-selective superconductivity in the FeSCs; and c) multi-orbital physics of chromium-based systems.

Recent Progress (September 2017 – July 2018)

Topic #1 -- Orbital-selective correlations in iron-based systems

1.A New approach for orbital-selective Mott physics. There is an increasing recognition that the multiorbital nature of the *3d* electrons is important to the normal state of the iron-based superconductors and related quantum materials. An important characteristic of the pertinent multi-orbital Hubbard models is that the orbitals are kinetically coupled, *i.e.*, hybridized, to each other (Fig. 1), which makes the orbital-selective Mott phase to be counter-intuitive. Here we develop a Landau free-energy functional to put the microscopic analysis from the U(1) slave-spin approach [1,2,3] in this perspective. We show that the Landau functional

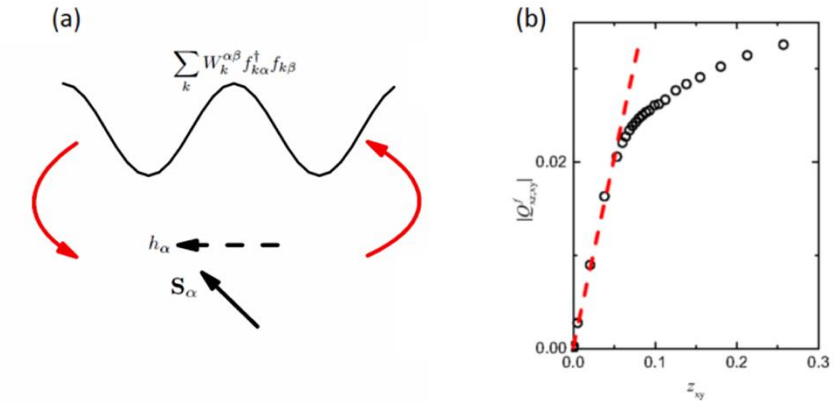

Fig. 1: (a) The coupling between the spin (*f*-spinon) and charge (*S*-slave-spin) degrees of freedom, which underlies the Landau free-energy functional constructed in this work; (b) A key prediction of the Landau theory is supported by numerical result. From publication P1.

contains only biquadratic (as opposed to bilinear) couplings between the quasiparticle weights of different orbitals. This leads to the stability of a dynamically suppressed hybridization and the concomitant orbital-selective Mott transition against fluctuations beyond the mean-field level.

1.B Orbital-selective correlations in the nematic phase of FeSe. Motivated by the recent low-temperature experiments on bulk FeSe, we study the electron correlation effects in a multiorbital model in the nematic phase using the U(1) slave-spin theory. We find that a finite nematic order helps to stabilize an orbital selective Mott phase. Moreover, we propose that when the d- and s-wave bond nematic orders are combined with the ferro-orbital order, there exists a surprisingly large orbital selectivity between the xz and yz orbitals even though the associated band splitting is relatively small (Fig. 2). Our results explain that a strong orbital selectivity exists in the nematic phase of FeSe, even though the band splitting is weak as seen in the ARPES experiments. The co-existing bond and site orders provide new clues to the nature of the nematic order.

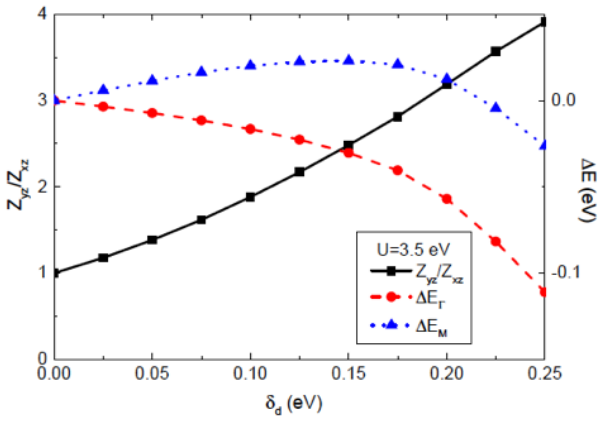

Fig. 2: Nematic state of bulk FeSe: Large orbital selectivity, measured by the ratio of the quasiparticle weights of the xz and yz orbitals, occurs even though the associated band splitting is relatively small, shown here for the Γ and M points, when site and bond nematic orders coexist. From publication P2.

Topic #2 -- Electronic orders and their fluctuations in iron-based systems

2.A Emergent double-Q C4 antiferromagnetism and enhanced nematic correlations. Electron correlations produce a rich phase diagram in the iron pnictides. Our earlier theoretical studies on the correlation effect demonstrated how quantum fluctuations weaken and concurrently suppress a C2-symmetric single-Q AF order and a nematic order [4]. Here we find that a C4-symmetric collinear double-Q AF order (Fig. 3a) appears as an emergent phase near the quantum phase transition. For this double-Q AF order, we show that it is accompanied not only by a charge order but also by an enhanced nematic susceptibility, as illustrated in Fig. 3b. Our results provide a natural understanding for

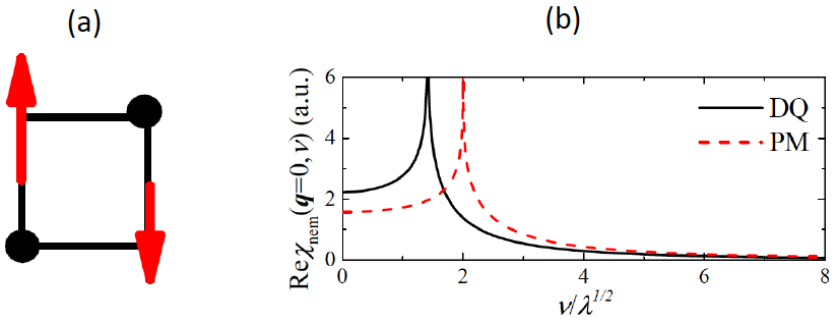

Fig. 3: The collinear double-Q AF order is C4-symmetric (a), but has an enhanced nematic susceptibility (b). From publication P3.

several intriguing recent experiments in hole-doped iron arsenides, and bring out common physics that underlies the different magnetic phases of various iron-based superconductors.

A collaboration with the Birgeneau group revealed a) the first evidence for the charge order in the C4 magnetic phase, based on spectroscopy measurements in $Ba_{1-x}Na_xFe_2As_2$ (publication P4); and b) the instantaneous local structure to comprise fluctuating orthorhombic regions with a length scale of a few nanometers, in the C4 magnetic phase of $Sr_{1-x}Na_xFe_2As_2$, implying an exceptionally large nematic susceptibility in this C4-symmetric phase (publication P5), which is consistent with our theory summarized in the previous paragraph.

2.B Quasi-degenerate magnetic orders in FeTe. FeTe has the unusual $(\pi/2,\pi/2)$ bicollinear order. As a step towards a unified description of magnetism in iron-based systems, we have preliminary theoretical results that the bicollinear order is nearly degenerate with another $(\pi/2,\pi/2)$ plaquette AF order. Evidence for this quasi-degeneracy has been found: While the low-energy spin excitations are indeed transverse spin waves, at energies above 20 meV, the magnetic scattering is dominated by an isotropic continuum (publication P6).

Topic #3 -- Orbital-selective superconductivity in the nematic phase of FeSe.

Motivated by recent experiments on the superconductivity of the bulk FeSe, we study the pairing structure of this compound in its nematic phase using a multiorbital model with frustrated spin-exchange interactions. We find that the electron correlations, which generate strong orbital selectivity in the normal state, naturally give rise to an orbital-selective superconducting pairing. The orbital selectivity in the pairing amplitudes is enhanced by nematicity, and produces a large gap anisotropy (Fig. 4). Our results naturally explain the observed gap anisotropy in bulk FeSe, and have broad implications to the superconductivity of other iron-based superconductors.

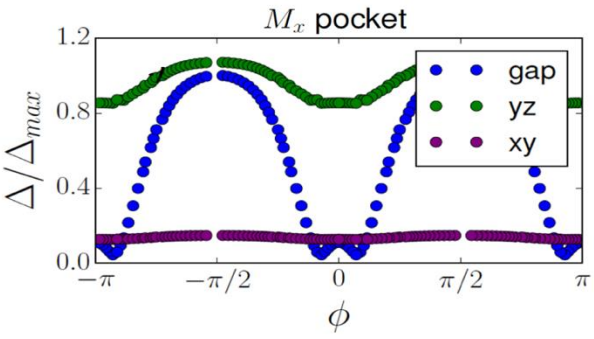

Fig. 4: Superconductivity in the nematic FeSe: Orbital selective pairing amplitude produces a large gap anisotropy. From publication P7.

Topic #4 – Bad metals and quantum phase transitions in CrAs.

Our goal here is to carry out studies of correlated-electron physics in multi-orbital systems beyond FeSCs. At ambient pressure, CrAs undergoes a first-order transition into a double-helical magnetic state at T_N = 265 K, which is accompanied by a structural transition. The recent discovery of pressure-induced superconductivity in CrAs makes it important to clarify the nature of quantum phase transitions out of its coupled structural/helimagnetic order. In a theory-experiment collaborative study, the coupled order is found to be suppressed by either pressure or

phosphorus doping. In addition, the *A* coefficient of the quadratic temperature dependence of the resistivity exhibits a dramatic enhancement as pressure or doping approaches its respective critical value, around which non-Fermi-liquid behavior and superconductivity develops. We advanced a theoretical approach and understood the quantum critical behavior in terms of a nearly second-order helimagnetic quantum phase transition.

Future Plans

Our plan for the coming year (Y2 of the grant) includes:

New theoretical approach to the correlated-electron physics of FeSCs. We plan to develop a Variational Monte Carlo method to study electron correlations in the intermediate coupling regime. This direction is pertinent to a variety of strongly correlated systems, but naturally we will start from the multi-orbital models for the FeSCs. The variational approach will treat the correlation effects of both the Hubbard and Hund's couplings. Preliminary results are quite encouraging, demonstrating a quantum phase transition between the coupled AF/nematic orders and disordered phase as a function of the interaction strength, with characteristics compatible with field-theoretical analyses.

Orbital-selective correlations and superconductivity in the nematic phase of FeSe. Our work during Y1 (publications P2 and P7) has opened up several important directions of future study on this topic. In particular, we plan to address the evolution of electron correlations and orbital-selective pairing for FeSe under either pressure or as a function of S-doping.

Frustrated magnetism and spin dynamics in FeTe. Our recent work on the quasi-degenerate magnetic order in FeTe (publication P6) provides the basis to study magnetic dynamics in this system. We expect this planned work to be particular instructive in uncovering the ingredients of a unifying description of magnetism and related electronic orders in the FeSCs in general.

Orbital-selective correlations in Cr-based systems. Our recent studies on the quantum phase transitions in the Cr-based systems (publication P8) sets the stage for the study of the bad-metal characteristics. We plan to analyze the orbital-selective correlations in this and related systems.

References

1. R. Yu and Q. Si, *Mott Transition in Multi-Orbital Models for Iron Pnictides*, Phys. Rev. B **84**, 235115 (2011).

2. R. Yu and Q. Si, *U(1) slave-spin theory and its application to Mott transition in a multi-orbital model for iron pnictides*, Phys. Rev. B **86**, 085104 (2012).

3. R. Yu and Q. Si, *Orbital-selective Mott Phase in Multiorbital Models for Alkaline Iron Selenides* $K_{1-x}Fe_{2-y}Se_2$, Phys. Rev. Lett. **110**, 146402 (2013).

4. J. Dai, Q. Si, J.-X. Zhu and E. Abrahams, *Iron pnictides as a new setting for quantum criticality*, PNAS **106**, 4118 (2009).

Publications (September 2017 – July 2018, acknowledging the DOE support)

P1. R. Yu and Q. Si, *Orbital-selective Mott phase in multiorbital models for iron pnictides and chalcogenides*, Phys. Rev. B **96**, 125110 (2017).

P2. R. Yu, J.-X. Zhu, and Q. Si, *Orbital selectivity enhanced by nematic order in FeSe*, Phys. Rev. Lett., submitted; arXiv:1803.01733.

P3. R. Yu, M. Yi, B. A. Frandsen, R. J. Birgeneau, and Q. Si, *Emergent phases in iron pnictides: Double-Q antiferromagnetism, charge order and enhanced nematic correlations*, Phys. Rev. Lett., submitted (2017).

P4. B. A. Frandsen, K. M. Taddei, M. Yi, A. Frano, Z. Guguchia, R. Yu, Qimiao Si, D. E. Bugaris, R. Stadel, R. Osborn, S. Rosenkranz, O. Chmaissem, and R. J. Birgeneau, Local orthorhombicity in the magnetic C4 phase of the hole-doped iron-arsenide superconductor Sr(1-x)Na(x)Fe_2As_2, Phys. Rev. Lett. **119**, 187001 (2017).

P5. M. Yi, A. Frano, D. H. Lu, Y. He, M. Wang, B. Frandsen, A. F. Kemper, R. Yu, Q. Si, L. Wang, M. He, F. Hardy, P. Schweiss, P. Adelmann, T. Wolf, M. Hashimoto, S.-K. Mo, Z. Hussain, M. Le Tacon, C. S. Nelson, A. E. Boehmer, D.-H. Lee, Z.-X. Shen, C. Meingast, and R. J. Birgeneau, Emergent Charge Order in Ba(1-x)Na(x)F e_2As_2, Phys. Rev. Lett., submitted (2018).

P6. Y. Song, X.Y. Lu, L.-P. Regnault, Y. Su, H.-H. Lai, W.-J. Hu, Q. Si, and P. C. Dai, Isotropic continuum of spin excitations in antiferromagnetically ordered $Fe_{1.07}Te$, Phys. Rev. B **97**, 024519 (2018).

P7. H. Hu, R. Yu, E. M. Nica, J.-X. Zhu, and Q. Si, *Orbital-selective superconductivity in the nematic phase of FeSe*, Phys. Rev. Lett., submitted; arXiv:1805.05915.

P8. M. Matsuda*, F. K. Lin*, R. Yu*, J.-G. Cheng, W. Wu, J. P. Sun, J. H. Zhang, P. J. Sun, K. Matsubayashi, T. Miyake, T. Kato, J.-Q. Yan, M. B. Stone, Q. Si, J. L. Luo, and Y. Uwatoko, *Evolution of Magnetic Double Helix and Quantum Criticality near a Dome of Superconductivity in CrAs*, Phys. Rev. X, in press (2018).

Many-Body Theory of Energy Transport and Conversion at the Nanoscale

Principal Investigator: Charles A. Stafford
Department of Physics, University of Arizona
1118 E. 4th Street, Tucson, AZ 85721
staffordphysics92@gmail.com

Keywords: Quantum thermodynamics, thermoelectrics, nonequilibrium statistical mechanics

Program Scope

This project addresses the fundamental challenge of understanding interacting quantum systems far from equilibrium, while simultaneously exploring the potential of nanostructured materials for applications in energy-conversion technologies.

The main focus of the project is quantum thermoelectrics. The experimental observation of a thermoelectric voltage across a single molecule, first reported[1] in 2007, begs the question, "What is the temperature difference between the hot side and cold side of the molecule?" Can temperature vary from one place to another in a small quantum system such as a molecule or even an atom? To date, experimental probes of temperature lack the spatial resolution needed to answer these fundamental questions, but this project will investigate some promising scenarios to break the nanometer barrier, including a single-atom thermometer.

To elucidate the local quantum mechanisms responsible for thermoelectricity, the project will investigate the local thermodynamics of nonequilibrium quantum systems. The flow of entropy and heat in quantum conductors will be investigated from fundamental principles, and the complex nature of the quantum-classical crossover will be explored.

Fundamental research on the nonequilibrium many-body theory of nanostructures will be conducted in parallel, to enable the applied research on nanoscale energy conversion. The local properties of interacting quantum systems far from equilibrium will be investigated using nonequilibrium Green's functions (NEGF) to treat general protocols in stochastic thermodynamics. Various nonequilibrium fluctuation-dissipation theorems will be derived, one of which underlies the operation of the proposed single-atom thermometer.

Recent Progress

Emergence of Fourier's law of heat transport in quantum electron systems

The microscopic origins of Fourier's venerable law of thermal transport in quantum electron systems has remained somewhat of a mystery, given that previous derivations[2,3] were forced to invoke intrinsic scattering rates far exceeding those occurring in real systems. The PI, together with former undergraduate researcher Sosuke Inui and collaborator Justin Bergfield devised an alternative hypothesis [2], namely, that Fourier's law emerges naturally if many quantum states participate in the transport of heat across the system. The hypothesis was tested systematically in a graphene flake junction (see Fig. 1) and it was shown that the temperature

distribution becomes nearly classical and the heat flow laminar when the broadening of the individual quantum states of the flake exceeds their energetic separation. In contrast, when one or a few quantum states dominate the thermal transport, the temperature distribution is non-monotonic and the heat flow is highly non-classical, with quantum vortices and backflow. A thermal resistor network model was developed to investigate the scaling of the sample and contact thermal resistances and it was shown that the latter is consistent with classical thermal transport theory in the limit of large level broadening.

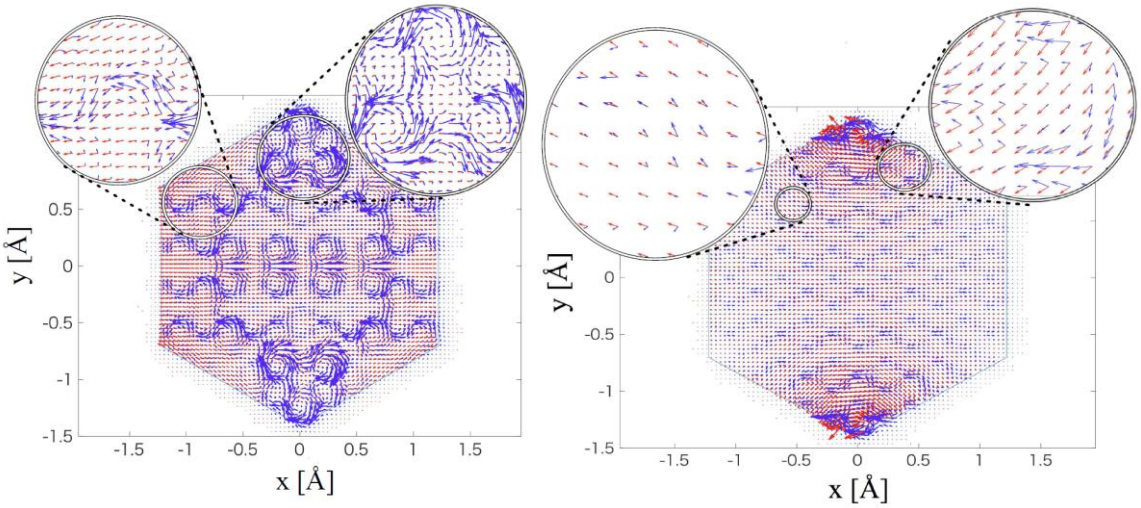

FIG. 1. Classical (red arrows) and quantum (blue arrows) heat flow across a graphene nanoflake. Left panel: Quantum regime, with vortices and backflow. Right panel: Fourier regime, with laminar flow along the C-C bonds.

Scanning tunneling thermometry

Former Ph.D. student Abhay Shastry and the PI invented a new method [1] to measure temperature in conductive materials with sub-nanometer spatial resolution, a two-order-of-magnitude improvement over the current state of the art. The method relies on purely electrical measurements effectuated by a conductive scanning probe operating in the tunneling regime. The key concept is to bypass the difficult direct measurement of heat currents by using the Wiedemann-Franz law, which has a broad range of validity in conducting materials, and has recently been confirmed experimentally in atomic-scale junctions. Then, measuring just the electrical current into the probe under a specific sequence of thermoelectric bias conditions is sufficient to determine the local temperature with high precision. This invention was described in Abhay Shastry's Ph.D. thesis, and is the subject of a provisional U.S. patent application filed in March, 2018.

Local entropy of a nonequilibrium fermion system

The local entropy of a nonequilibrium system of independent fermions was investigated, and analyzed in the context of the laws of thermodynamics [3]. It was shown that the local temperature and chemical potential can only be expressed in terms of derivatives of the local

entropy for linear deviations from local equilibrium. The first law of thermodynamics was shown to lead to an inequality, not an equality, for the change in the local entropy as the nonequilibrium state of the system is changed. The maximum entropy principle (second law of thermodynamics) was proven: a nonequilibrium distribution has a local entropy less than or equal to a local equilibrium distribution satisfying the same constraints.

Thermoelectric probes of nonequilibrium quantum systems

In collaboration with Abhay Shastry, it was shown that a local measurement of temperature and voltage for a quantum system in steady state, arbitrarily far from equilibrium, with arbitrary interactions within the system, is unique and exists [4]. A positive temperature solution exists whenever there is no net population inversion. However, when there is a net population inversion, the measurement results in an absolute negative temperature (see Fig. 2). Our analysis also provides a proof of the positivity of the Onsager matrix[4] of thermoelectric linear response theory, a statement of the second law of thermodynamics that had lacked an independent proof for 85 years.

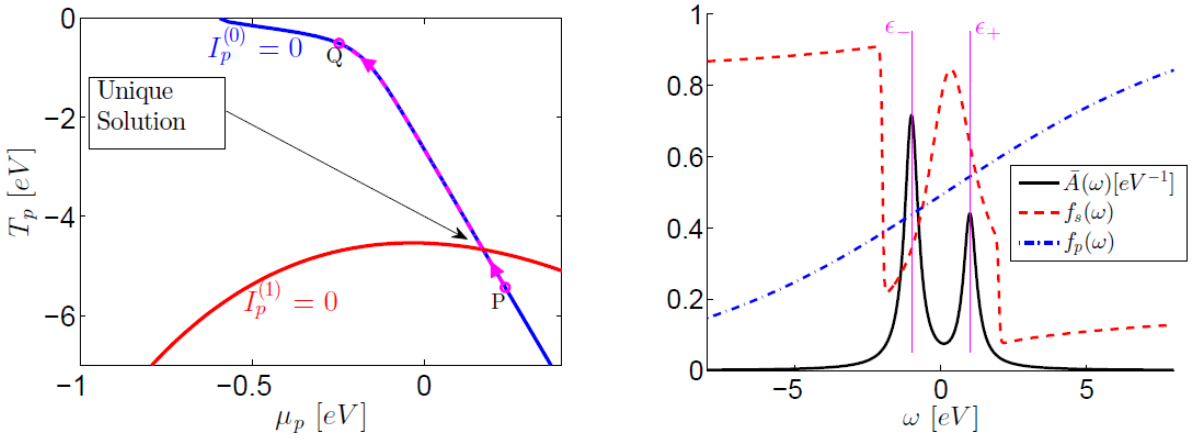

FIG. 2. Equilibration of a thermoelectric probe with a strongly-driven two-level quantum system. Left panel: Curves along which the electric current $I_p^{(0)}$ and heat current $I_p^{(1)}$ into the probe vanish. Right panel: The local spectrum $\bar{A}(\omega)$, local nonequilibrium distribution $f_s(\omega)$, and probe distribution $f_p(\omega)$ corresponding to the unique negative temperature solution on the left.

Future Plans

Single-atom thermometer

Measuring temperature with nanoscale resolution has proven extraordinarily difficult because scanning probes lack the thermal isolation needed to achieve high spatial resolution. The PI, along with former Ph.D. student Abhay Shastry and former undergraduate researcher Marcus Rosales has proposed a novel method to measure temperature with subnanometer resolution using individual physisorbed atoms as surface thermometers. We study the diffusive dynamics of aluminum adatoms adsorbed on graphene nanoflakes subject to a thermoelectric bias leading to a nontrivial spatial temperature distribution. The adatoms couple to local thermal fluctuations of both the vibrational and electronic degrees of freedom. The electronic coupling is mediated by

Coulomb interactions, and is treated using NEGF. The adatom motion can be followed by STM in real time, and we find that they seek out the cold spots on the surface, thereby serving as thermometers. The theory underlying these phenomena has been worked out, and small-scale simulations have been carried out that are consistent with theoretical predictions. Large-scale simulations are currently underway.

Quantum thermodynamics in the time domain

To this point, the project has focused on nonequilibrium steady-state systems, with a few results derived for systems with adiabatic time dependence. However, the NEGF formalism that is the workhorse for our research is equally applicable to more general time-dependent systems. Time-dependent thermodynamic processes (e.g., work, particle and energy transfer) in open quantum systems will therefore be investigated. Both aperiodic and period driving will be considered, the later using Floquet-NEGF based on the PI's prior work.[5]

Nonlinear Peltier effect

Together with former undergraduate researcher Marco Jimenez (an exchange student from University of Sonora who is entering the UA physics Ph.D. program in Fall 2018) and former Ph.D. student Abhay Shastry, the PI has been investigating the maximum cooling power of a model quantum thermocouple consisting of a double quantum dot with three electrical terminals. Promising preliminary results have been obtained for the noninteracting case, indicating that substantial cooling power (several nanowatts) can be achieved with a single nanoscale thermocouple. In principle, the nonlinear response depends strongly on the electron-electron interactions required to enforce gauge invariance. The cooling power of a double quantum dot with electron-electron interactions will therefore be systematically investigated. Since the Coulomb interaction is typically the largest energy scale in the problem for such a system, it is possible that even larger cooling powers may be realized in the interacting system.

References

1. P. Reddy, S.-Y. Jang, R. A. Segalman, and A. Majumdar, “Thermoelectricity in Molecular Junctions,” Science, vol. 315, no. 5818, pp. 1568–1571, 2007.
2. Y. Dubi and M. Di Ventra, “Fourier's Law: insight from a simple derivation,” Physical Review E **79**, 042101 (2009).
3. Y. Dubi and M. Di Ventra, “Reconstructing Fourier’s law from disorder in quantum wires,” Physical Review B **79**, 115415 (2009).
4. L. Onsager, “Reciprocal relations in irreversible processes. i.,” Phys. Rev. **37**, pp. 405–426 (1931).
5. C. A. Stafford and Ned S. Wingreen, “Resonant Photon-Assisted Tunneling Through a Double Quantum Dot: An Electron Pump From Spatial Rabi Oscillations,” Phys. Rev. Lett. **76**, 1916 (1996).

Publications

[1] Abhay Shastry and Charles A. Stafford, “Scanning Tunneling Thermometry using Electrical Measurements,” Provisional U.S. Patent Number: 62/642,359, filed March 13, 2018.

[2] Sosuke Inui, Charles A. Stafford, and Justin P. Bergfield, Emergence of Fourier's law of heat transport in quantum electron systems, ACS Nano **12**, 4304-4311 (2018).

[3] Charles A. Stafford and Abhay Shastry, Local entropy of a nonequilibrium fermion system, Journal of Chemical Physics **146**, 092324 (2017).

[4] Abhay Shastry and Charles A. Stafford, Temperature and voltage measurement in quantum systems far from equilibrium, Physical Review B **94**, 155433 (2016).

Non-equilibrium Relaxation and Aging Scaling of Driven Topological Defects in Condensed Matter

And

Non-equilibrium Relaxation, Aging Scaling, and Critical Depinning Dynamics of Skyrmions in Disordered Magnetic Films

Principal Investigator: Uwe C. Täuber (tauber@vt.edu)
Co-Principal Investigator: Michel Pleimling (pleim@vt.edu)
Department of Physics (MC 0435), Virginia Tech
Robeson Hall, 850 West Campus Drive, Blacksburg, Virginia 24061

Keywords: driven topological defects, skyrmions, type-II superconductors, non-equilibrium relaxation, aging scaling

Project Scope

This project aims at understanding relaxation processes in systems with different types of topological defects. (1) Technical applications of type-II superconductors, especially high-T_c compounds, in external magnetic fields require an effective flux pinning mechanism to reduce Ohmic losses due to flux creep and flow. Consequently, the properties of interacting vortex lines subject to strong thermal fluctuations and point-like or extended disorder have been a major research focus in condensed matter physics. (2) Skyrmion topological defects are particle-like spin textures encountered in magnetic thin films and bulk materials with broken inversion symmetry and strong spin-orbit coupling that promise novel avenues for highly efficient magnetic data storage and logic operations. While both equilibrium and stationary transport properties (typically in the linear response regime) of interacting skyrmions have been intensely studied, much less is known about their relaxation processes away from stationarity. Supported through DOE-BES, we have earlier developed an efficient and versatile Langevin molecular dynamics algorithm to investigate the dynamics of interacting magnetic flux lines in disordered type-II superconductors. We have gained extensive expertise in the analysis of the ensuing complex steady-state as well as non-equilibrium relaxation phenomena of vortex matter. In addition, we utilize a coarse-grained particle-like representation of the dynamics of magnetic skyrmions in terms of stochastic equations of motion to probe their relaxation features and gain a comprehensive understanding of the interplay between the crucial Magnus force, repulsive skyrmion-skyrmion interactions, and thermal as well as non-equilibrium fluctuations in disordered magnetic films.

Recent Progress

Non-equilibrium kinetics of relaxing skyrmions

We have initiated a detailed investigation of the relaxation dynamics of systems of interacting magnetic skyrmions. Similar to vortices in type-II superconductors, these topological defects

repel each other through mutual screened logarithmic interactions, and thus at low temperatures and in pure samples form a triangular lattice. We have generated and tested a Langevin dynamics code utilizing a recently developed particle model derived for skyrmions [1] that yields equations of motion in two dimensions which are very similar to those used for the effective two-dimensional description of vortices in type-II superconductors, when the latter are treated as point-like objects. The most important distinction resides in the strong effect of the Magnus force on a magnetic skyrmion, which acts in the direction perpendicular to its velocity. After initializing the system by distributing the skyrmions at randomly selected positions, we have followed the subsequent non-equilibrium relaxation kinetics of skyrmions towards the equilibrium (quasi-) ordered triangular lattice. We found that the interplay between Magnus force, repulsive interactions, and thermal noise yields different relaxation regimes (Figure 1). In the noise-dominated case, the Magnus force enhances the disordering effects of extrinsic thermal fluctuations. Conversely, when the Magnus force is prevalent, it cooperates with the skyrmion interaction to generate a dynamic regime with slowly decaying correlations. Quite interestingly, in both these regimes the two-time skyrmion density autocorrelation function satisfies simple aging scaling behavior, yet the distinct regimes are characterized by different values of the aging exponent. Further physical insight into the non-equilibrium properties as functions of noise and Magnus force strengths can be gained from single-time quantities such as the mean skyrmion nearest-neighbor distance, which provides a growing length scale. Generally, we observe that the Magnus force markedly accelerates the approach to the steady state.

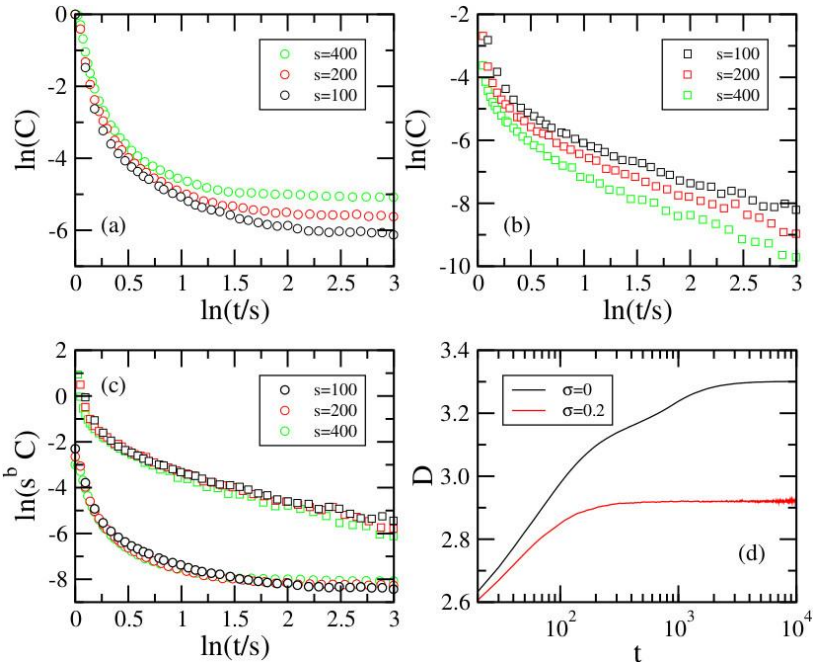

Fig. 1: Unscaled two-time skyrmion autocorrelation function $C(s,t)$ as a function of the time ratio t/s for different values of the waiting time $s < t$: (a) at vanishing temperature or noise ($\sigma = 0$; circles), and (b) for non-zero noise strength $\sigma = 0.2$ (squares). (c) Scaled two-time autocorrelations, and (d) average nearest-neighbor distances $D(t)$ for these same two cases. Upon decreasing σ, the aging exponent changes sign: $b = 0.60$ for $\sigma = 0.2$, whereas $b = -0.50$ for $\sigma = 0$.

Vortex matter flow regimes in the presence of extended pinning centers

We have explored the dynamical properties of driven magnetic vortices in type-II superconductors in the presence of extended planar defects, meant to model naturally occurring twin boundaries, commonly found in materials like YBCO. We have first considered the simplest scenario, where the flux lines are driven perpendicular to the defect planes. A study of

the non-equilibrium steady states for several sample thicknesses and drive strengths has revealed a rich collection of at least four dynamical regimes spanning a remarkably broad depinning transition region that separates the pinned and moving-lattice states of vortex matter. We have performed novel direct measurements of flux line excitations such as half-loops and double kinks, and quantitatively analyzed their excitation occurrence distributions to characterize the various flux flow profile and generated a boundary curve separating the regions of linear and non-linear transport that matches a previous theoretical prediction [2]. Static and dynamic visualizations of the vortices nicely supplement the quantitative results obtained. We are now studying the even more complex scenarios that emerge when the parallel defect planes are tilted with respect to the external driving current.

Future Plans

Physical aging of interacting skyrmions with random disorder

As demonstrated in our recent paper [3], the interplay between Magnus force, mutually repulsive skyrmion interactions, and thermal noise results in intriguing relaxation processes following a temperature quench. Depending on the relative strengths of the thermal noise and the Magnus force, different regimes can be identified through their distinct aging scaling properties of certain two-time quantities such as the density autocorrelation function. Whereas these predictions should be experimentally verifiable, our analysis was only a partial one as we assumed that the skyrmion-skyrmion interactions and the thermal noise dominate any influence of material defects on the skyrmion kinetics. However, the known wide range of possible defects in magnetic materials that can interact with skyrmions [4] indicates that for a complete understanding of relaxation processes in skyrmion systems our previous study needs to be expanded to include the effect of attractive and/or repulsive as well as point-like or extended (linear) defect sites. Since most material defects tend to attract skyrmions, it is natural to first extend our study to include point-like pinning centers, and investigate how their presence affects the non-equilibrium relaxation of the skyrmion system. As in experimental systems the material defects can have very different origins, more than one pinning strength is expected to be encountered. In order to study these more realistic situations, we will also consider situations where not all defects are endowed with identical strengths, but are instead drawn from a distribution of pinning strengths. We also note that magnetic skyrmions can interact with material defects through very different mechanisms. This opens the intriguing possibility that some types of defects may act as repulsive point-like defects. Indeed, some theoretical studies show that regions of high magnetic anisotropy as well as holes in the magnetic layer can result in an effective repulsive interaction between material defects and skyrmions. We note that this is quite different to the defect pinning mechanism in type-II superconductors which is invariably attractive. In order to obtain a full picture of the non-equilibrium relaxation in skyrmion matter, we therefore propose to also consider situations (i) where all pinning sites are repulsive, and (ii) where there is a mixture of attractive and repulsive defects. Our goal is to fully understand how relaxation properties of skyrmion matter change when an increasing fraction of attractive pins is replaced with repulsive ones. This should provide information that experimentalists may use in order to characterize the material defects in magnetic films by analyzing the observed skyrmion relaxation dynamics.

Relaxation processes following a drive quench

Upon applying an external electric current, interacting skyrmion systems settle into driven non-equilibrium stationary states, whose physical features are accessible in experiments. Different moving phases have been identified: for weak attractive pins only a moving crystal is observed, whereas for strong pins a moving liquid is encountered that for stronger drive orders into a moving crystal [5]. This ordering is unexpected and is due to the Magnus force. Driven skyrmion matter affords us with the intriguing opportunity to probe relaxation kinetics in situations where the ultimate stationary configuration is a non-equilibrium steady state. For the proposed investigation of different quench scenarios, in addition to sudden changes in temperature, one may also tune the strength of the driving force. Based on our earlier experience in studying non-stationary kinetics in driven vortex matter beyond the linear response regime, we would not expect to observe slow relaxation processes and the consequent emergence of an aging scaling window following a quick increase or drop in the current, provided the system remains in an essentially equivalent moving driven state. However, if the system is suddenly forced into a dynamical critical regime through a sudden drive quench down to the critical current, one would definitely anticipate the emergence of very rich non-equilibrium dynamics governed by exceedingly slow relaxation time scales. These effects should be especially prominent at very low temperatures, where skyrmion matter depinning at a critical current becomes a genuine continuous non-equilibrium phase transition. For this sub-project we need first to write the code for Langevin molecular dynamics simulations of skyrmion matter in the presence of an external drive. This code will then be used to map out the associated dynamic phase diagram in parameter space in detail. Based on this phase diagram we will select the initial and final values of the drive strength in order to quench (1) from the moving phase deep into the pinned regime or skyrmion glass phase and (2) from the moving phase to the dynamical critical point. Our goal is to identify experimentally realizable protocols and accessible observables that will aid us in separating generic universal from unique material-specific features. We also expect that this investigation will allow us to gain considerable new insights into the universal properties of transitions between pinned and moving non-equilibrium steady states.

References

1. S.-Z. Lin, C. Reichhardt, C. D. Batista, and A. Saxena, *Particle model for skyrmions in metallic chiral magnets: Dynamics, pinning, and creep,* Phys. Rev. B **87**, 214419 (2013).
2. M. C. Marchetti and V. M. Vinokur, *Twin-boundary pinning of superconducting vortex arrays,* Phys. Rev. B **51**, 16276 (1995).
3. B. L. Brown, U. C. Täuber, and M. Pleimling, *Effect of the Magnus force on skyrmion relaxation dynamics,* Phys. Rev. B **97**, 020405(R) (2018).
4. J. Sampaio, V. Cros, S. Rohart, A. Thiaville, and A. Fert, *Nucleation, stability and current-induced motion of isolated magnetic skyrmions in nanostructures*, Nat. Nanotechn. **8**, 939 (2013).
5. C. Reichhardt, D. Ray, and C. J. Olson Reichhardt, *Collective transport properties of driven skyrmions with random disorder,* Phys. Rev. Lett. **114**, 217202 (2015).

Publications (August 2016 - July 2018)

1. H. Assi, H. Chaturvedi, U. Dobramysl, M. Pleimling, and U. C. Täuber, *Disordered vortex matter out of equilibrium: a Langevin molecular dynamics study,* Molecular Simulation **42**, 1401 (2016) [arXiv:1509.02227].
2. H. Assi, H. Chaturvedi, , M. Pleimling, and U. C. Täuber, *Structural relaxation and aging scaling in the Coulomb and Bose glass models,* Eur. Phys. J. B **89**, 252 (2016) [arXiv:1606.02971].
3. H. Chaturvedi, H. Assi, U. Dobramysl, , M. Pleimling, and U. C. Täuber, *Flux line relaxation kinetics following current quenches in disordered type-II superconductors,* J. Stat. Mech. 2016, 083301 (2016) [arXiv:1606.06100].
4. W. Liu and U. C. Täuber, *Critical initial-slip scaling for the noisy complex Ginzburg-Landau equation,* J. Phys. A: Math. Theor. **49**, 434001 (2016) [arXiv:1606.08263].
5. U. C. Täuber, *Phase transitions and scaling in systems far from equilibrium,* Annu. Rev. Condens. Matter Phys. **8**, 14 (2017) [arXiv:1604.04487].
6. B. L. Brown, U. C. Täuber, and M. Pleimling, *Effect of the Magnus force on skyrmion relaxation dynamics,* Phys. Rev. B **97**, 020405(R) (2018) [arXiv:1801.00774].
7. H. Chaturvedi, N. Galliher, U. Dobramysl, M. Pleimling, and U. C. Täuber, *Dynamical regimes of vortex flow in type-II superconductors with parallel twin boundaries,* submitted to Eur. Phys. J. B [arXiv:1710.03679].

Unconventional Metals in Strongly Correlated Systems

Principal Investigator: Senthil Todadri
Department of Physics
Massachusetts Institute of Technology
Cambridge MA 02139 -4307
senthil@mit.edu

Project scope:

This theoretical project seeks a description of metals in regimes where the quasiparticle description fails, and their relationship with conventional phases and broken symmetry order in materials with strong electron correlations. The most notorious empirical example of such non-Fermi liquid behavior is in the normal state of the optimally doped cuprates but over the past decade has been demonstrated in a number of non-cuprate materials. The non-Fermi liquid behavior often occurs at intermediate energy scales but the scale at which conventional behavior is restored may be low compared to microscopic scales. Further the unconventional metal also gives way to broken symmetry orders at low temperature such as superconductivity or magnetism. A major component of the project seeks to develop methods capable of dealing with non-fermi liquid physics and its relation with superconductivity.

Recent progress:

1 Correlated electronic states in twisted bilayer graphene

A remarkable recent experiment has observed Mott insulator and proximate superconductor phases in twisted bilayer graphene when electrons partly fill a nearly flat mini-band that arises at a `magic' twist angle. In two recent papers (with my student Liujun Zou and collaborators H.C. Po and Ashvin Vishwanath) we described many pertinent aspects of the physics of this system. We proposed a Mott insulator with intervalley coherence that spontaneously breaks U(1) valley symmetry, and described a mechanism that selects this order over the competing magnetically ordered states favored by the Hunds coupling. We also identified symmetry related features of the nearly flat band that are key to understanding the strong correlation physics and constrain any tight binding description. First, although the charge density is concentrated on the triangular

lattice sites of the moir\'e pattern, the Wannier states of the tight-binding model must be centered on different sites which form a honeycomb lattice. Next, spatially localizing electrons derived from the nearly flat band necessarily breaks valley and other symmetries within any mean-field treatment, which is suggestive of a valley-ordered Mott state, and also dictates that additional symmetry breaking is present to remove symmetry-enforced band contacts. Tight-binding models describing the nearly flat mini-band were derived, which highlight the importance of further neighbor hopping and interactions. We discuss consequences of this picture for superconducting states obtained on doping the valley ordered Mott insulator. We show how important features of the experimental phenomenology may be explained and suggest a number of further experiments for the future.

2. Pair density wave, charge density wave, and vortex in high-Tc cuprates

A recent scanning tunneling microscopy (STM) experiment reports the observation of charge density wave (CDW) with period of approximately 8a in the halo region surrounding the vortex core, in striking contrast to the approximately period 4a CDW that are commonly observed in the cuprates. Inspired by this work, we study a model where a bi-directional pair density wave (PDW) with period 8 is at play. This further divides into two classes, (1) where the PDW is a competing state of the d wave superconductor and can exist only near the vortex core where the d wave order is suppressed, and (2) where the PDW is the primary order, the so called mother state that persists with strong phase fluctuations to high temperature and high magnetic field and lies behind the pseudogap phenomenology. With MIT students Ya-Hui Zhang, Zhehao Dai and my colleague Patrick Lee we studied the charge density wave structures near the vortex core in these models. We emphasized the importance of the phase winding of the d-wave order parameter. The PDW can be pinned by the vortex core due to this winding and become static. Furthermore, the period 8 CDW inherits the properties of this winding, which gives rise to a special feature of the Fourier transform peak, namely, it is split in certain directions. There are also a line of zeros in the inverse Fourier transform of filtered data. We proposed that these are key experimental signatures that can distinguish between the PDW-driven scenario from the more mundane option that the period 8 CDW is primary.

3. Physics of non-fermi liquid metals

I (together with Debanjan Chowdhury (MIT), Yochai Werman (Berkeley), and Erez Berg (Chicago)) constructed examples of translationally invariant solvable models of strongly-correlated metals. A key building block of these models is a dot of N orbitals with interactions described by the currently topical Sachdev-Ye-Kitaev (SYK) model. The SYK model is well known to be solvable in the large-N limit. The innovation in our work was to assemble these dots into a translation invariant lattice (building on earlier work on disordered lattices by Balents and collaborators) and to study, in a controlled manner, the properties of the resulting strongly correlated metal. These lattice models display crossovers as a function of temperature into regimes with local quantum criticality and marginal-Fermi liquid behavior. In the marginal Fermi liquid regime, the dc resistivity increases linearly with temperature over a broad range of temperatures. By generalizing the form of interactions, we also constructed examples of non-Fermi liquids with critical Fermi surfaces. The self-energy has a singular frequency dependence, but lacks momentum dependence, reminiscent of a dynamical mean field theory-like behavior but in finite dimensions. In the low temperature and strong-coupling limit, a heavy Fermi liquid is formed. The critical Fermi-surface in the non-Fermi liquid regime gives rise to quantum oscillations in the magnetization as a function of an external magnetic field in the absence of quasiparticle excitations. We discussed the implications of these results for local quantum criticality and for fundamental bounds on relaxation rates.

4. Novel phases of mixed valence systems

Samarium hexaboride - SmB6 - is a classic three-dimensional mixed valence system with a high- temperature metallic phase that evolves into a paramagnetic charge insulator below 40 kelvin. In recent years this material has been extensively studied as a possible topological Kondo insulator (a correlated version of the celebrated topological band insulators). A number of recent experiments have however suggested the possibility that the low-temperature insulating bulk hosts electrically neutral gapless fermionic excitations. If correct this makes SmB_6 even more novel than a correlated topological insulator. Similar surprising bulk phenomena have been reported in another mixed valence system YbB_{12}. Inspired by this situation, I, together with Debanjan Chowdhury and Inti Sodemann (MIT post-docs), described a new phase of matter---dubbed a

composite exciton Fermi liquid--- in a mixed valence insulator with a three dimensional fermi-surface of a neutral fermion, that we named the "composite exciton". We described the mechanism responsible for the formation of such excitons, and showed how it might help explain some of the mysteries of SmB6. In a subsequent paper we studied in detail the possibility that electrically insulating states - such as the composite exciton fermi liquid - may show quantum oscillations in a magnetic field (a much needed elaboration of an old idea from Olexei Motrunich).

Planned activities:

I am currently studying electronic properties of nearly flat band in a number of graphene moire strictures. It is imperative to first understand the phenomenology of near magic angle twisted bilayer graphene. The work already completed sets the stage for a full pronged attack on this problem. I am also studying other graphene moire structures that are being investigated experimentally at MIT and elsewhere.

Recent publications supported by DOE:

1. Origin of Mott insulating behavior and superconductivity in twisted bilayer graphene, Hoi Chun Po, Liujun Zou, Ashvin Vishwanath, T. Senthil, https://arxiv.org/abs/1803.09742 (under review in Phys Rev X).
2. Band Structure of Twisted Bilayer Graphene: Emergent Symmetries, Commensurate Approximants and Wannier Obstructions, Liujun Zou, H.-C. Po, A. Vishwanath, and T. Senthil,https://arxiv.org/abs/1806.07873 (under review in Phys Rev B).
3. Pair density wave, charge density wave and vortex in high Tc cuprates, Zhehao Dai, Ya-Hui Zhang, T. Senthil, Patrick Lee, Phys. Rev. B 97, 174511 (2018)
4. Translationally invariant non-Fermi liquid metals with critical Fermi-surfaces: Solvable models, Debanjan Chowdhury, Yochai Werman, Erez Berg, T. Senthil, Phys. Rev. X 8, 031024 (2018)
5. Mixed-valence insulators with neutral Fermi-surfaces, Debanjan Chowdhury, Inti Sodemann, T. Senthil, Nature Communications 9, 1766 (2018)
6. Quantum oscillations in insulators with neutral Fermi surfaces, Inti Sodemann, Debanjan Chowdhury, T. Senthil, Phys. Rev. B 97, 045152 (2018)

Orbital-free Quantum Simulation Methods for Applications to Warm Dense Matter

Principal Investigator: Samuel B. Trickey
Dept. of Physics and Dept. of Chemistry, Univ. Florida, Gainesville FL 32611-8435
trickey@qtp.ufl.edu
co-PI: J.W. Dufty (Physics, Univ. Florida)
10 July 2018
Keywords: free energy density functional theory, ab initio molecular dynamics, transport coefficients, warm dense matter

Project Scope

Predictive simulation of materials under extreme state conditions - such as encountered in giant planet interiors and in the state trajectory of inertial confinement fusion - is highly challenging. The electronic temperature T typically is of the order of the Fermi temperature (T_F). Pressures (P) range from ambient to well into the 100s of GPa. Sometimes called the warm dense matter (WDM) regime, the system state trajectory involved (from ambient to final conditions) has limited experimental accessibility. Even that limited access often involves difficult experimental techniques. Achieving predictive simulation would have high payoff therefore. That, in turn, is the driver for pursuing significant progress in the predictive capacity and speed of ab initio molecular dynamics (AIMD) simulations.

AIMD is the current and foreseeable best practice for studying materials under extreme conditions because they are most even-handedly approached as complicated condensed phase systems, not (as still is sometimes) as a plasma. Ion thermodynamics in AIMD is generated by classical dynamics with forces from quantum electrons in the Born-Oppenheimer approximation. Cost-accuracy balance makes the Mermin free-energy version of density functional theory (DFT) the best choice for the quantum part. This leads to a clear requirement and a highly desirable objective.

The *requirement* is a suitably accurate approximation for the exchange correlation (XC) free energy F_{XC}. Ground-state DFT development provides a paradigm of increasing refinement, the Perdew-Schmidt "Jabob's ladder": local density approximation (LDA; density *n* alone), generalized gradient approximation (GGA; ∇n added), meta-GGA (τ= KE density or ∇^2n added) etc. Before this project, there was no well-founded XC free-energy functional analogous with the Perdew-Zunger or Vosko-Wilk-Nussair ground-state LDA. As discussed below, we this year published the first ever non-empirical, constraint-based GGA XC free energy functional. We also corrected an inconsequential technical error in our 2014 LDA (the first of its kind), and confirmed that the so-called ground-state approximation, $F_{XC}[n;T] \approx E_{xc}[n(T)]$ with the latter a ground state functional, is not reliable.

The *highly desirable objective* is linear scaling of computational cost with system size and with T. Thermal occupation of high-energy (relative to ground state) Kohn-Sham (KS) states exacerbates the unfavorable KS computational cost scaling (cubic) with T and system size. Typical linear-scaling methods all eventually depend on some form of sparse Hamiltonian matrix or equivalent sparse structure. Therefore they are inapplicable to WDM, which often is metallic. Orbital-free DFT (OF-DFT) depends only on the density, so it is intrinsically linear scaling. OF-DFT requires two approximate free-energy functionals, the XC functional already discussed and the non-interacting free energy (KS KE F_τ and entropy F_σ components). Note that simple OF-DFT schemes such as Thomas-Fermi plus scaled von Weizsäcker are completely inadequate.

In support of these functional developments (F_{XC} , F_τ , F_σ), the third project thrust is to seek deeper and broader theoretical underpinnings that provide constraints, bounds, and other rigorous results for free-energy DFT approximations and extensions, e.g. for transport coefficients. The fourth thrust is development, implementation, testing, and distribution of open-source simulation software which exploits the advances in the other three thrusts. After progress summaries on these four thrusts, we outline important components of research presently underway or in prospect.

Recent Progress

Free-energy XC functionals – In publication [3] we presented KDT16, the first full GGA $F_{XC}[n;T]$. Fig. 1 (from [3]) shows the superior agreement of KDT16 pressures with path integral Monte Carlo values compared to the deviations of as much as 20% for ground-state PBE. Fig. 2 shows what happens when first one adds explicit T-dependence [finite-T LDA, our "KSDT", Phys. Rev. Lett. **112**, 076403 (2014)] and then adds spatial inhomogeneity at the level of the GGA "KDT16", Ref. [3]. Notice that use of the ground state GGA shifts the pressure in the wrong direction from ground-state LDA. This is much stronger evidence of the inadequacy of the ground-state approximation than we had been able to provide before. Publication [3] also provided (in Supplemental Material) a correction to the KSDT LDA which removed a minor technical error in the original use of zero temperature quantum Monte Carlo data. The corrected functional, corrKSDT, both removes a very small magnitude negative entropy error and demonstrates conclusively that the criticisms of KSDT from the Kiel group are essentially vacuous.

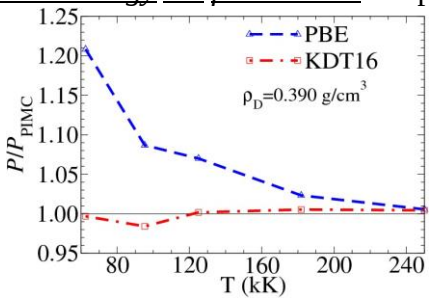

1. *Ratio of DFT pressure to PIMC pressure for new KDT16 functional vs. ground-state PBE functional (deuterium).*

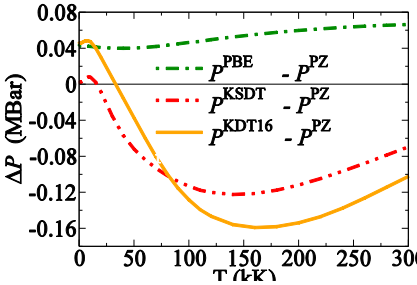

2 *Static fcc Al pressure shifts with respect to ground-state PZ results*

Orbital-free KS kinetic energy functional – An obvious pre-requisite for OFDFT at non-zero T is a reliable orbital-free ground-state non-interacting KE functional. Publication [1] addresses this with a new $T_s[n]$ specifically designed in the context of DFT non-universality. The essential insight is that the pseudo-densities used in AIMD simulations do not conform to the Kato cusp condition densities used to constrain the previous best one-point $T_s[n]$, our non-empirical VT84F [Phys. Rev. B **88,** 161108(R) (2013)]. Our new LKT (Luo-Karasiev-Trickey) GGA in contrast is specifically adapted to the local-pseudo potentials that are inescapable in plane-wave-based AIMD. LKT is non-empirical and constraint-based, with a single parameter that is calibrated by satisfying positivity constraints for pseudo-atom densities. (There is no parametrization to experimental data or to calculations on any aggregated systems.) In static lattice tests on simple metals and semi-conductors, the new LKT functional both outperforms VT84F, and remarkably, is reasonably competitive with more costly parametrized two-point functionals such as Wang-Govind-Carter, Huang-Carter, and Constantin et al.'s KGAP.

Orbital-free mGGA XC functional – Emerging consensus about ground-state DFT applied to solids and nanostructures is that the mGGA level of refinement of the XC functional is needed (sometimes in combination with van der Waals corrections, a distinct issue). In their ordinary form, however, mGGAs are out of reach of OFDFT because of their explicit dependence on the Kohn-Sham

orbitals through the positive-definite kinetic energy density $\tau = (1/2)\sum|\nabla\varphi|^2$. Given our work on the OFDFT kinetic energy density functionals, it was a fairly obvious step to try to deorbitalize mGGA XC functionals. Because of the number of constraints it satisfies and its rather broadly good performance, much attention has been given in recent years to the SCAN mGGA [Phys. Rev. Lett. 115, 036402 (2015)]. We have successfully deorbitalized it as discussed in Publication [6] for molecules with a non-empirical Laplacian-dependent KE density. *Completely unmodified*, the resulting Laplacian-dependent functional (SCAN-L) also is *equally successful* in matching the original SCAN on tests of lattice parameters, cohesive energies, and bulk moduli of 55 solids [D. Mejía Rodríguez and S.B. Trickey, in preparation]. In VASP, standard KS calculations with original SCAN are about 30-50% slower than with SCAN-L. For long AIMD runs at many temperatures, this is an important performance gain with no apparent loss of predictive reliability. We will provide the VASP code to the VASP developers shortly (see below). Another advantage of deorbitalization is that it yields a true KS solution, not a generalized KS solution. Also for those who need the SCAN optimized effective potential, SCAN-L may be an approximate alternative.

Foundational theory – Publications [2] and [7] explore and extend the connections among classical kinetic theory of transport, the Kubo-Greenwood approximation, and time-dependent DFT. The analysis involves another paper during this period from our group [4]. In it, short-time correlation functions were examined to expose how, at least at the semi-classical level, the DFT-based Kubo-Greenwood approximation arises in the context of kinetic theory. The net result is to provide a substantial rationale for the K-G approximation, which generally has been used *ad hoc* and without rationalization.

In [5] we showed that supposed constraints on the allowed order of spatial derivatives in an orbital-free kinetic energy density approximation are, in fact, not constraints at all, but complicated yet trivial rearrangements of the Kohn-Sham Euler equation. This resolves a long-standing but little noticed conflict between those supposed constraints and the reality of modern gradient and Laplacian dependent KE density functional approximations.

Software and data – Publication [10] presented the detailed analysis underlying our algorithmic formulation of the Kubo-Greenwood frequency- dependent electrical conductivity and the algorithms and data flow in the new code KGEC. It was released under GPL from our web site at the same time. KGEC is a post-processor to QuantumEspresso and has been advertised as such on the QuantumEspresso web site. All of our software is downloadable from www.qtp.ufl.edu/ofdft under GNU GPL.

We began a new online OFDFT reference data resource. Its purpose is to save time by avoiding duplicative effort by those interested in developing and/or testing orbital-free non-interacting functionals (approximate KS kinetic energy density functionals "KEDFs" at T = 0K). At www.qtp.ufl.edu.ofdft/referencedata.shtml one can click on an element in a graphical periodic table and bring up computed post-scf KS KE values of for 36 approximate KEDFs.

Investigations Underway and Planned

Extension of the ground-state LKT KEDF and the SCAN-L mGGA XC functional into free-energy functionals has begun. Such extensions use formulations previously developed in this project: publication [3] and Phys. Rev. B **86**, 115101 (2012). No major barriers to success are anticipated. The result will be the most refined finite-T OFDFT pair of functionals ever.

We have had some initial successes with machine-learnt KEDFs for deorbitalization of conventional mGGA XC functionals. These can be thought of as the ML counterparts of SCAN-L discussed below. The intent therefore is to make a focused exploration of machine-learnt KEDFs *per se* and of finite-T counterparts. Challenges include imposition of constraints, fabrication of appropriate training sets, and technical details of the artificial neural networks employed.

Currently, we are testing and debugging new modules for the KGEC code (see above) that compute the frequency-dependent dielectric function and the opacity. Some peculiar and so-far undiagnosed difficulties with parallelization of the new modules are the current focus. KGEC now is collaborative with Univ. of Arizona (L. Calderín) and Laboratory for Laser Energetics, Univ. of Rochester (V.V. Karasiev). Both were group members when the KGEC project began and the first version was published. We also will provide our SCAN-L code for VASP to the VASP developers, with the expectation that this will drive usage up substantially.

We intend to restart and bring to completion a project suspended by departures (V.V. Karasiev) and by higher priorities for limited personnel. This is development of non-interacting OFDFT functionals in tunable form. Those are built to extrapolate and/or interpolate finite-T KS calculations on static lattice systems. They do so by parametrizing a constraint-based functional form to those calculations. The resulting tuned functional then can be used with AIMD. This approach was motivated by the computational challenge of computing the Al liquid-vapor critical point. We have done massive conventional KS AIMD calculations which rather clearly confirm that prior such calculations were more fortunate than predictive. The question is whether the OFDFT-AIMD can demonstrate success with linear scaling on such a difficult problem.

We will extend the corrKSDT LSDA XC functional (recall above) to fully polarized systems and include recent Quantum Monte Carlo data [Phys. Rev. Lett. 117, 156403 (2016) and arXiv 1703.08074) for low r_s. This also is collaborative work with V.V. Karasiev (LLE, U. Rochester).

As to formal underpinnings, we are working to complete derivation of the quantum version of the short-time kinetic equation (recall above) including comparative analysis with respect to our already proposed quantization of classical result. We will continue, and hopefully conclude, analysis of the effects of ion motion upon electrical conductivity. The intent is to quantify these effects with practical relaxation time models. And we will revisit phenomenological models for quantum hydrodynamics to show the proper role of DFT for WDM conditions of WDM and the relation to tdDFT results.

Since this project began (Fall 2009), we have worked to bring free-energy DFT substantially along a logical, formal, and practical path akin to the celebrated evolution of ground-state DFT. For context, before this project there was not even a purely Monte Carlo based LSDA XC free-energy functional. . We are catching up rapidly. Free-energy DFT now is at about the level of a soundness, accuracy, and utility that characterized ground-state DFT in 2000. The next steps are better functionals rooted in deeper understanding of the theory, along with paradigmatic calculations to illustrate the power and reach of the approach.

Publications (2016 – present)

All publications, codes, and other software are available from http://www.qtp.ufl.edu/ofdft

[1] "A simple generalized gradient approximation for the non-interacting kinetic energy density functional", Kai Luo, V.V. Karasiev, and S.B. Trickey, Phys. Rev. B Rapid Commun. [submitted 13 June 2018; provisionally accepted 09 July; arXiv 1806.05205].

[2] "Density response from kinetic theory and time dependent density functional theory for matter under extreme conditions", J. W. Dufty, K. Luo, and S.B. Trickey, Phys. Rev. E [submitted 15 May 2018; arXiv 1805.06509].

[3] "Nonempirical semi-local free-energy density functional for matter under extreme conditions", V. V. Karasiev, J. W. Dufty, and S.B. Trickey. Phys. Rev. Lett. **120**, 076401 (2018).

[4] "Kinetic theory for strongly coupled coulomb systems", J.W. Dufty and J. Wrighton. Phys. Rev. E **97**, 012149 (2018).

[5] "Trivial constraints on orbital-free kinetic energy density functionals", K. Luo and S.B. Trickey [Chem. Phys. Lett., **695** 190 (2018).

[6] "Deorbitalization strategies for meta-GGA exchange-correlation functionals", D. Mejia-Rodriguez and S.B. Trickey, Phys. Rev. A 96, 052512 (2017).

[7] "On the Kubo-Greenwood model for electron conductivity", J.W. Dufty, J. Wrighton, K. Luo, and S.B. Trickey, Contrib. Plasma Phys. **58**, 150 (2018).

[8] "Accurate anisotropic gaussian type orbital basis sets for atoms in strong magnetic fields". Wuming Zhu and S.B. Trickey, J. Chem. Phys. **147**, 244108 (2017).

[9] "Long-range exchange limit and dispersion in pure silica zeolites", A.M. Albavera-Mata, C.M. Zicovich-Wilson, J.L. Gázquez, S.B. Trickey, and A.Vela; Theor. Chem. Acc. **137**, 26 (2018)

[10] "Kubo-Greenwood electrical conductivity formulation and implementation for projector augmented wave datasets", L. Calderín, V.V. Karasiev, and S.B. Trickey, Comput. Phys. Commun. **221**, 118 (2017).

[11] "Density functional theory for the electron gas and for jellium", J. W. Dufty. Langmuir **33**, 11570 (2017).

[12] "Comment on 'Communication: Simple and accurate uniform electron gas correlation energy for the full range of densities'" [J. Chem. Phys. **145**, 021101 (2016)] V.V. Karasiev, J. Chem. Phys. **145**, 157101 (2016).

[13] "Temperature effects in static and dynamic polarizabilities from distinct generalized gradient approximation exchange-correlation functionals", J. Carmona-Espíndola, J.L. Gázquez, A. Vela and S.B. Trickey, Chem. Phys. Lett. **664**, 77 (2016).

[14] "A PW91-like exchange with a simple analytical form", J.C. Pacheco-Kato, J.M. del Campo, J.L. Gázquez, S.B. Trickey, and A. Vela, Chem. Phys. Lett **651**, 268 (2016).

[15] "Unexpected cold curve sensitivity to GGA exchange form", S.B. Trickey, Theor. Chem. Acc. **135,** 219 (2016).

[16] "Global hybrid exchange energy functional with correct asymptotic behavior of the corresponding potential" J. Carmona-Espíndola, J.L. Gázquez, A. Vela and S.B. Trickey, Theor. Chem. Acc. **135**, 120 (2016).

[17] "Revised Thomas-Fermi approximation for singular potentials", J.W. Dufty, and S.B. Trickey, Phys. Rev. B **94**, 075158 (2016).

[18] "Finite temperature quantum effects on confined charges", J. Wrighton, J. Dufty, and S. Dutta, Phys. Rev. E, **94**, 053208 (2016).

Novel Phases and Dynamics of Multi-orbital Mott Insulator

PI: Nandini Trivedi, The Ohio State University

Keywords: Quantum spin-liquid, frustrated magnetism, quantum phase transition, spin dynamics

Project Scope

The goal of this project is to gain theoretical insight into magnetism in the presence of spin-orbit coupling (SOC) for multi-orbital Mott insulators. Inspired by the exact solution of the Kitaev model that harbors a quantum spin liquid with novel excitations and struck by its relevance for materials with anisotropic orbital interactions, we explore various new classes of 4d and 5d transition metal oxides. Starting with all electron Hamiltonians, we derive minimal magnetic models. Our aim is to understand the role played by orbital frustration, even in the absence of any geometric frustration, in creating orbitally ordered as well as spin-orbital liquid phases. Orbital frustration arises primarily from the directional or anisotropic nature of d-orbitals in contrast to the isotropic nature of the spin degree of freedom. These models are investigated by a variety of theoretical and numerical methods, including exact diagonalization, mean field theories, density matrix renormalization group and quantum Monte Carlo methods. Testable predictions for three experiments: nuclear magnetic resonance (NMR) and resonant x-ray scattering (RXS) to probe orbital ordering and pump-probe experiments to probe quantum dynamics test the validity of these models for materials.

Quantum Spin Liquids: Frustration in strongly correlated electronic materials results from competing interactions between localized magnetic moments (spins) which cannot be simultaneously satisfied while simultaneously minimizing a system's global energy. In some solids at zero temperature, quantum fluctuations together with the particular details of the frustrated lattice may yield a massively degenerate ground state characterized by massive many-body quantum entanglement. Such globally entangled ground states, termed *quantum spin-liquids* (QSL), harbor *fractional* quasiparticle excitations (FQE) whose quantum number is only a fraction of the elementary local degrees of freedom. In two-dimensions, FQE's have the fascinating property of obeying *fractional statistics*, and are termed *anyons* if they obtain an arbitrary phase factor upon mutual exchange, or *non-Abelian anyons* when this phase factor is a higher-dimensional unitary matrix. Much of the current interest in exploring frustrated materials has to do with potentially exploiting non-Abelian anyons for use in performing physically fault-tolerant operations in a possible quantum computing device [1].

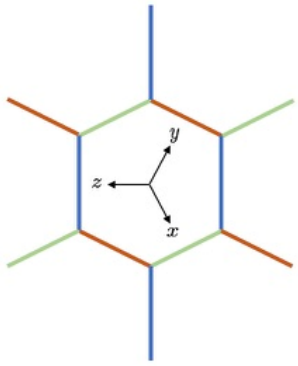

Fig. 1: Plaquette of the Kitaev honeycomb model in two dimensions.

In searching for a candidate material that may harbor these kinds of exotic excitations, the transition metal compound α-$RuCl_3$ has recently received considerable attention [2]. The physical properties of α-$RuCl_3$ are believed to be well described by an extended Kitaev honeycomb model. The exactly solvable Kitaev model consists of $S = 1/2$ degrees of freedom that are frustrated by anisotropic bond-dependent, nearest-neighbor, interactions $H_K = \sum_\alpha \sum_{\langle j,k \rangle_\alpha} J_\alpha \sigma_j^\alpha \sigma_k^\alpha$, where J_α is the Kitaev exchange constant, $\alpha \in \{x, y, z\}$, j and k are nearest-neighbor sites lying along the bond α, and σ_j^α, σ_k^α are corresponding Pauli matrices. For isotropic Kitaev exchange interactions ($J_x = J_y = J_z$), this model is known to harbor non-Abelian anyons under an externally applied magnetic field. Recently, much of the theoretical interest has been to perform numerical simulations on extended Kitaev models with an externally applied field, and to try to fit the results of these numerics to the experimental data [3].

We use exact diagonalization on finite site clusters to offer an unambiguous signature of fractionalization of spin-flip quanta in the dynamical local spin-spin correlations of the pure Kitaev model as a function of an externally applied magnetic field. Whereas recent attention has been focused on observing a broad continuum in the dynamical structure factor as indicative of the fractional excitations of a non-ordered ground state [4], we propose investigating the real-time dynamics of spin-spin correlations where we expect the signatures of fractionalization to be sharp and distinct. We also determine the effect of rotating an externally applied field, relative to the plane of the honeycomb lattice, on the various phases and phase transitions identifiable in the local dynamical response. Our aim is to expand the exploration from spectroscopy to probing the nature of fractionalized excitations directly in the real-time dynamics. We propose future experiments using pump-probe THz spectroscopy on candidate materials such as α-$RuCl_3$. In these experiments, the pump excites photocarriers in the system, and the THz probe pulse measures the photoconductivity as a function of time [5]. After passing through the sample the terahertz waveform of the electric field $E(t)$ is measured in the time domain. Based on our estimates using an exchange coupling of about 5 meV, we expect signatures of fractionalization to appear at time scales lying within the range $10^{-13}\text{s} < t < 10^{-12}\text{s}$, or for frequencies in the 1-10 THz regime.

Recent Progress

We use exact diagonalization, on eight to sixteen site clusters of the Kitaev honeycomb model with periodic boundary conditions, under an externally applied magnetic field pointing along [111], [001], and [-110]. We obtain this model's energy spectrum, as well as its local spin-spin correlator, and local dynamical response as functions of the field strength (beyond the perturbative limit) and orientation. We find phase transitions from a gapped Kitaev QSL to an intermediate gapless QSL, to a partially polarized phase with increasing field along [111] for antiferromagnetic (AF) Kitaev interactions. These are deduced from level crossings in the energy spectrum (vertical red dashed lines in Fig. 2) and are detectable in the on-site dynamical response as sharp discontinuities in the trajectories of distinct frequency modes. The intermediate QSL

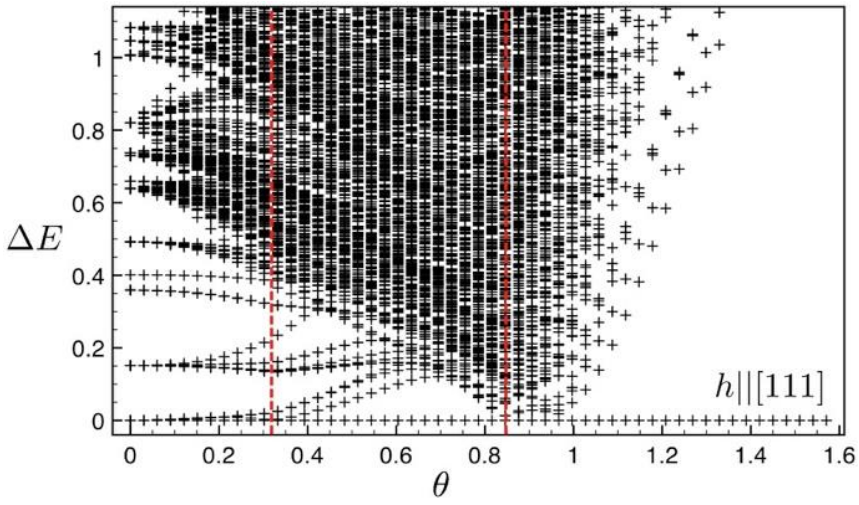

Fig. 2: Energies of the lowest lying excitations of the AF Kitaev honeycomb model as a function of the field strength parameter θ for a field pointing along [111].

phase is characterized by a large density of low energy states. The corresponding plethora of modes in the local dynamical response along [111] is considerably reduced upon changing the orientation toward [001] (Fig. 3), resulting in a clearly discernible beating pattern between a few modes of comparable strength and energy, possibly observable in pump probe experiments (Fig. 4).

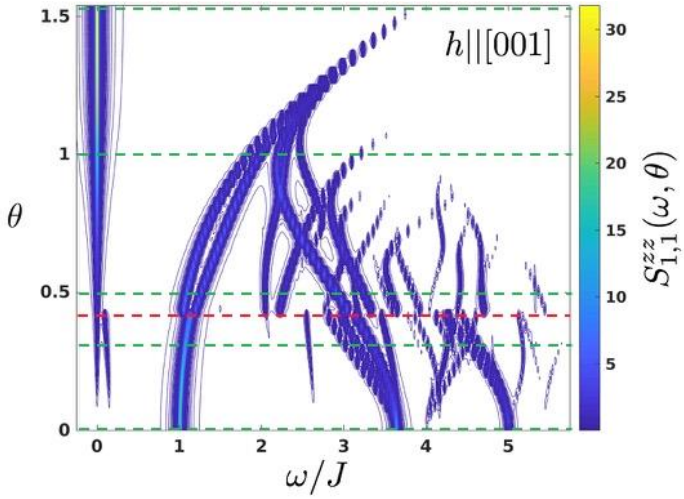

Fig. 3: The on-site dynamical response for the AF Kitaev honeycomb model for a field pointing along [001]. Horizontal dashed red line corresponds to location of level crossing in the energy spectrum.

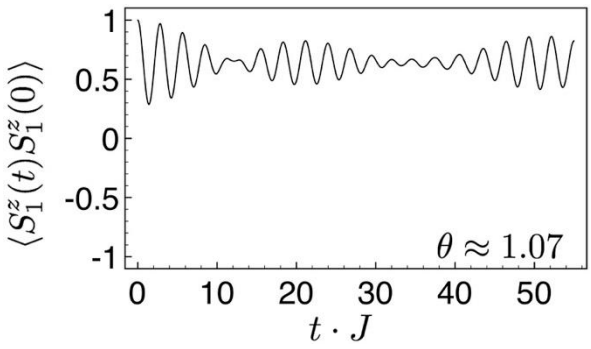

Fig. 4: On-site dynamical spin-spin correlatior for AF Kitaev exchange, for a field pointing along [001]. A clear nodal, beat pattern, or wave-packet feature is evident for this value of the field strength, θ = 1.07.

Future Plans

We propose a multi-pronged approach to investigate QSLs:

(1) DMRG calculations on larger sized systems of entanglement spectra and spin-spin correlations
(2) Semi- analytic approaches to understand the intermediate quantum spin liquid phase
(3) Calculation of the thermal Hall effect as a function of orientation of the external magnetic field and temperature
(4) Disorder as a probe of QSLs; build on previous work funded by DOE on self-consistent calculations of disordered superconductors
(5) Collaborate with experimental groups to explore real-time dynamics to detect salient features of fractionalization in the QSL.

References

1. C. Nayak, S. H. Simon, A. Stern, M. Freedman, S. D. Sarma, *Rev. Mod. Phys.* **80**, 1083 (2008).
2. A. Banerjee, J. Yan, J. Knolle, C. A. Bridges, M. B. Stone, M. D. Lumsden, D. G. Mandrus, D. A. Tennant, R. Moessner, and S. E. Nagler, *Science*, 1055 (2017).
3. S. M. Winter, K. Riedl, D. Kaib, R. Coldea, and R. Valentí, *Phys. Rev. Lett.* **120**, 077203 (2018).
4. J. Knolle, D. L. Kovrizhin, J. T. Chalker, and R. Moessner, *Phys. Rev. Lett.* **112**, 207203 (2014).
5. J. Zhang and R. Averitt, *Annual Review of Materials Research*, **44**, 19 (2014).

Publications (August 2016-July 2018)

1. D. C. Ronquillo and N. Trivedi, arXiv:1805.03722v1

2. Y. L. Loh, M. Randeria, N. Trivedi, C.-C. Chang, and R. Scalettar. Superconductor-insulator transition and Fermi-Bose crossovers. **Phys. Rev. X 6** 021029 (2016).

3. L. Huang, T. M. McCormick, M. Ochi, Z. Zhao, M.-T. Suzuki, R. Arita, Y. Wu, D. Mou, H. Cao, J. Yan, N. Trivedi, and A. Kaminski. Spectroscopic evidence for a type II Weyl semimetallic state in MoTe2. **Nature Materials 15** 1155 EP (2016).

Nonequilibrium thermodynamics in magnetic nanostructures

Yaroslav Tserkovnyak (University of California, Los Angeles)

Keywords: Spintronics, nonequilibrium magnetism, spin superfluidity, topological hydrodynamics, Bose-Einstein condensation of magnons

Project Scope

Recent strides within the fields of spintronics and spin caloritronics have established versatile thermoelectric tools for studying spin dynamics in diverse classes of magnetic heterostructures. Of particular relevance to this proposal is the ability to induce and control spin transport and collective dynamics in (ferro- and antiferro-)magnetic insulators. Theoretical research within the scope of this project has been playing an important role, over the past $\sim$3 years, in guiding the pertinent experimental efforts. Notable achievements here include the observation of a Spin caloritronic nanooscillator based on the heat-induced bosonic condensation of magnons, the development of a Spin-current probe for phase transitions in insulators, which was demonstrated by spin pumping through an antiferromagnetic insulator, and Control and local measurement of the spin chemical potential in a magnetic insulator using nitrogen vacancies in diamond.

Emboldened by these and related developments on the experimental fronts, and bolstered by the recent progress in theoretical understanding of nonequilibrium thermodynamics and collective kinetics in magnetic nanostructures, we are setting out to continue our work with a focus on three thrusts: (i) Emergent (topological) hydrodynamics in ferromagnets, antiferromagnets, and spin liquids; (ii) Thermal control of spin condensates, superfluids, and soliton dynamics; and (iii) Production and control of macroscopic quantum entanglement in magnetic insulators by thermal means. This proposal builds organically on our work of the past several years within this Award, which is evolving hand-in-hand with the remarkable experimental progress.

Our efforts on the topological hydrodynamics will build on the evolution of spin superfluids from mere analogs of the conventional neutral superfluids to systems that exhibit novel dynamics of conserved topological invariants (such as winding chirality in one dimension, which is the closest analog of superfluids and superconductors; skyrmion number in two dimensions; and more exotic topological quantities in quantum magnets, whose conservations and the associated hydrodynamics are rooted in the topological invariance). Central to our agenda are thermal means to couple to and exhibit the underlying physics. One of the key themes here will be the interplay and interaction between collective spin superfluids, as robust low-dissipation signal carriers, and magnetic solitons, as the building blocks of spin memory and logic functionalities.

Recent Progress

Here, I will touch upon three highlights from the most recent work. The full publication list for the work supported by this Award is appended below, for the last two years.

In Ref. [1], we studied *Hydrodynamics and topological spin currents in amorphous magnets*. Spin superfluidity, i.e., coherent spin transport mediated by topologically stable textures, offers promising perspectives for the design of energetically efficient devices for applications in spintronics. In contrast to spinor condensates and 3He, superfluid spin transport in solid state is limited by parasitic anisotropies rooted in relativistic interactions and spatial inhomogeneities. Here, we showed how structural disorder in amorphous materials can average out the effect of these undesired couplings. We established nonlinear equations describing the hydrodynamics of spin in insulating amorphous magnets, where the currents are defined in terms of coherent rotations of a noncollinear texture. Our theory includes dissipation and nonequilibrium torques at the interface with metallic reservoirs. This framework allowed us to determine different regimes of coherent dynamics and their salient features in nonlocal magneto-transport measurements. Our work paves the way for future studies on macroscopic spin dynamics in materials with frustrated interactions.

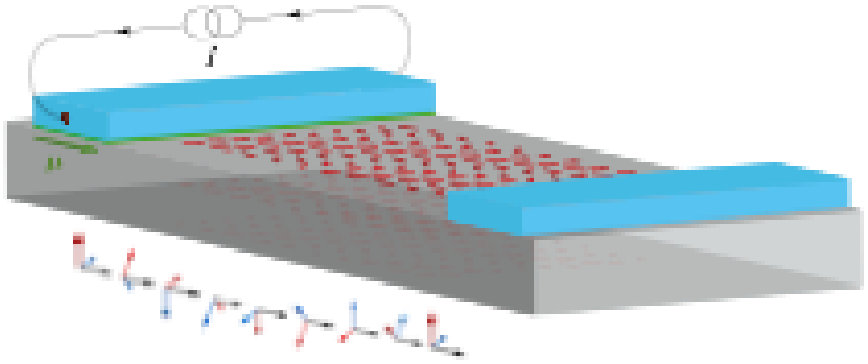

Two-terminal geometry for the generation and detection of coherent spin transport in amorphous magnets. The electric current in the injector induces a spin accumulation (green arrow) via the spin Hall effect. The spin-transfer torque triggers the dynamics of the spin texture in the spin-glass state (red arrows), which take the form of a uniform precession of the order parameter in the steady state. The latter is depicted as a rotating triad of vectors, which represents the internal spin frame of the texture adapted to the instantaneous state of the magnet. The spin dynamics pumps angular momentum into the metals, which is detected as a voltage in the second terminal via the inverse spin-Hall effect.

Ref. [2] is a theory-experiment collaboration between UCLA and Harvard on *Control and local measurement of the spin chemical potential in a magnetic insulator*. The spin chemical potential characterizes the tendency of spins to diffuse. Probing this quantity could provide insight into materials such as magnetic insulators and spin liquids and aid optimization of spintronic devices. Here, we introduced single-spin magnetometry as a generic platform for nonperturbative,

nanoscale characterization of spin chemical potentials. We experimentally realized this platform using diamond nitrogen-vacancy centers and use it to investigate magnons in a magnetic insulator, finding that the magnon chemical potential can be controlled by driving the system's ferromagnetic resonance. We introduced a symmetry-based two-fluid theory describing the underlying magnon processes, measure the local thermomagnonic torque, and illustrate the detection sensitivity using electrically controlled spin injection. Our results pave the way for nanoscale control and imaging of spin transport in mesoscopic systems.

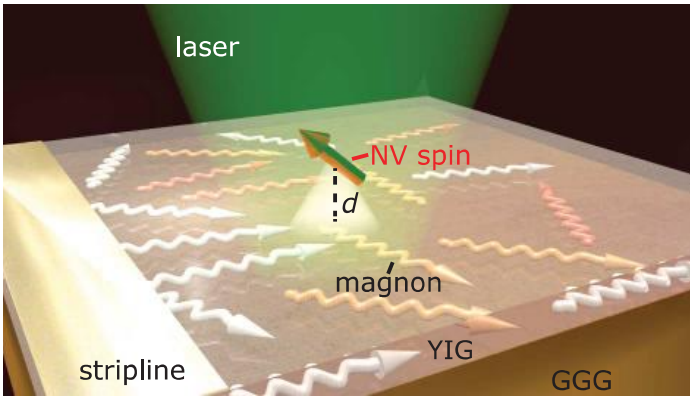

Sketch of an NV spin locally probing the magnetic fields generated by magnons in a 20-nm-thick YIG film grown on a GGG substrate.

Finally, Ref. [3], is a proposal on *Exploiting coherence in nonlinear spin-superfluid transport*. We showed how the interference between superfluid spin currents can endow spin circuits with coherent logic functionality. While the hydrodynamic aspects of the linear-response collective spin transport obviate interference features, we focused on the nonlinear regime, where the critical supercurrent is sensitive to the phase accumulated by the condensate in a loop geometry. We proposed to control this phase by electrical gating that tunes the spin-condensate coherence length. The nonlinear aspects of the spin superfluidity thus naturally lend themselves to the construction of logic gates, uniquely exploiting the coherence of collective spin currents. Vice versa, this functionality can be used to reveal the fundamental properties of spin superfluids.

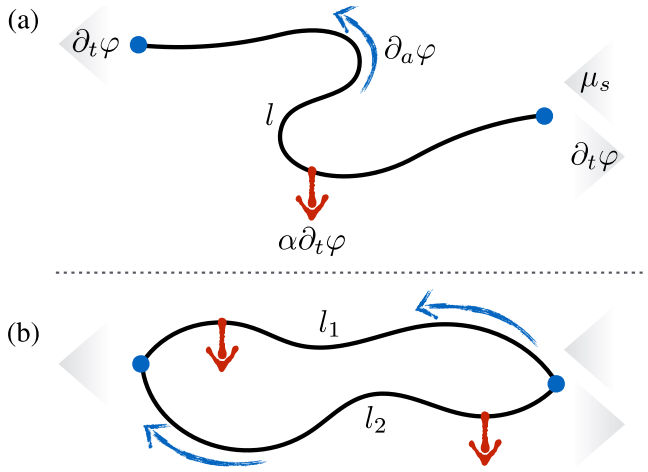

Hydrodynamic spin transport in linear response. (a) Single channel collectively transmitting spin current, which is injected on the right. Spin pumping ejects spin currents at both ends, and along the length of the conduits Gilbert damping leads to an attenuation. (b) Superposition of two similar spin flows in a loop geometry composed of two branches. The phase corresponds to the azimuthal angle of easy-plane magnetic dynamics.

Future Plans

The field of the proposed research, which addresses the problem of coupled spin and heat transport in magnetic and topological heterostructures, with a focus on nonlinear spin condensates, superfluids, and solitonic dynamics, continues to prosper and rapidly develop. In fact, recent observations of a long-distance transfer of spins through magnetic insulators, controlled production and motion of magnetic skyrmions, spin supercurrents, thermally-induced Bose-Einstein condensation of magnons, and control and local measurement of spin chemical potential, all at room temperature, are certain to fuel an avalanching growth of the field. This project is positioned in the midst of these developments, with the PI collaborating or closely interacting with most of the relevant experimental groups in the US and abroad.

Specifically, I plan to focus on the following three thrusts over the next years:

• Emergent (topological) hydrodynamics in ferromagnets, antiferromagnets, and frustrated spin systems.

• Thermal control of spin condensates, superfluids, topological hydrodynamics, and soliton dynamics.

• Production of macroscopic quantum entanglement in magnetic insulators by thermal means.

Publications (August 2016 – July 2018)

1. H. Ochoa, R. Zarzuela, and Y. Tserkovnyak, *Hydrodynamics and Topological Spin Currents in Amorphous Magnets,* submitted to Phys. Rev. Lett. (arXiv:1803.01309).
2. C. Du, T. Van der Sar, T. X. Zhou, P. Upadhyaya, F. Casola, H. Zhang, M. C. Onbasli, C. A. Ross, R. L. Walsworth, Y. Tserkovnyak, and A. Yacoby, *Control and Local Measurement of the Spin Chemical Potential in a Magnetic Insulator,* Science **357**, 195-198 (2017).
3. Y. Tserkovnyak and M. Kläui, *Exploiting Coherence in Nonlinear Spin-Superfluid Transport,* Phys. Rev. Lett. **119**, 187705 (2017).
4. Y. Tserkovnyak and H. Ochoa, *Generalized Boundary Conditions for Spin Transfer,* Phys. Rev. B (Rap. Comm.) **96**, 100402(R) (2017).
5. H. Ochoa, S. K. Kim, O. Tchernyshyov, and Y. Tserkovnyak, *Gyrotropic Elastic Response of Skyrmion Crystals to Current-Induced Tensions,* Phys. Rev. B (Rap. Comm.) **96**, 020410(R) (2017).
6. H. Ochoa, R. Zarzuela, and Y. Tserkovnyak, *Emergent Gauge Fields from Curvature in Single Layers of Transition-Metal Dichalcogenides,* Phys. Rev. Lett. **118**, 026801 (2017).
7. M. Evelt, H. Ochoa, O. Dzyapko, V. E. Demidov, A. Yurgens, J. Sun, Y. Tserkovnyak, V. Bessonov, A. B. Rinkevich, and S. O. Demokritov, *Chiral Charge Pumping in Graphene Deposited on a Magnetic Insulator,* Phys. Rev. B **95**, 024408 (2017) (Editors' Suggestion).

8. C. Safranski, I. Barsukov, H. K. Lee, T. Schneider, A. A.Jara, A. Smith, H. Chang, K. Lenz, J. Lindner, Y. Tserkovnyak, M. Wu, and I. N. Krivorotov, *Spin Caloritronic Nano-Oscillator*, Nature Comm. **8**, 117 (2017).
9. S. K. Kim, H. Ochoa, R. Zarzuela, and Y. Tserkovnyak, *Realization of the Haldane-Kane-Mele Model in a System of Localized Spins*, Phys. Rev. Lett. **117**, 227201 (2016).
10. Z. Qiu, J. Li, D. Hou, E. Arenholz, A. T. NDiaye, A. Tan, K. Uchida, K. Sato, S. Okamoto, Y. Tserkovnyak, Z. Q. Qiu, and E. Saitoh, *Spin-Current Probe for Phase Transition in an Insulator*, Nature Comm. **7**, 12670 (2016).

Fractional Quantum Number Excitations in Yb-based compounds.

Alexei Tsvelik, Igor Zaliznyak, Brookhaven National Laboratory

Keywords: Quantum criticality**,** spinons, phasons, effective spins.

Project Scope

The purpose of the project is to study materials with strong spin-orbit (SO) coupling where the emergent low energy dynamics of large magnetic moments leads to unusual quantum-entangled magnetic states. These states can be described by effective low energy theoretical models that can be solved affording a predictive theoretical analysis. In the presence of conduction electrons the interaction between the electrons and the critical fluctuations of the Yb-moments leads to non-Fermi liquid behavior of the transport. The prime examples are magnetic metal Yb_2Pt_2Pb and related insulating perovskites of $YbAlO_3$ family which display unique magnetic and transport properties originating in quantum dynamics of Yb magnetic moments. Yb_2Pt_2Pb is a 3D metallic compound which has quasi-1D fractionalized magnetic excitations (spinons) originating from Yb ions arranged in 1D structures. Despite the fact that the ground state Kramers doublet of Yb ions includes only orbitals with high projection of the total angular moment $|m_J| = 7/2$, the spin dynamics is fully quantum and is well described by the spin-1/2 XXZ chain with modest Ising anisotropy. When the magnetic field overcomes the spectral gap and the chains become quantum critical we observe various effects originating from the interchain coupling and interaction with the conduction electrons. These ones include T-linear electrical resistivity and 3D dispersive phason modes.

Recent Progress

As was first observed in Ref. 1, 3D metallic compound Yb_2Pt_2Pb has the most unusual and unexpected magnetic spectrum (see Fig. 1) in the form of a continuum dispersing in one direction. The source of magnetism is Yb ions arranged in an array of one dimensional chains The best description of the spectrum and all related effects is obtained by modeling the system by arrays of spin-1/2 Heisenberg chains with nearest and next-to-nearest neighbor exchange interaction:

$$H = \sum_{n,m>0} \mathrm{J}_m \left(S_n^x S_{n+m}^x + S_n^y S_{n+m}^y + \Delta_m S_n^z S_{n+m}^z \right),$$

The best fit to the experimental data is obtained with $J_2 / J_1 = 1/2$ and $\Delta_1 = 2–3$. This was unexpected since the strong crystal field projects the total angular momentum of Yb-ions onto the Kramers doublet $|m_J| = 7/2$. However, it turns out that the superexchange in rare earth materials has matrix elements between all states of total angular momentum and therefore can flip between +7/2 and -7/2 states. This is because the superexchange interaction has a form of the permutation operator which has matrix elements between all states. Although this fact was

established theoretically by Dirac and reemphasized in the 60-ties by Coqblin and Schrieffer, its experimental relevance has not been appreciated.

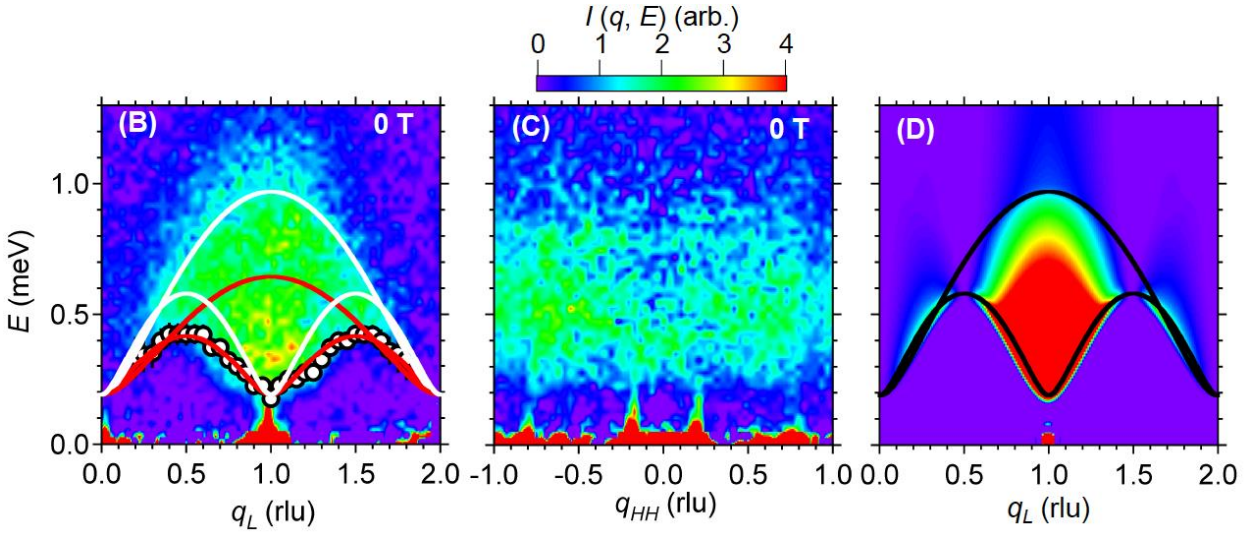

Fig.1 The magnetic excitation spectrum and dispersion along the q_L direction in reciprocal space measured at T = 0.1 K, summed over 1 < q_{HH} <1 rlu. The lower boundary of the spectrum (white circles) is shown along with the boundaries of the two-spinon continuum obtained by fitting the lower boundary (red lines, Δ= 3.46) and comparing the total measured spectrum to theory (white lines, Δ = 2.6). The color scale for parts B-D is shown above part C. Error bars represent one standard deviation. (C) The magnetic excitation spectrum along the q_{HH} direction in reciprocal space measured at T = 0:1 K, summed over 0 < q_L < 2 r.l.u. (D) The spinon spectrum obtained from tDMRG calculations for the XXZ model (1) with Δ = 2.6 on the 96-site chain. The continuum boundary (black lines) is the same as that shown in (B) for Δ = 2.6.

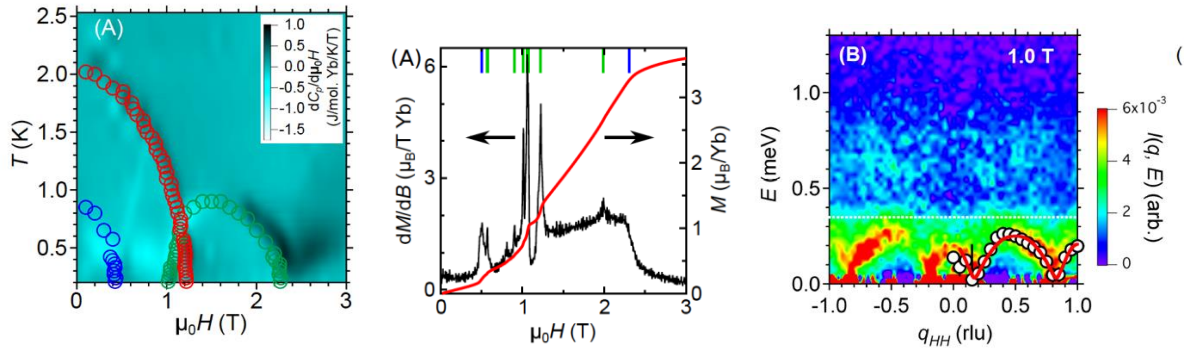

Fig.2 (A) The phase diagram of YbPtPb in magnetic field. (B) The magnetization and the static magnetic susceptibility as function of magnetic field, (C) The excitation spectrum in the transverse direction.

At the same time external magnetic field couples to the total angular momentum **J** ($E = g_L \mathbf{BJ}$) and so does neutron magnetic moment. As a consequence, at the low energy where only $|m_J| = 7/2$ states are active, the neutron scattering is dominated by the longitudinal excitations polarized along the local Ising axes.

The experiments in magnetic field reveal a rich phase diagram. When the magnetic field exceeds the gap (H > 0.5 T) we enter a state where individual chains are critical and represent Luttinger

liquid. The interchain interactions establish incommensurate spin density wave order. Fig. 2C shows the dispersion of the corresponding longitudinal phason mode.

The electrical resistivity in the region of the phase diagram shows T-linear behavior. As was explained in Ref. 2, this behavior arises when 3D electrons with almost spherical Fermi surface interact with 1D spin excitations. The absence of transverse dispersion of these excitations makes the entire Fermi surface "hot".

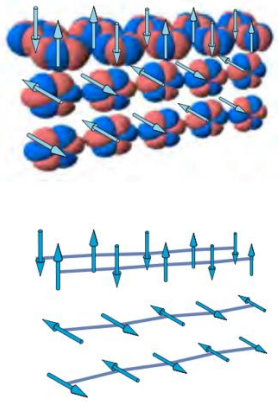

Fig. 3 Magnetic structure of Yb-chains.

Future Plans

Yb-based compounds of the Yb_2Pt_2Pb family and related $YbAlO_3$ perovskite family present a new and very interesting examples of materials where essentially 1D spin subsystem coexists with 3D conduction electrons. The relative smallness of the superexchange interaction and large magnetic moments associated with the effective spins-1/2 allows one to explore the phase diagram applying magnetic field. The results obtained so far have demonstrated very satisfactory agreement with theoretical expectations. There are several aspects which require clarification. The theory predicts that when the magnetic field exceeds the saturation limit and only the transverse excitations remain, they will become virtually invisible due to the extreme anisotropy of the Landee factor. The drastic (two orders of magnitude) reduction of the neutron scattering intensity could be expected based on the g-factor estimates. However, the observed suppression near the saturation field is less than expected which is likely a result of the electron-spin interaction. These results are yet unpublished and require a theoretical analysis. It turns out that Yb_2Pt_2Pb is just one member of an extensive class of Yb-chain materials. There are many others including those like $YbAlO_3$ which are insulators. The magnetic spectrum is very similar to Yb_2Pt_2Pb, although there are differences in magnetic field [1]. On one hand this is a clear indication that the interaction between Yb magnetic moments and the conduction electrons in Yb_2Pt_2Pb is indeed small. On the other hand, these interactions have distinct consequences for transport and a study of differences between the metallic and insulating compounds will clarify

the structure of the electron-spin interactions. We plan to explore these materials and try to elucidate the differences coming from the presence of conduction electrons.

References

1. L. S. Wu, S. E. Nikitin, Z. Wang, W. Zhu, C. D. Batista, M. Brando, L. Vasylechko, M. Frontzek, A. T. Savici, G. Sala, G. Ehlers, A. D. Christianson, M. D. Lumsden, and A. Podlesnyak, *Tomonaga-Luttinger liquid behavior and spinon confinement in $YbAlO_3$* , unpublished.

Publications (August 2016 – July 2018)

If more than 10 publications, list only the 10 most relevant.

1. L. S. Wu, W. J. Gannon, I. A. Zaliznyak, A. M. Tsvelik, M. Brockmann, J.-S. Caux, M.-S. Kim, Y. Qiu, J. R. D. Copley, G. Ehlers, A. Podlesnyak, M. C. Aronson, *"Orbital Exchange and Fractional Quantum Number Excitations in an f-electron Metal Yb_2Pt_2Pb"*, Science **352**, 1206-1210 (2016).
2. L. Classen, I. Zaliznyak and A. M. Tsvelik, *``Field-induced quantum criticality from fractionalized local moments coupled to itinerant electrons in Yb2Pt2Pb"*, Phys. Rev. Lett. **120**, 156404 (2018).
3. W. J. Gannon, L. S. Wu, I. A. Zaliznyak, A. E. Feiguin, A. M.Tsvelik, F. Demmel, Y. Qiu, J. R. D. Copley, and M. C. Aronson, *"The Longitudinal Excitations of Weakly Coupled Tomonaga-Luttinger Liquids: Spinon Confinement and Sharp Longitudinal Mode in Yb2Pt2Pb in Magnetic Field"*, accepted to Nature Communications.

Time-dependent density-functional approaches for spin-dependent nonequilibrium phenomena

Carsten A. Ullrich
Department of Physics and Astronomy, University of Missouri, Columbia, MO 65211

Keywords: femtomagnetism, density-functional theory for noncollinear magnetism, spin-orbit coupling, spin waves in itinerant magnetic systems, Hubbard model

Project Scope

The objective of this research is to develop new approaches for spin-dependent nonequilibrium phenomena in quantum materials, and to apply these methods in linear response and in the real-time nonlinear regime. This work is motivated by a growing interest in noncollinear magnetism in systems of interacting electrons, occurring in the ground state, during spin-wave excitations, or driven by strong, ultrafast fields. The standard density-functional approaches for noncollinear magnetism, the local spin-density and generalized gradient approximations, assume a local spin quantization axis for the exchange-correlation (xc) functional. This does not produce any xc magnetic torques, thus missing an important aspect of magnetization dynamics. The PI will develop a new class of orbital-dependent xc functionals for noncollinear magnetism by generalizing the local Slater exchange and the Singwi-Tosi-Land-Sjölander (STLS) method for the case of general mixed two-component spinor wave functions. These new functionals will be applied to the following situations. *1. Spin waves in 2D materials.* We will extend our prior work under DOE support, where we studied 2D electron systems in the presence of Rashba and Dresselhaus spin-orbit coupling. We will calculate spin-wave dispersions with noncollinear Slater and STLS and compare with experimental data from inelastic light scattering, and study spin waves in graphene and related 2D topological materials. *2. Strongly driven Hubbard dimers.* We will solve the time-dependent Kohn-Sham equation for two electrons in a Hubbard dimer driven by noncollinear magnetic fields, testing the Slater and STLS xc magnetic fields and torques by comparison with exact benchmark results from the two-body Schrödinger equation. *3. Ab initio noncollinear spin dynamics*. We will implement our new xc functionals for noncollinear magnetism in the open source codes Abinit and Octopus. We will calculate the magnetization of typical noncollinear materials such as lattices of Cr atoms. With Octopus, we will simulate the ultrafast magnetization dynamics of small Fe or Cr clusters and of magnetic molecules, in particular graphene fragments. The proposed research will have fundamental and practical impact in the area of noncollinear magnetic phenomena in a broad spectrum of materials in and out of equilibrium.

Recent Progress

1. Spin-helix Larmor mode. This work was carried out in collaboration with Irene D'Amico (York, UK) and the experimental group of Florent Perez (UPMC Paris). A two-dimensional electron gas (2DEG) in the presence of equal-strength Rashba and Dresselhaus spin-orbit coupling ($\alpha = \beta$) sustains persistent helical spin-wave states, which have remarkably long lifetimes [1]. In the presence of an in-plane magnetic field, we found that there exist single-particle excitations that have the character of propagating helical spin waves. For magnon-like collective excitations in such systems, the spin-helix texture reemerges as a robust feature, giving rise to a decoupling of spin-orbit and electronic many-body effects [2]. We were able to prove that the resulting spin-flip wave dispersion is the same as in a magnetic 2DEG without spin-orbit coupling, apart from a shift by the spin-helix wave vector $\boldsymbol{Q}$ (see Fig. 1). In particular, there is a collective mode in which the electronic spins precess about the persistent spin-helix texture. This mode is shown to have an energy given by the bare Zeeman splitting, in analogy with Larmor's theorem. This is a new and exact many-body result, which we call the spin-helix Larmor mode. Fig. 2 shows a proposal to observe the spin-helix Larmor mode experimentally.

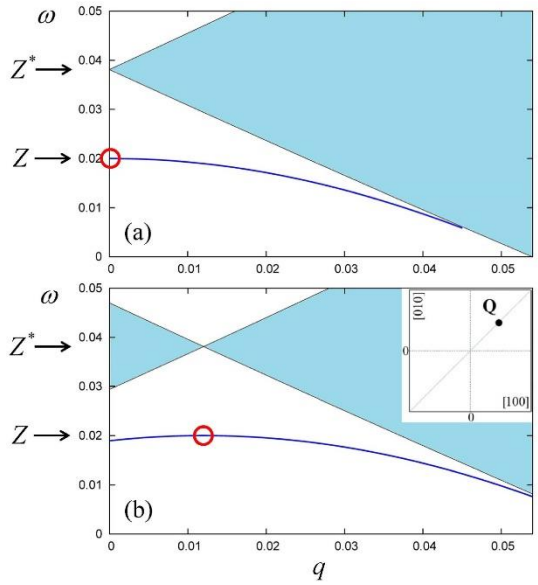

Fig.1. Continuum of single-particle excitations (shaded areas) and spin-wave dispersions (blue line) for a 2DEG with an in-plane magnetic field. Top: no spin-orbit coupling. Bottom: with $\alpha = \beta$ Rashba and Dresselhaus spin-orbit coupling. The red circles indicate Larmor's theorem. *Z*: bare Zeeman energy.

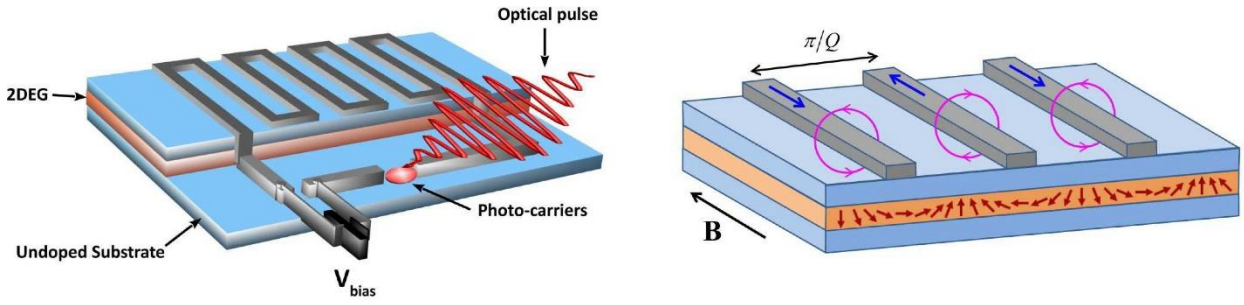

Fig.2. Proposed experimental design for the excitation of the spin-helix Larmor mode. Left: photo-conductive antenna on top of the sample, converting infrared optical pulses into a current pulses. Right: close-up view of the metal stripes on top of the spin-polarized 2DEG. The currents (blue arrows) are in alternating directions in neighboring stripes; the induced magnetic fields (pink circles) trigger a standing spin wave in the 2DEG.

2. Density-functional theory for systems with noncollinear spin: orbital-dependent exchange-correlation functionals and their application to the Hubbard dimer. A new class of orbital-dependent exchange-correlation (xc) potentials for application in noncollinear spin-density-functional theory has been developed [3]. Starting from the optimized effective potential (OEP) formalism for the exact exchange potential – generalized to the noncollinear case – correlation effects are added via a self-consistent procedure inspired by the Singwi-Tosi-Land-Sjölander (STLS) method [4]. Schematically, the procedure works as follows. We express the response function (omitting spin indices) as

$$c(\mathbf{r},\mathbf{r}',w) = c_0(\mathbf{r},\mathbf{r}',w) + \int d\mathbf{x}\int d\mathbf{x}'\, c_0(\mathbf{r},\mathbf{x},w)\, f_{\rm xc}^{\rm STLS}(\mathbf{x},\mathbf{x}')\, c(\mathbf{x}',\mathbf{r}',w)$$

The fluctuation-dissipation theorem gives the static structure factor,

$$S(\mathbf{r},\mathbf{r}') = -\frac{1}{p}\int_0^\infty \mathrm{Re}\, c(\mathbf{r},\mathbf{r}',w)\, dw$$

and then we construct the xc kernel as

$$f_{\rm xc}^{\rm STLS}(\mathbf{r},\mathbf{r}') = \frac{S(\mathbf{r},\mathbf{r}') - \delta(\mathbf{r}-\mathbf{r}')n(\mathbf{r})}{n(\mathbf{r})n(\mathbf{r}')\,|\mathbf{r}-\mathbf{r}'|}$$

which closes the self-consistent cycle. The limit without correlations is the exact-exchange (EXX) Slater kernel. From the xc kernel (including spin dependence) we then construct xc potentials and magnetic fields.

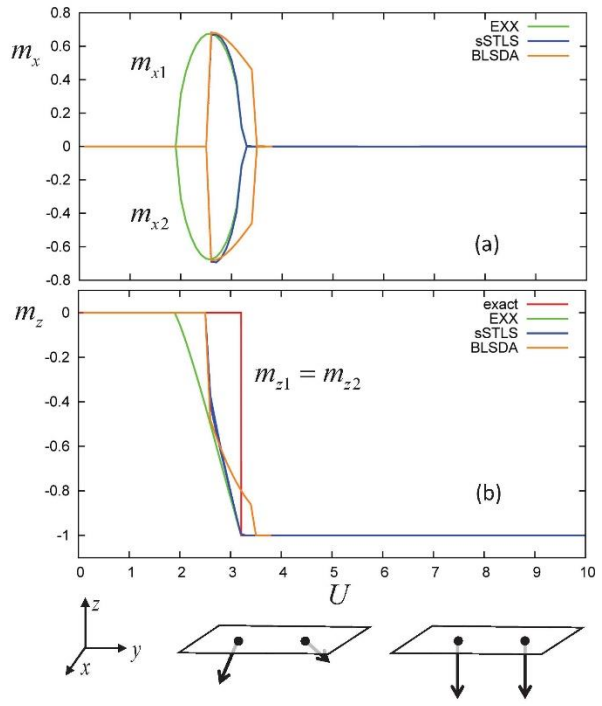

Fig.3. Magnetization components of a Hubbard dimer in a magnetic field along the *z*-direction. The calculation is unrestricted, allowing a symmetry breaking in the transverse *x*-direction. Exact results are compared with DFT results (EXX, sSTLS and BLSDA).

This general formalism was then applied to the asymmetric Hubbard dimer in uniform and noncollinear external magnetic fields and compared to exact diagonalization and to the Bethe-ansatz local spin-density approximation (BLSDA) [5]. The STLS gives the overall best performance for total energies, densities and magnetizations, particularly in the weakly to moderately correlated regime. Fig. 3 gives an illustration of the performance: here, the Hubbard dimer is in the presence of a uniform magnetic field along *z*, but a spin-unrestricted calculation leads to symmetry-broken solutions, where a magnetization along the *x*-direction appears in the crossover region between the weakly and strongly correlated regime (around the Hubbard interaction strength U=3). We also carried out calculations for noncollinear external magnetic fields, which confirm the good performance of the STLS [3].

Future Plans

Spin waves in graphene. The PI and a graduate student, Matthew Anderson, are currently studying collective spin dynamics in doped graphene. The goal is to obtain spin-wave dispersions in the presence of SOC, and identify regimes and parameters where the expected modulation effects would be strong enough to facilitate experimental observation (this will be in collaboration with Florent Perez at UPMC Paris).

Exchange-correlation magnetic torques. The PI and a graduate student, Edward Pluhar, are currently using the density-functional formalism for noncollinear spin to construct xc magnetic torques for the Hubbard dimer and compare this to exact results, obtained by inverting the Kohn-Sham equation to construct the exact xc potentials and magnetic fields. These will be the first exact benchmarks for xc magnetic torques, and a stringent test for our STLS formalism.

Real-time TDDFT for femtomagnetism. We plan to implement the orbital-dependent xc potentials for noncollinear magnetism in the ab-initio codes octopus and Abinit, to study the ultrafast magnetization dynamics in frustrated noncollinear spin systems such as Cr clusters. To perform this work, a postdoctoral researcher will be identified to join the group in early 2019.

References

1. B. A. Bernevig, J. Orenstein, and S.-C. Zhang, *Exact SU(2) symmetry and persistent spin helix in a spin-orbit coupled system,* Phys. Rev. Lett. 97, 236601 (2006)

2. S. Karimi, C. A. Ullrich, I. D'Amico, and F. Perez, *Spin-helix Larmor mode,* Sci. Rep. **8**, 3470 (2018)

3. C. A. Ullrich, *Density-functional theory for systems with noncollinear spin: orbital-dependent exchange-correlation functionals and their application to the Hubbard dimer,* to appear in Phys. Rev. B (2018)

4. K. S. Singwi, M. P. Tosi, H. R. Land, and A. Sjölander, *Electron correlation at metallic densities*, Phys. Rev. **170**, 589 (1968)

5. V. V. Franca, D. Vieira, and K. Capelle, *Simple parametrization for the ground-state energy of the infinite Hubbard chain incorporating Mott physics, spin-dependent phenomena and spatial inhomogeneity,* New J. Phys. **14**, 073021 (2012).

Publications (2016-2018)

1. F. Baboux, F. Perez, C. A. Ullrich, G. Karczewski, and T. Wojtowicz, *Spin-orbit stiffness of the spin-polarized electron gas,* Physica Status Solidi RLL **10**, 315-319 (2016)

2. F. Perez, F. Baboux, C. A. Ullrich, I. D'Amico, G. Vignale, G. Karczewski, and T. Wojtowicz, *Spin-orbit twisted spin waves: group velocity control*, Phys. Rev. Lett. **117**, 137204 (2016)

3. S. Karimi, F. Baboux, F. Perez, C. A. Ullrich, G. Karczewski, and T. Wojtowicz, *Spin precession and spin waves in a chiral electron gas: beyond Larmor's theorem,* Phys. Rev. B **96**, 045301 (2017)

4. S. Karimi, C. A. Ullrich, I. D'Amico, and F. Perez, *Spin-helix Larmor mode,* Sci. Rep. **8**, 3470 (2018)

5. C. A. Ullrich, *Density-functional theory for systems with noncollinear spin: orbital-dependent exchange-correlation functionals and their application to the Hubbard dimer,* to appear in Phys. Rev. B (2018)

6. I. D'Amico, F. Perez, and C. A. Ullrich, *Chirality and dissipation of spin modes in two-dimensional electron liquids,* in preparation for J. Appl. Phys. D Topical Reviews (2018)

Computational studies of hydrogen interactions with materials

PI: Chris G. Van de Walle

Materials Department, University of California, Santa Barbara, CA 93106-5050
vandewalle@mrl.ucsb.edu

Keywords: fuel cells, proton conductors, battery electrodes, electrochromism, first-principles calculations

Project Scope

We are conducting computational studies with the goal of developing new insights for hydrogen interactions with materials. Using state-of-the-art density functional calculations, our research addresses the energetics and electronic structure of hydrogen interactions with materials used for hydrogen storage, ionic conductors, or battery electrodes. In addition, we address the mechanisms governing the electrochromic behavior that is observed upon intercalation of hydrogen or other monovalent dopants into tungsten oxide and related materials. Overall, our studies are aimed at elucidating a number of aspects of the physics, and to develop promising strategies for improving existing materials as well as developing novel materials. Central themes include investigations of charge localization and of solid-light interactions.

Recent Progress

1. Ion-transport engineering of alkaline-earth hydrides for hydride electrolyte applications

The heavier alkaline-earth hydrides (CaH_2, SrH_2, and BaH_2) are promising materials for hydrogen energy applications, due to their excellent ionic conductivity and thermal stability. Transport in these materials has been attributed to hydride ions. We have studied the defect chemistry and ion-transport mechanisms. We find that hydride ion transport is mediated by hydrogen vacancies, with a migration barrier that depends strongly on the charge state of the vacancy (V_H). As shown in **Figure 1**, vacancies in the positive charge state have a much lower barrier than neutral vacancies.

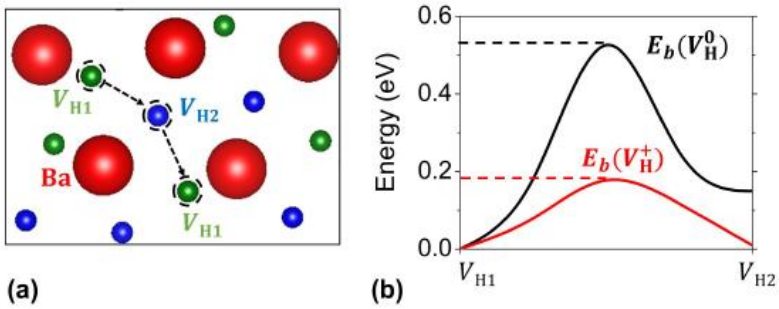

Figure 1: (a) Schematic pathway for migration of a hydrogen vacancy (V_H) between H1 and H2 sites in BaH_2. (b) Potential energy change along the migration path for vacancies in the neutral and positive charge states.

It is therefore advantageous to enhance the concentration of positive vacancies. We are proposing a strategy for enhancing the ionic conductivity by lowering the formation energy of positively charged vacancies. This can be accomplished by doping with acceptors, in particular alkali-metal impurities. We find that optimal synthesis conditions can produce ionic conductivities for hydride conduction that are equivalent to proton conductivities in the best proton conducting oxides.

Our results indicate that the alkaline-earth hydrides are promising candidates for hydrogen electrolytes, with the potential to match or surpass the performance of solid-state proton conductors. Their properties make them well-suited for energy applications in systems requiring fast hydrogen kinetics. A paper describing these results is under review at *Chemistry of Materials*.

2. Mechanisms of electrochromism

Tungsten oxide (WO_3) is well known for its electrochromic properties. While broadly used for applications such as smart windows, electrochromism is still poorly understood. Several mechanisms based on polarons and/or defects have been proposed. We have demonstrated that these mechanisms are not viable [6]. Instead, we focus on absorption of photons by electrons in the conduction band. These carriers originate from dopants that are diffused into the material when a voltage is applied. We have investigated the behavior of WO_3 under such high doping [4]. Most importantly, in a paper that has been accepted for publication in MRS Commun. [7], we demonstrate that the presence of these electrons can explain the large increase in optical absorption in the visible region of the spectrum.

For both crystalline and disordered structures, doping induces strong absorption in the infrared. Absorption in the visible range (**Figure 2)** increases with the degree of structural distortion; the absorption coefficient in the blue exceeds 10^3 cm^{-1} at doping levels above 10^{20} cm^{-3} in the monoclinic phase. Increased disorder in disordered structures significantly enhances the visible-range absorption. Our results demonstrate that carrier-induced absorption provides a consistent explanation for electrochromism.

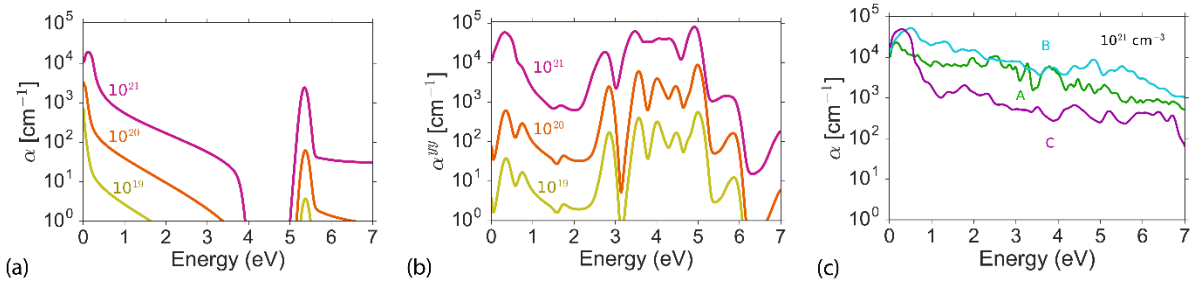

Figure 2: Optical absorption spectra for transitions involving carriers added by doping for (a) the cubic, (b) the monoclinic phase, and (c) for three disordered structures of WO_3. For the cubic and monoclinic phases, results are shown for three doping levels (10^{19}, 10^{20}, and 10^{21} cm^{-3}); for the disordered phase, the doping level is 10^{21} cm^{-3}.

3. Efficient n-type doping of MoO_3

MoO_3 is another material that exhibits electrochromic behavior. It is also an attractive layered material that is widely used for transparent contacts for organic photovoltaics or organic light-emitting diodes. For these and other applications, a thorough understanding of the behavior of point defects and impurities and their impact on conductivity is essential. Using our expertise in including van der Waals interactions in hybrid functionals (developed with DOE support), we studied the electronic properties of native defects and intentional dopant impurities to obtain controllable *n*-type doping in MoO_3.

We have found that electron polarons play an important role in understanding the properties of MoO_3. Electrons can be self-trapped, or bind to defects. Oxygen vacancies can lead to the experimentally observed unintentional *n*-type doping. Our calculations also show that Tc and Re impurities on the Mo site and halogens (F, Cl, and Br) on the O site all act as shallow donors. Our calculated binding energies will guide the choice of impurity. However, they also trap electron polarons [**Figure 3**]. Surprisingly, Fe, Ru, and Os impurities are amphoteric, i.e., they can act as acceptors and will compensate *n*-type MoO_3. While not suitable for *n*-type doping, Mn atoms exhibit interesting magnetic behavior and may enable new applications of this versatile material.

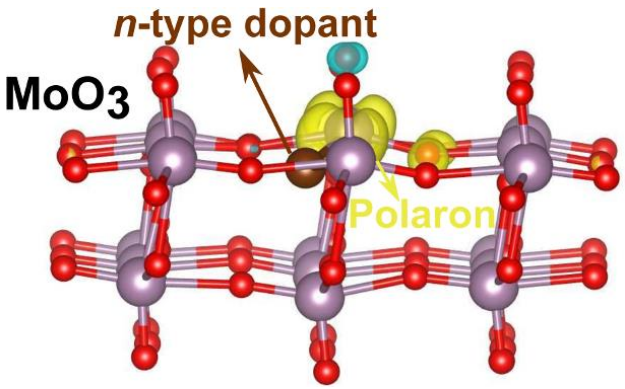

Figure 3. *n*-type dopant (Br on an O site) in MoO_3, with an associated electron polaron localized on a nearby Mo site.

These results have been published in *Chemistry of Materials* [2].

4. Enhancing ionic conductivity in proton conductors

In the course of our project, we have conducted systematic investigations of ionic conductivity in proton conductors, including a study of cerates such as $BaCeO_3$ and $SrCeO_3$. More recently, we focused attention on perovskite zirconates such as $SrZrO_3$, which are among the best proton conducting oxides, with applications as electrolyte materials in solid oxide fuel cells. To achieve high proton concentrations, $SrZrO_3$ is doped with trivalent cations which act as acceptor dopants when substituting at the Zr site; this leads to the formation of compensating oxygen vacancies, which enable proton incorporation. We have conducted an investigation into the properties of acceptor dopants (Sc and Y) in $SrZrO_3$, including their interaction with protons, and the tendency to self-compensate by forming donor defects at the Sr site [3].

We have found that under Sr-rich conditions, both Sc and Y will substitute at a Zr site and act as deep acceptors, where the deep level originates from a small hole polaron. Under Zr-rich

growth conditions, Sc again forms an acceptor, however Y forms self-compensating donor species by substituting at the Sr site, and this is detrimental to proton conductivity since oxygen vacancies no longer form. The increased tendency for Y to self-compensate originates from the larger ionic radius. We also investigated the proton–dopant association (**Figure 4**); we found that the binding energy of a proton to a negatively charged acceptor impurity is 0.41 eV for Sc and 0.31 eV for Y. This indicates that proton transport is limited by trapping at impurity sites.

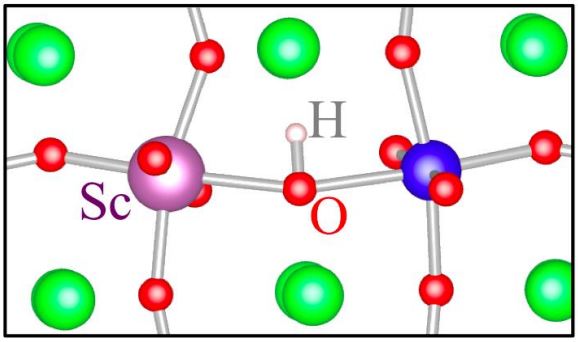

Figure 4. Protons in acceptor-doped $SrZrO_3$ can be trapped by forming a complex.

Future Plans

We continue our studies of hydride ion transport by turning our attention to oxyhydrides. In the context of electrochromism, we plan a further assessment of mechanisms of carrier-induced optical absorption in WO_3 and MoO_3. For proton conductors, we will study protonic and electronic conduction in double perovskites. We also conduct studies of conductivity in battery electrodes and are engaged in an investigation of Na intercalation in $NaMnO_2$.

Publications (August 2016 – July 2018)

1. Z. Zhu, H. Peelaers, and C. G. Van de Walle, *Hydrogen intercalation in MoS_2*, Phys. Rev. B **94**, 085426 (2016).

2. H. Peelaers, M. L. Chabinyc, and C. G. Van de Walle, *Controlling n-type doping in MoO_3*, Chem. Mater. **29**, 2563 (2017).

3. L. Weston, A. Janotti, X. Y. Cui, C. Stampfl, and C. G. Van de Walle, *Acceptor doping in the proton conductor $SrZrO_3$*, Phys. Chem. Chem. Phys. **19**, 11485 (2017).

4. W. Wang, A. Janotti, and C.G. Van de Walle, *Phase transformations upon doping in WO_3*, J. Chem. Phys. **146**, 214504 (2017).

5. Z. Zhu, H. Peelaers, and C. G. Van de Walle, *Electronic and protonic conduction in $LaFeO_3$*, J. Mater. Chem. A **5**, 15367 (2017).

6. W. Wang, H. Peelaers, J.-X. Shen, A. Janotti, and C. G. Van de Walle, *First-principles characterization of defects in WO_3*, in *Oxide-based Materials and Devices IX*, edited by D. J. Rogers, D. C. Look, and F. H. Teherani, Proc. SPIE **10533**, 105332C (2018).

7. W. Wang, H. Peelaers, J.-X. Shen, and C. G. Van de Walle, *Carrier-induced absorption as a mechanism for electrochromism in WO_3*, MRS Commun. (in press).

X-ray Spectroscopy on Excited and Decaying Systems

Michel van Veenendaal
Northern Illinois University

Keywords: Nonequilibrium dynamics, strongly-correlated systems, magnetism, X-ray spectroscopy

Project Scope

The goal of this project is to study the dynamics of a variety of systems excited away from equilibrium predominantly by visible light. Special attention is paid to the X-ray spectroscopic response of these systems in order to connect to experiments performed at Department of Energy's user facilities. The focus lies on the following nonequilibrium processes: (i) *Spin crossover complexes.* In a number of transition-metal compounds, the transition metal has two competing spin states, usually characterized as low and high spin. Upon photoexcitation, an electron is transferred to the ligands or between different transition-metal sites. This causes the system to cascade from one spin state to another. These transitions are very amenable to X-ray spectroscopy and are therefore often used as a model system for the study of nonequilibrium dynamics. (ii) *Non equilibrium spin dynamics.* Initial pump-probe RIXS experiments have been performed on antiferromagnetic iridates (Dean *et al*, Nature Mat. 15, 602 (2016)) demonstrating the feasibility of measuring the time-dependent spin-density wave spectrum. The goal is to obtain an understanding of the time evolution of the spin-density wave spectrum after creating spin excitations using visible light. (iii) *Ultrafast charge-order melting.* Upon photoexcitation, the charge order in a system can often be melted for sufficiently high fluences. This is often combined with a disappearance of the charge-density wave gap. These systems can be studied using pump-probe type experiments, where the pump is in the visible or terahertz region. Suitable probes are X-ray diffraction and resonant X-ray scattering, which are sensitive to the long-range order. The goal is to increase the realism in the models describing the ultrafast charge-order melting.

Recent Progress

Measuring ultrafast spin crossovers using short-pulsed X-ray probes – Understanding intersystem crossings on a femtosecond time scale is of the upmost importance for progress in fields such as ultrafast magnetism and phase transitions, catalysis, and energy conversion processes. Unfortunately, few experimental tools allow the measurement of the nonequilibrium electronic structure on this time scale. Recent years have seen the construction of several X-ray free-electron laser facilities based on the principle of self-amplified spontaneous emission enabling the creation of femtosecond X-ray pulses with a few hundred meV resolution. Despite the tremendous experimental progress, our understanding of the nonequilibrium X-ray response function is virtually uncharted territory, which complicates experimental progress and hampers

our ability to extract information from these crucial experiments. Recent experiments have pushed the spin crossover switching time below 50 fs, which is less than the oscillation period of the breathing mode of the ligands surrounding the magnetic ion.

As an initial system, the low-to-high spin crossover on cobalt in Fe-Co Prussian blue analogues was studied. Here the cobalt ion undergoes a spin transition after a photoexcitation from Fe to Co. The d^7 state quickly relaxes from low-to-high spin. A model was used that included the local many-body electronic structure described by the full Coulomb multiplet effects, crystal-field effects, and the spin-orbit interaction. The transition-metal is coupled to a quantum-mechanical breathing mode describing the elongation of the metal-ligand distance during the spin transition. The calculations demonstrated a spin crossover from the doublet to the quartet within 20 fs, see Fig. 1. Concurrently, the total spin increases from a 1/2 to 3/2 and the number of holes in the t_2 orbitals increases from 0 to 1. At the same time, the metal-ligand distance increases due to the stronger repulsion of the ligands in the high-spin state. The system fully relaxes to the lowest quartet state in 150-200 fs. Strong oscillations in spin-orbit coupling and the involvement of higher-lying quartets were found. The model used includes the details necessary for a description

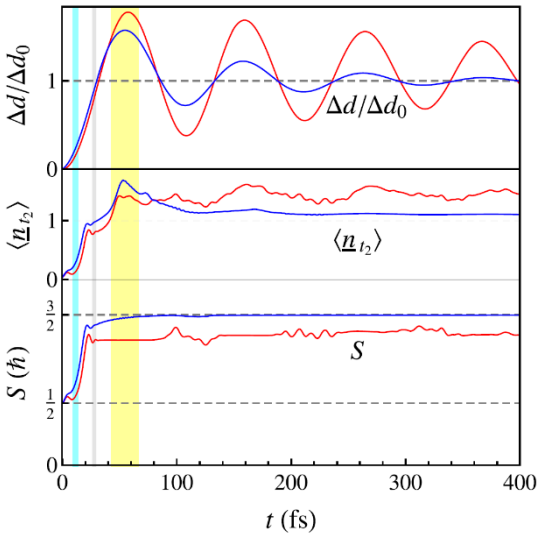

Figure 1. The time dependence of the expectation value of some important operators during the ultrafast spin crossover in a divalent cobalt ion. A comparison is made between the results without damping (red) and with a damping constant $\hbar\Gamma$ = 13 meV (blue). From top to bottom: the normalized displacement $\Delta d/\Delta d_0$, the number of holes in the t_2 orbitals, and the total spin S.

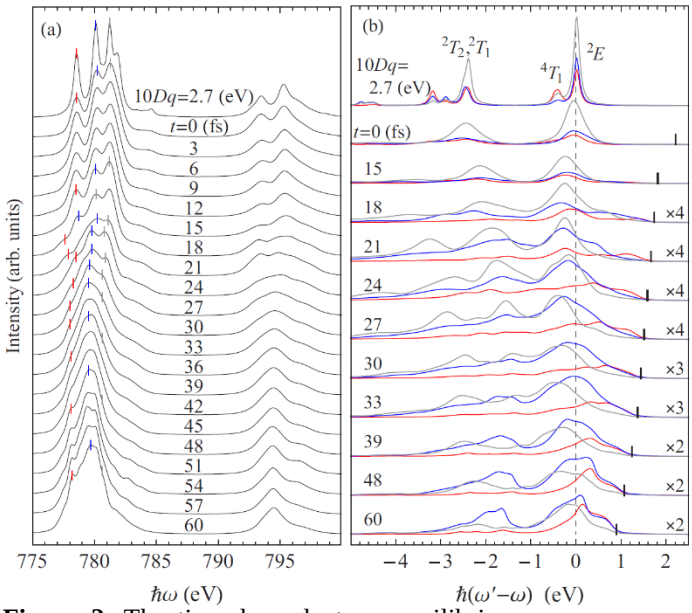

Figure 2. The time-dependent nonequilibrium x-ray response functions for the cobalt ion. (a) X-ray absorption intensity as a function of incoming photon energy ∇ω for selected times indicated in the figure. The metal-ligand separation, spin, and t_2 occupation at these times can be found in Fig. 1. (b) RIXS intensity as a function of the change in photon energy ∇(ω′−ω) for selected times indicated in the figure. RIXS was calculated for the incoming photon energies indicated by the small vertical lines of corresponding color in the absorption spectra in (a). Some spectra are scaled by the amount shown in the figure. The small black vertical lines indicate the highest ∇(ω′−ω). The top spectra show an atomic multiplet calculations with a static cubic crystal field of 10Dq = 2.7 eV.

of core-level X-ray spectroscopy on the cobalt ion. The response in the soft-X-ray region was calculated demonstrating the sensitivity of time-dependent X-ray spectroscopic tools to changes in the local electronic structure. Figure 2 clearly shows the effects of the spin transition on the *L*-edge X-ray absorption and resonant inelastic X-ray scattering (RIXS) spectra. Changes in local spin and symmetry and the underlying mechanism are reflected in strong broadenings, a collapse of clear selection rules during the intersystem crossing, fluctuations in the isotropic branching ratio in x-ray absorption, crystal-field collapse and/or oscillations, and time-dependent anti-Stokes processes in RIXS. This work demonstrates that X-ray absorption and resonant inelastic x-ray scattering at transition-metal L edges can provide insight into ultrafast intersystem crossings of importance for energy conversion, ultrafast magnetism, and catalysis.

Spin-density wave spectra in nonequilibrium systems – Experimentally, the collapse of the spin- density wave spectrum as a result of spin flips induced by photoexcitations with visible light can be studied using resonant inelastic X-ray scattering at X-ray free electron lasers, as was shown by Dean *et al*, Nature Mat. 15, 602 (2016). The ultrafast demagnetization and recovery of the spin system was studied using a semiclassical model based on the Landau-Lifshitz-Gilbert (LLG) model. The advantage of this model is that larger systems can be treated and the inclusion of spin damping is straightforward. The size of the system was 40×40=1600 spins. The demagnetization and subsequent recovery was studied for different numbers of flipped spins. For 25% excited spins, the lowest magnetization of a few percent is reached around 150 fs after excitation. The magnetization then recovers in about 1 ps. The RIXS experiment measures the spin-density response $S_{\mathbf{q}}(\omega)$. The created spin excitation in the experiment moves in the background described by the LLG model. In the absence of photoexcitations, this model gives a typical spin density wave (SDW) spectrum. The spin background is used to calculate the spin density wave spectrum which is averaged over different initial states. These calculations, see Fig. 3, show a collapse of the magnon dispersion with a significant transfer of spectral weight from the magnon dispersion to low-energy. It also shows the temporary opening of a spin gap. For the used relaxation time, this spin gap disappears

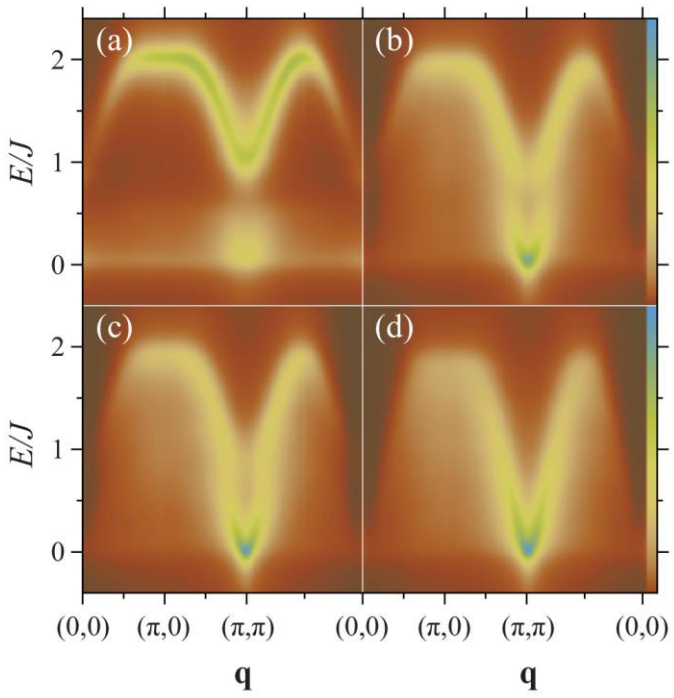

Figure 3. Time dependent spin-density wave spectra of a two-dimensional spin model after photoexciting 25% of the spins. (a) Spectrum directly after photoexcitation. (b),(c) Spectra at 16 and 19 fs when the spin gap is closing. (d) Spectrum at 100 fs after photoexcitation.

around 15-20 fs. The quickest recovery of the SDW spectrum is observed around the (π,π) point. This is understandable since (π,π) corresponds to the short-range correlations, which are expected to recover first. The higher-lying spectral weight is strongly broadened although the outlines of the original SDW spectrum are still clearly visible. This is different from the experimental data (Dean *et al*, Nature Mat. 15, 602 (2016)) which show the largest changes around the reciprocal lattice point (π,π) at 2 ps. However, it is possible that the short-range interactions are already restored at this delay and that the additional, which is found close to zero energy loss, is mainly due to diffuse scattering resulting from changed in the long-range order. Additional measurements at times closer to the photoexcitations are needed to verify this.

Future Plans

Nonequilbrium spin dynamics using exact diagonalization. Spin waves can be calculated using model systems that describe the material in terms of quantum-mechanical Heisenberg spins. The postdoctoral researcher hired on this grant, Tsezar Seman, is performing high-performance exact diagonalizations of Heisenberg-like models. The time-dependence is calculated using Krylov methods for linear chains of 16-24 sites. Currently different photoexcitations (bimagnon, magnon) are under investigation. The calculations show additional melting of the magnetic order after the photoexcitation. A significant increase in spectral weight with energy higher than the magnon dispersion is observed. Also, additional low-energy spectral weight is created. The time-dependence shows a clear oscillatory behavior.

Spin crossover in Fe complexes. The spin crossover in the Prussian-blue analogues was chosen for the relative simplicity of the process (one spin flip and a photoexcitation causing a direct transfer from the iron to the cobalt). The much more commonly studied spin crossover in Fe complexes requires two spin flips from low-to-high spin state. Additionally, the spin crossover is initiated by a photoexcitation from the iron to the ligands, thereby further complicating the spin crossover. The fastest reported spin crossover is less than 50 fs. This spin crossover has been studied with a wide variety of X-ray spectroscopies. Additional interesting spin crossovers occur in nickel complexes, which can be accompanied by the breaking of the bond in the apical direction. The Jahn-Teller distortion plays an important role in these systems. Initial calculations on the iron complexes are being performed graduate student William Baker and postdoc Tsezar Seman.

Publications (August 2016 – July 2018)

1. L. Zhu, T. F. Seman, M. van Veenendaal, and K. H. Ahn, *Photo-induced nonequilibrium dynamics in charge-density wave materials*, J. Appl. Phys. **123**, 115112 (2018).

2. M. van Veenendaal, *Nonequilibrium X-ray spectroscopy as a probe of spin crossover in Fe-Co Prussian blue analogues*, Phys. Rev. B **97**, 125108 (2018).

3. L. S. I. Veiga, M. Etter, K. Glazyrin, F. Sun, G. Fabbris, J. R. L. Mardegan, P. S. Malavi, Y. Deng, P. Stavropoulos, H. -Y. Kee, W. G. Yang, M. van Veenendaal, J. S. Schilling, T. Takayama, H. Takagi, and D. Haskel, *Electronic and structural response at pressure-driven magnetic transition in hyperhoneycomb iridate β-Li2IrO$_3$*, Phys. Rev. B Rapid Comm. **96**, 140402 (2017).

4. M. van Veenendaal, *Ultrafast intersystem crossings in Fe-Co Prussian blue analogues*, Scientific Reports **7**, 6672 (2017).

5. M. van Veenendaal, *Photoinduced ultrafast charge-order melting: Charge-order inversion and non-thermal effects*, Phys. Rev. B **94**, 115101 (2016).

6. Y. Ding, C.-C. Chen, Heung-Sik Kim, Myung Joon Han, Zhenxing Feng, Yufeng Peng, Mary Upton, Diego Casa, Jungho Kim, Ayman Said, Thomas Gog, Gang Cao, Ho-kwang Mao, and Michel Van Veenendaal, *Pressure-Induced Confined Metal from the Mott Insulator Sr$_3$Ir$_2$O$_7$*, Phys. Rev. Lett. 116, 216402 (2016).

7. J. W. Freeland, M. van Veenendaal, and J. Chakhalian, *Evolution of electronic structure across the RNiO$_3$ series*, J. El. Spec. Rel. Phenom. 208, 56 (2016).

8. Y. Wang, B. Moritz, C.-C. Chen, C. J. Jia, M. van Veenendaal, and T. P. Devereaux, *Using Non-Equilibrium Dynamics to Probe Competing Orders in a Mott-Peierls System*, Phys. Rev. Lett. **116**, 086401 (2016).

MATERIALS GENOME INNOVATION FOR COMPUTATIONAL SOFTWARE (*MAGICS*)

Priya Vashishta
Collaboratory for Advanced Computing and Simulations, Department of Chemical Engineering & Materials Science, Department of Physics & Astronomy, and Department of Computer Science, University of Southern California, Los Angeles, CA 90089-0242

Keywords: Computational synthesis; Reactive force fields; Non-adiabatic QMD software; Thermal conductivity software; GEARS software; ultra-fast X-ray laser experiments for validation

***MAGICS* Center Team** consists 11 investigators from 4 universities and 2 national laboratories. The Center supports 9 postdocs and software engineers, and 10 graduate students.

- ***USC***: Priya Vashishta–PI, Malancha Gupta, Rajiv K. Kalia, Aiichiro Nakano, Oleg Prezhdo
- ***Rice University***: Pulickel M. Ajayan
- ***SLAC National Accelerator Laboratory***: Uwe Bergmann and David Fritz
- ***California Institute of Technology***: William A. Goddard, III
- ***Lawrence Berkeley National Laboratory***: Kristin A. Persson
- ***University of Missouri***: David J. Singh

Project Scope

The MAGICS (Materials Genome Innovation for Computational Software) Center is about layered materials genome. Our goal is to develop and deliver validated first-principles based computational synthesis and characterization software and carry out ultrafast pump-probe X-ray laser experiments at LCLS. The software will aid the synthesis of stacked layered materials (LMs) by chemical vapor deposition (CVD), exfoliation, and intercalation. The software will provide function-property-structure relationships and will be sufficiently general to help synthesis and characterization of other functional nanomaterials.

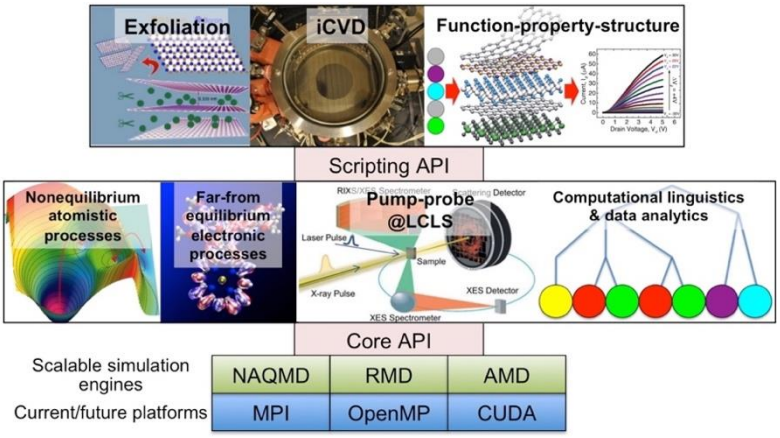

Overview of MAGICS research and software stack. API–application programming interface; LCLS–Linac Coherent Light Source; NAQMD–non-adiabatic quantum molecular dynamics; RMD–reactive molecular dynamics; AMD–accelerated molecular dynamics; MPI–message passing interface; OpenMP–open multi-processing; CUDA–compute unified device architecture.

Research Completed and Materials Software Delivered in 2016-2018

A. MAGICS software stack

1. RXMD – ***Reactive molecular dynamics software for peta-to-exa-scale***

RXMD is a scalable parallel software for reactive MD based on the first principles-informed reactive force-fields (ReaxFF). RXMD follows atomic trajectories that include chemical bond breakage and formation based on a reactive bond-order and charge transfer based on a charge-equilibration scheme. ***RXMD source code is available on GitHub and pre-compiled executables are available for DOE supercomputers, Mira, Theta and Cetus at ALCF.***

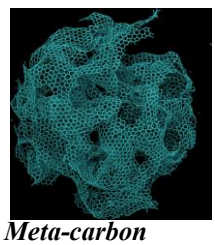

Meta-carbon synthesis simulated with RXMD

2. QXMD – *Quantum dynamics software with non-adiabatic quantum dynamics extensions*

A scalable parallel software for quantum molecular dynamics (QMD) with various extensions (X), where X currently supported include adiabatic and non-adiabatic (NA). In QMD, interatomic forces are computed quantum mechanically based on DFT. NAQMD describes electronic excitations using linear-response time-dependent DFT. Transitions between excited states are treated using surface hopping algorithm. ***Pre-compiled executables are available for DOE supercomputers, Mira, Theta and Cetus at ALCF.***

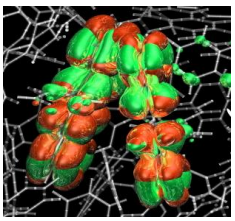

Electron and hole charges from QXMD

3. Thermal Conductivity Plugins – *Software plugins for LAMMPS to calculate thermal properties*

Thermal conductivity tools are a set of plugins for thermal properties — velocity autocorrelation functions, phonon density of states, specific heat and thermal conductivity with isotopic mass distribution — using LAMMPS. Source code and documentation for the plugins are publicly available on the MAGICS software distribution website.

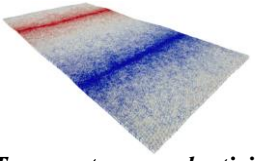

Temperature conductivity calculations using plugins

4. GEARS – *Real-time virtual reality visualization of molecular simulations*

Game-Engine-assisted Research platform for Scientific Computing is a hardware-agnostic workflow that leverages game engines to adapt scientific visualization and simulation techniques for virtual reality (VR). It allows researchers to port existing codebases to VR. ***Source code and associated documentation for GEARS are publicly available on GitHub and the MAGICS software distribution website.***

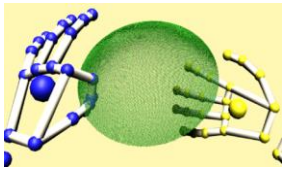

Manipulating atomic structures in GEARS VR

B. Research Completed at the MAGICS center

1. Optical control of lattice motion in monolayer crystals

Photo-induced non-radiative energy dissipation is a pathway to induce structural phase transitions in 2D materials. ***In our pump-probe experiments, we use ultrafast electron diffraction to directly probe the sub-picosecond conversion of photoenergy to lattice vibrations in 2D $MoSe_2$ and $MoTe_2$.*** NAQMD simulations reproduce this ultrafast increase in lattice temperature and the corresponding conversion of photoenergy to lattice vibrations.

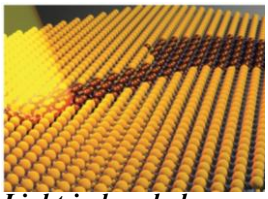

Light-induced phase transition

2. Scalable synthesis of layered materials by exfoliation

We have investigated exfoliation of MoS_2 into nanosheets in a mixture of water and isopropanol. MD simulations are performed to examine shock-induced collapse of cavitation bubbles and the resulting exfoliation of MoS_2. Collapse of cavitation bubbles generates high-speed nanojets and shock waves in the solvent. Large shear stresses due to the nanojet impact initiate exfoliation, and reflected shock waves enhance exfoliation.

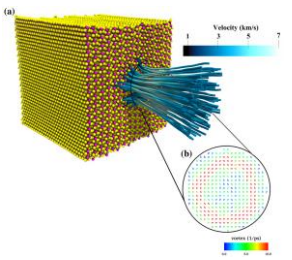

Cavitation bubble collapse leading to a nanojets

3. Emergent magnetism in two dimensional alloys

Tailoring structural phase transitions using alloying is a novel idea with implications in designing all-2D architectures. We have grown 2D alloys of Re-doped $MoSe_2$ which show composition-tunable structural phase variations. ***None of the ingredients, Re, Mo and Se are magnetic materials, yet a magnetic phase is observed in 2D alloys of Re-doped $MoSe_2$. The compositions where the magnetic phase is observed agree with predictions from quantum simulations.***

4. Machine learning-based prediction of structure and properties of 2D materials

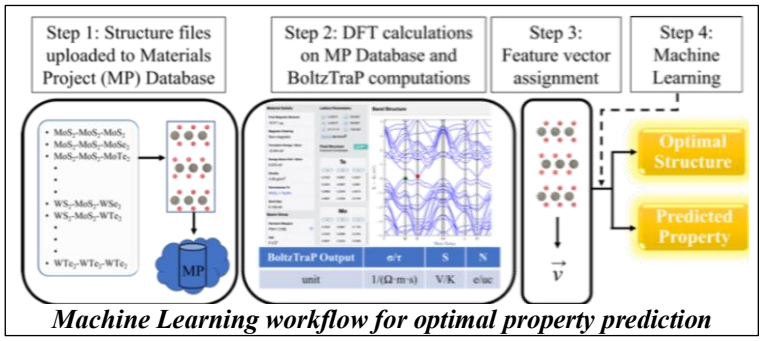

Machine Learning workflow for optimal property prediction

We present two machine learning models, namely ***Gaussian process regression*** and ***Bayesian optimization*** for prediction of thermoelectric properties of layered materials. Bayesian optimization significantly reduces the computational cost of discovering the optimal structure compared to regression models. ***The models can be used for prediction of any material property and our software, including data preparation code based on the Python Materials Genomics (PyMatGen) library and python-based machine learning code, is available open-source to materials science and engineering community.***

Research in Progress and Future Plans

1. Time-to-solution methods for ReaxPQ+

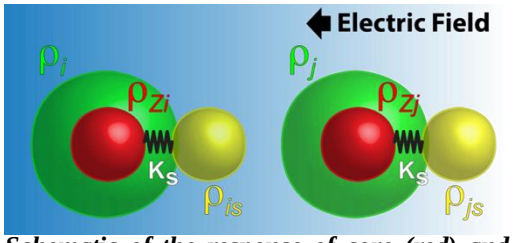

Schematic of the response of core (red) and shell (yellow) charges to an external electric filed in the new PQEq+ model

A recent reactive force-field model by ***Goddard*** *et al.* based on a ***polarizable charge equilibration scheme (ReaxPQ)*** improves accuracy in describing reactions but is inadequate for calculating polarizabilities. We have generalized ReaxPQ to ReaxPQ+, in which atomic polarizations respond to both internal and external electric fields, thus achieving near-quantum accuracy. *We accelerate computationally expensive ReaxPQ+ using (1) a new extension of the shift-collapse algorithm to compute dynamic n-tuples with minimal data transfers, (2) multithreading with round-robin data privatization, and (3) data reordering to reduce computation and allow vectorization.*

2. Synthesis of 2D ternary alloys and in-plane heterostructures

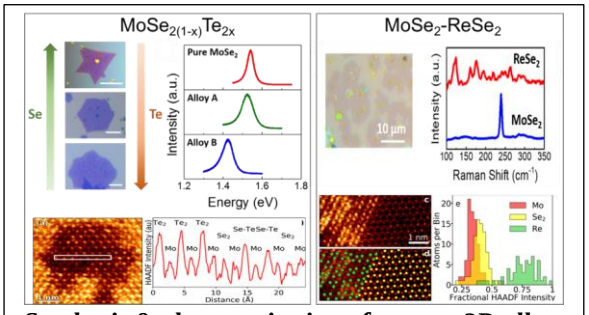

Synthesis & characterization of ternary 2D alloys

The stability of $MoSe_2$-$ReSe_2$ in-plane 2D heterostructures is being investigated by joint experiment/simulation effort. STEM imaging shows an atomically-sharp interface and quantum simulations are used to characterize the electronic/magnetic structure. We are also successful in selectively synthesizing ternary alloys by doping the chalcogen lattice of $MoSe_2$ with Te. Stability and electronic structures of both alloys were confirmed by *ab initio* and MD simulations.

3. Machine learning using neural networks for defect identification in computational synthesis

Identification of structural phases during computational synthesis requires complex structural analysis. ***This can be formulated as a classification problem and can be solved using machine learning techniques such as neural networks and support vector machines. We have used feed-forward neural network with three hidden layers to identify the different phases present during CVD computational synthesis of MoS_2.*** We used a 300-dimensional feature vector that captures radial and angular distribution around each atom. ***We find that our neural network model has learned about different phases present in the system and separate them from each other.***

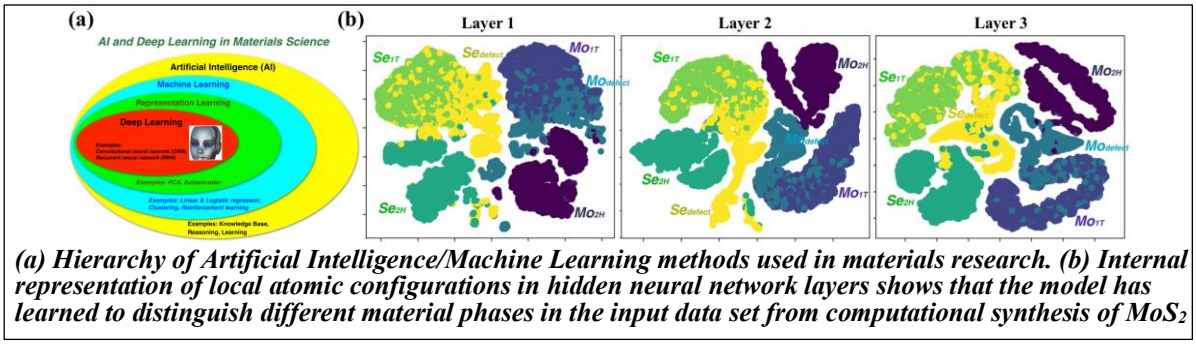

(a) Hierarchy of Artificial Intelligence/Machine Learning methods used in materials research. (b) Internal representation of local atomic configurations in hidden neural network layers shows that the model has learned to distinguish different material phases in the input data set from computational synthesis of MoS_2

MAGICS Software Distribution and Training

The MAGICS center has conducted two workshops for the distribution of materials software from the center and for the training of the materials community in the use of center software.

Participants at the 2nd MAGICS workshop in March 2018

The first MAGICS workshop on materials software was held at USC Radisson Hotel, November 12 – 15, 2017. The workshop had 36 participants - graduate students, post-docs and early-career faculty from 21 universities and 3 DOE labs. Travel, accommodation and all meals were fully paid for all participants. **The second MAGICS workshop was held at the USC Radisson Hotel, March 2-4, 2018**. 22 students, postdocs and early-career faculty from 14 Universities and DOE Labs attended the workshop. **Dr. James Davenport** and **Dr. Harriet Kung** from the DOE – Basic Energy Sciences were present for a part of the workshop.

References and Selected Publications

1. S. Hong, A. Krishnamoorthy, P. Rajak, S. Tiwari, M. Misawa, F. Shimojo, R. K. Kalia, A. Nakano and P. Vashishta, *Computational Synthesis of MoS_2 Layers by Reactive Molecular Dynamics Simulations: Initial Sulfidation of MoO_3 Surfaces*, Nano Lett., **17**, 4866 (2017)

2. S. Hong, C. Sheng, A. Krishnamoorthy, P. Rajak, S. Tiwari, K.-i. Nomura, M. Misawa, F. Shimojo, R. K. Kalia, A. Nakano and P. Vashishta, *Chemical Vapor Deposition Synthesis of MoS_2 Layers from the Direct Sulfidation of MoO_3 Surfaces Using Reactive Molecular Dynamics Simulations*, J. Phys. Chem. C, **122**, 7494 (2018)

3. V. Kochat, A. Apte, J. A. Hachtel, H. Kumazoe, A. Krishnamoorthy, S. Susarla, J. C. Idrobo, F. Shimojo, P. Vashishta, R. Kalia, A. Nakano, C. S. Tiwary and P. M. Ajayan, *Re Doping in 2D Transition Metal Dichalcogenides as a New Route to Tailor Structural Phases and Induced Magnetism*, Adv. Mater., **29**, 1703754 (2017)

4. M.-F. Lin, V. Kochat, A. Krishnamoorthy, L. Bassman, C. Weninger, Q. Zheng, X. Zhang, A. Apte, C. S. Tiwary, X. Shen, R. Li, R. Kalia, P. Ajayan, A. Nakano, P. Vashishta, F. Shimojo, X. Wang, D. M. Fritz and U. Bergmann, *Ultrafast non-radiative dynamics of atomically thin $MoSe_2$*, Nat. Comm., **8**, 1745 (2017)

5. A. Krishnamoorthy, L. Bassman, R. K. Kalia, A. Nakano, F. Shimojo and P. Vashishta, *Semiconductor-metal structural phase transformation in $MoTe_2$ monolayers by electronic excitation*, Nanoscale, **10**, 2742 (2018)

6. K. Hiroyuki, K. Aravind, B. Lindsay, K. Rajiv, N. Aiichiro, S. Fuyuki and V. Priya, *Photo-induced lattice contraction in layered materials*, J. Phys.: Condens. Matt., accepted (2018)

7. L. Bassman, A. Krishnamoorthy, H. Kumazoe, M. Misawa, F. Shimojo, R. Kalia, A. Nakano and P. Vashishta, *Electronic Origin of Optically-Induced Subpicosecond Lattice Dynamics in $MoSe_2$ Monolayer*, Nano Lett., accepted (2018)

8. L. Bassman, P. Rajak, R. K. Kalia, A. Nakano, F. Sha, M. Aykol, P. Huck, K. Persson, J. Sun, D. J. Singh and P. Vashishta, *Efficient Discovery of Optimal N-Layered TMDC Hetero-Structures*, MRS Adv., **3**, 397 (2018)

9. A. Apte, V. Kochat, P. Rajak, A. Krishnamoorthy, P. Manimunda, J. A. Hachtel, J. C. Idrobo, S. A. Syed Amanulla, P. Vashishta, A. Nakano, R. K. Kalia, C. S. Tiwary and P. M. Ajayan, *Structural Phase Transformation in Strained Monolayer $MoWSe_2$ Alloy*, ACS Nano, **12**, 3468 (2018)

10. N. Payam and J. S. David, *Thermal conductivity of single-layer WSe_2 by a Stillinger–Weber potential*, Nanotechnology, **28**, 075708 (2017)

Time-dependent density functional theory and quantum continuum mechanics

GRANT DE-FG02-05ER46203

Principal Investigator:
Giovanni Vignale, Department of Physics, University of Missouri, Columbia (MO).
E-mail: vignaleg@missouri.edu

Project scope

The goal of the proposed research activities is to develop new theoretical tools for the treatment of non-equilibrium phenomena in a broad range of materials and structures, while deepening our understanding of thermal effects at the nanoscale and developing a description of the electronic structure in terms of mechanical concepts such as the electronic stress tensor. The three major activities associated with this goal are: (1) development of the time-dependent *thermal* density functional theory (DFT), (2) development of quantum continuum mechanics, and (3) studies of quantum thermal and electric transport in electron liquids in the hydrodynamic regime.

Recent progress

1. With my current postdoc, Dr. Mohammad Zarenia, we have started a comprehensive study of the thermoelectric transport properties of two-dimensional electronic systems such as monolayer and bilayer graphene. While the electrical resistivity is largely controlled by extrinsic effects (disorder and phonons), the thermal resistivity of these systems has a large contribution from electron-electron (e-e) scattering. The e-e contribution can be calculated in a completely parameter-free way and constitutes an important addition to our understanding of interacting electron liquids, as well as a crucial input for the thermal density functional theory. It is well established in the literature and supported by recent experiments, see e.g. Refs. [1, 2], that e-e scattering can dominate the transport properties of 2D electron liquids in a suitable temperature range, neither too low nor too high: this is called the hydrodynamic regime. Once in the hydrodynamic regime, the different scattering mechanism which contribute to electrical and thermal resistivity can give rise to large deviations from the conventional Wiedemann-Franz (WF) law. Some of these deviations have been observed in recent experiments, and they are believed to be important in the quest for high-ZT (Figure of merit) materials and efficient thermo-electric power conversion. Previous theoretical work on 2D electrons in graphene had focused either on the single-band Fermi liquid regime (temperature much lower than the extrinsically controlled Fermi energy), or on the Dirac electron-hole liquid regime, where the carriers are thermally generated in both bands. In the former case, the WF ratio is reduced relative to the standard value (see Ref. [3]); in the latter case it is enhanced (this has been seen in the experiments of Ref. [2]).

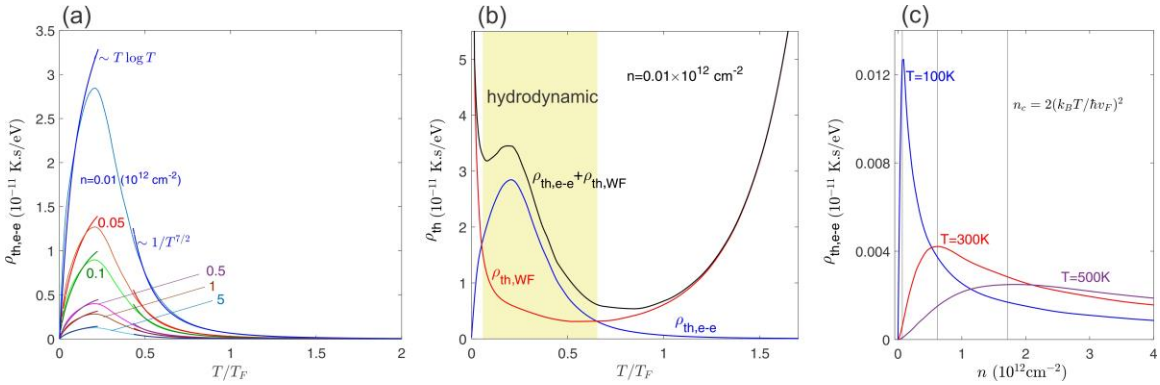

Fig. 1: **(a)** Intrinsic thermal resistivity $\rho_{th,e-e}$ from e-e interactions only as a function of temperature (T_F is the Fermi temperature) for different carrier densities as labeled. The thick curves are fitted functions, indicating the limiting behaviors of $\rho_{th,e-e}$. **(b)** Comparison between $\rho_{th,e-e}$ and the hypothetical thermal resistivity $\rho_{th,WF}$, which would be obtained by applying the standard Wiedemann-Franz law to a simple model of the electric resistivity in which e-e collisions play no role. The total resistivity $\rho_{th,e-e}+\rho_{th,WF}$ is also shown. The highlighted region indicates the hydrodynamic regime. **(c)** $\rho_{th,e-e}$ as a function of carrier density at fixed temperatures as labeled. The vertical lines correspond to the critical density n_c at which a crossover from Fermi liquid (high doping) to Dirac fluid (low doping) occurs, i.e., where the density of thermally excited electrons in the conduction band exceeds the density of extrinsically doped electrons.

Our theory is the first to present the complete evolution of the thermal resistivity ρ_{th} from the Fermi liquid regime to the Dirac electron-hole liquid regime. The two regimes are found to be separated by a thermal resistivity maximum, which we have studied either as a function of temperature (at fixed electron density), see Figs. 1(a) and 1(b), or as a function of electron density at fixed temperature, Fig. 1(c). While a maximum in the intrinsic ρ_{th} is also predicted for Galilean invariant 2DEGs (e.g. in traditional doped GaAs), we find that the decrease of $\rho_{th,e-e}$ with increasing temperature beyond the maximum is much faster in graphene than in 2DEG, reflecting the existence of an essentially conserved thermal current in the electron-hole Dirac liquid. More precisely, the $\sim 1/T^{7/2}$ behavior of $\rho_{th,e-e}$ for $T>T_F$, see Fig. 1(a), is linked to the fact that the thermal e-e relaxation time, $\tau_{th,e-e}$, scales according to $1/\tau_{th,e-e} \propto \mu^2$, where the chemical potential at constant density decreases as $\mu \sim 1/T$. In order to better understand the interplay between momentum-non-conserving collisions (with impurities and phonons) and momentum-conserving (e-e) collisions, we have shown in Fig. 1(b) the hypothetical thermal resistivity $\rho_{th,WF}$ which would be obtained by applying the standard Wiedemann-Franz (WF) law to a simple model of the electric resistivity in which e-e collisions play no role. $\rho_{th,WF}$ is seen to grow rapidly at the low and high temperature ends, crossing the intrinsic $\rho_{th,e-e}$ at two points. The two crossing points define the hydrodynamic regime as the temperature region for which $\rho_{th,e-e}>\rho_{th,WF}$. This shows unequivocally that the WF ratio is *reduced* in the hydrodynamic regime and should show a minimum corresponding to the crossover between Fermi liquid and electron-hole Dirac liquid. Observation of a minimum in the WF ratio will therefore provide strong evidence for the occurrence of our predicted crossover within the hydrodynamic regime.

We have also calculated the Seebeck coefficient of carriers in graphene, and we have shown that, at variance with Galilean-invariant systems, it does not coincide with the

entropy per particle, although it reduces to this quantity in the Fermi liquid regime. Similar calculations are planned for more complex systems such as graphene bilayers and Weyl semimetals. Lastly, we clarify the relative importance of inter-band and intra-band Coulomb collisions in graphene and resolve the singular behavior of the electric resistivity, including the effect of disorder at low densities.

2. With my former postdoc, Dr. Mohammad Sherafati, we have worked on the Hall viscosity of *gapped graphene* in the presence of an external magnetic field – a preprint based on this work has just been published on arXiv (Publication 3) and will soon be submitted for publication in PRB. This is the continuation of the work we did previously on the Hall viscosity of graphene and is part of our activity on quantum continuum mechanics. The system studied is "gapped graphene", where the gap arises from broken inversion symmetry, i.e., as a "Semenoff mass" in the Hamiltonian of graphene (the interesting possibility of a Haldane mass will be considered in a near future). We focus on the relation between the Hall viscosity and the coefficient of q^2 in the small wave vector expansion of the nonlocal Hall conductivity. In gapless monolayer graphene (in a magnetic field) two degenerate valleys contribute equally to both quantities, and the relation is summarized by a generalized Hoyos-Son formula (Ref. [4]), which expresses the order q^2 Hall conductivity in terms of the viscosity and the orbital magnetic susceptibility. A novel feature emerges in gapped graphene, due to the fact that the two valleys are no longer equivalent: as a result, valley-resolved quantities such as the single-valley Hall conductivity and the single-valley Hall viscosity are no longer quantized, even when the Fermi level is in a gap between Landau levels: the single-valley Hall viscosity diverges. Quantization and the Hoyos-Son formula are recovered only when one sums over the valleys, but do not hold separately in each valley. This demonstrates the crucial difference that exists between Hall conductivity/Hall viscosity and valley Hall conductivity/valley Hall viscosity when it comes to their topological properties.

3. With my former postdoc, Florian Eich, I have completed a theoretical study of the temperature dependence of the exchange-correlation free energy of the homogeneous electron gas – a crucial input for the implementation of the thermal DFT. We have presented a critical assessment of a recently proposed parametrization of this quantity, and we have discussed the advantages of calculating the effective mass of quasiparticles in the interacting electron liquid from the low-temperature free energy vis-à-vis conventional approaches (Publication 1).

4. With my former postdocs, Stefano Pittalis and Florian Eich, we have completed the construction of energy functionals for non-collinear spin-density functional theory, making use of "natural building blocks" that are invariant under $U(1) \times SU(2)$ local gauge transformations (Publication 2).

References

1. R. Krishna Kumar, D.A. Bandurin, F.M.D. Pellegrino, Y.Cao, A. Principi, H. Guo, G. H. Auton, M. Ben Shalom, L. A. Ponomarenko, G. Falkovich, K. Watanabe, T. Taniguchi, I.V. Grigorieva, L.S. Levitov, M. Polini, and A.K. Geim, *Superballistic flow of viscous electron fluid through graphene constrictions*, Nature Physics **13**, 1182–1185 (2017).

2. J. Crossno, J.K. Shi, Ke Wang, X. Liu, A. Harzheim, A. Lucas, S. Sachdev, Ph. Kim, T. Taniguchi, K. Watanabe, Th. A. Ohki, and K. Ch. Fong, *Observation of the Dirac fluid and the breakdown of the Wiedemann-Franz law in graphene*, Science 10.1126/science.aad0343 (2016).
3. A. Principi and G. Vignale, *Violation of the Wiedemann-Franz law in hydrodynamic electron liquids*, Phys. Rev. Lett. 115, 056603 (2015).
4. C. Hoyos and D. T Son, *Hall viscosity and electromagnetic response*, Phys. Rev. Lett. **108**, 066805 (2012).

Planned activities

1. We will extend our study of thermal transport and thermoelectric power to more complex systems, such as bilayer graphene, where experimental studies are already underway. We will also study the "trans-Seebeck effect", which arises from Coulomb drag in bilayer systems.

2. With Dr. Paolo Emilio Trevisanutto at the National University of Singapore (NUS), I will work on the continuum mechanics formulation of the exciton problem. I will also try to derive a general condition/criterion to assess the stability of the ground-state of a quantum many-electron system against spontaneous geometric deformations.

Publications 2017-2018

1) "*Effective mass of quasiparticles from thermodynamics*", F. G. Eich, Markus Holzmann, and G. Vignale, arXiv:1704.04076, Phys. Rev. B **96**, 035132 (2017).

2) "U(1)×SU(2) gauge invariance made simple for density functional approximations", S. Pittalis, G. Vignale, F. G. Eich, arXiv:1704.07304, Phys. Rev. B **96**, 035141 (2017).

3) *"Hall Viscosity and nonlocal conductivity of gapped graphene",* M. Sherafati and G. Vignale, arXiv:1802.09616 (2018).

Quantum Mesoscopic Materials

Principal Investigator: Valerii M. Vinokour; Co-PIs: Andreas Glatz, Alexey Galda (MSD)
Argonne National Laboratory

Keywords: Quantum information, quantum engine, non-Hermitian Hamiltonian, confinement.

Project Scope

The QMM explores physics arising from the direct interplay between quantum coherence and entanglement, quantum evolution, topological excitations, disorder, and fluctuations, both in equilibrium and in far-from-equilibrium states and focuses on the following intertwined directions:
1. *Ultraquantum thermodynamics for quantum information science*: Building on our discovery of quantum *H*-theorem and quantum formulation of the second law of thermodynamics, we will pursue the design of quantum engines based on the entropy teleportation, error-correction protocols for quantum computing, ultrafast measurements for quantum metrology, and material platform for quantum sensing.
2. *Non-equilibrium processes in open dissipative systems*: Having established a non-Hermitian Hamiltonian approach to quantitative description of non-equilibrium processes, we (i) Continue constructing fundamental nonequilibrium thermodynamics including into our PT symmetry-based approach the Lee-Yang Zero technique and nonequilibrium quantum phase transitions and (ii) Use our approach to investigate into the physics of the qubit coherence and nonreciprocal quantum systems for quantum information sciences.
3. *Topological matter and new quantum materials for fundamental physics and applications*: We develop gauge field theory approach for comprehensive description of intertwined fundamental topological states: superconductivity, superinsulation, and bosonic topological insulator, which according to G. t'Hooft's conjecture, are the condensed matter realization of quark physics. We will pursue and explore fundamental implications of confinement, asymptotic freedom, and related QED phenomena for creating material platform for supersensitive sensors, qubits, and logical units for quantum information science.
4. *Topological excitations in ferroelectrics*: Confinement in finite systems stabilizes exotic topological excitations (TE) in ferroelectric materials (FE), which will constitute a new class of multivalued logical units and low-dissipation circuits for quantum information technology, and neuromorphic computing.

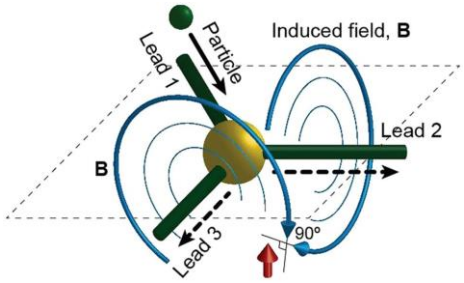

Fig. 1. A particle incident from the lead 1 is scattered into two other leads 2 and 3. Propagating particle induces magnetic field perpendicular to the lead direction. The spin is placed at the point where the respective fields induced by particles propagating along leads 2 and 3 are perpendicular to each other. To simplify consideration, we choose the setup design allowing to neglect the field induced by the particle in the lead 1.

Recent Progress

1. Building on the mathematical formalism provided by the quantum information theory (QIT) we formulated the quantum *H*-theorem in terms of physical observables. We discussed the second law of thermodynamics in quantum physics and uncovered situations where it can be locally violated. We considered examples of quantum evolution and found physical systems which being energy-

isolated evolve with the diminishing entropy. An example of such a system is presented in Fig. 1, where the particle scatters on the spin, playing the role of the thermal reservoir. Such a system offers a quantum realization of the Maxwell demon, quantum Maxwell demon (QMD) and lays the ground for design of quantum heat engines utilizing the possibility of the local violation of the second law of thermodynamics. Our findings led to establishing a new discipline – ultraquantum thermodynamics – dealing with the quantum systems with a few degrees of freedom (e.g. qubits).

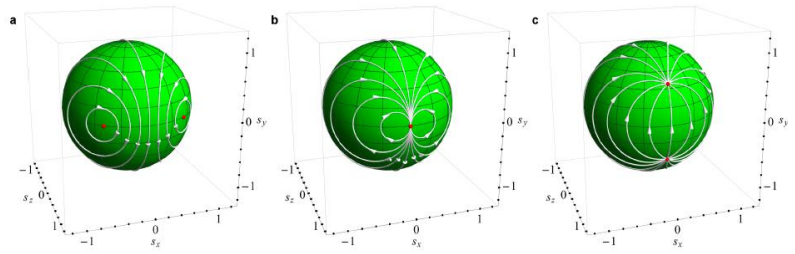

Fig. 2. Transition between the elliptic (a) and loxodromic (c) Möbius transformations by increasing the ratio of imaginary-to-real magnetic field. In classical spin dynamics, this corresponds to the PT symmetry-breaking.

2. Vast majority of processes in nature occurs in the non-equilibrium. Yet, the existing theories, can handle mostly only slight deviations from equilibrium. Moreover, it has been long believed that the general systematic approach to nonequilibrium cannot exist because of the lack of a general foundational principle equivalent to minimal energy principle in equilibrium. We developed a general approach for quantitative treatment of open dissipative systems far from equilibrium based on the description of far from equilibrium system by the non-Hermitian Hamiltonian, the non-Hermiticity of which is proportional to the applied driving force. The dynamic phase transition from stationary to nonstationary motion is described as a loss of the parity-time reversal (PT) symmetry by eigenstates of the Hamiltonian at some threshold drive. We applied our technique to dynamic Mott transition and classical spin systems. In the former, our approach enabled the analytical derivation of the critical behavior of the dynamic Mott transition. In spin systems, establishing the correspondence between the PT symmetry breaking transition and the Moebius transformation unraveled that dynamic phase transitions in open dissipative systems are in fact topological phase transitions in configurational space. We found PT symmetry-breaking transition between precession and exponentially damped spin dynamics and showed that transition properties can be derived from the distribution of Yang-Lee zeros of the system's partition function. The physical interpretation of imaginary magnetic field as describing the action of nonconservative forces opens the possibility of direct observations of Lee-Yang zeros in nonequilibrium physical systems.

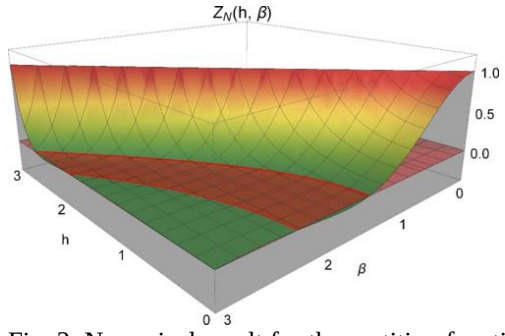

Fig. 3. Numerical result for the partition function of N=4 ferromagnetically coupled spins (J=1) with open boundary condition placed in magnetic field h=hˆx+iβˆy. Zeros of the partition function (Lee-Yang zeros) are only observed in the regime of broken PT symmetry, i.e., when |h|<|β|. Partition function takes strictly positive values in the regime of unbroken PT symmetry, |h|>|β|.

1. In 1976, G. t'Hooft found that confined quarks form the state, which in many respects is similar to superconductivity but is completely opposite in a sense that it has an infinite resistance rather than infinite conductance. He called the novel state "superinsulator." In 1996, Diamantini *et al*, independently constructed the field theory of the Josephson junction arrays and found that on the insulating side of the superconductor-insulator transition (SIT) a new ground state dual to

superconductivity with the infinite resistance forms and re-coined the name "superinsulator." Finally, superinsulators were re-discovered by Vinokur and coauthors experimentally and theoretically in 2008. Existence of superinsulators was derived from the duality of the uncertainty principle, and they were identified as confined Berezinskii-Kosterlitz-Thouless phase. Using the mathematical formalism of Diamantini *at al.*, we developed a comprehensive field theory of the SIT and unraveled the topological nature of the SIT and phases that emerge in its critical vicinity. We unraveled the topological nature of the superinsulating phase as a confined state of Cooper pairs bound by Polyakov strings, in a full concert with the 't Hooft's conjecture, and constructed the phase diagram of the SIT. We resolved the decades lasting enigma of why some materials exhibit the direct SIT and others go via the intermediate metallic phase which we demonstrated to be a bosonic topological insulator.

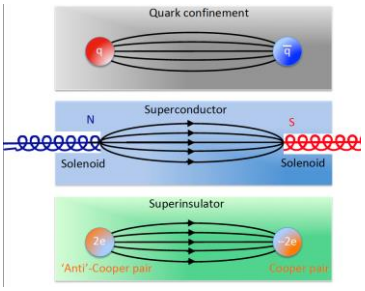

Fig. 4. Quark confinement, vortex in a superconductor, and the Polyakov string confining Cooper pairs in a superinsulator.

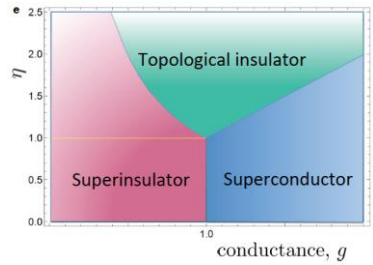

Fig. 5. Phase diagram of the critical vicinity of the SIT. The conductance is a tuning parameter and η quantifies the strength of quantum fluctuations.

4. We discovered that strained ferroelectric films harbor more than two discrete states of polarization which is manipulated by electric field. This offered a roadmap for adopting ferroelectric nanodots for information processing based on the multivalued logics, hence to function like a human brain. We demonstrated the multi-stable polarization states that enable the design of the ferrolectric multibit cells are found from Ginzburg-Landau functional for films of ferroelectric perovskite oxides. Using the catastrophe theory we demonstrated that these states are topologically protected.

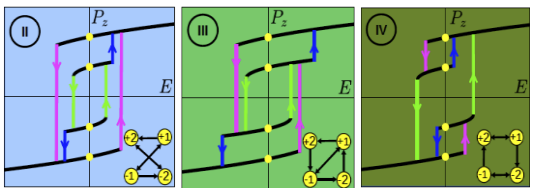

Fig. 6. Typical multibit switching processes in topologically-controlled access memory (TAM) units. Stored information is quantified by *logical quantum* (loq)-*numbers*, which for the shown processes may assume values |-2), |-1), |1),| 2). Panel (II) presents 4-loq unit with two hidden states; panels (III) and (IV) display topologically different full-access 4-loq units. Right bottom corners of the respective panels show maps of the switching logical operations.

Future Plans

1. *Ultraquantum thermodynamics for quantum information science*: We will pursue a theoretical platform for Non-local quantum Maxwell demon acting over macroscopic distances. A quantum Maxwell demon is a device that can lower the entropy of an energy-isolated quantum system by providing it with purity. The functionality of such a quantum demon is rooted in a quantum mechanical SWAP operation between mixed and pure states that can be separated in space. Lowering the entropy of an isolated system from a

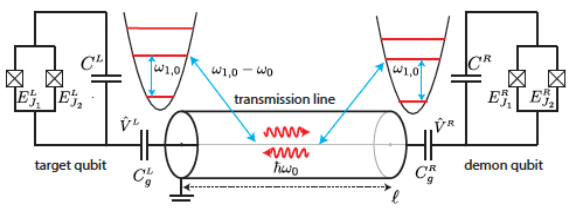

Fig. 7. Schematic setup for a non-local quantum Maxwell demon swapping the mixed state of the target qubit (left) with the pure state of the demon qubit (right) via an autonomous and energy-conserving process.

distance then raises the question of nonlocality in the discussion of the Second Law. We will determine the extent of the non-locality attainable in the operation of a quantum Maxwell demon and will find, assuming the present-day performance of a cQED setup, that macroscopic distances on the order of meters can be bridged using a transmission line as a coupling medium at elevated temperatures of the order of a few Kelvin. We further will apply the concept of the coherent transformation of the quantum states to develop quantum metrology. At variance to the quantum system, the qubit can be coherently transferred into a state which is the superposition of its ground and first excited energy levels. The level spacing depends on the magnitude of the magnetic flux. Therefore, the qubit that is prepared as a superposition of these states, acquires a phase depending on the magnetic flux. Making use of quantum algorithms for the phase estimation (according to Kitaev), we will measure this phase with the high precision.

2. ***Non-equilibrium processes in open dissipative systems:*** Non-Hermitian Hamiltonians admit a special class of degeneracy points, called exceptional points (EPs), where some of their eigenvalues and eigenvectors coalesce. These degeneracies are stable against both Hermitian or non-Hermitian perturbations and have unusual physical implications. We will show that we can construct protocols of encircling individual EPs in parameter space, such that the unique combination of the Riemannian structure of energy surfaces, accumulation of Berry phase and non-adiabaticity of system's dynamics result in non-reciprocal character of evolution. We will consider the non-reciprocal spin wave transfer via the spin system promising to realize the anti-symmetric spin diode for spintronics.

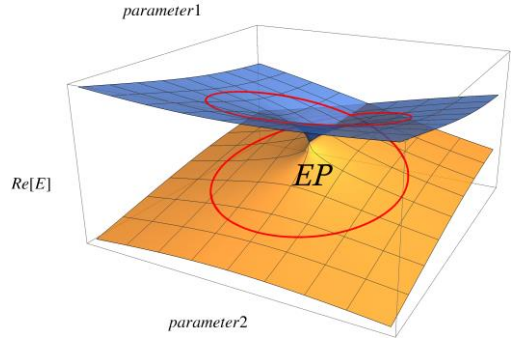

Fig. 8. Exceptional point in energy spectrum (E) of non-Hermitian Haimltonian. Encircling the EP by 2π brings system to a new state, revealing the system's non-trivial topological properties.

We will show that we can build a non-equilibrium Ising computer in which the annealing process brings the system to a steady state, rather than ground state, offering an unprecedented degree of control and speed. We will develop a microscopic theory of impeding coherence in the field-driven qubits weakly coupled to environment by taking the system out of equilibrium while preserving the inherent PT symmetry. This will enable a dramatic improvement of coherence times.

3. *Topological matter and new quantum materials for fundamental physics and applications*: Building on the comprehensive field theory of the SIT we will develop theories of quantum coherent states, superconductor, superinsulator, and Bose metal, and the deconfinement transition. We will generalize the BKT theory onto three dimensions and demonstrate that superinsulators are not restricted to 2D but can also exist in 3D. We will show that in 3D, the Kosterlitz exponential criticality transforms into more singular Vogel-Fultcher criticality which is a benchmark of the glassy behavior. Thus our field theory approach will establish the topological nature of the glass transition. Achieving the full understanding of the nature of quantum coherent states in the vicinity of the SIT will break ground for using superinsulator- and superconductor-based supercapacitors and superinductors for quantum information and telecommunication technologies.

4. *Topological excitations in ferroelectrics*: We will investigate quantum dynamics of topological excitations and explore the implications of negative capacitance in ferroelectric nanodots. To take into account that the nature of domain walls is strongly determined by microscopic long-range dipolar interactions and to capture atomistic effects, we will use molecular dynamics simulations instead of the commonly used (coarse grained) phase field approaches.

Selected publications

1. I. Luk'yanchuk, A. Sene, V. M. Vinokur, Electrodynamics of ferroelectric films with negative capacitance, Phys. Rev. B **98**, 024107 (2018).

2. A. Galda, V. M. Vinokur, Parity-time symmetry breaking in spin chains, Phys. Rev. B **97**, 201411 (2018).

3. A. Yu. Mironov, D. M. Silevitch, T. Proslier, S. V. Postolova, M. V. Burdastyh, A. K. Gutakovskii, T. F. Rosenbaum, V. M. Vinokur, T. I. Baturina, Charge Berezinskii-Kosterlitz-Thouless transition in superconducting NbTiN films, Scientific Reports, **8**, 4082 (2018).

4. N. S. Kirsanov, A. V. Lebedev, M. V. Suslov, V. M. Vinokur, G. Blatter, G. B. Lesovik, Entropy Dynamics in the System of Interacting Qubits, Journal of Russian Laser Research, **39**, 120-127 (2018).

5. M. Lankhorst, N. Poccia, M. P. Stehno, A. Galda, H. Barman, F. Coneri, H. Hilgenkamp, A. Brinkman, A. A. Golubov, V. Tripathi, T. I. Baturina, V. M. Vinokur, Scaling universality at the dynamic vortex Mott transition, Phys. Rev. B **97**, 020504 (2018).

6. S. V. Postolova, A. Yu. Mironov, M. R. Baklanov, V. M. Vinokur, T. I. Baturina, Reentrant Resistive Behavior and Dimensional Crossover in Disordered Superconducting TiN Films, Scientific Reports, **7**, 1718 (2017).

7. A. Galda, V. M. Vinokur, Linear dynamics of classical spin as Mobius transformation, Scientific Reports, **7**, 1168 (2017).

8. L. Baudry, I. Lukyanchuk, V. M. Vinokur, Ferroelectric symmetry-protected multibit memory cell, Scientific Reports, **7**, 42196 (2017).

9. G. P. Papari, A. Glatz, F. Carillo, D. Stornaiuolo, D. Massarotti, V. Rouco, L. Longobardi, F. Beltram, V. M. Vinokur, F. Tafuri, Geometrical vortex lattice pinning and melting in YBaCuO submicron bridges, Scientific Reports **6**, 38677 (2016).

10. G. B. Lesovik, A. V. Lebedev, I. A. Sadovskyy, M. V. Suslov, V. M. Vinokur, *H*-theorem in quantum physics, Scientific Reports **6**, 32815 (2016).

First-Principles Calculation of Correlated Electron Systems Based on Gutzwiller Many-Body Wave Functions

Principle Investigators: Cai-Zhuang Wang (FWP leader), Kai-Ming Ho, Yongxin Yao, Vladimir Antropov
Ames Laboratory, Ames, Iowa, 50011
wangcz@ameslab.gov

Keywords: Correlated electron; First-principles calculation; Gutzwiller many-body wave function; Equation of states; spin-multiplet.

Project Scope

Understanding and controlling the properties of matter that emerge from its complex correlations of atomic or electronic constituents requires accurate and efficient methods to calculate the energies and properties of strongly-correlated electron materials. While density functional theory (DFT) and computational codes based on the Kohn-Sham approach are highly effective and have been applied successfully to the prediction of the structures and properties of many materials, it fails for materials with strongly-correlated electrons. The scope of this project is to pursue the development of first-principles theory, algorithms, and computational codes for calculating the total energy and electronic structures of correlated-electron materials without using *adjustable* Coulomb interaction U and J parameters while retaining computational efficiency. Computationally efficient and tractable algorithms and approaches for treating strong correlation, spin-orbit coupling, as well as crystal field effects based on Gutzwiller many-body wave functions will be developed and implemented to quantitatively describe the electronic properties and energetics of strongly correlated electron materials. Such computational algorithms and codes are highly desirable and would be widely applicable to many systems. This development is new and therefore should be considered as high risk, but it also has the potential for high payoff.

Recent Progress

A correlation matrix renormalization (CMR) theory and related computational methods for calculating the total energies and electronic structures of correlated materials have been developed [1-5]. The CMR method is based on Gutzwiller wave function (GWF) [6] but it efficiently incorporates electron correlation effects into self-consistent first-principles calculations without using adjustable Hubbard U and Hund's J parameters. In our CMR theory, the commonly-adopted Gutzwiller approximation [7-13] for evaluating the one particle density matrix is extended to treat the two-particle correlation matrix of correlated electron systems with the help of Wick's theorem [1-5]. Therefore, both one-particle density and two-particle correlation matrices can be evaluated at the speed of Hartree-Fock (HF) calculations and then been renormalized according to the local electron correlation effects to reach the accuracy comparable to high-level quantum chemistry calculations. Several key technical implementations of the CMR theory have been developed to significantly improve the accuracy of the CMR method. These new developments include (a) Using sum-rule correction to correct the

inaccuracy due to the use of Wick's theorem to factorize the two-particle correlation matrix in the CMR theory; (b) Adopting new renormalization z-factors that are different from those derived by Gutzwiller approximation to more accurately capture the correlation effects in systems with finite dimensions; (c) Incorporating dynamical correlation effects in addition to the static correlations from the Gutzwiller wave function.

The CMR method has been validated by studying the binding and dissociation behavior of various small molecules, where results from accurate quantum chemistry calculations or from experiment are available for comparison. In these systems, electron correlation changes from weak to strong regime as the bond lengths between the atoms increase. We found the binding and dissociation behavior of the molecules with singlet ground state in G2 test-set calculated from the CMR method agrees well with the results from high-level quantum chemistry configuration interaction (CI) calculations and available experimental data [3,4]. Some examples are shown in **Figure 1**.

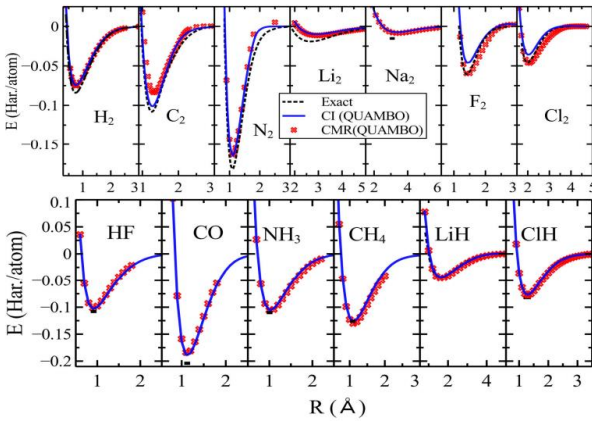

Figure 1. Binding energy curves of some molecules from the G2 test-set. The CMR and CI calculations are based on quasiatomic minimal basis orbitals (QUAMBOs). The results from CMR agree well with CI and experimental results.

We also extend the CMR method to study the electron correlations in periodic solid systems [5]. Using the linear hydrogen chain as a benchmark system, we show the results from the CMR method compare very well with those obtained recently by accurate auxiliary field quantum Monte Carlo (AFQMC) calculations [14] as shown in **Figure 2**. The excellent agreement between the results of CMR calculation and that of accurate AFQMC on 1D atomic hydrogen chain is intriguing since many other methods fail to describe this system accurately [14]. We also study the equation of states of three-dimensional crystalline phases of atomic hydrogen [5]. Considering the computational cost of CMR being similar to HF and its outstanding performance on the atomic hydrogen lattice systems, we believe it is very promising to extend CMR to systems with more electrons to address the long-standing issues in complex strongly correlated materials.

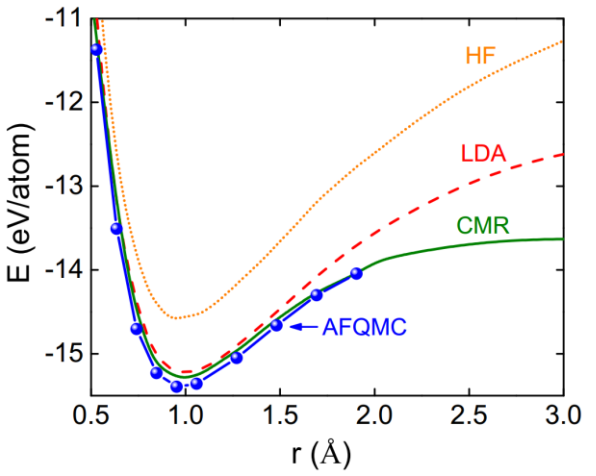

Figure 2. Equation of state of the one dimensional hydrogen chain calculated from our CMR theory is compared with the results from LDA, HF, and AFQMC. (The AFQMC data are from Phys. Rev. X, **7**, 031059 (2017)

Future Plans

The progress made over the preceding two years enables us to address more complex and challenge problems in correlated electron materials. We will continue to develop key theoretical and computational approaches to address correlated electron problems.

We will further develop CMR theory and computational code for studying more complex strongly-correlated bulk materials containing d and f electrons without using the adjustable Coulomb U and J parameters. We selected two widely-studied cases for realistic benchmark of our CMR approach: *fcc*-Ce and rock-salt phase of MnO. *fcc*-Ce shows a volume collapse transition in paramagnetic state due to the Kondo screening effect. The benchmark of our CMR approach on *fcc*-Ce represents a very stringent test as no adjustable parameters are involved, in contrast to DFT+Gutzwiller and LDA+DMFT calculations with adjustable Hubbard interaction parameters. MnO is a complex correlated insulator, which shows simultaneous volume collapse, magnetic moment collapse and metallization by applying pressure [15]. It involves a delicate interaction between strong electron correlation effects, crystal field effect and magnetism. We will apply our CMR approach to MnO and compare the theoretical equation of states with the experimental data [16,17]. Other important physical observables, such as orbital occupations, local magnetic moment, will also be compared with reliable data from DFT+DMFT calculation [17]. The knowledge gained from these benchmark calculations will be used to further improve and optimize the accuracy and efficiency of the CMR theory and computational code for studying strongly-correlated materials.

We will also explore new theory and method that can treat electron correlation effects beyond the conventional Gutzwiller approximation. The foundation of our theory and computational approaches for correlated electron calculations is Gutzwiller variational many-body wave function (GWF). Currently, almost all the studies in the literature based on GWF adopt the Gutzwiller approximation to make the evaluation of physical properties of correlated electron systems feasible. Since Gutzwiller approximations effectively amount to neglecting spatial correlations between the spins of the electrons, some correlation effects would be overlooked. Very recently, we have been exploring a new approach to bypass the factorization of correlation renormalization factor $z_{i\alpha\sigma}^{j\beta}$ while retaining the Wick's theorem through the sum-rule correction scheme. We refer to this new approach as "Gutzwiller conjugate gradient minimization" (GCGM) approach [18]. The feasibility of the GCGM approach has been

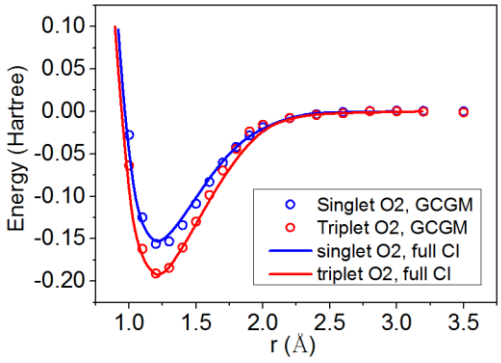

Figure 3. Binding energy curves of O_2 molecule in the singlet and triplet spin states obtained from GCCM approach are compared with large-basis full CI calculations.

preliminarily explored by calculating the binding energies of H_2, N_2, and O_2 molecules where results from exact CI calculations are available for comparison. As shown in **Figure 3**, the results from this new GCGM approach agree well with CI calculations, even for the triplet state of O_2 molecule where spin correlations are very subtle and important. We will further development the GCGM method to treat more complex correlation effects in larger molecules and periodic bulk systems.

References

1. Y. X. Yao, J. Liu, C. Z. Wang, and K. M. Ho, Phys. Rev. B **89**, 045131 (2014).
2. Y. X. Yao, J. Liu, C. Liu, W. C. Lu, C. Z. Wang, and K. M. Ho, Sci. Rep. **5**, 13478 (2015).
3. C. Liu, J. Liu, Y. X. Yao, C. Z. Wang, and K. M. Ho, Mol Phys, **115**, 667 (2017).
4. C. Liu, J. Liu, Y. X. Yao, P. Wu, C. Z. Wang, and K. M. Ho, J. Chem. Theory Comput. **10**, 4806 (2016).
5. X. Zhao, J. Liu, Y. X. Yao, C. Z. Wang and K. M. Ho, Phys. Rev. B **97**, 075142 (2018).
6. M. Gutzwiller, Phys. Rev. Lett. **10**, 159 (1963); Phys. Rev. **137**, A1726 (1965).
7. D. Vollhardt, Rev. Mod. Phys. 56, 99 (1984).
8. G. Kotliar and A. E. Ruckemstein, Phys. Rev. Lett. **57**, 1362 (1986).
9. J. Bünemann, F. Gebhard, and W. Weber, Foundations of Phys. **30**, 2011 (2000).
10. J. Bünemann, W. Weber, and F. Gebhard, Phys. Rev. B, **57**, 6896 (1998).
11. J Bünemann and F. Gebhard, Phys. Rev. B **76**, 193104 (2007).
12. T. Schickling, F. Gebhard, and J. Bunemann, Phys. Rev. Lett. **106**, 146402 (2011).
13. T. Schickling, F. Gebhard, J. Bunemann, L. Boeri, O. K. Andersen, and W. Weber, Phys. Rev. Lett. **108**, 036406 (2012).
14. M. Motta, D. M. Ceperley, G. K.-L. Chan, J. A. Gomez, E. Gull, et al. Phys. Rev. X **7**, 031059 (2017).
15. J. Kunes, A. V. Lukoyanov, V. I. Anisimov, R. T. Scalettar, and W. E. Pickett, Nature Mater **7**, 198–202 (2008).
16. J. R. Patterson, C. M. Aracne, D. D. Jackson, V. Malba, S. T. Weir, P. A. Baker, and Y. K. Vohra, Phys. Rev. B **69**, 220101 (2004).
17. C. S. Yoo, B. Maddox, J.-H. P. Klepeis, V. Iota, W. Evans, A. McMahan, M. Y. Hu, P. Chow, M. Somayazulu, D. Häusermann, R. T. Scalettar, and W. E. Pickett, Phys. Rev. Lett. **94**, 115502 (2005).
18. Z. Ye, Y. X. Yao, X. Zhao, C. Z. Wang, K. M. Ho, J. Chem. Theory Comput. *under review*

Selected Publications

[1] C. Liu, J. Liu, Y. X. Yao, P. Wu, C. Z. Wang, and K. M. Ho, "Correlation matrix renormalization theory: improved description of intersite electron interactions with sum-rule corrections", J. Chem. Theory Comput. **10**, 4806 (2016).

[2] C. Liu, J. Liu, Y. X. Yao, C. Z. Wang, and K. M. Ho, "Sum-rule corrections: A route to error cancellations in correlation matrix renormalization theory", Mol Phys, **115**, 667 (2017).

[3] X. Zhao, J. Liu, Y. X. Yao, C. Z. Wang and K. M. Ho, "Correlation matrix renormalization theory for correlated-electron materials and application to crystalline phases of atomic hydrogen", Phys. Rev. B, **97**, 075142 (2018).

[4] Z. Ye, Y. X. Yao, X. Zhao, C. Z. Wang, K. M. Ho, "First-principles calculation of correlated electron materials based on Gutzwiller wave function beyond Gutzwiller approximation", J. Chem. Theory Comput. *under review.*

[5] A. L. Wysocki, A. Kutepov, and V. P. Antropov, "Strength and Scales of Itinerant Spin Fluctuations in 3d Paramagnetic Metals," Phys. Rev. B, **94**, 140405 (2016).

[6] M. Kim, C. Z. Wang, and K. M. Ho, "Coexistence of Type-II Dirac Point and Weak Topological Phase in Pt_3Sn," Phys. Rev. B, **96**, 205107 (2017).

[7] B. Q. Song, M. C. Nguyen, C. Z. Wang, and K. M. Ho, "Stability of the 1144 phase in Iron Pnictides," Phys. Rev. B, **97**, 094105 (2018).

[8] M. C. Nguyen, Y. X. Yao, C. Z. Wag, K. M. Ho, and V. P. Antropov, "Magnetocrystalline anisotropy in cobalt based magnets: A choice of correlation parameters and the relativistic effects" J. Phys. Condens. Matter, **30**, 195801 (2018).

[9] M. C. Nguyen, V. Taufour, S. L. Bud'ko, P. C. Canfield, V. P. Antropov, C. Z. Wang and K. M. Ho, "Using first-principles calculations to screen for fragile magnetism: Case study of $LaCrGe_3$ and $LaCrSb_3$", Phys. Rev. B. **94**, 184401 (2018).

[10] M. Kim, C. Z. Wang, and K. M. Ho, "Topological states in A15 superconductors", Nature Communications. *Submitted*. http://arxiv.org/abs/1807.03405

Disorder and Interaction in Correlated Electron Materials

Principal investigator: Ziqiang Wang
Department of Physics, Boston College, Chestnut Hill, MA 02467
wangzi@bc.edu

Project Scope

The program has two main themes. The first one investigates the electronic structure, emergent quantum electronic states, low energy excitations, and unconventional superconductivity in correlated electron materials such as the transition metal oxides, pnictides, and chalcogenides. Recent focuses have been on the high-T_c cuprates, the Fe-pnictides and Fe-chalcogenides superconductors, and the strongly spin-orbit coupled strontium iridates. This part of the program is motivated by and stays close to current experimental discoveries. The outcome will advance the theoretical understanding of the low-temperature collective quantum mechanical properties of the charge, spin, orbital, and lattice degrees of freedom as well as their interplay with topology. This part of the program maintains close collaborations with experimental groups in angle resolved photoemission (ARPES), scanning tunneling microscopy (STM), neutron scattering, nuclear magnetic resonance (NMR), and transport, etc. The second theme of the program investigates fundamental, yet unresolved problems of strong correlation by developing reliable, analytical methods and approaches. The primary focus here has been the ``standard models'' of correlated electrons in Mott-Hubbard systems; namely the Hubbard model with charge excitations and its necessary physical extensions. Examples include the Mott transition; Mott insulator and fractionalized spin liquids; the interplay between strong correlation and spin orbit coupling; the nature of AF insulators; the interplay among interaction, geometric frustration, disorder, and topological order.

Recent Progress

Below are some highlights of the recent progress.

Quantum anomalous vortex and Majorana zero mode in Fe(Te,Se) superconductors – Back in 2015, in collaboration with the STM group of Prof. Shuheng Pan, we discovered robust zero-bias conductance peaks at the interstitial/excess Fe sites in Fe(Te,Se) superconductors. These zero-energy bound states defy all known properties of impurity states, but behave in many ways similar to the Majorana zero-energy mode (MZM). Since then, theories have shown that the spin-orbit coupling (SOC) in Fe(Te,Se) is strong and produces a topological Dirac fermion surface state, which has been detected by ARPES experiments recently. The lightly electron doped surface state acquires a pairing gap below T_c by the natural proximity to the fully gapped bulk Fe(Te,Se) superconductor.

In recent months, we have been working towards a theoretical understanding of these fascinating phenomenon orchestrated by superconductivity, SOC, magnetism, and

topology. We discovered that the local moments induced by the excess Fe and the SOC generate superconducting vortices in the absence of external magnetic fields. We termed such a spontaneous vortex a quantum anomalous vortex (QAV). The QAV nucleates around an excess Fe due to the coupling of the angular momentum and the local magnetization that lowers its energy compared to the energy of the vortex-free state. We find that the MZM emerges spontaneously from the topological surface state at the vortex core of the QAV without applying an external magnetic field. Thus, the zero-bias conductance peaks observed originally in the STM experiments at the excess Fe sites are indeed the localized Majorana zero energy modes. Moreover, the finite angular momentum Caroli-de Gennes states inside the QAV are found to be pushed to the energy of the bulk pairing gap, which significantly enhances the stability of the MZM. The obtained tunneling conductance is in remarkable agreement with the data from the STM experiments. The QAV thus provides a new and advantageous platform for the realization and manipulation of robust and localized MZMs, which should useful for investigating their non-abelian statistics, interactions, and their potential for quantum computing.

Antiferromagnetic Chern Insulators in Noncentrosymmetric Systems – We continued to work on the topological properties of interaction-driven electronic states. An example of the latter common in systems and materials with strong local correlation is the antiferromagnetic (AF) insulator. To the extent that the low energy physics of such AF insulators are adiabatically connected to band insulating states in the magnetic unit cell and protected by the magnetic gap, they can be topological insulators. We showed that, in addition to Z_2 or AF topological crystalline insulators, there is a new class of AF Chern insulators (AFCI) in 2D systems without inversion symmetry. Despite the absence of a net magnetization, AFCI possess a nonzero Chern number C and exhibit the quantum anomalous Hall effect (QAHE) due to spontaneous time-reversal symmetry breaking. As shown in the figure, their existence is guaranteed by the bifurcation of the boundary line of Weyl points between a 2DTI or a quantum spin Hall (QSH) insulator and a topologically trial band insulator (BI) with the emergence of AF long-range order with increasing interaction. As a concrete example, we studied the phase structure of the honeycomb lattice Kane-Mele model as a function of the inversion-breaking ionic potential Δ and the Hubbard interaction U. Using a combination of weak- and strong-coupling approaches, we found an easy z-axis C=1 AFCI phase and a spin-flop transition to a topologically trial collinear AF insulator in the xy-plane. Thus, the topological AFCI can be obtained near the phase boundary between band and Mott insulators if the inversion symmetry breaking ionic potential is comparable to the Hubbard U. The results demonstrate the existence of two kinds of AF insulators: the conventional topologically trial AF Mott insulator and the topological AF Chern insulator with unquenched charge fluctuations. We proposed possible experimental realizations of the AFCI and QAHE in correlated transition-metal di-chalcogenides and in cold atoms on optical lattices where recent experiments have shown that both the sublattice potential and the SOC can be tuned optically.

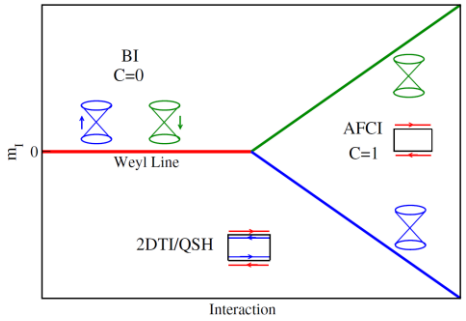

Hidden Spin-orbit Entangled Electronic Order in Parent and Electron-Doped Iridates Sr_2IrO_4 – Since the discovery of high-T_c superconductivity in 1986, analogs of the cuprate have been long sought after in other transition metal oxides. The perovskite iridate Sr_2IrO_4 has emerged recently as a promising candidate. Atomically, Sr_2IrO_4 is isostructural to the cuprate La_2CuO_4. The strong spin-orbit coupling of the 5d iridium further makes the low-energy electronic structure of the iridates remarkably similar to the cuprates, raising the hope that they may share certain quantum electronic states. Recent experiments discovered that the electronic states in the parent and electron doped iridates are highly unconventional and strikingly analogous to the cuprates, including Fermi surface pockets, Fermi arcs (shown in the Figure), and the pseudogap phenomena. It is important to understand the origin of these correlated and highly spin-orbit entangled electronic states and their implications for the possible unconventional superconductivity. Our theoretical studies show that the experimental observations can be described by a hidden d-wave spin-orbit density wave order with staggered pseudospin currents depicted in the inset of the Figure.

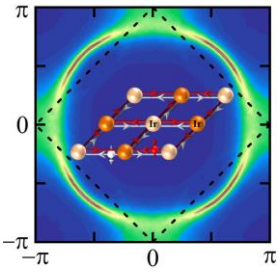

We studied the correlation and disorder effects in a five 5d-orbtial model derived from the band theory, in both parent and electron doped iridates. Our previous work on understanding the symmetry and electronic nematicity in the multiorbital Fe-based superconductors supported by the DOE grant played an important part in the study of the iridates. The conjectured pseudospin current order is time-reversal invariant, but breaks a hidden symmetry under a joint two-fold spin-orbital rotation followed by a lattice translation. This lifts the degeneracy of the electronic states at certain high-symmetry points in the Brillouin zone, which is responsible for the fascinating properties observed by angle-resolved photoemission and scanning tunneling microscopy. Direct experimental detection of the spin current is proposed. The pseudospin current order turns the iridate metallic state into an electron doped quasi-2D Dirac semimetal with important implications on the possible superconducting state suggested by recent experiments. These findings will stimulate further experimental and theoretical studies of the perovskite iridates for unconventional superconductivity.

Nodeless high-T_c superconductivity in hole-rich monolayer CuO_2– Our work was motivated, among other things, by the recent experimental advance and discovery in high-T_c cuprate superconductors. (1) Monolayer CuO_2 has been grown successfully by the state-of-the-art ozone molecular beam epitaxy (MBE) on $Bi_2Sr_2CaCu_2O_{8+\delta}$ (BSCCO) substrate, making it possible to directly probe the superconducting state in the copper-oxygen plane. (2) Scanning tunneling microcopy (STM) performed on the monolayer CuO_2/BSCCO revealed new and surprising physics beyond the bulk cuprates. In contrast to the widely observed V-shaped local density of states (LDOS) typical of a nodal d-wave superconductor as in the bulk cuprates, STM finds remarkably a robust U-shaped LDOS characteristic of a **nodeless** superconducting gap, which is further shown to be insensitive to nonmagnetic impurities. We studied theoretically the monolayer CuO_2/BSCCO and showed that the new physics originates from a significant charge transfer across the interface that pushes the CuO_2 monolayer into the heavily overdoped, hole-rich regime yet

inaccessible in bulk cuprates. As a consequence, the Cu $d_{3z^2-r^2}$ orbital is activated in addition to the $d_{x^2-y^2}$ orbital such that the Fermi surface contains one electron and one hole pocket. The liberated orbital degrees of freedom, which are quenched in bulk cuprates, introduce the important new physics. Constructing a minimal two-orbital model and carrying out the strong coupling analysis, we discovered that the spin and the new spin-orbital entangled exchange interactions produce a nodeless superconductor with extended s-wave pairing symmetry and a pairing energy gap comparable to the bulk d-wave gap, in good agreement with experiments. Thus, we conclude that the monolayer CuO_2 in the hole-rich regime is a nodeless multiorbital high-T_c superconductor of a different pairing symmetry than in the bulk cuprates. The findings led to the global phase diagram over the extended doping regime shown in the Figure and provide the much needed insights into the strong correlation effects of the electron's spin and orbital degrees of freedom in realizing unconventional high-T_c superconductivity, as exemplified in both the cuprate and the Fe-based superconductors. More importantly, these findings open a new direction to search for high-T_c superconductors with liberated orbitals via interface charge transfer over extended range of carrier concentrations in transition-metal oxide heterostructures.

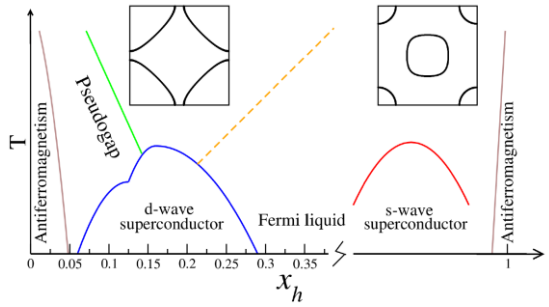

Future Plans

In the coming year, the research activities will be centered on our new finding of the Quantum Anomalous Vortex (QAV). The QAV refers to the spontaneous SC vortex generated by the local moment of interstitial magnetic ions in an s-wave superconductor with strong spin-orbit coupling (SOC) in the absence of external magnetic fields. The situation is formally analogous to the quantum anomalous Hall effect (QAHE) on the surface of topological insulators doped with magnetic transition metal elements due to combined effects of SOC and ferromagnetic order. We have shown that the QAV provides a remarkably consistent description of the localized Majorana zero-energy model (MZM) observed at the interstitial Fe sites in Fe(Te,Se) superconductors. The ability to produce such nonabelian charge neutral excitations without applying magnetic field means that the localized MZM can be manipulated by moving the transition metal ions, which holds great potential for studying their interactions and entanglement for quantum computing. We will collaborate with STM groups to carry out experimental tests of these ideas. We will also study the QAV and the MZM under different physical settings, e.g. in s-wave superconductor with strong Rashba SOC and Zeeman coupling. In parallel, we will investigate the important RKKY type of interactions between the local moments and their implications on the stability of the QAV and the MZM with increasing density of the transition metal ions. The outcome will, among other things, provide the much needed insights into the highly unconventional superconductor to metal transition in Fe(Te,Se) with increasing density of the excess Fe impurities.

Recent Publications

1. Kun Jiang, Sen Zhou, Xi Dai, and Ziqiang Wang, "Antiferromagnetic Chern Insulators in Noncentrosymmetric Systems", **Physical Review Letters** 120, 157205 (2018).

2. Jiaxin Yin, Songtian S. Zhang, Hang Li, Kun Jiang, Guoqing Chang, Bingjing Zhang, Biao Lian, Cheng Xiang, Ilya Belopolski, Hao Zheng, Tyler A. Cochran, Suyang Xu, Guang Bian, Kai Liu, Tay-Rong Chang, Hsin Lin, Zhongyi Lu, Ziqiang Wang, Shuang Jia, Wenhong Wang, and M. Zahid Hasan, "Giant and anisotropic spin-orbit tunability in a kagome magnet", accepted and to be published in **Nature**, (2018).

3. Shang Gao , Felix Flicker , Raman Sankar , He Zhao , Zheng Ren , Bryan Rachmilowitz , Sidhika Balachandar , Fangcheng Chou , Kenneth S. Burch , Ziqiang Wang , Jasper van Wezel , and Ilija Zeljkovic, "Atomic-Scale Strain Manipulation of a Charge Density Wave", **Proc. Nat. Acad. Sci.** 10.1073/pnas.1718931115, (2018).

4. He Zhao, Bryan Rachmilowitz, Zheng Ren, Ruobin Han, J. Schneeloch, Ruidan Zhong, Genda Gu, Ziqiang Wang, and Ilija Zeljkovic , "Superconducting proximity effect in a topological insulator using Fe(Te,Se)", **Physical Review B** 97, 224504 (2018).

5. Kun Jiang, Xianxin Wu, Jiangping Hu, and Ziqiang Wang, "Nodeless high-T_c superconductivity in highly-overdoped monolayer CuO_2", arXiv:1804.05072 (2018).

6. Haiwen Liu, Hua Jiang, Ziqiang Wang, Robert Joynt, and X. C. Xie, "Discrete Scale Invariance in Topological Semimetals", arXiv:1807.02459 (2018).

7. Y. G. Zhong, J. Y. Guan, X. Shi, J. Zhao, Z. C. Rao, C. Y. Tang, H. J. Liu, G. D. Gu, Z. Y. Weng, Z. Q. Wang, T. Qian, Y. J. Sun, and H. Ding, "Continuous doping of a cuprate surface: new insights from in-situ ARPES", arXiv:1805.06450 (2018).

8. Wei Zhang, Lei Wang, and Ziqiang Wang, "Interpretable Machine Learning Study of Many-Body Localization Transition in Disordered Quantum Ising Spin Chains", arXiv:1807.02954 (2018).

9. Kunkun Li, Shifeng Jin, Jiangang Guo, Yanping Xu, Yixi Su, Erxi Feng, Yu Liu, Shengqiang Zhou, Tianping Ying, Shiyan Li, Ziqiang Wang, Gang Chen, and Xiaolong Chen, "Unusual double-peak specific heat and spin freezing in a spin-2 triangular lattice antiferromagnet $FeAl_2Se_4$", arXiv:1805.12569 (2018).

10. Jiaxin Yin, Songtian S. Zhang, Guangyang Dai, Hao Zheng, Guoqing Chang, Ilya Belopolski, Xiancheng Wang, Hsin Lin, Ziqiang Wang, Changqing Jin, and M. Zahid Hasan, "Vector field based emergent phase diagram in a correlated superconductor", arXiv:1802.10059 (2018).

11. Sen Zhou, Kun Jiang, Hua Chen, and Ziqiang Wang, "Correlation effects and hidden spin-orbit entangled electronic order in parent and electron-doped iridates Sr_2IrO_4". **Physical Review X** 7, 041018 (2017).

12. Guo-Yi Zhu, Ziqiang Wang, Guang-Ming Zhang, "Nodeless and topological superconducting phases of d-wave superconductors in proximity to antiferromagnets", **Europhys Letters** 118, 37004 (2017).

13. P. S. Wang, P. Zhou, S. S. Sun, Y. Cui, T. R. Li, Hechang Lei, Ziqiang Wang, and Weiqiang Yu, "Robust short-range-ordered nematicity in FeSe evidenced by high-pressure NMR". **Physical Review B** 96, 094528 (2017).

Electronic structure using tensor networks, machine learning, and quantum computing

Principal Investigator: Professor Steven R. White
Department of Physics & Astronomy, University of California, Irvine, CA 92697
srwhite@uci.edu
Principal Investigator: Professor Kieron Burke
Department of Chemistry and of Physics, University of California, Irvine, CA 92697
kieron@uci.edu

Project Scope

The overarching theme of this project is to bring an unprecedented combination of high accuracy and efficiency to correlated electronic structure calculations of solids using the density matrix renormalization group and tensor networks, and to make this accuracy widely available for complicated systems by incorporating it in a highly accurate density functional. In a nutshell, by using several novel techniques, including entirely new ways of choosing optimal basis sets for strongly correlated systems, we can make correlated wavefunction calculations with DMRG far more efficient than before. We then use recently developed machine learning techniques to create density functionals which correct the errors in standard semilocal approximations, to yield 'chemical' accuracy (errors less than 1.6 milliHartree) for strongly correlated systems.

Progress so far has been driven by the meticulous creation of a 1D mimic of real electronic structure calculations, in which approximate density functionals make errors that are quantitatively similar to those in realistic simulations. We have developed algorithms and tuned the interaction so that DMRG calculations are extremely efficient in this 1D world, and even include a mimic of the electron-electron cusp. This has allowed us to run a near endless sequence of calculations to create/refine/test our new basis set approaches, and to generate sufficient data to create machine-learned density functionals on strongly correlated systems, and in the thermodynamic limit.

We have already demonstrated how efficient our basis functions are in (quasi-one-dimensional) realistic calculations. In the last year we have further developed a new approach, multi-sliced gausslet DMRG, which is now able to calculate hydrogen chain systems in the complete-basis-limit with exact correlation, something no other approach can achieve. We will also extend this method to treat arbitrary small to medium sized molecules. Simultaneously, we are creating the machinery to train machine-learned density functionals on the output from these multi-sliced calculations, thus reproducing this high accuracy in routine low-cost DFT calculations. The DMRG approach is crucial for rapidly generating data for training functionals, and for treating the most correlated systems. For a broad range of other systems, the machine-learned density functional will provide high accuracy ground-state energies and densities with much lower computational cost.

Recent Progress

Software: The ITensor library for DMRG and tensor networks was developed by White and Miles Stoudenmire, who was a postdoc on this project. Miles has now become a permanent researcher at the Flatiron Institute with about half of his time devoted to ITensor and software. ITensor just had a major new release and its use is growing rapidly. Graduate student Thomas E. Baker (supported by this project, now a postdoc at U. Sherbrooke) contributed substantially to ITensor documentation, and other group members use and help develop ITensor. ITensor is publicly available through its website (itensor.org) and on github.

Machine Learning Electronic Structure: Most applications of machine-learning (ML) to materials problems involve scanning the properties of many systems, often using DFT, in order to find new systems with given target properties. We have pursued finding density functionals themselves using ML methods. Previously our methods have not been applied to the full interacting problem, because of the cost of generating accurate energies and densities to train on. But our 1D laboratory is ideally suited to do this, since we have worked so hard to reduce computational cost for the many-body problem. We applied ML directly to F[n], the complete universal functional of Hohenberg and Kohn, which contains the non-interacting kinetic energy, the Hartree energy, and the XC energy. This was only possible because we already had our 1D mimic of electronic structure, and could perform a very large number of DMRG calculations in a reasonable amount of time on our local cluster.

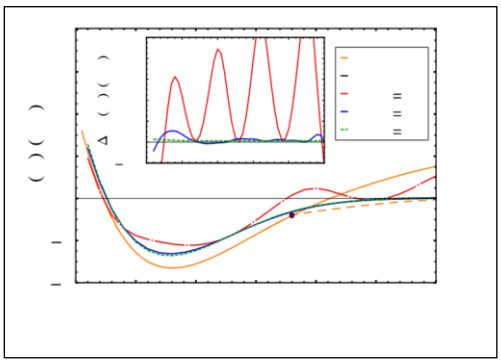

Machine Learning can achieve high accuracy based on only a few training points N_T and reproduce the exact bond dissociation curve with quantum chemical accuracy.

A key breakthrough came in a very simple algorithm devised by supported student Li Li. For each molecule, the molecular density is reduced to a sum of smooth atomic densities, via Hirschfeld partitioning (a popular scheme in quantum chemistry). For a given number of H atoms, N_C, these atomic densities were combined into data sets. The shape and spread of these atomic densities varied for different molecular bond lengths, and numbered in the hundreds. A principal component analysis was performed on these 'atomic' densities, which could be extremely accurately represented with just the largest 7 principal components. Thus all the molecular densities could be described with a basis of just 7 N_C components. This reduced calculational time by several orders of magnitude, and produced densities that were sufficiently accurate that the error in the density led to energy errors smaller than 1.6 mHa. With this breakthrough, we had an ML algorithm that was computationally feasible, and in this basis, had much better learning curves than any other procedure. By extrapolating to infinite chain length, we could then extract the total

energy of an infinite chain to high accuracy. The paper where this is described has already been cited more than 30 times in the year since publication [Google scholar, Jun 26, 2018].

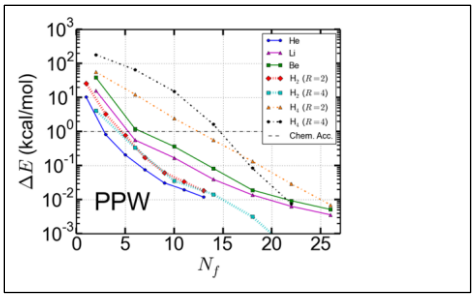

Energy errors for 1D atoms and molecules when evaluated in a basis of N$_f$ product plane waves (PPW's) adapted to DFT orbitals

Wavelet Coarse Graining - A crucial intermediate step leading to the development of gausslets was the idea of wavelet coarse-graining (Baker:2018). Here we developed a unique combination of existing types of basis set(atom-centered gaussians, plane waves, and wavelets) to create a system-specific basis designed to yield the natural orbitals of a quantum system with relatively few basis functions (2-3 more than the number of significantly occupied natural orbitals). Such a basis could provide convergence to milliHartree accuracy for an accurate quantum solver with much fewer basis functions than in a standard basis. The gausslets discussed below are a generic version of this.

For a 10 atom (1D) chain, we found we achieve high accuracy with about 5 basis functions per atom, for all interatomic separations, ranging from equilibrium to extremely stretched. This serves as a proof that such small basis sets can be constructed for 1D systems.

Sliced Basis DMRG- Exploiting the locality inherent in electronic structure is crucial both to the algorithms themselves (e.g. the *local* density approximation of DFT) and to improved computational scaling, as in the various linear-scaling electronic structure methods. In sliced basis DMRG, we use a completely localized basis in one of the three dimensions, with standard Gaussian basis functions in the two transverse directions. This representation where one dimension is special is very useful for DMRG, which is based on a 1D representation. The slicing dramatically improves the scaling of DMRG. By utilizing a matrix product operator compression method, we are able to achieve linear scaling of the computation time in the number of atoms, in a hydrogen chain system. In these calculations, correlation is treated exactly (via DMRG) within the degrees of freedom of the basis. With this method, we could obtain exact correlation for systems as large as 1000 hydrogen atoms.

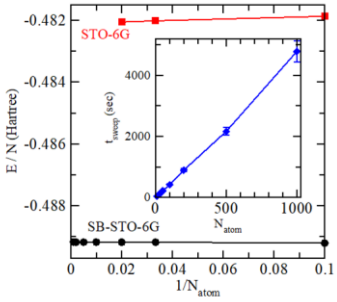

Sliced basis calculation for long hydrogen chains. The key plot is the inset, which shows the calculation time on a desktop for one DMRG sweep, as a function of the number of atoms.

Gausslets and Diagonal Approximations- To facilitate the adaptation of our methods to 3D, we developed wavelet-like functions made out of sums of Gaussians, called gausslets. A grid of gausslets makes a basis with a number of desirable properties, including

orthonormality, completeness, smoothness, and most important, a diagonal property. The diagonal property allows for a dramatic improvement in scaling of electronic structure: the N^4 tensor representing the electron-electron interaction of conventional bases can be replaced by a N^2 scaling matrix, just as if one were on a grid. Such an approximation can only be made in special basis functions; in fact, it was discovered for sinc basis functions, where the sampling theorem tells one that a band limited signal can be treated as if it were on a grid. Sincs would be a very poor choice for a DMRG basis, owing to their long tails.

Future Plans

Multisliced Gausslets – The progression to 3D is the crucial part of this development, currently being written up. We have improved on the 1D Gausslet approach by using coordinate transformations to increase basis resolution near nuclei, while maintaining orthogonality and the diagonal approximation. To go to 3D, we implement a new approach called multislicing, which forms basis functions as products of 1D functions, in a tree-like construction where z functions are created first, then for each z specific y functions, and then for each y and z, specific x functions are created. This structure makes constructing the Hamiltonian matrix elements very simple. Our initial test case for a real 3D system is a linear chain of evenly space hydrogen atoms, where with DMRG we can approach the complete basis set limit with exact correlation for fairly long chains.

Machine learning - We will redo the calculations of Ref [4] with a Kohn-Sham methodology, instead of a pure density functional, which should further improve the learning efficiency. We will also begin calculations on chains that are not equal-spaced, as a first attempt to generalize our ML methods to more arbitrary densities. In each case, our atoms-in-molecules density representation should prove very effective. If we succeed, we will have constructed a general-purpose XC functional that works for strong correlation. All the methodology should apply directly to 3D systems, using the basis sets developed in the other parts of our project.

Publications

1. Hybrid grid/basis set discretizations of the Schrodiner Equation, Steven R. White, *Journal of Chemical Physics.* **147**, 244102 (2017). (Editor's Pick)
2. Sliced Basis Density Matrix Renormalization Group for Electronic Structure, E.M. Stoudenmire and Steven R. White, Phys. Rev. Lett. 119, 046401 (2017).
3. Towards the solution of the many-electron problem in real materials:
equation of state of the hydrogen chain with state-of-the-art many-body methods, Mario Motta, David M Ceperley, Garnet Kin-Lic Chan, John A Gomez, Emanuel Gull, She
ng Guo, Carlos A Jiménez-Hoyos, Tran Nguyen Lan, Jia Li, Fengjie Ma, Andrew J Millis, Nikolay V Prokof'ev, Ushnish Ray, Gustavo E Scuseria, Sandro Sorella, Edwin M Stoudenmire, Qiming Sun, Igor S Tupitsyn, Steven R White, Dominika Zgid, Shiwei Zhang, Phys. Rev. X} 7, 031059 (2017).
4. Pure density functional for strong correlation and the thermodynamic limit from machine learning Li Li, Thomas E. Baker, Steven R. White, Kieron Burke, Phys. Rev. B **94**, 245129 (2016).

Thermodynamic Stability of Solid Solutions and High Entropy Alloys

Michael Widom, Carnegie Mellon University

Keywords: Entropy, Thermodynamics, Phase stability, intrinsic disorder

Project Scope

Solid solutions contain chemically similar elements that can mix freely within a crystalline lattice. High entropy alloys (HEAs[1-3]) are a recently discovered special case characterized by their large number of principal components. This proposal addresses the thermodynamic phase stability and mechanical response of solid phases. The work utilizes first principles total energy calculations and molecular dynamics simulations, augmented with novel Monte Carlo techniques and data analysis methods, and free energy modeling[4,5].

A central issue is to quantify the entropy because it plays a central role in thermodynamic stability of solid solutions, and to validate the claim of high entropy in HEAs. Among the many different sources of entropy, two are expected to be most relevant: vibrational entropy, which is typically the largest contribution; discrete configurational entropy of mixing among chemical species, which is the defining character of the solid solution. Because direct calculation of entropy is generally not feasible, parallel tempering molecular dynamics is used to enrich ensemble sampling. Histogram analysis of the resulting trajectories allows accurate calculation of relative free energies. Decomposition of the entropy into vibrational and configurational contributions is performed using cluster occupation statistics to isolate the configurational part, while vibrational densities of states calculated from dynamical matrices provides the vibrational entropy.

Recent Progress

The central goal of the project, prediction of the thermodynamic stability of a high entropy alloy entirely from first principles, was accomplished (publication 5) by calculating the free energies of CrMoNbV and its many potentially competing phases of simpler stoichiometry (Fig. 1). This compound presents an interesting challenge because of the phase separation of several of its binary and ternary alloy subsystems and the presence of potentially competing complex crystalline phases. We predicted that the equiatomic HEA was stable above T=1700K but that it would decompose into a mixture of a medium entropy alloy and an intermetallic Laves phase at low temperatures. This prediction was strikingly confirmed by the experimental observation of a reversable phase transformation (Fig. 2). This observation validates the defining concept of the field of HEAs, the stabilization of single phase solid solutions at high temperature by their configurational entropy.

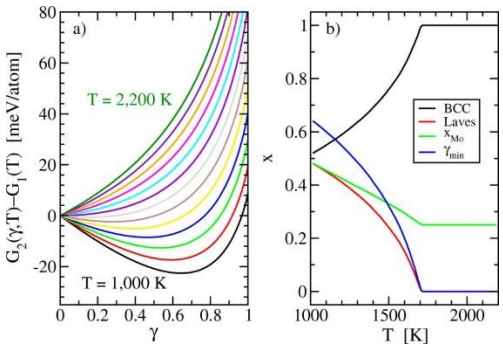

Fig. 1. (a) Free energy, $G_2(\gamma,T)$, for a two-phase BCC + Laves mixture of phase fraction γ, relative to G_1, the free energy of the equiatomic BCC HEA. (b) Minimizing values of x_{Mo}, γ, and BCC and Laves-phase fractions as functions of temperature.

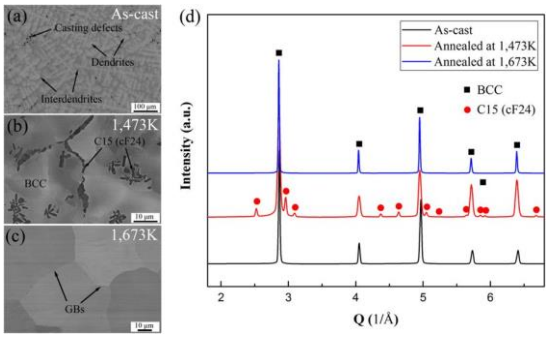

Fig. 2. Electron micrographs of the (a) as-cast Cr–Mo–Nb–V sample (scale bar 100 μm), (b) following the T = 1473 K anneal (scale bar 10 μm), and (c) following the T = 1673 K anneal (scale bar 10 μm). (d) Synchrotron x-ray patterns.

While the entropy of an N-component HEA is ideally log(N), short-range chemical order reduces the entropy below its ideal value. We can account for this decrease by subtracting the mutual information content, $I[y_{\alpha\beta};x_\alpha] = \sum_{\alpha\beta} y_{\alpha\beta} \ln y_{\alpha\beta}/x_\alpha x_{\beta,}$ of the nearest neighbor pair correlation function $y_{\alpha\beta}$ from the ideal mixing entropy. Generalizing this approach to second neighbors and multi-point correlations results in the entropy expressions from Kikuchi's cluster variation method. Remarkably, this notion can also be generalized to liquids, in which case we subtract the mutual information content, $I[g(r)] = \frac{1}{2}\rho \int d\boldsymbol{r}\, g(r) \ln g(r)$, of the radial distribution function $g(r)$ from the ideal gas entropy. In the grand canonical ensemble it is also necessary to add a term due to fluctuations in particle number, $\Delta S_{Fluct} = \frac{1}{2} + \frac{1}{2}\rho \int d\boldsymbol{r}\, [g(r) - 1]$ (see Fig. 3). This approach yields absolute entropies in excellent agreement with experimental data (Fig. 4).

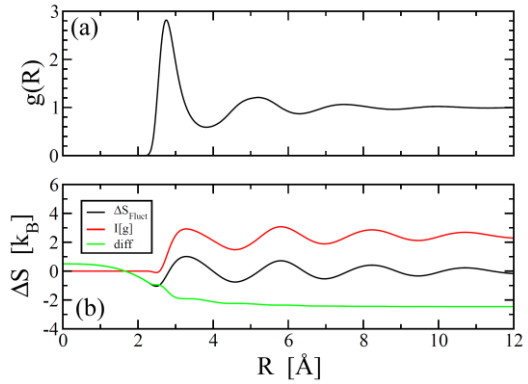

Fig. 3. (a) Radial distribution function of liquid aluminum simulated from first principles at T=1000K. (b) Contributions to the entropy due to number fluctuations (black), mutual information (red), and their net entropy reduction (green).

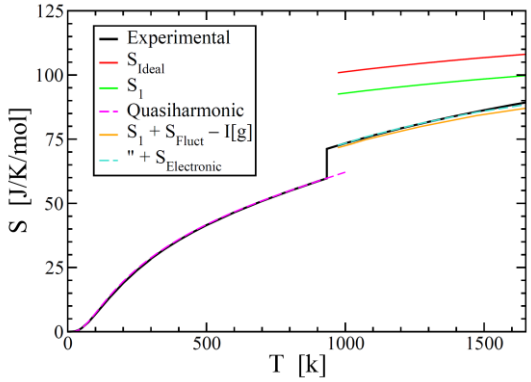

Fig. 4. Experimental (black) and predicted entropies of aluminum. The ideal gas (red) and single particle entropies (green) must be reduced by the contributions of Fig. 3 (oran) and increased by the electronic entropy (turquoise). The quasiharmonic approximation is excellent (magenta) in the solid state.

We also investigate the mechanical stability of HEAs. An interesting comparison can be found among the refractory HEAs. In publication 8 we created HEA structures with elements taken from four overlapping squares from the Periodic Table, NbTiVZr, HfNbTaZr, CrMoNbV, and MoNbTaW, annealed using hybrid Monte Carlo/molecular dynamics to generate representative short-ranged chemical order. This set of compounds is interesting because the elements Ti, Zr and Hf are BCC at high temperatures but transform to HCP at low temperatures, while the remaining elements are normal BCC structures at all temperatures. The BCC states of the BCC/HCP elements are mechanically unstable at low temperatures and are stabilized at high temperatures by their vibrational entropy. The elastic constants of HEAs containing both BCC/HCP elements and normal BCC elements are on the borderline of violating the Born stability criteria. Moreover, their lattice distortion is unusually large and their Debye-Waller factors exhibit strong temperature variation.

The BCC to HCP transformation of the BCC/HCP elements turns out to be a type of Jahn-Teller-Peierls transition. We demonstrated this by following the total energy, the electronic density of states, the band structure, and the charge density along the Burgers distortion pathway from BCC to HCP via a family of orthorhombic intermediate states. A pseudogap at the Fermi level deepens in the density of states as the energy drops along the Burgers pathway. The origin of the pseudogap can be traced to the opening of a gap at the S-point of the orthorhombic Brillouin zone (Fig. 5). The energy reduction is due to accumulation of charge density adjacent to interatomic bonds, as is evident from inspection of the occupied S-point wavefunction (Fig. 6).

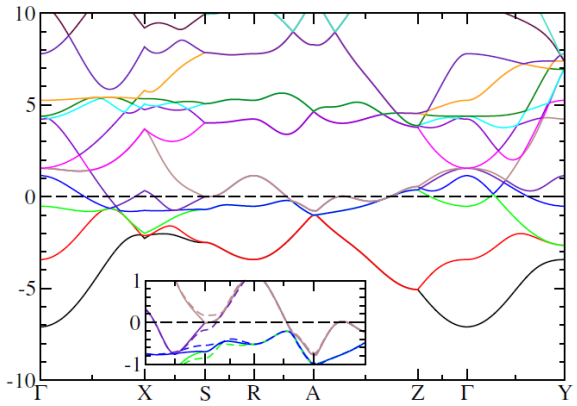

Fig. 5. Band structure of Hf in an orthorhombic setting. Solid lines are the limiting case of BCC, exhibiting degeneracy at E_F at the S point in the Brillouin zone. Applying the Burgers distortion lifts the degeneracy as shown in the inset.

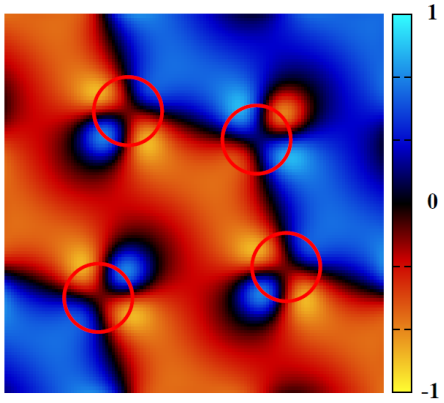

Fig. 6. Wavefunction of the occupied state below E_F at the S-point with applied Burgers distortion. Red circles show positions of the atoms. Note the d_{xy} character of the wave functions and the hybridization of wavefunctions on short bonds.

Future Plans

In the future we will examine more HEA compositions, specifically the Cantor alloy[2] CoCrFeMnNi and the Yeh-type alloys[1] that are Cantor-type plus Al. The complicating feature here is the presence of mixed ferro- and antiferromagnetism due to the combination of middle and late transition metal elements. The magnetism presents two challenges: first, ab-initio methods for calculation of magnetic entropy are poorly developed; second, the magnetism is partially frustrated leading to multiple self-consistent solutions of the Kohn-Sham equations. Magnetism also has important structural consequences such as an effective repulsion of the antiferromagnetic elements from the ferromagnetic ones.

Great opportunities are also present in the study of liquids. We will apply our information-theoretic approach to liquid alloys with special attention to phase separating compounds. Given our ability to accurately predict both solid and liquid state absolute entropies (Fig. 6) and enthalpies, entirely from first principles, we should be able to predict melting temperatures based on the crossing of absolute free energies.

References

1. J.-W. Yeh, S.-K. Chen, S.-J. Lin, J.-Y. Gan, T.-S. Chin, T.-T. Shun, C.-H. Tsau, and S.-Y. Chang. *Nanostructured high-entropy alloys with multiple principal elements: Novel alloy design concepts and outcomes*, Adv. Eng. Mater. **6**, 299-303 (2004)

2. B. Cantor, I. T. H. Chang, P. Knight, and A. J. B. Vincent. *Microstructural development inequiatomic multicomponent alloys*, Mat. Sci. Eng. A **375-77**, 213-8 (2004)

3. D. B. Miracle and O. N. Senkov. *A critical review of high entropy alloys and related concepts*, Acta Mat. **122**, 448-511 (2017)

4. M. Widom, *Prediction of structure and phase transformations*, in M.C. Gao, J.-W. Yeh, P.K. Liaw, and Y. Zhang, editors, High entropy alloys: fundamentals and applications, chapter 8, pages 267-298 (Springer, 2016)

5. R. Feng, P.K. Liaw, M. Gao and M. Widom, *First-principles prediction of high-entropy-alloy stability*, npj Comp. Mater. **3**, 50 (2017)

Publications (August 2016 – July 2018)

1. M.C. Gao and M. Widom, "Information entropy of liquid metals" *J. Phys. Chem. B* **122**, 3550-3555 (2018)

2. Z. Yu, P.R. Cantwell, Q. Gao, D. Yin, Y. Zhang, N. Zhou, G.S. Rohrer, M. Widom, J. Luo and M.P. Harmer, "Segregation-induced ordered superstructures at general grain boundaries in a nickel-bismuth alloy", *Science* **358**, 97-101 (2017)

3. S. Yao, Q. Gao, M. Widom, C. Marvel and M. Harmer, "Phase diagram of carbon nickel tungsten: Superatom Model", *Phys. Rev. Mater.* **1**, 043402 (2017)

4. M. Gao, P. Gao, J. Hawk, L. Ouyang, D. Alman and M. Widom, "Computational modeling of high-entropy alloys: structures, thermodynamics and elasticity", *J. Mater. Res.* **32**, 3627-3641 (2017)

5. R. Feng, P.K. Liaw, M. Gao and M. Widom, "First-principles prediction of high-entropy-alloy stability", *npj Comp. Mater.* **3**, 50 (2017)

6. T. Ogitsu, V. Lordi, E. Schwegler and M. Widom, "Comment on 'New Ground-State Crystal Structure of Elemental Boron'", *Phys. Rev. Lett.* **118**, 159601 (2017)

7. A. Acharya and M. Widom, "A microscopic continuum model for defect dynamics in metallic glasses", *J. Mech. Phys. Solids* **104**, 1-11 (2017)

8. B. Feng and M. Widom, "Elastic stability and lattice distortion of refractory high entropy alloys" *Mat. Chem. Phys.* **210**, 309-14 (2017)

9. P.C. Mende, Q. Gao, A. Ismach, H. Chou, M. Widom, R. Ruoff, L. Colombo and R.M. Feenstra, "Characterization of hexagonal boron nitride layers on nickel surfaces by low-energy electron microscopy", *Surf. Sci.* **659**, 31-42 (2017)

10. S. Yao, Q. Gao and M. Widom, "Phase diagram of boron carbide with variable carbon composition", *Phys. Rev. B* **95**, 054101 (2017)

Fluctuation Induced Interactions in Novel Materials

Principal investigator: Professor Lilia M. Woods
Department of Physics, University of South Florida, Tampa FL, 33620
lmwoods@usf.edu

Keywords: electromagnetic fluctuations, Dirac materials, Casimir and van der Waals forces

Project Scope

One of the most intriguing manifestations of zero-point fluctuations are the Casimir and van der Waals (vdW) forces, which arise from the confinement of fluctuating electromagnetic fields between objects. The common origin associated with the vacuum fluctuations of the electromagnetic field ensures that the Casimir and vdW interactions are actually the two sides of the same coin, meaning they are the same type of long-ranged, dispersive force. VdW forces are characteristic for molecular scale separations and are typically associated with mediating physisorption phenomena and gluing together chemically inert layers, such as graphene, for example. Casimir forces, on the other hand, typically act at micrometer scale separations, where the speed of light matters, and they are important for sticktion and adhesion phenomena, usually present in Nano and Micro Electro Mechanical Sensors (NEMS and MEMS devices). The scope of the current project is to investigate how novel materials affect this ubiquitous interaction and find ways to control it at different length scale by taking advantage of the fundamental properties of the materials as well as the application of external fields. Pursuing directions towards broadening the basic science of fluctuation interaction is also part of this project.

Recent Progress

Some highlights of our progress regarding Dirac-like materials, their properties, and schemes of calculations for their vdW/Casimir interactions are provided below. An accompanying list of supporting publications is also given.

The expanding graphene family – nonlocal optical response – Graphene has served as a template of studying Dirac-like physics in reduced dimensions. The library of graphene-type of materials is expanding, however, and silicene, germanene, and stanene (2D hexagonal arrangements of Si, Ge, and Sn atoms) have recently been discovered. While C atoms in graphene are in a planar configuration with sp^2 orbital hybridization, silicene, germanene, and stanene are characterized by a buckled structure with sp^3 orbital hybridization. These materials also have significant spin orbit coupling (SOC), which is unlike graphene whose SOC is negligible. The interaction of 2D honeycomb systems with external laser light irradiation and/or perpendicular to the surface electrostatic field can be used to achieve an array of electronic Hall phases. These topologically protected states can be characterized by their Chern number C (an integer) and they can be arranged in a phase diagram for the entire graphene family. Fluctuation induced forces depend strongly on the optical response of the interacting objects, thus significant efforts are directed towards the calculation of the optical conductivity tensor for the materials in the graphene family. A unified description based on the Kubo formalism is developed for all components of

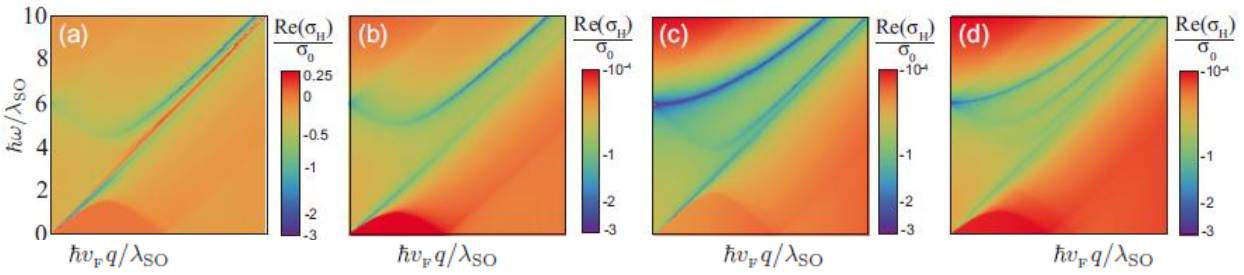

Figure 1 Density plots of the real part of the Hall dynamical conductivity of the graphene family materials in (a) Quantum Spin Hall Insulator; (b) Spin Polarized Metal; (c) Anomalous Quantum Hall Insulator; (d) Polarized Spin Quantum Hall Insulator phases. λ_{SO} is the spin orbit coupling constant.

the conductivity tensor in order to understand the interplay between frequency and spatial dispersion and Hall phase transitions in these systems. In Fig. 1 contour plots of the Hall dynamical conductivity response are shown. The figure highlights that by driving Hall transitions via external fields the optical spectra is determined by graphene-like features as dictated by the Chern number of the specific phase. Our calculations also show that spatial dispersion can affect the plasmonic properties of the graphene family, especially at large wave vectors. Our Ref. [1] constitutes a full description of the nonlocal optical response in 2D topological phase transitions in staggered layers and similar analysis can be carried out in other materials with Dirac-like spectra.

Casimir force phase transitions in the graphene family – The Dirac-like physics in the graphene family can be probed via the long ranged dispersive Casimir interactions they experience [2]. In fact, this type of force has a rich structure precisely due to materials unique electronic and optical properties. We have considered a Fabry-Perot cavity formed by two sheets of silicene/silicene, germanene/germanene, or stanene/stanene (Fig. 2a). An applied external electric field E_z and circularly polarized light with strength Λ are applied perpendicular to the layers and are used to drive the different Hall phase transitions. In Fig. 2b the Casimir energy is shown at chemical potential $\mu = 0$ and distance $d = \hbar c/\lambda_{s_O}$. It is found that the interaction becomes quite strong along the lines where the Chern number is $C = \pm 1$ (bright lines). When the interacting layers are in an Anomalous Quantum Hall Insulator phase, quantized and repulsive force is also possible, as indicated by the purple region in Fig. 2b. Additionally, the phase transitions induce an array of scaling laws, which are markedly different than the scaling laws of typical materials. Fig. 2c further indicates that the finite dissipation Γ affects the scaling laws as well, especially at shorter separations. It turns out that temperature may affect the Casimir interaction significantly. It can reduce the contrast in magnitude between the energies for different points in phase space, which ultimately results in blurred phase transitions. It is also possible that the effect of quantization and repulsion be reduced or completely eliminated depending on the separation. Nevertheless, it is possible to observe such unique effects by properly choosing the distance, temperature, and external field strengths. The measurement of some of these effects should be within reach with current state of the art Casimir force experiments.

During this investigation, it was realized that the role of temperature is quite strong in interactions originating from zero-point vacuum fluctuations in Dirac materials. The remarkable manifestation of thermal fluctuation is studied in a stack of N graphene layers by examining their Casimir energy as well as the Casimir-Polder energy of an atom positioned on top of the stack [3]. By employing the full polarization tensor in the entire frequency plane, regimes in terms of distance separations and temperature ranges are determined in order to understand the dominance

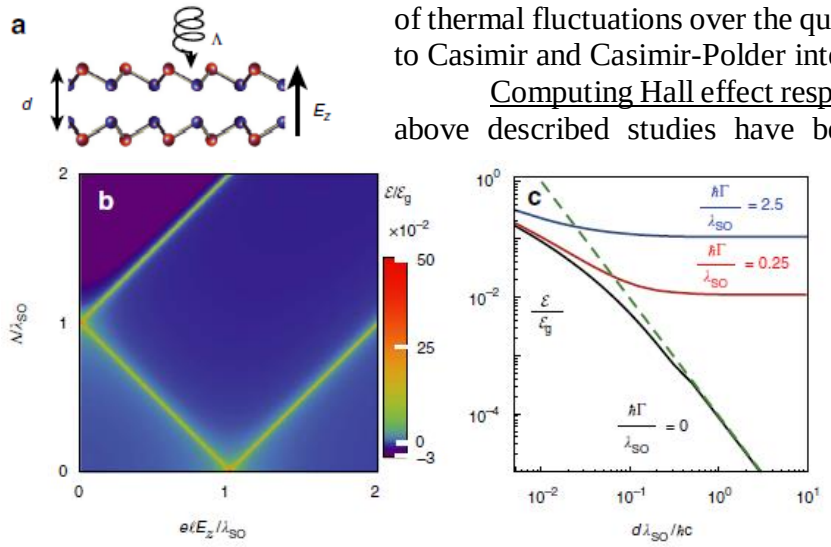

Figure 2 (a) Fabry-Perot cavity of two layers under externally applied fields. (b) Casimir energy phase diagram for two dissipationless identical parallel layers for $\frac{d\lambda_{SO}}{\hbar c} = 1$. (c) Distance dependence of the Casimir energy at $\Lambda = E_z = 0$ for various values of dissipation.

of thermal fluctuations over the quantum mechanical contributions to Casimir and Casimir-Polder interactions.

Computing Hall effect responses from first principles – The above described studies have been performed using effective models for the optical response and underlying dispersive interactions, which essentially rely on the Dirac-like band structure within low wave vector expansions. However, for many materials, including Weyl semi-metals and honeycomb bilayers, such simplified band structure may not be enough and the atomistic nature of the materials must be taken in to account in the calculation of the response properties. In this project, initial steps are made towards a Wannier function interface with standard *ab initio* density functional theory (DFT) codes, such as VASP and Quantum Espresso. The Wannier function representation is convenient in the Kubo formalism for computing the optical conductivity tensor by taking into account the full electronic structure of the materials in terms of wave vector, frequency, temperature, and external field dependences. This elaborate computational scheme was tested on FeRh, a typical metal that experiences antiferromagnetic/ferromagnetic (AFM/FM) phase transition at $T \approx 350\ K$. It appears that FeRh is a good playground to test the Wannier function representation applied to a material, not studied before, and more importantly, to find a unique application in spintronics, which further broadens the scope of this project.

It is important to note that the conductivity calculations, that enable us to examine the different Hall effects in the material [4], require an active control of the wave functions, Hamiltonian, and energies (well beyond the currently available "black box" tool in VASP, for example). After computing the electronic structure via DFT (as implemented in Quantum Espresso), the Wannier function interpolation scheme based on 18 maximally localized functions per atom in the unit cell the DFT electronic structure for both phases (AFM and FM) are reproduced and effective Hamiltonians are generated. We calculate a range of conductivities describing the inverse spin Hall effect (ISHE), anomalous Hall effect (AHE), and the anomalous Nernst effect (ANE) for both phases. It is found that these Hall conductivities experience dramatic changes across the phase transition, which can further be used to analyze the properties of the material. Perhaps one of the most interesting features is that $\sigma_{yx}^{(SH)}$ has an almost linear behavior as a function of temperature and it flips its sign as FeRh changes from an AFM to a FM, as shown in Fig. 3. At the same time, $\sigma_{yx}^{(AH)}$ and $\sigma_{yx}^{(AN)}$ are zero for the AFM phase as expected from the time reversal symmetry, but they are non-zero in the FM phases.

Future Plans

Bilayers of honeycomb Dirac layers – With the graphene family expanding, bilayer materials composed of staggered hexagonal layers becomes a natural direction of exploration. Our *ab initio* simulations show that the structure bilayers formed by silicenes, germanenes, or stanenes, experience rather strong atomic registry dependence as compared to bilayer graphenes [5]. The composition and stacking are expected to play significant role on the optical response as well as their fluctuation induced interactions. This is a direction to be explored in the immediate future.

Weyl materials and optical response – Weyl materials can be characterized as 3D versions of graphene and their surfaces have distinct properties from bulk as the projection of the Weyl nodes (topologically robust features) on surfaces give rise to Fermi arcs. The different electronic structure for bulk and surface will result in different optical response which undoubtedly will have different contributions in their vdW/Casimir interactions. The PI plans to develop reliable models for such interactions relying on first principles methods as well as analytical theories.

VdW interactions – Another direction in the intermediate future of this project is the development of *ab initio* methods for dispersion forces capable of revealing how Dirac-like features in the spectra, band crossings in the energy band structure, and other topological and geometrical characteristics affect such interactions. Through the DFT/Wannier Functions calculations, we are able to connect specific intrinsic materials properties to the optical response. Since vdW forces are closely associated with the correlated electronic fluctuations, it is clear that the nontrivial topology of the interacting materials is of importance as well. This route may ensure finding pathways for manipulation and control of vdW interactions by enhancing (or inhibiting) particular electronic structure features.

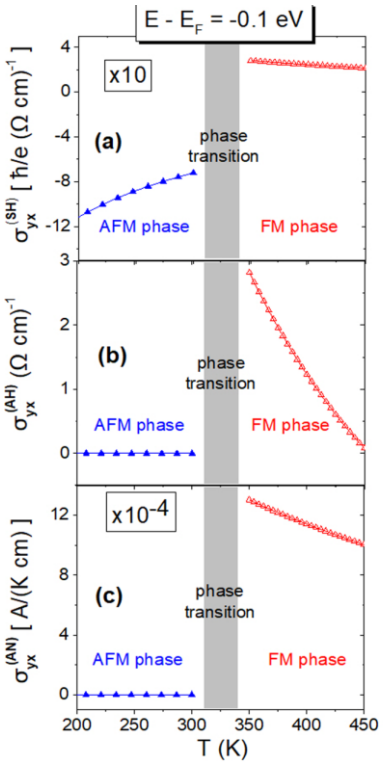

Figure 3 Temperature dependence for the (a) spin Hall conductivity; (b) the anomalous Hall conductivity; (c) anomalous Nernst conductivity at a particular Fermi level.

References

1. P. Rodriguez-Lopez, W. J. M. Kort-Kamp, D. A. R. Dalvit, and L. M. Woods, *Nonlocal optical response in topological phase transitions in the graphene family*, Phys. Rev. Materials **2**, 014003 (2018).
2. P. Rodriguez-Lopez, W. J. M. Kort-Kamp, D. A. R. Dalvit, and L. M. Woods, *Casimir force phase transitions in the graphene family*, Nat. Comm. **8**, 14699 (2017).
3. N. Khusnutdinov, R. Kashparov, and L.M. Woods, *Thermal Casimir and Casimir-Polder interactions in N parallel 2D Dirac materials*, 2D Materials **5**, 035032 (2018).
4. A. Popescu, P. Rodriguez-Lopez, P. Haney, and L. M. Woods, *Thermally driven anomalous Hall effect transitions in FeRh*, Phys. Rev. B **97**, 140407 (R) (2018).
5. A. Popescu, P. Rodriguez-Lopez, and L. M. Woods, *Composition and stacking dependent topology in bilayers from the graphene family*, under preparation.

Publications (August 2016 – July 2018)

1. L. M. Woods, D. A. R. Dalvit, A. Tkatchenko, P. Rodriguez-Lopez, A. W. Rodriguez, and R. Podgornik, *A materials perspective of Casimir and van der Waals interactions*, Rev. Mod. Phys. **88**, 045003 (2016)
2. P. Rodriguez-Lopez, W. J. M. Kort-Kamp, D. A. R. Dalvit, and L. M. Woods, *Casimir force phase transitions in the graphene family*, Nat. Comm. **8**, 14699 (2017).
3. P. Rodriguez-Lopez, W. J. M. Kort-Kamp, D. A. R. Dalvit, and L. M. Woods, *Nonlocal optical response in topological phase transitions in the graphene family*, Phys. Rev. Materials **2**, 014003 (2018).
4. N. Khusnutdinov, R. Kashparov, and L.M. Woods, *Thermal Casimir and Casimir-Polder interactions in N parallel 2D Dirac materials*, 2D Materials **5**, 035032 (2018).
5. A. Popescu, P. Rodriguez-Lopez, P. Haney, and L. M. Woods, *Thermally driven anomalous Hall effect transitions in FeRh*, Phys. Rev. B **97**, 140407 (R) (2018).
6. A.R. Khabibullin, A. Karolak, M.M. Budzevich, M.L. McLaughlin, L.M. Woods, and D.L. Morse, *Structure and properties of DOTA-chelated radiopharmaceuticals within the ^{225}Ac decay pathway*, MedChemComm, accepted (2018) (DOI: 10.1039/C8MD00170G)

First Principles Investigations of Innovative Materials

Ruqian Wu

Department of Physics and Astronomy, University of California, Irvine, CA 92697-4575

We develop and apply density functional approaches to address fundamental issues in the development of innovative materials for use in spintronics, quantum information, energy conversion and storage technologies. Explicitly, we study 1) how to use the newly discovered van der Waals (vdW) two-dimensional (2D) magnetic materials to magnetize the surface bands of 2D and three-dimensional topological insulators for the realization of quantum anomalous Hall effect at a reasonably high temperature; 2) how to effectively imprint the exchange and spin orbit coupling (SOC) in graphene and its siblings through the proximity effect from other vdW 2D materials; 3) how to use the giant electric field at the surface of ferroelectric substrate to manipulate the spin Hall effect, magnetic anisotropy, Rashba SOC and *Dzyaloshinskii-Moriya interaction*; (4) how to develop the phonon breakdown feature of intercalated vdW materials for energy harvesting and storage applications. Following are a few examples of our recent studies.

Recent major progress

Quantum spin hall effect in graphene: We further extend our studies of graphene-related systems to two directions: 1) using Bi_2Se_3 clusters to imprint SOC in graphene bands; and 2) placing graphene on other two-dimensional materials such as WS_2. Graphene played a key historical role in the development of topological insulators materials that exhibit an electrically inert interior yet form exotic metals at their boundary. Kane and Mele predicted that coupling between the spin and orbital motion of electrons turns graphene into a 'quantum-spin-Hall' insulator that hosts spin-filtered metallic edge states with inherent resilience from scattering. These novel edge states underlie tantalizing technological applications for low-power electronics, spintronics devices, and fault-tolerant quantum computing. Graphene's intrinsic spin-orbit coupling is far too weak to produce an observable quantum-spin-Hall (QSH) phase in practice, external ways are needed to boost graphene's spin-orbit coupling to stabilize a robust QSH phase.

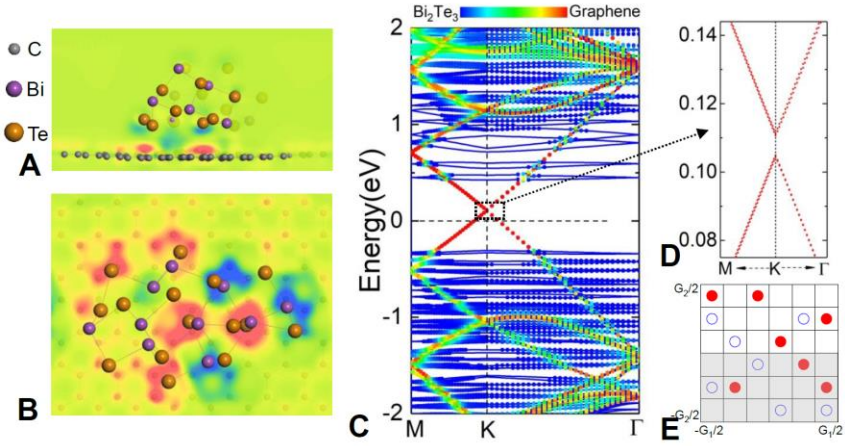

Fig. 1. A) and (B) *Side and top views of the atomic structure and charge-density difference of Bi_2Te_3/Graphene. Red and blue colors respectively indicate charge depletion and accumulation.* ***(C) and (D)*** *Band structure of Bi_2Te_3/Graphene.* ***(E)*** *The n-field configuration with red solid, blue hollow circles and blank boxes denoting n= -1, n= 1, and n=0, respectively. Summing the n-fields over half of the torus yields a nontrivial Z_2 invariant.*

In collaborations with J. Haruyama and J Alicea, we experimentally and theoretically study artificially enhanced spin-orbit coupling in graphene via random decoration with dilute Bi_2Te_3 nanoparticles. Remarkably, multi-terminal resistance measurements suggest the presence of helical edge states characteristic of a quantum-spin-Hall phase; X-ray photoelectron spectra, scanning tunneling spectroscopy, and first-principles calculations further support this scenario. These observations highlight a pathway to spintronics and quantum-information applications in graphene-based quantum-spin-Hall platforms.

Since the atomic structure of the nanoparticle is unknown, we performed ab initio molecular dynamics (AIMD) simulations by baking it at 600K for 6 picoseconds and then cooling it down to 300 K in 5 picoseconds. The structures obtained through AIMD simulations were further relaxed at 0 K, with the inclusion of the van der Waals correction in DFT calculations. Figures 4A and 4B show side and top views of the optimized structure of the Bi_2Te_3 nanoparticle on graphene. Due to the weak van der Waals interaction, the composite system's band structure continues to exhibit Dirac cones (Fig. 4C). Electronic states of the Bi_2Te_3 nanoparticle reside rather far from the Fermi level and disperse weakly, indicating adequacy of the 7×7 supercell for minimizing direct interaction among adjacent nanoparticles. Significantly, the Bi_2Te_3 nanoparticles nevertheless yield a sizeable band gap $E_g \approx 6$ meV at the Dirac point. By counting the positive and negative n-field numbers over the half of the torus—see Fig. 4E—one obtains a nontrivial Z_2 invariant. Therefore, DFT predicts that Bi_2Te_3-nanoparticle-decorated graphene realizes a QSH phase.

1/f Magnetic Flux Noise in Superconducting Device: A major obstacle to using superconducting quantum interference devices (SQUIDs) as qubits is flux noise. Several proposals for the microscopic source of spins have been put forth such as surface spin clusters and correlated fluctuations, electron spin exchange via the hyperfine interactions and adsorbed OH or O_2 molecules. As shown in Fig. 2(a) with curves of density of state (DOS) and spin density, our DFT calculations indicate that states of an O_2 molecule are spin polarized and has a magnetic moment of each O_2 has 1.8 μ_B on the α-alumina surface that is often used to model native oxide layer on Al SQUIDs. When the spin is oriented perpendicular to the axis of the O–O bond, the barrier to spin rotations is only about 10 mK and, therefore, we proposed that the mysterious spins producing flux noise on SQUID surfaces could be O_2 molecules. Following this theoretical prediction, our work demonstrated that 1) that O_2 molecules indeed condense on aluminum oxide surfaces and retain their magnetization; and 2) magnetic noise can be significantly suppressed by appropriate surface treatment such as NH_3 passivation. As shown in Figure 2, the static spin susceptibility is reduced by more than an order

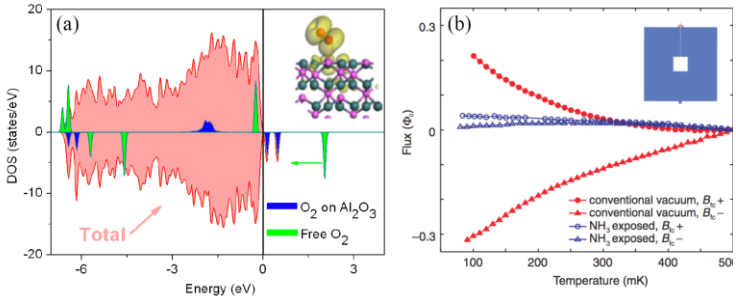

Figure 2. (a) Density of states (red for total, blue for adsorbed oxygen, and green for isolate oxygen) and isosurface of spin density for O_2 on α-Al_2O_3(0001). (b) Temperature dependent flux threading a square-washer SQUID (350 pH; see inset) cooled in a conventional vacuum (closed red symbols) and cooled following vacuum bake and NH_3 passivation (open blue symbols).

of magnitude e and the 1/f magnetic flux noise power drops by a factor of 5 after the NH_3 treatment. This work represents a breakthrough for the control of magnetic noise in SQUIDs.

Recent experiments have also implicated hydrogen (H) atoms as a source for the remaining flux noise even though the presence of hydrogen is rarely associated with magnetism. One evidence is the finding of an energy splitting of ~1.42 GHz in electron spin resonance (ESR) measurements on (α-Al_2O_3(0001), a value that coincides with the hyperfine splitting of a free H atom. Our DFT calculations indicate that H atoms may indeed produce a sizeable local spin polarization and ESR splitting. Furthermore, we found that H adatoms on α-Al_2O_3(0001) facilitate the adsorption of other molecules such as O_2 and N_2, both bring in additional fluctuating spins. Based on extensive studies, we suggested that graphene coating may remove unpaired electrons from H/α-Al_2O_3(0001) and prevent other magnetic adsorbates. Clearly, these results are important for the elimination of flux noise on SQUIDs.

Emergent magnetic phenomena at interfaces of oxides: While the inherent chemical contraindication limits the fabricability of many bulk materials, heterointerfaces and multilayer films have attracted increasing attention and a multitude of intriguing physical properties have been discovered. The emergent phenomena, such as the presence of high mobility electron gas, quantum Hall effect, superconductivity, ferromagnetism polarization enhancement and metal-insulator transition, have greatly enriched fundamental science and provide new platforms for technological innovations. The coexistence of ferromagnetism, superconductivity and conducting two-dimensional electron gas (2DEG) at the interface between two insulators, e.g. $LaAlO_3$ and $SrTiO_3$ (LAO/STO), are among the most exciting discoveries in this realm and a number of new opportunities may appear on the horizon. Ferroic-based heterostructures are gems of modern materials physics and nanoscience for the realization of novel properties, since the electron spin, electric dipole and lattice strain in these materials can be continuously manipulated by magnetic, electric and stress fields.

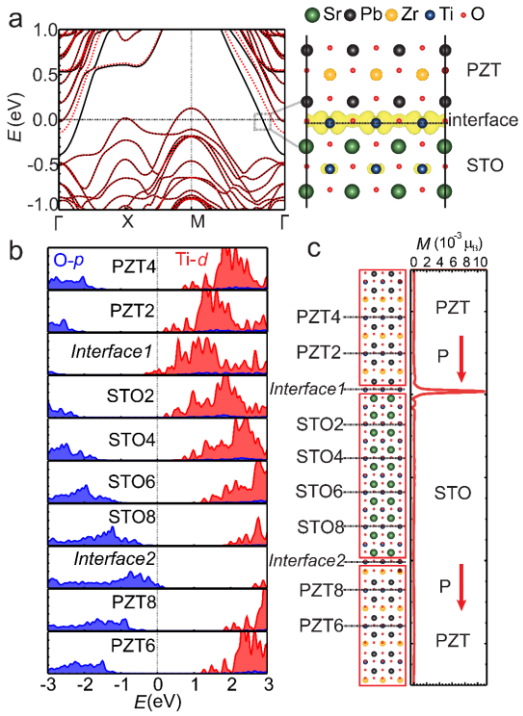

Fig. 3. (a) Calculated band structure of the STO/PZT heterostructure with U_{eff}=2.3 eV for Ti and Zr d-orbitals. The right panel gives charge of states near the Fermi level. The majority-spin and minority-spin bands are represented by black solid and red dashed lines, respectively. (b) Atom-resolved DOS of the STO/PZT heterostructure. The vertical dashed line at E=0 represents the position of the Fermi level. Blue and red colors denote O-p and Ti-d contributions, respectively. (c) The planar-average of spin density of the STO/PZT heterostructure along the axis of polarization. The corresponding atomic structure is shown in the left side.

In a collaborative work with Profs. X.Q. Pan and J. Xia at UC Irvine, we recently demonstrated the possibility of producing spin-polarized two-dimensional electron gas at the interface of $SrTiO_3$ and $PbZr_{0.2}Ti_{0.8}O_3$ (PZT). As shown in Fig. 3, spin-polarized metallic states appear at the interface between STO and PZT layers even though both are insulators. The curves of atom-resolved DOS for different O and Ti atoms show that the conduction and valence bands are almost linearly shifted along the *c*-axis due to the internal electric field produced by the polarization in the

ferroelectric PZT layers (Fig. 3b). Note that we have two STO/PZT interfaces in our theoretical model and both interfaces are metallic, but magnetization only arises at the interface where the electric polarization of PZT is pointing towards STO (*Interface1* in Fig. 3c). The *Interface2* has hole conducting via states from O-2p orbitals. It is intriguing that one may manipulate the carrier type and magnetic state of the STO/PZT interface with a bias to switch the electric polarization of PZT. This adds a new knob to tune the magnetic state of oxide films, as desired for multiferroic materials.

Planned activities: 2018-2019

We have several research topics in the next year.

1. Search for axion materials
2. Study emergent 2D magnetic materials
3. Explore the possibility of realizing the quantum anomalous Hall effect with 2D magnetic layers on topological insulators
4. Study the spin the Seebeck effect in nanowires and nanoribbons
5. Study magnetic and topological properties of transition metal adatoms on 2D materials
6. Simulate segregation of alkali atoms in layered materials

Selected Publications through 2015

1. J. Hu, Z.Y. Zhu, and R.Q. Wu, *"*Chern Half Metal: The Case of Graphene With Co or Rh Adatom*"*, Nano. Lett. **15**, 2074 (2015).
2. H. Wang, C.T. Shi, J. Hu, S. Han, C. Yu and R.Q. Wu, "Candidate source of flux noise in SQUIDs: adsorbed oxygen molecules", Phys. Rev. Lett. **115**, 077002 (2015).
3. Bowen Yang, Min-Feng Tu, Jeongwoo Kim, Yong Wu, Hui Wang, Jason Alicea, Ruqian Wu, Marc Bockrath, and Jing Shi, "*Tunable spin-orbit coupling and symmetry-protected edge states in graphene/WS_2*", 2D Materials, **3**, 031012 (2016).
4. W.C. Yu, J. Lan, R.Q. Wu, and J. Xiao, "*Magnetic Snell's law and spin-wave fiber with Dzyaloshinskii-Moriya interaction*", Phys. Rev. B **94**, 140410(R), (2016).
5. P. Kumar, S. Sendelbach, M. A. Beck, J. W. Freeland, Z. Wang, H. Wang, C. C. Yu, R. Q. Wu, D. P. Pappas, R. McDermott, *"Origin and Suppression of 1/f Magnetic Flux Noise*", Phys. Rev. Appl(Lett), **6**, 041001 (2016).
6. Z.M. Han, G. Czap, C-l Chiang, C. Xu, X.Y. Wei, Y.X. Zhang, R.Q. Wu, and W. Ho, "*Imaging Halogen Bond: Self-assembly of Hexahalogenbenzene*" Science, **358**, 206 (2017).
7. S. Thomas, B. Kuiper, J. Hu, J. Smit, Z. Liao, Z. Zhong, G. Rijnders, A. Vailionis, R. Wu, G. Koster, J. Xia, "Localized Control of Curie Temperature in Perovskite Oxide Film by Capping-layer-induced Octahedral Distortion", Phys. Rev. Lett. **119**, 177203 (2017).
8. B. Li, H. Wang, Y. Kawakita, Q. Zhang, M. Feygenson, H. L. Yu, D. Wu, K. Ohara, T. Kikuchi, K. Shibata, T. Yamada, Y. Chen, J. Q. He, D. Vaknin, R. Q. Wu, K. Nakajima and M. G. Kanatzidis, "*Liquid-like thermal conduction in a crystalline solid*", Nature Mater. **17**, 226 (2018).
9. Yi Zhang, Lin Xie, Jeongwoo Kim, Alex Stern, Hui Wang, Kui Zhang, Henry Liu, Hang Chi, Ctirad Uher, Yinghao Chu, Jing Xia, Ruqian Wu, and Xiaoqing Pan, "*Spin-Polarized Conductive Two-Dimensional Electron Gas Emergent at the Ferroelectric/Insulator Interface*", Nature Communications, **9**, 685 (2018).
10. Z. Wang, H. Wang, C. Yu and R.Q. Wu, *"Hydrogen as a source of magnetic flux noise in superconducting quantum devices"*, Phys. Rev. B, **98**, 020403R (2018).

Interfacial Magnetic Skyrmions and Proximity Effects

Principal investigator: Jiadong Zang
Department of Physics, University of New Hampshire

Keywords: Skyrmions, topological charge, Dzyaloshinskii-Moriya interaction, perpendicular magnetic anisotropy, hopfion

Project Scope

Magnetic skyrmion is a nanostructured spin texture in which magnetic moments point in all directions wrapping a unit sphere. The aim of this project is to realize and manipulate skyrmions on the interface and other confined geometries, and control their dynamical or electrical behaviors. We are systematically exploring new approaches to create/annihilate skyrmions and studying their proximity effect once attached to other orders. Our theoretical efforts are supported by partnership with the experimental collaborator Dr. Axel Hoffmann from Argonne National Laborotory.

The skyrmion, being topologically nontrivial, not only attracts interests from fundamental physics, but also offers game-changing strategy in future low-dissipative information technology. However, the major challenge is to realize precise control of skyrmions. To this end, the overarching investigations in this project highlight the formation of skyrmions in geometrical confinement, manipulations of skyrmions by phonons and magnons, and engineering of the semiconducting skyrmion properties.

Recent Progress

Thermally driven topology in chiral magnets – Nontrivial topology of the skyrmion is characterized by integer values of the topological charge defined as $Q = \frac{1}{4\pi}\int \mathbf{S}\cdot(\partial_x\mathbf{S}\times\partial_y\mathbf{S})$, but the presence of nonzero topological charge does not necessarily indicates the presence of skyrmions. By calculating the topological charge of a 2D chiral magnet model in the *B*-*T* phase diagram, we found a broad distribution of the topological charge, which exists even in random spin states at high temperatures. This phenomenon is originated from unbalanced spin canting induced by the Dzyaloshinskii-Moriya interaction D and external field B . We have employed CP^1 representation of spin and carried out field-theoretic analysis. It reveals that thermal fluctuation nature of topological charge and shows $Q \propto D^2B/T^3$, consistent with numerical results shown

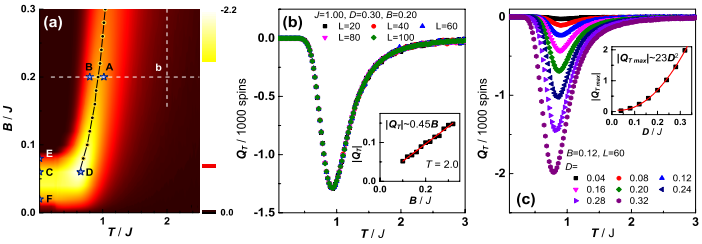

Fig. 1: (**a**) Distribution of the topological charge in *B*-*T* diagram. (**b**) Finite size scaling of the topological charge. The inset shows the linear relation between topological charge and field. (**c**) Topological charge as a function of DM interaction.

in Fig. 1 (b-c). We propose that the thermally driven topological charge can be detected by thermal Hall effect measurements.

Discovery of target skyrmions in nanodisks – A new type of skyrmion texture, the target skyrmion, was discovered in ultra small FeGe nanodisk at zero magnetic field. This is the first realization of zero-field skyrmions of the Bloch type. The target skyrmion, shown in Fig. 2, consists of a series of concentric helical strips. In particular, the target skyrmion we observed in nanodisk is a composite of a conventional skyrmion at the center and an incomplete twist at the edge. Depending on the center spin polarization, two types of target skyrmions being time reversal to each other exist, as shown in Fig. 2(a-b). We addressed, in this work, the importance of the disk thickness, which not only induces a surface twist of the skyrmion states, but also gives rise to a demagnetization field perpendicular to the disk, both reducing the energy of the target skyrmion. Our experimental collaborators from PGI Germany and CAS China employed advanced electron holography technique and truly observed zero-field target skyrmion in a FeGe nanodisk with 160nm in diameter and 90nm in thickness [Fig.2(c-d)]. Target skyrmion from one type can be switched to to other by magnetic field. Monopole and anti-monopole are emergent in the switch process.

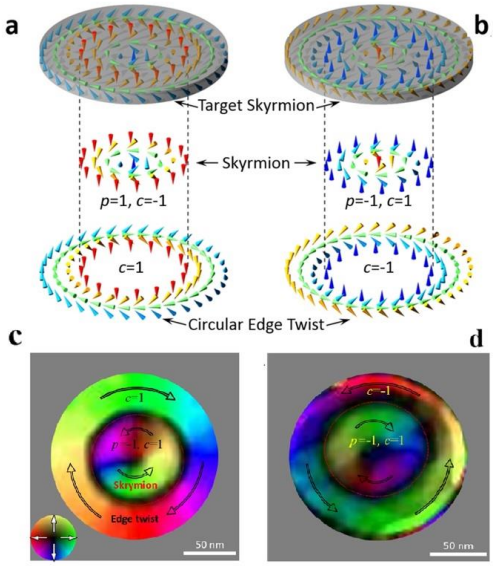

Fig. 2: (**a-b**) Schematic magnetization configurations of two types of target skyrmions in a nanodisk. *p* stands for the polarity and *c* stands for circularity, namely the rotation sense of in-plane magnezation. (**c-d**) Experimental observation of two target skyrmions.

Giant perpendicular magnetic anisotropy in iron-based thin films – Induced by the spin-orbit coupling (SOC), magnetic thin films might have perpendicular magnetic anisotropy (PMA) under which magnetic moments tend to stick out-of-plane. A significant PMA is a pathway towards nanometer-sized interfacial skyrmions. Using the first-principles calculation, we found Fe film on BN, AlN, GaN, and InN ($000\bar{1}$) substrates has a giant PMA of 24.1 meV, 34.3 meV, 32.5 meV, and 53.7meV per iron, respectively. That is more than one order of magnitude larger than PMA in any 3d transition metal based thin films. Such giant PMA is originated from half filling of degenerate x^2-y^2 and xy orbitals. Under first order perturbation of the SOC, this degeneracy is lifted, leading to a net nonzero spin (S_z=2) and orbital angular momentum (L_z=2), both in the perpendicular direction.

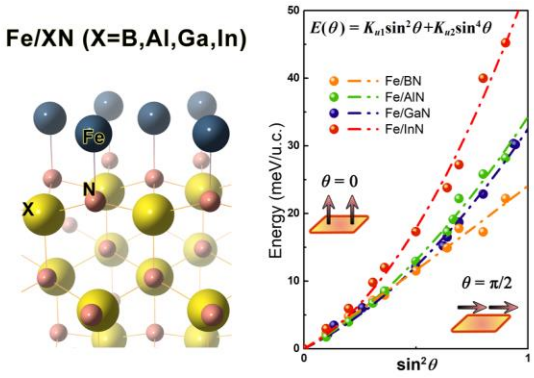

Fig. 3: (**a**) lattice structure of Fe monolayer on top of XN($000\bar{1}$) substrate. Fe sitting at nitrogen-top sites has the lowest energy. (**b**) Calculated system energy as a function of spin polarization direction.

3D Hopfion texture in chiral magnet heterostructures – Skyrmion is a 2D topological spin texture. Its generalization into 3D is the hopfion. In each hopfion, spins with the same z-component form a torus plane. Spins pointing onto the same direction form a closed loop called preimage. Preimages of two directions are always linked in the Hopfion texture. Using GPU-enabled micromagnetic simulations, we predicted the presence of zero-field stable hopfion texture in the chiral magnet nanodisk sandwiched by two perpendicular magnetic films. Another state, the monopole-antimonople pair was also observed. Switching between the hopfion and monopole-antimonopole pair states can be enabled by an external magnetic field. This is the first prediction of magnetic hopfion state.

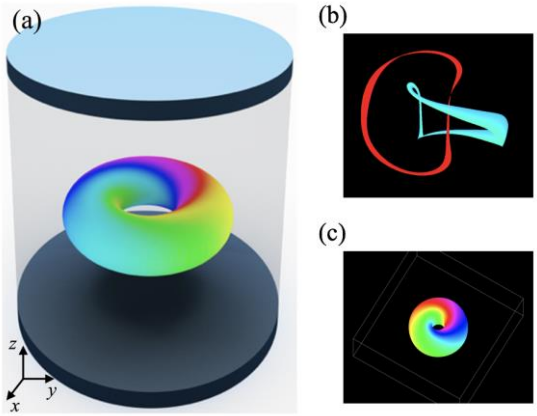

Fig. 4: (**a**) Schematic of proposed structure. A chiral magnetic disk is sandwiched by two PMA layers. (**b**) Preimages of spins in x(red) and -x(cyan) directions. (**c**) Preimages of all spins with zero z-component. They form a torus plane.

Future Plans

In the coming two years, we will mostly focus on the following problems in this new program.

Skyrmionics in 3D– Inspired by works on target skyrmions and hopfions, we plan to systematically analyze skyrmions and other 3D topological charges in three dimensions. Their static structure, dynamics, and material realization will be studied. Recently, in collaboration with Prof. Tokura's group in Japan, we are studying skyrmions in other confined geometries, especially nano-tetrahedra. Skyrmions in these geometries are found to be stable even at zero magnetic field. Due to the 3D nature, micromagnetic simulations are extremely challenging. High performance calculations enabled by GPU will be carried out. We will also study resonant spin wave modes of skyrmion in 3D and these confined geometries.

Thermally driven topological charge – In two dimensional chiral magnets, the thermally driven topology we observed coexists with the skyrmion crystal phase. A fundamental question we asked is that whether we can find thermally driven topology in spin models without the skyrmion phase. In recent attempts, we have already found some examples. In our model square system, inversion symmetry is globally respected, but locally broken. As a result, the DM interaction is staggered from one bond to the other and stable skyrmion phase becomes impossible. But still the topological charge becomes nonzero at finite temperature and finite magnetic field. We need to determine different phases in this model both numerically and analytically, and reveal the correlation between topology and these phases.

Searching materials – Following discovery of giant PMA materials in Fe/GaN heterostructures, more first-principles calculations will be employed to design new skyrmion materials by manipulating interfacial chemistry. More skyrmions materials in the bulk will be searched as well. We are aiming at skyrmions on the atomic scales.

Electron dynamics in skyrmions – Electrons traversing skyrmions exhibit novel properties like Hall effects. We are working on electron transport of skyrmion materials in proximity to other magnetic and electronic orders. An example work being wrapped up is on the skyrmion-topological insulator interface. Ultimately we will work out a quantum theory of electron and magnetization dynamics of semiconducting skyrmions. To this end, micromagnetic simulation described by the Landau-Lifshitz-Gilbert (LLG) equation will be coupled to the non-equilibrium Green's function (NEGF)- based quantum transport theory.

Publications (August 2016 – July 2018)

1. Y. Liu, R. K. Lake, and J. Zang, *Braiding Hopfion knots in chiral magnets*, arXiv:1806. 01682. submitted to Phys. Rev. Lett.

2. Y. Liu, and J. Zang, *An overview and outlook of magnetic skyrmions*, Acta Physica Sinica, **67**, 131201 (2018).

3. J. Yu and J. Zang, *Giant perpendicular magnetic anisotropy in Fe/III-V nitride thin films*, Science Advances **4**, ee7814 (2018).

4. J. Zang, and J. Yu, *Giant Perpendicular Magnetic Anisotropy In Fe/GaN Thin Films For Data Storage And Memory Devices*, US Provisional Patent No. 62/589,399.

5. Y. Liu, R. Lake, and J. Zang, *Shape dependent resonant modes of skyrmions in magnetic nanodisks*, J. Magn. Magn. Mater **455**, 9 (2018).

6. Z. Dai, W. Jin, J. X. Yu, M. Grady, J. T. Sadowski, Y. D. Kim, J. Hone, J. Zang, R. M. Osgood, Jr. and K. Pohl, *Surface buckling of phosphorene materials: determination, origin and influence on electronic structure*, Phys. Rev. Mat. **1**, 074203 (2017).

7. F. Zheng, H. Li, S. Wang, D. Song, C. Jin, W. Wei, A. Kovacs, J. Zang, M. Tian, Y. Zhang, H. Du, and R. E. Dunin-Borkowski, *Direct imaging of zero-field target skyrmion and its polarity switch in chiral magnetic nanodisk*, Phys. Rev. Lett. **119**, 197205 (2017).

8. W. T. Hou, J. X. Yu, M. Daly, and J. Zang, *Thermally driven topology in chiral magnets*, Phys. Rev. B (Rapid Communications) **96**, 140403 (2017).

9. Y. Liu, H. Yan, M. Jia, H. Du., A. Du, J. Zang, *Field-driven oscillation and rotation of multi-skyrmion cluster in a nanodisk*, Phys. Rev. B **95**, 134442 (2017).

10. W. Jiang, G. Chen, K. Liu, J. Zang, S. G. E. te Velthuis, and A. Hoffmann, *Skyrmions in Magnetic Multilayers*, Physics Report **704**, 1 (2017).

Laser-induced ultrafast magnetization in ferromagnets

Principal investigator: Dr. Guoping Zhang
Department of Physics, Indiana State University
gpzhang@indstate.edu

Keywords: Ultrafast, laser, magnetization, reversal, magnetism

Project Scope

Our project aims to understand laser-induced ultrafast demagnetization in ferromagnets and targets an unexplored frontier in magnetic storage devices. The idea is based on whether a single femsecond (fs) laser pulse is able to manipulate the spin on an ultrafast time scale. This will have a direct impact on the future magnetic storage devices since it will exceed the current record of magnetic storage speed by several orders of magnitude. The scope of this program is (a) to investigate why an ultrafast laser pulse can induce so great demagnetization within so short time scales (a few hundred femtoseconds), by investigating the intraband transitions, which has been ignored so far, and (b) whether a single laser pulse with a weak intensity is able to reverse the spins permanently. Our objectives are (1) to reveal the interaction between the laser and magnetic systems on the real time scale, and (2) to establish the link between the laser-induced spin-orbit torque and the spin reversal. We will employ the time-dependent Liouville equation with the first-principles density functional theory. This will enable us to reveal the entire picture with the crystal momentum domain, so our theoretical results can be tested experimentally. We will spend next two years to investigate the all-optical helicity-dependent spin reversal. This becomes increasingly promising for the future applications, in particular coupled with the Hall cross, so the interconnection between the optical communication and electrons can be developed precisely.

Recent Progress

Below are some highlights of progress made in the past 2 years (a more comprehensive publication list is appended below the highlights).

Generating high-order optical and spin harmonics from ferromagnetic monolayers

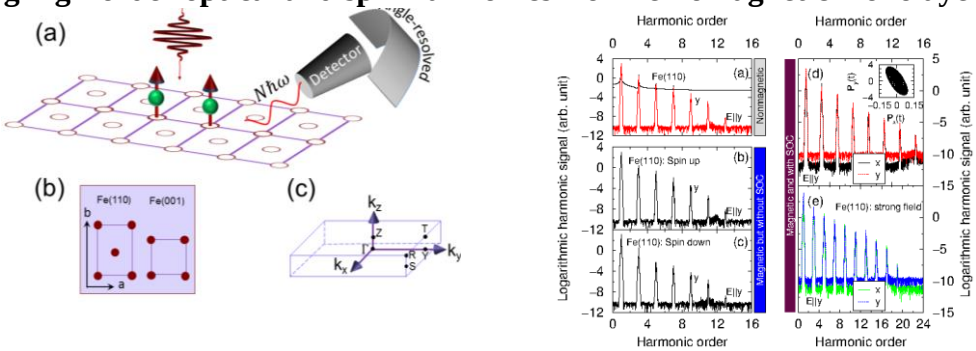

High-order harmonic generation (HHG) in solids has entered a new phase of intensive research, with envisioned band-structure mapping on an ultrashort time scale. This partly benefits from a

flurry of new HHG materials discovered, but so far has missed an important group. HHG in magnetic materials should have profound impact on future magnetic storage technology advances. Here we introduce and demonstrate HHG in ferromagnetic monolayers. We find that HHG carries spin information and sensitively depends on the relativistic spin-orbit coupling; and if they are dispersed into the crystal momentum k space, harmonics originating from real transitions can be k-resolved and carry the band structure information. Geometrically, the HHG signal is sensitive to spatial orientations of monolayers. Different from the optical counterpart, the spin HHG, though probably weak, only appears at even orders, a consequence of SU(2) symmetry. Our findings open an unexplored frontier – magneto-high-order harmonic generation.

Switching ferromagnetic spins by an ultrafast laser pulse: Emergence of giant optical spin-orbit torque

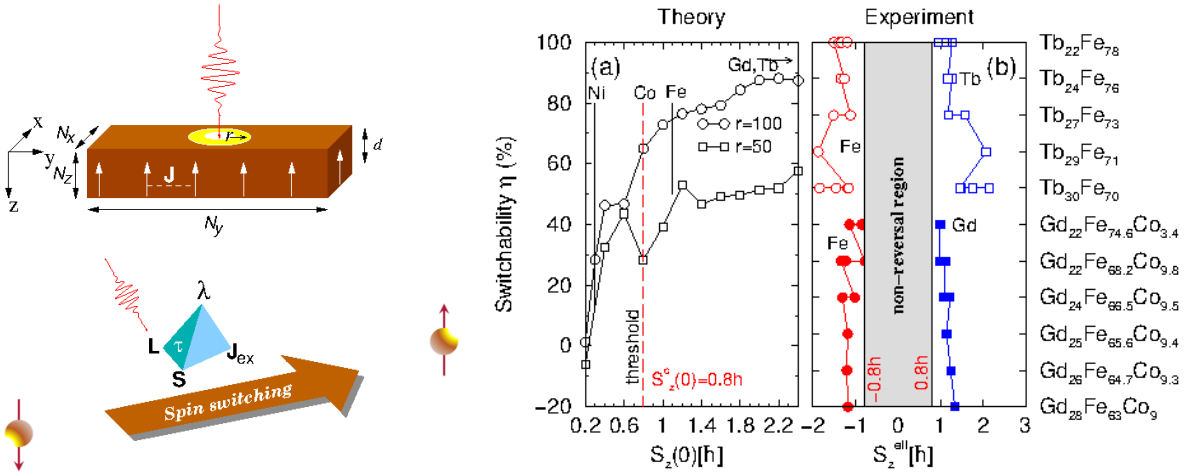

Faster magnetic recording technology is indispensable to massive data storage and big data sciences. All-optical spin switching offers a possible solution, but at present it is limited to a handful of expensive and complex rare-earth ferrimagnets. The spin switching in more abundant ferromagnets may significantly expand the scope of all-optical spin switching. Here by studying 40000 ferromagnetic spins, we show that it is the optical spin-orbit torque that determines the course of spin switching in both ferromagnets and ferrimagnets. Spin switching occurs only if the effective spin angular momentum of each constituent in an alloy exceeds a critical value. Because of the strong exchange coupling, the spin switches much faster in ferromagnets than weakly coupled ferrimagnets. This establishes a paradigm for all-optical spin switching. The resultant magnetic field (65T) is so big that it will significantly reduce high current in spintronics, thus representing the beginning of photospintronics.

Experimental demonstration of 55-fs spin canting in photoexcited iron nanoarrays

As magnetic storage density approaches 1TB/in2, a grand challenge is looming as how to read/write such a huge amount of data within a reasonable time. The ultrafast optical manipulation of magnetization offers a solution, but little is known about the intrinsic speed limit of quantum spin switching. Here, we report that low-energy 50-fs laser pulses can induce

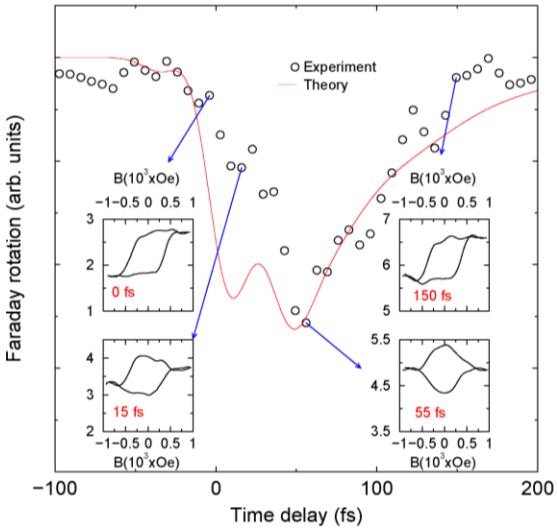

spin canting in Fe nanoparticles within 55 fs, breaking the previous record by at least one order of magnitude. Both linearly and circularly polarized light can be used to tilt spins. In our model, the incident laser field first excites the orbital angular momentum, and through spin-orbit coupling, the spin cants out-of-plane and results in a distinctive diamond hysteresis loop. The spin canting time decreases with spin angular momentum. This spin canting is not limited to Fe nanoparticles and is also observed in Fe/Pt and Fe3O4 nanoparticles. Our results demonstrate the potential of magnetic nanostructures as a viable magnetic medium for high density and fast-switching magnetic storage devices.

First-principles and model simulation of all-optical spin reversal

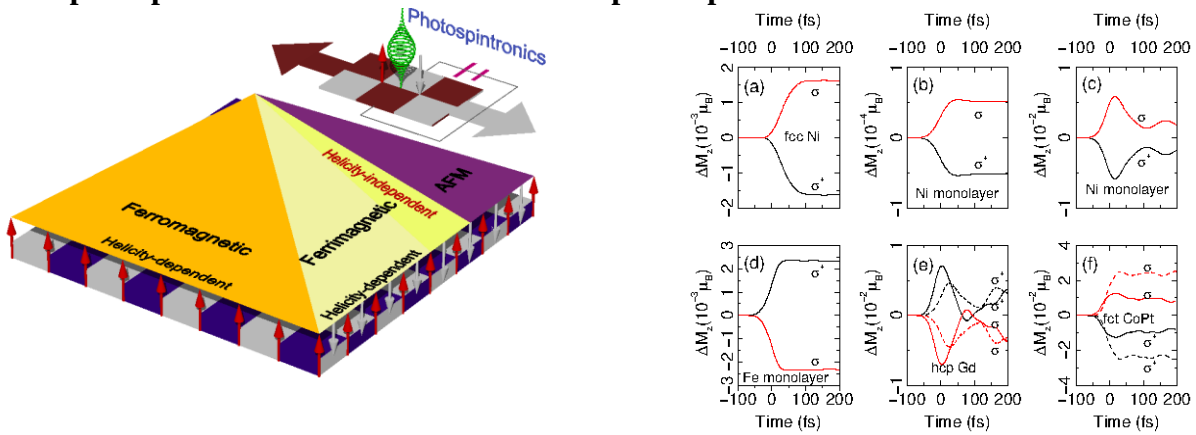

All-optical spin switching is a potential trailblazer for information storage and communication at an unprecedented fast rate free of magnetic fields. However, the current wisdom is largely based on semiempirical models of effective magnetic fields and heat pulses, so it is difficult to provide high-speed design protocols for actual devices. Here, we carry out a massively parallel first-principles and model calculation for 13 spin systems and magnetic layers, free of any effective field, to establish a simpler and alternative paradigm of laser-induced ultrafast spin reversal and to point out a path to a full-integrated photospintronic device. It is the interplay of the optical selection rule and sublattice spin orderings that underlines seemingly irreconcilable helicity-dependent and -independent switchings. Using realistic experimental parameters, we predict that strong ferrimagnets, in particular, Laves phase C_{15} rare-earth alloys, meet the telecommunication energy requirement of 10 fJ, thus allowing a cost-effective subpicosecond laser to switch spin in the gigahertz region.

Future Plans

Intraband transition – It has been hotly debated whether laser-induced spin transport affects the demagnetization. We will develop a scheme that can take into account both processes. We will extend our time-dependent Liouville formalism into the crystal-momentum space where the transitions among different crystal momenta are included. We expect this will yield some important insights into how photodoping and photoexcitation affect the demagnetization in ferromagnets.

Element-resolved demagnetization processes – In an element ferromagnet, such as fcc Ni, bcc Fe and hcp Co, all the atoms demagnetize at the same rate because they are equivalent. However, what happens to the demagnetization rate if they form an alloy, such as permalloy ($Fe_{20}Ni_{80}$). Experimentally, Matthias et al. showed there is a clear delay between Fe and Ni, but more recently experiments did not observe the delay. The question is which is correct or maybe both are correct. In fact, these experiments employed different techniques. We plan to introduce an element-resolved technique by using the same idea that is very popular in resonant x-ray scattering that we compute the absorption at each element edge, so the information of the spin moment at different atom sites can be resolved.

Publications

1. G. P. Zhang, M. S. Si, Mitsuko Murakami, Y. H. Bai and T. F. George, Generating high-order optical and spin harmonics from ferromagnetic monolayers, Nat. Comm. (in press, 2018).
2. Mitsuko Murakami, Guo-ping Zhang, Dmitry Telnov, and Shih-I Chu, Photoelectron momentum distribution of ground- and excited-state lithium atoms induced by extreme-ultraviolet photon absorption, Journal of Physics B: Atomic, Molecular and Optical Physics, (in press, 2018).
3. G. P. Zhang, Z. Babyak, Y. Xue, Y. H. Bai and T. F. George, First-principles and model simulation of all-optical spin reversal, Phys. Rev. B **96**, 134407 (2017).
4. Mitsuko Murakami and G. P. Zhang, Resonant two- or three-photon ionization of noble-gas atoms captured by time-resolved photoelectron momentum spectroscopy, Phys. Rev. A **96**, 063403 (2017).
5. G. P. Zhang, T. Jenkins, M. Bennett and Y. H. Bai, Manifestation of intra-atomic 5d6s-4f exchange coupling in photoexcited gadolinium , J. Phys.: Condens. Matter **29**, 495807 (2017).
6. G. P. Zhang, Y. H. Bai and Thomas F. George, Is perpendicular magnetic anisotropy essential to all-optical ultrafast spin reversal in ferromagnets? J. Phys.: Condens. Matter **29**, 425801 (2017).
7. Mitsuko Murakami, G. P. Zhang, and Shih-I Chu, Multielectron effects in the photoelectron momentum distribution of noble-gas atoms driven by visible-to-infrared-frequency laser pulses: A time-dependent density-functional-theory approach, Phys. Rev. A **95**, 053419 (2017).
8. Mitsuko Murakami, Zach Babyak, Michael Giocolo, and G. P. Zhang, Quantum mechanical interpretation of the ultrafast all-optical spin switching, J. Phys.: Condensed Matter **29**, 184002 (2017).
9. Yuhang Ren, Wei Lai, Zehra Cevher, Yu Gong, and G. P. Zhang, Experimental demonstration of 55-fs spin canting in photoexcited iron nanoarrays, Appl. Phys. Lett. **110**, 082404 (2017).
10. G. P. Zhang, A. Gardner, T. Latta, K. Drake and Y. H. Bai, Superintermolecular orbitals in the C60/pentacene complex, Phys. Rev. A **94**, 062501 (2016).
11. G. P. Zhang, Y. H. Bai and T. F. George, Switching ferromagnetic spins by an ultrafast laser pulse: Emergence of giant optical spin-orbit torque, EPL **115**, 57003 (2016).
12. Mingqiang Gu, Kang Wang, Yiming Wang, Qiyun Xie, Hongling Cai, Guo-Ping Zhang and Xiaoshan Wu, Enhancement of orbital ordering and spin polarization by controlling the dimensionality of the octahedra network, npj Quantum Materials **1**, 16011 (2016).
13. G. P. Zhang, T. Latta, Z. Babyak, Y. H. Bai, and T. F. George, All-optical spin switching: A new frontier in femtomagnetism A short review and a simple theory, Modern Physics Letters B **30**, 16300052 (2016).

Project Title: Fundamental and Defect Properties of Electronic Materials

Principal Investigator: Shengbai Zhang
Department of Physics, Applied Physics & Astronomy, Rensselaer Polytechnic Institute, Troy, NY 12180
Email: zhangs9@rpi.edu
Keywords: bulk band alignment, semiconductor 2D limit, carbon topological physics, 2D charged defect

Project Scope:

The scope of this project includes theoretical developments of fundamental physics and improved defect methodologies, and perform, in parallel, cutting-edge researches utilizing our theoretical breakthroughs and study defect properties. New physics in lower dimensions is also a focus for potential applications. Our objectives include (1) the development of a common reference energy for infinitely large systems. While the preliminary breakthrough has been made recently, a lot needs to be done in order to firmly establish our new theory. (2) A formulation of charged defect formation energy free of model parameters. (3) We propose to study the physics of defects under non-equilibrium growth conditions, which hopefully can replace the current theory that the PI and John Northrup had developed 27-years ago. As direct applications of the discovery in (1), we will calculate (4) *ab-initio* deformation potentials and electron-phonon coupling parameters in solids and (5) the band offsets across *unstrained* interfaces. We will also pursue (6) the effects of charged defects and doping on interfacial atomic structures and properties in 2D systems.

Recent Progress:

(1) Formalism for Charged Defects in Two- and Quasi Two-Dimensions - Two-dimensional (2D) materials are promising candidates for future high-performance electronics and optoelectronics due to their intriguing properties. One of the prerequisites for achieving this goal is to understand the properties of defects. This is not only because native defects and unintentional impurities are usually unavoidable and can strongly affect the physical properties of the materials, but also because intentional doping is a primary means to control n- or p-type conductivity, which is a key ingredient for the design of optoelectronic devices. About three years ago, we developed a formalism for defects in 2D systems and applied it to defects in monolayer BN, which is an isolated and flat 2D system. However, when a monolayer material is placed in a dielectric environment, such as on a substrate, its defect properties can be strongly altered. Also, few-layer 2D materials are common in electronic applications. Recently, we generalized the formalism to quasi-2D systems of arbitrary thickness and geometry [1].

Using black phosphorus (BP) as a prototype, we have calculated the formation and ionization energies (IEs) of phosphorus vacancy (V_P) and substitutional group-VI impurities (O_P, S_P, Se_P, and Te_P), as depicted in Fig. 1. We have studied these defects in mono-, bi-, and tri-layer BPs and showed that due to the increased screening in the thicker layers, the IEs can change considerably,

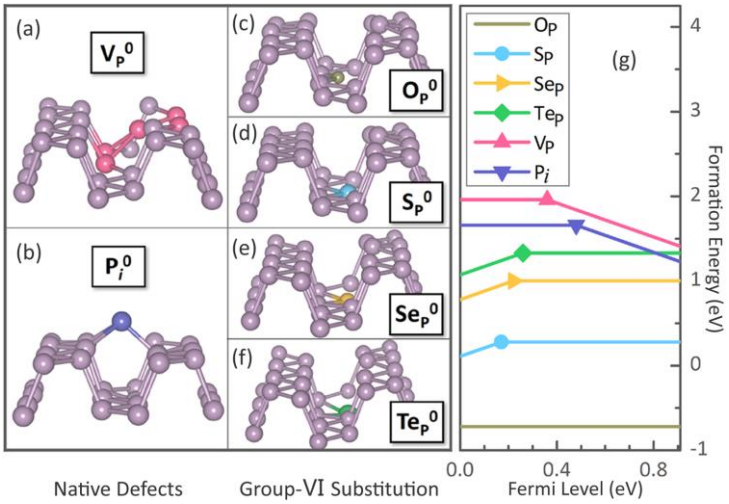

Fig. 1. (a)-(f) Atomic structures and (g) the corresponding formation energies for selected defects in monolayer BP. In (a), atoms with noticeable relaxations are marked in pink.

e.g., for Te_P it is reduced from 0.67 eV for ML BP to 0.47 eV for bilayer BP and to 0.33 eV for trilayer BP.

(2) Topological Nanostructured Carbon Allotropes - Recently, research on topological metals and semimetals (TMs) has attracted considerable interests. In these materials, topologically-protected quasiparticles emerge at protected band-crossing points around Fermi Level, giving rise to condensed matter realizations of many peculiar fermions with a variety of distinct electronic properties. The search for TMs has been focused on compounds involving heavy elements, hoping that the strong spin-orbit coupling could help to achieve a nontrivial band structure. On the other hand, light elements such as carbon may offer a distinct yet fruitful alternative. For example, graphene is well-known with two-dimensional (2D) Dirac fermions. With a negligible spin–orbit coupling, the real spin here can be considered as a dummy variable. Since 2015, we have been working on carbon allotropes with Weyl points, nodal loops, as well as Weyl surfaces.

Recently, we proposed [2] yet another low-energy carbon allotrope, which is entirely composed of pentagonal carbon rings (see Fig. 2). Under equilibrium, the pentagon carbon is a narrow-gap semiconductor. However, a semiconductor-to-metal quantum phase transition takes place when a strain is applied. Remarkably, at the critical point, a novel low-energy isospin-1 triplet fermion emerges. Passing the transition point, the system possesses triply degenerate fermion points. Upon a breaking of the screw-rotational symmetry, these triple points transform into inter-connected Hopf-link Weyl loops protected by a mirror symmetry. The associated Landau-level spectra exhibit distinct features tied to topological fermions, which is an indication of pronounced anomalies in magneto-transport.

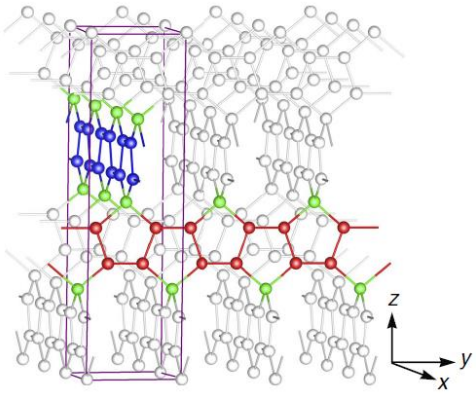

Fig. 2. Atomic structure of pentagonal carbon where purple framework depicts the unit cell, while red and blue atoms form mutually orthogonal armchair chains which are linked together by green atoms.

(3) Traditional Semiconductors in the Two-Dimensional Limit - Most known 2D materials are derivatives of layered 3D materials. From a coordination chemistry viewpoint, however, the crystal structure of any 2D system, or thin film, need not be that of bulk. For example, atomic-layer-thin semiconductors exist in the single-layer honeycomb (SLHC) structure such as graphene and silicene. Recent experiment also suggests that GaN, a traditional 3D semiconductor, may form a 2D structure.

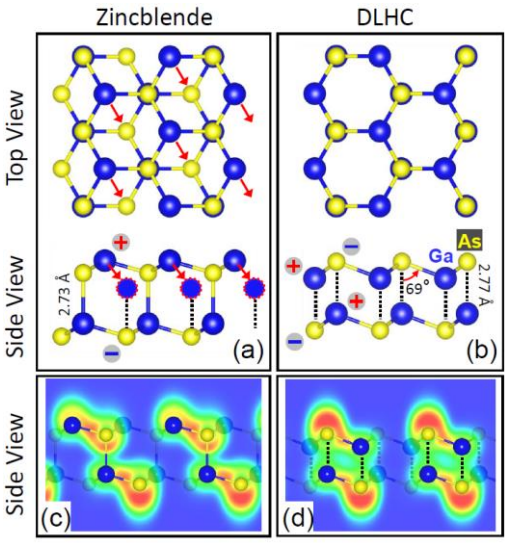

Fig. 3. Top and side views of (a) bilayer-thick truncated bulk (TB) and (b) DLHC GaAs. Red arrows indicate atomic displacements from TB to DLHC. Charged atoms are denoted by (+) and (−) signs. (c), (d) Electron localization functions with contours ranging from 0 (blue) to 0.8 (red).

Recently, we showed [11] by first-principles calculations that traditional 3D semiconductors can exist in layered forms with structures that are distinct from their 3D counterparts (see Fig. 3). In the ultrathin limit of binary semiconductors, the most stable form can be neither truncated bulk (TB) nor SLHC, but instead a TB slab along (111) tends to spontaneously relax to a double-layer honeycomb (DLHC) where individual SLHCs are bound together through dative bonding. The DLHC is not only kinetically stable, but can also be energetically stable. Intereatingly, multiple-layer DLHCs may also form with van der Waals interactions between the layers. A fascinating property of DLHC is the parity of the conduction band which alternates with number of layers. In the case of InSb, InAs, GaSb, GaAs, and HgTe, this leads to not only a gap reduction but also an alternation between normal and topological insulators.

Future Plans (2018-2019):

Development of a common reference energy for infinitely large systems – Through years of seemingly fruitless efforts, we finally made a breakthrough by establishing a universal theory of built-in potential. It provides the key elements for understanding the common energy reference of dissimilar bulk materials. While it is customary to use the planar-averaged potential in surface, interface, and defect calculations to determine the workfunction, band alignment, and defect transition level positions, it has not been recognized that the hidden physics behind such a simple average. Due to the superposition principle, the planar-averaged potential above satisfies the Poisson equation: $\nabla^2\bar{V}(z) = -\bar{\rho}(z)$ where $\bar{\rho}(z) = \frac{1}{S}\int dxdy\rho(\boldsymbol{r})$ is the planar averaged charge density. This transforms the 3D electrostatic problem into one with homogeneous charge distribution in the x-y plane, leaving only the z coordinate as its variable. By an extensive analysis backed by numerous first-principles calculations, we recently showed that the 1D potential above may be used to define a characteristic orientation-dependent quantity $V^{(m)}$. The built-in potential at an arbitrary A-B interface, which has long being a widely-used concept but without a clear definition, can then be uniquely defined as the offset between $V_A^{(m)}$ and $V_B^{(m)}$.

We will formulate the above built-in potential expression using a formal Berry-phase approach, putting everything on the same footing as the one developed for electrical polarization in periodic solids. A seemingly ill-defined quantity of an infinitely-large system is the bulk-average of the electrostatic potential $V(\boldsymbol{r})$, which is related to $\bar{V}(z)$ by $V_0 = \frac{1}{L}\int dzV(z)$, where L is the length of the unit cell. In most first-principles calculations, V_0 is set to zero. Recently, we proved rigorously that V_0 of an infinite bulk equals to its hidden vacuum level and the difference between $V^{(m)}$ and V_0 is due entirely to the existence of a bulk qudrupole, which can in fact be precisely defined and accurately calculated from the charge distribution in a unit cell. Even without the Berry-phase approach, our finding here sets the stage for accurately determining the absolute

deformation potentials and for the calculations of band edge/Fermi level positions of various solids, which will then be used to understand the physics behind surface work functions, the formation of Schottky barriers, the origin for electrode potentials, and the nature of redox potentials, all of which have been used extensively across a wide-range of fields and disciplines.

List of key publications (2017-2018):

(1) D Wang, D Han, XB Li, NK Chen, D West, V Meunier, S Zhang, HB Sun, "Charged defects in two-dimensional semiconductors of arbitrary thickness and geometry: Formulation and application to few-layer black phosphorus", Phys. Rev. B 96, 155424 (2017).
(2) C. Zhong, Y. Chen, Z.-M. Yu, Y. Xie, H. Wang, S. A. Yang & S. Zhang, "Three-dimensional Pentagon Carbon with a genesis of emergent fermions", Nature Comm. 8, 15641 (2017).
(3) L. Wang, P. Guan, J. Teng, P. Liu, D. Chen, W. Xie, D. Kong, S. Zhang, T. Zhu, Z. Zhang, E. Ma, M. Chen & X. Han, "New twinning route in face-centered cubic nanocrystalline metals", Nature Comm. 8, 2142 (2017).
(4) J. Zhang, W. Xie, J. Zhao and S. Zhang, "Band alignment of two-dimensional lateral heterostructures", 2D Mater. 4 (2017) 015038.
(5) Z. Lou, Y. Li, L. Zhu, W. Xie, W. Niu, H. Song, Z. Ye, S. Zhang, "The crystalline/amorphous contact in Cu 2 O/Ta 2 O 5 heterostructures: increasing its sunlight-driven overall water splitting efficiency", J. Mater. Chem. A 5, 2732 (2017).
(6) XP Wang, XB Li, NK Chen, QD Chen, XD Han, S Zhang, HB Sun, "Element-specific amorphization of vacancy-ordered GeSbTe for ternary-state phase change memory", Acta Mat. 136, 242 (2017).
(7) ML Agiorgousis, YY Sun, S Zhang, "The Role of Ionic Liquid Electrolyte in an Aluminum–Graphite Electrochemical Cell", ACS Energy Letters 2, 689 (2017).
(8) N-K Chen, D Han, X-B Li, F Liu, J Bang, X-P Wang, Q-D Chen, H-Y Wang, S Zhang, H-B Sun, "Giant lattice expansion by quantum stress and universal atomic forces in semiconductors under instant ultrafast laser excitation", Phys. Chem. Chem. Phys.19, 24735 (2017).
(9) J. Wang, X. Sui, W. Shi, J. Pan, S. Zhang, F. Liu, S.-H. Wei, Q. Yan, and B. Huang, "Prediction of Ideal Topological Semimetals with Triply Degenerate Points in the NaCu3Te2 Family", Phys. Rev. Lett. 119, 256402 (2017).
(10) NK Chen, XB Li, XP Wang, WQ Tian, S Zhang, HB Sun, "Strong electron-polarized atom chain in amorphous phase-change memory GeSbTe alloy", Acta Materialia 143, 102 (2018).
(11) M. C. Lucking, W. Xie, D.-H. Choe, D. West, T.-M. Lu, and S. B. Zhang, "Traditional Semiconductors in the Two-Dimensional Limit", Phys. Rev. Lett. 120, 086101 (2018).
(12) N.-K. Chen, X.-B. Li, J. Bang, X.-P. Wang, D. Han, D. West, S. Zhang, and H.-B. Sun, "Directional Forces by Momentumless Excitation and Order-to-Order Transition in Peierls-Distorted Solids: The Case of GeTe", Phys. Rev. Lett. 120, 185701 (2018).
(13) J. Zhang, W. Xie, M. L. Agiorgousis, D.-H. Choe, V. Meunier, X. Xu, J. Zhao and S. Zhang, "Quantum oscillation in carrier transport in two-dimensional junctions", Nanoscale 10, 7912 (2018).
(14) H Tan, Y Li, SB Zhang, W Duan, "Effect of Hartree–Fock pseudopotentials on local density functional theory calculations", Physical Chemistry Chemical Physics 20, 18844 (2018).
(15) Y Gao, Y Chen, Y Xie, PY Chang, ML Cohen, S Zhang, "A class of topological nodal rings and its realization in carbon networks", Phys. Rev. B 97, 121108 (2018).

Understanding and Control of Charge Carriers in Quantum Materials

Alex Zunger
University of Colorado, Boulder Colorado 80309

Project Scope

Project Period: 08/15/2016 - 08/14/2019

Scope 1: Sort out what are the minimal theory ingredients needed to explain the observed trends in gaps, structure and magnetism in binary and ternary 3d oxides. We note that Electronic structure calculations generally require two kinds of inputs (a) An underlying *description of interelectronic interactions* (dynamic or static correlation, single determinant or many body; type of exchange-correlation used in DFT, U or no U, etc.) and (b) A *framework for describing the structure of the compounds* (allowing energy lowering symmetry breaking or not; single site structural models (CPA) or a polymorphous description, supercells or single primitive cells etc.). Our observation is that many of the articles published on correlated oxides tested DFT while making rather naïve and highly restrictive assumptions on (b) above, got poor results, and concluded that DFT itself (part a) fails, requiring heavy-duty beyond DFT methodology instead. Our scope is to examine the performance of properly executed DFT (including reasonable (a) and (b)) for addressing the basic structural, metal/insulator (ie gaping) and magnetic states (AFM vs PM) along the series of binary (NiO, MnO, CoO, FeO) and ternary perovskite (ABO3 with B=3d). This could establish what is the *minimal* theoretical framework required to explain these basic observed trends.

Scope 2: Testing whether theoretically predicted exciting new effects do actually 'live' in reasonably stable compounds: To maintain theory-experiment friendship, it may be wise to examine if some of the exciting theoretically predicted effects are likely to 'live' in stable, or not too unstable structures. This includes exciting effects such as topological insulation in doped, **wide-gap cubic** BaBiO3; Unique Wyle semimetal Ba2CuO2 with remarkable **8-fold degenerate** semi-metallic bands, or bulk Dirac Semimetals **with 4-fold degenerate bands** in BiO2. We will examine these and other cases on an ongoing basis.

Scope 3: Realistic doping of Quantum Materials: Many of the envisioned functionalities of quantum materials such as superconductivity, interesting QSL, wide gap topological insulators, Li ion batteries, etc. require changing their Fermi energy, via doping. Sometimes this is done by naïve models where the Fermi energy is displaced at will in a given band structure, assuming that the host solid stays indifferent. The "modern theory of doping", however, has often shown that compounds react adversely to arbitrarily shifting their Fermi level by developing structural deformations, polaronic localization,

and even phase transitions that defeat the original effect being sought. We will investigate some relevant cases.

Recent Progress-selected items

Progress on Scope 1: the origin of band gaps in 3d perovskite oxides:

Transition metal perovskite oxides ABO_3 show a broad range of magnetic, electronic, structural and ferroelectric properties and have long served as a platform for testing our understanding of condensed matter theories. In particular, their insulating character – found in most compounds – has long been thought to arise from dynamic electronic correlations through the celebrated Mott-Hubbard mechanism. We investigate the origin of band gap opening in the full family of 3d perovskite oxides, both in the low-temperature phase and in the high-temperature, paramagnetic phase. We enquire what is the minimal, essential theoretical picture needed to understand the trends in gaping, magnetism and structure for the ABO3 series. We find that insulation occurs via (i) energy-lowering crystal symmetry reductions (octahedral rotations, Jahn-Teller and bond disproportionation effects), as well as (ii) intrinsic electronic instabilities described by single determinant DFT band theory, all lifting orbital degeneracies. Instead of implying a universal role to dynamical correlations, our examination shows that the three basic properties — gapping, magnetism and crystal structures — are simultaneously accounted for by the same DFT band structure approach with static correlations, allowing for a general flexible framework for describing the structure of the compounds. This is a consequential result both because it suggests that whereas ABO_3 oxides may be complicated, they are not necessarily strongly correlated. Finally, our work establishes DFT as a simple platform to study reliably and with sufficient precision not only band gap formation, structure and magnetism in complex oxides, but also – in the future – doping, defect physics and interface effects. In collaboration with Julien Varignon and Manuel Bibes.

Progress on Scope 2: Thermodynamic (in) stability of some compounds predicted to host exciting new effects

- Topological insulators: BaBiO3 was predicted earlier to become a TI if doped n-type (shifting E_F by ~ 1 eV). We find that such doping destabilizes the cubic structure creating another phase that is not a TI.

- Wyle semimetals: Non-magnetic Ba_2CuO_2 in space group #130 was previously predicted to be a prototype Wyle semimetal with remarkable 8-fold degenerate semi-metallic bands. We find that spontaneous magnetism (spin-polarization) lowers the total energy, breaks symmetry, removes degeneracy and creates a wide-gap insulator, not semi metal.
- Bulk Dirac Semimetals: 4-fold degenerate bands in BiO_2 in the assumed beta

cristoblite (SiO_2) structure was previously predicted to form 3D bulk Wyle. We find that this assumed structure is far above the ground state convex hull of Bi and O_2, so its unlikely to ever be made.

- Stable **oxide** topological insulators (TI's): If made, these could bring together the traditional oxide functionalities with the dissipationless surface states of TI's have been sought for years but none was found. Yet, heavier chalcogenides (selenides, tellurides) were readily found to be TI's. We will clarify here the basic contradiction between TI-ness and stability which is maximal for oxides, and trace the basic design principles necessary to identify the window of opportunity for stable oxide TI's. We have first identified the electronic motif that can achieve topological band inversion ('topological gene') in ABO3 as being a lone-pair electron-rich B atom (e.g. Te, I, Bi) at the octahedral site. We then illustrated *that poorly screened oxide systems with large inversion energies can undergo energy-lowering atomic distortions that remove the band inversion*. We identified the coexistence windows of TI functionality and structure stability for different pressures and found that the common cubic ABO3 structures have inversion energies lying outside this coexistence window at zero pressure but could be moved into the coexistence window at moderate pressures.

Progress on Scope 3: Realistic doping of Quantum Materials:

- Quantum Spin Liquids: n- type doping of Kagome QSL candidate Cu3Zn[(OH)6Cl6] is desirable so as to convert this insulator into an important superconductor. We find via DFT modern theory of doping that such doping creates a self-trapped electron polaron that is insulating.

Planned activities

(1) Doping Kagome quantum spin liquids (continue scope 3 above)

(2) Theoretical characterization of Anti Doping:

Successful doping of insulators or semiconductors by electrons (holes), means that EF shifts towards the conduction band (valence band) and that the conductivity of free electrons (holes) increases. This is textbook predictable when the density of states of the host solid remain unperturbed by the doping process itself. Recently, however, some peculiar doping characteristics were sporadically noted in different electron doped systems: instead of shifting EF towards the conduction band and increasing conductivity, electron doping was observed to increase the band gap and thus lead to a decrease in conductivity. We will explain this peculiar effect.

Selected Publications (8/2016-)

[1] Yonggang G. Yu, Xiuwen Zhang, and Alex Zunger, *"Natural off-stoichiometry causes carrier doping in half-Heusler compounds"* Phy. Rev. B. 95, 085201 (2017).

[2] D. Yang, Jian Lv, X. Zhao, Q. Xu, Yuhao Fu, Y. Zhan, Alex Zunger, and Lijun Zhang, *"Functionality-Directed Screening of Pb-Free Hybrid Organic−Inorganic Perovskites with Desired Intrinsic Functionalities*" Chemistry of Materials 29, 524 (2017).

[3] Xin-Gang Zhao, Dongwen Yang, Yuanhui Sun, Tianshu Li, Lijun Zhang, Liping Yu, and Alex Zunger, *"Cu–In Halide Perovskite Solar Absorbers"* **J. Am. Chem. Soc**. 137, 6718 (2017).

[4] Ilya Sychugov, Fatemeh Sangghaleh, Benjamin Bruhn, Federico Pevere, Jun-Wei Luo, Alex Zunger, and Jan Linnros, *"Strong Absorption Enhancement in Si Nanorods"* **Nano Letters** 16, 7937 (2016).

[5] Q. Liu, X. Zhang, L. B. Abdalla and A. Zunger, *"Transforming common III-V and II-VI semiconductor compounds into two-dimensional topological heterostructures: The case of CdTe/InSb superlattices"* **Advanced Functional Materials** 26, 3259-3267.

[6] Q. Liu and Alex Zunger, "*Predicted Realization of Cubic Dirac Fermion in Quasi-One-Dimensional Transition-Metal Mono Chalcogenides*" **Phys Rev. X** 7, 021019 (2017).

[7] Jun-Wei Luo, Shu-Shen Li, and Alex Zunger, "Rapid saturation of the hole Rashba effect under electric field in semiconductor nanwires" **Phys. Rev. Lett**. 119, 126401 (2017).

[8] Jun-Wei Luo, Shu-Shen Li, Ilya Sychugov, Federico Pevere, Jan Linnros, and Alex Zunger, *"Absence of redshift in the direct band gap of silicon nanocrystals with reduced size"* **Nature Nanotechnology** 12, 930 (2017).

[9] X. Zhang, L. B. Abdalla, Q. Liu and Alex Zunger, *"Enabling electronic motif for topological insulation in ABO3 perovskites*" **Advanced Functional Materials** 27, 1701266 (2017).

[10] G. M. Dalpian, Q. Liu, C. C. Stoumpos, A. P. Douvalis, M. Balasubramanian, M. G. Kanatzidis and Alex Zunger, "Changes in charge density vs changes in formal oxidation states: The case of Sn halide perovskites and their ordered vacancy analogues" Phy. Rev. Materials 1, 025401;(2017).

[11] Giancarlo Trimarchi, Zhi Wang and Alex Zunger, *"Polymorphous band structure model of gapping in the antiferromagnetic and paramagnetic phases of the Mott insulators MnO, FeO, CoO, and NiO?"* Phys. Rev. B 97, 035107 (2018).

[12] Aron Walsh and Alex Zunger, *"Instilling defect tolerance in new compounds"* **Nature Materials** 16, 964 (2017).

[13] AlexZunger, "Inverse design in search of materials with target functionalities" **Nature Reviews Chemistry**, 2, 0121 (2018).

[14] P. V. Balachandran, A. A. Emery, J. E. Gubernatis, T. Lookman, C. Wolverton, and A. Zunger, *"Predictions of new ABO_3 perovskite compounds by combining machine learning and density functional theory"* Phys. Rev. Materials 2, 043802 (2018).

Semiconductor Nanostructures: Magnetism, Spin-Orbit Coupling, and Superconductivity

Principal Investigator: Igor Zutic, University at Buffalo, State University of New York zigor@buffalo.edu

Keywords: proximity effects, spin textures, quantum dots, topological materials, correlations

Project Scope

Semiconductor nanostructures provide both the key element for conventional electronics as well as a versatile platform to study fundamental phenomena. Impressive materials advances have enabled realizing novel states of matter and many surprising trends. In HgTe/CdTe quantum wells increasing the thickness of the HgTe layer, having a large spin-orbit coupling (SOC), leads to the quantum phase transition between the trivial and topological insulator. Through magnetic or superconducting proximity effects from a nearby material, initially trivial semiconductor nanostructures can also acquire topologically nontrivial states and unconventional superconductivity. Motivated by these experimental advances and stimulated by our collaborations with several experimental groups, we propose comprehensive studies of semiconductor nanostructures. We focus on two classes of systems: (i) magnetic quantum dots and (ii) heterostructures with magnetic, superconducting, and topological materials. In both cases we expect important implications of SOC and unexplored theoretical opportunities. Our approach that spans multiple techniques, from simple analytical methods and first-principle calculations, to developing Bethe-Salpeter equation for magnetic proximity effects in semiconductor nanostructures, will guide experimental realization of our predictions.

Recent Progress

Proximitized Materials While proximity effects are commonly viewed as just curious and specialized phenomena limited to cryogenic temperatures or disappearing beyond a few nanometers, we put forth a much broader picture and a notion of proximitized materials [1]. As shown in Fig. 1, given material can be transformed through proximity effects whereby it acquires properties of its neighbors, for example, becoming superconducting, magnetic, topologically nontrivial, or with an enhanced spin–orbit coupling. Such proximity effects not only complement the conventional methods of designing materials by doping or functionalization but also can overcome their various limitations. In proximitized materials, it is possible to realize properties that are not present in any constituent region of the considered heterostructure. Even though proximity effects usually imply equilibrium properties (zero applied bias), they can also alter the nonequilibrium behavior of materials, as further studied in the following two research projects.

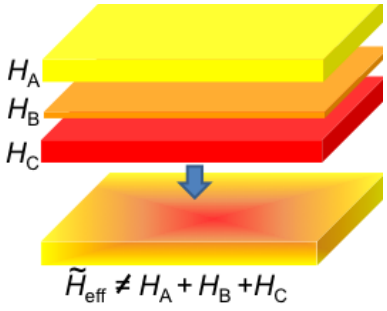

Fig. 1 Proximity-modified layer B in the presence of layers A and C, with the respective effective and individual Hamiltonians, H_{eff}, H_A, H_B, H_C [1].

Tunneling Planar Hall Effect Unlike previous manifestations of the Hall effect, such as the anomalous, tunneling anomalous, and planar Hall effects, we propose a tunneling planar Hall effect [2] emerging in ferromagnet/topological insulator junctions that has some key differences in terms of the relevant geometry and the magnetization configuration. The proposed effect, shown in Fig. 2, is maximized for a planar magnetization, **M**, parallel to the applied bias where other Hall effects vanish [2]. In contrast to conventional tunneling, a thick barrier with TIs can still lead to a large conductance due to Klein tunneling (known also from graphene). The asymmetry in the tunneling and the Hall voltage in Fig. 2(b) result from the interplay of strong SOC and Klein tunneling, modified by the proximity-induced spin splitting in the topological surface state of the 3D TI. Electrostatic control of the barrier enables a giant Hall angle, with the tunneling planar Hall conductance exceeding the longitudinal tunneling conductance [2]. This simple geometry differs from the usual studies of F/TI junctions with an out-of-plane **M** to open the band gap in the topological surface sate, commonly expected to be required for interesting phenomena, such as the quantum anomalous Hall effect.

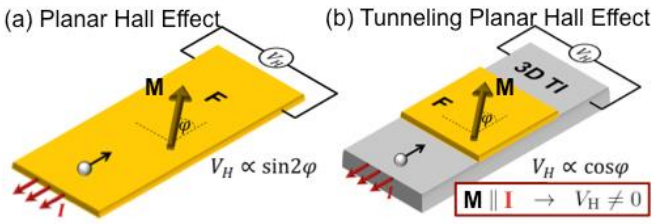

Fig. 2 (a) Planar and (b) tunneling planar Hall effect which in a TI/F junction leads to a Hall-like voltage, V_H, even for the magnetization, **M**, parallel to the current, I [2].

Magnetic Proximity Effects: Converting Excitons For the past 50 years magnetic proximity effects were studied within the single-particle description focusing on the induced magnetic moment and exchange splitting. However, the resulting neglect of Coulomb interaction and many-body effects is insufficient to describe monolayer transition metal dichalcogenides (TMDs). These van der Waals materials have unique optical properties that combine a direct band gap, huge excitonic binding energies (up to ~0.5 eV), strong SOC, and efficient light emission. While recent experiments demonstrate the proximity-induced exchange splitting in TMDs using magnetic substrates, the employed single-particle description poses large uncertainties and excludes detected excitons. By using Bethe-Salpeter equation to accurately include the interplay between the Coulomb

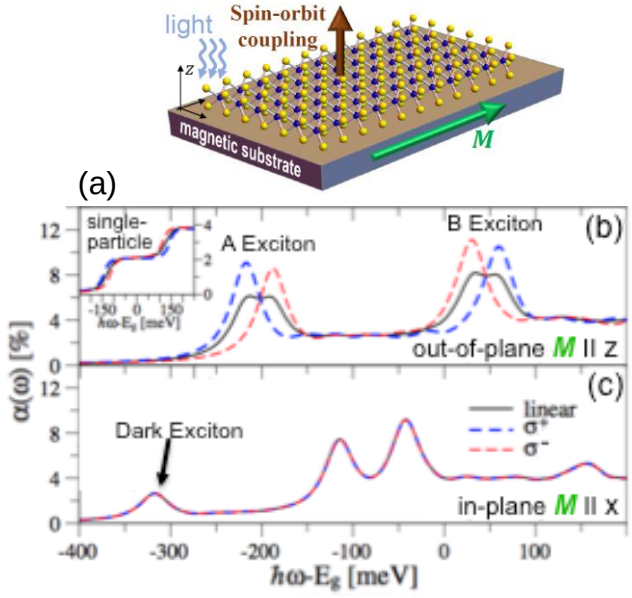

Fig. 3 A monolayer TMD on a magnetic substrate with magnetization, **M**. (b) and (c) Absorption spectra for different light polarizations and **M** directions, qualitatively different than within the common single-particle picture (inset) [3].

interaction and spin-orbit coupling in magnetic proximity effects, we predict how it transforms the optical response of TMDs for the geometry in Fig. 3(a). Depending on the **M** direction, excitonic lines can be split or excitons can be converted between dark and bright (corresponding to the optically forbidden and allowed dipole transitions, respectively), resulting in the new spectral features, shown in the absorption spectra in Fig. 3(c). While the value of interfacial SOC is generally not known at the TMD/F interfaces, we find that varying such SOC only yields negligible changes and preserves the spectral shape of the dark exciton. Our approach to accurately include Coulomb interaction could be readily used to elucidate novel phenomena from proximity effects in other van der Waals materials with reduced screening.

Magnetic and Superconducting Proximity Effects An interplay between magnetic and superconducting proximity effects can lead to many exotic states. Among them there is an increased interest to study Majorana bound states (MBS) which are emergent quasiparticles with exotic non-Abelian statistics and particle-antiparticle symmetry. Despite impressive progress in 1D semiconductor nanowires with proximity-induced superconductivity to implement MBS, these geometries pose inherent difficulties to braid (exchange) MBS and thus demonstrate their non-Abelian statistics. To overcome these challenges, we have proposed a versatile platform to realize and braid MBS [4], depicted in Fig. 4. Using magnetic tunnel junctions (MTJs), well-established in the research on magnetic hard drives and magnetic random access memory, we show how the resulting magnetic textures arising from the fringing fields can be used to localize and braid Majoranas [4]. In a subsequent work, through a collaboration with Javad Shabani and Andrew Kent (New York University) [5], we have considered other arrays of MTJs and materials which they plan to implement and experimentally demonstrate our proposal.

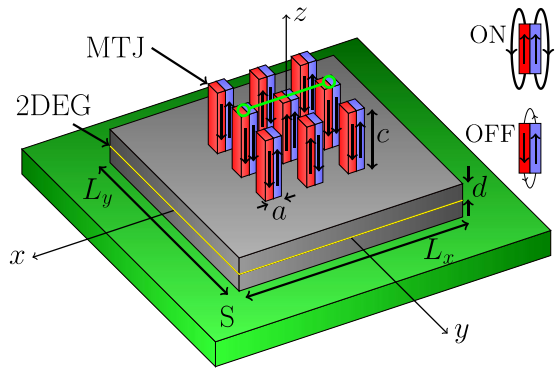

Fig. 4 2D electron gas (2DEG) on the s-wave superconductor (S). An array of magnetic tunnel junctions (MTJs) provides a magnetic texture, tunable by switching MTJs to the (anti)parallel (OFF/ON) configuration. Majorana bound states form at the ends of the middle row (green curve) [4].

Future Plans

Multiple Carrier Occupancy in Magnetic Quantum Dots We will provide a theoretical framework for experiments in the group of Athos Petrou (University at Buffalo) which support our prediction for the role Coulomb interaction on the optical and magnetic properties of Mn-doped quantum dots with the Type-II band alignment such that only the holes are confined. An optical control of magnetic interaction is obtained by using two different energies 3.06 eV and 2.54 eV of the photoexcitation in the system based on ZnTe quantum dots embedded in

(Zn,Mn)Se matrix. With the change to smaller of these two energies there is a three-fold increase of the photoluminescence saturation red shift induced by an external magnetic field. This effect can be viewed as the optical analog of the gate-controlled overlap between the carrier wavefunction and magnetic impurities in a quantum well. In contrast to the usual description of similar quantum dots, where the valence band structure and magnetic properties are dominated only by the heavy holes, we expect that light holes also play an important role.

Multiple Hall Effects in Bi Monolayers Recent experimental observation a large topologically nontrivial gap and the quantum spin Hall effect in Bi monolayers on SiC substrates suggests interesting opportunities to also observe other Hall effects in similar topologically-nontrivial systems. In collaboration with the group of Zhongqin Yang (Fudan University, China) we will use a tight-binding model and first-principles calculations to show that magnetic proximity effects from suitably chosen substrates could support multiple Hall effects, including quantum spin Hall and valley Hall effects in Bi monolayers with strong SOC. Observing these Hall effects has not yet been realized in a single materials system. To corroborate our findings, standard electronic structures calculations will be supplemented with results for spin Berry and Berry curvatures in different valleys.

Magnetic Anisotropy of Andreev Reflection In collaboration with the experimental group of Farkhad Aliev (University of Madrid, Spain) we will develop a theoretical analysis of the recent measurements which support predictions we put forth with the group of Jaroslav Fabian (University of Regensburg, Germany) that a ferromagnet/insulator/metal junction with a negligible magnetoresistance could undergo a striking transformation by cooling it below the superconducting transition temperature of a metal. Such a junction would have orders of magnitude higher magnetoresistance than in the normal state and support the formation of spin-triplet superconductivity. An important challenge is to understand the influence of an applied magnetic field on the conductance measurements and thus identify the intrinsic magnitude of the magnetic anisotropy.

References

1. I. Zutic, A. Matos-Abiague, B. Scharf, H. Dery, K. Belashchenko, *Proximitized Materials*, Mater. Today, (2018), https://doi.org/10.1016/j.mattod.2018.05.003 (open access)
2. B. Scharf, A. Matos-Abiague, J. E. Han, E. M. Hankiewicz, and I. Zutic, *Tunneling Planar Hall Effect in Topological Insulators: Spin-Valves and Amplifiers*, Phys. Rev. Lett. **117**, 166806 (2016).
3. B. Scharf, G. Xu, A. Matos-Abiague, and I. Zutic, *Magnetic Proximity Effects in Transition-Metal Dichalcogenides: Converting Excitons*, Phys. Rev. Lett. **119**, 129403 (2017).
4. G. L. Fatin, A. Matos-Abiague, B. Scharf, and I. Zutic, *Wireless Majorana Fermions: From Magnetic Tunability to Braiding*, Phys. Rev. Lett. **117**, 077002 (2016).
5. A. Matos-Abiague, J. Shabani, A. D. Kent, G. L. Fatin, B. Scharf, and I. Zutic, *Tunable Magnetic Textures: From Majorana Bound States to Braiding*, Solid. State Commun. **262**, 1 (2017)

Publications (August 2016 – July 2018)

1. I. Zutic, A. Matos-Abiague, B. Scharf, H. Dery, K. Belashchenko, *Proximitized Materials*, Materials Today, (2018), https://doi.org/10.1016/j.mattod.2018.05.003 (open access)
2. B. Scharf, A. Matos-Abiague, J. E. Han, E. M. Hankiewicz, and I. Zutic, *Tunneling Planar Hall Effect in Topological Insulators: Spin-Valves and Amplifiers*, Phys. Rev. Lett. **117**, 166806 (2016).
3. B. Scharf, G. Xu, A. Matos-Abiague, and I. Zutic, *Magnetic Proximity Effects in Transition-Metal Dichalcogenides: Converting Excitons*, Phys. Rev. Lett. **119**, 129403 (2017).
4. G. L. Fatin, A. Matos-Abiague, B. Scharf, and I. Zutic, *Wireless Majorana Fermions: From Magnetic Tunability to Braiding*, Phys. Rev. Lett. **117**, 077002 (2016).
5. A. Matos-Abiague, J. Shabani, A. D. Kent, G. L. Fatin, B. Scharf, and I. Zutic, *Tunable Magnetic Textures: From Majorana Bound States to Braiding*, Solid. State Commun. **262**, 1 (2017).
6. B. Scharf, T. Frank, M. Gmitra, J. Fabian, I. Zutic, and V. Perebeinos, *Excitonic Stark Effect in MoS_2 Monolayers*, Phys. Rev. B **94**, 245434 (2016).
7. D. Van Tuan, B. Scharf, I. Zutic, and H. Dery, *Marrying Excitons and Plasmons in Monolayer Transition-Metal Dichalcogenides*, Rev. X **7**, 041040 (2017)
8. I. Zutic and T. Zhou, *Tailoring Magnetism in Semiconductors*, Sci. China-Phys. Mech. Astron. **61**, 067031 (2018).

Author Index

Participant List

Name	Organization	Email
Allen, Philip	Stony Brook University	philip.allen@stonybrook.edu
Andreev, Anton	University of Washington	aandreev@uw.edu
Asta, Mark	Lawrence Berkeley National Laboratory	mdasta@lbl.gov
Balatsky, Alexander	Los Alamos National Laboratory	balatsky@hotmail.com
Balents, Leon	University of California, Santa Barbara	balents@spinsandelectrons.com
Bansil, Arun	Northeastern University	ar.bansil@northeastern.edu
Baranger, Harold	Duke University	baranger@phy.duke.edu
Barraza-Lopez, Salvador	University of Arkansas	sbarraza@uark.edu
Bhatt, Ravindra	Princeton University	ravin@princeton.edu
Bhowal, Sayantika	University of Missouri	bhowals@missouri.edu
Bondarev, Igor	North Carolina Central University	ibondarev@nccu.edu
Chamon, Claudio	Boston University	chamon@bu.edu
Chan, Garnet	California Institute of Technology	gkc1000@gmail.com
Chelikowsky, James	University of Texas	jrc@utexas.edu
Cheng, Hai-Ping	University of Florida	hping@ufl.edu
Chernyshev, Alexander	University of California, Irvine	sasha@uci.edu
Chudnovsky, Eugene	The City University of New York	eugene.chudnovsky@lehman.cuny.edu
Coleman, Piers	Rutgers University	coleman@physics.rutgers.edu
Cooper, Valentino	Oak Ridge National Laboratory	coopervr@ornl.gov
Daw, Murray	Clemson University	daw@clemson.edu
Devereaux, Thomas	SLAC National Accelerator Laboratory	tpd@stanford.edu
Dwaraknath, Shyam	Lawrence Berkeley National Laboratory	shyamd@lbl.gov
Feiguin, Adrian	Northeastern University	a.feiguin@northeastern.edu
Fernandes, Rafael	University of Minnesota	rfernand@umn.edu
Finkel'stein, Alexander	Texas A&M University	finkelstein@physics.tamu.edu
Flint, Rebecca	Iowa State University	flint@iastate.edu
Freericks, James	Georgetown University	james.freericks@georgetown.edu
Fu, Liang	Massachusetts Institute of Technology	liangfu@mit.edu
Galitski, Victor	University of Maryland	galitski@umd.edu

Glatz, Andreas	Argonne National Laboratory	glatz@anl.gov
Glazman, Leonid	Yale University	leonid.glazman@yale.edu
Govoni, Marco	Argonne National Laboratory	mgovoni@anl.gov
Graf, Matthias	US Department of Energy	matthias.graf@science.doe.gov
Gull, Emanuel	University of Michigan, Ann Arbor	egull@umich.edu
Haas, Stephan	University of Southern California	shaas@usc.edu
Hayes, Robin	US Department of Energy	robin.hayes@science.doe.gov
Heinonen, Olle	Argonne National Laboratory	heinonen@anl.gov
Hermele, Michael	University of Colorado Boulder	michael.hermele@colorado.edu
Jain, Anubhav	Lawrence Berkeley National Laboratory	ajain@lbl.gov
Jain, Jainendra	Pennsylvania State University	jkj2@psu.edu
Jordan, Andrew	University of Rochester	jordan@pas.rochester.edu
Kalia, Rajiv	University of Southern California	rkalia@usc.edu
Kent, Paul	Oak Ridge National Laboratory	kentpr@ornl.gov
Kharzeev, Dmitri	Stony Brook University	dmitri.kharzeev@stonybrook.edu
Kim, Eun-Ah	Cornell University	eun-ah.kim@cornell.edu
Kotliar, Gabriel	Rutgers University/Brookhaven National Laboratory	kotliar@physics.rutgers.edu
Kovalev, Alexey	University of Nebraska, Lincoln	alexey.kovalev@unl.edu
Lambrecht, Walter	Case Western Reserve University	walter.lambrecht@case.edu
Lee, Patrick	Massachusetts Institute of Technology	palee@mit.edu
Lee, Honyung	Oak Ridge National Laboratory	hnlee@ornl.gov
Louie, Steven	University of California, Berkeley/Lawrence Berkeley National Laboratory	sglouie@berkeley.edu
Lyanda-Geller, Yuli	Purdue University	yuli@purdue.edu
Maier, Thomas	Oak Ridge National Laboratory	maierta@ornl.gov
Marianetti, Chris	Columbia University	chris.marianetti@columbia.edu
Markiewicz, Robert	Northeastern University	markiewic@neu.edu
Matveev, Konstantin	Argonne National Laboratory	matveev@anl.gov
Mele, Eugene	University of Pennsylvania	mele@physics.upenn.edu
Mishchenko, Eugene	University of Utah	eugene.mishchenko@gmail.com

Mitas, Lubos	North Carolina State University	lmitas@ncsu.edu
Mitchell, John	Argonne National Laboratory	mitchell@anl.gov
Mitra, Aditi	New York University	aditi.mitra@nyu.edu
Moreo, Adriana	University of Tennessee/Oak Ridge National Laboratory	amoreo@utk.edu
Nagel, Sidney	University of Chicago	srnagel@uchicago.edu
Niu, Qian	University of Texas, Austin	niu@physics.utexas.edu
Park, Hyowon	University of Illinois, Chicago/Argonne National Laboratory	hyowon@uic.edu
Perkins, Natalia	University of Minnesota	nperkins@umn.edu
Pickett, Warren	University of California, Davis	pickett@physics.ucdavis.edu
Pleimling, Michel	Virginia Tech	pleim@vt.edu
Ponomareva, Inna	University of South Florida	iponomar@usf.edu
Raghu, Srinivas	SLAC National Accelerator Laboratory	sraghu@stanford.edu
Rahman, Talat	University of Central Florida	talat.rahman@ucf.edu
Rappe, Andrew	University of Pennsylvania	rappe@sas.upenn.edu
Reboredo, Fernando	Oak Ridge National Laboratory	reboredofa@ornl.gov
Rehr, John	University of Washington	jjr@uw.edu
Scalettar, Richard	University of California, Davis	scalettar@physics.ucdavis.edu
Sharifzadeh, Sahar	Boston University	ssharifz@bu.edu
Sheng, Dong-Ning	California State University Northridge	donna.sheng@csun.edu
Si, Qimiao	Rice University	QMSI@rice.edu
Stafford, Charles	University of Arizona	staffordphysics92@gmail.com
Todadri, Senthil	Massachusetts Institute of Technology	senthil@mit.edu
Trickey, Samuel	University of Florida	trickey@qtp.ufl.edu
Trivedi, Nandini	The Ohio State University	trivedi.15@osu.edu
Tserkovnyak, Yaroslav	University of California, Los Angeles	yaroslav@physics.ucla.edu
Tsvelik, Alexei	Brookhaven National Laboratory	tsvelik@gmail.com
Ullrich, Carsten	University of Missouri	ullrichc@missouri.edu
Van de Walle, Chris	University of California, Santa Barbara	vandewalle@mrl.ucsb.edu
van Veenendaal, Michel	Northern Illinois University	veenendaal@niu.edu

Vashishta, Priya	University of Southern California	priyav@usc.edu
Vinokour, Valerii	Argonne National Laboratory	vinokour@anl.gov
Wang, Cai-Zhuang	AMES Laboratory	wangcz@ameslab.gov
Wang, Ziqiang	Boston College	wangzi@bc.edu
Widom, Michael	Carnegie Mellon University	widom@cmu.edu
Woods, Lilia	University of South Florida	lmwoods@usf.edu
Wu, Ruqian	University of California, Irvine	wur@uci.edu
Xu, Bin	University of Arkansas	binxu@uark.edu
Zang, Jiadong	University of New Hampshire	jiadong.zang@unh.edu
Zarenia, Mohammad	University of Missouri	zareniam@missouri.edu
Zhang, Shengbai	Rensselaer Polytechnic Institute	zhangs9@rpi.edu
Zhang, Guoping	Indiana State University	gpzhang@indstate.edu
Zunger, Alex	University of Colorado, Boulder	alex.zunger@colorado.edu
Zutic, Igor	University at Buffalo	zigor@buffalo.edu